



U.S. Department of Transportation
Federal Highway Administration

Publication No. FHWA-NHI-16-009
FHWA GEC 012 – Volume I
July 2016

NHI Courses No. 132021 and 132022

Design and Construction of Driven Pile Foundations – Volume I

Developed following:

AASHTO LRFD Bridge Design Specifications, 7th Edition, 2014, with 2015 Interim.

AASHTO LRFD Bridge Construction Specifications, 3rd Edition, 2010, with '11, '12, '13, '14, and '15 Interims.



NATIONAL HIGHWAY INSTITUTE

Training Solutions for Transportation Excellence

NOTICE

The contents of this report reflect the views of the authors, who are responsible for the facts and accuracy of the data presented herein. The contents do not necessarily reflect policy of the Department of Transportation. This report does not constitute a standard, specification, or regulation. The United States Government does not endorse products or manufacturers. Trade or manufacturers' names appear herein only to illustrate methods and procedures, and are considered essential to the objective of this document.

1. REPORT NO. FHWA-NHI-16-009	2. GOVERNMENT ACCESSION NO.	3. RECIPIENT'S CATALOG NO.	
4. TITLE AND SUBTITLE Geotechnical Engineering Circular No. 12 – Volume I Design and Construction of Driven Pile Foundations		5. REPORT DATE July 2016	
		6. PERFORMING ORGANIZATION CODE	
7. AUTHOR(S) Patrick J. Hannigan, PE, Frank Rausche, PhD, PE, Garland E. Likins, PE, Brent R. Robinson, PhD, PE, and Matthew L. Becker, EI.		8. PERFORMING ORGANIZATION REPORT NO.	
9. PERFORMING ORGANIZATION NAME AND ADDRESS Ryan R. Berg & Associates, Inc. 2190 Leyland Alcove Woodbury, MN 55125		10. WORK UNIT NO.	
		11. CONTRACT OR GRANT NO. DTFH61-11-D-00049	
12. SPONSORING AGENCY NAME AND ADDRESS National Highway Institute U.S. Department of Transportation Federal Highway Administration, Washington, DC 20590		13. TYPE OF REPORT & PERIOD COVERED Final Report	
		14. SPONSORING AGENCY CODE	
15. SUPPLEMENTARY NOTES <i>FHWA COTR: Heather Shelsta</i> <i>FHWA Technical Working Group: Naser Abu-Hejlal, PhD, PE; Scott Anderson, PE; and Silas Nichols, PE</i>			
16. ABSTRACT This document presents information on the analysis, design, and construction of driven pile foundations for highway structures. This document updates and replaces FHWA NHI-05-042 and FHWA NHI-05-043 as the primary FHWA guidance and reference document on driven pile foundations. The manual addresses design aspects including subsurface exploration, laboratory testing, pile selection, aspects of geotechnical and structural limit states, as well as technical specifications. Construction aspects including static load tests, dynamic tests, rapid load tests, wave equation analyses, dynamic formulas and development of driving criteria, as well as pile driving equipment, pile driving accessories, and monitoring of pile installation inspection are also covered. Step by step procedures are included for most analysis procedures and design examples.			
17. KEY WORDS Driven pile foundations, foundation economics, site characterization, geomaterial properties, axial compression resistance, axial tension resistance, lateral resistance, pile groups, specifications, nominal resistance determination tests, construction monitoring and quality assurance.		18. DISTRIBUTION STATEMENT No restrictions.	
19. SECURITY CLASSIF. Unclassified	20. SECURITY CLASSIF. Unclassified	21. NO. OF PAGES 517	22. PRICE

CONVERSION FACTORS

Approximate Conversions to SI Units			Approximate Conversions from SI Units		
When You Know	Multiply By	To Find	When You Know	Multiply By	To Find
(a) Length					
inch (in.)	25.4	millimeter (mm)	millimeter (mm)	0.039	inch (in.)
foot (ft)	0.305	meter (m)	meter (m)	3.28	foot (ft)
yard (yd)	0.914	meter (m)	meter (m)	1.09	yard (yd)
mile (mi)	1.61	kilometer (km)	kilometer (km)	0.621	mile (mi)
(b) Area					
square inches (in ²)	645.2	square millimeters (mm ²)	square millimeters (mm ²)	0.0016	square inches (in ²)
square feet (ft ²)	0.093	square meters (m ²)	square meters (m ²)	10.764	square feet (ft ²)
Acres (ac)	0.405	hectares (ha)	hectares (ha)	2.47	Acres (ac)
square miles (mi ²)	2.59	square kilometers (km ²)	square kilometers (km ²)	0.386	square miles (mi ²)
square inches (in ²)	645.2	square millimeters (mm ²)	square millimeters (mm ²)	0.0016	square inches (in ²)
(c) Volume					
fluid ounces (oz)	29.57	milliliters (mL)	milliliters (mL)	0.034	fluid ounces (oz)
Gallons (gal)	3.785	liters (L)	liters (L)	0.264	Gallons (gal)
cubic feet (ft ³)	0.028	cubic meters (m ³)	cubic meters (m ³)	35.32	cubic feet (ft ³)
cubic yards (yd ³)	0.765	cubic meters (m ³)	cubic meters (m ³)	1.308	cubic yards (yd ³)
(d) Mass					
ounces (oz)	28.35	grams (g)	grams (g)	0.035	ounces
pounds (lb)	0.454	kilograms (kg)	kilograms (kg)	2.205	pounds
short tons (2000 lb) (T)	0.907	megagrams (tonne) (Mg)	megagrams (tonne) (Mg)	1.102	short tons (2000 lb)
(e) Force					
pound (lb)	4.448	Newton (N)	Newton (N)	0.2248	pound (lb)
(f) Pressure, Stress, Modulus of Elasticity					
pounds per square foot (psf)	47.88	Pascals (Pa)	Pascals (Pa)	0.021	pounds per square foot (psf)
pounds per square inch (psi)	6.895	kiloPascals (kPa)	kiloPascals (kPa)	0.145	pounds per square inch (psi)
(g) Density					
pounds per cubic foot (pcf)	16.019	kilograms per cubic meter (kgm ³)	kilograms per cubic meter (kgm ³)	0.0624	pounds per cubic feet (pcf)
(h) Temperature					
Fahrenheit temperature (°F)	5/9(°F- 32)	Celsius temperature (°C)	Celsius temperature (°C)	9/5(°C)+ 32	Fahrenheit temperature (°F)

Notes:

A compliant version can be found here: <https://www.fhwa.dot.gov/publications/convtbl.cfm>

- 1) The primary metric (SI) units used in civil engineering are meter (m), kilogram (kg), second (s), Newton (N), and Pascal (Pa=N/m²).
- 2) In a "soft" conversion, an English measurement is mathematically converted to its exact metric equivalent.
- 3) In a "hard" conversion, a new rounded metric number is created that is convenient to work with and remember.

PREFACE

The purpose of this manual is to provide updated, state-of-the-practice information for the design and construction of driven pile foundations in accordance with the Load and Resistance Factor Design (LRFD) platform. Engineers and contractors have been designing and installing pile foundations for many years. During the past three decades, the industry has experienced several major improvements including newer and more accurate methods of predicting and measuring geotechnical resistance, vast improvements in design software, highly specialized and sophisticated equipment for pile driving, and improved methods of construction control. Previous editions of the FHWA Design and Construction of Driven Pile Foundations manual were published 1985, 1996, and 2006 and chronicle the many changes in design and construction practice over the past 30 years. This two volume edition, GEC-12, serves as the FHWA reference document for highway projects involving driven pile foundations.

Volume I, FHWA-NHI-16-009, covers the foundation selection process, site characterization, geotechnical design parameters and reporting, selection of pile type, geotechnical aspects of limit state design, and structural aspects of limits state design. Volume II, FHWA-NHI-16-010, addresses static load tests, dynamic testing and signal matching, rapid load testing, wave equation analysis, dynamic formulas, contract documents, pile driving equipment, pile accessories, driving criteria, and construction monitoring. Comprehensive design examples are presented in publication FHWA-NHI-16-064.

Throughout this manual, numerous references will be made to the names of software or technology that are proprietary to a specific manufacturer or vendor. Please note that the FHWA does not endorse or approve commercially available products, and is very sensitive to the perceptions of endorsement or preferred approval of commercially available products used in transportation applications. Our goal with this development is to provide recommended technical guidance for the safe design and construction of driven pile foundations that reflects the current state of practice and provides information on advances and innovations in the industry. To accomplish this, it is necessary to illustrate methods and procedures for design and construction of driven pile foundations. Where proprietary products are described in text or figures, it is only for this purpose.

The primary audience for this document is: agency and consulting engineers specialized in geotechnical and structural design of highway structures; engineering geologists and consulting engineers providing technical reviews, or who are engaged in the design, procurement, and construction of driven pile foundations. This document is also intended for management, specification and contracting specialists, as well as for construction engineers interested in design and contracting aspects of driven pile systems.

This document draws material from the three earlier FHWA publications in this field; FHWA-DP-66-1 by Vanikar (1985), FHWA HI 97-013 and FHWA HI 97-014 by Hannigan et al. (1998), and FHWA NHI-05-042 and FHWA NHI-05-043 by Hannigan et al. (2006). Photographs without specific acknowledgement in this two volume document are from these previous editions, their associated training courses, or from the consulting practice of GRL Engineers, Inc.

The following individuals were part of the Ryan R. Berg & Associates internal peer review team and are acknowledged for their technical advice and contributions to this version of the document:

Mr. Jerry DiMaggio – Applied Research Associates, Inc.

Mr. Van E. Komurka – Wagner Komurka Geotechnical Group, Inc.

Mr. Billy Camp – S&ME, Inc.

Dr. Brian Anderson – Auburn University

TABLE OF CONTENTS

LIST OF TABLES	xi
LIST OF FIGURES	xv
1 DRIVEN PILE FOUNDATION MANUAL	1
1.1 INTRODUCTION	1
1.2 PURPOSE OF THE MANUAL.....	1
1.3 SCOPE OF MANUAL.....	3
1.4 HISTORY OF DRIVEN PILE FOUNDATIONS.....	4
1.5 INFORMATION SOURCES	4
REFERENCES.....	6
2 OVERVIEW OF PILE FOUNDATION DESIGN & CONSTRUCTION.....	7
2.1 INTRODUCTION	7
2.2 LIMIT STATES	7
2.3 LOADS, LOAD COMBINATIONS, AND LOAD FACTORS	9
2.4 NOMINAL AND FACTORED RESISTANCE	14
2.5 STRENGTH LIMIT STATES	15
2.6 SERVICE LIMIT STATES.....	15
2.7 EXTREME EVENT LIMIT STATES	16
2.8 CONSTRUCTION OF PILE FOUNDATIONS	16
2.9 FOUNDATION SPECIALIST INVOLVEMENT.....	17
2.10 THE DRIVEN PILE DESIGN AND CONSTRUCTION PROCESS	18
2.11 COMMUNICATION.....	39
REFERENCES.....	42
3 CONSIDERATIONS IN FOUNDATION SELECTION.....	45
3.1 FOUNDATION DESIGN APPROACH	46
3.2 FOUNDATION ALTERNATIVES.....	47
3.2.1 Shallow Foundations.....	49
3.2.2 Shallow Foundations with Ground Improvement	49
3.2.3 Deep Foundations	49
3.2.3.1 Driven Piles	50
3.2.3.2 Drilled Shafts.....	50
3.2.3.3 Micropiles.....	50
3.2.3.4 Continuous Flight Auger (CFA) Piles	51

3.3	ESTABLISHMENT OF A NEED FOR A DEEP FOUNDATION.....	51
3.4	ECONOMIC ASPECTS OF FOUNDATION SELECTION.....	54
3.4.1	Foundation Support Cost.....	54
3.4.1.1	Cost Optimization Example.....	55
3.5	OTHER CONSIDERATIONS	61
3.5.1	Constructability	62
3.5.2	Consideration of Pile Driving Noise	62
3.5.5	Durability Considerations.....	68
3.6	UNANTICIPATED OCCURRENCES	72
3.6.1	Fill Stockpile	73
3.6.2	Adjacent Construction	74
	REFERENCES.....	75
4	SITE CHARACTERIZATION.....	79
4.1	INTRODUCTION	79
4.2	SITE CHARACTERIZATION PROGRAM	80
4.2.1	Data Collection	80
4.2.2	Field Reconnaissance Survey.....	83
4.2.3	Detailed Field Exploration.....	85
4.2.3.1	Geophysical Surveys	85
4.2.3.2	Depth, Spacing, and Frequency of Boring & In-Situ Tests	86
4.2.3.3	Soil Boring Methods	88
4.2.3.4	Soil Sampling Methods	88
4.2.3.5	Rock Exploration Methods (Coring / Drilling) ...	91
4.2.3.6	Groundwater	94
4.2.4	Information Required for Construction	95
	REFERENCES.....	96
5	GEOMATERIAL DESIGN PARAMETERS AND GEOTECHNICAL REPORTS.....	99
5.1	IN-SITU SOIL TESTING	99
5.1.1	Standard Penetration Test.....	102
5.1.2	Cone Penetration Test	109
5.1.3	Vane Shear Test.....	112
5.1.4	Other In-Situ Tests.....	113
5.1.4.1	Dilatometer Test	114
5.1.4.2	Pressuremeter Tests.....	114
5.1.4.3	Dynamic Cone	114
5.2	SOIL PARAMETERS	115

5.2.1	Soil Classification and Index Properties	115
5.2.2	In-Situ Stress.....	118
5.2.3	Shear Strength	119
5.2.3.1	Laboratory Tests for Soil Shear Strength	121
5.2.3.1.1	Direct Shear	121
5.2.3.1.2	Unconfined Compression	121
5.2.3.1.3	Triaxial Compression Test.....	122
5.2.3.2	Effective Stress Friction Angle Correlations, Cohesionless Soils.....	122
5.2.3.3	Fully Drained Shear Strength of Fine- Grained Cohesive Soils	127
5.2.3.4	Undrained Shear Strength of Fine-Grained Cohesive Soils.....	127
5.2.4	Deformation	130
5.2.4.1	Elastic Deformation.....	130
5.2.4.2	Primary Consolidation Settlement	132
5.2.5	Electro Chemical Properties	134
5.3	ROCK PARAMETERS	134
5.3.1	Rock Index Properties and Classification.....	135
5.3.2	Rock Mass Shear Strength.....	135
5.3.3	Rock Mass Deformation	136
5.4	CONSIDERATIONS FOR PILE DRIVABILITY	136
5.5	SELECTION OF PARAMETERS FOR DESIGN AND CONSTRUCTION.....	137
5.5.1	Soil Parameters.....	138
5.5.2	Rock Parameters.....	138
5.5.3	Site Variability	140
5.6	GEOTECHNICAL REPORTING.....	142
5.6.1	Geotechnical Data Reports.....	142
5.6.2	Geotechnical Foundation Design Reports.....	144
5.6.3	Geotechnical Baseline Reports.....	148
	REFERENCES.....	149
6	PILE TYPES FOR FURTHER EVALUATION.....	155
6.1	OVERVIEW OF TYPICAL PILE TYPES	155
6.2	TIMBER PILES.....	164
6.3	STEEL H-PILES	166
6.4	STEEL PIPE PILES	168
6.4.1	Closed End Steel Pipe	168
6.4.2	Open End Steel Pipe	170

6.5	MONOTUBE PILES	173
6.6	TAPERTUBE PILES	174
6.7	SPIN FIN PILES	174
6.8	PRESTRESSED CONCRETE PILES	176
6.9	CONCRETE CYLINDER PILES	178
	6.9.1 Spun-Cast Cylinder Piles.....	179
	6.9.2 Bed-Cast Cylinder Piles	180
	6.9.3 Industrial Concrete Products (ICP) Piles.....	180
6.10	COMPOSITE PILES	181
	6.10.1 Precast Concrete - Steel H-pile Composite Piles.....	181
	6.10.2 Steel Pipe - H-pile Composite Piles.....	182
	6.10.3 Corrugated Shell - Timber Composite Piles	182
	6.10.4 Corrugated Shell - Pipe Composite Piles	183
6.11	PILE TYPES INFREQUENTLY USED ON TRANSPORTATION PROJECTS	183
	6.11.1 Fundex Piles	183
	6.11.2 Tubex Piles	184
	6.11.3 Pressure Injected Footings (PIF).....	184
	6.11.4 Mandrel Driven Piles	185
	6.11.5 Reinforced Concrete Piles	185
6.12	DESIGN CONSIDERATIONS IN AGGRESSIVE SUBSURFACE ENVIRONMENTS	187
	6.12.1 Corrosion of Steel Piles.....	188
	6.12.1.1 Corrosion in Non-Marine Environments	188
	6.12.1.2 Corrosion in Marine Environments	192
	6.12.2 Sulfate and Chloride Attack on Concrete Piles	193
	6.12.3 Bacteria, Fungi, Insect, and Marine Borer Attacks on Timber Piles	194
	6.12.4 Design Options for Piles Subject to Degradation or Abrasion	195
6.13	SELECTION OF PILE TYPE AND SIZE FOR FURTHER EVALUATION.....	196
6.14	HISTORICAL PRICE INFORMATION	199
	6.14.1 California.....	200
	6.14.2 Florida	201
	6.14.3 Indiana.....	202
	6.14.4 Maryland.....	203
	6.14.5 North Carolina	204
	6.14.6 Pennsylvania.....	205
	6.14.7 Texas.....	206

7.2.3.2	Axial Tension Resistance of Pile Groups	290
7.2.3.2.1	Axial Tension Resistance of Groups in Cohesionless Soils	291
7.2.3.2.2	Axial Tension Resistance of Groups in Cohesive Soils.....	292
7.2.4	Nominal Axial Resistance Changes after Pile Driving ..	293
7.2.4.1	Relaxation	293
7.2.4.2	Soil Setup.....	294
7.2.4.2.1	Estimation of Pore Pressures During Driving	299
7.2.4.3	Implementation of Time Effects During Construction	300
7.2.5	Nominal Lateral Resistance	301
7.2.6	Pile Length Estimates for Contract Documents	301
7.2.7	Groundwater Effects and Buoyancy	302
7.2.8	Site Dewatering	302
7.2.8.1	Artesian Conditions	303
7.2.9	Scour	304
7.2.10	Downdrag	307
7.3	SERVICE LIMIT STATES.....	308
7.3.1	Tolerable Vertical Deformations and Angular Distortion.....	309
7.3.1.1	Load Factor for Vertical Deformations	310
7.3.2	S-0 Concept for Vertical Deformations	310
7.3.3	Construction Point Concept	312
7.3.4	Recommended Procedure for Vertical Deformation Analysis	314
7.3.5	Pile Group Settlement	316
7.3.5.1	Elastic Compression of Piles.....	317
7.3.5.2	Group Settlement in Cohesionless Soils	317
7.3.5.2.1	Method Based on SPT Test Data.....	319
7.3.5.2.2	Method Based on CPT Test Data.....	319
7.3.5.3	Group Settlement in Cohesive Soils	320
7.3.5.4	Time Rate of Settlement in Cohesive Soils ...	325
7.3.5.5	Group Settlement in Layered Soils	326
7.3.5.6	Group Settlement Using the Janbu Tangent Modulus Approach.....	328
7.3.5.7	Group Settlement Using the Neutral Plane Method.....	334
7.3.6	Settlement Due to Downdrag.....	336

	7.3.6.1	Recommended Approach for Downdrag	341
	7.3.6.2	Methods for Reducing Downdrag and Drag Force	348
	7.3.7	Horizontal Pile Foundation Deflection.....	351
	7.3.7.1	Pile Head Fixity.....	353
	7.3.7.2	Lateral Design Methods.....	355
	7.3.7.3	p-y Method	356
	7.3.7.4	Strain Wedge Method.....	362
	7.3.7.5	Single Piles	364
	7.3.7.6	Pile Groups	364
	7.3.7.6.1	Lateral Resistance Increases Through Ground Improvement	371
	7.3.8	Lateral Squeeze of Foundation Soil and Solutions	374
	7.3.9	Overall Stability	375
7.4		EXTREME EVENT LIMIT STATES	376
	7.4.1	Extreme Event Scour During Check Flood.....	376
	7.4.2	Seismic and Seismic Induced Downdrag.....	377
	7.4.2.1	AASHTO Recommendations for the Equivalent Static Seismic Force	378
	7.4.2.2	Liquefaction.....	382
	7.4.3	Ice and Collisions	385
	7.4.3.1	Ice Loads	386
	7.4.3.2	Vehicle Collison	387
	7.4.3.3	Vessel Collision	387
	7.4.4	Combined Extreme Events.....	388
7.5		DETERMINATION OF MINIMUM PILE PENETRATION.....	388
7.6		DETERMINATION OF R_{ndr} TO ESTABLISH CONTRACT DRIVING CRITERIA	390
7.7		DRIVABILITY ANALYSIS	391
	7.7.1	Factors Affecting Drivability	392
	7.7.2	Methods for Determining Pile Drivability	393
	7.7.3	Drivability versus Pile Type.....	395
7.8		CONSIDERATIONS FOR BATTER PILE DESIGN AND CONSTRUCTION.....	395
7.9		CORROSION AND DETERIORATON.....	397
7.10		ADDITIONAL DESIGN AND CONSTRUCTION CONSIDERATIONS.....	398
	7.10.1	Minimum Pile Spacing, Clearance, and Cap Embedment.....	398
	7.10.1.1	Special Considerations for Large Pile Sizes ..	399

7.10.2	Identification of High Rebound Soils	400
7.10.3	Soil and Pile Heave.....	400
7.10.4	Piles Driven Through Embankment Fills	402
7.10.5	Effect of Predrilling, Jetting and Vibratory Installation on Nominal Resistance	403
7.10.6	Densification Effects on Nominal Resistance and Installation Conditions	404
7.10.7	Plugging of Open Pile Sections.....	405
REFERENCES.....		411
8	STRUCTURAL ASPECTS AND LIMIT STATES.....	427
8.1	INTRODUCTION	427
8.2	BASIC STRUCTURAL PROPERTIES OF DRIVEN PILES.....	428
8.2.1	Material Properties.....	428
8.2.2	Pile Section Definitions.....	430
8.2.3	Effective Length and Buckling.....	433
8.3	STRUCTURAL CONSIDERATIONS AND RESISTANCE FACTORS.....	434
8.3.1	Depth to Fixity	435
8.3.2	Limiting Slenderness Ratio	436
8.3.3	Resistance Factors	436
8.4	TIMBER PILES.....	439
8.4.1	Driving Stresses	440
8.4.2	Structural Resistance	441
8.4.2.1	Axial Compression Parallel to Grain	441
8.4.2.2	Flexure.....	443
8.4.2.3	Combined Flexure and Axial Compression ...	444
8.5	STEEL PILES.....	445
8.5.1	Driving Stresses	445
8.5.2	Structural Resistance	445
8.5.2.1	Axial Compression.....	445
8.5.2.2	Flexure.....	449
8.5.2.3	Combined Axial Compression and Flexure ...	452
8.5.2.4	Shear	453
8.5.3	Example Calculations for H Pile Structural Resistance.	454
8.6	CONCRETE PILES.....	459
8.6.1	Driving Stresses	459
8.6.2	Structural Resistance	460
8.6.2.1	Axial Compression.....	460

8.6.2.2	Biaxial Flexure	461
8.7	COMPOSITE PILES	464
8.7.1	Driving Stress	464
8.7.2	Structural Resistance	464
8.7.2.1	Axial Compression	464
8.8	LAYOUT OF PILE GROUPS	467
8.9	PRELIMINARY DESIGN OF PILE BENT AND GROUP CAPS	470
8.9.1	Cap Considerations for Large Pile Sizes	481
REFERENCES	482
A	LIST OF FHWA/ NHI RESOURCES RELEVANT TO DEEP FOUNDATIONS	485
B	LIST OF ASTM AND AASHTO PILE DESIGN AND TESTING SPECIFICATIONS	491
C	PILE HAMMER INFORMATION	495

LIST OF TABLES

Table 2-1	Limit State, Load Case, and Load Combination (after AASHTO 2014).....	8
Table 2-2	Load Combinations and Load Factors (after AASHTO 2014)...	10
Table 2-3	Load Factors for Permanent Loads (after AASHTO 2014).....	11
Table 2-4	Design Stage Communication.....	40
Table 2-5	Construction Stage Communication.....	41
Table 3-1	Foundation Information Sources Provided by the Federal Highway Administration.....	45
Table 3-2	Foundation Types and Typical Uses (Modified from Bowles 1977).....	48
Table 3-3	Pile Length Estimates Based on Field Methods and Factored Resistances.....	59
Table 3-4	Compression Factor, α , for Sand Based on Soil Density and Level of Driving Energy (after Massarsch and Fellenius 2014).....	67
Table 4-1	Subsurface Exploration Phases.....	81
Table 4-2	Sources of Subsurface Information and Use.....	82
Table 4-3	Minimum Number of Exploration Points per Substructure (modified from Sabatini et al. 2002).....	87
Table 4-4	Soil Boring Methods.....	89
Table 4-5	Summary of Rock Coring Methods.....	92
Table 4-6	Rock Quality Designation.....	94
Table 5-1	Field and Laboratory Tests for Geomaterial Parameter Determination.....	100
Table 5-2	Summary of In-Situ Methods.....	103
Table 5-3	Soil Index Tests used for Driven Pile Design (modified from Brown et al. 2010).....	116
Table 5-4	Typical Values of Sensitivity (after Sowers 1979).....	117
Table 5-5	AASHTO (2014) Correlation Between SPT (N_1) ₆₀ values to Drained Friction Angle of Granular Soils (modified after Bowles 1997).....	123
Table 5-6	Correlation Between Relative Density, SPT N value, and Internal Friction Angle for Cohesionless Soils in GEC-5 (2002) (after Meyerhof 1956).....	123

Table 5-7	Correlation Between Relative Density, CPT Cone Resistance, and Angle of Internal Friction for Clean Sands (after Meyerhof 1976).....	125
Table 5-8	Unconfined Compressive Strength of Particles for Rockfill Grades in Figure 5-12.....	126
Table 5-9	Empirical Values for Unconfined Compressive Strength, q_u , and Consistency of Cohesive Soils Based on Uncorrected N- Value (after Bowles 1977)	129
Table 5-10	Estimating Soil Modulus, E_s , Based on Soil Type (after AASHTO 2014).....	131
Table 5-11	Estimating Soil Modulus, E_s , from SPT N value (after AASHTO 2014).....	132
Table 5-12	Estimating Soil Modulus, E_s , from Cone Resistance, q_c (after AASHTO 2014)	132
Table 5-13	Usual Types of Soft Rocks (after Kanji 2014).	139
Table 5-14	Coefficients of Variation for Geotechnical Properties and In-Situ Tests (after Duncan and Wright 2005).....	141
Table 5-15	Pile Foundation Decisions Influenced by Subsurface Information	143
Table 5-16	Information Included in Geotechnical Data Reports (after Brown et al. 2010).....	144
Table 6-1	Timber Piles Technical Summary	157
Table 6-2	Steel H-Piles Technical Summary	158
Table 6-3	Steel Pipe Piles Technical Summary	159
Table 6-4	Precast, Prestressed Concrete Technical Summary	160
Table 6-5	Monotube Pile Technical Summary	161
Table 6-6	Tapertube Piles Technical Summary	162
Table 6-7	Composite Piles Technical Summary.....	163
Table 6-8	Preservative Retention Requirements (after Collin 2002)	195
Table 6-9	Pile Type Selection Based on Subsurface and Hydraulic Conditions.	198
Table 6-10	Pile Type Selection Based on Pile Shape Effects.	199
Table 6-11	CALTRANS, 2014 Contract Cost Data.....	200
Table 6-12	FDOT 2015 Historical Cost Information.....	201
Table 6-13	INDOT 2015 Unit Price Summaries	202
Table 6-14	MDSHA Price Index Published July 2015.....	203
Table 6-15	2015 NCDOT Bid Quantities and Averages.....	204
Table 6-16	2015 PennDOT Bid Quantities and Averages.....	205
Table 6-17	TxDOT 12-Month Project Bid Averages	206

Table 7-1	Resistance Factors for Static Analysis Methods Presented in this Manual (modified from AASHTO 2014)	224
Table 7-2	Resistance Factors for Field Determination Methods (after AASHTO 2014).....	226
Table 7-3	Summary of Static Analysis Methods in GEC-12 and AASHTO (2014) for Determination of Nominal Resistance ..	228
Table 7-4	Methods of Static Analysis for Piles in Cohesionless Soils	230
Table 7-5	Methods of Static Analysis for Piles in Cohesive Soils.....	231
Table 7-6	Design Table for Evaluating K_s for Piles when $\omega = 0^\circ$ and $V = 0.10$ to 1.00 ft ³ /ft.....	240
Table 7-7	Design Table for Evaluating K_s for Piles when $\omega = 0^\circ$ and $V = 1.0$ to 10 ft ³ /ft.....	241
Table 7-8	Design Parameter Guidelines for Cohesionless Siliceous Soil (after API 1993)	253
Table 7-9	Approximate Range of β and N_f Coefficients (after Fellenius 2014).....	256
Table 7-10	Input Factors for Brown's Method.....	260
Table 7-11	C_s Values for Eslami and Fellenius Method (after Fellenius 2014).....	261
Table 7-12	CPT C_f VALUES	264
Table 7-13	Published Nominal Shaft Resistance Values in Weak Rock Materials.....	270
Table 7-14	Published Nominal Toe Resistance Values in Weak Rock Materials.....	271
Table 7-15	Summary of Computer Analysis Software for Axial Single Pile Analysis	275
Table 7-16	Soil Setup Factors (after Rausche et al. 1996)	299
Table 7-17	Hydraulic Design, Scour Design, and Scour Design Check Flood Frequencies per HEC-18 (after Arneson et al. 2012) ...	305
Table 7-18	Tolerable Movement Criteria for Bridges.....	310
Table 7-19	Time Factors for Settlement	326
Table 7-20	Typical Modulus and Stress Exponent Values (after Canadian Geotechnical Society 1985)	333
Table 7-21	Representative Values of ϵ_{50} for Clays.....	358
Table 7-22	Representative Modulus of Subgrade Reaction Values, k_s and k_c , for Clays and Sands	359
Table 7-23	Laterally Loaded Pile Group Studies.....	367
Table 7-24	Summary of Ground Improvement Method and Increase in Lateral Resistance (after Rollins and Brown 2011).....	373

Table 7-25	Summary of Ground Improvement Method and Associated Costs for Increase in Lateral Resistance after (Rollins and Brown 2011)	373
Table 7-26	Site Class Definition	379
Table 7-27	Site Factor Values, F_{pga} , at Zero Period Acceleration	380
Table 7-28	Site Factor Values, F_a , for Short Period Coefficient S_s	380
Table 7-29	Site Factor Values, F_v , for Long Period Coefficient, S_1	380
Table 7-30	Seismic Zones	382
Table 7-31	Blow Count Correction, N_{corr} , for the Equivalent Clean Sand Blow Count, $(N_1)_{60-e}$	384
Table 7-32	Summary of Load and Resistance Information	390
Table 8-1	Common Steel Pipe Pile Grades and Yield Stress.....	429
Table 8-2	Common Steel H-pile Grades and Yield Stress	429
Table 8-3	Timber Pile Compression Stress and Elastic Modulus Reference Values (after AASHTO 2014).....	430
Table 8-4	Rate of Increase of Soil Modulus with Depth for Sands (ksi/ft) (after AASHTO 2014)	436
Table 8-5	Resistance Factors During Pile Driving	438
Table 8-6	Structural Limit Resistance Factors for Piles in Compression	438
Table 8-7	Reference Design Values for Timber Piles, ksi (after AASHTO 2014).....	439
Table 8-8	Time Effect Factors (after AASHTO 2014)	439

LIST OF FIGURES

Figure 2-1	Structural analysis of bridge used to establish foundation force effects (modified from Brown et al. 2010).....	12
Figure 2-2	Example of factored load calculation.....	13
Figure 2-3	Driven pile design and construction process.....	19
Figure 3-1	Situations in which deep foundations may be needed (modified from Vesic 1977).	53
Figure 3-2	Soil profile and nominal geotechnical resistances versus depth.....	56
Figure 3-3	Pile cost versus pile penetration depth.	57
Figure 3-4	Nominal resistance of pile support cost versus penetration depth.....	57
Figure 3-5	Nominal and factored resistances for axial compression loads.	58
Figure 3-6	Nominal resistance and pile support cost.....	60
Figure 3-7	Nominal and factored resistances for axial tension loads.....	61
Figure 3-8	Predicted vibration levels for class II and class III soils (after Bay 2003).	65
Figure 3-9	Settlement area and magnitude around a pile in homogeneous sand deposit (after Massarsch and Fellenius 2014).....	67
Figure 3-10	Corrosion and resulting buckling of foundation pile (courtesy Wisconsin Department of Transportation).....	69
Figure 3-11	Concrete pile damage from corrosion effects on concrete pile reinforcement (courtesy of Moser 2011).....	70
Figure 3-12	Concrete surface abrasion and deterioration in tidal zone (courtesy of Moser 2011).....	71
Figure 3-13	Examples of timber pile deterioration (courtesy Bridge Engineering Center at Iowa State University).	72
Figure 3-14	Tilting columns adjacent to stockpile (courtesy DeIDOT).	73
Figure 3-15	Cracked pile cap from lateral soil movements (courtesy DeIDOT).....	74
Figure 4-1	Typical field reconnaissance form.....	84
Figure 4-2	Standard split spoon sampler.....	91
Figure 4-3	Shelby tubes (after Mayne et al. 2002).....	91
Figure 4-4	Rock core samples.....	93

Figure 5-1	Schematic of common of in-situ tests (after Mayne et al. 2001).....	102
Figure 5-2	Standard Penetration Test schematic (after Mayne et al. 2001).....	104
Figure 5-3	Standard Penetration Test hammer types.	105
Figure 5-4	Instrumented 2 foot long AW rod atop drill string for SPT hammer energy measurements.	106
Figure 5-5	Adjacent borings with different SPT hammer types (after Finno 1989).	107
Figure 5-6	Cone penetrometers (after Mayne et al. 2001).....	110
Figure 5-7	CPT rig.	110
Figure 5-8	Soil behavior type classification chart based on normalized CPT data (after Robertson 1990).....	112
Figure 5-9	Vane shear test schematic (after Mayne et al. 2001).....	113
Figure 5-10	Typical ranges of friction angle for rockfills, gravels and sands (Note: 1 kPA = 0.145 psi) (after Terzaghi et al. 1996).....	126
Figure 5-11	Relationship between ϕ' and PI (after Terzaghi et al. 1996)...	127
Figure 5-12	Soil stress strain curve and 50% secant modulus (after Brown et al. 2010).....	131
Figure 5-13	Plot of Void Ratio vs Vertical Effective Stress from consolidation test.	133
Figure 6-1	Pile classification chart.	156
Figure 6-2	Timber pile typical illustration.	157
Figure 6-3	Steel H-pile typical illustration.....	158
Figure 6-4	Steel pipe piles typical illustration.	159
Figure 6-5	Precast, prestressed concrete typical illustration.....	160
Figure 6-6	Monotube pile typical illustration.	161
Figure 6-7	Tapertube pile typical illustration.....	162
Figure 6-8	Composite piles typical illustration.	163
Figure 6-9	Timber piles.	164
Figure 6-10	H-piles with driving shoes.	166
Figure 6-11	Typical 16 inch closed end pipe pile.....	169
Figure 6-12	42 inch diameter, spiral weld, open end, pipe for main river pier.....	171
Figure 6-13	Large diameter open end pipe piles.	171
Figure 6-14	Constrictor plate.....	172
Figure 6-15	Constrictor plate installed inside pipe pile.	172
Figure 6-16	Tapered Monotube section (right) with add-on sections (left).	173

Figure 6-17	Tapertube piles (courtesy DFP Foundation Products, LLC). ...	174
Figure 6-18	Spin Fin pile load transfer illustration.	175
Figure 6-19	30 inch diameter Spin Fin pile.	176
Figure 6-20	Typical prestressed concrete piles.	177
Figure 6-21	Square prestressed concrete piles.	177
Figure 6-22	Typical spun-cast concrete cylinder pile section.	179
Figure 6-23	Concrete cylinder pile.	180
Figure 6-24	Precast concrete piles each with H-pile stinger.	181
Figure 6-25	Steel pipe - H-pile composite piles.	182
Figure 6-26	Soil sampling and testing protocol for corrosion assessment of steel piles in non-marine applications.	189
Figure 6-27	Procedure for uniform or macrocell corrosion assessment of steel piles in non-marine applications.	190
Figure 6-28	Procedure for determination of electrochemical testing, corrosion monitoring and corrosion mitigation techniques.	191
Figure 6-29	Loss of thickness by corrosion for steel piles in seawater (after Morley and Bruce 1983).	193
Figure 7-1	Compaction of cohesionless soils during pile driving (after Broms 1966).	215
Figure 7-2	Disturbance of cohesive soils during pile driving (after Broms 1966).	216
Figure 7-3	Situation where two static analyses are necessary due to scour.	218
Figure 7-4	Situation where two static analyses are necessary due to fill materials.	218
Figure 7-5	Typical load transfer profiles.	220
Figure 7-6	Effective stress diagram – water table below ground surface.	222
Figure 7-7	Effective stress diagram – water table above ground surface.	222
Figure 7-8	Nordlund’s general equation diagram for nominal resistance.	234
Figure 7-9	Relationship of δ/ϕ and pile soil displacement, V , for various pile types (after Nordlund 1979).	235
Figure 7-10	Design curve for evaluating K_δ for piles when $\phi = 25^\circ$ (after Nordlund 1979).	235
Figure 7-11	Design curve for evaluating K_δ for piles when $\phi = 30^\circ$ (after Nordlund 1979).	236
Figure 7-12	Design curve for evaluating K_δ for piles when $\phi = 35^\circ$ (after Nordlund 1979).	237

Figure 7-13	Design curve for evaluating K_δ for piles when $\phi = 40^\circ$ (after Nordlund 1979).	237
Figure 7-14	Correction factor for K_δ when $\delta \neq \phi$ (after Nordlund 1979).....	238
Figure 7-15	Relationship between maximum unit toe resistance and friction angle for cohesionless soils (after Meyerhof 1976).....	238
Figure 7-16	Chart for estimating α_t coefficient and bearing capacity factor N'_q (after Bowles 1977).....	239
Figure 7-17	Adhesion values for piles in cohesive soils (after Tomlinson 1979).....	248
Figure 7-18	Adhesion factors for driven piles in clay (Tomlinson 1980).....	249
Figure 7-19	Penetrometer design curves for pile shaft friction in sand (after FHWA Implementation Package, FHWA-TS-78-209). .	265
Figure 7-20	Design curve for pile shaft friction in clay (after Schmertmann 1978).	265
Figure 7-21	Illustration of Nottingham and Schmertmann Procedure for estimating pile toe resistance (FHWA-TS-78-209).	266
Figure 7-22	Bearing capacity factors for foundations on rock (modified from Pells and Turner 1980).....	273
Figure 7-23	Soil profile for computer software comparison.	276
Figure 7-24	Nominal resistance from DRIVEN program using FHWA method.	276
Figure 7-25	Nominal resistance from APILE program using FHWA Method.	277
Figure 7-26	Nominal resistance from UNIPILE program using Beta Method.	277
Figure 7-27	Nominal resistance versus depth for three pile types calculated by the APILE program with the FHWA Method.	278
Figure 7-28	Design chart of nominal resistance, R_n , and factored resistance, R_r , versus depth for one pile type with different field control methods.	280
Figure 7-29	Overlap of stress zones for friction pile group (after Bowles 1988).....	283
Figure 7-30	Measured dissipation of excess pore water pressure in soil surrounding full scale pile groups (after O'Neill 1983).....	285
Figure 7-31	Three dimensional pile group configuration (after Tomlinson 1994).....	287
Figure 7-32	Design chart for nominal and factored resistance in axial tension.	290
Figure 7-33	Uplift of pile group in cohesionless soil (after Tomlinson 1994).....	292

Figure 7-34	Uplift of pile group in cohesive soils (after Tomlinson 1994)...	293
Figure 7-35	Excess pore water pressure due to pile driving (after Poulos and Davis 1980).....	300
Figure 7-36	Local and channel degradation scour.....	305
Figure 7-37	Angular distortion due to non-uniform bridge settlement.	309
Figure 7-38	Example settlement and angular distortion profile (after Modjeski and Masters 2015).	311
Figure 7-39	Settlement profile with design differential settlement and design angular distortion from S-0 concept (after Modjeski and Masters 2015).	312
Figure 7-40	Construction point concept: (a) identification of key construction points, (b) estimated load-deformation behavior (after Modjeski and Masters 2015).....	313
Figure 7-41	Settlement profile with angular distortion from construction point concept (after Modjeski and Masters 2015).....	314
Figure 7-42	Stress zone from single pile and pile group (after Tomlinson 1994).....	316
Figure 7-43	Values of the bearing capacity index, C' , for granular soil (data from Hough 1959).....	318
Figure 7-44	Equivalent footing concept.	320
Figure 7-45	Stress distribution below equivalent footing for a pile group in firm clay (after Duncan and Buchignani, 1976).....	321
Figure 7-46	Stress distribution below equivalent footing for a pile group (modified from Cheney and Chassie 2000).....	322
Figure 7-47	Plot of void ratio vs. vertical effective stress from consolidation test.	323
Figure 7-48	Non-linear relation between stress and strain in soil (after Fellenius 1990).	329
Figure 7-49	Neutral plane (after Goudrealt and Fellenius 1994).	335
Figure 7-50	Calculated load versus depth in 12.75 inch O.D. concrete filled pipe pile as a function of time (after MnDOT Geotechnical Manual).....	338
Figure 7-51	Change in neutral plane, negative shaft resistance, and drag force during transition to geotechnical strength limit (after MnDOT Geotechnical Manual).	339
Figure 7-52	Conceptual illustration of soil and pile movement (left) and resulting neutral plane and pile forces (right) (adapted from Siegel et al. 2013).	339
Figure 7-53	Common downdrag situation due to fill weight.	340
Figure 7-54	Common downdrag situation due to ground water lowering. ...	340

Figure 7-55	Plot of static analysis results (after Siegel et al. 2013).....	342
Figure 7-56	Plot of normalized toe resistance versus toe movement (after Siegel et al. 2013).....	343
Figure 7-57	Axial load and resistance plot of cumulative shaft resistance vs. depth (after Siegel et al. 2013).....	344
Figure 7-58	Axial load and resistance plot of unfactored permanent load plus cumulative shaft resistance vs depth (after Siegel et al. 2013).....	345
Figure 7-59	Axial load and resistance plot including mobilized resistances (after Siegel et al. 2013).....	345
Figure 7-60	Axial Load and resistance plot including neutral plane location based on mobilized toe resistance (after Siegel et al. 2013).....	346
Figure 7-61	Geofoam block approach embankment (courtesy MnDOT). ...	349
Figure 7-62	Over-sized collar for bitumen coating protection.	350
Figure 7-63	Soil resistance to a lateral pile load (after Smith 1989).	352
Figure 7-64	Effect of pile head fixity on translation at service limit state (after Wilson et al. 2006).....	354
Figure 7-65	Effect of pile head fixity on moment in piles at strength limit state (after Wilson et al. 2006).....	354
Figure 7-66	Typical lateral analysis pile-soil model.	357
Figure 7-67	Typical p-y curves for ductile and brittle soil (after Coduto 1994).....	358
Figure 7-68	Graphical presentation of p-y analysis results (after Reese 1986).....	361
Figure 7-69	Comparison of measured and COM624P predicted load- deflection behavior versus depth (after Kyfor et al. 1992).	361
Figure 7-70	Strain wedge developed in soil (after Ashour et al. 1998a). ...	362
Figure 7-71	Proposed geometry of compound passive wedge (after Ashour et al. 1998a).....	363
Figure 7-72	Soil-pile interaction with multiple soil layers (after Ashour et al. 1998a).	364
Figure 7-73	Illustration of p-multiplier concept for lateral group analysis. ...	366
Figure 7-74	Typical plots of (a) Load versus deflection and (b) Bending moment versus deflection for pile group analysis (adapted from Brown and Bollman 1993).	369
Figure 7-75	Ground improvement treatment areas for increased lateral resistance of pile groups in weak soils (Rollins and Brown 2011).....	372
Figure 7-76	Examples of abutment tilting due to lateral squeeze.....	375

Figure 7-77	Design response spectrum (after AASHTO 2014).....	381
Figure 7-78	Correlation between the Residual Undrained Strength Ratio, s_r / σ'_{vo} and equivalent clean sand SPT blow count, $(N_1)_{60-e}$ (Idriss and Boulanger 2007).....	383
Figure 7-79	Application of equivalent impact force (after AASHTO 2014).....	388
Figure 7-80	Variation of foundation response depending on group configuration and batter (after Wilson et al. 2006).....	396
Figure 7-81	Balance of forces on pile subject to heave (after Haggerty and Peck 1971).....	402
Figure 7-82	Variation in expected static resistance from API method based on plugged, unplugged, and automatic calculated plugging.....	408
Figure 7-83	Plugging of open end pipe piles (after Paikowsky and Whitman 1990).....	409
Figure 7-84	Plugging of H-piles (after Tomlinson 1994).....	409
Figure 8-1	H-pile section dimensions.	430
Figure 8-2	Table of H-pile section properties (modified from Skyline Steel 2015).	431
Figure 8-3	Pipe pile section dimensions.	431
Figure 8-4	Effective length factors, K (after AASHTO 2014).....	434
Figure 8-5	Moment interaction diagram.....	463
Figure 8-6	Pile group layout.	469
Figure 8-7	Cap section and notation.	472
Figure 8-8	Critical punching (two-way) shear sections around column....	474
Figure 8-9	Critical section from overlapping critical perimeters (after AASHTO 2014).....	475
Figure 8-10	Pile punching shear for: (a) circular pile; (b) rectangular H pile; (c) circular pile near corner of cap; and (d) two nearby circular piles.....	476
Figure 8-11	One-way beam shear critical sections from column.....	478
Figure 8-12	One-way beam shear critical sections from pile(s).	478

LIST OF SYMBOLS

- A - Pile cross sectional area (7.3).
- A_b - Brown's regression analysis factor based on soil type (7.2).
- A_d - Angular distortion (7.3).
- A_{dm} - Modified angular distortion (7.3).
- A_p - Pile toe area (7.1);
Cross sectional area of pile material at pile toe (7.2) (7.10).
- A_{pp} - Cross sectional area of soil plug in open end pipe or H-piles at pile toe (7.2); Cross sectional area of pile and soil plug at pile toe (7.10).
- A_{ps} - Cross sectional area of prestressing steel (8.6).
- A_s - Pile shaft surface area (7.1) (7.2) (7.10);
Peak seismic ground acceleration coefficient modified by short-period site factor (7.4).
- A_{si} - Pile shaft interior surface area (7.10).
- A_{so} - Pile shaft exterior surface area (7.10).
- A_{st} - Cross sectional area of steel (8.5). (8.7) (9.5).
- A_{stc} - Cross sectional area of compression reinforcing steel (8.9).
- A_{str} - Cross sectional area of longitudinal reinforcing steel (8.6) (8.7).
- A_{stt} - Cross sectional area of tension reinforcing steel (8.9).
- A_{stv} - Area of transverse reinforcement within distance, s (8.9).
- A_1 - Constant based on soil type and subsurface condition (7.2).
- A_2 - Constant based on pile type (7.2).
- $a(t)$ - Acceleration measured at the gage location (10.4).
- B - Width of pile group (7.2) (7.3);
- B_b - Database calibrated regression factor (7.2).
- b - Pile width or diameter (3.5) (7.1) (8.4);
Width/ Height of square (8.2);
Depth of beam or width of dimension lumber (8.4);
Width of the compression face (8.9).
- b_c - Column side for square columns (8.9).
- b_f - Flange width of pile section (8.2) (8.5).
- b_o - Critical punching shear perimeter (8.9).
- b_v - Width of interface (8.9).
- C - Perimeter of pier excluding half circles at ends of oblong pier (7.4).

- C' - Dimensionless bearing capacity index, determined from average corrected SPT N value, for layer with consideration of SPT hammer type (7.3).
- C_a - Pile adhesion (7.2) (7.10).
- C_c - Compression index (5.2) (7.3).
- C_d - Pile perimeter at depth d (7.2);
Deck factor for timber pile structural resistance (8.4).
- C_F - Correction factor for K_δ when $\delta \neq \phi$ (7.2).
- C_F - Size factor for timber pile structural resistance (8.4).
- C_f - Conversion factor for cone tip resistance to sleeve friction (7.2).
- C_{fu} - Flat-use factor for timber pile structural resistance (8.4).
- C_h - Pore water pressure dissipation factor (7.2).
- C_i - Incising factor for timber pile structural resistance (8.4).
- C_M - Wet service factor for timber pile structural resistance (8.4).
- C_n - Correction factor for SPT N value (5.1).
- C_p - Toe correction coefficient for Eslami and Fellenius CPT Method (7.2).
- C_r - Recompression index (5.2) (7.3).
- C_s - Swell index (5.2);
Shaft correlation coefficient for Eslami and Fellenius CPT Method (7.2).
- C_{sm} - Elastic seismic response coefficient (7.4).
- C_v - Coefficient of consolidation (5.2) (7.3);
Volume factor for timber pile structural resistance (8.4).
- C_α - Secondary compression index (5.2).
- C_λ - Time effect factor for timber pile structural resistance (8.4).
- C_1 - Composite column constant 1 (8.7).
- C_2 - Composite column constant 2 (8.7).
- C_3 - Composite column constant 3 (8.7).
- C_4 - Damping constant for Statnamic test (11.4).
- c - Cohesion (5.2) (7.1);
Distance from centroid to outer edge (8.2);
Distance between the neutral axis and the compressive face (8.9).
- c' - Effective cohesion (5.2).
- c_o - Column diameter (8.9).
- c_1 - Small column side for rectangular columns (8.9).
- c_2 - Large column side for rectangular columns (8.9).
- D - Pile embedded length (3.5) (7.2) (7.3) (7.10);
Pile penetration below the rock surface (7.2).
Outside pile diameter (8.2);
- DA - Design angular distortion (7.3).
- DWT - Deadweight tonnage (7.4).

- D_B - Pile embedded length into bearing stratum (7.3).
- D_{il} - Depth from reference to top of incompressible layer (7.3).
- D_{np} - Depth from reference to neutral plane (7.3).
- D_r - Relative density (5.1) (5.2).
- D_δ - Design differential settlement (7.3).
- D' - Effective depth, 2/3 pile embedded length (7.1).
- D_1 - Inside pile diameter (8.2).
- d - Equilibrium depth (7.10).
- d_c - Clear space (8.9).
- d_f - Depth to fixity below the ground (8.3); Pile embedment into cap (8.9).
- d_s - Distance to center of steel (8.9).
- d_{sc} - Distance from extreme compression fiber to the centroid of the compression reinforcement (8.9).
- d_{st} - Distance from extreme compression fiber to the centroid of the tensile reinforcement (8.9).
- d_v - Vane diameter (for Vane Shear Test) (5.2);
Effective depth to reinforcement (8.9).
- d_w - Web depth of pile section (8.5).
- E - Elastic modulus of material (Youngs modulus) (5.2) (7.3);
Elastic modulus of pile material (7.3) (8.3).
- E_c - Elastic modulus of concrete (8.2).
- E_e - Modified elastic modulus of steel for composite column (8.7).
- E_m - Rock Mass Modulus (5.1).
- E_n - Rated hammer energy (5.1).
- E_o - Timber reference value for elastic modulus (8.2).
- ER - SPT Hammer efficiency as determined by energy measurements in accordance with ASTM D4633 (5.1).
- E_r - Manufacturers rated hammer energy (3.5);
Modulus of Intact Rock (5.1).
- E_s - Elastic modulus of soil (5.1) (5.2) (7.3) (8.3) .
- E_{sm} - Secant modulus (7.3).
- E_{st} - Elastic modulus of steel (8.5);
Elastic modulus of prestressing steel (8.6).
- E_{50} - 50% secant modulus (5.4).
- e - Void ratio (7.3).
- e_o - Initial soil layer void ratio (5.2.4) (7.3).
- F - Vertical force (7.4).
- F_a - Short period site factor (7.4);
- F_b - Adjusted timber pile structural flexural resistance (8.4).
- F_{bo} - Timber reference value for strength in flexure (8.4).

- F_c - Adjusted timber pile structural axial resistance (8.4).
- F_{co} - Timber reference value for compressive stress parallel to grain (8.2) (8.4).
- F_e - Nominal compressive resistance of composite section (8.7).
- F_p - Plug mobilization factor (7.2).
- F_{PGA} - Zero period site factor (7.4).
- F_v - Long period site factor (7.4).
- F_{vo} - Timber reference value for strength in shear (8.4).
- F_{vs} - Factor for pile driving method (1.0 for impact or 0.68 for vibratory) (7.2).
- F_y - Yield stress of steel (8.2) (8.5) (8.7) (8.8).
- F_{yf} - Minimum yield strength of lower strength flange (8.5).
- F_{yr} - Yield stress of reinforcing steel (8.6) (8.7).
- F_{yw} - Yield stress of web (8.5).
- f_c - Consolidation factor (non-dimensional regression factor) (7.2).
- f'_c - Ultimate compression strength for concrete,
Concrete compressive strength at 28 days (8.2) (8.6) (8.7).
- f_{cr} - Elastic local buckling stress (8.5).
- f_n - Unit negative shaft resistance (7.3).
- f_{pe} - Effective prestress in concrete (8.6).
- f_r - Remolding recovery rate (non-dimensional regression factor) (7.2).
- f_s - Unit sleeve friction; Average unit sleeve friction (5.1) (7.2).
- f_s - Unit shaft resistance over the pile surface area (7.1) (7.2);
Unit positive shaft resistance (7.3).
- f_{sc} - Stress in the mild steel compression reinforcement at nominal flexural
resistance (8.9).
- f_{si} - Interior unit shaft resistance (7.10).
- f_{so} - Exterior unit shaft resistance (7.10).
- f_{st} - Stress in the mild steel tension reinforcement at nominal flexural
resistance (8.9).
- f_1 - Correction factor for undrained shear strength determination (5.2).
- G - Shear modulus (5.2) (8.5).
- G_s - Specific Gravity (5.2).
- H_o - Initial soil layer thickness (5.2) (7.3).
- H_v - Maximum vertical drainage path in cohesive layer (7.3).
- h - Total Thickness of sublayers (7.3);
Distance between flange and centroid for warping torsional constant
(8.5); Structural depth, thickness of cap less pile embedment (8.9).
- h_f - Height of embankment fill (7.3).
- h_i - Thickness of soil strata (5.2).
- h_v - Vane height (for Vane Shear Test) (5.2).

- h_w - Height of water (pressure head) for calculation of pore water pressure (5.2).
- I - Moment of inertia (8.2);
Weak axis moment of inertia (8.3).
- I_f - Influence factor for group embedment (7.3).
- I_x - Moment of inertia about the major principal axes of cross section (8.5).
- I_y - Moment of inertia about the minor principal axes of cross section (8.5).
- j - Stress exponent (7.3).
- K - Effective length factor for buckling (7.2) (8.2) (8.5) (8.7).
- K_o - At rest earth pressure coefficient (5.2) (7.2).
- K_s - Ratio of unit pile shaft resistance to cone unit sleeve friction for cohesionless soils (7.2).
- K_δ - Coefficient of lateral earth pressure (7.2).
- k_c - Modulus of subgrade reaction for cyclic lateral loading (7.3).
- k_s - Modulus of subgrade reaction for static lateral loading (7.3).
- k_1 - Regression factor (0.17 for PSC, 0.12 for CEP and 0.15 for OEP) (7.2).
- k_2 - Regression factor (0.00044 for PSC piles, 0.00078 for CEP, and 0.00060 for OEP) (7.2).
- L - Total pile length (7.3).
- $L\%$ - Pile length subject to heave (7.10).
- L_e - Effective pile length considering unbraced length (8.4).
- L_o - Embedded pile length at the time of initial driving (7.2).
- L_s - Span length (7.3).
- L_t - embedded pile length at time "t" after initial driving (7.2).
- l - Unbraced length, or laterally unsupported length plus d_f (8.3) (8.5) (8.7).
- M_b - Bending moment (7.3).
- M_n - Nominal flexural resistance (structural) (8.4) (8.5) (8.6).
- M_p - Plastic moment about the weak axis (8.5).
- M_r - Factored flexural resistance (structural) (8.3) (8.5) (8.6).
- M_{rx} - Factored flexural resistance about x-axis (8.5) (8.6).
- M_{ry} - Factored flexural resistance about y-axis (8.5) (8.6).
- M_u - Factored moment load (structural) (2.3) (8.3).
- M_{ux} - Factored moment about x-axis (8.5) (8.6) (8.8).
- M_{uy} - Factored moment about y-axis (8.5) (8.6) (8.8).
- m_n - Dimensionless modulus number (7.3).
- m_{nr} - Dimensionless recompression modulus number (7.3).
- m_s - Semilog-linear slope of R_s vs t from multiple restrrike tests (7.2).
- N - Uncorrected field SPT resistance value (5.1) (5.2) (5.4) (5.5) (7.2) (7.3) (7.4).
- N_a - Average SPT N-Value over pile length (7.2).

- N_c - Dimensionless bearing capacity factor (7.2).
- N_k - Bearing capacity factor, typically from 15 to 20 (5.2).
- N_q - Dimensionless bearing capacity factor (API Method) (7.2).
- N_q^* - Dimensionless bearing capacity factor (7.2).
- N_t - Toe resistance coefficient (7.2).
- N_{60} - SPT N value corrected for 60% energy transfer (5.1.1) (7.2) (7.3).
- $(N_1)_{60}$ - SPT N value corrected for energy and overburden stress (5.1) (5.2) (7.2) (7.4) (7.10);
Average corrected SPT N value within a depth B below pile toe (7.3).
- $(N_1)_{60e}$ - Equivalent clean sand blow count (7.4).
- N_{corr} - SPT N value corrected for percent fines (7.4.).
- N_v - Bearing capacity factor (7.2).
- n - Exponent typically equal to 1 in clays (e.g., Olsen 1997) and 0.5 in sandy soils (e.g. Lio and Whitman 1986) (5.1);
Number of piles in pile group (7.2) (7.3) (8.8).
- n_h - Rate of increase of soil modulus with depth (8.3).
- n_i - Number of piles whose centers lie inside the two-way shear critical section (8.9).
- n_o - Number of piles whose centers lie outside the two-way shear critical section (8.9).
- P_e - Elastic critical buckling resistance (8.5).
- $P_e(x)$ - Equivalent static horizontal seismic force acting on superstructure (7.4).
- PGA - Peak ground acceleration coefficient (7.4).
- P_m - P-multiplier for p-y curve (7.3).
- P_n - Nominal axial resistance (structural) (8.4.2) (8.5) (8.6) (8.7).
- P_o - Equivalent nominal axial yield resistance (structural) (8.5) (8.6).
- P_r - Factored axial resistance (structural) (3.4.1) (8.3) (8.5) (8.6) (8.7).
- P_{rx} - Factored axial resistance determined on the basis that only eccentricity, e_y , is present (8.6).
- P_{rxy} - Factored axial resistance in biaxial flexure (8.6).
- P_{ry} - Factored axial resistance determined on the basis that only eccentricity, e_x , is present (8.6).
- P_s - Pile shape factor (7.2);
- P_s - Equivalent static vessel impact force (7.4).
- P_t - Pile base factor (7.2).
- P_u - Factored axial load (structural) (8.3.3) (8.6) (8.8) (8.9).
- P_{ui} - Maximum single pile axial load (8.8).
- P_{uz} - Factored axial load from superstructure/substructure acting upon pile cap (8.8).
- p - Soil resistance per unit pile length (7.3).

- p_a - Atmospheric pressure (5.1) (5.2).
- p_f - Design foundation pressure (7.3.4).
- Q - Total factored load (2.3); Factored axial load (7.3) (7.6);
Slender element reduction factor (8.5).
- Q_c - Scour Design Check Flood Frequency (7.2).
- Q_d - Hydraulic design flood frequency (7.2);
Unfactored permanent load (7.3).
- Q_{max} - Maximum axial compressive force in the pile (7.3).
- Q_l - Live load on a pile (7.3).
- Q_i - Force effect (2.3) (7.3) (7.4).
- Q_L - Lateral pile load (7.3).
- Q_s - Scour Design Flood Frequency (7.2).
- q - Surcharge (7.3).
- q_c - Cone tip resistance (5.1) (5.2) (7.2).
- q_{ca} - Average cone tip resistance within a depth of B below the pile toe (7.3).
- q_{c1} - Average q_c over a distance of x_b below the pile toe (7.2).
- q_{c2} - Average q_c over a distance of $8b$ above the pile toe (7.2).
- q_{DMT} - Dilatometer test tip resistance (5.5).
- q_E - Eslami cone stress (7.2).
- q_{Eg} - Geometric average of the corrected cone tip resistance over the
influence zone (7.2).
- q_L - Limiting unit toe resistance (7.2).
- q_p - Unit toe resistance (7.1) (7.2) (7.1).
- q_t - Corrected cone tip resistance (5.1) (7.2).
- q_u - Unconfined compressive strength (5.1) (5.2) (5.3) (5.5) (7.2).
- R - Radius of pier (7.4).
- R_f - Friction ratio or f_s/q_t (5.1).
- R_n - Nominal resistance (2.4) (3.4) (7.1) (7.2) (7.3) (7.6) (7.10).
Nominal resistance of each individual pile in the group (7.2).
- R_{ndr} - Nominal driving resistance (3.4) (7.6).
- R_{ng} - Nominal resistance of pile group (7.2).
- R_{no} - Initial nominal resistance at time “ t_o ” of driving (7.2).
- R_p - Nominal toe resistance (7.1) (7.2) (7.3).
- R_r - Factored resistance (2.4) (7.2) (8.8) (8.9).
- R_{relax} - Resistance loss from relaxation (7.6).
- R_{rg} - Factored resistance of the pile group (7.3).
- R_s - Nominal shaft resistance (3.4) (7.1) (7.2) (7.3) (12.7).
- R_{scour} - Resistance loss from scour (7.6).
- R_{so} - Initial shaft resistance at “ t_o ” of driving (7.2).
- R_s^+ - Positive Shaft Resistance (7.3).

- R_s^- - Negative Shaft Resistance (7.3).
- R_{ug} - Nominal uplift resistance of the pile group (7.2).
- r_p - Equivalent pile radius (7.2).
- r_s - Minimum radius of gyration (8.3);
Radius of gyration about axis normal to plane of buckling (8.5) (8.7).
- S - Settlement (7.1); Estimated total settlement (7.3);
Elastic section modulus (8.2) (8.4).
- S_{avg} - Average settlement (3.5).
- S_d - Differential settlement of the foundation (7.3).
- S_{dd} - downdrag movement (7.3).
- S_c - Settlement from primary consolidation (5.2) (7.3).
- S_{DS} - C_{sm} value with a period of 0.2 seconds = $F_a S_s$ (7.4).
- S_{D1} - C_{sm} value with a period of 0.2 seconds = $F_v S_1$ (7.4).
- S_h - Horizontal abutment movement (7.3).
- S_{max} - Maximum settlement (3.5).
- S_p - Pile slope (7.3).
- S_s - Short period spectral acceleration (7.4).
- S_t - Sensitivity of a cohesive soil (5.2).
- S_{ta} - Total foundation settlement (7.3).
- S_{tp} - Total foundation settlement before construction (7.3).
- S_{tr} - Relevant total settlement (7.3).
- S_v - Vertical fill settlement (7.3).
- S_y - Elastic section modulus about weak axis (8.5).
- S_1 - Long period coefficient (7.4).
- s - Spacing of the transverse reinforcement (8.9).
- s_r - Residual shear strength (7.4).
- s_u - Undrained shear strength (3.4) (5.1) (5.2) (5.5) (7.2) (7.4) (8.3);
Vane Shear Test undrained shear strength (5.5);
Average undrained shear strength (7.3);
Undrained shear strength of soft cohesive soil (7.3) (7.10).
- T - Theoretical time factor for percentage of primary consolidation (7.3).
- T_m - Period of vibration of m^{th} mode(s) (7.4).
- T_o - Reference period to define spectral shape = $0.2T_s$ (7.4).
- T_s - Corner period when spectrum changes from independent to inversely
proportional = S_{D1} / S_{DS} . (7.4).
- T_v - Input torque during shear (for Vane Shear Test) (5.2).
- t - Time after driving (7.2);
Time for settlement to occur (7.3);
- t - Pipe pile wall thickness (8.2) (8.5).
- t_{cap} - Thickness of pile cap (8.9).

- t_f - Flange thickness of pile section (8.2) (8.5).
- t_i - Ice thickness (7.4).
- t_o - Time after driving from which the increase in resistance is linear in logarithmic time (days) (typically 0.5 for sand, 1.0 for clay) (7.2).
- t_{soil} - Thickness of compressible soil beneath neutral plane (7.3).
- t_w - Web thickness of pile section (8.2) (8.5).
- U - Displacement (7.3).
- u - Pore water pressure (5.1) (5.2) (7.1).
- u_e - Excess pore water pressure (7.2).
- u_h - Hydrostatic pore water pressure (7.2).
- V - Volume of soil displaced per unit length of pile (7.2);
Vessel impact velocity (7.4).
- V_c - Nominal shear resistance provided by concrete tensile strength (8.9).
- V_n - Nominal shear resistance (8.9).
- V_r - Factored shear resistance (structural) (8.3).
- V_s - Shear wave velocity (7.4);
Nominal shear resistance provided by steel reinforcement (8.9).
- V_u - Factored shear load (structural) (2.3) (8.3) (8.9).
- W - Pier or Abutment Width (4.2);
Equivalent weight of the superstructure (7.4).
- W_c - Estimated weight of pile cap (8.8).
- W_g - Effective weight of the pile/soil block including pile cap weight (7.2).
- W_p - Weight of soil plug (7.10).
- W_s - Estimated weight of soil above pile cap (8.8).
- w - Moisture Content (5.1) (5.2) (7.2) (7.4).
- x - Distance along x-axis from the center of the column to each pile center (8.8).
- Y_o - Pile head deflection (7.3).
- y - Lateral soil (or pile) deflection (7.3);
Distance along y-axis from the center of the column to each pile center (8.8).
- Z - Length of pile group (7.2) (7.3).
- Z_y - Plastic section modulus about weak axis (8.5).
- α - Compression factor for settlement (3.4) (3.5);
Dimensionless adhesion factor (7.2).
- α' - Ratio of pile unit shaft resistance to cone unit sleeve friction for cohesive soils (7.2).
- α_t - Dimensionless factor in Nordlund method (7.2).
- β - Bjerrum-Burland beta coefficient (7.2).
- β_c - Ratio of the long side to the short side of the load (8.9).

- β_m - Mobilized angle for strain wedge analysis (7.3).
- β_1 - Stress block factor (8.9).
- Δ - Elastic compression (7.3).
- Δd - Length of pile segment (7.2).
- ΔH - Total settlement at Pier or Abutment (7.3).
- ΔH_{100} - Differential settlement over 100 Feet within a pier or abutment, or the differential settlement between piers (7.3).
- Δ_{um} - Maximum excess pore pressure (7.2).
- $\Delta\sigma$ - Additional stress at mid-point of soil layer from loading (5.2);
Additional pressure from structural loading (7.3).
- $\Delta\sigma_h$ - Changes in deviator stress in the direction of loading (7.3).
- $\Delta\varepsilon$ - Strain from the increase in effective stress (7.3);
- δ - Friction angle between pile and soil (7.2) (7.3);
- ε - Strain (5.2) (7.3).
- ε_{cu} - Failure strain of concrete in compression (8.6).
- ε_v - Vertical strain (5.2).
- ε_{50} - Strain at one half the maximum principal stress (7.3) (7.4).
- η_g - Pile group efficiency (7.2).
- η_i - Load modifier based on ductility, redundancy, or operation classification (2.3) (2.4).
- γ - Total unit weight of soil (5.1) (5.2) (5.5).
- γ' - Buoyant unit weight of soil (5.5).
- γ_d - Dead Load Factor (7.3).
- γ_f - Unit weight of embankment fill (7.3).
- γ_i - Load factor, statistically based multiplier applied to force effect (2.3) (2.4) (7.4) (7.3);
Unit weight of soil strata for calculation of in-situ stress (5.2).
- γ_l - Load factor for force effect due to live loads (7.3).
- γ_p - Load factor for force effect due to permanent loads (2.3) (7.3) (7.4).
- γ_{SE} - Load factor for force effect due to vertical settlement (7.3).
- γ_{TG} - Load factor for force effect due to temperature gradient (2.3).
- γ_w - Unit weight of water (5.2).
- λ - Normalized column slenderness factor (8.7).
- λ_f - Slenderness ratio for flange (8.5).
- λ_{pf} - Limiting slenderness ratio for a compact flange (8.5).
- λ_{nf} - Limiting slenderness ratio for a non-compact flange (8.5).
- ν - Poisson ratio (5.2) (5.4).
- σ - Normal stress (pressure) on plane of failure, stress (5.2).
- σ' - Effective normal stress (pressure) on plane of failure ($\sigma - u$) (5.2).

- σ'_d - Vertical effective stress at the center of depth increment d (7.2).
- σ_{dr} - Driving stress (8.4) (8.5) (8.6).
- σ'_{ho} - Horizontal effective stress at the sample depth (5.2).
- σ'_o - Effective stress prior to stress increase (7.3).
- σ_p - Preconsolidation pressure or stress (5.1) (5.2) (7.3).
- σ'_p - Vertical effective stress at the pile toe (7.2).
- σ_r - Reference stress for settlement with Janbu Tangent Modulus (7.3).
- σ_v - Total stress (7.1).
- σ'_v - Vertical effective stress (7.1).
- σ'_{vi} - Initial vertical effective stress prior to pile driving (7.2).
- σ'_{vo} - Vertical effective stress at the sample depth (5.1.1) (5.2) (7.2);
Vertical effective stress at midpoint of each layer (prior to stress increase) (7.3).
- σ'_1 - Effective stress after stress increase (7.3).
- τ - Shear stress at failure (shear strength) (5.2); Shear strength of soil (7.1).
- ϕ - Resistance factor, statistically based multiplier on nominal resistance (2.4); Angle of internal friction (2.4) (5.1) (5.2) (5.5) (7.1) (7.2) (7.3).
- ϕ' - Effective Stress Friction Angle (5.1) (5.5) (7.2.) (7.10).
- ϕ_c - Resistance factor (pile structural resistance in compression) (8.3) (8.5) (8.6).
- ϕ_{b1} - Block Failure (7.1).
- ϕ_{da} - Resistance factor (pile structural resistance during driving) (8.3) (8.4) (8.5) (8.6).
- ϕ_{dyn} - Resistance factor (based on the construction control method) (2.10) (3.4) (7.1) (7.2) (7.6).
- ϕ_f - Resistance factor (pile structural resistance in flexure) (8.3) (8.5) (8.6).
- ϕ_m - Mobilized angle of internal friction (7.3).
- ϕ_{stat} - Resistance factor (based on the static analysis method) (7.1) (7.2).
- ϕ_{ug} - Resistance factor for group uplift (based on the uplift analysis method) (7.1) (7.2).
- ϕ_{up} - Resistance factor (based on the uplift analysis method) (3.4) (7.1) (7.2).
- ϕ_v - Resistance factor (pile structural resistance in shear) (8.3).
- ψ - Ratio of undrained shear strength divided by effective overburden pressure, s_u / σ'_{vo} (7.2).
- ω - Angle of pile taper from vertical (7.2).
- μ - Correction factor (5.2).

LIST OF ACRONYMS

AASHTO	- American Association of State Highway and Transportation Officials
ASTM	- American Society for Testing and Materials
BL	- Blast load
BOR	- Beginning of Restrike
BR	- Vehicular braking force
CD	- Consolidated Drained triaxial test
CE	- Vehicular centrifugal force
CED	- Closed End Diesel hammer
CEP	- Closed End Pipe
CFA	- Continuous Flight Auger
COR	- Coefficient of Restitution
CPT	- Cone Penetration Test
CPTu	- Piezo Cone Penetration Test
CR	- Force effects due to creep
CT	- Vehicular collision force
CU	- Consolidated Undrained triaxial test
CV	- Vessel collision force
DA	- Design Angular Distortion
DC	- Dead load components and attachments
DD	- Downdrag
DF	- Drag force
DLT	- Dynamic Load Test
DMT	- Dilatometer test
DW	- Wearing surface and utilities
DWT	- Deadweight tonnage
EH	- Horizontal earth pressure
EL	- Locked-in stress
EOD	- End of Drive
EQ	- Earthquake load
ER	- SPT hammer efficiency as determined by energy measurements
ES	- Earth surcharge
EV	- Vertical earth pressure
FHWA	- Federal Highway Administration
FR	- Friction load
I.D.	- Inner diameter

IC	- Ice load
IM	- Vehicular dynamic load allowance
KE	- Kinetic Energy
LL	- Liquid Limit; Vehicular live load
LS	- Live Load Surcharge
LVDT	- Linear Variable Differential Transformer
MUP	- Modified Unloading Point Method
NHI	- National Highway Institute
O.D.	- Outer Diameter
OED	- Open Ended Diesel hammer
OEP	- Open Ended Pipe
PE	- Potential Energy
PGA	- Peak Ground Acceleration coefficient
PI	- Plasticity Index
PL	- Plastic Limit; Pedestrian live load
PS	- Secondary forces from post-tensioning
RSA	- Residual Stress Analysis
SA	- Static Analysis
SE	- Force effect due to settlement
SH	- Force effects due to shrinkage
SLT	- Static Load Test
SPT	- Standard Penetration Test
SRD	- Soil Resistance to Driving
SUP	- Segmental Unloading Point Method
TG	- Force effect due to temperature gradient
TU	- Force effect due to uniform temperature
UPM	- Unloading Point Method
UU	- Unconsolidated Undrained triaxial test
VST	- Vane shear test
WA	- Water load and steam pressure
WD	- Downward traveling wave, Wave Down
WE	- Wave Equation
WEAP	- Wave Equation Analysis Program
WL	- Wind on live load
WS	- Wind load on structure
WU	- Upward traveling wave, Wave Up

CHAPTER 1

DRIVEN PILE FOUNDATION MANUAL

1.1 INTRODUCTION

In 1985 the Federal Highway Administration (FHWA) published the first edition of this manual. Subsequent editions were published in 1997 and 2006. Since the last published update, significant changes in pile design, construction, and performance requirements have occurred which make it necessary to once again update the manual. This 2015 update is primarily dictated by the need to revise and update manual content in accordance with the Load and Resistance Factor Design (LRFD) methodology which replaced the Allowable Strength Design (ASD) method for the design of transportation substructures in 2007. Other significant changes in practice addressed by this edition of the manual include:

- emphasis on a rational economic evaluation of the foundation design,
- use of higher strength pile materials and/or larger driven pile sections to support greater foundation loads,
- updates in computer programs for pile foundation analysis and design,
- use and quantification of soil setup in pile design and construction,
- improvements in pile installation equipment and equipment performance monitoring,
- increased use of instrumented static load test programs, and
- improvements in QA/QC methods for nominal resistance and pile integrity verifications.

1.2 PURPOSE OF THE MANUAL

The purposes of the previous driven pile foundation manual editions remain largely unchanged. It is worthwhile to restate the purpose and objectives of the manual.

1. There exists a vast quantity of information on driven pile foundations which presently is not compiled in a form which is useful to most practicing engineers. There are proven rational design procedures, information on construction materials, equipment and techniques, and useful case histories.

Unfortunately, much of this information is fragmented and scattered. Standard textbooks and other publications on the subject tend to be theoretically oriented and practicing design and construction engineers often find them lacking in practical aspects. One of the primary goals of this manual is to meet that need for the practicing engineer.

2. Many historical design methods lead to unnecessarily conservative designs because they were based solely on experience and tradition with little theoretical background. Well established rational design procedures and techniques are summarized herein that provide more economical driven pile foundation systems that can safely support the applied structural loads.
3. There are opportunities for substantial cost savings on driven pile foundation projects through the use of improved methods of design and construction technology. A minimum of fifteen percent of the substructure cost can be easily saved by utilizing such methods and, in most cases, the savings are more significant.
4. Since the adoption of LRFD methodology for all transportation projects, a comprehensive driven pile foundation manual has been needed. This manual is intended to fulfill that need as well as to establish minimum design standards and recommendations.
5. Design criteria for bridges and other structures are becoming more complex and sophisticated. Extreme design events such as scour, debris loading, vessel impact, and seismic events require that foundation performance be evaluated under lateral and uplift loading, group behavior, and substructure - superstructure interaction. In addition, deformation performance requirements (lateral and vertical deflections) are routinely included in project requirements. This new series of performance criteria frequently results in foundations which are more costly, more complex to design, and more difficult to construct.
6. The loading conditions noted above have can have a substantial impact on the structural design of the piles. In the past, driven piles were often designed structurally for axial loads only using an allowable stress approach. The allowable stresses had been established primarily to assure pile drivability. However, the requirement that piles be analyzed for combined horizontal and axial loads requires a change in the evaluation procedure. The pile top is subjected to both horizontal and axial loads and in a pile group the

pile resistance to lateral loads varies with each pile row. Of course this complicates the geotechnical analysis. It also complicates the pile structural analysis. A combined bending and axial load analysis of the structural behavior of the pile must be performed. Particularly for concrete piles this analysis must be based on an ultimate strength analysis and it is not always obvious which pile within a group is the critical one. Comprehensive software is now available to perform the necessary analyses and is discussed herein.

7. Alternative contracting methods (ACM), design-build (D-B) and CM/GC (construction manager/general contractor), are increasingly replacing the conventional design-bid-build (DBB) method as the preferred methods of project development and delivery. Among the changes which these ACM's affect is an intentional, but yet aggressive challenge to existing design specifications.
8. Final pile design selection should involve a cost evaluation. In the past, such evaluations have been implied but they were not a routine part of the design process. Methods have been developed to perform cost evaluations of pile foundations that include the effects of soil setup. These concepts will be presented in this edition of the manual.
9. A larger selection of pile hammer types and sizes, improvements in hammer performance, advancements in equipment controllability and installation aids allow efficient pile installation in most subsurface conditions.

1.3 SCOPE OF MANUAL

The manual is limited to driven piles and consists of eighteen chapters and four appendices. The first half of the manual covers the design aspects of pile foundations including cost evaluations, geotechnical data collection and analysis, selection of pile type, as well as geotechnical and structural aspects of limit state design. The second half of the manual covers methods of nominal resistance verification as well as chapters on pile driving equipment, accessories and inspection procedures. Theoretical discussions have been included only where necessary. Specific recommendations are made where appropriate. Example problems are included to provide hands-on knowledge to manual users.

The manual is a standalone document that provides guidance for engineers on the design and construction of driven pile foundations. A separate training course will

be used to transfer knowledge in this area and will continue with the original goal of updating transportation department practice. Also, new engineers continue to join transportation agencies and require expanding their knowledge in the practical aspects of pile design and installation.

1.4 HISTORY OF DRIVEN PILE FOUNDATIONS

The detailed history of driven pile foundations has been lost to time. It has been postulated that some of the earliest use of driven timber piles dates back to 800 BC where the piles were installed with mauls or drop hammers. Reinforced concrete piles debuted in Europe in 1897 and in Chicago in 1901. Structural steel piles including, pipe, I-beams, and H-piles followed not too long thereafter. Octagonal and square, precast, prestressed concrete piles as well as 36 inch and 54 inch diameter post-tensioned concrete cylinder piles developed in the 1950's.

As noted above, the first pile hammers were simple drop hammers. The first modern pile driving hammer was a Scottish steam hammer patented by Naysmith in 1839. In the U.S., steam pile driving hammers were reported between the mid- to late 1800's. In the mid 1920's, the diesel pile hammer was invented in Germany. Vibratory hammers were invented in the Soviet Union in the 1940's and made their way into the U.S. market in the 1960's. The first hydraulic pile hammers were developed in Scandinavia in the 1960's. In the 1960's, Bodine developed a resonant pile hammer but the hammer had limited use in the market due to mechanical reliability issues. The resonant pile driver re-emerged in the 2000's. Many improvements in hammer features and operation have occurred over the years for all hammer types. Rausche (2000) summarized the development of pile driving equipment along with equipment capabilities and properties.

1.5 INFORMATION SOURCES

The information presented in this manual has been collected from several sources. The primary references are the 7th Edition of the AASHTO LRFD Bridge Design Specifications (2014) with 2015 Interim Revisions and the 3rd Edition of the AASHTO LRFD Bridge Construction Specifications with 2010, 2011, 2012, and 2014 Interim Revisions. Additional sources of information include: "Evaluation of Soil and Rock Properties," GEC-5 by Sabatini et al. (2002), "Implementation of AASHTO LRFD Design Specifications for Driven Piles" by Abu-Hejleh et al. (2013), "Drilled Shafts: Construction Procedures and LRFD Design Methods" GEC-10 by Brown et

al. (2010), “LRFD Seismic Analysis and Design of Transportation Geotechnical Features and Structural Foundations” GEC-3 by Kavazanjian et al. (2011) as well as “Evaluating Scour at Bridges, Fifth Edition” HEC-18 by Arneson et al. (2012).

The information within has been condensed, modified and updated as needed. The sources also include state-of-the-art technical publications, manufacturers' literature, existing Federal Highway Administration (FHWA), National Highway Institute (NHI) and Transportation Research Board (TRB) publications, standard textbooks, and information provided by State and Federal transportation engineers. Reference lists are provided at the end of each chapter.

Many of the documents used in the development or updating of this manual, as well as useful industry links are available at

<https://www.fhwa.dot.gov/engineering/geotech/>.

REFERENCES

- Abu-Hejleh, N., Kramer, W.M., Mohamed, K., Long, J.H., and Zaheer, M.A. (2013). Implementation of AASHTO LRFD Design Specifications for Driven Piles, FHWA-RC-13-001. U.S. Dept. of Transportation, Federal Highway Administration, 71 p.
- American Association of State Highway and Transportation Officials (AASHTO). (2014). AASHTO LRFD Bridge Design Specifications, US Customary Units, Seventh Edition, with 2015 Interim Revisions. American Association of State Highway and Transportation Officials, Washington, D.C., 1960 p.
- Arneson, L.A., Zevenbergen, L.W., Lagasse, P.F., and Clopper, P.E. (2012). Evaluating Scour at Bridges, Fifth Edition, FHWA-HIF-12-003, Hydraulic Engineering Circular (HEC) No. 18. U.S. Dept. of Transportation, Federal Highway Administration, 340 p.
- Brown, D. A., Turner, J.P. and Castelli R.J. (2010). Drilled Shafts: Construction Procedures and LRFD Design Methods, FHWA-NHI-10-016, Geotechnical Engineering Circular (GEC) No. 10. U.S. Dept. of Transportation, Federal Highway Administration, 970 p.
- Kavazanjian, E., Wan, J-N. J., Martin, G.R., Shamsabadi, A., Lam, I., Dickenson, S.E., and Hung, C.J. (2011). LRFD Seismic Analysis and Design of Transportation Geotechnical Features and Structural Foundations, FHWA-NHI-11-032, Geotechnical Engineering Circular (GEC) No. 3. U.S. Dept. of Transportation, Federal Highway Administration, 592 p.
- Rausche, F. (2000). Keynote Lecture: Pile Driving Equipment: Capabilities and Properties, Proceedings of the Sixth International Conference on the Application of Stress Wave Theory to Piles, A.A. Balkema, pp. 75-90.
- Sabatini, P.J., Bachus, R.C., Mayne, P.W., Schneider, J.A., and Zettler, T.E. (2002). Evaluation of Soil and Rock Properties, FHWA-IF-02-034, Geotechnical Engineering Circular (GEC) No. 5. U.S. Dept. of Transportation, Federal Highway Administration, 385 p.

CHAPTER 2

OVERVIEW OF PILE FOUNDATION DESIGN & CONSTRUCTION

2.1 INTRODUCTION

As stated by Professor R. B. Peck, “driving piles for a foundation is a crude and brutal process.” The interactions among the piles and the surrounding soil are complex. Insertion of piles alters the character of the soil and intense strains are set up locally near the piles. The non-homogeneity of soils, along with the effects of the pile group and pile shape, adds further difficulties to the understanding of soil-pile interaction. For piles driven to hard rock or into soft rock, the strength and structure of the rock mass including joints, bedding planes, and the degree of weathering complicate our understanding of rock-pile interaction.

Broad generalizations about pile behavior are unrealistic. An understanding of the significance of several factors involved is required to be successful in the design of pile foundations. Because of the inherent complexities of pile behavior, it is necessary to use practical semi-empirical methods of design, and to focus attention on significant factors rather than minor or peripheral details.

To arrive at the optimum driven pile foundation solution, the foundation engineer must have a thorough understanding of the subsurface conditions including soil/rock parameters and behavior, the applicable limit states, the factored loads and load combinations, project performance requirements, foundation costs, and the current foundation design and construction practices where the foundation is located.

2.2 LIMIT STATES

Four limit states are identified in the AASHTO LRFD Bridge Design Specifications (AASHTO 2014): strength, service, extreme event, and fatigue. In addition, these limit states have several load combination cases such that up to thirteen limit states may require evaluation in a bridge design. There are five strength limit cases, two extreme event limit cases, four service limit cases, and two fatigue limit cases as described in Table 2-1.

Limit states that commonly govern driven pile foundation designs include: Strength I, Strength IV, Extreme Event I (earthquake), Extreme Event II (ice, vessel, blast, and vehicle collision), and Service I. All applicable limit states have equal importance in a driven pile foundation design. Service Limit States II, III, and IV and Fatigue Limit States I and II are relevant to the behavior of superstructure elements and are not generally applicable to foundation design.

Table 2-1 Limit State, Load Case, and Load Combination (after AASHTO 2014)

Limit State and Load Case	Load Combination
Strength I	Basic load combination related to normal vehicular use of the bridge without wind.
Strength II	Load combination relating to use of the bridge by owner-specified special vehicles, evaluation permit vehicles, or both, without wind.
Strength III	Load combination for bridge exposed to wind velocity exceeding 55 mph without live loads.
Strength IV	Load combination for very high dead load to live load force effect ratios. (Typical for bridge spans greater than 250 feet).
Strength V	Load combination for normal vehicular use of the bridge with wind velocity of 55 mph.
Extreme Event I	Load combinations including earthquake.
Extreme Event II	Load combinations relating to ice load, collision by vessels and vehicles, and certain hydraulic events with a reduced live load other than that which is part of the vehicular collision load.
Service I	Load combinations relating to normal operational use of the bridge with a 55 mph wind and all loads taken at their nominal values.
Service II	Load combinations intended to control yielding of steel structures and slip of slip-critical connections due to vehicular live load.
Service III	Load combinations relating to tension in prestressed concrete superstructures with the objective of crack control and to principal tension in the webs of segmental concrete girders.
Service IV	Load combinations intended to control tension in prestressed concrete columns with the objective of crack control.
Fatigue I	Fatigue and fracture load combination related to infinite load-induced fatigue life.
Fatigue II	Fatigue and fracture load combination related to finite load-induced fatigue life.

2.3 LOADS, LOAD COMBINATIONS, AND LOAD FACTORS

The total factored load, Q , associated with a given limit state is calculated based on the applicable force effect, load modifiers, and load factors.

$$Q = \sum \eta_i \gamma_i Q_i \quad \text{Eq. 2-1}$$

Where:

- η_i = load modifier based on ductility, redundancy, or operation classification.
- γ_i = load factor, a statistically based multiplier applied to force effect.
- Q_i = force effect.

A specific load combination applies for each limit state case. A general description of the applicable load, load combinations and load factors associated with each limit state is presented in Table 2-2. The two letter codes in the second column in Table 2-2 correspond to permanent loads and the remaining two letter code descriptions correspond to transient loads.

For example, the total factored load, Q , for Strength Limit State I is defined as follows:

$$Q = \gamma_p DC + \gamma_p DD + \gamma_p DW + \gamma_p EH + \gamma_p EV + \gamma_p ES + \gamma_p EL + \gamma_p PS + \gamma_p CR + \gamma_p SH + 1.75LL + 1.75IM + 1.75CE + 1.75BR + 1.75PL + 1.75LS + WA + FR + 1.20TU + \gamma_{TG} TG + \gamma_{SE} SE$$

The load factor for permanent loads, γ_p , has maximum and minimum values as prescribed in Table 2-3. For permanent force effects, the load factor that produces the more critical load combination is selected from Table 2-3.

Table 2-2 Load Combinations and Load Factors (after AASHTO 2014)

Load Combination Limit State	DC DD DW EH EV ES EL PS CR SH	LL IM CE BR PL LS	WA	WS	WL	FR	TU	TG	SE	EQ*	BL*	IC*	CT*	CV*
Strength I	γ_p	1.75	1.00	---	---	1.00	0.50/1.20	γ_{TG}	γ_{SE}	---	---	---	---	---
Strength II	γ_p	1.35	1.00	---	---	1.00	0.50/1.20	γ_{TG}	γ_{SE}	---	---	---	---	---
Strength III	γ_p	---	1.00	1.40	---	1.00	0.50/1.20	γ_{TG}	γ_{SE}	---	---	---	---	---
Strength IV	γ_p	---	1.00	---	1.00	1.00	0.50/1.20	-- -	---	---	---	---	---	---
Strength V	γ_p	1.35	1.00	0.40	---	1.00	0.50/1.20	γ_{TG}	γ_{SE}	---	---	---	---	---
Extreme Event I	γ_p	γ_{EQ}	1.00	---	---	1.00	---	-- -	---	1.00	---	---	---	---
Extreme Event II	γ_p	0.50	1.00	---	---	1.00	---	-- -	---	---	1.00	1.00	1.00	1.00
Service I	1.00	1.00	1.00	0.30	1.00	1.00	1.00/1.20	γ_{TG}	γ_{SE}	---	---	---	---	---
Service II	1.00	1.30	1.00	---	---	1.00	1.00/1.20	-- -	---	---	---	---	---	---
Service III	1.00	0.80	1.00	---	---	1.00	1.00/1.20	γ_{TG}	γ_{SE}	---	---	---	---	---
Service IV	1.00	---	1.00	0.70	---	1.00	1.00/1.20	-- -	1.00	---	---	---	---	---
Fatigue I -** LL, IM & CE	---	1.50	---	---	---	---	---	-- -	---	---	---	---	---	---
Fatigue II -** LL, IM & CE	---	0.75	---	---	---	---	---	-- -	---	---	---	---	---	---

* - Use one of these at a time

** - Load factors only applied to LL, IM and CE

The two letter load descriptions correspond to permanent and transient loads as follows:

DC – dead load components and attachments
 DD – downdrag
 DW – wearing surface and utilities
 EH – horizontal earth pressure
 EV – vertical earth pressure
 ES – earth surcharge
 EL – locked-in stress
 PS – secondary forces from post-tensioning
 CR – force effects due to creep
 SH – force effects due to shrinkage
 LL – vehicular live load
 IM – vehicular dynamic load allowance
 CE – vehicular centrifugal force
 BR –vehicular braking force

PL – pedestrian live load
 LS – live load surcharge
 WA – water load and steam pressure
 WS – wind load on structure
 WL – wind on live load
 FR – friction load
 TU – force effect due to uniform temp.
 TG – force effect due to temp. gradient
 SE – force effect due to settlement
 EQ – earthquake load
 BL – blast load
 IC – ice load
 CT – vehicular collision force
 CV – vessel collision force

Table 2-3 Load Factors for Permanent Loads (after AASHTO 2014)

Type of Load	Max. Load Factor, γ_p	Min. Load Factor, γ_p
DC: Components and Attachments	1.25	0.90
DC: Strength IV only	1.50	0.90
DD: Downdrag (Tomlinson α -Method)	1.40	0.25
DD: Downdrag: (λ Method)	1.05	0.30
DW: Wearing Surface and Utilities	1.50	0.90
EH: Horizontal Earth Pressure (Active)	1.50	0.90
EH: Horizontal Earth Pressure (At-rest)	1.35	0.90
EH: Horizontal Earth Pressure (AEP for anchored walls)	1.35	N/A
EL: Locked-in Construction Stresses	1.00	1.00
EV: Vertical Earth Pressure (overall stability)	1.00	N/A
EV: Vertical Earth Pressure (retaining walls and abutments)	1.35	1.00
EV: Vertical Earth Pressure (rigid buried structures)	1.30	0.90
EV: Vertical Earth Pressure (rigid frames)	1.35	0.90
EV: Vertical Earth Pressure (flexible buried str. - metal box, plate, fiberglass)	1.50	0.90
EV: Vertical Earth Pressure (flexible buried str. - thermoplastic)	1.30	0.90
EV: Vertical Earth Pressure (flexible buried str. - all others)	1.95	0.90
ES: Earth Surcharge	1.50	0.75

Brown et al. (2010) summarized the basic limit state design process for a bridge or other structure. For each limit state, the structural engineer determines the foundation force effects using a preliminary structural model of the proposed structure. This structural model is developed and analyzed under the limit state load combinations described in Table 2-2. Factored loads are used in the analyses.

Figure 2-1 illustrates the reactions at a column-cap joint computed by the structural analysis. These are the force effects transmitted to the deep foundation supported cap. For driven pile designs, these reactions are resolved into vertical, horizontal, and moment components, and are taken as the factored values of axial, lateral, and moment force effects, respectively at the top of the pile cap. Multiple iterations are typically performed to obtain agreement between deformations and forces calculated by the structural analysis and those based on geotechnical analysis at the structure/foundation (column-cap) interface. The resulting factored force effects must be less than the factored resistance. This is an oversimplified description of

the process but it describes the general procedure by which factored foundation force effects are determined for each applicable limit state.

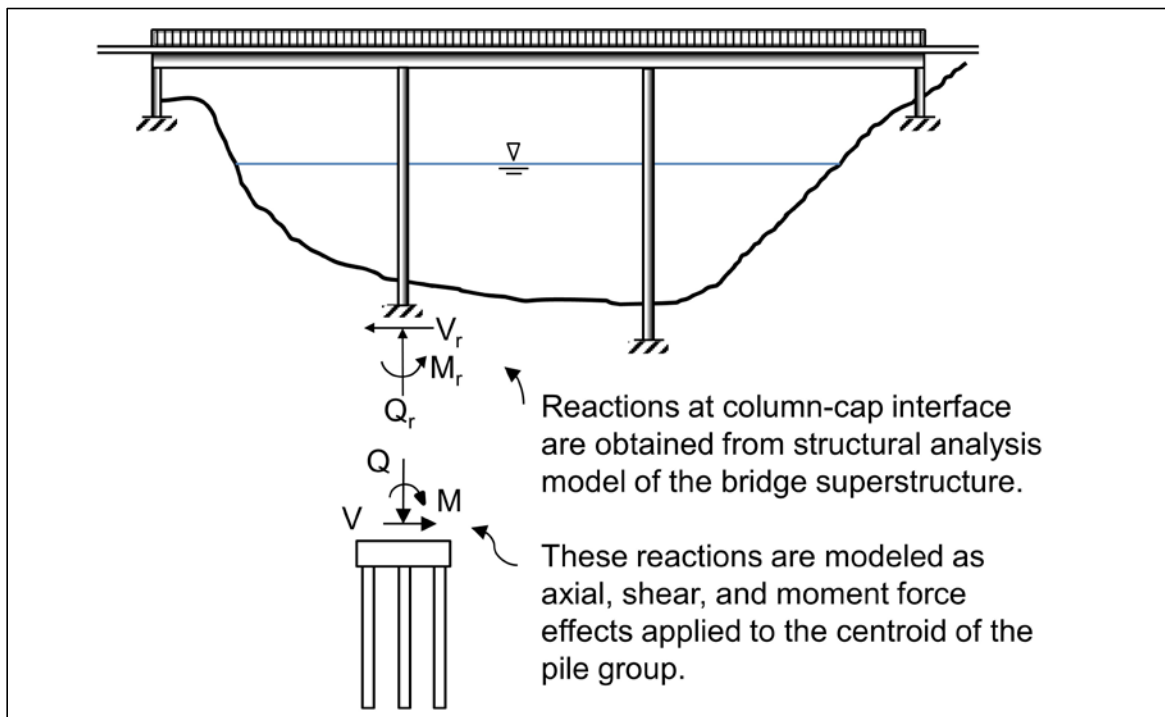


Figure 2-1 Structural analysis of bridge used to establish foundation force effects (modified from Brown et al. 2010).

In the structure model, the load factors in Tables 2-2 and 2-3 are varied over the specified ranges to determine the load combinations resulting in maximum force effects on the foundation. These maximum force effects are then used in the limit state checks.

An example of the final structure loads determined for a 45 foot wide, three span structure having a total length of 350 feet and a main span length of 100 feet is presented in Figure 2-2. The structure will be subjected to both scour and seismic events. At Abutment 1, the highest factored axial loads are 2548 kips for the Strength I limit state and 1982 kips for the Service II limit state. The abutment also has a lateral shear load of 1980 kips transverse to the bridge for the Extreme Event I limit state. At Pier 2, the highest factored axial loads are 5542 kips for the Strength I limit state and 4307 kips for the Service II limit state. The pier is also subjected to a lateral shear load of 1267 kips longitudinal to the bridge, and a moment of 40,800 ft-kips at the Extreme Event I limit state. Each limit state load combination is then checked independently based on all appropriate factored loads and moments and compared to the corresponding factored resistance and performance criteria (tolerable deformations) for each case.

Load Combination Limit State	DC DD DW EH EV ES EL PS CR SH	LL IM CE BR PL LS	WA	WS	WL	FR	TU	TG	SE	EQ*	BL*	IC*	CT*	CV*
Strength I	70	1.75	1	---	---	1	0.50/1.20	770	750	---	---	---	---	---
Strength II	70	1.35	1	---	---	1	0.50/1.20	770	750	---	---	---	---	---
Strength III	70	---	1	1.4	---	1	0.50/1.20	770	750	---	---	---	---	---
Strength IV	70	---	1	---	1	1	0.50/1.20	---	---	---	---	---	---	---
Strength V	70	1.35	1	0.4	---	1	0.50/1.20	770	750	---	---	---	---	---
Extreme I	70	700	1	---	---	1	---	---	---	---	1	---	---	---
Extreme II	70	0.5	1	---	---	1	---	---	---	---	1	1	1	1
Service I	1	1	1	0.3	1	1	1.00/1.20	770	750	---	---	---	---	---
Service II	1	1.3	1	---	---	1	1.00/1.20	---	---	---	---	---	---	---
Service III	1	0.8	1	---	---	1	1.00/1.20	770	750	---	---	---	---	---
Service IV	1	---	1	0.7	---	1	1.00/1.20	---	1	---	---	---	---	---
Fatigue I	---	1.5	---	---	---	---	---	---	---	---	---	---	---	---
Fatigue II	---	0.75	---	---	---	---	---	---	---	---	---	---	---	---

Abutment 1 Load (kips)	Axial loads at base of abutment							Perpendicular (or transverse) to Bridge							Total
	1252	562	0	0	0	0	0	0	0	0	1980	0	0	0	
Strength I	1565	1184	0	0	0	0	0	0	0	0	0	0	0	0	2548
Strength II	1565	758	0	0	0	0	0	0	0	0	0	0	0	0	2324
Strength III	1565	0	0	0	0	0	0	0	0	0	0	0	0	0	1566
Strength IV	1878	0	0	0	0	0	0	0	0	0	0	0	0	0	1878
Strength V	1565	758	0	0	0	0	0	0	0	0	0	0	0	0	2324
Extreme I	0	0	0	0	0	0	0	0	0	1980	0	0	0	0	1980
Extreme II	0	0	0	0	0	0	0	0	0	0	0	0	0	0	0
Service I	1252	562	0	0	0	0	0	0	0	0	0	0	0	0	1814
Service II	1252	730	0	0	0	0	0	0	0	0	0	0	0	0	1982
Service III	1252	450	0	0	0	0	0	0	0	0	0	0	0	0	1702
Service IV	1252	0	0	0	0	0	0	0	0	0	0	0	0	0	1252
Fatigue I	0	422	0	0	0	0	0	0	0	0	0	0	0	0	422
Fatigue II	0	211	0	0	0	0	0	0	0	0	0	0	0	0	221

Extreme I - Lateral shear load: 1980 kips (transverse to bridge)

Pier 2 Load (kips)	Axial loads at base of pier					Longitudinal (or transverse) to Bridge					Total			
	2660	1267	0	0	0	0	0	0	0	3840		0	0	0
Strength I	3325	2217	0	0	0	0	0	0	0	0	0	0	0	5542
Strength II	3325	1710	0	0	0	0	0	0	0	0	0	0	0	5035
Strength III	3325	0	0	0	0	0	0	0	0	0	0	0	0	3325
Strength IV	3990	0	0	0	0	0	0	0	0	0	0	0	0	3990
Strength V	3325	1710	0	0	0	0	0	0	0	0	0	0	0	5035
Extreme I	0	0	0	0	0	0	0	0	0	1267	0	0	0	1267
Extreme II	0	0	0	0	0	0	0	0	0	0	0	0	0	0
Service I	2660	1267	0	0	0	0	0	0	0	0	0	0	0	3927
Service II	2660	1647	0	0	0	0	0	0	0	0	0	0	0	4307
Service III	2660	1014	0	0	0	0	0	0	0	0	0	0	0	3674
Service IV	2660	0	0	0	0	0	0	0	0	0	0	0	0	2660
Fatigue I	0	950	0	0	0	0	0	0	0	0	0	0	0	950
Fatigue II	0	475	0	0	0	0	0	0	0	0	0	0	0	475

Extreme I - Moment at base: 40,800 k-ft
 Extreme I - Lateral shear load: 1267 kips (longitudinal to bridge)

Figure 2-2 Example of factored load calculation.

2.4 NOMINAL AND FACTORED RESISTANCE

The nominal resistance, R_n , is calculated and then multiplied by the applicable resistance factor to determine the factored resistance, R_r . Nominal geotechnical resistances and associated resistance factors are discussed in Chapter 7. Nominal structural resistances and applicable resistance factors are presented in Chapter 8. The factored resistance must be greater than or equal to the sum of all factored force effects in all applicable limit states. The basic LRFD methodology equation is given as:

$$\sum \eta_i \gamma_i Q_i \leq \phi R_n = R_r \quad \text{Eq. 2-2}$$

Where:

- η_i = load modifier based on ductility, redundancy, or operation classification, applied to the force effect.
- γ_i = load factor, statistically based multiplier applied to force effect.
- Q_i = force effect.
- ϕ = resistance factor, statistically based multiplier applied to nominal resistance.
- R_n = nominal resistance.
- R_r = factored resistance.

The load modifiers for redundancy, η_r , described in AASHTO Article 1.3.4 were developed for superstructures. Paikowsky (2004) in NCHRP Report 507 defined redundancy in driven pile foundation designs based on the number of piles in a pile cap with redundant piles defined as 5 or more piles per pile cap and non-redundant piles defined as 4 piles or less per pile cap. For non-redundant driven pile foundation designs, AASHTO Article C10.5.5.2.3 recommends the resistance factor be reduced by 20%.

2.5 STRENGTH LIMIT STATES

The strength limit states ensure local and global strength and stability against statistically significant load combinations occurring during the structure design life. Strength limit state design of driven pile foundations includes an evaluation of the nominal geotechnical and structural resistances as well as the loss of lateral and vertical support in the design flood event (100 year) due to scour. For driven pile designs, strength limit state considerations include:

- axial compression resistance of single piles and pile groups,
- uplift resistance of single piles and pile groups,
- lateral resistance of single piles and pile groups,
- bearing stratum punching failure,
- structural resistance in axial compression, combined axial and flexural loading, and shear, and
- drivability including and driving stresses.

Geotechnical and structural strength limit state considerations are described in detail in Chapters 7 and 8, respectively of this manual.

2.6 SERVICE LIMIT STATES

The service limit states provide limits on stress, deformation, and cracking under regular service conditions. Service limit state considerations in driven pile foundation designs include:

- vertical deformation – settlement,
- horizontal movements,
- rotation,
- overall stability, and
- deformations due to scour at the design flood (100 year event).

Service limit state considerations are further discussed in AASHTO (2014) Articles 10.5.2.1 through 10.5.2.4 and associated commentary. All applicable service limit state load combinations must be evaluated.

2.7 EXTREME EVENT LIMIT STATES

Extreme event limit states ensure structural survival of a bridge under unique major occurrences such as earthquakes, floods, and vehicle, vessel collisions, or blasts with return periods significantly greater than the bridge design life. Extreme event limit states for driven pile foundation design include:

- the check flood (500 year event) for scour,
- vessel collision,
- vehicle collision,
- blast loading,
- seismic loading, and
- other site-specific situations determined by the design engineer.

A liquefaction assessment is required as part of the design for multi-span bridges if the site is classified as Seismic Zone 2, 3, or 4. Extreme event limit states are discussed further in Section 7.4 of this manual.

2.8 CONSTRUCTION OF PILE FOUNDATIONS

Construction of a successful driven pile foundation that meets the design objectives depends on relating the load requirements to the resistance requirements of the field installation and resistance determination method. The means for obtaining such a foundation must be explicitly incorporated into the plans and specifications as well as adhered to in the construction administration.

A pile foundation must be installed to meet the limit state requirements for compressive, lateral and uplift resistance. This may dictate driving piles for a required nominal resistance or to a predetermined penetration depth established by the designer to satisfy strength, service and extreme event limit state performance requirements. It is equally important to avoid pile damage or foundation cost overruns by excessive driving. These objectives can all be satisfactorily achieved by use of wave equation analysis, dynamic monitoring of pile driving, and/or static load testing. Some agencies have calibrated and/or developed new dynamic formulas for nominal resistance verification to replace more unreliable dynamic formulas such as the Engineering News formula.

Knowledgeable construction supervision and inspection are the keys to proper installation of piles. State-of-the-art designs and detailed plans and specifications

must be coupled with good construction supervision to achieve desired results. Post construction review of pile driving results versus predictions regarding pile penetration resistances, pile lengths, field problems, and static and/or dynamic load test nominal resistances is essential.

These reviews add to the experience of all engineers involved on the project and will enhance their skills. In addition, the implementation of LRFD in pile foundation design with rationally determined resistance factors makes it possible to use data from the post construction review to improve the resistance factors for future projects.

2.9 FOUNDATION SPECIALIST INVOLVEMENT

The input of an experienced foundation specialist is essential to produce a successful driven pile foundation. A foundation specialist has both a structural and geotechnical background in design and construction. The foundation specialist is the most knowledgeable person for selecting the pile type, estimating pile length, and choosing the most appropriate and cost effective method to determine the nominal resistance. In some agencies, the role of the foundation specialist may be divided amongst individuals and disciplines. Regardless of how the foundation specialist role is fulfilled, geotechnical and structural expertise in both design and construction knowledge is essential as design input.

The foundation specialist should be involved from the planning stage through the design and construction process. In some project phases (i.e. preliminary explorations, preliminary design, and final design), the foundation specialist will have significant involvement. In other project phases, such as construction, and post construction review, the foundation specialist's involvement may be more of a technical support role. The foundation specialist's involvement provides the needed continuity of design personnel in dealing with design related issues that develop throughout the construction stage. The importance of this continuity of knowledge, experience, and communication applies to all types of contracting methods.

2.10 THE DRIVEN PILE DESIGN AND CONSTRUCTION PROCESS

The driven pile design and construction process includes aspects that are unique in all of structural design. Because pile driving characteristics are related to the nominal geotechnical resistance for most soils, they can be used to improve the accuracy of the estimated nominal geotechnical resistance. In general, the various methods of determining nominal geotechnical resistance from dynamic data such as penetration resistance with wave equation analysis or with dynamic measurements are more accurate than the static analysis methods based on subsurface exploration information. It should be clearly understood that the static analysis based on the subsurface exploration information has the primary function of providing an estimate of the pile length for contractor bidding purposes.

Pile drivability is a critical aspect of the design process and must be considered during the design phase. If the design is completed, a contractor is selected, and then the piles cannot be driven, large additional costs can often result. Therefore, it is absolutely necessary that driven pile foundation design and construction be linked to a greater degree than in the design and construction of other foundation types.

During construction, the pile driving criterion is usually a blow count criterion that is established at the early stage of field installation, and individual pile penetration depths may vary depending on the subsurface variability. In some instances, piles may need to meet a minimum penetration depth and a blow count criterion. Minimum pile penetration depths are sometimes established to satisfy uplift or lateral loads, or for serviceability consideration. In other cases, satisfying a required pile penetration depth established from static analysis may be the sole pile installation criterion.

The driven pile design-construction process is outlined in the flow chart of Figure 2-3. The design and construction process will be discussed block by block using the numbers in the blocks as a reference and will serve to guide the designer through all of the tasks that must be completed. The block border depicts whether the structural engineer, geotechnical engineer, or construction engineer has the lead role for a given step in the design or construction process. This highlights the importance of interdisciplinary communication. The foundation specialist may perform some or a portion of the outlined structural and geotechnical steps based on their background and the organizational structure of the transportation agency.

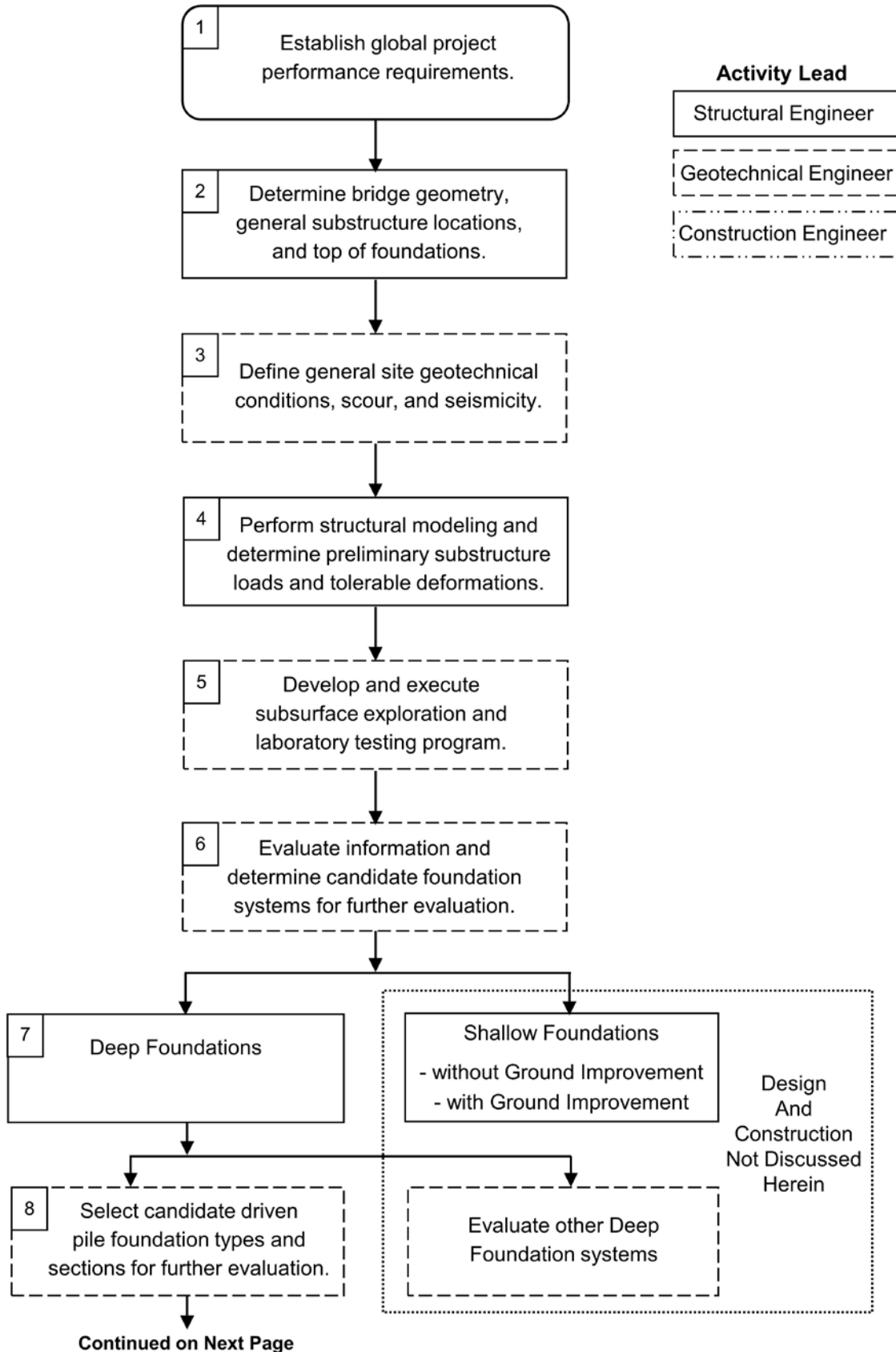


Figure 2-3 Driven pile design and construction process.

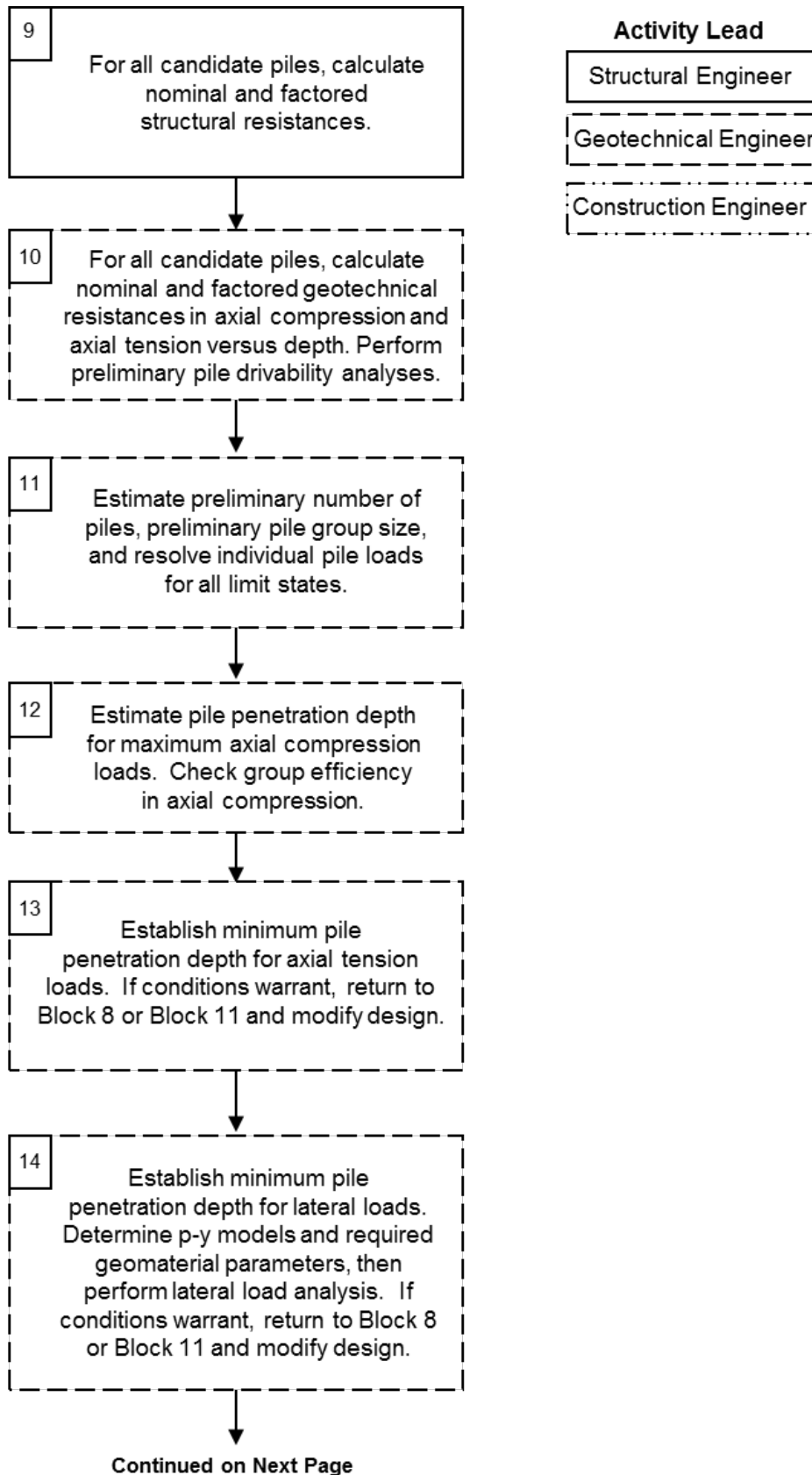


Figure 2-3 Driven pile design and construction process (continued).

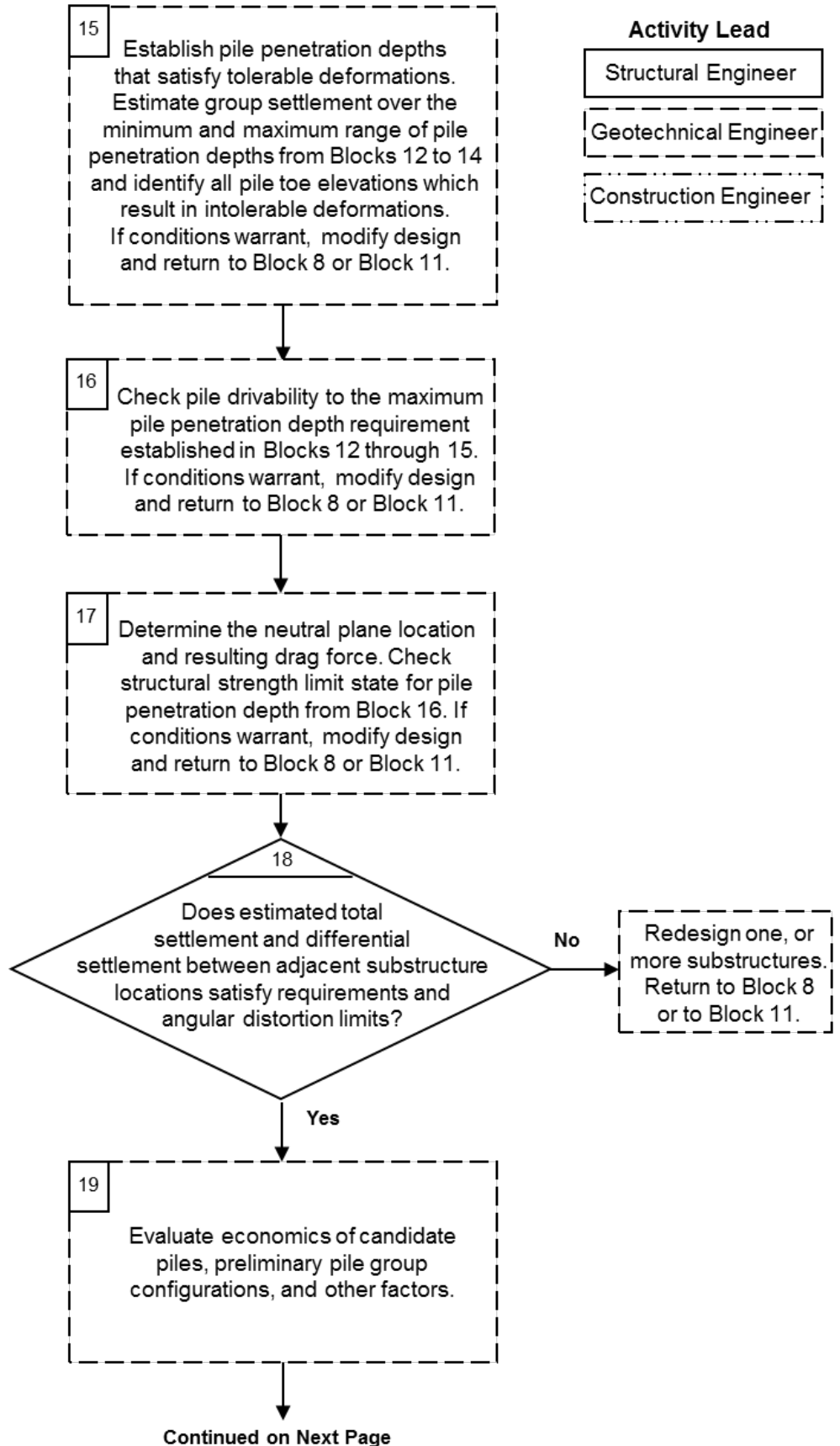


Figure 2-3 Driven pile design and construction process (continued).

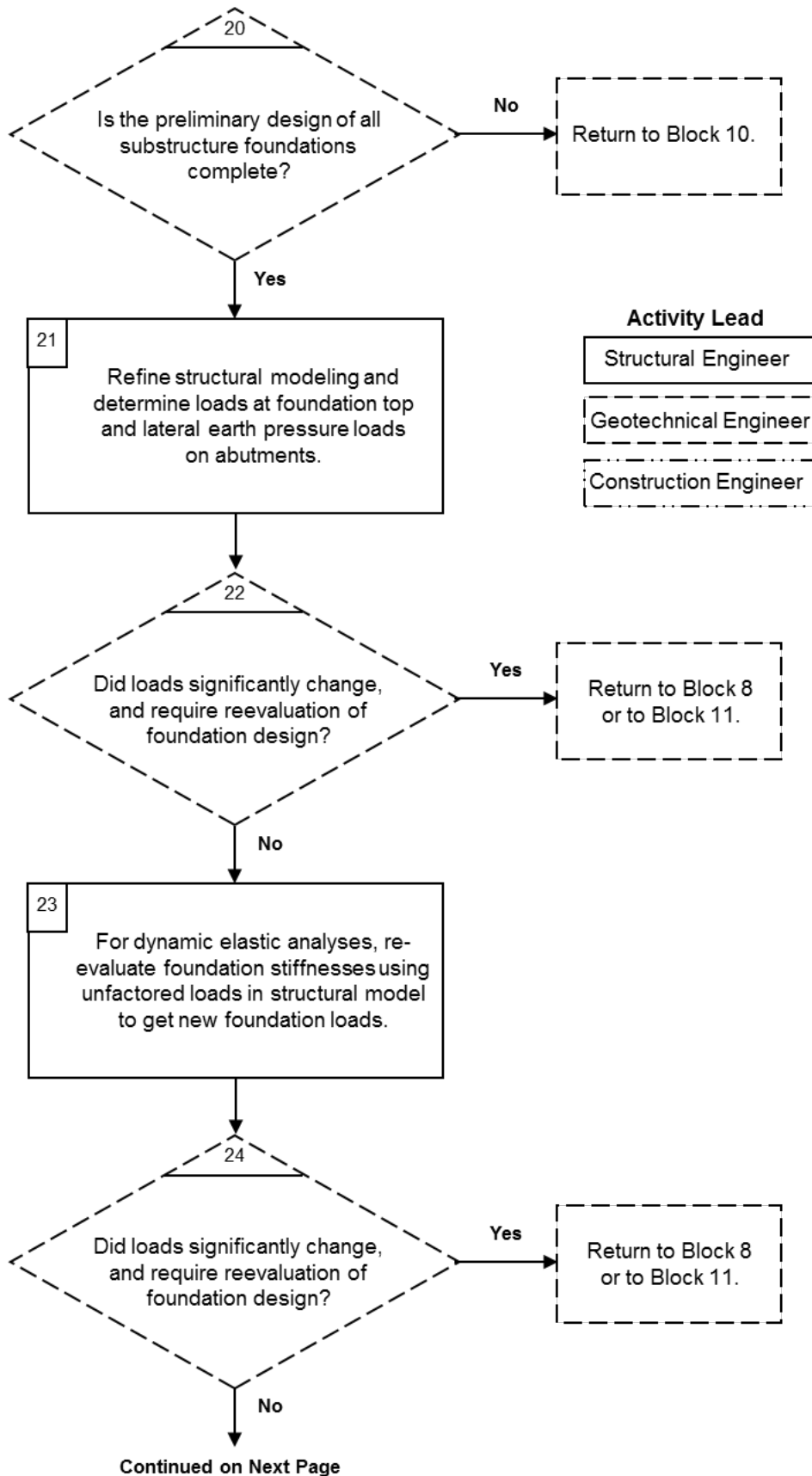


Figure 2-3 Driven pile design and construction process (continued).

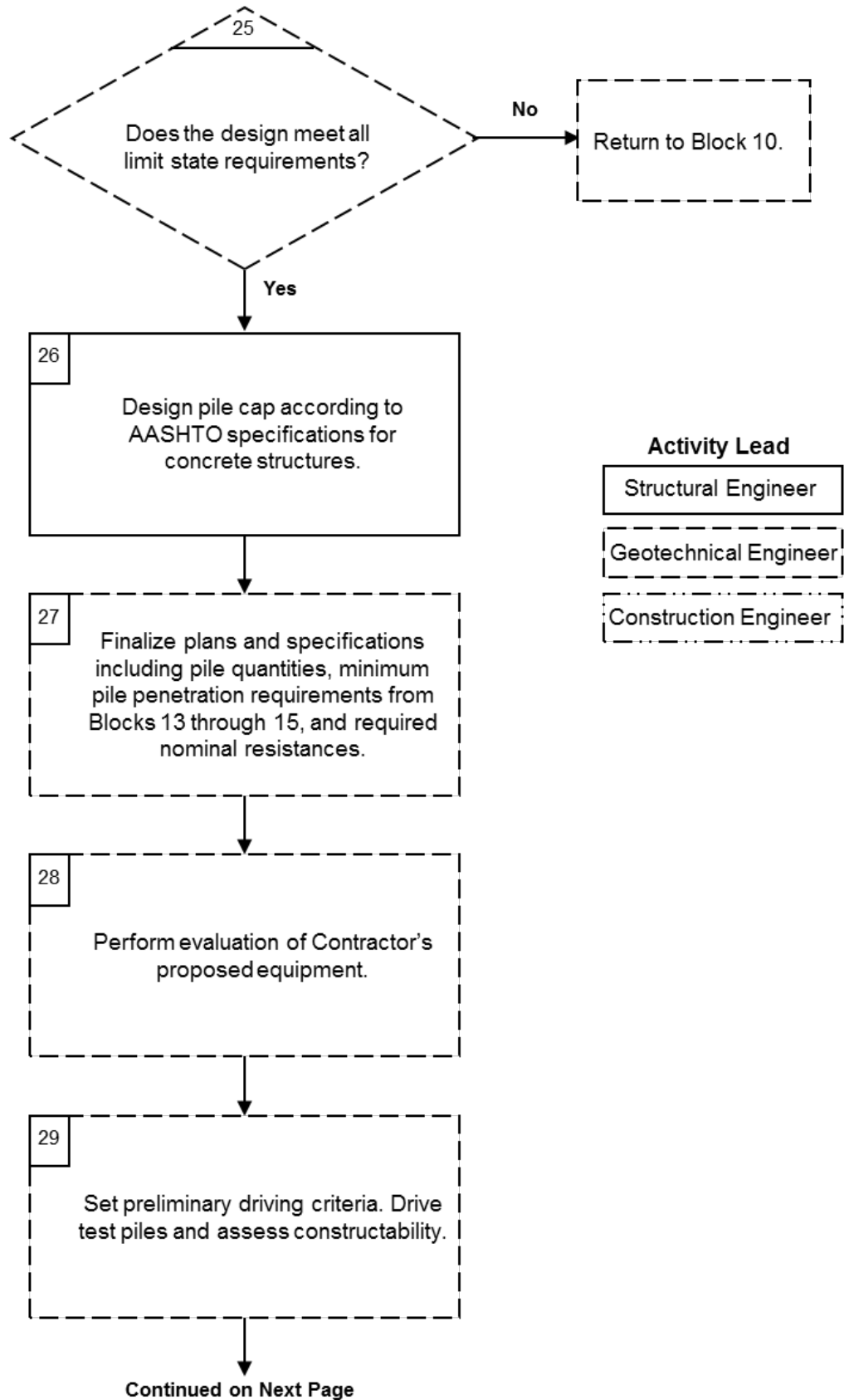


Figure 2-3 Driven pile design and construction process (continued).

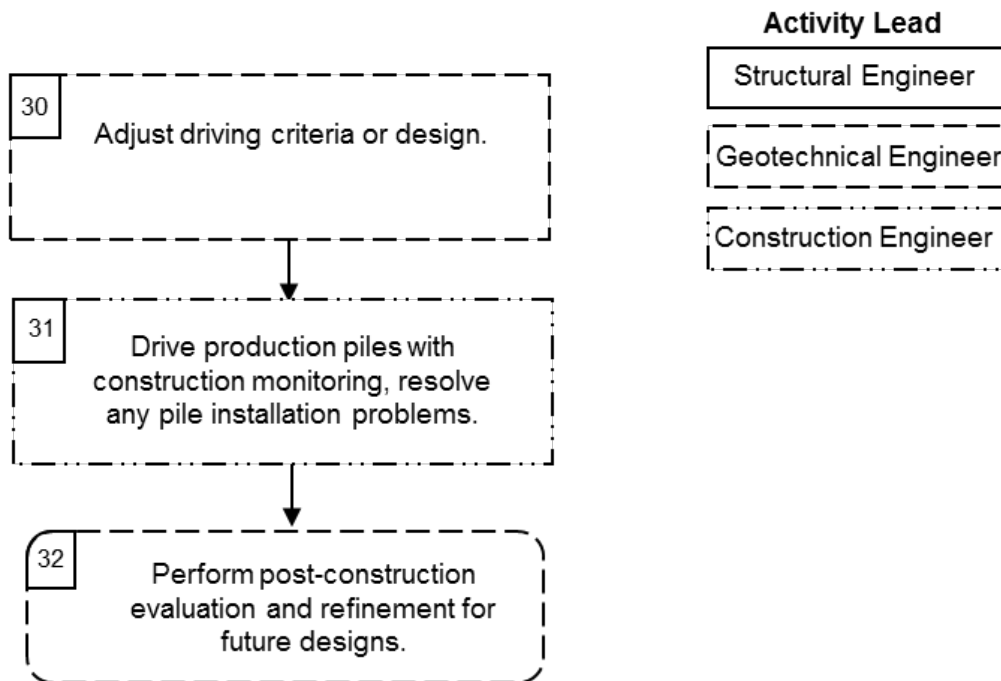


Figure 2-3 Driven pile design and construction process (continued).

Figure 2-3 is representative of the key steps in a typical design-bid-build project. The contractor in a design-bid-build project would be retained between Blocks 27 and 28, however the design and construction tasks for projects delivered using design-build or construction manager/general contractor contracts will vary. In a design-build contract, the contractor would be retained early on in the process once the project's general requirements and preliminary supporting information has been established. Hence, the early steps of the flow chart in a design-build contract will vary. While the responsibility for the individual tasks will differ in alternative contracting methods, the identified key design or construction activities are still performed.

Block 1: Establish Global Project Performance Requirements.

The first step in the design process is to determine the structure requirements.

1. Is the project a new bridge, a replacement bridge, a bridge renovation, a bridge widening, a retaining wall, a noise wall, or sign or light standard?
2. Will the project be constructed in phases or all at one time?
3. What are the general structure layout and approach grades?
4. What are the surficial site characteristics?
5. What are the approximate foundation loads? What are the deformation or deflection limits (total settlement, differential settlement, and lateral deformations) for the service and extreme event limit states?
6. Will the structure be subjected to any extreme event limit states such as seismic, scour, debris loading, vessel or vehicle impact, etc.?
7. Are there any special considerations to be evaluated such as lateral squeeze?
8. Are there modifications in the design that may be desirable for the site under consideration such as changes in substructure locations or span length?
9. Are there site or surrounding environmental considerations that must be considered in the design (low headroom, utility conflicts, aggressive soil environments, environmentally impacted soil and/or groundwater, limitations on noise, vibrations, etc.)? These factors may influence the selection of suitable deep foundation types, the deep foundation installation equipment, as well as the need for installation aids such as predrilling for driven pile options.
10. Are there other factors influencing bridge span lengths including river navigation channel width, road or railroad crossings; or avoidance of previous foundations?

Block 2: Determine Structure (bridge) Geometry, Substructure Locations and Elevations.

The general bridge geometry, probable substructure locations, and the top of foundation elevations should be established at this time.

Block 3: Define General Site Geotechnical Conditions, Scour, and Seismicity.

A great deal can be learned about the foundation requirements with even a very general understanding of both the site geology and area geotechnical conditions. Frequently there is information available on foundations that have been constructed in the area. This information can be of assistance in avoiding problems. Both subsurface exploration information and foundation construction experience should be collected prior to beginning the foundation design. This step is sometimes overlooked in practice.

If scour will be a design consideration, the hydraulic engineer should be consulted to determine probable scour depths that may impact the foundation selection.

Block 4: Perform Preliminary Structure Modeling. Determine Preliminary Substructure Loads and Tolerable Deformations.

Preliminary structural analysis and modeling of the proposed bridge or structure is performed at this time. The strength, service and extreme event limit states load demands and performance requirements at the foundation top have been established. For major bridge structures such as cable-stayed and balanced cantilever bridges, construction stage loads may govern the foundation design.

Many agencies also have total and differential settlement criteria for typical bridges which must be satisfied by the design. Lateral deformation limits for the proposed structure should also now be known and conveyed to the foundation specialist.

It is imperative that the foundation specialist obtain a completely defined and unambiguous set of foundation loads and deformation limits in order to proceed through the foundation design process. Accurate load information and deformation criteria are essential in the development and implementation of an adequate subsurface exploration program for the planned structure. It is important for the foundation specialist to address the level of uncertainty in their deformation

predictions and distinguish between total final loads and incremental loading such that post-construction deformation can be distinguished from total deformations. Of course, post-construction deformations are those of most interest.

Block 5: Develop and Execute Subsurface Exploration and Laboratory Testing Program for Feasible Foundation Systems.

Based on the information obtained in Blocks 1-4, it is possible to make decisions regarding the necessary information that must be obtained for the technically feasible foundation systems at the site. The subsurface exploration program including the associated laboratory testing must meet the project needs for design and construction at a cost consistent with the size and complexity of the project. Depending upon the project size and complexity, it may be advantageous to perform the subsurface exploration program in phases, one for preliminary planning and general site evaluation and a second phase for final design.

The results of the subsurface exploration soil boring and in-situ testing program along with laboratory test results are used to prepare a subsurface profile; define soil and rock parameters including strength, compressibility, parameter variation, liquefaction susceptibility, and seismic earth pressure parameters; subsurface water conditions, as well as identify critical cross sections for design. The design profile for each substructure location will be developed from the information gathered in this block and used in later blocks. Site characterization and design parameter selection are covered in detail in Chapters 4 and 5.

Block 6: Evaluate Information and Determine Candidate Foundation Systems.

The information collected in Blocks 1-5 must be evaluated and candidate foundation systems selected. The question to be answered is what candidate foundation systems are appropriate for consideration based on the site conditions. This question will be answered based primarily on the strength and compressibility of the geomaterials, the proposed loading conditions, the project deformation limits, the project schedule, and the foundation cost. Shallow foundations may be determined to be technically feasible and the most economical solution provided all project performance requirements can be addressed. Ground improvement techniques in conjunction with shallow foundations should also be evaluated. Shallow and deep foundation interaction with approach embankments and approach slabs must also be considered.

If the performance of a shallow foundation exceeds the established deformation limit, or if excessive scour is a concern, a deep foundation must be used. The design of shallow foundations and ground improvement techniques are not covered in this manual. Information on design consideration for shallow foundations can be found in Munfakh et al. (2001), Kimmerling (2002), Samtani et al. (2010), and in Abu-Hejleh et al. (2014). The effects of settlement can be more comprehensively examined by using a construction point concept and estimating the differential settlement between supports as discussed by Modjeski and Masters, Inc, et al. (2015) in SHRP 2 Report S2-R19B-RW-1. Information on ground improvement techniques can be found in Elias et al. (2006) and at <http://www.geotechtools.org>. The selection of the appropriate foundation system including cost considerations is discussed in greater detail in Chapter 3, while Chapter 6 presents pile type selection along with advantages and disadvantages.

Block 7: Determine if a Deep Foundation is Required.

Once candidate foundation systems have been identified in Block 6, it has been determined that a deep foundation system is required. Therefore, driven piles and other deep foundation systems must be further evaluated. These other deep foundation systems are primarily drilled shafts, but also include micropiles, continuous flight auger (CFA) piles, and other drilled-in deep foundation systems. The questions that must be answered in deciding between driven piles and other deep foundation systems will center on both the technical feasibility and the relative costs of available systems. Foundation support cost can be conveniently calculated based on the cost per unit of load carried. The foundation cost analysis should address all temporary and permanent requirements (e.g., pile caps, effects of pile cap elevation, cofferdams, use of vertical and/or batter piles, load tests, construction control tests) for that specific foundation type. In addition, constructability and productivity (i.e., schedule) must be considered. This manual is concerned with driven piles; therefore other types of deep foundations will not be further discussed. Design guidance on drilled shafts can be found in Brown et al. (2010). For micropile design guidance refer to Sabatini et al. (2005), and for CFA piles refer to in Brown et al. (2007). Economic considerations in the foundation selection process are discussed in Chapter 3.

Block 8: Select 2 to 5 Candidate Driven Pile Types and Sections for Further Evaluation.

At this point on the flow chart, the primary concern is for the design of a driven pile foundation. The pile type must be selected consistent with the factored loads (compression, tension, and lateral) to be resisted per pile. Consider this problem. The general magnitude of the pier load is known from the information obtained in Blocks 1 and 4. However, a large number of combinations of pile types and nominal geotechnical resistances can satisfy the nominal resistance requirements for the factored loads. In the case of axial compression resistance, should twenty piles with a nominal resistance of 225 kips be used to support a 4,500 kip factored load, or would it be better to use ten piles with a nominal resistance of 450 kips, or five piles with a nominal resistance of 900 kips? This decision should consider the nominal structural resistance of the piles, the realistic geotechnical nominal resistances and deformations for the soil conditions at the site, the cost of the different pile types, and the capability of construction contractors to install the piles. Changes in the foundation selection from twenty 225 kip piles to five 900 kip piles will also affect structure and foundation response and therefore adjust the lateral and axial loads as well as pile cap requirements and costs. At this point in the design process, 2 to 5 candidate pile types and/or sections that meet the general project requirements should be selected for further evaluation. Pile type and selection considerations are covered in greater detail in Chapter 6.

Approximate loads determined in Block 1 were refined in Block 4. At those stages of the design process, the other aspects of the total structural design were probably insufficiently advanced to establish the final factored loads. By the time that Block 7 has been reached, the foundation loads and deformation limits should be closer to being finalized.

If there are extreme event limit states applicable to the structure, the design must satisfy those load and deformation requirements. Vessel impact will be evaluated primarily by the structural engineer and the results of that analysis will give factored loads for that case. There may be stiffness considerations in dealing with vessel impact since the design requirement is basically that some vessel impact energy be absorbed.

Scour presents a different requirement. AASHTO (2014) Article 3.7.5 requires changes in foundation conditions resulting from the design flood (100 year event) be evaluated at the strength and service limit states. Foundation condition changes from the check flood (500 year event) must be considered and evaluated at the

extreme event limit state. Scour is not a force effect. However, scour can change the substructure conditions and alter the consequences of force effects acting on the structure. It must be assured that after scour, the pile will still satisfy geotechnical and structural resistance demands.

In many locations, seismic design will be an important factor. Since the 1971 San Fernando Earthquake, significant emphasis has been placed on the design of highway bridges in seismic events. AASHTO (2014), Section 10, Appendix A10 discusses seismic analysis and design requirements. Additional seismic design guidance is available in GEC-3, LRFD Seismic Analysis and Design of Transportation Geotechnical Features and Structural Foundations, by Kavazanjian et al. (2011), as well as in the AASHTO (2011) Guide Specifications for LRFD Seismic Bridge Design, 2nd Edition, with 2012, 2014, and 2015 Interims.

Block 9: Calculate Nominal and Factored Structural Resistance.

The maximum nominal and factored structural resistances of all candidate pile types in axial compression, bending, and combined axial compression and flexure resistance are calculated at this time. Pile structural resistance is covered in Chapter 8.

The maximum factored resistance for a given pile type is the lesser of the factored structural resistance or the factored geotechnical resistance for that pile.

Block 10 Calculate the Nominal and Factored Geotechnical Resistance, as well as Perform a Preliminary Drivability Assessment of Candidate Pile Types.

The maximum nominal and factored geotechnical resistance in axial compression and uplift are calculated as a function of pile penetration depth for all candidate pile types. A static analysis method(s) appropriate for the pile type(s), the soil conditions, and the loading condition should be selected. These methods are presented in detail in Chapter 7. Factored geotechnical resistances are most often calculated based on the resistance determination method used in the field but can also be calculated solely on the basis of an appropriate static analysis method. Review of the nominal and factored geotechnical resistances versus depth for candidate pile sections and various resistance determination methods assists the designer in selecting the foundation type and associated resistance determination method.

Deposits within the subsurface strata which are unsuitable as load carrying geomaterial must be identified. The geotechnical resistance from these layers must be determined by static analysis. Unsuitable layers may include urban fills, organic deposits, soft and very soft cohesive soils, as well as potentially scourable or liquefiable materials.

Preliminary wave equation drivability assessments of candidate pile sections should be performed at this time. These analyses must consider the geotechnical resistance from suitable as well as unsuitable layers. A commonly available pile hammer having a ram weight of 1 to 2% of the required nominal resistance is a good initial trial hammer size for preliminary drivability assessments.

Block 11: Estimate the Preliminary Number of Piles, Preliminary Group Size, and Resolve Individual Pile Loads at All Limit States.

The preliminary number of piles at a substructure location can be estimated by dividing the largest factored axial load by an individual pile's factored geotechnical resistance. Axial compression and axial tension requirements should both be considered. In some cases, lateral load requirements may control the design. Therefore, similar past experience may also be used to estimate the preliminary number of piles, trial group configurations, and pile spacing. Using the factored loads with the trial group configurations, determine the limit state reactions on the substructure unit and the resulting maximum factored load per pile at the strength, service, and extreme limit states for each candidate pile type.

Block 12: Estimate Pile Penetration Depth for Axial Compression Loads and Check Group Efficiency in Axial Compression.

For each candidate pile section and each group configuration, determine the estimated pile penetration depth where the factored geotechnical resistance exceeds the factored load. Note that the factored geotechnical resistance will vary based on the resistance verification method. Block 12 establishes an estimated pile penetration depth for compression loading for each of the candidate pile types. Note this estimated depth is a function of the resistance determination method. Check that group axial compression resistance meets design requirements. If the group resistance group does not satisfy requirements, modify the design.

Block 13: Establish Minimum Pile Penetration Depth for Axial Tension Loads.

Determine the maximum factored axial tension load to be resisted in any limit state. From the nominal axial tension resistance versus depth results calculated in Block 10, determine the minimum pile penetration depth necessary to obtain a factored geotechnical resistance greater than the maximum factored axial tension load. Block 13 establishes a minimum pile penetration depth for tension loading for each of the candidate pile types. Note that this minimum depth is a function of the resistance determination method. Check that group axial tension resistance meets design requirements. If axial tension requirements cannot be achieved, modify the design. Return to Block 8 and select a new pile type or new pile section, or return to Block 11 and evaluate new group configurations.

Block 14: Establish Minimum Pile Penetration Depth for Lateral Loads.

Determine p-y models and required geomaterial properties for each layer in the subsurface profile. The p-y model and parameters chosen depend on the soil or rock response being modelled in the service or extreme event limit case. Results of this analysis will be compared to the tolerable lateral deformation requirements. Check that the deformation and lateral resistance of the trial group configuration meets design requirements. Determine the minimum pile penetration depth necessary to resist the maximum applied lateral loads within the permissible deformation limit. This depth establishes the minimum pile penetration depth for lateral loading for the candidate pile type and group. This topic is covered in greater detail in Section 7.3.4.2. If lateral deformation requirements cannot be achieved, modify the design. Return to Block 8 and select a new pile type or pile section, or return to Block 11 and evaluate new group configurations.

Block 15: Establish Pile Penetration Depths that Satisfy Tolerable Deformations Based on Group Settlement Computations.

Preliminary group configurations should now be evaluated for settlement. One of the primary objectives at this stage is to determine if a minimum pile penetration depth is required and, if so, to determine the required minimum pile toe elevation. In some subsurface profiles, piles could attain the requisite nominal resistance near the bottom of a dense layer overlying a compressible layer. In order to satisfy tolerable deformation limits, it may be necessary to drive through, or otherwise penetrate, the higher, suitable layer to preclude large future settlements. Hence, in some

stratigraphy cases, it is necessary to calculate group settlements over a range of pile termination depths to determine the minimum (highest pile toe elevation) and, in unique stratigraphy cases, the maximum (lowest pile toe elevation) acceptable for tolerable group settlements. Any penetration depths that will result in intolerable deformations should be identified. Where appropriate, Block 15 establishes a minimum pile penetration depth, maximum pile penetration depth, or both. If tolerable deformation requirements cannot be achieved, modify the design. Return to Block 8 and select a new pile type, or return to Block 11 and evaluate new group configurations.

Block 16: Check Pile Drivability.

Identify the maximum pile penetration depth required by each block in Block 12 through Block 15. Perform a wave equation drivability analysis for each candidate section to the maximum pile penetration depth determined in any of these blocks. Candidate pile types that cannot be driven to the required nominal resistance and/or the minimum pile penetration depth without exceeding material stress limits and within a reasonable blow count of 30 to 120 blows per foot with appropriately sized driving systems are eliminated at this time. It should be noted that 120 blows per foot or 10 blows per inch is considered refusal driving conditions by many hammer manufacturers. Therefore, depending on the expected driving conditions (e.g., an extended duration of hard driving compared to a quick transition onto hard rock), it may more reasonable to assess candidate pile drivability based on an upper limit of 96 blows per foot or 8 blows per inch. In some cases pile installation aids such as jetting or predrilling may be evaluated subject to other design limitations.

The drivability analyses should also consider what influence the group configuration (pile spacing) and construction procedures and constraints (i.e., predrilling, cofferdams, etc.) may have on pile installation conditions. If the selected pile type does not meet drivability requirements, a different pile section, pile type, or group configuration is required. Return to Block 8 and select a new pile type, or return to Block 11 and evaluate new group configurations.

Block 17: Determine Location of Neutral Plane and Magnitude of Drag Force.

The neutral plane location for drag force evaluation is performed in this step. Note that the neutral plane location may have already been determined in Block 15 depending upon the settlement analysis approach selected by the designer. The

neutral plane is defined as the location where the sum of the permanent structure load and drag force is balanced by the sum of the shaft and toe resistances occurring below the neutral plane. The maximum drag force, caused by differential movement between the pile and the geomaterials, occurs at the neutral plane. The drag force magnitude is related to the pile properties, loading conditions, soil stress state, and deformation. The sum of the permanent structure load plus the maximum drag force should be less than the pile's factored structural resistance. If it is not, a different pile section or pile type is required, and the design process returns to Block 8, or a new group configuration is required and the design process returns to Block 11. Determination of the neutral plane location and drag force is discussed further in Section 7.2.10.

It should be noted that the AASHTO (2014) design specifications do not specifically address drag force considerations relative to the pile structural resistance. For example, the factored structural resistance of an H-pile is the nominal structural resistance multiplied by the resistance factor for axial compression, ϕ_c . This resistance factor is 0.70 for combined axial and flexural resistance of undamaged piles, 0.60 for the axial resistance of piles in compression under good driving conditions, and 0.50 for the axial resistance of piles in compression subject to damage due to severe driving conditions. While not equivocally stated, it follows that if the neutral plane is located below the point of fixity and above the depth where H-piles are subject to potential damage during driving, then the sum of the permanent load plus drag force at the neutral plane is limited to 0.70 of the nominal structural resistance.

Block 18: Does the Computed Total Settlement, Differential Settlement, and Angular Distortion Satisfy Design Requirements?

In this block, the total settlement should be computed and compared to project deformation limits. At the same time, the computed differential settlement between the current substructure location and adjacent substructure units should be compared to differential settlement and angular distortion limits. The construction point concept described in Section 7.3.3 and the recommended procedure for vertical deformation analysis in Section 7.3.4 should be followed.

If the total settlement, differential settlement, or angular distortion limits are exceeded, the design process returns to an earlier block. If a new pile type or section needs to be considered, the design process returns to Block 8. If existing

candidate pile types or sections are considered for the redesign of one or more of the substructure units, then the design process returns to Block 11.

Block 19: Evaluate Economics of Candidate Pile Types and/or Sections.

The next step is to determine the pile support cost versus pile penetration depth for each candidate pile type and/or section. The support cost, which is the cost per ton supported, is the pile cost at a given penetration depth divided by the nominal resistance at that penetration depth. The pile cost can be calculated from the unit cost per foot multiplied by the pile length between the pile cutoff elevation and the pile penetration depth. These plots should be evaluated to identify possible pile termination depths to obtain the lowest pile support cost. In some instances, uplift load rather than axial compression load may control the design in which case the same concept could be used for nominal tension resistance. The pile cost should include all costs associated with a given candidate section including material, transportation, and installation. In addition, the cost of the pile cap, cofferdams, dewatering or other related construction items should be included. This economic assessment should be modified appropriately in cases where lateral load demand and deformation control the design. The cost of the resistance determination method should be considered when evaluating the economics of candidate piles. Economic evaluation is presented in detail in Chapter 3.

Block 20: Is the Preliminary Design Complete at All Substructure Locations?

The preliminary design process in Blocks 9 through 19 is completed for each substructure location until the preliminary design is complete at all foundation units.

Block 21: Refine Structural Modeling and Loads.

At this point, the structure and foundation response to the loading cases can be further refined based on the structural and geotechnical analyses completed in Block 9 through Block 17. The structural model is now reanalyzed using the results from these preliminary substructure analyses to better determine the structure loads at the foundation top, and lateral earth pressure loads on the abutments.

Block 22: Did the Loads Significantly Change Requiring Reevaluation of the Foundation Design?

Based on the refined structural modeling, review the preliminary design based on the refined loads. If necessitated by the refined modelling, return to Block 8 and modify the design.

Block 23: Re-evaluate Foundation Stiffness and Loads.

For dynamic elastic analyses in seismic or other dynamic extreme events, the structural engineer now re-evaluates foundation stiffness. The structural model will be rerun to get new foundation loads.

Block 24: Did the Loads Significantly Change Requiring Reevaluation of the Foundation Design?

Review the preliminary design based on the refined loads from the dynamic elastic analyses. If loads from lateral pile analysis do not match the new foundation top loads within 5%, re-iterate the process until convergence is achieved. See Section 7.4.2.1 and GEC 3, (Kavazanjian et al. 2011). If necessary, return to Block 8 and modify the design.

Block 25: Does the Design Meet All Limit State Requirements?

The foundation specialist checks the estimated and/or minimum pile toe elevation for nominal geotechnical resistance in axial compression and tension, deformation under lateral load, serviceability, and drivability. If any limit state checks are not satisfied, the design process returns to Block 8.

Block 26: Design Pile Caps and Abutments.

The final design of the pile cap (and abutment walls) is completed according to AASHTO specifications for concrete structures. The size and thickness of the pile cap in evaluating trial group configurations should have been previously evaluated and the cost of the resulting pile cap estimated. Pile cap cost is a key component in selecting the most cost effective foundation and should not be overlooked in the

design process. A procedure for preliminary sizing of pile caps is provided in Chapter 8.

Block 27: Prepare Plans and Specifications, Set Nominal Resistance Field Verification Procedure.

When the design has been finalized, the structural engineer prepares the project plans and the geotechnical engineer the project specifications. It is important that all of the quality assurance procedures are clearly defined for the bidders to avoid claims after construction is underway. The factored pile load should be shown on the plans along with nominal resistance, the resistance determination method and the method's resistance factor, ϕ_{dyn} . If changes in the resistance determination method are later appropriate, the required nominal resistance with the new method can readily be evaluated. Any minimum or maximum pile penetration depth requirements should also be clearly identified. This information should also be readily apparent in the project specifications so that the contractor has no question regarding the installation requirements. Quality assurance procedures should be in place that address commonly occurring pile installation issues such as obstructions, drivability and construction records. Contract documents and specifications are discussed in Chapter 14, and the foundation report is covered in Chapter 5.

Block 28: Perform Evaluation of Contractor's Equipment Submission.

At this point the engineering effort shifts to the field. The contractor will be required to submit a description of the pile driving equipment that is intended to be used on the project for the engineer's evaluation. On most projects, a wave equation analysis is performed to estimate the blow count that must be achieved in the field to meet the required nominal driving resistance as well as to check if the pile can be driven to the required pile penetration depth, if specified. Driving stresses are also determined and evaluated. If all conditions are satisfactory, the equipment is approved for driving. Some design specifications make this information advisory to the contractor rather than mandatory. Chapters 12 and 14 provide additional information in this area.

Block 29: Set Preliminary Driving Criteria, Drive Test Pile(s), Perform Resistance Evaluation Tests, and Evaluate the Nominal Resistance Achieved.

Depending on the specified resistance determination method, the blow count needed to achieve the required nominal resistance can be established and used as the preliminary driving criteria. With some methods, the preliminary criteria can be determined before driving a pile and with other methods a pile must be driven, tested, and results evaluated. Preliminary driving criteria are generally established using wave equation analysis or a dynamic formula since these can be performed before driving a pile. Additional details on wave equation analysis and dynamic formulas are presented in Chapters 12 and 13, respectively.

The test pile(s), if required, are driven to the preliminary criteria. Driving requirements may be defined by blow count, minimum penetration depth, dynamic monitoring results, or a combination of these conditions. The nominal resistance can be evaluated using the observed blow count and hammer performance (e.g., stroke, energy readout) in a wave equation analysis or dynamic formula. Alternatively, the nominal resistance achieved by the test pile can be evaluated by more reliable methods such as a static load test, dynamic load test, or rapid load test. Details on static load testing are presented in Chapter 9, dynamic load testing in Chapter 10, rapid load testing in Chapter 11.

Each field resistance determination method has its own resistance factor, ϕ_{dyn} . Therefore, it is important to determine the resistance determination method during the design process. The selected resistance determination method determines the required nominal resistance. Post-design modification to the resistance determination method changes the resistance factor and the required nominal resistance. Changing to a more reliable resistance determination method reduces the required nominal resistance, which generally shortens the piles. Conversely, changing to a less reliable resistance determination method increases the required nominal resistance. This may result in the original design no longer meeting design or constructability requirements.

On smaller projects, a dynamic formula might be used to evaluate the nominal resistance. The modified Gates Formula is frequently used for this purpose but some transportation agencies have also developed or adopted other dynamic formulas. If a dynamic formula is used, then drivability and hammer selection will be based on the blow count given by the formula only, since stresses and drivability to a penetration depth are not determined. Dynamic formula usage is covered in Chapter 13.

Block 30: Adjust Driving Criteria or Design.

At this stage the final installation criteria can be set or, if test results from Block 29 indicate the nominal resistance is inadequate, the driving criteria may have to be changed. Occasionally, it may be necessary to make changes in the design as far back as Block 8. It may also be possible to change to a more reliable resistance determination method with a higher resistance factor and thereby reduce the required nominal resistance to a nominal resistance that can be achieved without a major design change.

In some cases, it is desirable to perform preliminary field testing before final design. When the project is very large and the subsurface conditions are difficult, it may be possible to achieve substantial cost savings by having results from a design stage test pile program, including actual driving records at the site. Such results can be used to optimize the design, and reduce contractor contingencies when included as part of the bid package.

Block 31: Drive Production Piles with Construction Monitoring.

After the driving criteria is established, the production pile driving begins. Quality control and quality assurance procedures have been established and are applied. Construction inspection items are discussed in greater detail in Chapter 18. Problems may arise and must be handled as they occur in a timely fashion.

Block 32: Post-Construction Evaluation and Refinement of Design.

After completion of the foundation construction, the design should be reviewed and evaluated for its effectiveness in satisfying the design requirements and also its cost effectiveness. This review benefits future similar projects constructed in similar conditions.

2.11 COMMUNICATION

Good communication between all organizations and disciplines involved in the design and construction of a pile foundation is essential to reach a successful completion of the project. In the design stage, communication and interaction is needed between the structural, geotechnical, geologic, hydraulic, and construction

disciplines, as well as with consultants, drill crews and laboratory personnel. In the construction stage, structural, geotechnical and construction disciplines need to communicate for a timely resolution of construction issues as they arise. Tables 2-4 and 2-5 highlight some of the key issues to be communicated in the design and construction stages.

Table 2-4 Design Stage Communication

Subject	Structural	Geotechnical	Hydraulic	Construction	Field Crews	Laboratory
Preliminary Structure Loads and Performance Criteria.	X	X	X			
Determination of Scour Potential.	X	X	X			
Determination of Applicable Extreme Events.	X	X	X			
Review of Past Construction Problems in Project Area.	X	X	X	X		
Implement Subsurface Exploration and Testing Programs.	X	X	X	X	X	X
Determination of Pile Type, Length and Nominal Resistance.	X	X		X		
Select Construction Control and Quality Assurance Methods.	X	X		X		
Effects of Approach Fills on Design.	X	X				
Prepare Plans and Specifications.	X	X	X	X		

Table 2-5 Construction Stage Communication

Subject	Structural	Geotechnical	Construction
Perform Required Methods of Construction Control and Quality Assurance.	X	X	X
Perform Wave Equation Analysis of Contractors Driving System to Establish Driving Criteria.	X	X	X
Perform Static Load Test(s) and/or Dynamic Monitoring and Adjust Driving Criteria.	X	X	X
Resolve Pile Installation Problems / Construction Issues.	X	X	X

REFERENCES

- Abu-Hejleh, N., Kramer, W.M., Mohamed, K., Long, J.H., and Zaheer, M.A. (2013). Implementation of AASHTO LRFD Design Specifications for Driven Piles, FHWA-RC-13-001. U.S. Dept. of Transportation, Federal Highway Administration, 71 p.
- American Association of State Highway and Transportation Officials (AASHTO). (2011). Guide Specifications for LRFD Seismic Bridge Design, 2nd Edition, with 2012, 2014, and 2015 Interim Revisions. American Association of State Highway and Transportation Officials, Washington, D.C., 331 p.
- American Association of State Highway and Transportation Officials (AASHTO). (2014). AASHTO LRFD Bridge Design Specifications, US Customary Units, Seventh Edition, with 2015 Interim Revisions. American Association of State Highway and Transportation Officials, Washington, D.C., 1960 p.
- Brown, D.A., Dapp, S.D., Thompson, W.R., and Lazarte, C.A. (2007). Design and Construction of Continuous Flight Auger (CFA) Piles. FHWA-HIF-07-03, Geotechnical Engineering Circular (GEC) No.08. U.S. Dept. of Transportation, Federal Highway Administration, 289 p.
- Brown, D. A., Turner, J.P. and Castelli R.J. (2010). Drilled Shafts: Construction Procedures and LRFD Design Methods, FHWA-NHI-10-016, Geotechnical Engineering Circular (GEC) No. 10. U.S. Dept. of Transportation, Federal Highway Administration, 970 p.
- Elias, V., Welsh, J.P., Warren, J., Lukas, R.G., Collin J.G., and Berg, R.R. (2006). Ground Improvement Methods Volumes I and II, FHWA-NHI-06-019 and FHWA NHI-06-020. National Highway Institute, Federal Highway Administration, U.S. Department of Transportation, Washington D.C.
- Kavazanjian, E., Wan, J-N. J., Martin, G.R., Shamsabadi, A., Lam, I., Dickenson, S.E., and Hung, C.J. (2011). LRFD Seismic Analysis and Design of Transportation Geotechnical Features and Structural Foundations, FHWA-NHI-11-032, Geotechnical Engineering Circular (GEC) No. 3. U.S. Dept. of Transportation, Federal Highway Administration, Washington, D.C., 592 p.

- Kimmerling, R.E. (2002). Shallow Foundations, FHWA-IF-02-054, Geotechnical Engineering Circular (GEC) No. 6. U.S. Dept. of Transportation, Federal Highway Administration, Washington, D.C., 310 p.
- Modjeski and Masters, Inc. (2015). Bridges for Service Life Beyond 100 Years: Service Limit State Design. SHRP2 Report S2-R19B-RW-1. Transportation Research Board, Washington D.C., 268 p.
- Munfakh, G., Arman, A., Collin, J.G., Hung, J.C.-J., and Brouillette, R.P. (2001). Shallow Foundations Reference Manual, FHWA-NHI-01-023. National Highway Institute, Federal Highway Administration, Washington, D.C., 222 p.
- Paikowsky, S.G. (2004), with contributions from Birgisson, B., McVay, M., Nguyen, T., Kuo, C., Baecher, G., Ayyub, B., Stenersen, K., O'Malley, K., Chernauskas, L., and O'Neill, M., Load and Resistance Factor Design (LRFD) for Deep Foundations, NCHRP Report 507. Transportation Research Board, Washington, D.C., 76 p.
- Sabatini, P.J., Tanyu, B., Armour, P., Groneck, P., and Keeley, J. (2005). Micropile Design and Construction, FHWA-NHI-05-039. National Highway Institute, U.S. Dept. of Transportation, Federal Highway Administration, Washington, D.C., 436 p.
- Samtani, N.C., Nowatzki, E.A., and Mertz, D.R. (2010). Selection of Spread Footings on Soils to Support Highway Bridge Structures, FHWA-RC TD-10-001. U.S. Department of Transportation, Federal Highway Administration, Washington, D.C., 98 p.

CHAPTER 3

CONSIDERATIONS IN FOUNDATION SELECTION

A foundation is the interfacing element between the superstructure, substructure, and the underlying geomaterial (i.e., soil or rock). The loads transmitted by the foundation to the underlying geomaterial must not cause shear failure or damaging deformations of the superstructure. It is essential to systematically consider various foundation types and to select the most appropriate alternative based on the superstructure requirements, the subsurface conditions, and foundation cost. Foundation types include shallow foundations consisting of spread footing or mat foundations with or without ground improvement; or deep foundations consisting of driven piles, micropiles, drilled shafts, or continuous flight auger (CFA) piles.

Subsequent chapters of this manual provide guidance on driven pile foundation design and construction. FHWA guidance for other foundation solutions is shown in Table 3-1 below.

Table 3-1 Foundation Information Sources Provided by the Federal Highway Administration

Foundation Solution	FHWA Reference	Author(s)
Spread Footings	GEC-6, FHWA-SA-02-054	Kimmerling (2002)
Ground Improvement	FHWA-NHI-06-019/020	Elias et al. (2006)
Micropiles	FHWA-NHI-05-039	Sabatini et al. (2005)
Drilled Shafts	GEC-10, FHWA NHI-10-016	Brown et al. (2010)
CFA Piles	GEC-8, FHWA-HIF-07-03	Brown et al. (2007)

Complete references for the above design manuals are provided at the end of this chapter. Information on the availability of these documents is provided at <https://www.fhwa.dot.gov/bridge/geopub.htm>

3.1 FOUNDATION DESIGN APPROACH

The following design approach is recommended to determine the most appropriate foundation alternative.

1. Determine the foundation loads to be supported, structure layout, limits on total and differential settlements, lateral deformations, lateral loads, scour, seismic and other extreme event loading conditions, and special requirements such as construction phasing and time constraints on construction. A complete knowledge of these issues is of paramount importance.
2. Evaluate the subsurface exploration and laboratory testing data. Ideally, the subsurface exploration and laboratory testing programs were performed with knowledge of the foundation loads and the needed geomaterial resistances. If the subsurface information is insufficient, perform a second subsurface exploration program, laboratory testing program, or in-situ testing program.
3. Prepare a final subsurface profile and critical cross sections. Determine subsurface layers suitable or unsuitable for spread footings, pile foundations, or drilled shaft load transfer. Also consider if ground improvement techniques could modify unsuitable layers into suitable bearing layers.
4. Determine the most feasible foundation alternatives. Both shallow foundations and deep foundations should be considered. Deep foundation alternatives include driven piles, drilled shafts, micropiles, and CFA piles. Proprietary deep foundations systems should not be excluded as they may be the most economical alternative in a given condition. Consideration should be given to the following foundation options.

Shallow Foundations:

- a. Spread footings (without ground improvement).
- b. Mat foundations.

Deep Foundations:

- a. Driven pile foundations.
 - b. Candidate pile types.
 - c. Viable pile sections.
 - d. Drilled shafts.
 - e. Micropile.
 - f. Continuous Flight Auger (CFA) piles.
5. Prepare cost estimates for technically feasible alternative foundation designs including all associated substructure and construction control method costs. The cost estimates should consider the concept of foundation support cost introduced in Section 3.4.1. The foundation support cost should include all associated temporary and permanent substructure costs required for foundation construction (e.g. sheeting or cofferdam requirements, concrete tremie seal, pile cap requirement and size), the effect of environmental or construction limitations (noise, vibration, low overhead, access restrictions), as well as any required mitigation procedures (noise shrouds, predrilling, bubble nets, etc.).
 6. Select the most appropriate foundation alternative. Generally the most economical alternative (lowest foundation support cost) should be selected and recommended. The ability of the local construction force as well as the availability of materials and equipment should also be considered.

For major projects, if the estimated costs of technically feasible foundation alternatives (during the design stage) are within 15 percent of each other, then alternate foundation designs should be considered for inclusion in the contract documents. The most economical foundation design will then be determined by construction demand and material pricing rather than subtleties in the design estimate.

3.2 FOUNDATION ALTERNATIVES

To determine the most preferred foundation alternatives, both shallow foundations and deep foundations should be considered. Table 3-2 summarizes shallow and deep foundation types and uses, as well as applicable and non-applicable subsurface conditions.

Table 3-2 Foundation Types and Typical Uses (Modified from Bowles 1977)

Foundation Type	Use	Applicable Soil Conditions	Non-suitable or Difficult Soil Conditions
Spread footing, wall footings.	Individual columns, walls, bridge piers.	Any conditions where bearing capacity is adequate for applied load. May use on single stratum; firm layer over soft layer, or weaker layer over firm layer. Check immediate, differential and consolidation settlements.	Any conditions where foundations are supported on soils subject to excessive scour or liquefaction.
Mat foundation.	Same as spread and wall footings. Very heavy column loads. Usually reduces differential settlements and total settlements.	Generally soil bearing value is less than for spread footings. Over one-half area of structure covered by individual footings. Check settlements.	Same as footings.
Driven pile foundations.	In groups to transfer heavy column and bridge loads to suitable soil and rock layers. Also to resist uplift and/or lateral loads.	Poor surface and near surface soils. Geomaterials suitable for load support 15 to 300 feet below ground surface. Check settlement and lateral deformation of pile groups.	Shallow depth to hard stratum. Sites where pile driving vibrations or heave would adversely impact adjacent facilities. Boulder fields.
Drilled shafts.	In groups to transfer heavy column loads. Mon shafts and small groups sometimes used. Cap sometimes eliminated by using drilled shafts as column extensions.	Poor surface and near surface soils. Geomaterial suitable for load support located 25 to 300 feet below ground surface.	Caving formations difficult to stabilize. Artesian conditions. Boulder fields. Contaminated soil. Areas with concrete delivery or concrete placement logistic problems.
Micropiles.	Often used for seismic retrofitting, underpinning, very difficult drilling through overburden materials, in low head room situations, and for projects with noise or vibration restrictions.	Any soil, rock, or fill conditions including areas with rubble fill, boulders, and karstic conditions.	High slenderness ratio may present buckling problems from loss of lateral support in liquefaction susceptible soils. Low lateral resistance. Offshore applications.
CFA Piles.	In groups to transfer heavy loads to suitable geomaterials. Projects with noise and vibration restrictions.	Medium to very stiff clays, cemented sands or weak limestone, residual soils, medium dense to dense sands, rock overlain by stiff or cemented deposits.	Very soft soils, loose saturated sands, hard bearing stratum overlain by soft or loose soils, karst conditions, areas with flowing water. Highly variable subsurface conditions. Conditions requiring long piles due to deep scour, liquefiable layers, or penetrating very hard strata or rock, offshore conditions.

3.2.1 Shallow Foundations

The feasibility of using spread footings for shallow foundation support should be considered in any foundation selection process. Spread footings are generally more economical than deep foundations in situations where geomaterial and loading conditions are conducive for their use. Favorable conditions include: competent soils within shallow depth; foundation width is expected to be relatively small; spread footing can be placed at an economical depth (e.g., 10-feet); quality granular fills are available (Abu-Hejleh et al. 2014). Spread footings on engineered compacted granular fills and mechanically stabilized earth (MSE) granular fills to support bridge abutments provide a satisfactory alternative to deep foundations with good performance and significant cost savings (Abu-Hejleh et al. 2014). Bridge foundations that are subject to scour, liquefaction, or large settlement, as well as those with large uplift or lateral load demand are typically not suitable for shallow foundations. Additional details on spread footings for highway bridges may be found in FHWA GEC-6, Shallow Foundations by Kimmerling (2002).

3.2.2 Shallow Foundations with Ground Improvement

In some situations, ground improvement methods can be used to improve subsurface conditions thereby allowing the use of shallow spread footing foundations. Ground improvement in conjunction with spread footings should be economically evaluated provided they meet strength and service limit state requirements as this combination may be more cost effective than deep foundation solutions. Additional information on ground improvement may be found in FHWA-NHI-06-019/020 Ground Improvement Methods (Elias et al. (2006), and at <http://www.GeoTechTools.org>.

3.2.3 Deep Foundations

Deep foundations are generally needed where the axial compression, axial tension, lateral load demand or a combination of the above cannot be satisfied by the near surface soil conditions. However, deep foundations should not be used indiscriminately for all subsurface conditions and for all structures. There are subsurface conditions where a driven pile, drilled shaft, micropile, or CFA pile may be very difficult or costly to install. Ground improvement techniques can also be used with deep foundations as an economical means to improve lateral resistance in weak surficial soils (Rollins and Brown 2011).

3.2.3.1 Driven Piles

Driven piles are the most commonly used deep foundation system for transportation projects. Piles are typically installed in groups using an impact pile driving hammer. Multiple pile types with various section properties are available to resist almost any load demand. Pile lengths for some pile types can be easily adjusted and spliced in the field to accommodate variations in subsurface conditions. Further guidance on pile selection, pile type advantages and disadvantages, as well as the best pile type for a given subsurface condition may be found in Chapter 6.

3.2.3.2 Drilled Shafts

Drilled shafts are frequently used for transportation projects with large axial compression or lateral load demand. They are installed by mechanically or percussion drilling a hole to the required depth and filling the hole with concrete. Sometimes an enlarged base or bell is formed mechanically to increase the toe bearing area. Drilling slurry and/or temporary casings can be used when the sides of the hole are unstable. Reinforcing steel is installed as a cage inserted prior to concrete placement. For complete details on drilled shafts, reference should be made to FHWA GEC-10, Drilled Shafts: Construction Procedures and LRFD Design Methods by Brown et al. (2010) and AASHTO (2014) design specifications Section 10.8.

3.2.3.3 Micropiles

Micropiles are often used for transportation projects in karst areas as well as for underpinning, seismic retrofitting, and projects with difficult drilling conditions. Micropiles are a small diameter (< 12 inches), reinforced, drilled, and grouted deep foundation element. Many different tools and installation methods are available to construct micropiles. They are often installed by rotating a casing with a cutting edge into the geomaterial or by percussion methods. Cuttings are removed with circulating drilling fluid. Reinforcing steel is then inserted and a sand-cement grout is pumped through a tremie. Pressurized two-stage grouting techniques are also used. The casing can be partially or fully withdrawn. Due to the wide variety of micropile types and construction techniques, reference should be made to FHWA-05-039, Micropile Design and Construction, Sabatini et al. (2005), and AASHTO (2014) design specifications Section 10.9 for complete details.

3.2.3.4 Continuous Flight Auger (CFA) Piles

Continuous Flight Auger (CFA) or alternatively Auger Cast-in-Place (ACIP) piles are usually installed by turning a continuous-flight hollow-stem auger into the ground to the required depth. As the auger is withdrawn, grout or concrete is pumped under pressure through the hollow stem, filling the hole from the bottom up. Vertical reinforcing steel is pushed down into the grout or concrete column before it hardens. Uplift tension reinforcing can be installed by placing a single high strength steel bar through the hollow stem of the auger before grouting. After reinforcing steel is placed, the pile head is cleaned of any lumps of soil which may have fallen from the auger. For complete details on CFA piles, reference should be made to FHWA GEC-8, Design and Construction of Continuous Flight Auger Piles by Brown et al. (2007).

3.3 ESTABLISHMENT OF A NEED FOR A DEEP FOUNDATION

The first difficult problem facing the foundation designer is to establish whether or not the site conditions dictate that a deep foundation must be used. Vesic (1977) summarized typical situations in which piles may be needed. These typical situations as well as additional uses of deep foundations are shown in Figure 3-1.

Figure 3-1(a) shows the most common case in which the upper soil strata are too compressible or too weak to support heavy vertical loads. In this case, deep foundations transfer loads to a deeper competent stratum and act as predominantly toe bearing foundations. In the absence of a competent stratum within a reasonable depth, the loads must be gradually transferred, mainly through soil resistance along the shaft, Figure 3-1(b). An important point to remember is that deep foundations transfer load through unsuitable layers to suitable layers. The foundation designer must define at what depth suitable soil layers begin in the soil profile.

Deep foundations are frequently needed because of the relative inability of shallow footings to resist inclined, lateral, or uplift loads and overturning moments or excessive deformations. Deep foundations resist uplift loads by shaft resistance, Figure 3-1(c). Lateral loads are resisted either by vertical deep foundations in bending, Figure 3-1(d), or by groups of vertical and battered piles, which combine the axial and lateral resistances of all piles in the group, Figure 3-1(e). Lateral loads from overhead highway signs and noise walls may also be resisted by groups of deep foundations, Figure 3-1(f).

Deep foundations are often required when scour around footings could cause loss of bearing capacity at shallow depths, Figure 3-1(g). In this case the deep foundations must extend below the depth of scour and develop their full nominal resistance in the support zone below the level of expected scour. FHWA scour guidelines using the Hydraulics Engineering Circular No. 18 (Arneson et al. 2012) require the geotechnical analysis of bridge foundations to be performed on the basis that all stream bed materials in the scour prism have been removed and are not available for bearing or lateral support. Costly damage and the need for future underpinning can be avoided by properly designing for scour conditions.

Liquefaction and other seismic effects on deep foundation performance must be considered for deep foundations in seismic areas. Soils subject to liquefaction in a seismic event may dictate that a deep foundation be used, Figure 3-1(h). Seismic events can also induce significant lateral loads to deep foundations. During a seismic event, liquefaction susceptible soils offer less lateral resistance, reduced shaft resistance, and can add drag load to a deep foundation.

Deep foundations are often used as fender systems to protect bridge piers from vessel impact, Figure 3-1(i). Fender system sizes and group configurations vary depending upon the magnitude of vessel impact forces to be resisted. In some cases, vessel impact loads must be resisted by the bridge pier foundation elements. Single deep foundations may also be used to support navigation aids.

In urban areas, deep foundations may occasionally be needed to support structures adjacent to locations where future excavations are planned or could occur, as in Figure 3-1(j). Use of shallow foundations in these situations could require future underpinning in conjunction with adjacent construction.

Deep foundations are also used in areas of expansive or collapsible soils to resist undesirable seasonal movements of the foundations. Under such conditions, deep foundations are designed to transfer foundation loads, including uplift or downdrag, to a level unaffected by seasonal moisture movements, Figure 3-1(k).

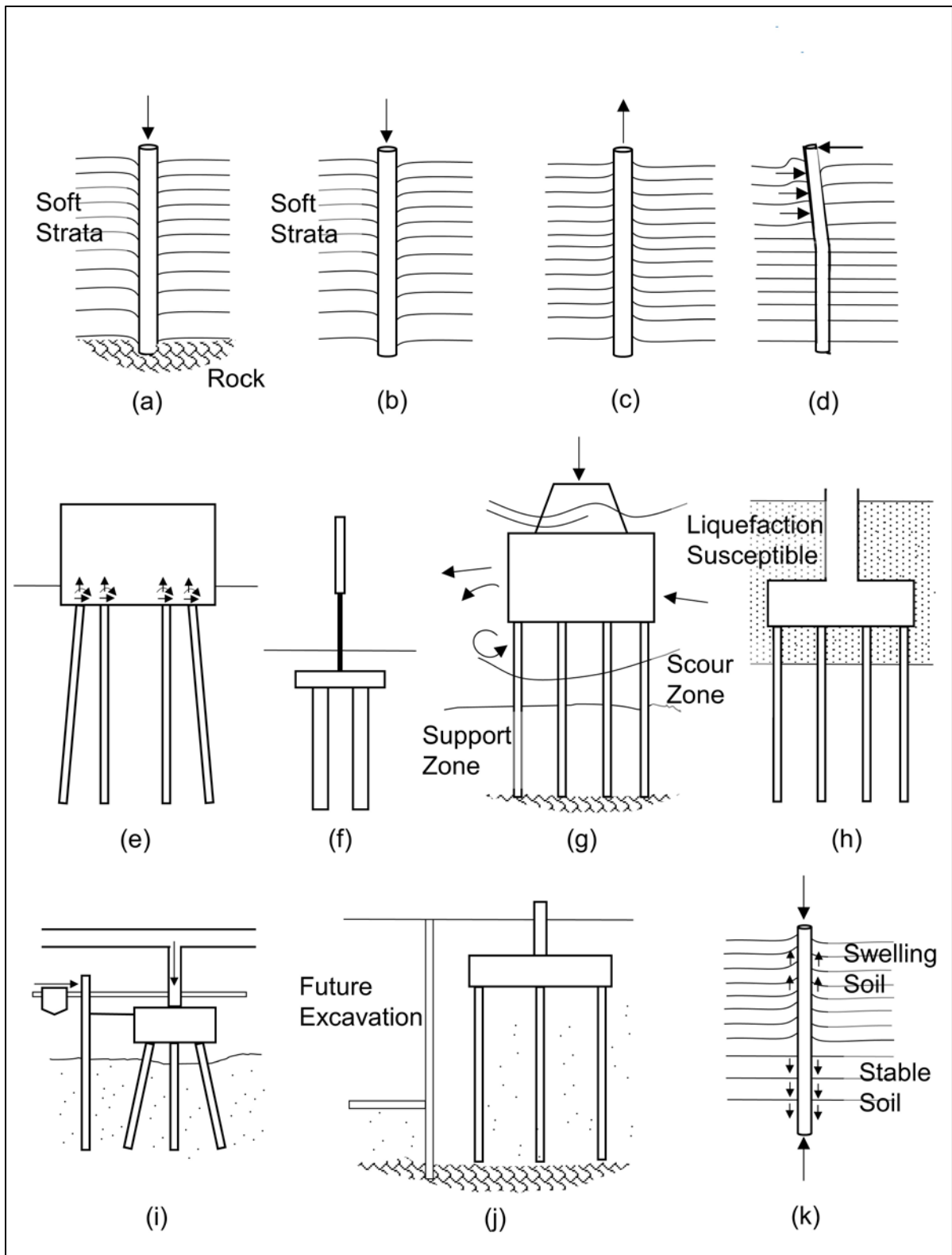


Figure 3-1 Situations in which deep foundations may be needed (modified from Vesic 1977).

3.4 ECONOMIC ASPECTS OF FOUNDATION SELECTION

In many instances, either a shallow or deep foundation alternative is technically feasible. Feasible conditions for the use of a shallow spread footing foundation are summarized in Abu-Hejleh et al. (2014). Under these circumstances, an evaluation of the shallow foundation should include; 1) the dimensions and depth of shallow footings based on bearing resistance, 2) the magnitude and time rate of settlement under anticipated loads, and 3) detailed cost analysis including such factors as need for cofferdams, overall substructure cost, dewatering and foundation seals, construction time, construction risk, claims potential, and other project constraints. A comparative analysis of feasible deep foundation alternatives should also be performed. The cost analysis of feasible alternatives generally has a significant role in final selection of the foundation type.

Because this manual deals only with driven pile foundations, other types of foundations will not be discussed further.

3.4.1 Foundation Support Cost

A rational comparison of technically viable foundation systems can be made based on the foundation support cost of each candidate foundation type. The foundation support cost is defined as the total cost of the foundation divided by the factored load the foundation supports in tons or kips. Factored loads are used since resistance factors vary by foundation type. For driven pile foundation projects, the total foundation support cost where axial loading governs can be separated into three major components; the pile support cost, the pile cap support cost, and the construction control method support cost. The total foundation cost should also include all costs associated with a given foundation system including the need for excavation or retention systems, dewatering, pile caps and cap size, environmental restrictions on construction activities, etc. A detailed discussion on foundation support cost applications to driven pile design is presented in Komurka (2015).

It should be noted that the above discussion assumes that the axial compression load controls the foundation design. On projects where the axial tension load, lateral load, or combined axial and lateral loads govern the foundation design, the support cost concept can still be applied. In those situations, the cost per ton of factored uplift load or factored lateral load should be used in the selection process.

3.4.1.1 Cost Optimization Example

Figure 3-2 presents a layered soil profile that will be used to illustrate the cost optimization process. The first step in the cost optimization of a candidate pile section is to perform a static analysis to determine its nominal geotechnical resistance versus the pile penetration depth. Static analysis methods are described in greater detail in Chapter 7. A static analysis was performed for an HP 14x117 H-pile using the FHWA method in the APILE computer program. The results of that static analysis are presented in Figure 3-2, and include the nominal geotechnical resistance which is comprised of the nominal shaft resistance and the nominal toe resistance at a given pile penetration depth.

Several possible pile penetration termination depths and associated nominal resistances are apparent in Figure 3-2. Piles could be driven into the medium dense sand layer at a depth of 60 feet for a nominal resistance of 150 kips; seated into the medium dense sand layer near a depth of 70 feet for 300 kips; driven through the medium dense sand layer and underlying stiff clay layer and into the extremely dense sand layer at 110 feet for 1000 kips; or driven to bedrock near 118 feet for 1700 kips. A rational economic assessment of these potential pile termination depths and nominal resistances is needed for cost effective design. For most pile types, the pile cost can usually be assumed as linear with depth based on unit price as illustrated in Figure 3-3. However, this may not be true for very long concrete piles or long, large section steel piles. These exceptions may require the cost analysis to reflect special transportation, handling, or splicing costs for the concrete piles or extra splice time and cost for steel piles.

Figure 3-4 presents a plot of nominal resistance pile support cost versus pile penetration depth. This figure is obtained by dividing the pile cost at a given depth from Figure 3-3 by the nominal resistance at that same depth from Figure 3-2. Note that Figure 3-4 includes the nominal resistance versus depth in addition to the pile support cost. For the H-pile section evaluated, a general conclusion can quickly be reached; piles penetrating to more than 60 feet will be more cost effective than shorter piles. At the top of the sand layer near 60 feet, the pile has a nominal resistance of 150 kips and a nominal resistance support cost of \$39 per kip. Near the middle of this sand layer at a penetration depth of 70 feet, the pile has a nominal resistance of 300 kips and a much lower nominal resistance support cost of \$19 per kip. The nominal resistance pile support cost drops further to \$9 per kip at a depth of 110 feet and a nominal resistance of 1000 kips. Finally, the nominal resistance pile support cost continues to decrease to \$5.50 per kip at a depth of 118 feet and a nominal resistance of 1722 kips.

An HP 14x117 H-pile section with a yield strength of 50 ksi has a nominal structural resistance of 1720 kips when fully embedded. An example detailing the calculation of the nominal structural resistance of an H-pile is provided in Section 8.5.3. The maximum factored load that can be placed on the pile is the lesser of the factored structural resistance or the factored geotechnical resistance. For the H-pile section used, the maximum factored structural resistance is 1032 kips when good driving conditions are anticipated based on the subsurface conditions, pile damage is unlikely, and a driving shoe is therefore not required. The maximum factored structural resistance decreases to 860 kips when severe driving conditions are anticipated based on the subsurface conditions, damage is possible, and a driving shoe is required. Figure 3-5 includes the nominal and factored structural resistances in the strength limit state under axial compression loading. The structural resistance for all pile types is discussed in Chapter 8.

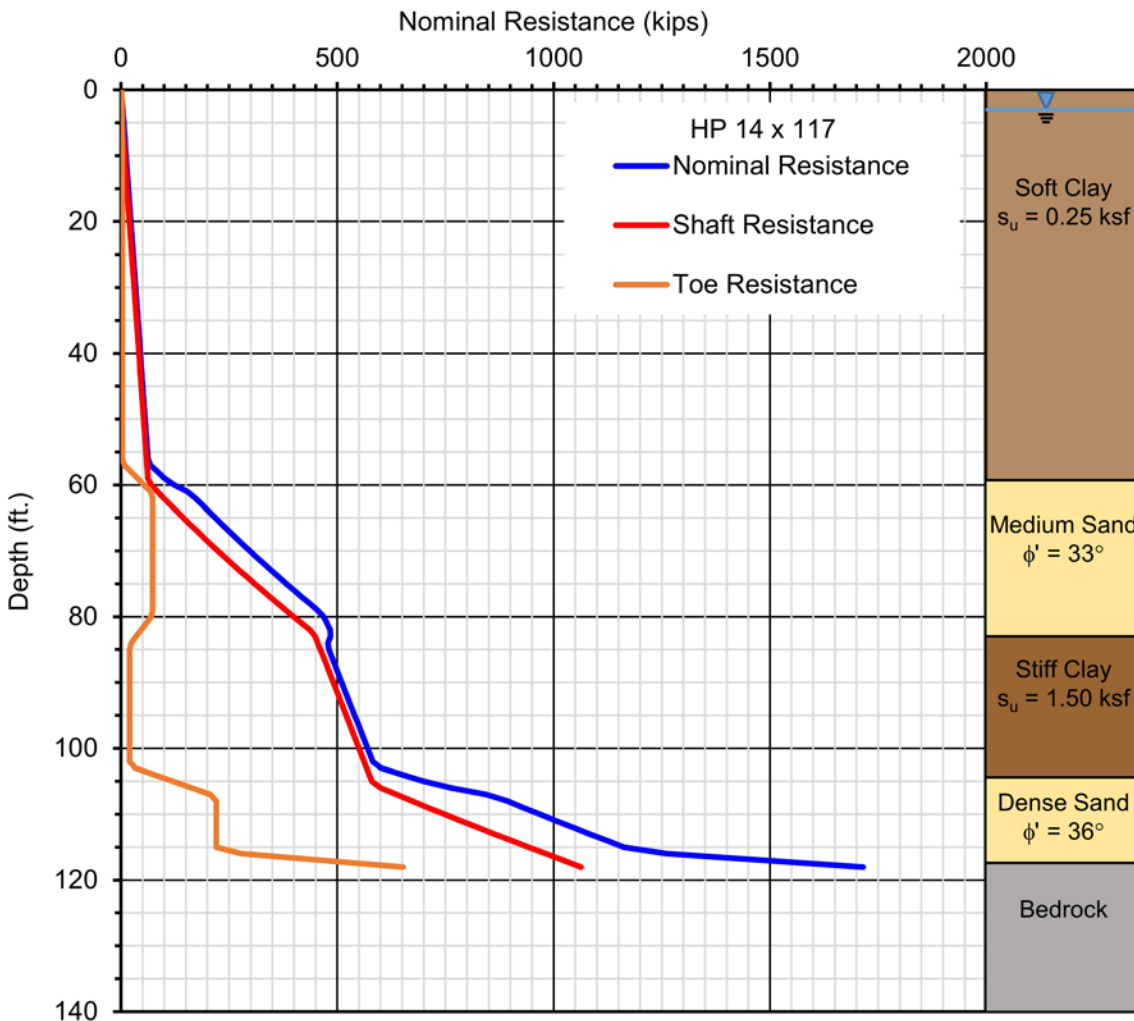


Figure 3-2 Soil profile and nominal geotechnical resistances versus depth.



Figure 3-3 Pile cost versus pile penetration depth.

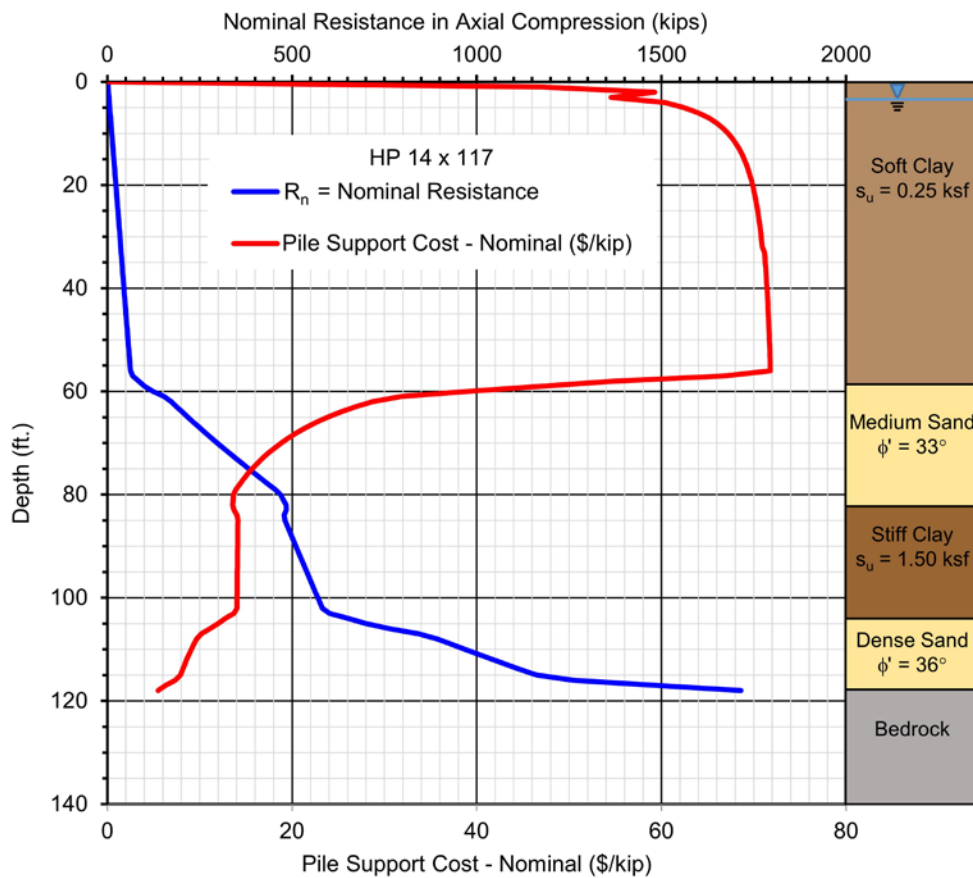


Figure 3-4 Nominal resistance of pile support cost versus penetration depth.

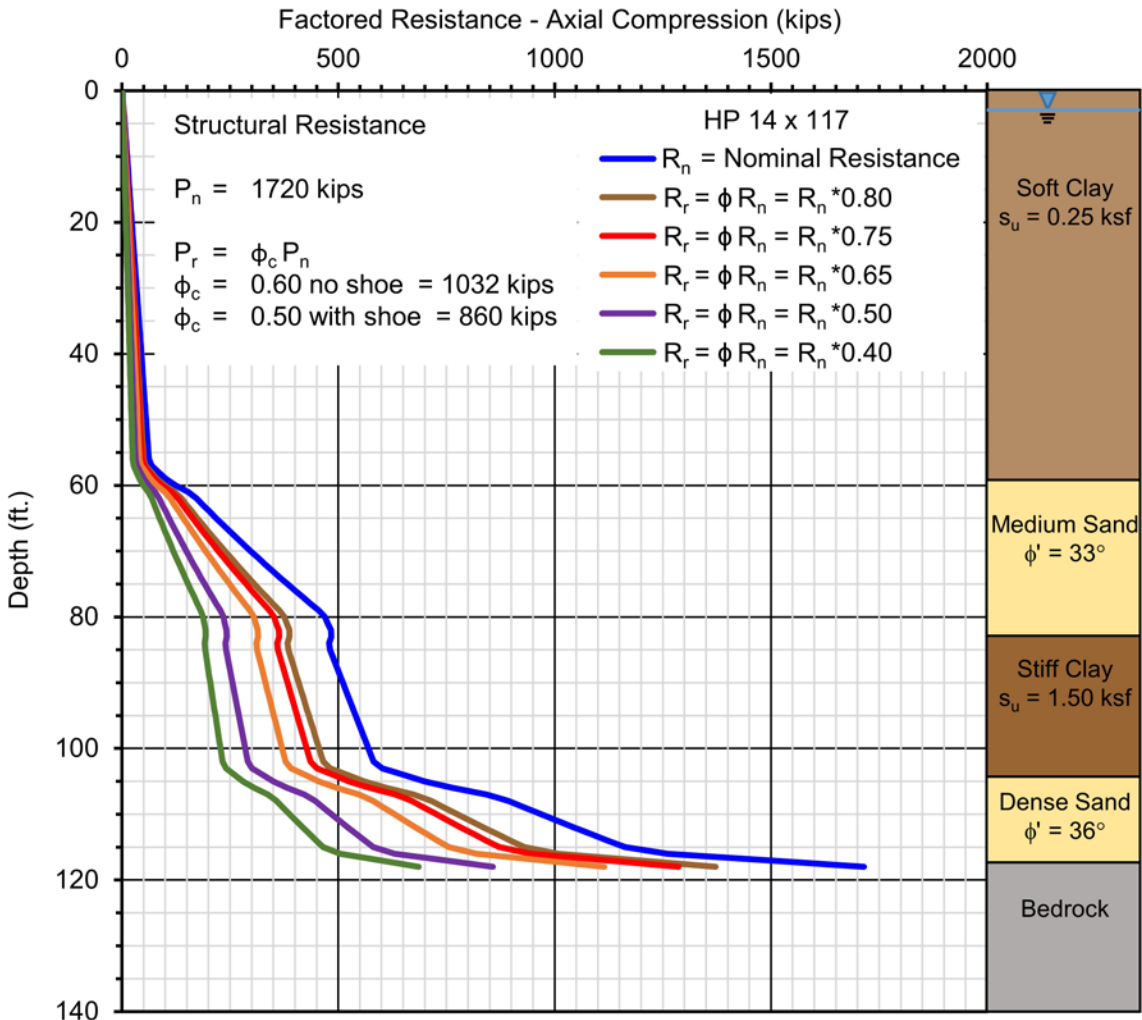


Figure 3-5 Nominal and factored resistances for axial compression loads.

Figure 3-5 also includes the nominal and factored geotechnical resistances in the strength limit state under axial compression loading. Geotechnical aspects of limit state design are covered in Chapter 7. The factored geotechnical resistances versus pile penetration depth shown in Figure 3-5 are based on construction control with the following field verification methods:

$\phi_{dyn} = 0.80$ Driving criteria established by successful static load test of at least one pile per site condition and dynamic testing with signal matching of at least two piles per site condition, but no less than 2% of production piles.

$\phi_{dyn} = 0.75$ Driving criteria established by successful static load test of at least one pile per site condition without dynamic testing or by dynamic testing with signal matching on 100% of the production piles.

$\phi_{dyn} = 0.65$ Driving criteria established by dynamic testing with signal matching of at least two piles per site condition, but no less than 2% of production piles.

$\phi_{dyn} = 0.50$ Driving criteria established by wave equation analysis based on end of drive conditions only.

$\phi_{dyn} = 0.40$ Driving criteria established by FHWA modified Gates dynamic formula based on end of drive conditions only.

The required nominal driving resistance, R_{ndr} , needed to utilize the full factored structural resistance, P_r , of either 1032 or 860 kips with a given resistance verification field method is provided in Table 3-3. The required nominal driving resistance for full utilization of the factored structural resistance can be calculated by dividing the factored structural resistance by the resistance factor of the field verification method, ϕ_{dyn} .

The estimated pile length for the nominal driving resistance, R_{ndr} , can then be determined from Figure 3-5 by the depth where the nominal geotechnical resistance, R_n equals the nominal driving resistance value for the field method. The abbreviations used in the table for the field verification methods are as described above with SLT for static load test, DLT for dynamic load test, WEA for wave equation analysis and DF for dynamic formula. Note that a drivability strength limit check will preclude use of the maximum factored structural resistance, P_r in some cases due to the nominal driving resistance, R_{ndr} , required by that field method.

Table 3-3 Pile Length Estimates Based on Field Methods and Factored Resistances

Field Method	ϕ_{dyn}	R_{ndr} $P_r = 1032$ kips	Estimated Length	R_{ndr} $P_r = 860$ kips	Estimated Length
SLT & 2% DLT	0.80	1290 kips	116 ft	1075 kips	113 ft
SLT or 100% DLT	0.75	1376 kips	117 ft	1147 kips	115 ft
2% DLT	0.65	1588 kips	118 ft	1323 kips	117 ft
WEA	0.50	2064 kips	118 ft+ Rock	1720 kips	118 ft
FHWA Gates DF	0.40	2580 kips	118 ft+ Rock	2150 kips	118 ft+ Rock

Figure 3-5 also illustrates the benefit of using a more reliable field verification method for piles terminated in the geomaterials above bedrock. If an HP 14x73 section is chosen for this subsurface condition instead of the HP 14x117 section, the maximum factored structural resistance for a fully embedded HP 14x73 section in severe driving conditions is 520 kips. For illustrative purposes, the static analysis

results are assumed unchanged for a HP 14x73 section compared to the HP 14x117 section based on roughly the same pile perimeter and the same plugged pile toe area. The estimated pile length from Figure 3-5 to geotechnically utilize the maximum factored structured resistance is 104 feet for field verification with a static load test and dynamic testing ($\phi_{dyn} = 0.80$) compared to an estimated length of 116 feet for field verification with the modified Gates dynamic formula ($\phi_{dyn} = 0.40$).

The results of the static analysis on the HP 14x117 H-pile section can be also used to evaluate the pile penetration requirements for the axial tension load demand. The shaft resistance from Figure 3-2 is presented once again in Figure 3-6 and labeled R_s for the nominal shaft resistance. The pile cost at a given depth from Figure 3-3 can be divided by the nominal shaft resistance at that same depth to obtain a plot of the pile support cost in dollars per kip of nominal uplift resistance versus pile penetration depth. Figure 3-6 presents plots of both the nominal uplift resistance pile support cost versus depth and the nominal uplift resistance versus depth. Two distinct plateaus in the pile support cost for tension loading are apparent, \$90 to \$100 per kip of nominal uplift resistance above 60 feet and \$15 to \$25 per kip of nominal uplift resistance below 70 feet.

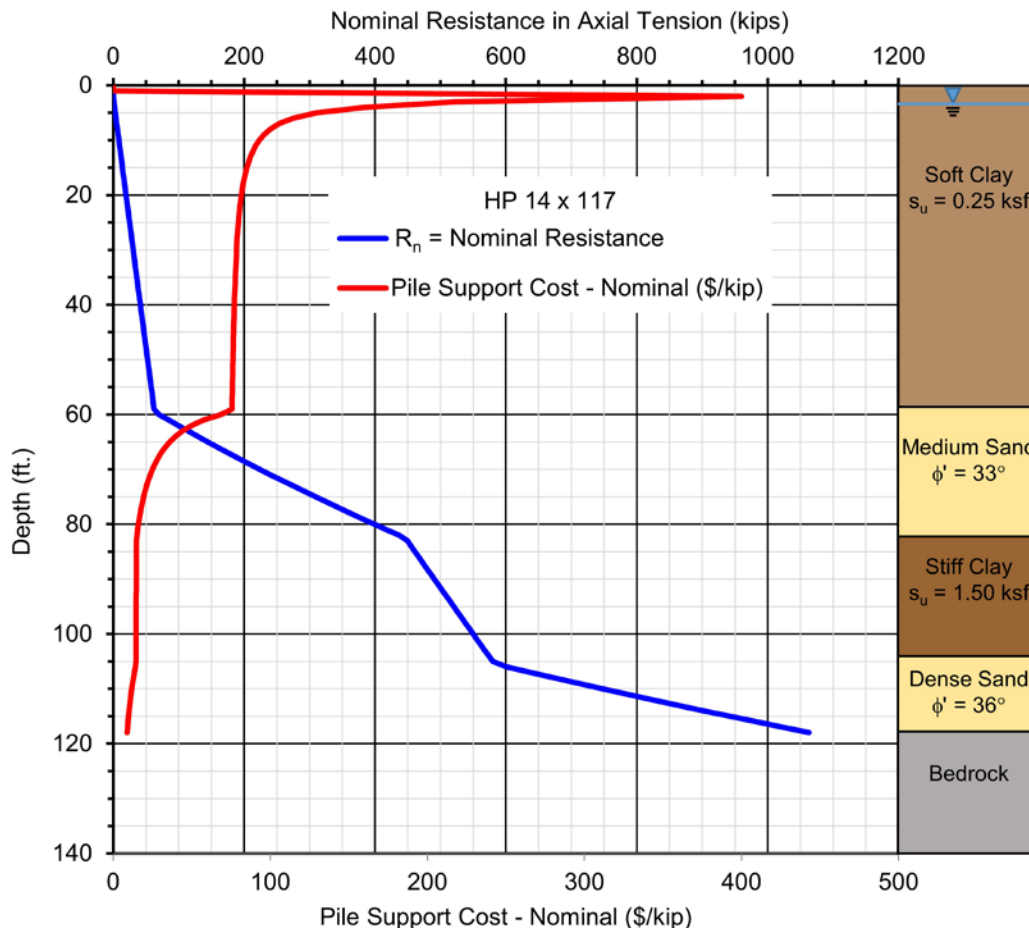


Figure 3-6 Nominal shaft resistance and pile support cost.

Figure 3-7 presents the nominal shaft resistance, R_s , and the factored axial tension resistance versus depth, R_r . In Figure 3-7, the nominal shaft resistance, R_s , is multiplied by the uplift resistance factors, ϕ_{up} , of 0.60 if the uplift resistance is determined with a static load test, 0.50 if obtained from a dynamic load test with signal matching, and 0.25 in clay layers and 0.35 in sand layers for uplift resistance determined by the α -method and Nordlund static analysis methods.

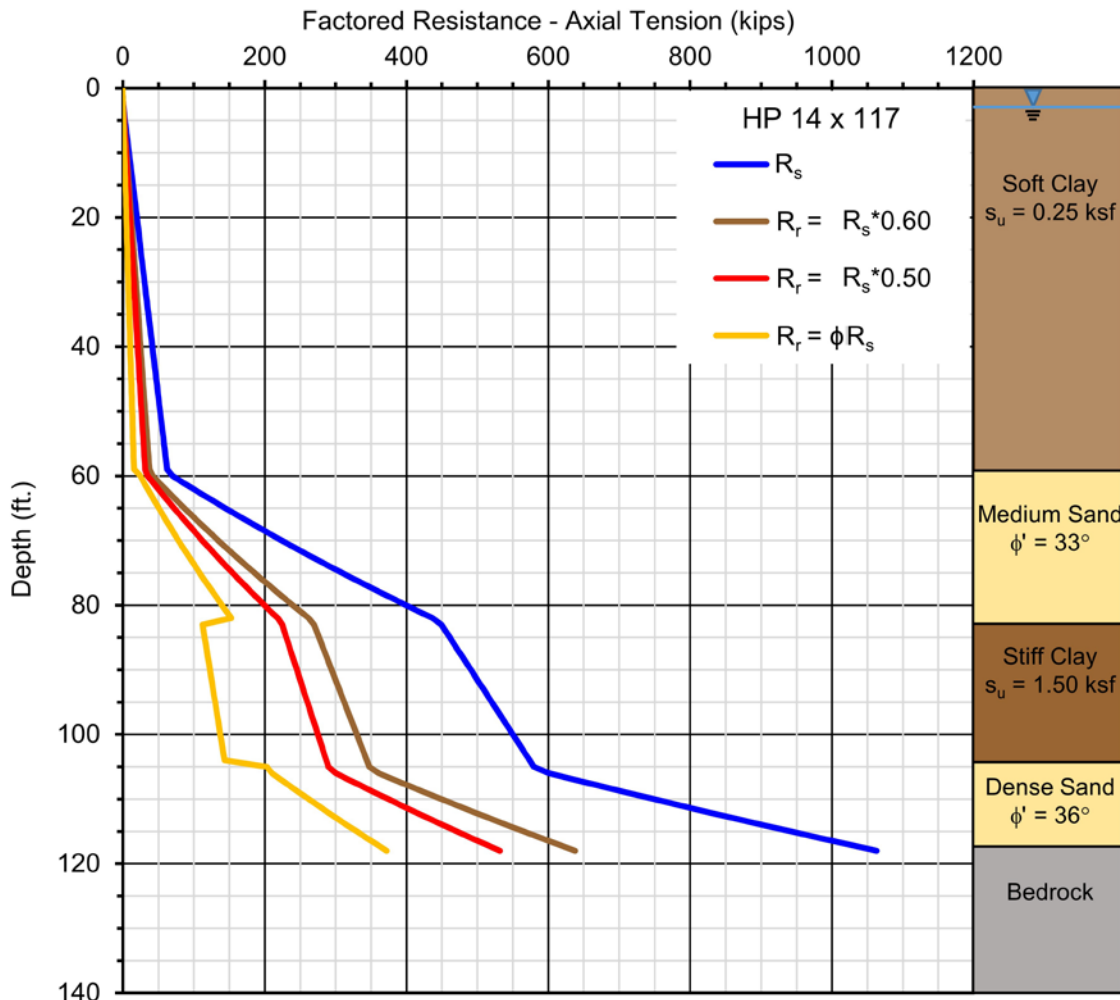


Figure 3-7 Nominal and factored resistances for axial tension loads.

3.5 OTHER CONSIDERATIONS

In many instances, several driven pile alternatives may be technically feasible for satisfying the project load and deformation requirements. Other considerations such as constructability, noise, vibrations, effects on nearby structures and utilities, durability, long term maintenance, and other considerations should also be evaluated to determine the most appropriate driven pile selection.

3.5.1 Constructability

Constructability should also be assessed during the design stage with any construction considerations factored into the pile selection and final design. Drivability is a key component of constructability and must be evaluated. The chosen pile section must be capable of being installed to the specified minimum penetration depth dictated by scour, extreme event or deformation considerations. The design and drivability assessment should consider the presence of any hard layers that must be penetrated to meet design requirements that could necessitate use of pile penetration aids such as predrilling or jetting. Constructability considerations and drivability analysis should also consider potential densification effects of soils constrained within cofferdams or soils that may densify from driving large pile groups. Similarly, the influence of soil heave on adjacent structures, utilities, or other piles from driving displacement piles in a cohesive deposit should be considered along with the need for pile penetration aids to mitigate the heave potential, if present. The cost of a driven pile foundation will increase on projects with limitations or restrictions on head room, work space, and construction access. Similarly, environmental restrictions on vibrations, noise, work hours, marine mammals, and fish will likely increase foundation costs.

3.5.2 Consideration of Pile Driving Noise

Driven piles are installed by impact hammers. Noise levels associated with typical impact pile driving activities depend upon the hammer and pile type used. Noise from impact pile driving operations typically ranges from around 80 to 135 dBa. If local ordinances dictate allowable noise levels at or below this level, some driving equipment may not meet these requirements. Manufacturers of a few diesel and hydraulic hammers can provide optional noise suppression devices that may reduce the pile driving generated noise by about 10 dBa. Independently manufactured devices are also available. Additional information on noise suppression equipment is presented in Chapter 15.

In noise sensitive areas, the foundation designer should review any noise ordinances to determine if pile driving noise suppression devices would be necessary and if so, the impact this may have on the contractor's equipment selection and productivity. If limits on work hours, pile equipment type, or noise suppression equipment are required, costs associated with these limitations should be considered in the foundation selection process.

3.5.3 Pile Driving Induced Vibrations

Since piles are driven by impact or vibratory hammers, ground vibrations of some magnitude are always induced into the surrounding soils during pile installation. In many situations these vibrations do not pose a significant threat or risk to structures. The vibrations created by pile driving depend on the soil type, pile type and section, pile hammer, installation techniques, penetration resistance, pile toe penetration depth, and distance from the pile. Therefore, the distance from a pile driving operation where these variables combine to cause vibration levels that are a threat to structures, facility operations, or utilities varies.

The ground vibration level where vibration induced soil densification and settlement or structural damage from direct vibrations may occur depends upon the vibration magnitude, frequency, and number of cycles as well as the type and condition of the existing structure or facility. In addition, nearby structures may house sensitive equipment whose operation may be adversely affected by pile driving vibrations. Establishing appropriate vibration limits for sensitive equipment can be difficult, which makes identifying and addressing such installations all the more important.

For pile driving projects with structures, facilities, or utilities within a zone potentially affected by pile driving vibrations, careful evaluation of the pile driving procedures and/or monitoring of ground vibrations during pile installations should be performed by personnel with vibration monitoring and mitigation experience. Even if a designer is satisfied the pile driving vibrations pose no threat to structures or equipment, advance notification to neighbors of pile driving activities, pre-construction condition surveys, and vibration monitoring plans promotes a “good neighbor” policy which can reduce the risk of claims.

Potential damage to nearby structures can result from two mechanisms:

1. Vibrations induced soil densification and settlement.
2. The effects of vibrations on the structure itself.

Lacy and Gould (1985) found that vibratory induced soil densification settlements and resulting structural damage can occur at ground surface peak particle velocities much less than 2 inches per second and that soil gradation is an important factor in this phenomenon. They reported that significant vibration induced settlements occurred at some sites with peak particle velocities measured on the ground surface as low as 0.1 to 0.2 inches per second. Sands particularly susceptible to vibratory

densification were late Pleistocene deposits with uniformity coefficients of up to 4 or 5 and relative densities of up to 50 or 55%.

Wiss (1981) reported typically recommended "safe" ground vibration levels for structures between 0.5 and 4 inches per second. In codes, such as NFPA 495 (2013), the maximum allowable particle velocity to prevent the onset or propagation of hairline cracks in plaster or drywall is a function of the vibration frequency. For example, a particle velocity of 1 inch per second at 30 Hz would be below NFPA 495 code limits but would be above code limits if the vibration frequency were 10 Hz.

Bay (2003) summarized relationships between peak particle velocity and the distance from the pile as a function of rated hammer energy. These results were plotted against typical damage thresholds for various types of structures. Charts for Class II and Class III soils were provided and are reproduced in Figure 3-8. Class II soils were defined as competent soils with SPT-N values of 5 to 15 blows per foot. Class III soils are hard soils with SPT N values of 15 to 50 blows per foot. Bay noted that stiff soil crusts near the ground surface can significantly increase the vibration levels from those noted in the charts and that other factors that can influence the vibration levels include nearby deep excavations, rock outcrops, and shallow bedrock. Soil-structure interaction should also be considered in assessing vibration levels and damage potential. Therefore, while informative, these charts should not be used to eliminate vibration monitoring.

If the potential for damaging ground vibrations is high, pile installation techniques should be specified to reduce vibration levels. Specifications could require predrilling or jetting, cutoff trenches, as well as use of a different pile type or use of a specific type of pile hammer. Since predrilling and jetting influence compression, uplift, and lateral pile capacities, a determination of probable vibration levels and remediation measures should be evaluated in the design stage. A case history illustrating how changing pile installation procedures reduced vibratory induced soil densification and off-site settlement damage was reported by Lukas and Gill (1992).

NCHRP Project 20-5, Dynamic Effects of Pile Installations on Adjacent Structures, by Woods (1997), provides a synthesis of pile driving induced vibrations and typical mitigation practices. This synthesis noted that vibration problem management is the key to minimizing vibration damage, delays and claims. Two important elements in vibration management are a vibration specification with limits on the frequency dependent maximum peak particle velocity and a predriving survey of surrounding structures. An example vibration specification that details the requirements of a preconstruction survey as well as particle velocity controls is included in the NCHRP

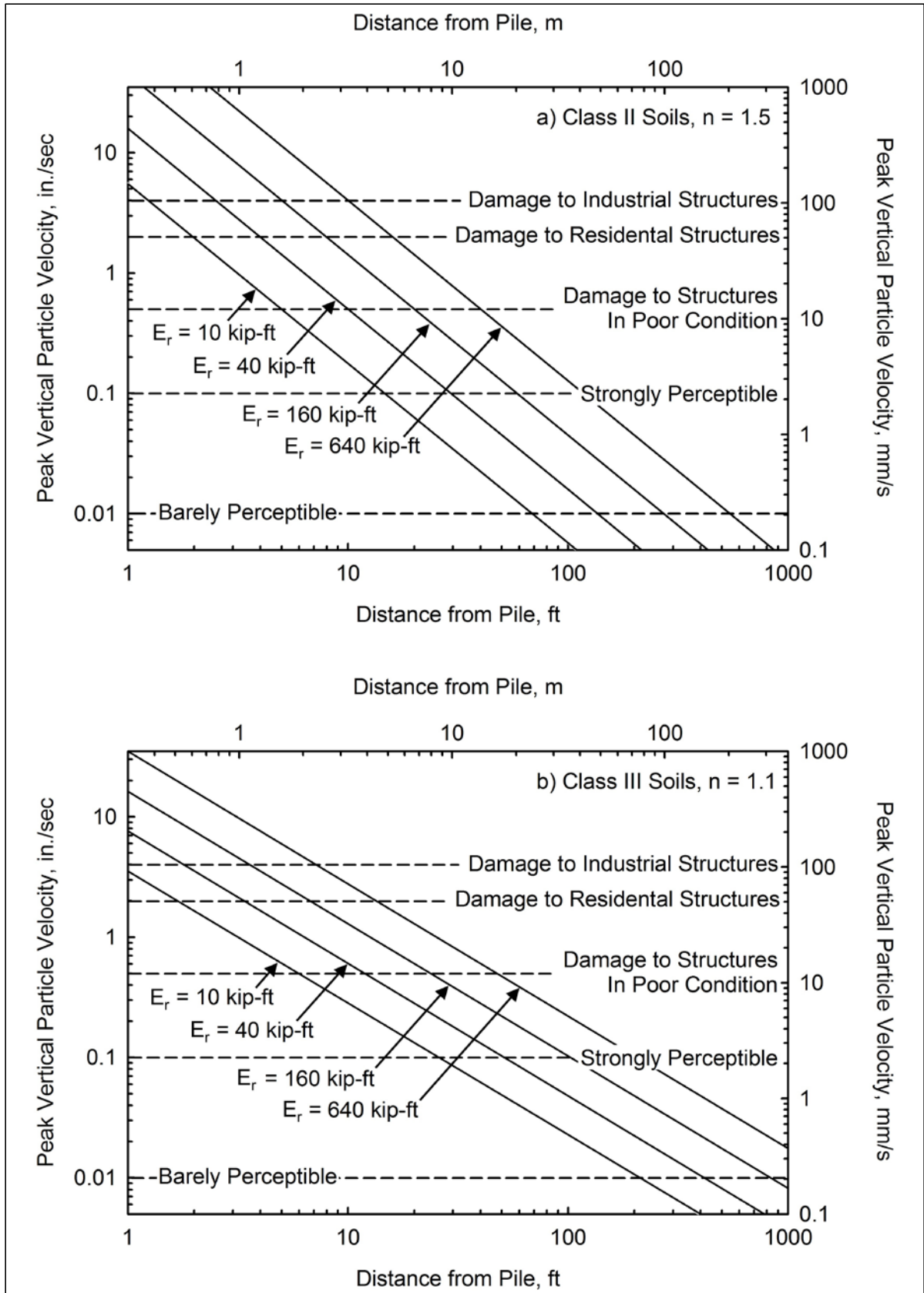


Figure 3-8 Predicted vibration levels for class II and class III soils (after Bay 2003).

synthesis. The predriving survey needs to document conditions within the potential effected area. Woods reported that vibration damage is not likely to occur at a distance from a driven pile of 50 feet for piles 50 feet long or less, or at a distance greater than one pile length away from driving for piles longer than 50 feet.

Piles with low impedances, EA/C , tend to transmit the hammer energy to the soils along the pile shaft and thus increase ground vibrations, whereas piles with higher impedances tend to more effectively transmit the hammer energy to the pile toe resulting in lower ground vibration levels (Woods 1997; Massarsch and Fellenius 2008). Hence, selection of a stiffer pile section at sites where vibrations are a concern may help reduce vibration problems.

Massarsch and Fellenius (2014) describe ground vibration effects on soil settlement. In loose sands and silts, vibratory densification beneath adjacent structures can occur, therefore causing deformation of the adjacent foundation. As discussed, pile dimensions influence the area affected by ground vibrations. Furthermore they propose that settlement occurs in an inverted 2(V):1(H) triangular region around the pile as depicted in Figure 3-9. Maximum settlement adjacent to the pile and average settlement within a distance of $3b + D/2$ from the pile are estimated using Equations 3-1 and 3-2. A compression factor is applied based on in-situ soil density and vibration magnitude, as shown in Table 3-4 for sands.

Maximum settlement	$S_{\max} = \alpha(D + 6b)$	Eq. 3-1
--------------------	-----------------------------	---------

Average settlement	$S_{\text{avg}} = \frac{\alpha(D + 3b)}{3}$	Eq. 3-2
--------------------	---	---------

Where:

- α = compression factor.
- D = pile embedded length (feet).
- b = pile diameter or width (feet).

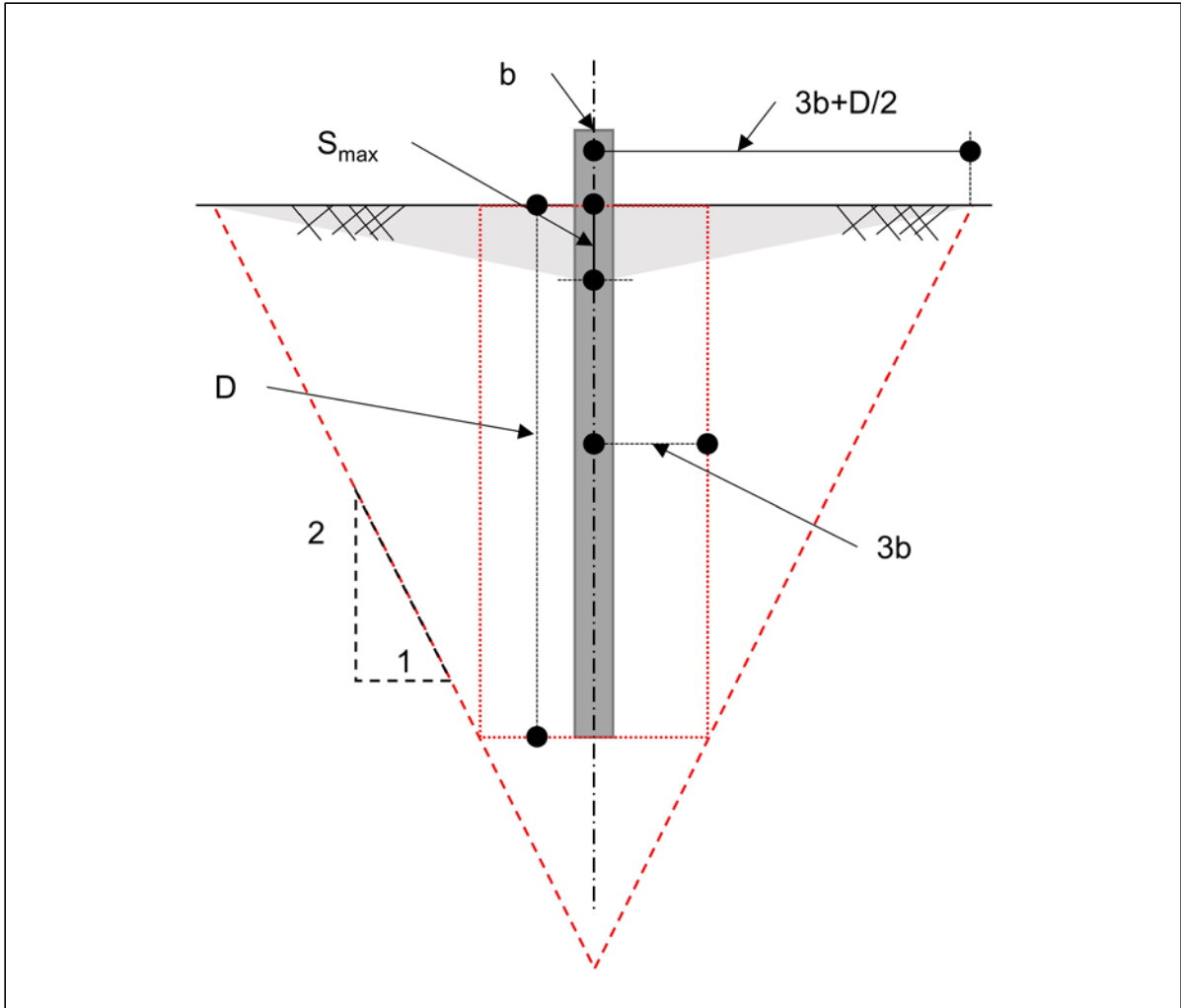


Figure 3-9 Settlement area and magnitude around a pile in homogeneous sand deposit (after Massarsch and Fellenius 2014).

Table 3-4 Compression Factor, α , for Sand Based on Soil Density and Level of Driving Energy (after Massarsch and Fellenius 2014)

Soil Density	Low Ground Vibration	Medium Ground Vibration	High Ground Vibration
Very Loose	0.02	0.03	0.04
Loose	0.01	0.02	0.03
Medium	0.005	0.01	0.02
Dense	0.00	0.005	0.01
Very Dense	0.00	0.00	0.005

The Pile Driving Contractors Association (2015) while working with The Citadel and WPC has a pile driving vibration database with 23 case histories and over 1800 individual pile-ground vibration measurements. Data has been submitted from a number of design and testing firms, with the goal of allowing contractors and designers to make reasonable assessments of the potential vibration effects from driven pile installations. This database should only be used for general guidance as differing site conditions, construction equipment and installation techniques may not be applicable in each unique situation.

3.5.4 Condition Surveys and Vibration Monitoring of Adjacent Facilities

Many projects are built in populated urban areas where existing condition surveys and vibration monitoring programs are warranted. Prior to starting construction, the internal and external condition of structures potentially affected by the construction activity should be documented using photos and videos. The condition of any existing cracks should be documented and crack monitors installed as needed. This documentation provides a preconstruction baseline of the existing conditions that can later be compared to any damage claims should they occur. Following construction, a similar survey should be performed with photos to document the change, if any, in the existing structures. Condition surveys should be performed using film rather than digital photography should damage claims be made.

The distance that should be surveyed on pile driving projects depends on the soil conditions, the pile type, the pile driving equipment, and the pile driving procedures. Many states have adopted a survey distance based on the rated pile hammer energy. Others agencies have policies based solely on the distance away from the pile driving operation. For most routine cases, a preconstruction and post construction survey along with a vibration monitoring program that documents conditions within 200 feet of the pile driving operation should be sufficient. However, this distance may need to be extended to as much as 500 feet for older structures, structures or utilities in poor condition, or highly vibration sensitive equipment.

3.5.5 Durability Considerations

The durability of a pile foundation can be defined by how long it performs satisfactorily, without unforeseen high maintenance costs relative to the foundations expected service life. AASHTO has mandated a design life of 75 years for new ordinary bridges. Complex major bridge structures may have a design life of 100 years. Hence, structure foundation durability over the design life is an important consideration. In general, driven piles have proved very durable in most

environments. However, environments exist for driven piles as well as any other deep foundation type where durability is an important design consideration to satisfy design life requirements.

In 2013, a pier supported on H-piles at the Leo Frigo bridge carrying I-43 over the Fox River in Green Bay, WI settled 2 feet during the night. The sudden settlement of the 32 year old structure resulted from severe corrosion and the resultant buckling and shearing of the foundation H-piles. Figure 3-10 illustrates the corrosion of the foundation piles uncovered at the pier location during the post event investigation. In the final investigation report on the event by Michael Baker, Jr. Inc., (2015) the corrosion and deterioration was attributed to a highly unusual set of occurrences at the pier location. Fill materials included the presence of porous, industrial fly ash in contact with the H-piles. The porous material permitted oxygen access to the piles. Also the fill material contained high amounts of sulfates and the water and soil surrounding the pile section contained high concentrations of chlorides. This unusual set of conditions created a highly aggressive environment for steel piles.



Figure 3-10 Corrosion and resulting buckling of foundation pile (courtesy Wisconsin Department of Transportation).

Gu et al. (2015) reported on the results of a corrosion study performed to evaluate the reuse of 34 year old H-pile foundations. The original project was for the Girard Avenue Bridge in Philadelphia, PA and piles were installed through a cinder ash fill located at the water table in close proximity to a tidal river. This study found that the piles had a 12% loss in section over their 34 year old life. This site specific corrosion rate was then used to assess future section loss over the rehabilitated structure life for both existing piles that were reused as well as new piles. The section loss rate was also used to evaluate the nominal pile resistance under axial and lateral loading. It was also noted that site specific corrosion rate of 0.0015 inches/year was less than published rates. Section 6.13 provides details on steel pile protection measures and design considerations for durability in aggressive environments.



Figure 3-11 Concrete pile damage from corrosion effects on concrete pile reinforcement (courtesy of Moser 2011).



Figure 3-12 Concrete surface abrasion and deterioration in tidal zone (courtesy of Moser 2011).

The durability of concrete piles should also be evaluated during design so that the foundation satisfies the target design life. Concrete piles can deteriorate due to chloride intrusion and resulting reinforcement and prestressing strand corrosion. Moser et al. (2011) noted the three main factors contributing to concrete deterioration in coastal structures include the high chloride content in seawater, the potential for high temperature and relative humidity, and the cyclic wetting due to tidal and splash action. Figure 3-11 shows two concrete piles with severe damage and cracking due to corrosion of the reinforcement steel. Abrasion of concrete piles in intertidal zone, as depicted in Figure 3-12, can also accelerate deterioration. Concrete abrasion can also occur at the mudline due to littoral drift of bottom sediments. Moser (2011) reported that some prestressed concrete piles in coastal Georgia have severe corrosion damage in the splash zone after less than 25 years of service which is well under the target design life.

Holland et al (2014) summarized multiple deterioration mechanisms affecting the concrete piles on a 38 year old I-95 bridge over Tuttle Creek. Their forensic investigation determined damage occurred from chloride-induced corrosion, severe deterioration of concrete from sulfate attack, and coarse aggregate attack from Cliona boring sponges.

To increase concrete pile durability in aggressive environments, high performance concrete mixes are being design and studied. The dense, impermeable, concrete that results with high performance concrete mixes should better protect reinforcement against the ingress of chlorides, sulfates, and seawater, as well as resist freeze/thaw and chemical attacks.

Timber piles also have durability considerations. Bigelow et al. (2007) evaluated several timber pile supported bridges in Iowa as part of a structure life assessment. Figure 3-13 illustrates the durability issues they documented as a result of a break down in the preservative barrier including a) mechanical damage, b) abrasion or debris damage, c) fire damage, and d) weathering. One of the most common durability issues occurred on piles in the stream channel as abrasion or debris damage from floating debris and/or ice. The study found that creosote treated timber piles up and away from the stream channel lasted 60 to 70 or more years and those in the stream channel have a life expectancy of 40 to 50 years.



Figure 3-13 Examples of timber pile deterioration (courtesy Bridge Engineering Center at Iowa State University).

3.6 UNANTICIPATED OCCURRENCES

The long term performance of a foundation is generally assessed by its total and differential settlement within and between substructure locations. Unanticipated occurrences can result from outside influences, such as a fill stockpile can affect a foundation's long term performance as shown in Figure 3-14 and Figure 3-15. Construction of a new pile foundation can also result in unanticipated outside influences as described in Section 3.6.2.

3.6.1 Fill Stockpile

During the summer of 2104, a portion of the 40 year old elevated section of I-495 near Wilmington, Delaware was noticed to have substantially tilted over a relatively short time period. The tops of some of the 50 feet tall columns supporting the elevated roadway were noted to be almost 2 feet out of alignment from their base as shown in Figure 3-14. Engineers determined a roughly 50,000 ton stockpile of fill material had been placed near the four affected piers. The weight of this fill had caused lateral movement of soil beneath the bridge, deformed the H-piles supporting the piers, and cracked the pile caps as illustrated in Figure 3-15. This caused four of the piers supporting the elevated roadway to tilt. In the above case, the structure was performing as expected based on its previous inspection report until being affected by the stockpile of fill material.

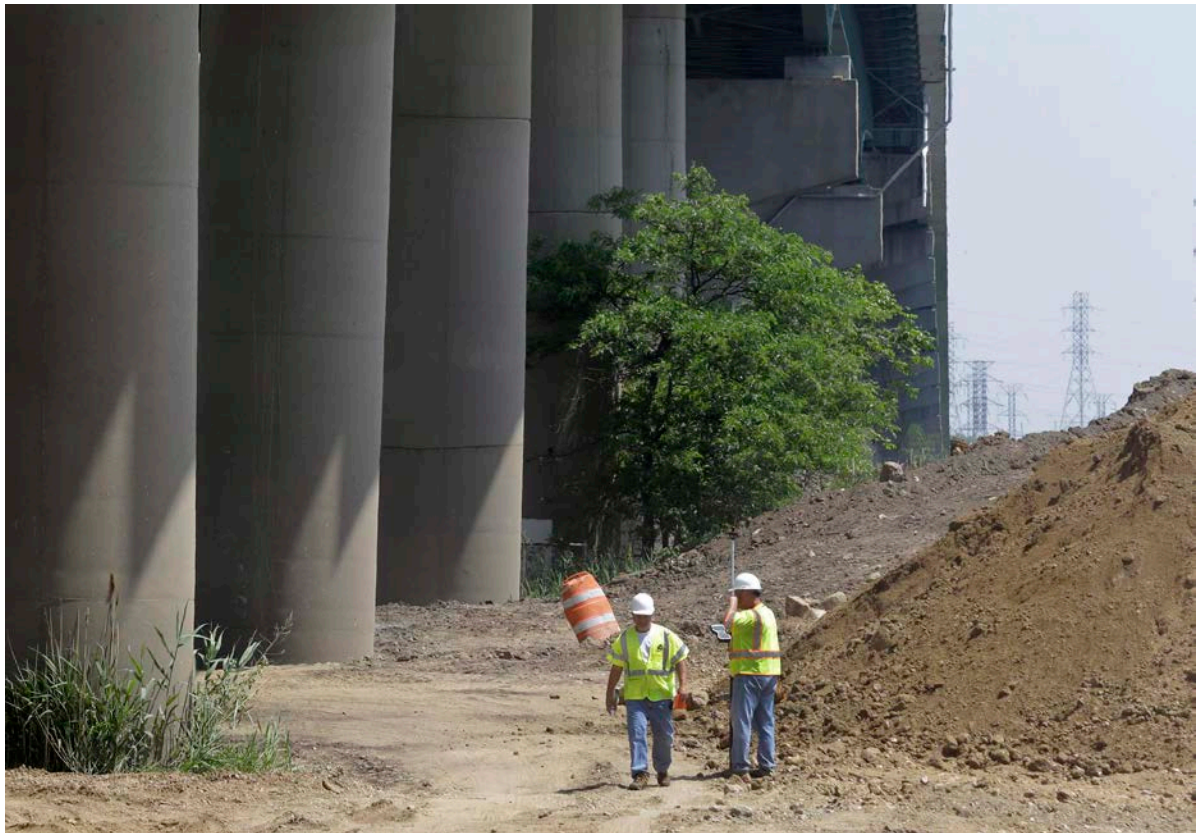


Figure 3-14 Tilting columns adjacent to stockpile (courtesy DeIDOT).



Figure 3-15 Cracked pile cap from lateral soil movements (courtesy DeIDOT).

3.6.2 Adjacent Construction

In 2015, the five span bridge carrying I-65 over Wildcat Creek was being widened from two to three travel lanes. Due to scour considerations, the new construction was supported on a driven H-pile foundation rather than spread footings. Shortly after production pile installation, the pier supported by the adjacent spread footing foundation settled as much as 10 inches and rotated 7 inches, ENR (2015). This resulted in closing the I-65 bridge to stabilize the pier. The movements were attributed to the release of artesian pressures and sand beneath the spread footing supported pier foundation.

REFERENCES

- Abu-Hejleh, N., Kramer, W.M., Mohamed, K., Long, J.H., and Zaheer, M.A. (2013). Implementation of AASHTO LRFD Design Specifications for Driven Piles, FHWA-RC-13-001. U.S. Dept. of Transportation, Federal Highway Administration, 71 p.
- Arneson, L.A., Zevenbergen, L.W., Lagasse, P.F., and Clopper, P.E. (2012). Evaluating Scour at Bridges, Fifth Edition, FHWA-HIF-12-003, Hydraulic Engineering Circular (HEC) No. 18. U.S. Dept. of Transportation, Federal Highway Administration, 340 p.
- Bay, J.A. (2003). A Summary of the Research on Pile Driving Vibrations. Proceedings of the Pile Driving Contractor's Association 7th Annual Winter Roundtable, Atlanta, 13 p.
- Bigelow, J., Clausen, C., Lebow, S., Greimann, L. (2007). Field Evaluation of Timber Preservation Treatments for Highway Applications, CRTE 06-252. Iowa Highway Research Board, Iowa Dept. of Transportation, Ames, IA, 104 p.
- Bowles, J.E. (1977). Foundation Analysis and Design. Second Edition, McGraw-Hill Book Company, Blacklick, OH, 750 p.
- Brown, D.A., Dapp, S.D., Thompson, W.R., and Lazarte, C.A. (2007). Design and Construction of Continuous Flight Auger (CFA) Piles. FHWA-HIF-07-03, Geotechnical Engineering Circular (GEC) No.08. U.S. Dept. of Transportation, Federal Highway Administration, 289 p.
- Brown, D. A., Turner, J.P. and Castelli R.J. (2010). Drilled Shafts: Construction Procedures and LRFD Design Methods, FHWA-NHI-10-016, Geotechnical Engineering Circular (GEC) No. 10. U.S. Dept. of Transportation, Federal Highway Administration, 970 p.
- Elias, V., Welsh, J.P., Warren, J., Lukas, R.G., Collin J.G., and Berg, R.R. (2006). Ground Improvement Methods Volumes I and II, FHWA-NHI-06-019 and FHWA NHI-06-020. National Highway Institute, Federal Highway Administration, U.S. Department of Transportation, Washington D.C.

- Engineering News Record (2015). Pile Driving and Poor Soils Prompt Indiana I-65 Shutdown.
- Gu, L., McInnes, S.E., Fenton, J.H., Welsh, S.J., and Mouradian, A.G. (2015). Corrosion Study of Existing Steel H-pile Installed Through Cinder-Ash Fill. Proceeding of the 2015 International Foundations Congress and Equipment Expo, San Antonio, TX, pp. 961-972.
- Holland, R.B., Kurtis, K.E., Moser, R.D. Kahn, L.F., Aguayo, F. and Singh, P.M. (2014). Multiple Deterioration Mechanisms in Coastal Concrete Piles, A Forensic Case Study, Concrete International, Vol. 36, No. 7, pp. 45-52.
- Kimmerling, R.E. (2002). Shallow Foundations, FHWA-IF-02-054, Geotechnical Engineering Circular (GEC) No. 6. U.S. Dept. of Transportation, Federal Highway Administration, Washington, D.C., 310 p.
- Komurka, V. (2015). Foundation Support Cost – Applications to Driven-Pile Design. Proceedings of the 2015 International Foundations Conference and Equipment Exposition, San Antonio, TX, pp. 990-1005.
- Lacy H.S. and Gould, J.P. (1985). Settlement from Pile Driving in Sands, Vibration Problems in Geotechnical Engineering. American Society of Civil Engineers (ASCE), Special Technical Publication, New York, NY, pp. 152-173.
- Lukas, R.G. and Gill, S.A. (1992). Ground Movement from Piling Vibrations. Piling-European Practice and Worldwide Trends, Proceeding of the Conference ICE Telford House, London, pp. 163-169.
- Massarsch, K.M, and Fellenius, G.H. (2008). Ground Vibrations Induced by Impact Pile Driving. The Sixth International Conference on Case Histories in Geotechnical Engineering, Arlington, VA, 38 p.
- Massarsch, K.R., and Fellenius, B.H. (2014). Ground Vibrations from Pile and Sheet Pile Driving. Part 1 Building Damage. Proceedings of the DFI-EFFC International Conference on Piling and Deep Foundations, Stockholm, Sweden, pp. 131-139.
- Michael Baker, Jr., Inc. (2015). Investigation Report, I-43 Leo Frigo Memorial Bridge, Volume I, 181 p.

- Moser, R., Holland, B. Kahn, L., Singh, P., and Kurtis, K. (2011). Durability of Precast Prestressed Concrete Piles in Marine Environment: Reinforcement Corrosion and Mitigation Part 1. GDOT Research Project No. 07-30. Office of Materials and Research Georgia Department of Transportation, 243 p.
- Munfakh, G., Arman, A., Collin, J.G., Hung, J.C.-J., and Brouillette, R.P. (2001). Shallow Foundations Reference Manual, FHWA-NHI-01-023. National Highway Institute, Federal Highway Administration, Washington, D.C., 222 p.
- National Fire Protection Association, (NFPA). (2013). Explosive Materials Code (495) - Chapter 11, Ground Vibration, Air Overpressure, Flyrock, and Gases, National Fire Protection Association, Quincy, MA, 58 p.
- Pile Driving Contractors Association (PDCA). (2015). National Pile Driving Noise and Vibration Database, <http://www.piledrivers.org>.
- Rollins, K.M., and Brown, D.A., (2011). Design Guidelines for Increasing the Lateral Resistance of Highway-Bridge Pile Foundations by Improving Weak Soils. NCHRP Report No. 697. Washington, D.C., 98 p.
- Sabatini, P.J., Tanyu, B., Armour., P., Groneck, P., and Keeley, J. (2005). Micropile Design and Construction, FHWA-NHI-05-039. National Highway Institute, U.S. Dept. of Transportation, Federal Highway Administration, Washington, D.C, 436 p.
- Vesic, A.S. (1977). Design of Pile Foundation, Synthesis of Highway Practice No. 42. National Cooperative Highway Research Program, Transportation Research Board, National Research Council, Washington, D.C., 68 p.
- Wiss, J.F. (1981). Construction Vibrations: State-of-the-Art. American Society of Civil Engineers (ASCE), Journal of the Geotechnical Engineering Division, , Vol. 107, No. 2, pp. 167-181.
- Woods, R.D. (1997). Dynamic Effects of Pile Installations on Adjacent Structures. NCHRP Synthesis 253, National Cooperative Highway Research Program, Transportation Research Board, Washington, D.C., 96 p.

CHAPTER 4

SITE CHARACTERIZATION

4.1 INTRODUCTION

The design of a structure's foundation requires adequate knowledge of the subsurface conditions at the construction site. The absence of a thorough foundation study or adequate geotechnical data often leads to (1) a foundation system with a large safety margin which is generally a more expensive foundation and in some cases one that may be difficult to construct, or to (2) an unsafe foundation, or to (3) construction disputes and claims.

Site characterization consists of a subsurface exploration program and subsequent testing to determine geomaterial parameters for foundation design. This information is also used in construction feasibility and planning decisions. For reliability based design, reducing uncertainty with respect to geomaterial properties may lead to more economical foundations, therefore a carefully implemented soil exploration and testing program is beneficial. This chapter will focus on site characterization based on the assumption that a driven pile deep foundation has been selected for design.

An experienced geotechnical engineer is of great value to the design team and assists with planning the subsurface exploration, ordering field and laboratory tests of geomaterials, determining the design subsurface profile, and recommending technically feasible and appropriate foundation systems. Subsurface exploration and/or laboratory testing results are often relayed in technical documents from specialty firms directly to the geotechnical engineer who then compiles this information into a geotechnical design report. This document is used by multiple engineering disciplines during the foundation design and construction phases. In some agencies, design memoranda and transmittals are used instead of geotechnical reports. In these situations, regular communication between engineering disciplines is essential for effective foundation design and construction.

Guidance on site characterization and the evaluation of geomaterial properties for geotechnical design is provided in several FHWA reference documents including FHWA-NHI-01-031, Mayne et al. (2002); GEC-5, Sabatini et al. (2002); and FHWA-NHI-06-088, Samtani and Nowarzki (2006). Laboratory and in-situ testing are also

integral to a site characterization program. These topics will be discussed further in Chapter 5 of this manual.

4.2 SITE CHARACTERIZATION PROGRAM

Site characterization encompasses the gathering and reporting of site conditions required to safely and economically design foundations and other earth structures, as well as to address constructability considerations. The information necessary to adequately characterize the site will vary depending upon the site geologic conditions, foundation types being considered for the structure, the structure performance requirements, the acceptable risk level for the structure, constructability, as well as owner preferences.

The site exploration should be carefully organized, and consists of three main phases. These are (1) planning the exploration program and data collection (office work), (2) completing a field reconnaissance survey, and (3) performing a detailed subsurface exploration program (boring, sampling, and in-situ testing). Each phase should be planned so that a maximum amount of information can be obtained at a minimum cost. Each phase also adds to, or supplements, the information from the previous phase. Table 4-1 lists the purpose of each exploration phase.

Depending upon the project size and contract delivery method, a single phase or staged subsurface exploration program may be appropriate. A single phase program is common for small project and staged subsurface exploration programs are often used for large projects. Staged programs are common for design-build projects where the owner performs a preliminary subsurface exploration program and the design-build team performs the final subsurface exploration program.

4.2.1 Data Collection

The purpose of this phase is to obtain information about the proposed structure and general information on subsurface conditions. The structural information can be obtained from studying the preliminary structure plan prepared by the bridge design office and by meeting with the structural designer. Approach embankment preliminary design and performance requirements can be obtained from the roadway office. General information about the subsurface conditions can be obtained from a variety of sources, some of which are listed in Table 4-2. Additional sources of historical data are listed in GEC-5, Sabatini et al. (2002). The data collection phase

Table 4-1 Subsurface Exploration Phases

Phase	Activity	Purpose	Remarks
1.	Planning the Exploration (Office Work).	<p>A. Obtain structure information and determine:</p> <ol style="list-style-type: none"> 1. Type of structure. 2. Preliminary location of piers and abutments. 3. Loading and special design events. 4. Allowable differential settlement, lateral deformations, and other performance criteria. 5. Any special features and requirements. <p>B. Obtain drilling records for nearby structures and from local well drillers.</p> <p>C. Perform literature reviews including maintenance records, pile driving records, scour history, etc.</p> <p>Obtain overall picture of subsurface conditions in the area.</p>	See Table 4-2 for sources of information.
2.	Field Reconnaissance Survey.	<p>Verify information gained from the office phase and plan the detailed subsurface exploration.</p> <p>A. Observe, confirm and collect information regarding:</p> <ol style="list-style-type: none"> 1. Topographic, geologic, and hydrologic features. 2. New and old construction in the area including utilities. Performance of existing structures. 3. Drilling equipment required, cost, and access for the equipment. <p>B. If appropriate, conduct geophysical testing to obtain preliminary subsurface information.</p>	Field reconnaissance is often conducted by a multi-disciplined team.
3.	Detailed Subsurface Exploration.	<p>Develop a preliminary boring plan based on phases 1 and 2. Conduct a preliminary evaluation for viable foundation systems including ground improvement. Determine subsurface requirements for all of the viable foundation systems. The boring plan should be modified if needed as the borings are performed and detailed subsurface information is obtained.</p> <p>The subsurface exploration should provide the following:</p> <ol style="list-style-type: none"> 1. Depth and thickness of strata (subsurface profile). 2. In-situ field tests to determine soil design parameters. 3. Samples to determine soil and rock design parameters. 4. Groundwater levels including perched, regional, and any artesian conditions. 	For major structures, the pilot boring program is often supplemented with control and verification boring programs.

Table 4-2 Sources of Subsurface Information and Use

Source	Use
Preliminary structure plans prepared by the bridge design office.	Determine: <ol style="list-style-type: none"> 1. Type of structure. 2. Preliminary locations of piers and abutments. 3. Footing loads and special design events. 4. Allowable differential settlement, lateral deformations, and performance criteria. 5. Any special features and requirements.
Geotechnical databases.	Nearby soil boring logs, laboratory test results, and in-situ test results.
Construction plans and records for nearby structures.	Foundation type, old boring data, construction information including construction problems.
Topographic maps prepared by the United States Coast and Geodetic Survey (USC and GS), United States Geological Survey (USGS) and State Geology survey.	Existing physical features shown; find landform boundaries and determine access for exploration equipment. Maps from different dates can be used to determine topographic changes over time.
County agricultural soil survey maps and reports prepared by the United States Department of Agriculture (USDA).	Boundaries of landforms shown; appraisal of general shallow subsurface conditions.
Aerial photos prepared by the United States Geological Survey (USGS) or satellite imagery such as Google Earth.	Detailed physical relief shown; gives indication of major problems such as old landslide scars, fault scarps, buried meander channels, sinkholes, or scour; provides basis for field reconnaissance.
Well drilling record or water supply bulletins from state geology or water resources department.	Old well records or borings with general soils data shown; estimate required depth of explorations and preliminary cost of foundations.
Geologic maps and Geology bulletins.	Type, depth and orientation of rock formations.

prepares the engineer for the field reconnaissance survey, and identifies possible problems and areas to scrutinize.

4.2.2 Field Reconnaissance Survey

Site visits by the geotechnical engineer and other members of the design team are necessary to properly characterize the site. Field reconnaissance presents an opportunity to locate and record many constructability issues such as site access, headroom restrictions, and other working conditions that may be otherwise overlooked from reviewing site or aerial photos and satellite images. This phase enables the engineer to substantiate the information gained from the office phase and to plan the detailed site exploration program.

The field reconnaissance for a structure foundation exploration includes, but is not limited to:

- a. Inspection of nearby structures to determine their performance with the particular foundation type used.
- b. Inspection of existing structure footings and stream banks for evidence of scour (for stream crossings) and movement. Large boulders in a stream are often an indication of obstructions which may be encountered in pile installations.
- c. Recording of the location, type and depth of existing structures which may be affected by the new structure construction.
- d. Visual examination of terrain for evidence of landslides.
- e. Location of trees and other vegetation, as well as surface water.
- f. Relating site conditions to proposed boring operations. This includes recording the locations of both overhead and below ground utilities, site access, private property restrictions, water depth and access points for marine borings, and other access restrictions or obstructions.
- g. Recording of any feature or constraint which may impact the constructability of potential foundation systems.

Figure 4-1 contains an example of a field reconnaissance form modified from the AASHTO Foundation Investigation Manual (1978) for recording data pertinent to a site. At conclusion of the data collection and field reconnaissance phases, the

Bridge Foundation Investigation
Field Reconnaissance Report
_____ Department of Transportation

Project No: _____ County _____ Sta. No. _____

Reported By: _____ Date _____

<p>1. Staking of Line Well Staked _____ Poorly Staked (We can work) _____ Request Division to Restake _____</p> <p>2. Bench Marks In Place: Yes _____ No _____ Distance from bridge - (ft) _____</p> <p>3. Property Owners Granted Permission: Yes _____ No _____ Remarks on Back _____</p> <p>4. Utilities Will Drillers Encounter Underground or Overhead Utilities? Yes _____ No _____ Maybe _____ At Which Holes? _____ What Type? _____ Who to See for Definite Location _____</p> <hr/> <p>5. Geologic Formation _____</p> <p>6. Surface Soils Sand _____ Clay _____ Sandy Clay _____ Muck _____ Silt _____ Other _____</p> <p>7. General Site Description Topography Level _____ Rolling _____ Hillside _____ Valley _____ Swamp _____ Gullied _____ Groundcover Cleared _____ Farmed _____ Buildings _____ Heavy Woods _____ Light Woods _____ Other _____ Remarks on Back _____</p> <p>8. Bridge Site Replacing _____ Widening _____ Relocation _____ Check Appropriate Equipment Truck Mounted Drill Rig _____ Failing 1500 _____ Track Mounted Drill Rig _____ Skid Rig _____ Truck Mounted Skid Rig _____ Rock Coring Rig _____ Wash Boring Equipment _____ Water Wagon _____ Pump _____ Hose _____ (ft) _____</p>	<p>8. Bridge Site – Continued Cut Section - (ft) _____ Fill Section - (ft) _____ If Stream Crossing: Will pontoons Be Necessary? _____ Can pontoons Be Placed in Water Easily? _____</p> <p>Can Cable Be Stretched Across Stream? How Long? _____</p> <p>Is Outboard Motorboat Necessary? _____ Current: Swift _____ Moderate _____ Slow _____ Describe Streambanks scour. If Present Bridge Nearby: Type of Foundation _____ Any Problems Evident in Old Bridge Including Scour _____ (describe on back) Is Water Nearby for Wet Drilling - (ft) _____ Are Abandoned Foundations in Proposed Alignment? _____</p> <p>9. Ground Water Table Close to Surface - (ft) _____ Nearby Wells - Depth - (ft) _____ Intermediate Depth - (ft) _____ Artesian head - (ft) _____</p> <p>10. Rock Boulders Over Area? Yes _____ No _____ Definite Outcrop? Yes _____ No _____ (show sketch on back) What kind? _____</p> <p>11. Special Equipment Necessary _____</p> <p>12. Remarks on Access (Describe any Problems on Access) _____</p> <p>13. Debris and Sanitary Dumps Stations _____ Remarks _____ _____ _____</p> <p>Reference: Modified from 1978 AASHTO Foundation Investigation Manual</p>
--	---

Figure 4-1 Typical field reconnaissance form.

engineer should have in mind geotechnical loading requirements, which would therefore dictate the planning of the field exploration program.

4.2.3 Detailed Field Exploration

The purpose of any field exploration program is to obtain representative information on subsurface conditions, to recover disturbed and undisturbed soil samples, to perform in-situ testing, and to determine groundwater levels. This information provides factual basis upon which all subsequent steps in the pile design and construction process are founded. Its quality and completeness are of paramount importance. Each step in the process directly or indirectly relies on this data. It is assumed that a preference to a driven pile foundation is given. Therefore, the field exploration plan will focus on items related to the design of driven pile foundations.

The first step in this phase is to prepare a preliminary boring, sampling, and in-situ testing plan. For major structures, pilot borings are usually performed at a few select locations during the preliminary planning stage. These pilot borings establish a preliminary subsurface profile and thus identify key soil strata for testing and analysis in subsequent design stage borings. Then, during the design stage of major structures, geophysical surveys and a two phase boring program are recommended. First, control borings are performed at key locations identified in the preliminary subsurface profile to determine what, if any, adjustments are appropriate in the design stage exploration program. Following analysis of the control boring data, verification borings are then performed to fill in the gaps in the design stage exploration program.

A preliminary structural design plan should also be established at this point such that borings are properly located with respect to structural or earthen elements. Geophysical surveys and in-situ testing are included in this category. Information on developing a site exploration program may be found in Sabatini et al. (2002).

4.2.3.1 Geophysical Surveys

Geophysical surveys aide in subsurface characterization over a wide area, and supplement borings and other invasive tests. Primarily, seismic and electrical methods are used to measure depth to groundwater and bedrock and to resolve intermediate soil strata thickness. These methods may identify and locate subsurface anomalies requiring further evaluation by soil borings or in-situ tests. Geophysical surveys may also locate voids, debris or buried objects as well as measure divisions in soil stiffness.

Seismic surface wave methods involve using an applied impact or simply ambient earthborn noise (traffic, wind, microtremors, etc.) to produce surface waves or vibrations that travel through the ground and reflect off changes in subsurface materials. These reflected waves are generally measured with geophones located on the surface. The collected data can be analyzed to compute soil stiffness, allowing the bedrock depth, groundwater depth, and other soil strata to be located. Additional details on seismic surface wave methods can be found in Wightman et al. (2003), Sirles (2006), Rosenblad and Li (2009), and Sirles et al. (2009).

Ground penetrating radar is a common geophysical option and is useful to detect near surface voids in the 20 to 30 feet depth range, buried objects, and to locate the water table. However, this technique decreases in effectiveness with depth, and is not effective in saturated clayey soils.

Electrical test methods employ electrical currents to measure resistivity which may be correlated to locate soil strata changes, as well as to detect voids or buried objects. DC resistivity testing does produce soil resistivity results below the groundwater table, as this medium conducts electrical current, Lucius et al. (2007). Results from this test can be modeled to show coarse versus fine grained material, as well as the groundwater table location, and bedrock.

It should be noted that geophysical surveys are often performed in the preliminary site exploration phase to provide a larger sense of site geology, and should further model soil stratigraphy. They should and always be performed in combination with direct exploration methods such as soil borings or in-situ testing.

4.2.3.2 Depth, Spacing, and Frequency of Boring & In-Situ Tests

The cost of a subsurface exploration program is comparatively small in relation to the foundation cost. For example, the cost of one 2.4 inch diameter boring is less than the cost of one 12 inch diameter pile. However, in the absence of adequate boring data, the design engineer must rely on extremely conservative designs with high safety margins. At the same time, the designer assumes enormous risk and uncertainty during the project's construction.

The number of borings required, their spacing, and sampling intervals depend on the uniformity of soil strata and loading conditions. Erratic subsurface conditions require closely spaced borings while more uniform soil profiles may require less frequent exploration. Structures sensitive to settlements or subjected to heavy loads require more detailed subsurface knowledge, and in this case, borings should be closely

spaced. Minimum guidelines for depth and quantity of borings for given structures are provided by Sabatini et al. (2002) and AASHTO (2014). For deep foundations, Table 4-3 provides minimum quantity guidelines.

Table 4-3 Minimum Number of Exploration Points per Substructure
(modified from Sabatini et al. 2002)

Pier or Abutment Width, W	Exploration Points per Substructure ¹
$W \leq 100\text{-ft}$	1
$W > 100\text{-ft}$	2

¹Additional exploration points should be provided if erratic subsurface conditions are encountered.

Minimum exploration depths should be met as well. Exploration points should extend a minimum of 20 feet below the expected pile toe elevation, or at least two times the pile group width. If piles will bear on rock, at least 10 feet of rock coring should be performed. Although these minimum values are provided by AASHTO (2014), additional boring and in-situ testing depths may be required due to site specific geology. Adjustments to the exploration program may be required as information becomes available, and likewise, additional rock coring length may be required if highly variable bedrock is present. Where unsuitable soil strata such as peat, highly organic materials, uncontrolled fills, soft fine grained soils, and loose coarse-grained soils are encountered, structure borings should extend through these deposits to reach and characterize suitable foundation support materials.

In-situ test spacing and frequency should be used to determine geomaterial design parameters based on project requirements. These tests generally supplement other aspects of the site exploration and will be performed after preliminary borings have been performed. In-situ tests are often done where undisturbed sampling is not easily performed. This includes both vane shear and pressuremeter testing among others. For in-situ testing and soil borings, many times a standard sampling interval is used. However, a customized soil boring and in-situ testing program may be formulated if general site geology or loading conditions warrant alternative intervals. This could aid with locating the contact between two soil strata, as well as discovering a thin layer of unsuitable material. Liquefaction and aggressive environment studies may also dictate appropriate sampling intervals.

4.2.3.3 Soil Boring Methods

Soil borings are the most frequently used soil exploration technique for projects in the public and private sector. Soil borings offer the ability to collect disturbed and undisturbed samples from various depths, as well as to perform in-situ tests. Common boring methods include augered borings, wash borings, and rotary drilling in soil. These methods, as well as sonic drilling, are presented in Table 4-4.

Continuous flight augers are either solid stem or hollow stem and are both used to bore into the subsurface and allow for sampling and/or in-situ testing. A solid stem auger is essentially a solid rod with flights, and must be removed in order to test native soil. They are therefore not useful in soft soils, sands or areas of high groundwater due to the probability of borehole collapse and are best used when soil sampling only at relatively shallow depths is required. Hollow stem augers act as a casing that stays in place during drilling, whereby subsequent sampling and testing is performed through the bottom of the hollow stem. This auger type is therefore practical for a variety of subsurface conditions and utilizes a plug when advancing the auger. Hollow stem auger diameters range from 2.25 inch I.D. up to 12.25 inch I.D with larger sizes reserved for more complex sampling and testing techniques.

Rotary drilling may be performed in soil or rock and involves inserting a drill bit to cut and grind the material. Water or drilling mud flushes out the cuttings, and provides borehole stability. Air has also been used to force out cuttings in lieu of drilling mud, however borehole stability issues remain. To sample soil or perform an in situ test, the drill bit is removed and a sampling device is then inserted to collect material.

Wash borings are advanced by the chopping action of a light bit in combination with the jetting action of water or drill fluid coming through the bit. Casing may be used to maintain an open bore hole, although typically a bentonite or drilling mud of similar properties is adequate. Drilling mud can contaminate recovered soil samples as well as add difficulty when trying to classify soil stratigraphy from wash cuttings. In addition, heavier particles such as gravel or cobbles may be left at the bottom of the hole if the wash system is undersized. Wash borings are infrequently used in the United States.

4.2.3.4 Soil Sampling Methods

Soil samples may be collected via disturbed or undisturbed methods. Disturbed soil samples contain representative material that may be used for visual classification and more routine laboratory testing which is further described in Chapter 5. These

Table 4-4 Soil Boring Methods

Method	Depth	Advantages	Disadvantages	Remarks
Auger Borings.	Most equipment can drill to depths of 100 to 200 feet.	Boring advanced without water or drilling mud. Hollow stem auger acts as a casing.	Difficult to detect change in material. Heavy equipment required. Water level must be maintained in boring equal to or greater than existing water table to prevent sample disturbance.	Boring advanced by rotating and simultaneously pressing an auger into the ground either mechanically or hydraulically.
Rotary Drilling.	Most equipment can drill to depths of 200 feet or more.	Suited for borings 4 to 6 inches in diameter. Most rapid method in most soils and rock. Relatively uniform hole with little disturbance to the soil below the bottom of hole. Experienced driller can detect changes based on rate of progress.	Drilling mud if used does not provide an indication of material change as the wash water does. Use of drilling mud hampers the performance of permeability tests.	Borehole advanced by rapid rotation of drilling bit and removal of material by water or drilling mud. Rock coring is performed by rotary drilling. Liquefaction evaluation methods require mud rotary drilling methods.
Wash Boring.	Most equipment can drill to depths of 100 feet or more.	Borings of small and large diameter. Equipment is relatively inexpensive. Equipment is light. Wash water provides an indication of change in materials.	Slow rate of progress. Not suitable for materials containing stones and boulders.	Boring advanced by a combination of the chopping action of a light bit and jetting action of the water coming through the bit.
Sonic Coring.	Up to 1000 feet.	Generally a 100% recovery rate. Can collect samples in soils and bedrock.	Expensive for large amounts of dense rock sampling.	Borehole advanced in 10 feet cased sections. Can collect any soil type with minimal to no fluids.

soil samples are not suitable for strength or compressibility testing as the sampling disturbance alters their condition. When in-situ particle arrangements, water content and other properties must be preserved for laboratory testing, undisturbed samples are taken. These samples are collected in devices designed to minimize sample disturbance. However, even while using utmost care for removal and transport, no sample will be completely undisturbed.

Disturbed soil samples may be collected with a split barrel sampler, sonic cores, or through test pits. Split barrel samplers typically range from 1.5 to 2.5 inches in diameter and are 18 or 24 inches long. Although multiple sizes exist, the standard split spoon sampler used for the Standard Penetration Test (SPT) has an inner diameter of 1.375 inches and outer diameter of 2 inches (ASTM D1586). A photograph of a standard SPT sampler is presented in Figure 4-2. This test is further discussed in Section 5.1.1.

Relatively undisturbed soil samples may be collected with thin walled tubes (Shelby tubes), a piston sampler or other specialized means. Thin walled tubes are produced in various sizes, and are typically used to collect fine grained soils as illustrated in Figure 4-3. These tubes are pushed into the soil and removed after a brief swelling of the soil occurs. ASTM D1587 provides detailed guidance on this sampling technique.

Piston samplers were developed to prevent soil from entering the sampling tube before the sample depth and to reduce sample loss during tube extraction. They are basically a thin wall tube sampler with a piston, rod, and a modified sampler head. There are numerous types of piston samplers; free or semi-fixed piston samplers, fixed-piston samplers, and retractable piston samplers.

The Pitcher sampler is a core barrel sampler that may be used for sampling a broad range of materials including undisturbed samples of stiff to hard clays, soft rocks and cemented sands. This sampler consists of a rotating outer core barrel with an inner thin walled sampling tube. The sampling tube leads the core barrel when sampling soft soils and the core barrel leads the sampling tube when sampling hard materials. This makes the Pitcher sampler particularly attractive for sampling materials with alternating hard and soft layers.



Figure 4-2 Standard split spoon sampler.



Figure 4-3 Shelby tubes (after Mayne et al. 2002).

4.2.3.5 Rock Exploration Methods (Coring / Drilling)

Rock drilling and coring is typically performed at the end of a soil boring once bedrock is encountered. Special drilling bits are used to cut and grind through rock, so that sampling can be performed. Fluid or air is circulated to flush out cuttings,

and an inner core barrel collects rock samples. The recovered rock core is classified by rock type, and the core recovery length and recovery percentage noted as a percentage of the core run. Table 4-5 summarizes several rock coring methods.

Conventional rotary coring is primarily used to collect rock samples. For this, a circular diamond or tungsten drill bit grinds rock so that a core is cut from the surrounding rock. To collect intact rock samples, the drill barrel typically has an inner and outer tube, of which the inner tube remains stationary during drilling. The inner tube is removable such that intact samples may be brought to the surface, while the outer tube acts as casing, and remains in place. However, several barrel types exist, which are discussed further in Sabatini et al. (2002).

Wire line rotary coring is similar to conventional rotary coring however; the inner barrel is connected to a wire retrieval line as opposed to a rod or tube. This retrieval method significantly speeds up sampling at deeper depths.

Table 4-5 Summary of Rock Coring Methods

Method	Depth	Type of Samples Taken	Advantages	Disadvantages	Remarks
Conventional Rotary Coring in Rock.	Most equipment can drill to depths of 200 feet or more.	Continuous Rock Cores.	Helps differentiate between boulders and bedrock.	Can be slow and fairly expensive.	Several types of core barrels are used.
Wire Line Rotary Coring in Rock.	Most equipment can drill to depths of 200 feet or more.	Continuous Rock Cores.	Improved recovery rate of fractured rock. Typically faster drilling rate when coring rock at deep depths.	Fairly expensive.	Inner tube retrieved by cable suspended lifting device. Preferred method for depths greater than 80 feet.
Rotary Coring of Swelling Clay or Soft Rock.	Most equipment can drill to depths of 200 feet or more.	Plastic tube encased sample.	Inner plastic tube protects soil and soft rock.	More complex equipment.	Smaller sample due to coring equipment.

A specialized barrel may be used when sampling swelling soil and soft rock. This barrel contains a third inner liner which contains the swelling soil or soft rock and is

more easily removed due to the 5% to 10% difference in liner and drill bit size (Acker 1974). A smaller diameter sample results from this barrel design, as opposed to samples collected via rotary coring. However, this collection method may exhibit less soil disturbance than thin walled sampling for some soil types.

Rock cores should be stored in a structurally sound box designed for the size of core collected as illustrated in Figure 4-4. Cores should be set carefully to retain natural bedding and fractures, and handled such that accidental breaks do not occur after retrieval. Features should be noted including bedding, fractures, and weathered zones, and photographs should be taken, always using a visible reference scale such as a tape measure. Sometimes wetting the rock surface can increase color contrast for photos. Labels identifying the project, borehole, depth interval and number of core runs should be written on the core box, in addition to standard field notes.

Rock cores are also given a rock quality designation (RQD). The RQD index test allows for a description of rock mass quality and should be performed in the field upon core recovery. The RQD index test, described in ASTM D6032, is used to provide estimates of overall rock quality. Deere and Deer (1989) proposed the RQD to be equal to the sum of the length of sound core pieces, 4 inches or greater in length, divided by the total length of core run. Core lengths should be measured from the axis centerline, while the RQD is expressed as a percentage. RQD designations are shown in Table 4-6, with a further discussion of rock quality index parameters provided in Section 5.4.



Figure 4-4 Rock core samples.

RQD values may be indicative of the pile penetration into the rock needed to satisfy resistance requirements when reviewed in combination with additional test results. However, the RQD value alone should not be used to correlate rock strength. In

addition to the coring methods presented here, various drill bits exist as well as core barrel types, which influence ease of drilling, core size and recovery rate. These should be selected accordingly based on experience and recovery requirements. Further descriptions of these may be found in Acker (1974), ASCE (2001), and ASTM D2113. Core samples should be retained for the duration of the project and beyond if needed due to any construction claims.

Table 4-6 Rock Quality Designation

Rock Mass Description	RQD
Excellent	90-100
Good	75-90
Fair	50-75
Poor	25-50
Very Poor	< 25

4.2.3.6 Groundwater

Accurate ground water level information is needed for the estimation of soil densities, determination of effective soil pressures and for the preparation of effective stress diagrams. Water levels will also indicate the construction difficulties which may be encountered in excavations and the dewatering effort required.

In most structure foundation explorations, water levels should be monitored during drilling of the boring, upon completion of the boring, and 24 hours after the completion of boring. More than one week may be required to obtain representative water level readings in low permeability cohesive soils or in bore holes stabilized with some drilling muds. In these cases, an observation well or piezometer should be installed in a boring to allow long term ground water monitoring. An observation well is typically used to monitor changes in the water level in a select aquifer whereas a piezometer is used to monitor changes in the hydrostatic pressure in a confined aquifer or specific stratum.

An observation well is usually a slotted section of small diameter PVC pipe installed in a bore hole. The bottom section of the slotted PVC pipe is capped and solid PVC sections are used to extend the observation well from the top of the slotted PVC section to a height above grade. The annulus between the slotted section and the sides of the bore hole is backfilled with sand. Once the sand is above the slotted PVC section, a bentonite seal is placed in the annulus sealing off the soil stratum in

which the water table fluctuations will be monitored. Grout or auger cuttings are used to backfill the remaining void, while a locking removable cover may be placed over the annulus top. The water level reading in the observation well will be the highest of the water table in any soil layer that the slotted section penetrates.

Piezometers are generally used to monitor hydrostatic pressure changes in a specific soil stratum. Piezometers may be either pneumatic or vibrating wire diaphragm devices and are installed in a sand pocket with a bentonite seal similar to an observation well. Single and multiple piezometers can be installed in a single bore hole using a cement-bentonite grout. Additional piezometer information is available in FHWA-NHI-01-031, Subsurface Investigations – Geotechnical Site Characterization (Mayne et al. 2002).

4.2.4 Information Required for Construction

The subsurface exploration and subsequent soil and rock testing program provides essential information for driven pile design and construction. Engineers and contractors use this information to select the most appropriate pile type for the loading requirements, size pile driving hammer equipment, determine if pile installation aids are needed to meet design objectives, prepare cost estimates and bid documents, establish construction control methods and generate construction schedules. To reduce the risk of unplanned cost and claims, a well-defined and executed site characterization program is vital.

As described in Chapter 6, a variety of driven pile types and sections exist and may derive their nominal resistance from end bearing, shaft resistance or both. The pile type is generally selected based on local practice, structural requirements and subsurface conditions, while size and length are contingent upon soil properties and bearing layers. Pile drivability and other construction considerations are affected by the overall site characterization including permeability, relative density, layering and soil response to pile driving.

REFERENCES

- Acker, W.L. III, (1974). Basic Procedures for Soil Sampling and Core Drilling, Acker Drill Company, Inc., Scranton, PA, 246 p.
- American Association of State Highway and Transportation Officials (AASHTO). (1978). Manual on Foundation Investigations Second Edition. AASHTO Highway Subcommittee on Bridges and Structures, Washington, D.C., 196 p.
- American Association of State Highway and Transportation Officials (AASHTO). (2014). AASHTO LRFD Bridge Design Specifications, US Customary Units, Seventh Edition, with 2015 Interim Revisions. American Association of State Highway and Transportation Officials, Washington, D.C., 1960 p.
- ASTM D1586-11. (2014). Standard Test Method for Standard Penetration Test (SPT) and Split-Barrel Sampling of Soils. Annual Book of ASTM Standards, Vol. 4.08, ASTM International, West Conshohocken, PA, 9 p.
- ASTM D1587-12. (2014). Standard Practice for Thin-Walled Tube Sampling of Soils for Geotechnical Purposes. Annual Book of ASTM Standards, Vol. 4.08, ASTM International, West Conshohocken, PA, 4 p.
- ASTM D2113-14. (2014). Standard Practice for Rock Core Drilling and Sampling of Rock for Site Investigation. Annual Book of ASTM Standards, Vol. 4.08, ASTM International, West Conshohocken, PA, 20 p.
- ASTM D6032-08. (2014). Standard Test Method for Determining Rock Quality Designation (RQD) of Rock Core. Annual Book of ASTM Standards, Vol. 4.09, ASTM International, West Conshohocken, PA, 5 p.
- ASTM Vol 4.08. (2014). Soil and Rock I, Vol. 4.08, ASTM International, West Conshohocken, PA, 1826 p.
- ASTM Vol 4.09. (2014). Soil and Rock II, Vol. 4.09, ASTM International, West Conshohocken, PA, 1754 p.

- Brown, D. A., Turner, J.P. and Castelli R.J. (2010). Drilled Shafts: Construction Procedures and LRFD Design Methods, FHWA-NHI-10-016, Geotechnical Engineering Circular (GEC) No. 10. U.S. Dept. of Transportation, Federal Highway Administration, 970 p.
- Cheney, R.S. and Chassie, R.G. (2000). Soils and Foundations Workshop Reference Manual. FHWA HI-00-045, U.S. Department of Transportation, National Highway Institute, Federal Highway Administration, Washington, D.C., 358 p.
- Federal Highway Administration (FHWA). (1996). Geotechnical Engineering Notebook DT-15. Differing Site Conditions. U.S. Dept. of Transportation, Federal Highway Administration, Washington, D.C., 36 p.
- Louie, J, N. (2001). Faster, Better: Shear-wave Velocity to 100 Meters Depth from Refraction Microtremor Arrays: Bulletin of the Seismological Society of America, V. 91.02, Alexandria, VA, pp. 347-364.
- Lucius, J.E., Langer W.H. and Ellefsen, K. (2007). An Introduction to Using Surface Geophysics to Characterize Sand and Gravel Deposits. U.S. Geological Survey Circular, Reston, VA, 1310, 33 p.
- Mayne, P.W., Christopher, B., Berg, R., and DeJong, J. (2002). Subsurface Investigations (Geotechnical Site Characterization), FHWA NHI-01-031, U.S. Dept. of Transportation, National Highway Institute, Federal Highway Administration, Washington, D.C., 300 p.
- Sabatini, P.J., Bachus, R.C., Mayne, P.W., Schneider, J.A., and Zettler, T.E. (2002). Evaluation of Soil and Rock Properties, FHWA-IF-02-034, Geotechnical Engineering Circular (GEC) No. 5, U.S. Dept. of Transportation, Federal Highway Administration, 385 p.
- Samtani, N.C. and Nowatzki, E.A. (2006). Soils and Foundations: Reference Manual, Vol. 1, FHWA-NHI-06-088, U.S. Dept. of Transportation, National Highway Institute, Federal Highway Administration, Washington, D.C., 462 p.
- Sirles, P.C. (2006). Use of Geophysics for Transportation Projects, NCHRP Synthesis 357, Transportation Research Board of the National Academies, Washington, D.C., 109 p.

Sirles, P., Shawver, J.B., Pullammanappallil, S., and Batchko, Z. (2009). Mapping Top-of-Bedrock and Soft-Soil Zones Beneath High-Traffic Areas Using 2D REMI, Symposium on the Application of Geophysics to Engineering and Environmental Problems (SAGEEP 2009), Environmental and Engineering Geophysical Society, Denver, CO, (available on CD; online: <http://www.eegs.org>).

Rosenblad B.L., and Li J. (2009). Comparative study of Refraction Microtremor (ReMi) and Active Source Methods for Developing Low-Frequency Surface Wave Dispersion Curves. *Journal of Environmental and Engineering Geophysics*. 14 (3), pp. 101-113.

Wightman, W., Jalinoos, F., Sirles., and Hanna, K. (2003). Applications of Geophysical Methods to Related Highway Problems. U.S. Dept. of Transportation, Federal Highway Administration, 716 p.

CHAPTER 5

GEOMATERIAL DESIGN PARAMETERS AND GEOTECHNICAL REPORTS

Properties of cohesive soil, cohesionless soil, soft rock, and hard rock affect the design and construction of driven piles. Depending on subsurface conditions, additional consideration may be given to aggressive soils or areas effecting pile integrity. As discussed in chapter 4, in-situ tests are performed during subsurface exploration while samples may be collected for further evaluation in a soils engineering laboratory. Results of in-situ and laboratory tests define material properties that are often correlated to design parameters, if not directly measured. Primary design parameters include shear strength and deformation values. This chapter will focus on the determination of soil and rock parameters that influence the design and construction of driven piles. Table 5-1 provides a summary of field and laboratory tests used for geomaterial characterization and determination of design parameters.

A discussion of in-situ and laboratory testing to acquire design parameters is provided in subsequent sections. For a more in depth discussion on the collection of design parameters, please refer to AASHTO (2014), Bowles (1992), Mayne et al. (2002), Duncan and Wright (2005) among other sources. In addition, the latest version of GEC-5, Evaluation of Soil and Rock Properties, should be consulted for updates in practice. The version at the time of this manual revision is Sabatini et al. (2002).

5.1 IN-SITU SOIL TESTING

In-situ testing provides soil parameters for the design of structure foundations especially in conditions where standard drilling and sampling methods cannot be used to obtain high quality undisturbed samples. Therefore, representative strength test data is difficult to obtain on these soils in the laboratory. To overcome these difficulties, test methods have been developed to evaluate soil properties, particularly strength and compressibility, in-situ.

Table 5-1 Field and Laboratory Tests for Geomaterial Parameter Determination

Design Parameter or Information Needed	Cohesionless Soil	Cohesive Soil	Rock
Subsurface Stratigraphy	Drilling and Sampling; SPT, CPT _u , CPT; Geophysical methods	Drilling and Sampling; SPT, USS, CPT _u , CPT, DMT; Geophysical methods	Drilling and Sampling; Rock Core Logging
Groundwater Conditions	Well / Piezometer	Well / Piezometer	Well / Piezometer
Classification	USCS Group	USCS Group	Rock Type
Gradation	Sieve Analysis	Sieve Analysis Hydrometer Analysis	N/A
Atterberg Limits	N/A	Liquid Limit Plastic Limit	N/A
Moisture Content, w	Wet and Oven-Dried Weights	Wet and Oven-Dried Weights	Lab
Unit Weight, γ	SPT, DMT	USS-Lab	USS-Lab
Sensitivity	N/A	VST, USS-Lab	N/A
RQD and GSI	N/A	N/A	Rock Core Recovery and Logging
Effective Stress Friction Angle, ϕ'	SPT, CPT _u , CPT, DMT	CD or CIU triaxial on USS	Correlate to GSI
Undrained Shear Strength, s_u	N/A	UU, CIU and UC on USS, VST, CPT	N/A
Preconsolidation Stress, σ_p	SPT, CPT	Consolidation test, DMT, CPT _u , CPT	N/A
Elastic Modulus of Soil, E_s	SPT, CPT, PMT, DMT; correlate with Index Properties	DMT, PMT, Triaxial Tests; correlate with Index Properties	N/A
Unconfined Compressive Strength, q_u	N/A	N/A	UC on Rock Core
Modulus of Intact Rock, E_r	N/A	N/A	Compression Test on Rock Core
Rock Mass Modulus, E_m	N/A	N/A	Correlate to GSI and q_u or E_r ; PMT

Table Key:

- CD – Consolidated Drained Triaxial Test (Section 5.2)
- CIU – Consolidated Undrained Triaxial test with pore pressure measurements (Section 5.2)
- CPT – Cone Penetration Test (Section 5.1.2)
- CPTu – Cone Penetration Test with pore water pressure measurements (Section 5.1.2)
- CU – Consolidated Undrained Triaxial Test (Section 5.2)
- DMT – Dilatometer Test (Section 5.1)
- GSI – Geological Strength Index
- PMT – Pressuremeter Test (Section 5.1)
- RQD – Rock Quality Designation Test (Section 4.2)
- SPT – Standard Penetration Test (Section 5.1.1)
- UU – Unconsolidated, Undrained Triaxial Test (Section 5.2)
- UC – Unconfined Compression Test (Section 5.2)
- USS – Undisturbed soil sample (Section 4.2)
- USCS – Unified Soil Classification System
- VST – Vane Shear Test (Section 5.1.3)

In-situ test methods can be effective when used to supplement conventional exploration programs. In addition, these methods help identify key strata for further conventional sampling and laboratory tests. In the absence of an adequate program to determine subsurface design parameters, the engineer must use a more conservative approach based on less certain data. This situation also results in additional uncertainty and risk and is not recommended.

Primary in-situ tests that provide data for foundation design are the Standard Penetration Test (SPT), cone penetration test (CPT), the cone penetration test with pore pressure measurements (CPTu), the seismic cone penetration test with pore pressure measurements (SCPTu), and the vane shear (VST). Other lesser used in-situ testing devices include the pressuremeter test (PMT) and flat dilatometer test (DMT). Each of these test methods apply different loading conditions (orientation and rate of strain) to gain information on strength and or/stiffness such as torsion for VST or axial loading for SPT. The net result is that all in-situ tests are index tests that require local correlations and where possible should be benchmarked to laboratory tests. In-situ test method schematics are depicted in Figure 5-1.

The applicability, advantages and disadvantages of all the in-situ testing methods are briefly summarized in Table 5-2. For a detailed discussion of a particular in-situ testing method, the reader is referred to the publications listed at the end of this chapter. NHI course 132031, Subsurface Investigations – Geotechnical Site Characterization and the accompanying course manual by Mayne et al. (2002) provides a thorough coverage of in-situ testing methods.

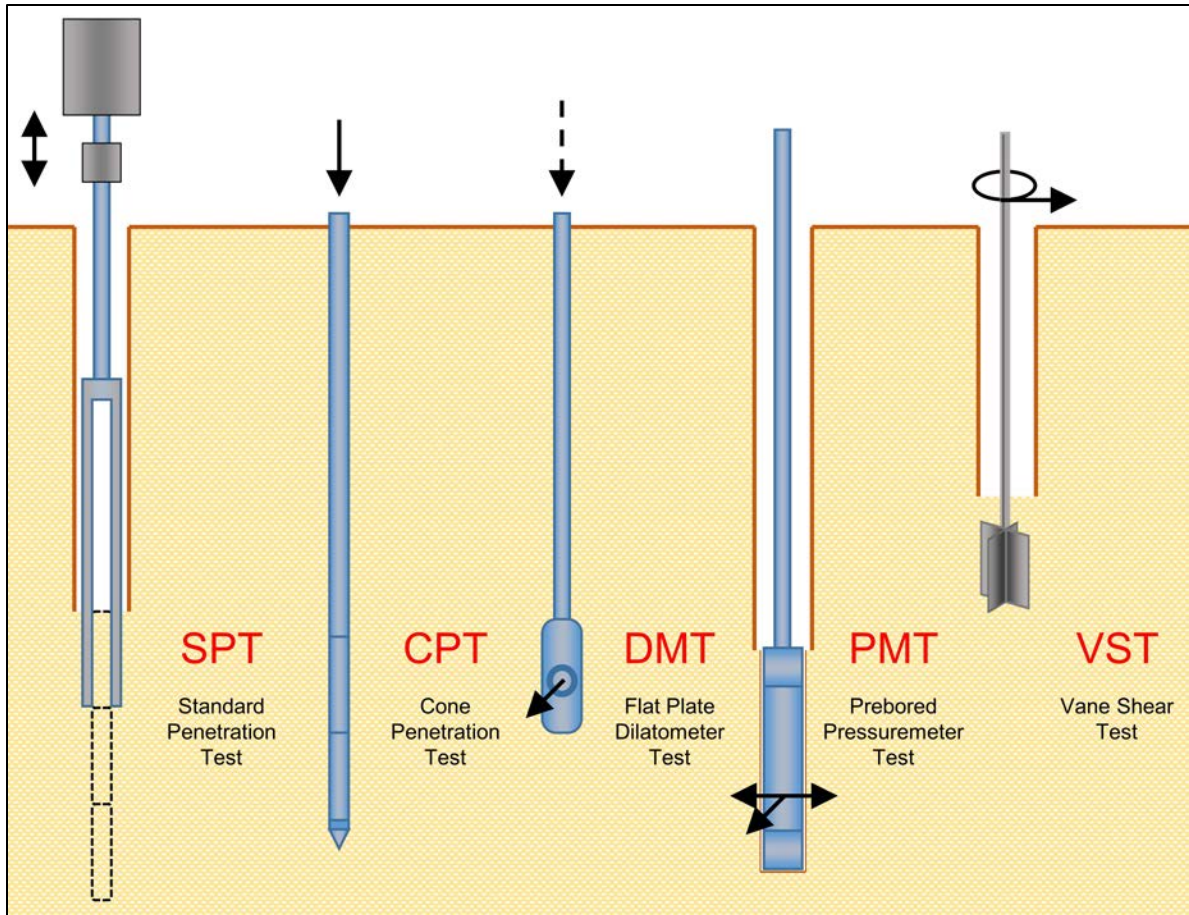


Figure 5-1 Schematic of common of in-situ tests (after Mayne et al. 2001).

5.1.1 Standard Penetration Test

The most common in-situ test in current use is the Standard Penetration Test (SPT) (ASTM D1586). During borehole advancement, the standard split spoon is driven using a 140 lb hammer from a 30 inch drop height. The sampler tip starts at the current borehole bottom and is driven 18 or 24 inches depending on sampler length. The number of blows for each 6 inch drive interval is counted, with the second and third interval summed to establish an N value. If the sampler penetrates over the increment under the weight of the drill rods or after the SPT hammer is set atop the rods, a WOR (weight of rods) or WOH (weight of hammer) designation is recorded on the boring log. Furthermore, if very dense or hard material is encountered and blow counts exceed 50 blows before finishing a 6 inch sampling interval, the SPT event is ended and the N value is designated as 50/x where x is the actual sampler penetration in inches measured for the 50 blows. This blow count and partial penetration increment should be recorded in lieu of an N value on the respective boring logs.

Table 5-2 Summary of In-Situ Methods

In-Situ Test	Information Obtained for Pile Foundation Design in Appropriate Soil Types	Advantages	Disadvantages
Standard Penetration Test (SPT) ASTM D1586	Collection of soil samples to confirm subsurface soil type. Correlations for determination of in-situ density, liquefaction susceptibility, and friction angle of sands, undrained shear strength of clays. Best suited for sand, silt, and clay materials. Not suitable in large gravel, rubble, and rock.	<ol style="list-style-type: none"> 1. Simple test. 2. Can retrieve samples to confirm soil type. 3. Equipment is widely available. 4. Correlations available for estimating soil parameters. 	<ol style="list-style-type: none"> 1. Operator and equipment dependent. 2. Samples are disturbed. 3. Cannot evaluate in-situ pore pressure. 4. Accuracy of estimated soil parameters.
Cone Penetration Test with Pore Pressure Measurements (CPTu) ASTM D5778	Continuous evaluation of subsurface stratigraphy. Correlations for determination of in-situ density and friction angle of sands, undrained shear strength of clays, and liquefaction susceptibility. Best suited for sand, silt, and clay materials. Not suitable in gravel, rubble, and rock.	<ol style="list-style-type: none"> 1. Cone can be considered as a model pile. 2. Quick and simple test. 3. Can reduce number of borings. 4. Relatively operator independent. 5. Pore pressure measurements can be used to assess soil setup effects. 6. Can help determine if penetration is drained or undrained. 	<ol style="list-style-type: none"> 1. Does not provide soil samples. 2. Should be used in conjunction with soil borings in an exploration program. 3. Local correlations can be important in data interpretation. 4. Location and saturation of porous filter can influence pore pressure measurements.
Pressuremeter Test (PMT) ASTM D4719	Bearing capacity from limit pressure and compressibility from pressure meter deformation modulus. Best suited in sand, silt, clay and soft rock. Not suitable in organic soils and hard rock.	<ol style="list-style-type: none"> 1. Tests can be performed in and below hard strata that may stop other in-situ testing devices. 2. Tests can be made on non-homogenous soil deposits. 	<ol style="list-style-type: none"> 1. Bore hole preparation very important. 2. Limited number of tests per day. 3. Limited application for axially loaded pile design.
Dilatometer Test (DMT) ASTM D6635	Correlations for soil type, earth pressure at rest, over consolidation ratio, undrained shear strength, and dilatometer modulus. Best suited for low to medium strengths sand and clay. Not suitable in dense deposits, gravel, and rock.	<ol style="list-style-type: none"> 1. Quick, inexpensive test. 2. Relatively operator independent. 	<ol style="list-style-type: none"> 1. Less familiar test method. 2. Intended for soils with particle sizes smaller than fine gravel. 3. Limited application for axially loaded pile design.
Vane Shear Test ASTM D2573	Undrained shear strength. Best suited in soft to medium clays. Not suitable in silt, sand or gravel.	<ol style="list-style-type: none"> 1. Quick and economical. 2. Compares well with unconfined compression test results at shallow depths. 	<ol style="list-style-type: none"> 1. Can be used to depths of only 13 to 20 feet without casing bore hole.
Dynamic Cone Test	Qualitative evaluation of soil density. Qualitative comparison of stratigraphy. Best suited in sand and gravel. Not suitable in clay.	<ol style="list-style-type: none"> 1. Can be useful in soil conditions where static cone (CPT) reaches refusal. 	<ol style="list-style-type: none"> 1. An unknown fraction of resistance is due to side friction. 2. Overall use is limited.

In addition to the penetration resistance that is recorded during driving, soil enters the hollow sampler, thus providing a disturbed soil sample. A schematic of the Standard Penetration Test is presented in Figure 5-2. A description of the SPT sampler was previously presented in Chapter 4 along with a photograph of the sampler in Figure 4-2.

The SPT hammer type and operational characteristics have a significant influence on the resulting SPT N values. There are two main hammer types currently in use in the U.S., the safety hammer and the automatic hammer. A third hammer type, the donut hammer, was used almost exclusively prior to about 1970 but not any longer due to safety considerations. Figure 5-3 provides illustrations of these SPT hammer types.

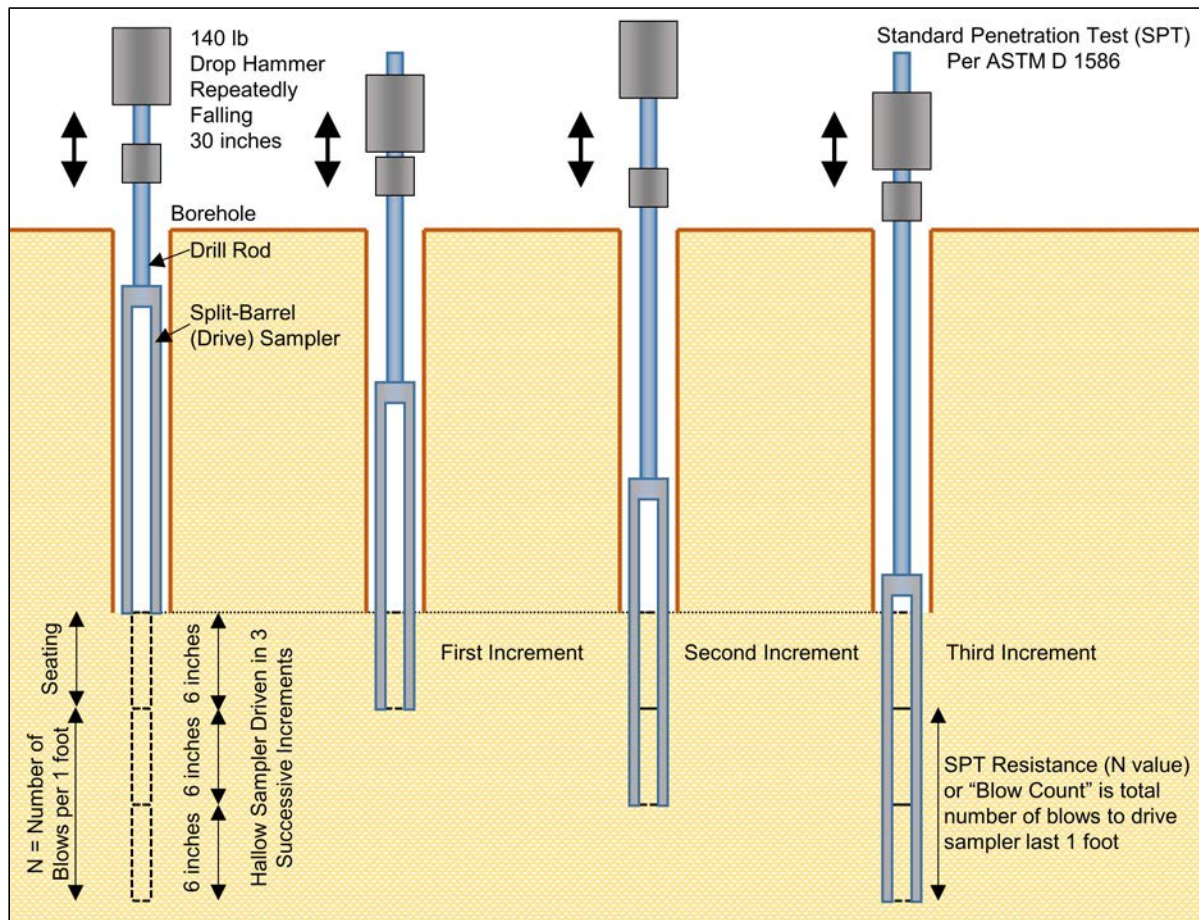


Figure 5-2 Standard Penetration Test schematic (after Mayne et al. 2001).

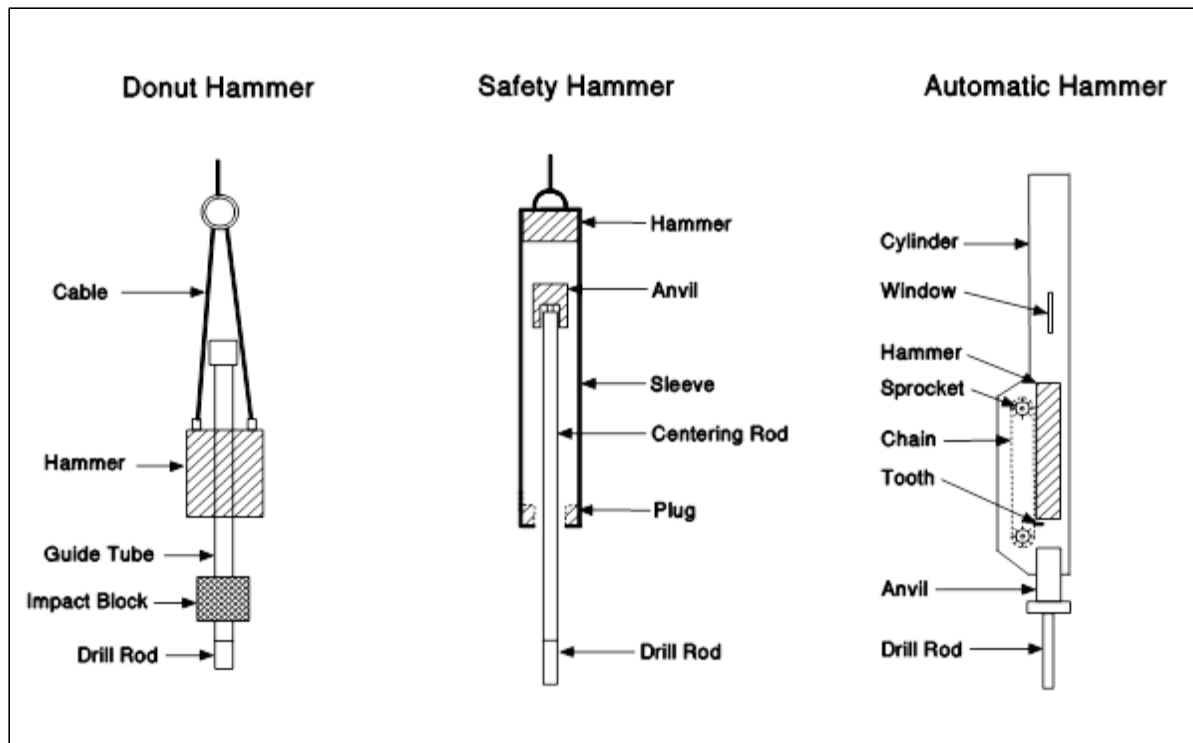


Figure 5-3 Standard Penetration Test hammer types.

Measurement studies on SPT energy transfer have been performed (e.g. Kovacs et al. 1983; Honeycutt et al. 2014). In general, these studies have indicated that the typical energy transfer from donut, safety, and automatic hammers are on the order of 45%, 60%, and 80% of the SPT test potential energy, respectively. It should not be assumed that all SPT hammers of a given type will have the energy transfer values noted above. Energy transfer for a given hammer type can and does vary according to hammer maintenance, hammer manufacturer, driller, and operating procedures. Because of these variations, it is recommended that SPT hammers undergo a yearly calibration in accordance with ASTM D4633 to document hammer performance. It may be particularly advantageous to conduct these calibrations prior to undertaking major projects. A photograph of energy transfer measurements being taken during a SPT sampling event is provided in Figure 5-4.

The use of reliable qualified drillers and adherence to recommended sampling practice cannot be overemphasized. Procurement practices should consider the drilling quality, sampling, and testing requirements needed for economical driven pile foundation design and construction.



Figure 5-4 Instrumented 2 foot long AW rod atop drill string for SPT hammer energy measurements.

The significance of the SPT hammer type and energy transfer on N values is very apparent in a pile capacity prediction symposium reported by Finno (1989). For this event, two soil borings were drilled less than 33 feet apart in a uniform sand soil profile. Figure 5-5 presents the results of the two borings, one with SPT N values obtained using a safety hammer and the other with an automatic hammer. The SPT N values from the safety hammer range from 1.9 to 2.7 times the comparable N value from the automatic hammer. This significant variation in N values clearly indicates that the type of SPT hammer used should be recorded on all drilling logs. It is recommended that SPT N values be corrected and reported as N_{60} values whenever possible. Cheney and Chassie (2000) identified ten common errors that influence SPT test results which should also be reviewed by designers and boring crews.

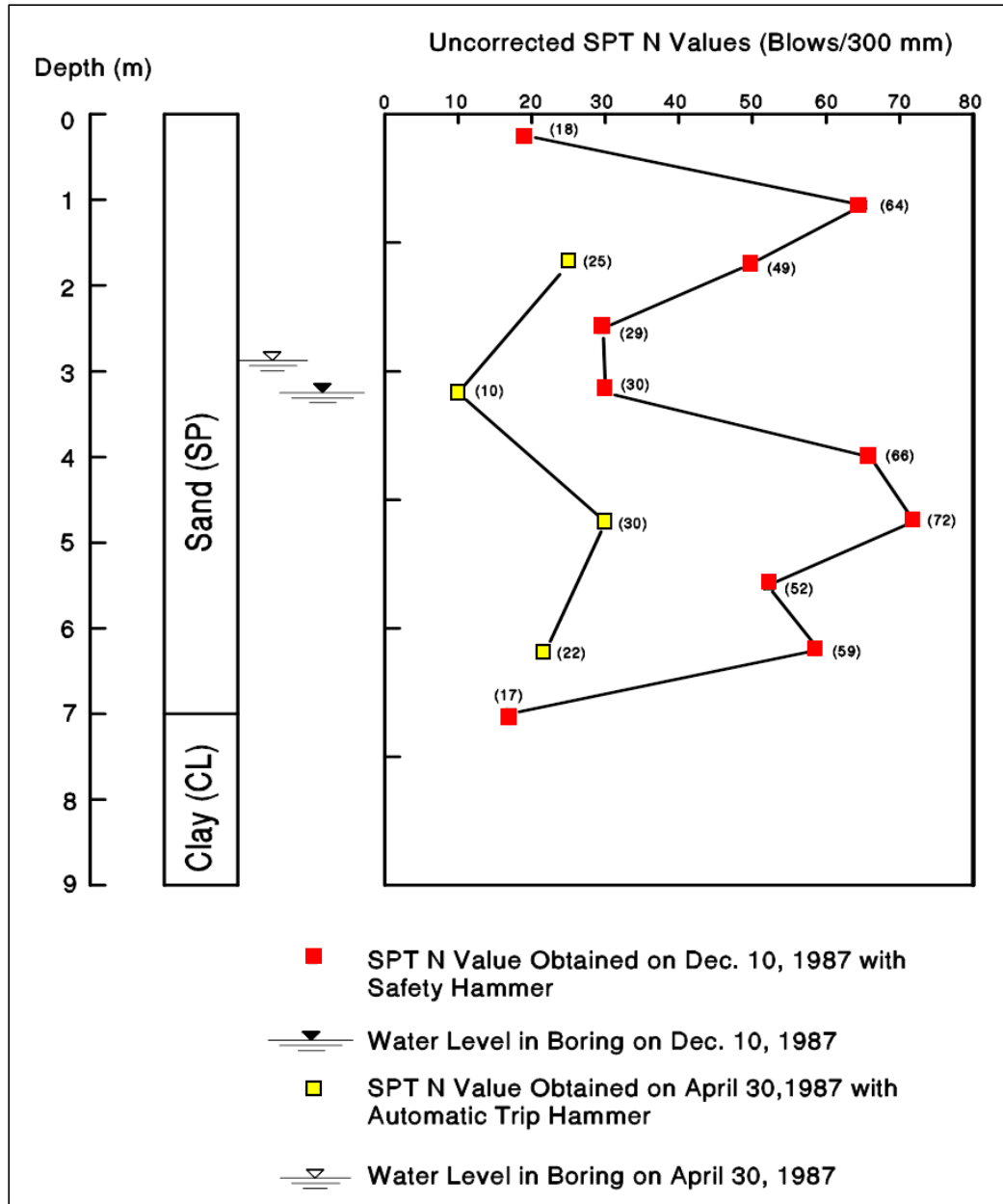


Figure 5-5 Adjacent borings with different SPT hammer types (after Finno 1989).

Although sources of error exist in the SPT test, correction and/or normalization factors have been developed to aid designers. The pile design charts and methods provided in this manual are the current standard of practice in the United States and use SPT N values based on safety hammer correlations, i.e., 60% energy transfer. Therefore SPT N values established on the basis of 60% energy transfer are referred to as N_{60} . Conversion of field SPT N values to N_{60} values based on energy transfer measurements are as follows:

$$N_{60} = N \left(\frac{ER}{60} \right) \quad \text{Eq. 5-1}$$

Where:

- N_{60} = SPT N value corrected for 60% energy transfer.
- N = uncorrected field SPT resistance value.
- ER = hammer efficiency as determined by energy measurements in accordance with ASTM D4633.

Typical SPT hammer efficiencies may also be found in geotechnical literature such as FHWA GEC-5, Sabatini et al. (2002) as well as Das (2007). The energy-corrected N_{60} value may be normalized for the effects of overburden stress, designated $(N_1)_{60}$, before being used in correlations between N values and soil properties. The general conversion is shown in Equation 5-2.

$$(N_1)_{60} = C_n N_{60} \quad \text{Eq. 5-2}$$

Where:

- $(N_1)_{60}$ = SPT N value corrected for energy and overburden stress.
- N_{60} = SPT N value corrected for 60% energy transfer.
- C_n = correction factor for SPT N value.

AASHTO specifications recommend SPT N values be corrected for overburden pressure using Equation 5-3 unless otherwise specified by the design method. Relationships for this factor have been published in the literature whereas Equation 5-3 is the recommended correction in AASHTO specifications from Peck et al. (1974). An alternate correction approach from Lio and Whitman (1986) is presented in Equation 5-4.

$$C_n = 0.77 \log \left[\frac{40}{\sigma'_{vo}} \right] \leq 2.0 \quad \text{Eq. 5-3}$$

$$C_n = \left(\frac{p_a}{\sigma'_{vo}} \right)^n \quad \text{Eq. 5-4}$$

Where:

- p_a = atmospheric pressure (ksf).
- σ'_{vo} = vertical effective stress at the sample depth (ksf).
- n = exponent typically equal to 1 in clays (Olsen 1997) and 0.5 in sandy soils (Lio and Whitman 1986).

Corrected N values are used for soil strength parameter correlations presented in Section 5.2. Note that correlations between cohesive soil and physical properties with N values are crude and, therefore, correction of N values in cohesive soils is generally not necessary.

5.1.2 Cone Penetration Test

The cone penetration test (CPT) was first introduced in the U.S. in 1965. By the mid 1970's, the electronic cone began to replace the mechanical cone, and in the early 1980's, the piezocone or cone penetration test with pore pressure measurements (CPTu) became readily available. A NCHRP synthesis by Mayne (2007) provides a good summary of cone penetration testing practices and use by transportation agencies in the US and Canada. The CPT/CPTu has developed into one of the most popular in-situ testing devices. Part of this popularity is due to the CPT's ability to provide large quantities of useful data quickly and at an economical cost. Depending upon equipment capability as well as soil conditions, 300 to 1200 feet of penetration testing may be completed in one day.

Current cone penetration testing relies on the use of electronic cone penetrometers with pore pressure measurements. In the cone penetration test, a cone penetrometer with a cross sectional area of 1.55 or 2.33 inch² and a 60° conical tip is attached to a series of rods and is continuously pushed into the ground. The cone also contains a friction sleeve located behind the conical tip. Pore pressure measurements are obtained with all modern cones from a pore pressure transducer located behind the conical tip and just before the friction sleeve. Pore pressure measurements at this location are referred to as the u_2 position.

Typically, a hydraulic ram with 10 to 40 kips of thrust is used to continuously advance the cone into the ground at a rate of 0.8 in/sec. Built in load cells are used to continuously measure the cone tip resistance, q_c , the unit sleeve friction resistance, f_s , and the pore pressure, u , during penetration. The pore pressure measurement is used to correct the measured cone tip resistance, q_c , for geometrical effects that reduce the measured value in proportion to the amount of pore pressure that is generated. The resulting corrected tip resistance is referred to as q_t . The friction ratio, R_f , is defined as f_s/q_t and is commonly used in the interpretation of test results. Careful porous element and cavity saturation is essential to obtain pore pressure measurements. Test procedures may be found in ASTM D5778. Both size cones are displayed in Figure 5-6 with a CPT rig shown in Figure 5-7.



Figure 5-6 Cone penetrometers (after Mayne et al. 2001).



Figure 5-7 CPT rig.

Modern cones may be further divided into three main types, the piezocone (CPTu), the seismic piezocone (SCPTu), and the resistivity piezocone (RCPTu). The CPTu can also be used to monitor pore pressure dissipation. The seismic cone includes a horizontal geophone above the friction sleeve which allows calculation of shear wave velocity at selected depths. The resistivity cone uses electrical conductivity or resistivity which allows detection of the freshwater – salt water interface or profiling of contaminated groundwater plumes. Since pore pressure measurements are made with all modern electronic cone penetrometers, the abbreviation CPT will be used hereafter and assume that pore pressure measurements are included.

Data collected with CPT can provide a continuous profile of the subsurface stratigraphy. A soil behavior chart developed by Robertson (1990) for CPT data is presented in Figure 5-8. From correlations with CPT data, evaluations of in-situ relative density, D_r , and effective friction angle, ϕ' , of cohesionless soils as well as the undrained shear strength, s_u , of cohesive soils can be made. Correlations for determination of other soil properties, liquefaction susceptibility, and estimates of SPT N_{60} values may also be determined. The accuracy of these correlations may vary depending upon geologic conditions. Correlation confirmation with local conditions is therefore important.

The primary advantage of CPT testing is the ability to rapidly develop a continuous profile of subsurface conditions more economically than other subsurface exploration or in-situ testing tools. Because the CPT collects continuous data, it can delineate fine changes in stratigraphy and characterize site variability better than other methods. Engineering properties can be assessed through empirical correlations. For cohesionless soils, these empirical engineering property correlations are accurate and commonly used. For cohesive soils, engineering property correlations are less accurate. CPT results are relatively operator independent and highly repeatable. Because of these advantages, the CPT is increasingly being used as an equal or superior subsurface exploration method in some stratigraphic conditions such as alluvial sites and liquefiable soils. In other subsurface conditions, CPT may be used to reduce the number of conventional borings needed on a project, or to focus attention on discrete zones for detailed soil sampling and testing.

Limitations of CPT testing include the inability to push the cone in dense or coarse soil deposits. In general, soils with SPT N values greater than about 30 to 40 are difficult to test with CPT equipment. To penetrate dense layers, cones are sometimes pushed in bore holes advanced through the dense strata. While CPT can be used in marine environments, the soundings must be performed from a fixed

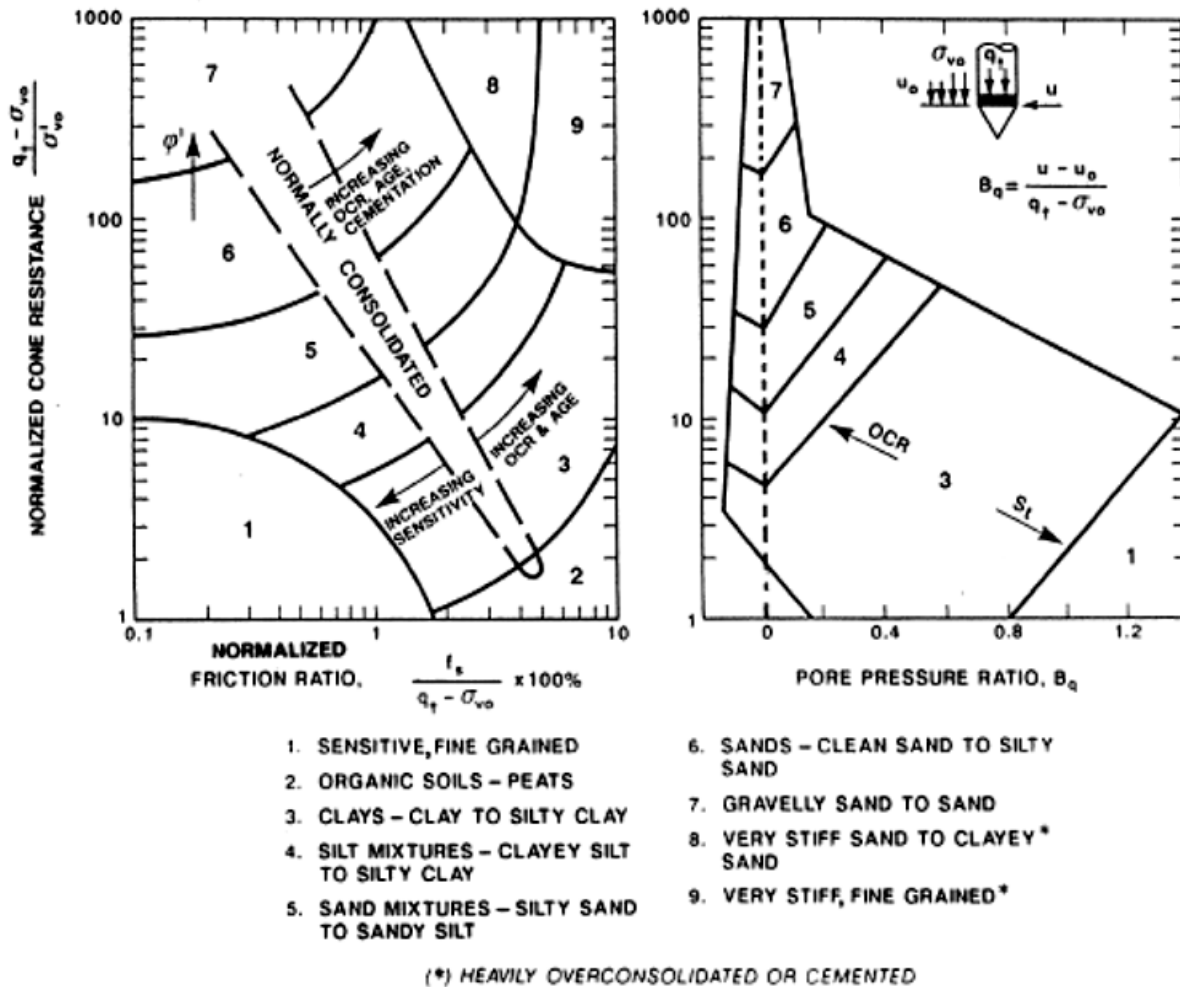


Figure 5-8 Soil behavior type classification chart based on normalized CPT data (after Robertson 1990).

platform (e.g., a jack-up barge) with sufficient casing to provide lateral support for the rods or specialized submersible equipment is will be required. Another limitation is that soil samples are generally not obtained during routine CPT programs for confirmation of stratigraphy. Local correlations are also important in data interpretation.

5.1.3 Vane Shear Test

The vane shear test is an in-situ test for determining the undrained shear strength of soft to medium clays. Figure 5-9 is a schematic drawing of the essential components and test procedure. The test consists of forcing a four bladed vane into undisturbed soil and rotating it until the soil shears. Two shear strengths are usually

recorded, the peak shearing strength and the remolded shearing strength. These measurements are used to determine the sensitivity of clay and allows for analysis of the soil resistance to be overcome during pile driving. It is necessary to measure skin friction along the steel connector rods which must be subtracted to determine the actual shear strength. The vane shear test generally provides the most accurate undrained shear strength values for clays when undrained shear strengths are less than 1 ksf. A detailed test procedure may be found ASTM D2573.

It should be noted that the sensitivity of clay determined from a vane shear test provides insight into the setup potential of the clay deposit. Soil setup may then be used for pile drivability and resistance evaluations. However, the sensitivity value is a qualitative and not a quantitative indicator of soil setup.

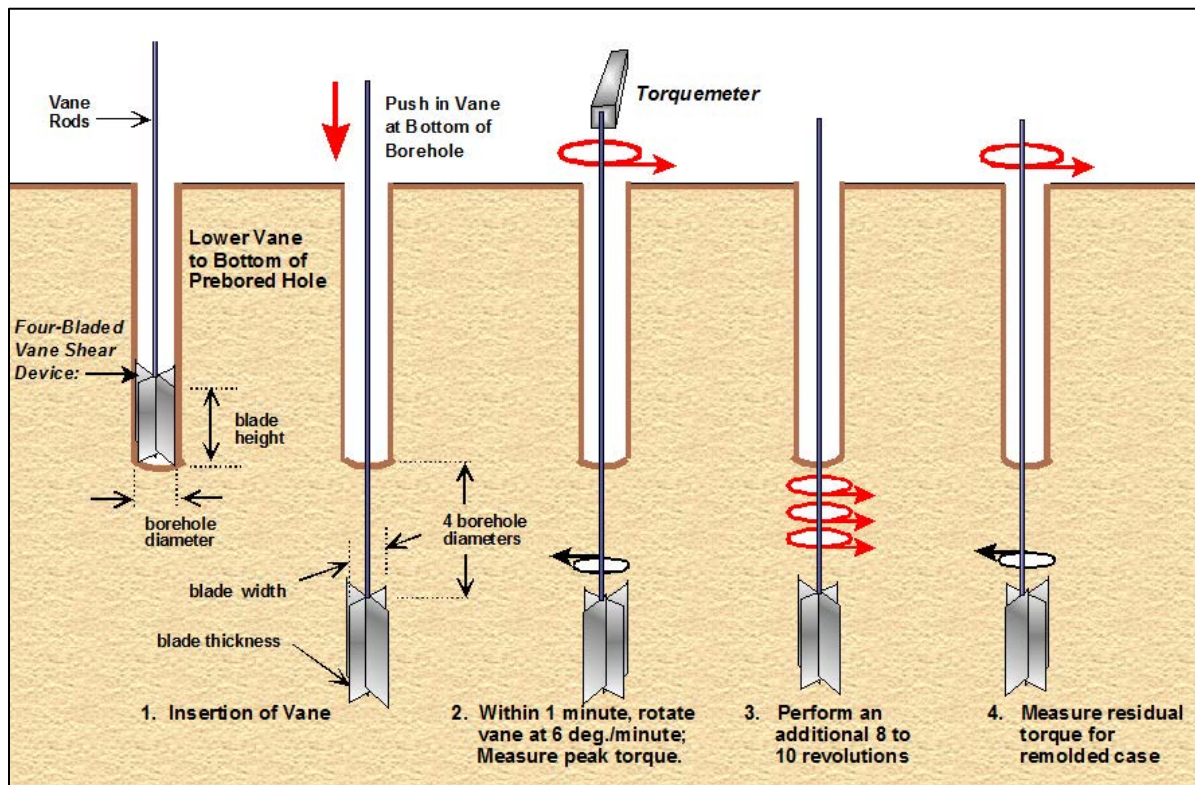


Figure 5-9 Vane shear test schematic (after Mayne et al. 2001).

5.1.4 Other In-Situ Tests

Other in-situ tests with limited application to pile foundation design include the dilatometer, the pressuremeter, and the dynamic cone. These are briefly discussed in the following sections.

5.1.4.1 Dilatometer Test

The dilatometer test (DMT) is an in-situ testing device that was developed in Italy in the early 1970's and first introduced in the U.S. in 1979. Like the CPT, the DMT is generally hydraulically pushed into the ground although it may also be driven. When the DMT can be pushed into the ground with tests conducted at 8 inch increments, 100 to 300 feet of DMT sounding may be completed in a day. The primary utilization of the DMT in pile foundation design is the delineation of subsurface stratigraphy and interpreted soil properties. However, it would appear that the CPT/CPTu is generally better suited to this task than the DMT. The DMT may be a potentially useful test for design of piles subjected to lateral loads. For axially loaded piles, the dilatometer test has limited direct value. The test procedures for DMT are presented in ASTM D6635.

5.1.4.2 Pressuremeter Tests

The pressuremeter test (PMT) is an in-situ device used to evaluate soil and rock properties, and imparts lateral pressures to the soil, allowing for soil shear strength and compressibility to be determined by interpretation of a pressure-volume relationship. Deposits such as soft clays, fissured clays, sands, gravels and soft rock can be tested with a pressuremeter. A pressuremeter test produces information on the elastic modulus of the soil as well as the at rest horizontal earth pressure, the creep pressure, and the soil limit pressure. For piles subjected to lateral loads, the pressuremeter test is a useful design tool and can be used for determination of p-y curves. However for design of vertically loaded piles, the pressuremeter test has limited value. Pile design procedures using pressuremeter data have been developed and may be found in FHWA-IP-89-008, The Pressuremeter Test for Highway Applications, Briaud (1989). Details on test procedures may be found in ASTM D4719, Standard Test Method for Pressuremeter Testing in Soils.

5.1.4.3 Dynamic Cone

There are two types of dynamic penetrometers with conical points. The dynamic cone type that is most often used has a shaft diameter that is smaller than the cone diameter. Theoretically, due to the cone being larger than the shaft, the penetrometer measures only point resistance. A lesser used cone type has a shaft and cone of the same diameter. This type of dynamic cone penetrometer records both skin friction and point resistance, but the two components cannot be analyzed independently. Equations have been developed for determining the geotechnical

resistance of pile foundations by using the dynamic cone test data. However, these are not used extensively and the dynamic cone penetrometer is not recommended for final foundation design unless specific local correlations with load tests to geotechnical failure have been taken.

5.2 SOIL PARAMETERS

Index properties and engineering properties for geomaterials are derived from field and laboratory testing. Differing soil and rock types may be segregated through index tests which aid in the division of subsurface strata for design. These properties are typically obtainable through routine sampling and testing methods, and assist with constructability limitations or preliminary pile selection based on soil type and loading conditions. Engineering properties for soil and rock include shear strength, compressibility and permeability. Shear strength values can be used to determine driven pile geotechnical resistances while compressibility information can be used to check service limit states. Permeability is not generally quantified for pile design purposes, however certain slow draining soils can influence pile drivability, and therefore knowledge of these areas may assist in constructability concerns. Further information on laboratory testing of soils may be found in Bowles (1992), as well as in GEC-5 by Sabatini et al. (2002) and Samtani and Nowatzki (2006) among other sources.

5.2.1 Soil Classification and Index Properties

Two soil classification systems are in common use for transportation projects. The AASHTO soil classification system is used by many transportation agencies for pavement features while the Unified Soil Classification System (USCS) is utilized for nearly all other geotechnical work. The USCS is better suited to deep foundation design and will therefore be solely used in this manual.

Routine index tests for classification include a particle size distribution, Atterberg limits and moisture content. Additional index tests include specific gravity and soil unit weight. A summary of these index tests is shown in Table 5-3.

Laboratory tests to determine the fine content and gradation of cohesionless soils and the remolded shear strength of cohesive soils are important in assessing pile drivability and potential soil setup effects (changes in nominal resistance with time).

Table 5-3 Soil Index Tests used for Driven Pile Design
(modified from Brown et al. 2010)

Test	Index Property Determined	Soil Type	Application	Standard Test Procedure
Particle Size Distribution (Mechanical and Hydrometer)	Grain Size Distribution	Sieve on all Soils; Hydrometer on Minus #200	USCS classification Aids in evaluation of densification and liquefaction potential for cohesionless soils	ASTM D422 AASHTO T88
Atterberg Limits	Liquid Limit (LL) Plastic Limit (PL) Plasticity index (PI) $PI = LL - PL$ Liquidity Index (LI) $LI = (w_n - PL) / PI$	Minus #40	USCS classification Soil consistency Engineering property correlations	ASTM D4318 AASHTO T89 AASHTO T90
Moisture Content	Moisture Content, w_n	Undisturbed Samples; Split-Spoon Samples with Moisture Change	Soil Consistency May aid in determination of water table elevation	ASTM D2216 AASHTO T265
Unit Weight (Undisturbed)	Total Unit Weight, γ OR Density, ρ	Fine-grained (Cohesive)	Aids evaluation of underground soil stresses	ASTM D7263 AASHTO T38
Specific Gravity	Specific Gravity, G_s	Minus #4	Aids evaluation of soil density and compressibility	ASTM D854 AASHTO T100
Soil Classification	USCS Group Name and Group Symbol;	All Soils	Physical characteristics define soil types	ASTM D2487

The relative density, gradation, and fine content of cohesionless soils provide useful information in assessing pile drivability. Soils with a high fine content generally have lower angles of internal friction than lower fine content soils of similar density. A high fine content can also affect soil drainage and pore pressures during shear, and thus, the effective stresses acting on a pile during driving. Depending upon soil density, cohesionless soils with high fine contents are also more likely to

demonstrate soil setup than cohesionless soils with little or no fines. The gradation and angularity of the soil grains also influences the angle of internal friction. Gradation information is also useful in assessing the densification and liquefaction potential of cohesionless soils.

Routine laboratory grain size analyses (mechanical and hydrometer) can quantify gradation and fine content. With this information, improved assessments of pile drivability and soil setup potential in cohesionless soils can be made. Cohesive soils may lose a significant portion of their shear strength when disturbed or remolded, as during the pile driving process. The ability to estimate the soil strength at the time of driving and the resulting strength gain with time or soil setup is a key component of economical pile design in cohesive soils. Soil setup is discussed further in Chapter 7. The sensitivity of a cohesive soil can provide a qualitative but not quantitative indication of potential soil setup. Sensitivity determined in-situ with a vane shear device provides the best assessment of cohesive soil sensitivity. However, the sensitivity of a cohesive soil can also be determined from laboratory tests on undisturbed and remolded samples to determine respective shear strength values.

The sensitivity of a cohesive soil, S_t , is defined as:

$$S_t = \frac{q_{u,undisturbed}}{q_{u,remolded}} \quad \text{Eq. 5-5}$$

Table 5-4 contains typical values of sensitivity as reported by Sowers (1979) which may be useful for preliminary estimates of remolded shear strength. Terzaghi and Peck (1967) noted that clays with sensitivities less than 16 generally regain a portion to all of their original shear strength with elapsed time. Based upon typical sensitivity values reported by Terzaghi et al. (1996) as well as by Sowers (1979), the remolded shear strength of many cohesive soils during pile driving would be expected to range from about 1/3 to 1/2 the undisturbed shear strength.

Table 5-4 Typical Values of Sensitivity (after Sowers 1979)

Soil Type	Sensitivity
Clay of medium plasticity, normally consolidated	2-8
Highly flocculent, marine clays	10-80
Clays of low to medium plasticity, overconsolidated	1-4
Fissured clays, clays with sand seams	0.5-2

Additional information on index testing of soil may be found in GEC-5 by Sabatini et al. (2002) as well as in Samtani and Nowatzki (2006). Section 5.4 provides additional insight and discussion on drivability considerations.

5.2.2 In-Situ Stress

For the design of driven piles, the in-situ state of stress at a given depth is needed to calculate geotechnical resistance. A basic assessment of stress calculation in soil is provided in this section. Further detail is provided in the literature including Sabatini et al. (2002), Samtani and Nowatzki (2006), and Das (2007) among other sources. The reader is directed to these resources for in depth coverage of this topic.

For geotechnical analyses, the effective soil stress is utilized for design. The effective stress, σ' , is the difference of total stress, σ , and pore water pressure, u , and may be expressed as Equation 5-6.

$$\sigma' = \sigma - u \quad \text{Eq. 5-6}$$

The total stress at a given depth is generally the product of total soil unit weight for each soil strata, γ_i , and strata thickness, h_i . Often multiple soils with ranges in unit weight exist at a given location. Therefore a summation of these layers accounts for the total stress calculation with depth as illustrated in Equation 5-7. Pore water pressure is a function of the unit weight of water, γ_w , and the pressure head, h_w , as shown in Equation 5-8.

$$\sigma = \sum_i^n (\gamma_i h_i) \quad \text{Eq. 5-7}$$

$$u = \gamma_w h_w \quad \text{Eq. 5-8}$$

The vertical effective stress at a given depth may be calculated as follows:

$$\sigma'_{vo} = \sum_i^n (\gamma_i h_i) - \gamma_w h_w \quad \text{Eq. 5-9}$$

Above the water table, free draining, coarse grained soils may be assumed dry. More likely however, this soil is partially saturated, particularly in the vadose zone where negative pore water pressure results from capillary effects. Accurate soil unit weights should be therefore be reflected in this effective stress calculation. The lateral resistance for deep foundations is affected by the horizontal effective stress. Determination of the effective horizontal stress at a given depth, σ'_{ho} , condition may

be evaluated by relating the vertical effective stress and the at rest lateral earth pressure coefficient, K_o , using Equation 5-10.

$$K_o = \frac{\sigma'_{ho}}{\sigma'_{vo}} \quad \text{Eq. 5-10}$$

Selection of effective stress or total stress usage for design is contingent upon the structural loading conditions and soil properties. For piles driven in free draining clean sands, an analysis would generally include the use of effective stress parameters since it may be assumed pore water pressure dissipates almost immediately after loading the soil. Conversely for clays or other slow draining soils, an increase in pore water pressure will be apparent immediately after loading. A total stress analysis may therefore be practical for this condition. The responsible engineer should exercise clear judgment involving loading conditions and the selection of design parameters.

5.2.3 Shear Strength

Shear strength is an internal resistance per unit area that the geomaterial can provide to resist failure along a plane. Compositional, environmental and in-situ factors combine to define the overall shear strength of a soil, which contributes to the geotechnical strength limit state for design. Geomaterial shear strength is also influenced by the manner (static, dynamic, cyclic) and rate of loading.

GEC-5 by Sabatini et al. (2002) notes several issues relevant to shear strength evaluations for driven pile designs. These include variation of the soil shear strength between the time the pile is driven and when load application occurs. Time dependent strength increases, referred to as soil setup, are often observed in saturated, normally consolidated to moderately over consolidated clays and fine-grained material. Conversely, a decrease in strength with time, referred to as relaxation, is often observed for heavily over consolidated clays, dense silts, dense fine sands, and weak laminated rock. Therefore, shear strength evaluations should consider both of these long and short term conditions.

Shear strength may also vary due to changes in site conditions that affect the in-situ effective stress state. Site conditions that may increase or decrease soil shear strength values include site dewatering, surface loading, and excavations. Granular soil strengths may also change over time due to densification from driving. This potential shear strength increase should be evaluated relative to pile drivability and constructability considerations.

The Mohr-Coulomb failure criterion will be the only model discussed herein and is shown in Equation 5-11.

$$\tau = c + \sigma \tan \phi \quad \text{Eq. 5-11}$$

Where:

- τ = shear stress at failure (shear strength).
- c = cohesion.
- σ = total normal stress (pressure) on plane of failure.
- ϕ = angle of internal friction.

Equation 5-11 is used for total stress analysis and uses an undrained friction angle and cohesion. For cases where effective stress or drained parameters are necessary, this equation is modified to Equation 5-12.

$$\tau = c' + \sigma' \tan \phi' \quad \text{Eq. 5-12}$$

Where:

- τ = shear stress at failure (shear strength).
- c' = effective cohesion.
- σ' = effective normal stress (pressure) on plane of failure.
- ϕ' = effective stress angle of internal friction.

In this drained situation, typically cohesionless soils exist, therefore c' is assumed equal to zero. However upon careful evaluation, c' may be included to account for certain conditions including cemented soils, partially saturated soils and heavily over consolidated clays. Determination of c' should be carefully selected on interpretation of the test data due to its strong influence on pile design results.

For short-term, undrained loading of cohesive soils, Equation 5-11 can be simplified to a total stress approach. Typically, cohesive soils exhibit a friction angle, ϕ , equal to zero, therefore Equation 5-13 reflects this behavior.

$$\tau = c = s_u \quad \text{Eq. 5-13}$$

Where:

- τ = shear stress at failure (shear strength).
- c = cohesion.
- s_u = undrained shear strength.

In addition to the above mentioned case, rapid loading of slow draining (low permeability) soil generates excess pore water pressure that is not easily quantified. Moreover, to simplify the shear stress calculation, the cohesion determined via testing may be assumed equal to the design shear strength while in-situ states of stress, water content, loading rate, and other variables are unknown.

5.2.3.1 Laboratory Tests for Soil Shear Strength

Three test methods are commonly used to measure shear strength in the laboratory. A brief description of each test method is provided in the subsequent sections. Further details on the test procedure and analysis may be found in GEC-5 by Sabatini et al. (2002), as well as the respective ASTM designations. The three test methods are as follows:

1. Direct shear test (AASHTO T236 / ASTM D3080).
2. Unconfined compression test (AASHTO T208 / ASTM D2166).
3. Triaxial compression test (AASHTO T234 / ASTM D2850).

5.2.3.1.1 Direct Shear

The direct shear test is performed by placing a sample of soil into a shear box which is split into two parts at mid height. A normal load is then applied to the top of the sample and one half of the shear box is pulled or pushed horizontally past the other half. The shear stress is calculated from the horizontal force divided by the sample area and is plotted versus horizontal deformation. A plot of at least three normal stresses and their corresponding maximum shear stresses provides the shear strength parameters c and ϕ . Bowles (1977) notes that the ϕ values determined from plane strain direct shear tests are approximately 1.1 times the ϕ values determined from triaxial tests. Direct shear tests are primarily performed on recompacted granular soils, which may not represent their in-situ conditions, and are generally not recommended for cohesive soils due to limitations on drainage control during shear.

5.2.3.1.2 Unconfined Compression

The unconfined compression test is a widely used laboratory test to evaluate the shear strength of cohesive soil and rock. In the unconfined compression test, an axial load is applied on a cylindrical sample while maintaining a zero lateral or confining pressure. Axial loading is increased to failure and the shear strength is

then considered to be one half the axial stress at failure. Unconfined compression tests are performed only on cohesive soil and rock samples.

Unconfined compression tests on cohesive soil samples recovered from deeper depths or samples with a secondary structure, such as sand seams, fissures, or slickensides, can give misleadingly low shear strengths. This is due to the removal of the in-situ confining stress normally present. Triaxial compression tests provide improved information on soil shear strength in these cases.

5.2.3.1.3 Triaxial Compression Test

The most versatile shear strength test is the triaxial compression test. Triaxial tests allow a soil sample to be subjected to three principal stresses under controlled conditions. A cylindrical test specimen is encased in a rubber membrane and is then subjected to a confining pressure. Drainage from the sample is controlled through its two ends as the shearing force is applied axially and increased to failure. A plot of normal stress versus shear stress is developed and parameters c and ϕ are determined. In triaxial tests where full drainage is allowed during shear, or in undrained tests with pore pressure measurements during shear, the effective stress parameters c' and ϕ' can be determined.

In triaxial compression tests, the drainage, consolidation, and loading conditions are selected to simulate the applicable field conditions for the shear strength evaluation. Triaxial compression tests are classified according to the consolidation and drainage conditions allowed during testing. The three test types normally conducted are unconsolidated undrained (UU) (ASTM D 2850), consolidated undrained (CU) (ASTM D 4767), and consolidated drained (CD) (ASTM D 7181). Unconsolidated undrained tests provide more reliable shear strength values than those obtained from unconfined compression tests. Consolidated undrained tests with pore pressure measurements provide both effective stress and total stress parameters.

5.2.3.2 Effective Stress Friction Angle Correlations, Cohesionless Soils

For pile design in cohesionless soil, the effective internal friction angle is typically correlated from in-situ test results. Usually, the SPT N value or CPT cone resistance provides this relationship. Care should be exercised when using any SPT N value to soil parameter correlation. Depending upon the date and method, the correlation may be based on an uncorrected N value from a certain SPT hammer type or a corrected $(N_1)_{60}$. AASHTO (2014) design specifications note that the designer should ascertain the basis of the correlation and use $(N_1)_{60}$ or N , as appropriate. The

SPT $(N_1)_{60}$ correlation to ϕ' in AASHTO is presented in Table 5-5 and is the basis of the AASHTO resistance factors associated with the AASHTO calibrations.

Table 5-5 AASHTO (2014) Correlation Between SPT $(N_1)_{60}$ values to Drained Friction Angle of Granular Soils (modified after Bowles 1997)

SPT Blow Count, $(N_1)_{60}$ (blows/ft)	Angle of Internal Friction ϕ' (degree)
< 4	25-30
4	27-32
10	30-35
30	35-40
50	38-43

FHWA GEC-5 (2002) provides a different correlation for effective friction angle based upon the SPT N value. This correlation, presented in Table 5-6, was originally tabulated in Meyerhof (1956) for relatively clean sands. Sabatini et al. (2002) in GEC-5 recommended ϕ' be reduced by 5° for clayey sand and increased by 5° for gravelly sand.

Table 5-6 Correlation Between Relative Density, SPT N value, and Internal Friction Angle for Cohesionless Soils in GEC-5 (2002) (after Meyerhof 1956)

State of Packing	Relative Density, D_r (%)	SPT Blow Count, N (blows/ft)	Angle of Internal Friction ϕ' (degree)
Very Loose	< 20	< 4	< 30
Loose	20-40	4-10	30-35
Compact	40-60	10-30	35-40
Dense	60-80	30-50	40-45
Very Dense	> 80	> 50	> 45

Note: In saturated fine sand or silty sand, $N = 15 + (N' - 15) / 2$ for $N' > 15$ where N is the blow count corrected for dynamic pore pressure effects during the SPT, and N' is the measured blow count.

Other correlation methods between corrected N values and laboratory test results have been published to provide drained friction angle equations for sands and gravels. Each method provides a correlation based upon the respective soil type, sampling method, and testing technique used.

Schmertmann (1975) assessed test data from clean sands and provides a correlation between friction angle, SPT N values and overburden stress. The data is interpreted for depths greater than 7-ft, for which Kulhawy and Mayne (1990) approximated a relationship as Equation 5-14.

$$\phi' = \tan^{-1} \left[\frac{N_{60}}{12.2 + 20.3 \left(\frac{\sigma'_{vo}}{P_a} \right)} \right]^{0.34} \quad \text{Eq. 5-14}$$

Hatanaka and Uchida (1996) utilized ground freezing to extract undisturbed samples of fine and medium sands. After subjecting samples to drained triaxial compression tests, an effective friction angle correlation to $(N_1)_{60}$ was established as shown in Equation 5-15.

$$\phi' = \sqrt{20(N_1)_{60}} + 20 \quad \text{Eq. 5-15}$$

Kulhawy and Chen (2007) performed strength tests on samples of sand and gravel. Although this study was performed to assess the uplift capacity of drilled shafts, a variable spread of sands and gravels were analyzed, and compared well with the Meyerhof (1956) correlations. For the combined 57 samples, a regression analysis ($r^2=0.356$, $n=57$) provided the relationship in Equation 5-16.

$$\phi' = 27.5 + 9.2 \log[(N_1)_{60}] \quad \text{Eq. 5-16}$$

Similar to correlations developed for the SPT, the effective friction angle may be compared to the CPT/CPTu generally via cone tip resistance, q_c . Meyerhof (1976) correlations are shown in Table 5-7 for relatively clean sands.

Table 5-7 Correlation Between Relative Density, CPT Cone Resistance, and Angle of Internal Friction for Clean Sands (after Meyerhof 1976)

State of Packing	Relative Density D_r (%)	Cone Tip Resistance q_c (tons/ft ²)	Angle of Internal Friction ϕ' (degree)
Very Loose	< 20	< 4	< 30
Loose	20-40	4-10	30-35
Compact	40-60	10-30	35-40
Dense	60-80	30-50	40-45
Very Dense	> 80	> 50	> 45

Robertson and Campanella (1983) compared cone resistance to drained triaxial compression tests results on clean, quartz sands. Using the cone tip resistance, a relationship to effective friction angle was presented by Kulhawy and Mayne (1990). This is shown in Equation 5-17.

$$\phi' = \tan^{-1} \left[0.1 + 0.38 \log \left(\frac{q_c}{\sigma'_{vo}} \right) \right] \quad \text{Eq. 5-17}$$

Where:

- ϕ' = effective stress angle of internal friction.
- q_c = cone tip resistance.
- σ'_{vo} = vertical effective stress at the sample depth.

For layers with cobbles and boulders, SPT N value correlations for the material friction angle can be problematic particularly when the material contains particles larger than the size of the split spoon sampler. The resultant inflated N values can result in overestimation of the friction angle of the rockfill materials. Therefore, the drained friction angle of rockfills, gravels, and sands can be estimated from Figure 5-10 using the appropriate rockfill grade from Table 5-8 in conjunction with the effective normal stress. The rockfill grades of A through E identified in Table 5-8 are based on the unconfined compressive strength of the rockfill particles. Once the rockfill grade is determined, a representative drained friction angle can be obtained from Figure 5-10 using the average effective normal stress in the layer. The secant friction angle is based on a straight line constructed from the origin of the Mohr circle diagram to the intersection with the strength envelope at the effective normal stress as detailed in Terzaghi et al (1996).

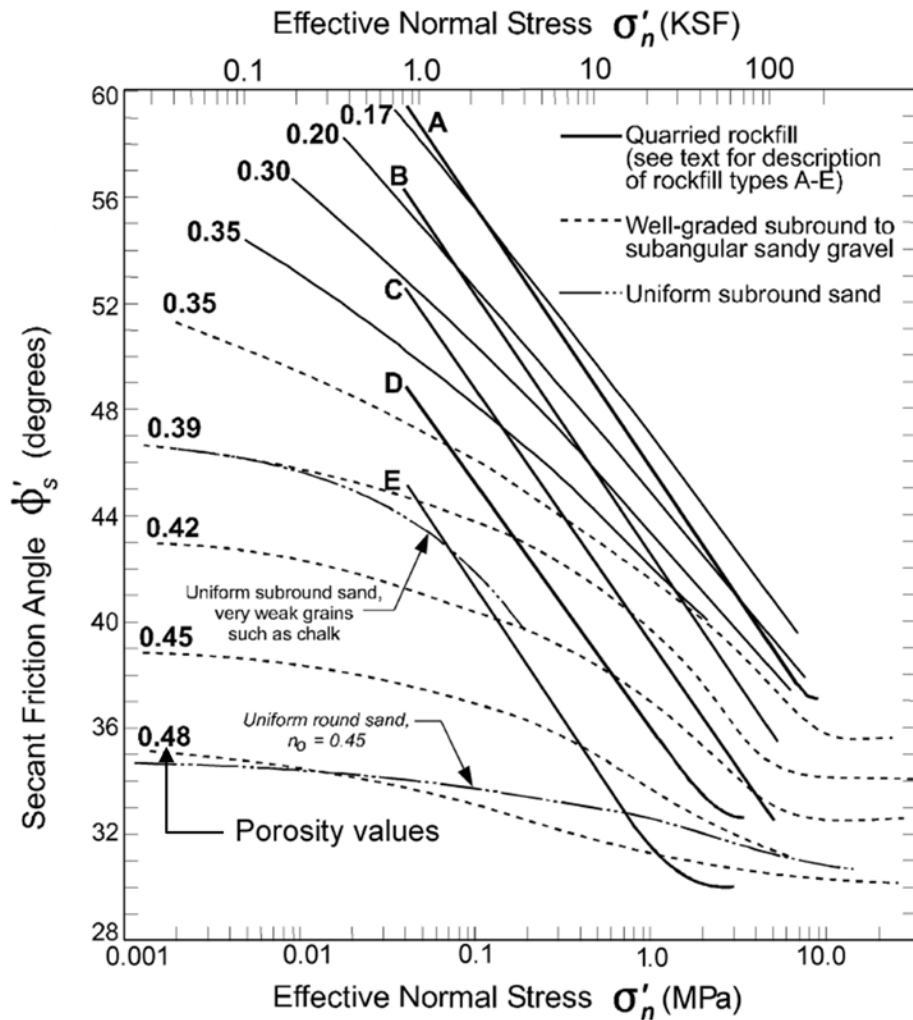


Figure 5-10 Typical ranges of friction angle for rockfills, gravels and sands (Note: 1 kPa = 0.145 psi) (after Terzaghi et al. 1996).

Table 5-8 Unconfined Compressive Strength of Particles for Rockfill Grades in Figure 5-12

Rockfill Grade	Particle Unconfined Compressive Strength (ksf)
A	≥ 4610
B	3460-4610
C	2590-3460
D	1730-2590
E	≤ 1730

5.2.3.3 Fully Drained Shear Strength of Fine-Grained Cohesive Soils

Effective stress analysis methods may be used for fine grained soils under fully drained loading. This approach is useful to assess driven pile resistances a significant time after pile installation when pore water pressure has stabilized. For these cases, laboratory testing is recommended by AASHTO (2014) to produce effective stress design parameters ϕ' and c' . Consolidated drained direct shear tests, consolidated drained (CD) triaxial tests or consolidated undrained (CU) triaxial tests with pore pressure measurements may be used to determine these shear strength parameters. Consideration for shear rate should be provided during these laboratory tests. Furthermore, complete dissipation of excess pore pressure for drained tests or equalization of pore pressure throughout the sample in undrained tests should be confirmed.

Preliminary estimates for effective friction angle may be interpreted from plasticity index (PI) tests. Terzaghi et al. (1996) assessed a range of clayey soils and shale to provide correlations between PI and effective friction angle. These results are presented in Figure 5-11. For these estimates FHWA GEC-5, Sabatini et al. (2002), recommends utilizing a cohesion value equal to zero ($c' = 0$).

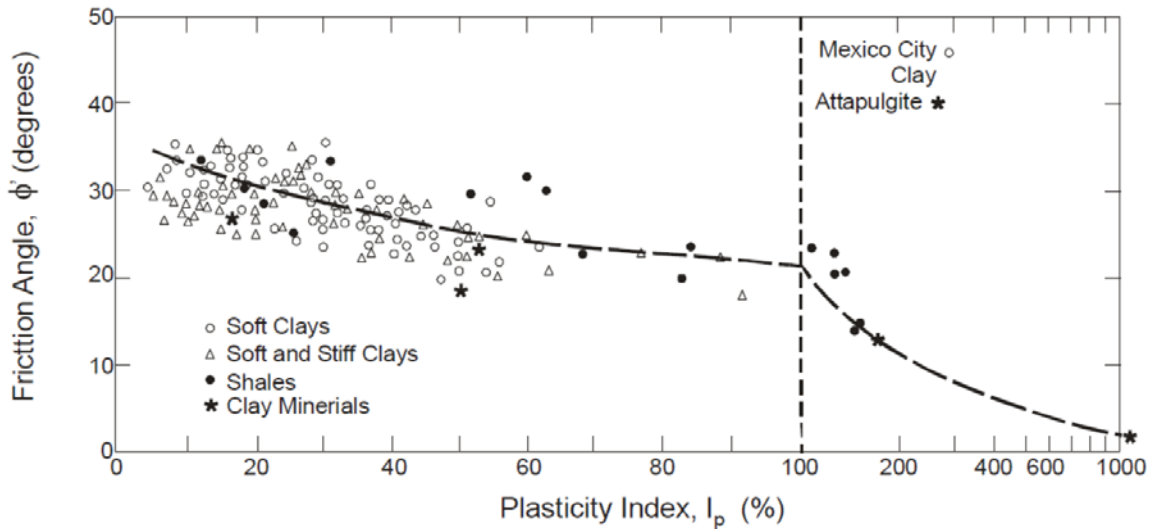


Figure 5-11 Relationship between ϕ' and PI (after Terzaghi et al. 1996).

5.2.3.4 Undrained Shear Strength of Fine-Grained Cohesive Soils

The undrained shear strength, s_u , of cohesive soils may be measured via laboratory testing or through correlations with in-situ tests. However, laboratory testing of undisturbed samples is recommended. This may be accomplished through simple

unconfined compression (UC) tests or by triaxial unconsolidated undrained (UU), or consolidated undrained (CU) testing. Sampler disturbance, strain rate variations and uncertain drainage conditions can affect shear strength results, although more conservative values are produced from these effects (Brown et al. 2010). CU triaxial tests offer the advantage of reconsolidating the sample to in-situ stress states before shearing, thus providing more representative shear strength values. AASHTO (2014) specifically recommends the use of CU and UU testing where possible.

For cases where undisturbed sampling is difficult or does not yield well preserved samples, in-situ testing may be implemented as an alternative. A discussion of in-situ test methods is provided in Section 5.1. Common correlations between the CPT, SPT, and VST are provided below. Additional correlations may be found in GEC-5 by Sabatini et al. (2002) among other sources.

A CPT to s_u correlation is provided in Equation 5-18. Local calibration of N_k is recommended.

$$s_u = \frac{q_c - \sigma'_{vo}}{N_k} \quad \text{Eq. 5-18}$$

Where:

- q_c = cone tip resistance.
- σ'_{vo} = vertical effective stress at the sample depth.
- N_k = cone factor, typically 14 to 16, may vary from approximately 10 to 18.

A preliminary estimate of undrained shear strength can be made from a corrected SPT N value in combination with atmospheric pressure, and a correction factor, f_1 , based on the plasticity index. Stroud (1974; 1989) utilized the f_1 empirical correction as follows:

$$s_u = \frac{f_1 N_{60} p_a}{100} \quad \text{Eq. 5-19}$$

Where:

- f_1 = 4.5 for PI = 50.
- f_1 = 5.5 for PI = 15.
- p_a = atmospheric pressure.
- N_{60} = SPT N value corrected for 60% energy transfer.

A preliminary estimate of s_u can also be made from uncorrected SPT N values (blows / ft). Table 5-9 contains an empirical relationship between the uncorrected SPT N value, unconfined compressive strength, and saturated unit weight for

cohesive soils. The undrained shear strength is one half of the unconfined compressive strength ($s_u = q_u / 2$). Correlation of N values to the undrained shear strength of clays is crude and unreliable for final design and as stated, should only be used for preliminary estimating purposes.

Table 5-9 Empirical Values for Unconfined Compressive Strength, q_u , and Consistency of Cohesive Soils Based on Uncorrected N- Value (after Bowles 1977)

Consistency	Very Soft	Soft	Medium	Stiff	Very Stiff	Hard
q_u , ksf	0-0.5	0.5-1.0	1.0-2.0	2.0-4.0	4.0-8.0	8.0+
Standard Penetration N value	0-2	2-4	4-8	8-16	16-32	32+
γ (saturated), lb/ft ³	100-120	100-120	110-130	120-140	120-140	120-140

The Vane Shear Test (VST) can be used for soft to medium clays and produces a correlation for s_u from the input torque, T_v , and vane diameter, d_v . During the VST both peak and residual shear strengths are measured, thus the sensitivity can be calculated (Equation 5-5). When the vane height to diameter ratio is equal to two, $h_v/d_v = 2$, a widely used relationship found in GEC-5 by Sabatini et al. (2002) is shown in Equation 5-20. Furthermore, Bjerrum (1972) developed a correction based on static equilibrium theory as shown in Equation 5-21.

$$s_u = \frac{6T_v}{7\pi(d_v)^3} \quad \text{For } \frac{h_v}{d_v} = 2 \quad \text{Eq. 5-20}$$

Where:

- s_u = undrained shear strength.
- T_v = input torque during shear.
- d_v = vane diameter.
- h_v = vane height.

$$\mu = 2.5(PI)^{-0.3} \leq 1.1 \quad \text{Eq. 5-21}$$

Where:

- μ = correction factor.
- PI = plasticity index.

5.2.4 Deformation

Deformation is a measure of the soil response to an applied load. For the design of driven piles, tolerable deformations relate to a structure's serviceability limit state. These values are obtained through tests that quantify strain to provide modulus and consolidation parameters.

5.2.4.1 Elastic Deformation

Modulus, E , is determined through direct measurement of a strain from an applied load via Hooke's Law (Equation 5-22) or through correlations with other laboratory and in-situ tests.

$$\sigma = E\varepsilon \quad \text{Eq. 5-22}$$

Where:

σ = stress.

E = elastic modulus of material.

ε = strain.

A stress-strain curve developed for modulus determination is shown in Figure 5-12. In this figure, the origin and half the peak stress are designated as points to develop the 50% secant modulus, E_{50} .

Shear modulus, G , is sometimes used in load-deformation calculations and is related to the elastic modulus, E , and Poisson ratio, ν , using Equation 5-23 below. Elastic deformation of soil will be further discussed in Chapter 7.

$$G = \frac{E}{2(1+\nu)} \quad \text{Eq. 5-23}$$

A compilation of soil elastic modulus and Poisson ratio values have been made by Bowles (1988) and Department of the Navy (1982). These values were tabulated by AASHTO (2014) so that preliminary estimates of elastic soil deformation could be established. Correlations to corrected SPT N values and CPT cone resistance are also included. Testing should be performed to confirm or supersede these tabulated values. Table 5-10 to Table 5-12 are modified from AASHTO (2014).

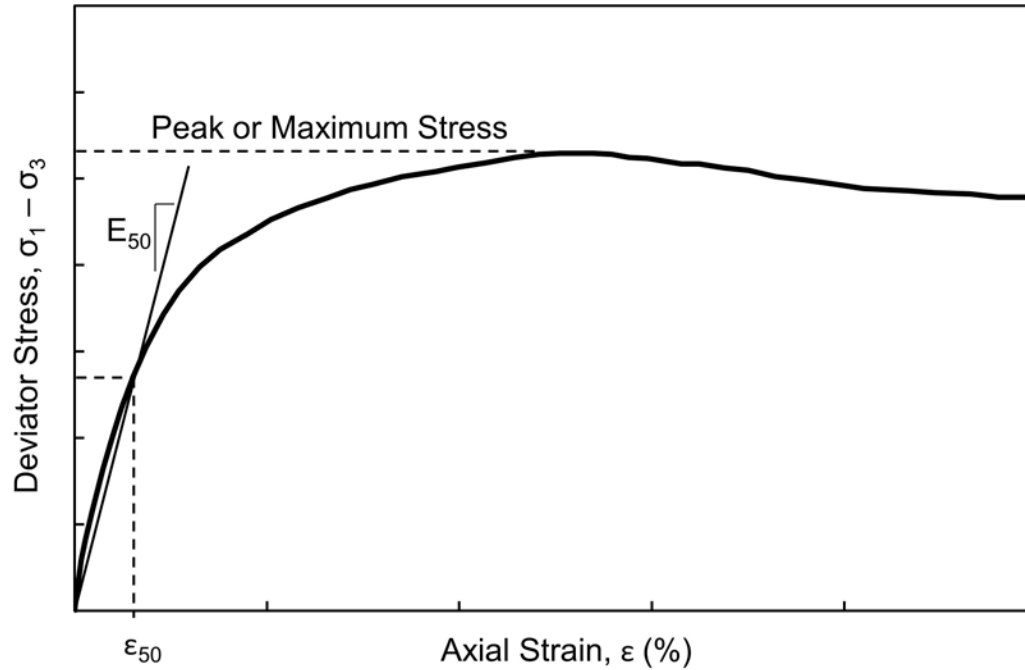


Figure 5-12 Soil stress strain curve and 50% secant modulus (after Brown et al. 2010).

Table 5-10 Estimating Soil Modulus, E_s , Based on Soil Type (after AASHTO 2014)

Soil Type	Typical Range of Young's Modulus, E_s (ksf)	Poisson Ratio, ν
Clay: Soft Sensitive Medium Stiff to Stiff Very Stiff	50-300 300-1,000 1,000-2,000	0.40-0.50 (undrained)
Loess	300-1,200	0.10-0.30
Silt	40-400	0.30-0.35
Sand: Loose Medium Dense Dense	200-600 600-1,000 1,000-1,600	0.20-0.36 0.30-0.40
Gravel: Loose Medium Dense Dense	600-1,600 1,600-2,000 2,000-4,000	0.20-0.35 0.30-0.40

Table 5-11 Estimating Soil Modulus, E_s , from SPT N value (after AASHTO 2014)

Soil Type	E_s (ksf)
Silts, Sandy Silts, Slightly Cohesive Mixtures	8 $(N_1)_{60}$
Clean Fine to Medium Sands, Slightly Silty Sands	14 $(N_1)_{60}$
Coarse Sands and Sands with Little Gravel	20 $(N_1)_{60}$
Sandy Gravels and Gravels	24 $(N_1)_{60}$

Table 5-12 Estimating Soil Modulus, E_s , from Cone Resistance, q_c
(after AASHTO 2014)

Soil Type	E_s (ksf)
Sandy Soils	2 q_c

5.2.4.2 Primary Consolidation Settlement

A one dimensional consolidation test (AASHTO T216 / ASTM D2435) is often performed to estimate the amount and rate at which a cohesive soil deposit will consolidate under an applied load. This test provides consolidation parameters including the coefficient of consolidation, C_v , compression index, C_c , recompression or swell index, C_r (alternatively C_s), and secondary compression index, C_{α} .

For this test, a saturated soil sample is constrained laterally while being compressed vertically. The vertical compression is measured and related to the change in the soil void ratio. Loading the cohesive sample increases pore water pressure within the soil voids. Over a period of time, as the water is squeezed from the soil, this excess water pressure will dissipate resulting in the soil grains (or skeleton) supporting the load. The amount of water squeezed from the sample is a function of load magnitude and compressibility of soil deposit while the rate of pressure dissipation is a function of the permeability of the soil. Test background and analysis information may be found in numerous sources such as Bowles (1977), GEC-5, Sabatini et al. (2002), and Samtani and Nowatzki (2006).

The results from the test are used to plot void ratio, e , versus vertical effective stress, σ'_{vo} , on a semi log scale to determine the preconsolidation pressure, σ_p , and other quantities. An illustration of a typical e -log σ'_v curve is presented in Figure 5-13. A plot of log time versus sample compression is used to determine coefficient of consolidation. Consolidation test results can be used to estimate magnitude and

settlement rate of pile foundations in cohesive soils. Consolidation tests can also be plotted as the vertical strain, ε versus vertical effective stress, σ'_v , on a semi log scale.

Equations 5-24 to 5-26 utilize the results of consolidation testing to determine primary consolidation settlement of cohesive soil.

For normally consolidated ($\sigma'_{vo} = \sigma_p$) cohesive soil layers:

$$S_c = \sum_i^n \frac{C_c}{1 + e_o} H_o \log \left(\frac{\sigma'_{vo} + \Delta\sigma}{\sigma'_{vo}} \right) \quad \text{Eq. 5-24}$$

For overconsolidated soil with ($\sigma'_{vo} + \Delta\sigma \leq \sigma_p$):

$$S_c = \sum_i^n \frac{C_r}{1 + e_o} H_o \log \left(\frac{\sigma'_{vo} + \Delta\sigma}{\sigma'_{vo}} \right) \quad \text{Eq. 5-25}$$

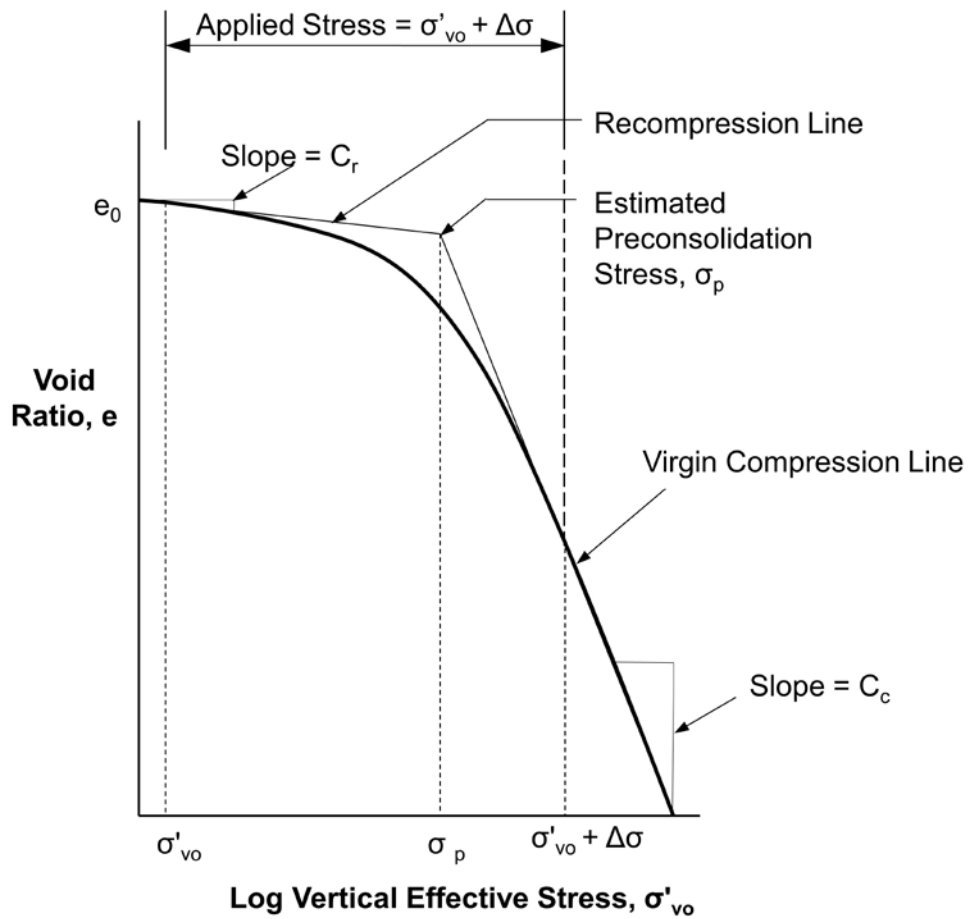


Figure 5-13 Plot of Void Ratio vs Vertical Effective Stress from consolidation test.

For overconsolidated soil with ($\sigma'_{vo} + \Delta\sigma > \sigma_p$):

$$S_c = \sum_i^n \frac{C_r}{1+e_o} H_o \log\left(\frac{\sigma_p}{\sigma'_{vo}}\right) + \frac{C_c}{1+e_o} H_o \log\left(\frac{\sigma'_{vo} + \Delta\sigma}{\sigma_p}\right) \quad \text{Eq. 5-26}$$

Where:

- S_c = settlement from primary consolidation.
- e_o = initial soil layer void ratio.
- H_o = initial soil layer thickness.
- σ_p = preconsolidation stress.
- σ'_{vo} = average vertical effective stress at the mid-point of the soil layer before loading.
- $\Delta\sigma$ = additional stress at mid-point of soil layer from loading.

5.2.5 Electro Chemical Properties

The soil and groundwater can contain constituents detrimental to pile materials. Electro chemical classification tests can be used to determine the aggressiveness of the subsurface conditions and the potential for pile deterioration. For pile design, corrosion rates for steel piles or disintegration rates for concrete may be required to evaluate long term structural resistance. These electro chemical tests include:

- a. pH (AASHTO T289 / ASTM D4972).
- b. Resistivity (AASHTO T288 / ASTM D1125).
- c. Sulfate ion content (AASHTO T290 / ASTM D4230).
- d. Chloride ion content (AASHTO T291 / ASTM D512).

Additional discussions on the influence of environmental conditions on pile section selection are presented in Section 6.14 of Chapter 6.

5.3 ROCK PARAMETERS

For the design of driven piles, rock property determination is necessary to assess end bearing resistance as well as long term deformation. Shallow rock profiles may necessitate predrilling pile locations into these materials to satisfy minimum penetration requirements. A designer's understanding of rock classification and associated rock characteristics is therefore essential. To properly classify and rate a given quantity of rock, a distinction between intact rock and rock mass should be

noted (Brown et al. 2010). Intact rock is a collection of consolidated and cemented particles forming rock material, where rock core samples are used to determine index and strength properties. Joints, faults, and other bedding features serve to break up intact rock, therefore this inclusive system combines to form a rock mass.

5.3.1 Rock Index Properties and Classification

When designing foundations that bear on rock, proper rock classification is essential. Physical and chemical properties of the rock should be noted during the subsurface exploration as the rock mass quality may affect design and construction. Rock classification should include color, texture, lithology (e.g. igneous, metamorphic, or sedimentary), field hardness, weathering, and geologic discontinuities.

The slake durability test (ASTM D4644) is useful to assess if rock will weather and deteriorate. The slake durability test is useful for weak rocks including shale, mudstone, and siltstone. These deposits are particularly susceptible to weathering or fracturing during the pile driving process. Low slake durability index results may help identify deposits in which driven piles are subject to relaxation.

The slake durability test requires representative rock fragments be dried to a constant weight in a wire mesh drum. After submerging and rotating the drum with containing rock fragments for 10-minutes in water, the sample is again dried to constant weight. This process is repeated a second time, and the ratio of final to initial dry weights results in the slake durability index, I_D . An I_D of less than 60% correlates to a rock prone to rapid degradation.

5.3.2 Rock Mass Shear Strength

Rock shear strength is typically measured in the laboratory through uniaxial compression testing where recovered core samples are prepared and subjected to loading in accordance with ASTM D7012. As load is applied during this test, axial strain is measured and plotted to determine the elastic modulus. The peak load is divided by the specimen's cross sectional area to provide an unconfined compressive strength, q_u . AASHTO and other methods for determining the nominal resistance of end bearing piles on rock utilizes the rock unconfined compressive strength.

5.3.3 Rock Mass Deformation

Rock deformation is typically elastic. Laboratory uniaxial compression test results can provide information on modulus values if rock deformation calculations are required. Rock deformation for most rock formations is generally not a design consideration as piles typically penetrate into weak rock or terminate on hard rock. If heavily loaded piles are terminated just into or above soil-like weak rock formations such as marl, rock mass deformation properties may be needed for design. To estimate the modulus values for rock, the designer should consider the RQD, GSI, and core recovery and use correlations of these parameters with rock mass modulus.

As noted in the previous section, the material modulus, E , is measured by plotting load versus strain during the uniaxial compression test. Careful axial and diametrical measurements also yield the material's Poisson ratio, ν . The modulus is the slope of the stress-strain curve. Figure 5-12 utilizes a 50% secant modulus, E_{50} , where a stress value equal to one-half of the maximum deviator stress was selected. Test result tables compiled by Kulhawy (1978) for numerous rock types have been in use to estimate elastic modulus and Poisson ratio. These tables are reproduced in a number of manuals including Samtani and Nowatzki (2006) and Table C10.4.6.5-1 of AASHTO (2014).

5.4 CONSIDERATIONS FOR PILE DRIVABILITY

AASHTO Article 10.7.8 stipulates that an evaluation of pile drivability should be performed during the design stage. Pile drivability is defined as the ability to drive the pile to the estimated nominal axial resistance anticipated during driving at or above the required penetration depth and to achieve penetration requirements within the driving stress limits of the pile material. To satisfy this objective, a detailed identification of the subsurface conditions and a thorough understanding of the soil behavior and its response to pile installation are needed.

Some subsurface issues that influence drivability are fairly obvious such as the presence of boulders above the bearing strata that increase the risk of pile damage or the identification of artesian conditions that can result in reduced geotechnical resistances. Other factors such as fine content, angularity, density, as well as high soil plasticity can all have a significant influence on drivability.

Cases of large soil shakes or high elastic behavior have been reported in dense silty sand, hard silty clay, glacial tills and other fine grained saturated soils (e.g., Likins 1983; Hannigan 1985; Hussein et al. 2006). Furthermore, Cosentino et al. (2010) researched cases of high rebound soils for the Florida DOT. High rebound is an effect of increased pore water pressure due to driving generally occurring near the pile toe. As driving continues, pore water pressure increases and causes a larger elastic response and rebound, leading to refusal driving conditions. If pile driving is paused, the pore water pressure dissipates and subsequently smaller rebound occurs. The research performed on the Hawthorn Group formation, a Florida soil formation, determined that high silt content and N value changes within the strata appeared to have strong correlations with soil zones of high elastic rebound.

Some sand deposits have also exhibited high dynamic resistances during pile driving. Thompson and Goble (1988) summarized details from nine projects that had this behavior. Unfortunately no clear relationship was identified between soil deposition, geologic, or mineralogical characteristics. This suggests drivability assessments should consider a range in dynamic soil properties rather than a specific value. Similarly, a range of dynamic soil properties should be evaluated in drivability analyses in highly plastic CH and MH soils where conventional values may underestimate the dynamic soil resistances encountered in these materials.

For certain weathered rock such as shale and siltstone, competent material is typically encountered during initial drive. However, a reduction in pile end bearing resistance can occur with time due to the release of locked in horizontal stresses in the laminated rock. Driving of adjacent piles to the same depth or below previously installed piles can also shatter the weak rock causing a reduction in end bearing resistance. Because rock types vary by region, local experience and analysis methods are advantageous in this regard.

5.5 SELECTION OF PARAMETERS FOR DESIGN AND CONSTRUCTION

Soil and rock parameters should be carefully selected based on site specific in-situ and laboratory testing results and relevant design methods for driven pile foundations. In some cases, resistance factors were developed for a specific design methodology based on a specific correlation approach between N and ϕ , between N and s_u , or a design method limit on the maximum friction angle.

5.5.1 Soil Parameters

Preliminary estimates of the soil shear strength and density parameters are often made from published correlations with SPT N values. Many of these correlations were provided in Section 5.2.3.3 and 5.2.3.4. While these correlations are very useful for preliminary design assessments, soil parameter confirmation and refinement should be obtained through additional in-situ and laboratory tests. Parameter variability for each layer must be considered for final soil parameter selection and final design. The shear strength, compressibility and index properties of each layer should be adequately quantified for design.

In coarse granular deposits, the selection of the design friction angle should be done conservatively. A comparison of nominal resistances from static load test results with static analysis predictions indicates that static analyses often overpredict the shaft resistance in these deposits. This is particularly true for coarse granular deposits comprised of uniform sized or rounded particles. Cheney and Chassie (1993) recommended limiting the shearing resistance by neglecting particle interlock forces. For shaft resistance calculations in gravel deposits, this results in a maximum ϕ' angle of 32° for gravels comprised of soft rounded particles, and in a maximum ϕ' angle of 36° for hard angular gravel deposits. The ϕ' angle used to calculate the toe resistance is determined using normal procedures.

Final design methods are often selected based on a given foundation type or from prior satisfactory design experience with the design method in similar subsurface conditions. The soil parameters required for method use must be acquired during the subsurface exploration program. Necessary parameters may include USCS classification, moisture content, density, grain size distribution, and Atterberg limits in addition to shear strength and compressibility information. In AASHTO Article 10.4, resistance factors have been developed for specific design method equations using specific procedural guidance. Hence, the soil parameters necessary to perform the analyses should be obtained in the prescribed manner. Design methods are discussed further in Chapter 7.

5.5.2 Rock Parameters

Design parameters for rock must be determined for piles driven either into soft rock or to hard rock. Rock cores should be collected for both soft and hard rock layers and the extent of rock weathering and fracturing should also be determined. The value of local experience with a given rock mass behavior cannot be overstated, as regional rock formations pose their own unique features.

A clear definition of soft and hard rock is not available in technical literature, in AASHTO, or in other building codes. In many intact rock classification systems, the transition between hard soil and soft rock occurs at an unconfined compression strength, q_u , of around 20 ksf. Similarly, the transition between soft rock and hard rock occurs between unconfined compression strength of 200 and 1000 ksf. In driven pile design and construction, soft rock is defined as rock that can be penetrated by pile driving and hard rock is defined as rock that cannot be penetrated. Hence, piles are driven into soft rock and driven to hard rock.

Soft and weak rocks are difficult materials to sample, test, and quantify. They have shear strengths greater than that of conventional soils and less than hard rock. Soft rock strengths can be too strong to be tested in soil laboratory equipment and too weak to be tested in rock mechanics equipment. Soft rocks often exhibit additional problematic characteristics such as crumbling, laminations, disaggregation, high plasticity, slaking, and variable strengths depending on weathering. All of these considerations complicate determination of representative parameter selection for pile design in soft rocks. Usual types of soft rock were identified by Kanji (2014) and are listed in Table 5-13.

Table 5-13 Usual Types of Soft Rocks (after Kanji 2014).

Rock Classification	Subclasses
Sedimentary Rocks	Mudstones, shales, siltstones, sandstones, conglomerates, breccias, marl, limestone, dolomites, gypsum, coal, salt rock, carnallite,
Igneous Rocks	Volcanic breccias and lahars, basaltic breccias, pyroclastic deposits, volcanic ash, tuff, ignimbrite, and weathering products of crystalline rocks (granite, gneiss)
Metamorphic Rocks	Slate, phyllite, schists, quartzite little cemented, and metavolcanic deposits.

As noted above, piles can be driven into soft and weak rocks. In these materials, rock classification, core recovery, RQD, unconfined compression strength, density, and slake durability index parameters should be quantified. Piles cannot be driven into hard rock as pile toe damage or yielding occurs before hard rock failure. As with soft and weak rocks, rock classification, core recovery, RQD, unconfined compression strength, and density parameters should be quantified for pile designs on hard rock.

5.5.3 Site Variability

After a thorough site investigation and characterization of material properties, a subsurface profile is then generated for design and constructability purposes. Often times, throughout a relatively uniform soil model, results of laboratory tests and in situ tests present conflicting information. Soil cohesion, relative density and permeability among other properties may vary within a given strata along a horizontal plane or with depth. Final selection of material parameters then becomes reliant upon the use of engineering judgment.

Chapter 8 of GEC-5, Sabatini et al. (2002), provides a detailed overview of incorporating engineering judgment into the selection of design parameters when site variability is encountered. When facing situations of this nature, the Engineer can reevaluate subsurface parameters by either (1) locating inconsistencies with reported test results or (2) using historical information (i.e. experience, published data) to assess the inherent site variability.

Site variability relates to the variability within similar site conditions of the same site, not between sites. Furthermore, determination of site variability should be performed for each substructure location. When pile designs are prepared (Chapter 7 and 8), they are done so with respect to the encountered subsurface conditions which directly correlate to performance criteria for construction and the resulting structure. Generally, the nearest boring(s) or in-situ test(s) are utilized for this purpose. Judgment may be applied when establishing a subsurface profile. However, the following three steps provided in Paikowsky et al. (2004) serve to aide this process.

1. Relate each significant bearing layer and determine average parameters used for strength analysis at each boring location.
2. Check the Coefficient of Variation (COV) between the average values for each identifiable significant layer obtained at each boring location.
3. Categorize site variability based on COV as low, medium, or high.
 - a. $COV < 25\%$ - Low
 - b. $25\% \leq COV < 40\%$ - Medium
 - c. $40\% \leq COV$ - High

When analysis results yield a high COV, additional tests, different tests, engineering judgement, or further division of the project site into smaller less variable sub-sites may be required.

A larger statistical analysis of design parameters can also serve as a means to identify variability. For this, a database of similar geomaterials is constructed with the goal of assessing variation within a particular property and the effect on the project at large. Duncan and Wright (2005) compiled Table 5-14 based on the variability of geotechnical properties from in situ tests. They present the COV for a select number of soil parameters, which have been compiled from a number of sources. It should be noted that these values are obtained from projects covering a wide range of material, and this should not be applied to specific cases.

Sabatini et al. (2002) suggests the use of statistics and sensitivity analyses as a minimum practice for design parameter selection. Based on reported test results, determination of the sample mean and standard deviation is a relatively straightforward process. The COV is a statistical measure of the extent of variability and is calculated by dividing the sample standard deviation by the sample mean. By applying these statistics to a sensitivity study for design methods, the influence of a given design parameter can be assessed. Several designs can then be completed efficiently with the use of computer software or spreadsheets.

Table 5-14 Coefficients of Variation for Geotechnical Properties and In-Situ Tests
(after Duncan and Wright 2005)

Property or In-Situ Test	COV (%)
Unit Weight (γ)	3-7
Buoyant Unit Weight (γ')	0-10
Effective Stress Friction Angle (ϕ')	2-13
Undrained Shear Strength (s_u)	13-40
Undrained Strength Ratio (s_u/σ'_{vo})	5-15
Standard Penetration Test N value (N)	15-45
Electric Cone Penetration Test (q_c)	5-15
Mechanical Cone Penetration Test (q_c)	15-37
Dilatometer Test Tip Resistance (q_{DMT})	5-15
Vane Shear Test Undrained Strength (s_u)	10-20

5.6 GEOTECHNICAL REPORTING

Upon conclusion of the site characterization program, the geotechnical engineer summarizes the factual data and prepares a geotechnical report. Three types of geotechnical reports are appropriate for driven piles: 1) geotechnical data reports; 2) geotechnical foundation design reports; and 3) geotechnical baseline reports. The type of geotechnical report prepared depends on project type and owner requirements.

Geotechnical data reports simply document and transmit a record of the exploration performed and the collected data. These data reports may be used on conventional Design-Bid-Build or Design-Build projects. Other agencies prefer foundation design reports that include the results of the subsurface exploration program as well as an assessment of the subsurface conditions with supporting design recommendations. The third type of report, a geotechnical baseline report, provides a contractual understanding of the subsurface conditions to be expected during construction. Geotechnical baseline reports are relatively uncommon on driven pile projects but are increasing in use particularly on Design-Build projects with highly variable site conditions. Dwyre et al. (2010) provides suggested guidelines for the application of geotechnical baseline reports to foundation projects. The various methods of geotechnical reporting are discussed in greater detail in the subsequent sections. Table 5-15 summarizes the decisions in driven pile design and construction that are influenced by the subsurface conditions.

5.6.1 Geotechnical Data Reports

A Geotechnical Data Report (GDR) contains only factual information from the performed site exploration. This includes a description of the geologic setting, site exploration program, and field and laboratory testing program. Also included are completed boring logs as well as field and laboratory test results. The GDR does not offer subsurface interpretations, or design recommendations, and is typically used when a subcontracted consultant performs the field exploration and associated soil or rock testing for the foundation designer. Information included in Geotechnical Data Reports is summarized in Table 5-16. The Owner's design team is responsible for interpreting the GDR. For design-build projects, the GDR may be used for construction bidding and must be included as a Contract Document.

Table 5-15 Pile Foundation Decisions Influenced by Subsurface Information

Decisions	Subsurface Information
Project Constraints and Auxiliary Equipment	<p>Old foundations, boulders, obstructions.</p> <p>Site accessibility and terrain.</p> <p>Site constraints, overhead and underground utilities, adjacent buildings.</p>
Pile Type and Accessory Selection	<p>Subsurface strata and installation conditions.</p> <p>Structural resistance needs.</p> <p>Geotechnical resistance available.</p> <p>Pile lengths.</p> <p>Need for pile splices.</p> <p>Bedrock type and depth.</p> <p>Water table.</p> <p>Coatings due to aggressive or abrasive environment.</p> <p>Pile driving shoes.</p>
Pile Driving Equipment Selection	<p>Hammer type requirements.</p> <p>Hammer size and energy requirements.</p> <p>Crane, leads, template, and other equipment.</p> <p>Drilling equipment, augers, spuds, jets.</p>
Construction Control	<p>Hammer energy control.</p> <p>Resistance determination method.</p> <p>Time dependent soil strength changes.</p>

**Table 5-16 Information Included in Geotechnical Data Reports
(after Brown et al. 2010)**

Background Information	<p>Overview of project (bridge, structure, retaining wall, or other facility).</p> <p>General site conditions (geology, topography, drainage, accessibility).</p> <p>Specific methods used for site exploration.</p>
Scope of Site Exploration	<p>Plans showing location of all borings, test pits, and in-situ test locations.</p> <p>Number, locations, and depths of all borings and in-situ tests.</p> <p>Types and frequency of samples obtained; standards used.</p> <p>Types and numbers of laboratory tests; standards used.</p> <p>Subcontractors performing the work and dates of work.</p>
Data Presentation	<p>Final logs of borings and test pits.</p> <p>Water level readings and other groundwater data.</p> <p>Data tabulations and plots from each in-situ test hole.</p> <p>Summary tables and data sheets for lab tests performed.</p> <p>Photographs of rock core.</p> <p>Results of geophysical tests.</p> <p>Geological mapping data sheets and summary plots.</p> <p>Existing information from previous site explorations (boring logs, data).</p>

5.6.2 Geotechnical Foundation Design Reports

A foundation design report is prepared to present the results of the subsurface explorations, laboratory test data, analysis, and specific design and construction recommendations for the foundation system of a structure. A foundation design report includes all the information noted in Table 5-16. In addition, the foundation design report includes an assessment of the subsurface conditions, identifies the soil and rock stratigraphy, provides design parameters for each soil and rock layer, presents analyses performed and their results, and provides recommendations for foundation design and construction. The report should make a clear distinction between factual and interpretive information. Foundation design reports are referred to frequently during the design and construction period as well as in resolving post construction issues such as claims. It is therefore important that the foundation design report be clear, concise and accurate. The foundation report is a very important document and should be prepared and reviewed accordingly.

Preliminary design recommendations based on, and/or transmitted with initial subsurface data does not constitute a foundation design report. A foundation design report must address each design issue such as axial compression resistance, uplift resistance, settlement, lateral resistance and response to lateral loading, seismic, scour, etc., in accordance with applicable limit state design methodologies. Only with this information can a foundation design report be prepared with appropriate content and quality.

The parts of a foundation design report are described below, and are modified from Cheney and Chassie (2000).

- I. Table of Contents.
- II. Introduction.
 - a. Summary of proposed construction, including factored foundation loads.
 - b. Summary of applicable extreme event limit states and loads.
 - c. Foundation performance criteria (total and differential settlements, lateral deformation).
 - d. Hydraulic information (if applicable).
 - e. Summary of site constraints including accessibility, environmental restrictions (noise, vibrations, contaminated soil or groundwater, marine mammals, fish, wildlife), utility conflicts, as well as any limitations on headroom or equipment.
- III. Scope of Explorations.
 - a. Field explorations (summary of dates and methods, appended results).
 - b. Laboratory testing (summary of types of tests, appended results).
- IV. Interpretation of Subsurface Conditions.
 - a. Description of formations.
 - b. Soil types.
 - c. Rock types.
 - d. Dip and strike of rock.
 - i. Regional.
 - ii. Local.
 - e. Water table data.
 - i. Perched.
 - ii. Regional.
 - iii. Artesian.

- V. Geomaterial Design Parameters. (Narrative to describe procedure for evaluating factual data to establish design values for all soil and rock layers).
 - a. Shear strength.
 - b. Compressibility.
 - c. Design analysis.

- VI. Description of Design Procedures.
 - a. Summary of results.
 - b. Explanation of interpretation.

- VII. Geotechnical Conclusions and Recommendations.

- VIII. Pile foundations.
 - a. Type of pile geotechnical resistance: shaft resistance, toe resistance, or both.
 - b. Delineation of unsuitable layers due to compressibility, scour, or liquefaction.
 - c. Suitable pile types: reasons for choice and/or exclusion of types and optimization of the recommended section.
 - d. Estimated pile toe elevation, (average estimated values with probable variation potential).
 - e. Estimated pile lengths.
 - f. Minimum pile penetration (AASHTO Article 10.7.7 summarizes reasons why a minimum penetration depth could be specified to satisfy all applicable limit states).
 - g. Nominal axial compression and axial tension resistances. Lateral load resistance and deformation.
 - h. Location of the neutral plane and drag force.
 - i. Estimated pile group settlement. Very important for pile groups in cohesive soils and large groups in a cohesionless soil deposit underlain by compressible soils.
 - j. Number of test piles and specific test pile locations for maximum utility.
 - k. Static pile load tests. If used, specify test locations for maximum utility.
 - i. Axial compression.
 - ii. Axial tension.
 - iii. Lateral.
 - l. Dynamic pile load tests. If used, specify test locations and restrike time and frequency.
 - m. Rapid load tests. If used, specify test locations.

- n. Resistance determination method (driving criteria). Nominal driving resistance depends on the resistance determination method per AASHTO Table 10.5.5.2.3-1.
- o. Nominal driving resistance.
- p. Pre-boring, pile toe reinforcement, or other requirements to reach pile penetration requirements or handle potential obstructions.
- q. Pile driving requirements: hammer size, alignment and location tolerances, sequence of driving, etc.
- r. Cofferdams and seals; seal design should consider potential conflicts between batter piles driven at alignment tolerance limits and depth of sheeting. Group densification inside sheeting for displacement piles in sands, or heave for displacement piles in clays should be considered.
- s. Corrosion effects or chemical attack; particular concern in marine environments, old dumps, areas with soil or groundwater contaminants.
- t. Effects of pile driving on adjacent construction; settlements from vibrations and development of excess pore water pressures in soil.
- u. Other pile foundation construction issues.
 - 1. Conflicts with existing foundations, foundation remnants, or other obstructions.
 - 2. Cobbles and boulders.
 - 3. Groundwater control and/or pile cap excavation stability.

IX. Appendix: Graphic Presentations.

- a. Map showing project location.
- b. Detailed plan of the site showing proposed structure(s) borehole locations and existing structures.
- c. Laboratory test data.
- d. Finished boring logs and interpreted soil profile.

X. Report Distribution.

Copies of the completed Foundation Report should be transmitted in accordance with agency protocol.

The foundation report should be widely distributed to design, construction and maintenance engineers involved in the project. The foundation report should also furnish information regarding anticipated construction problems and solutions. This will provide a basis for the contractor's cost estimates.

On conventional design-bid-build contracts, the foundation design report should be completed and available to the designer prior to final design. The foundation drawings, special provisions, and foundation design report should all be cross-checked for compliance upon completion of final design documents. Conflicts between any of these documents greatly increase the potential for construction problems. For design-build contracts, factual data is provided by the owner to the design-build team that then performs the final geotechnical exploration and foundation design report.

5.6.3 Geotechnical Baseline Reports

Uncertainties in subsurface construction and resulting claims resulted in the concept of a Geotechnical Baseline Report (GBR). This concept originated in the tunneling industry where due to the linear nature of construction activities an unexpected condition disrupting construction quickly had significant cost and schedule implications. Geotechnical Baseline Reports establish a single source document where the geotechnical conditions to be expected (or assumed) are established on a contractual basis. This allows the Owner and Contractor to allocate geotechnical construction risk according to the established baseline of expected subsurface conditions. Risks associated with subsurface conditions equivalent to or better than the baseline conditions are borne by the contractor and risk associated with more severe subsurface conditions are allocated to the owner.

A GBR represents what is assumed that will be encountered for contract purposes. Baselines stated in the GBR should be well defined, reasonable and realistic. These should be derived from the site exploration performed, and/or local experience, and provide rationale for specific requirements, designs or methods to be used. A GBR is not a warranty. It does provide a legal foundation for differing site condition claims. An example of a GBR statement relative to pile driving would be "Obstructions will be encountered between EL 610 and EL 605. For baseline purposes, these obstructions are reinforced concrete footing rubble, up to 3 feet thick, covering 15% of the substructure footprint at Pier 4."

A GDR also provides a summary of the site characterization and expected subsurface conditions. For projects where both a GDR and GBR exist, a GBR should take precedence over a GDR in the hierarchy of contract documents. More information on the GBR concept may be found in Essex (2007).

REFERENCES

- Acker, W.L. III, (1974). Basic Procedures for Soil Sampling and Core Drilling, Acker Drill Company, Inc., Scranton, PA, 246 p.
- American Association of State Highway and Transportation Officials (AASHTO). (2014). AASHTO LRFD Bridge Design Specifications, US Customary Units, Seventh Edition, with 2015 Interim Revisions. American Association of State Highway and Transportation Officials, Washington, D.C., 1960 p.
- ASTM D1452-09. (2014). Standard Practice for Soil Exploration and Sampling by Auger Borings. Annual Book of ASTM Standards, Vol. 4.08, ASTM International, West Conshohocken, PA, 6 p.
- ASTM D1586-11. (2014). Standard Test Method for Standard Penetration Test (SPT) and Split-Barrel Sampling of Soils. Annual Book of ASTM Standards, Vol. 4.08, ASTM International, West Conshohocken, PA, 9 p.
- ASTM D1587-12. (2014). Standard Practice for Thin-Walled Tube Sampling of Soils for Geotechnical Purposes. Annual Book of ASTM Standards, Vol. 4.08, ASTM International, West Conshohocken, PA, 4 p.
- ASTM D2113-14. (2014). Standard Practice for Rock Core Drilling and Sampling of Rock for Site Investigation. Annual Book of ASTM Standards, Vol. 4.08, ASTM International, West Conshohocken, PA, 20 p.
- ASTM D2573-08. (2012). Standard Test Method for Field Vane Shear Test in Cohesive Soil. Annual Book of ASTM Standards, Vol. 4.08, ASTM International, West Conshohocken, PA, 8 p.
- ASTM D4633-10. (2014). Standard Test Method for Energy Measurement for Dynamic Penetrometer. Annual Book of ASTM Standards, Vol. 4.08, ASTM International, West Conshohocken, PA, 7 p.
- ASTM D4719-07. (2014). Standard Test Methods for Prebored Pressuremeter Testing in Soils Annual. Annual Book of ASTM Standards, Vol. 4.08, ASTM International, West Conshohocken, PA, 10 p.

- ASTM D4971-02. (2014). Standard Test Method for Determining the In Situ Modulus of Deformation of Rock Using the Diametrically Loaded 76-mm (3-in.) Borehole Jack. Annual Book of ASTM Standards, Vol. 4.08, ASTM International, West Conshohocken, PA, 7 p.
- ASTM D5778-12. (2014). Standard Test Method for Electronic Friction Cone and Piezocone Penetration Testing of Soils. Annual Book of ASTM Standards, Vol. 4.08, ASTM International, West Conshohocken, PA, 20 p.
- ASTM D6635-07. (2014). Standard Test Method for Performing the Flat Dilatometer. Annual Book of ASTM Standards, Vol. 4.09, ASTM International, West Conshohocken, PA, 16 p.
- ASTM D7012-14. (2014). Standard Tests Method for Compressive Strength and Elastic Moduli of Intact Rock Core Specimens under Varying States of Stress and Temperatures. Annual Book of ASTM Standards, Vol. 4.09, ASTM International, West Conshohocken, PA, 9 p.
- ASTM Vol 4.08. (2014). Soil and Rock I, Vol. 4.08, ASTM International, West Conshohocken, PA, 1826 p.
- ASTM Vol 4.09. (2014). Soil and Rock II, Vol. 4.09, ASTM International, West Conshohocken, PA, 1754 p.
- Bowles, J.E. (1977). Foundation Analysis and Design. Second Edition, McGraw-Hill Book Company, Blacklick, OH, 750 p.
- Bowles, J E. (1992). Engineering Properties of Soils and Their Measurement. Fourth Edition. New York: McGraw-Hill, 480 p.
- Brown, D. A., Turner, J.P. and Castelli R.J. (2010). Drilled Shafts: Construction Procedures and LRFD Design Methods, FHWA-NHI-10-016, Geotechnical Engineering Circular (GEC) No. 10. U.S. Dept. of Transportation, Federal Highway Administration, 970 p.
- Cheney, R.S. and Chassie, R.G. (2000). Soils and Foundations Workshop Reference Manual. FHWA HI-00-045, U.S. Department of Transportation, National Highway Institute, Federal Highway Administration, Washington, D.C., 358 p.

- Cosentino, P.J., Kalajian, E., Misilo III, T.J., Fong, Y.C., Davis, K., Jarushi, F., Bleakley, A. (2010). Design Phase Identification of High Pile Rebound Soils. FL/DOT/BDK81 977-01. Florida Department of Transportation, Tallahassee, FL, 128 p.
- Das, B. M. (2007). Principles of Foundation Engineering. Sixth Edition. Toronto, Ontario, Canada: Thomson, 750 p.
- Department of the Navy, (1982). Foundations and Earth Structures Design Manual. DM 7.2. Naval Facilities Engineering Command, (NAVFAC), Alexandria, VA, 279 p.
- Duncan, J. M., and S. G. Wright. (2005). Soil Strength and Slope Stability, Hoboken, N.J.: John Wiley, 297 p.
- Dwyre, E.M., Batchko, Z., and Castelli, R.J. (2010). Geotechnical Baseline Reports for Foundation Projects, Proceedings, GeoFlorida 2010: Advances in Analysis, Modeling & Design, (GSP 199), Orlando, FL, pp. 1-10.
- Essex, R.J. (2007). Geotechnical Baseline Reports for Construction: Suggested Guidelines. The Technical Committee on Geotechnical Reports of the Underground Technology Research Council, Sponsored by the Construction Institute of ASCE and American Institute of Mining, Metallurgical, and Petroleum Engineers, ASCE. Reston, VA, 62 p.
- Hannigan, P.J. (1985). Large Quakes Developed During Driving of Low Displacement Piles. Proceedings of the Second International Conference on the Application of Stress-Wave Theory on Piles, Stockholm, 27-30, May, 1984 Rotterdam, The Netherlands: Balkema, pp. 118-125.
- Hatanaka, M., and Uchida, A. (1996). Empirical Correlation Between Penetration Resistance and Internal Friction Angle of Sandy Soils, Japanese Geotechnical Society, Soils and Foundations, Vol. 36, No. 4, pp. 1-9.
- Honeycutt, J., Kiser, S., and Anderson, J. (2014). Database Evaluation of Energy Transfer for Central Mine Equipment Automatic Hammer Standard Penetration Tests. Journal of Geotechnical and Geoenvironmental Engineering, 140(1), pp. 194-200.

- Hussein, M., Woerner, II, W., Sharp, M., and Hwang, C. (2006). Pile Driveability and Bearing Capacity in High-Rebound Soils. Proceeding of Geocongress 2006: Geotechnical Engineering in the Information Technology Age. Atlanta, GA, February 26-March 1, 2006, ASCE, Reston, VA, pp. 1-4.
- Kanji, M.A. (2014). Critical Issues in Soft Rocks. Journal of Rock Mechanics and Geotechnical Engineering 6, pp. 186-195.
- Kovacs, W. D. Salomone, L. A., and Yokal, F. Y. (1983). Comparison of Energy Measurements in the Standard Penetration Test Using the Cathead and Rope Method, US Nuclear Regulatory Commission, (NUREG) CR-3545, Washington, D.C.
- Kulhawy, F. H. (1978). Geomechanical Model for Rock Foundation Settlement. Journal of Geotechnical Engineering, Vol. 104, No. 2, pp. 211-227.
- Kulhawy, F.H. and Chen, J.-R. (2007). Discussion of 'Drilled Shaft Side Resistance in Gravelly Soils' by Kyle M. Rollins, Robert J. Clayton, Rodney C. Mikesell, and Bradford C. Blaise. Journal of Geotechnical and Geoenvironmental Engineering, ASCE, Vol. 133, No. 10, pp. 1325-1328.
- Kulhawy F. H. and Mayne, P. W. (1990). Manual on Estimating Soil Properties for Foundation Design, EL-6800, Electrical Power Research Institute (EPRI), Palo Alto, CA, 306 p.
- Liao, S.S.C. and Whitman, R.V.(1986). Overburden Correction Factors for SPT in Sand. Journal of Geotechnical Engineering, American Society of Civil Engineers (ASCE), Vol. 112, No. 3, pp. 373-377.
- Likins, G. E. (1983). Pile Installation Difficulties in Soils with Large Quakes. Dynamic Measurement of Piles and Piers, American Society of Civil Engineers, Geotechnical Engineering Division: Philadelphia, PA, 13 p.
- Mayne, P.W., Christopher, B., Berg, R., and DeJong, J. (2002). Subsurface Investigations (Geotechnical Site Characterization), FHWA NHI-01-031, U.S. Dept. of Transportation, National Highway Institute, Federal Highway Administration, Washington, D.C., 300 p.
- Mayne, P.W. (2007). Cone Penetration Testing. National Cooperative Highway Research Program (NCHRP) Synthesis 368, Washington D.C., 117 p.

- Meyerhof, G. G. (1956). Penetration Tests and Bearing Capacity of Piles, American Society of Civil Engineers (ASCE), Journal of the Soil Mechanics and Foundation Division, Vol. 82, No. 1, paper 886, pp. 1-29 .
- Meyerhof, G.G. (1976). Bearing Capacity and Settlement of Pile Foundations, American Society of Civil Engineers (ASCE), Journal of Geotechnical Engineering, Vol. 102, No. 3, pp. 195-228.
- Mokwa, R. L. and Brooks, H. (2008). Axial Capacity of Piles supported on Intermediate Geomaterials. FHWA/ MT Report No. 08-008/8117-32. Montana DOT, Helena, MT, 79 p.
- Peck, R.B., Hanson, W.E., and Thornburn, T.H. (1974). Foundation Engineering, Second Edition., Wiley, New York, NY, 544 p.
- Robertson, P.K. (1990). Soil Classification Using the Cone Penetration Test. Canadian Geotechnical Journal, Vol. 27, No. 1, pp. 151-158.
- Robertson, P.K. and Campanella, R. G. (1983). Interpretation of Cone Penetration Tests. Part I: Sand. Canadian Geotechnical Journal, Vol. 20, No. 4, pp. 718-733.
- Robertson P.K., Campanella, R.G., Gillespie, D. and Grieg, J. (1986). Use of Piezometer Cone Data. Proceedings of Use of In-Situ Tests in Geotechnical Engineering 1986, ASCE Special Publication No. 6, Blacksburg, pp 1263-1280.
- Sabatini, P.J., Bachus, R.C., Mayne, P.W., Schneider, J.A., and Zettler, T.E. (2002). Evaluation of Soil and Rock Properties, FHWA-IF-02-034, Geotechnical Engineering Circular (GEC) No. 5, U.S. Dept. of Transportation, Federal Highway Administration, 385 p.
- Samtani, N.C. and Nowatzki, E.A. (2006). Soils and Foundations: Reference Manual, Vol. 1, FHWA-NHI-06-088. U.S. Dept. of Transportation, National Highway Institute, Federal Highway Administration, Washington, D.C., 462 p.
- Schmertmann, J.H. (1975). Measurement of In Situ Shear Strength, Proceedings of the Conference on In Situ Measurement of Soil Properties, Vol. 2, ASCE, New York, NY, pp. 57-138.

- Sowers, G.F. (1979). *Introductory Soil Mechanics and Foundations. Geotechnical Engineering, Fourth Edition*, MacMillan Publishing Co. Inc., New York, NY, 592 p.
- Stroud, M.A. (1974). *The Standard Penetration Test in Insensitive Clays and Soft Rocks*, Proceedings of the European Symposium on Penetration Testing, Vol. 2 No. 2, Stockholm, Sweden, pp. 367-375.
- Stroud, M.A. (1989). *Standard Penetration Test: Introduction Part 2, Penetration Testing in the U.K.*, Thomas Telford, London, pp. 29-50.
- Terzaghi, K., and Peck, R.B. (1967). *Soil Mechanics in Engineering Practice, Second Edition*, Wiley and Sons, Inc., New York, NY, 729 p.
- Terzaghi, K., Peck, R.B., and Mesri, G. (1996). *Soil Mechanics in Engineering Practice, Third Edition*, Wiley and Sons, Inc., New York, NY, 592 p.
- Thompson, C.D., and Goble, G.G. (1988). *High Case Damping Constants in Sand. Proceedings of the Third International Conference on the Application of Stress-wave Theory to Piles 1988*, Ottawa, Canada, BiTech Publishers, Vancouver, B.C., pp. 555-566.

CHAPTER 6

PILE TYPES FOR FURTHER EVALUATION

The economic selection of a pile foundation type and section for a structure should be based on the specific subsurface conditions as well as the foundation loading requirements, performance criteria, construction limitations and schedule, as well as the foundation support cost. Piles can be broadly categorized in two main types: foundation piles for support of structural loads and piles for earth retention systems. The use of piles for earth retention systems is outside the scope of this manual. This chapter focuses on the characteristics of driven pile types typically used for highway structure foundations. Additional details on pile splices and toe protection devices are presented in Chapter 16.

6.1 OVERVIEW OF TYPICAL PILE TYPES

There are numerous types of piles used for foundation support. Figure 6-1 shows a pile classification system based on type of material, configuration, installation technique and equipment used for installation. Foundation piles can also be classified on the basis of their method of load transfer from the pile to the surrounding geomaterial. Load transfer can be by shaft resistance, toe resistance or a combination of both.

Tables 6-1 to 6-7, modified from NAVFAC (1982), summarize characteristics and uses of common driven pile types. The tables are for preliminary guidance only, and should be confirmed by local practice. The typical factored resistance may be controlled by the structural or available geotechnical resistance which may in turn be limited by installation conditions or performance requirements. Although drilled and bored piles are included in the pile classification chart shown in Figure 6-1, these foundation types are outside the scope of the FHWA driven pile foundation manual. Reference should be made to the FHWA reference manuals for drilled shafts (Brown et al. 2010), continuous flight auger (CFA) piles (Brown et al. 2007) and micropiles (Sabatini et al. 2005) for detailed information on these deep foundation types.

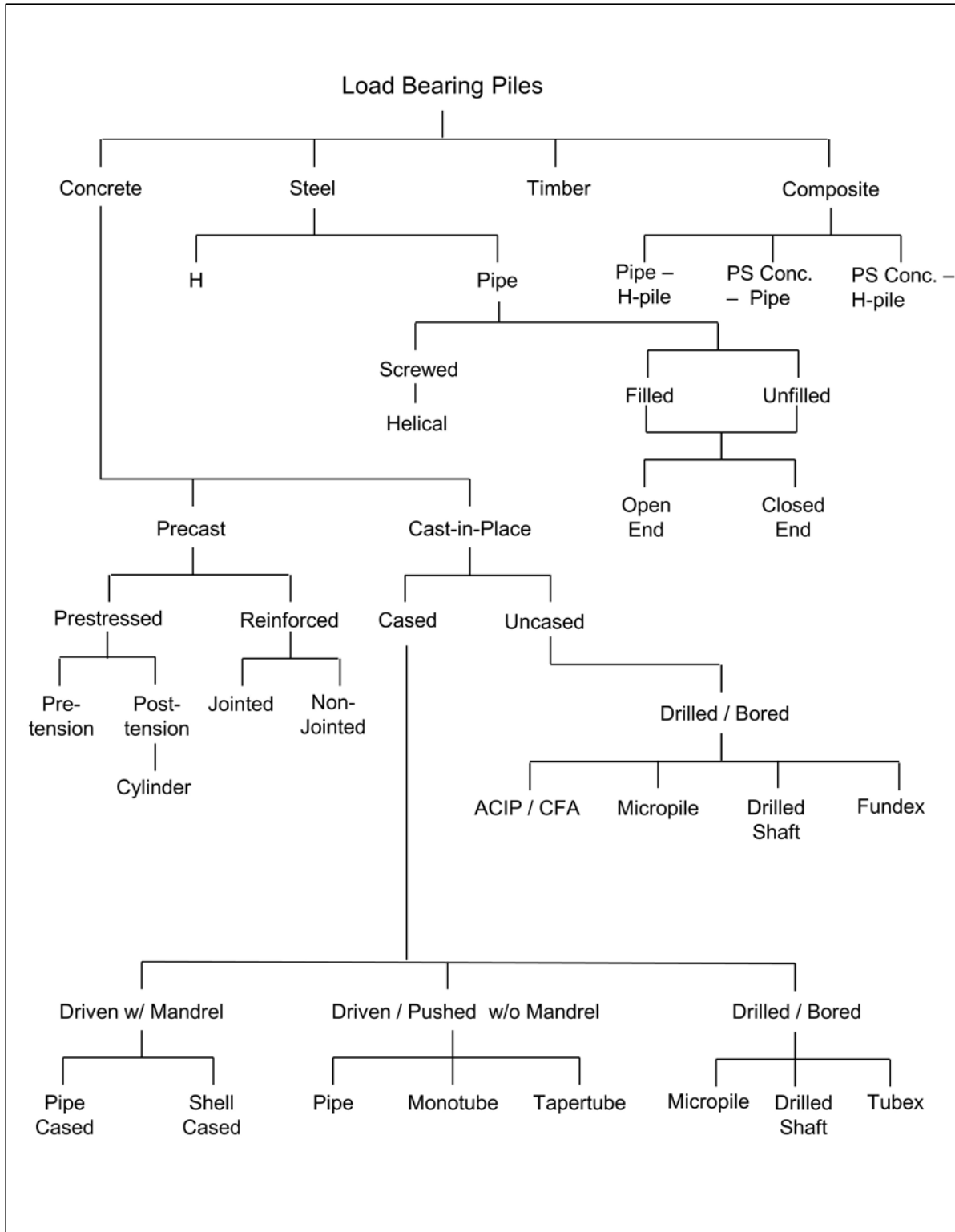


Figure 6-1 Pile classification chart.

Table 6-1 Timber Piles Technical Summary

PILE TYPE	TIMBER PILES
TYPICAL LENGTHS	15 to 75 feet for Southern Pine. 15 to 120 feet for Douglas Fir.
MATERIAL SPECIFICATIONS	ASTM D25. AWPA UC4A, UC4B, UC4C, UC5A, UC5B and UC5C.
TYPICAL FACTORED RESISTANCE	50 to 120 kips.
MAXIMUM DRIVING STRESS	$\sigma_{dr} = \phi_{da} (2.6 F_{co})$. $\phi_{da} = 1.15$. $F_{co} = 1.25$ ksi for Douglas Fir, 1.20 ksi for Southern Pine.
ADVANTAGES	<ul style="list-style-type: none"> • Comparatively low in initial cost. • Permanently submerged piles are resistant to decay. • Easy to handle.
DISADVANTAGES	<ul style="list-style-type: none"> • Difficult to splice. • Vulnerable to damage in hard driving; both pile head and pile toe may need protection. • Intermittently submerged piles are vulnerable to decay unless treated.
REMARKS	<ul style="list-style-type: none"> • Best suited for friction piles in granular material. • Suitable for friction piles with lower factored resistances in cohesive soils.

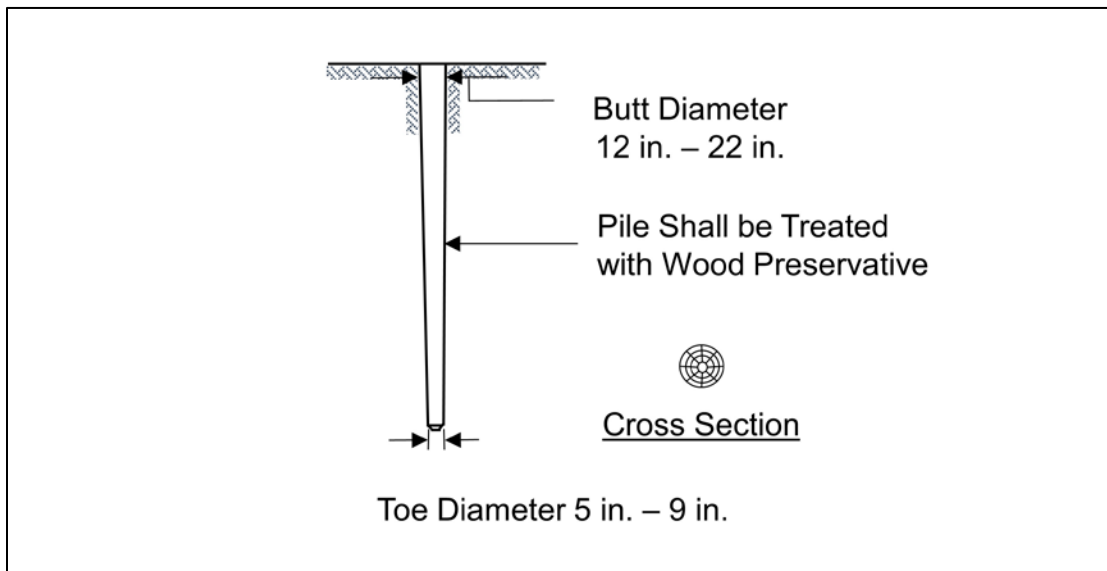


Figure 6-2 Timber pile typical illustration.

Table 6-2 Steel H-Piles Technical Summary

PILE TYPE	STEEL – H-PILES
TYPICAL LENGTHS	15 to 200 feet.
MATERIAL SPECIFICATIONS	ASTM - A572, A588, or A690 Grade 50, 60. (A572 Grade 50 is standard).
TYPICAL FACTORED RESISTANCE	260 to 1,600 kips.
MAXIMUM DRIVING STRESS	$\sigma_{dr} = 0.9 \phi_{da} F_y$ $\phi_{da} = 1.00$ F_y = Yield strength of steel (ksi).
ADVANTAGES	<ul style="list-style-type: none"> • Available in various lengths and sizes. • High factored resistance. • Small soil displacement. • Easy to splice. • Pile toe protection will assist penetration through harder layers and some small obstructions.
DISADVANTAGES	<ul style="list-style-type: none"> • Vulnerable to corrosion where exposed and in corrosive soil conditions. • HP section may be damaged or deflected by major obstructions.
REMARKS	<ul style="list-style-type: none"> • Best suited for toe bearing on rock. • Factored resistance reduced in corrosive environments. • Length and cost overruns often occur when used as a friction pile in granular materials.

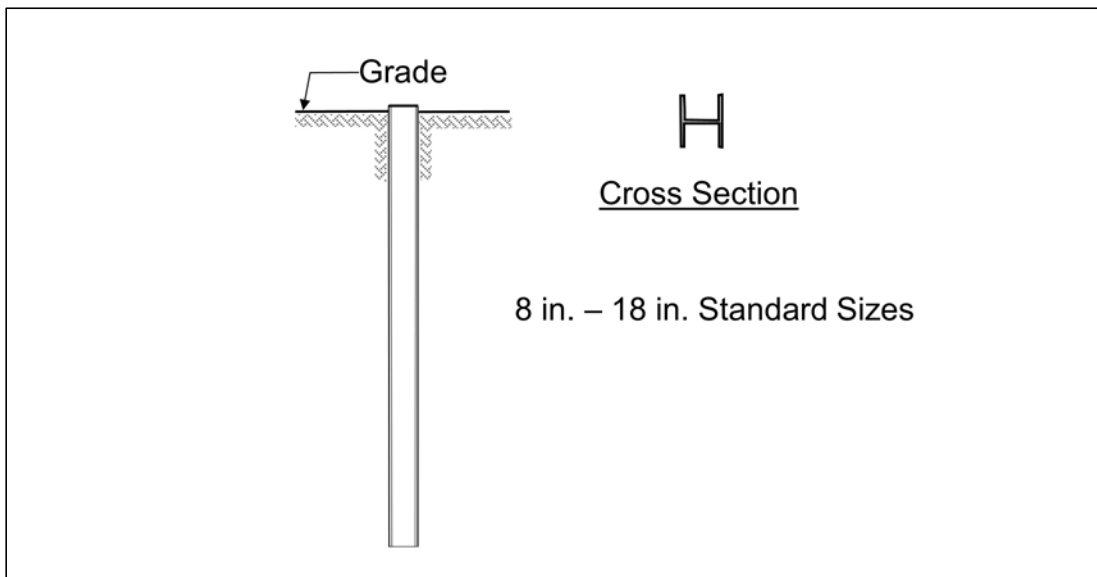


Figure 6-3 Steel H-pile typical illustration.

Table 6-3 Steel Pipe Piles Technical Summary

PILE TYPE	STEEL – PIPE PILES
TYPICAL LENGTHS	15 to 200 feet.
MATERIAL SPECIFICATIONS	ASTM A252 Grade 2 or 3, API 5L, or API 2B - for pipe. ACI 318 - for concrete (if filled). ASTM A572 - for core (if used).
TYPICAL FACTORED RESISTANCE	100 to 1,250 kips (closed end, $D \leq 30$ in.) with concrete fill. 660 to 6,500 kips (open end, $16 \text{ in.} \leq D \leq 72 \text{ in.}$) no concrete.
MAXIMUM DRIVING STRESS	$\sigma_{dr} = 0.9 \phi_{da} F_y$. $\phi_{da} = 1.00$ for non-composite during driving. F_y = Yield strength of steel (ksi).
ADVANTAGES	<ul style="list-style-type: none"> • Closed end pipe can be internally inspected after driving. • Low soil displacement for open end installation. • High factored resistances depending on section. • Open end pipe with shoe can be used for obstructions. • Open end pipe can be cleaned out and driven further. • Easy to splice.
DISADVANTAGES	<ul style="list-style-type: none"> • Vulnerable to corrosion where exposed and in corrosive soil conditions. • Potential soil displacement from larger closed end pipe.
REMARKS	<ul style="list-style-type: none"> • Provides high bending resistance where unsupported length is loaded laterally. • Open end not recommended as a friction pile in granular material due to tendency for length and cost overruns.

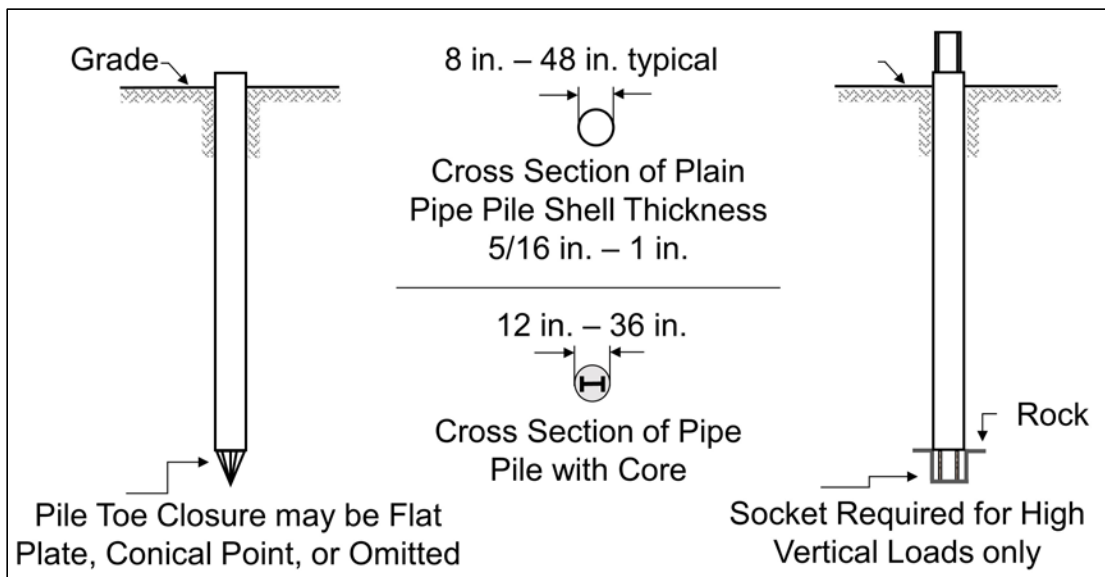


Figure 6-4 Steel pipe piles typical illustration.

Table 6-4 Precast, Prestressed Concrete Technical Summary

PILE TYPE	PRECAST PRESTRESSED CONCRETE PILES
TYPICAL LENGTHS	30 to 150 feet.
MATERIAL SPECIFICATIONS	ACI 318 - for concrete. ASTM - A82, A615, A722, and A884 - for reinforcing steel. ASTM - A416, A421, and A882 - for prestressing.
TYPICAL FACTORED RESISTANCE	350 to 2,200 kips on solid square piles. 1,500 to 3,000 kips on spun cast cylinder piles.
MAXIMUM DRIVING STRESS	$\sigma_{dr} = \phi_{da} (0.85 f'_c - f_{pe})$, In compression. $\sigma_{dr} = \phi_{da} (0.095 \sqrt{f'_c} + f_{pe})$, In tension (normal conditions). $\sigma_{dr} = \phi_{da} (f_{pe})$, In tension (severe conditions). $\phi_{da} = 1.00$. f'_c = Concrete compressive strength (ksi). f_{pe} = Effective prestress (ksi).
ADVANTAGES	<ul style="list-style-type: none"> • High factored resistances. • Corrosion resistance obtainable. • Hard driving possible.
DISADVANTAGES	<ul style="list-style-type: none"> • Vulnerable to handling damage. • Can have relatively high breakage rate. • Potential soil displacement effects from large sections. • Difficult to splice when insufficient length ordered.
REMARKS	<ul style="list-style-type: none"> • Cylinder piles are well suited for bending resistance.

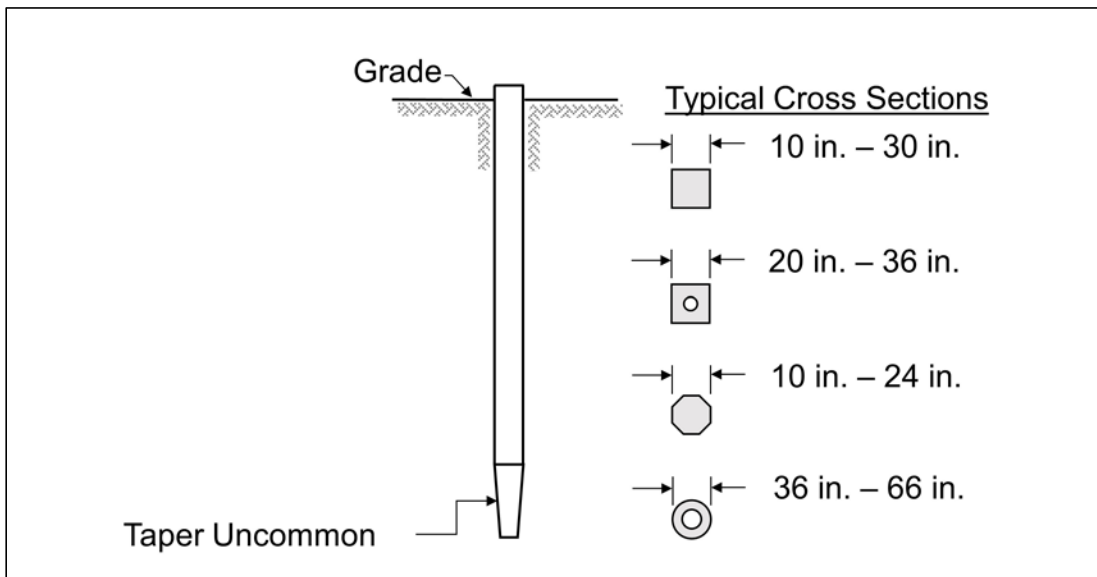


Figure 6-5 Precast, prestressed concrete typical illustration.

Table 6-5 Monotube Pile Technical Summary

PILE TYPE	MONOTUBE PILES
TYPICAL LENGTHS	15 to 100 feet.
MATERIAL SPECIFICATIONS	ACI 318 - for concrete. ASTM A252 - for steel pipe.
TYPICAL FACTORED RESISTANCE	100 to 450 kips.
MAXIMUM DRIVING STRESS	$\sigma_{dr} = 0.9 \phi_{da} F_y$ $\phi_{da} = 1.00$ for non-composite during driving. F_y = Yield strength of steel (ksi).
ADVANTAGES	<ul style="list-style-type: none"> • High factored resistance for relatively shorter lengths. • Increased shaft resistance from tapered section. • Fluted shell not easily damaged.
DISADVANTAGES	<ul style="list-style-type: none"> • Potential soil displacement effects. • Vulnerable to corrosion where exposed and in corrosive soil conditions.
REMARKS	<ul style="list-style-type: none"> • Best suited as a friction pile in granular soils.

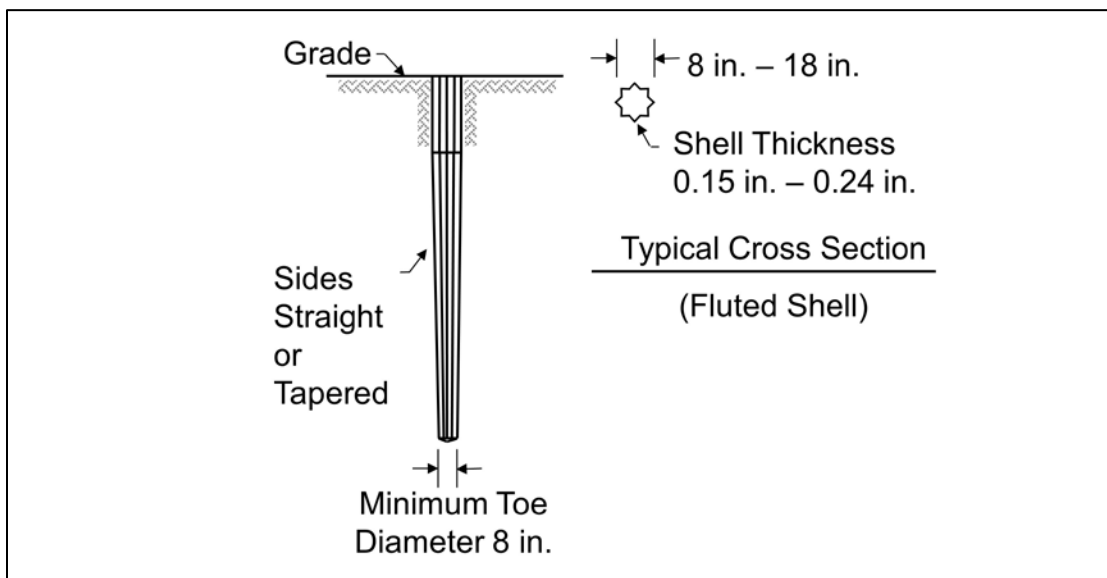


Figure 6-6 Monotube pile typical illustration.

Table 6-6 Tapertube Piles Technical Summary

PILE TYPE	TAPERTUBE PILES
TYPICAL LENGTHS	50 to 150 feet.
MATERIAL SPECIFICATIONS	ACI 318 - for concrete. ASTM A252 - for steel pipe.
TYPICAL FACTORED RESISTANCE	200 to 850 kips.
MAXIMUM DRIVING STRESS	$\sigma_{dr} = 0.9 \phi_{da} F_y$. $\phi_{da} = 1.00$ for non-composite during driving. F_y = Yield strength of steel (ksi).
ADVANTAGES	<ul style="list-style-type: none"> • High factored resistance for relatively shorter lengths. • Standard pipe piles may be spliced to tapered sections. • Increased shaft resistance from tapered section. • Reduced concrete fill volume in tapered section.
DISADVANTAGES	<ul style="list-style-type: none"> • Potential soil displacement effects. • Vulnerable to corrosion where exposed and in corrosive soil conditions.
REMARKS	<ul style="list-style-type: none"> • Best suited as a friction pile in granular soils.

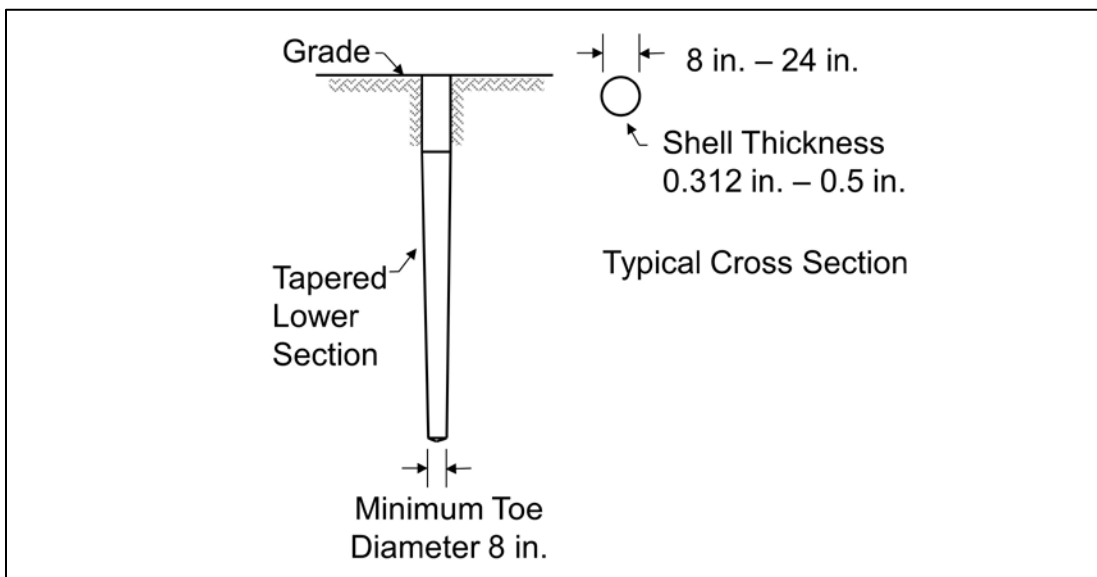


Figure 6-7 Tapertube pile typical illustration.

Table 6-7 Composite Piles Technical Summary

PILE TYPE	COMPOSITE PILES
TYPICAL LENGTHS	50 to 200 feet.
MATERIAL SPECIFICATIONS	ASTM A572 - for HP section. ASTM A252 - for steel pipe. ASTM D25 - for timber. ACI 318 - for concrete.
TYPICAL FACTORED RESISTANCE	100 to 1,250 kips.
MAXIMUM DRIVING STRESS	Varies depending on pile materials.
ADVANTAGES	<ul style="list-style-type: none"> • Composite section can be designed to address loading conditions and/or specific site requirements. • Considerable length can be provided at comparatively low cost for wood composite piles. • High factored resistance for some composite piles. • Internal inspection for pipe composite piles.
DISADVANTAGES	<ul style="list-style-type: none"> • More complex pile fabrication. • Difficult to attain good joints between two materials except for concrete and H or pipe composite piles.
REMARKS	<ul style="list-style-type: none"> • The weakest of any material used will govern the structural design and factored resistance.

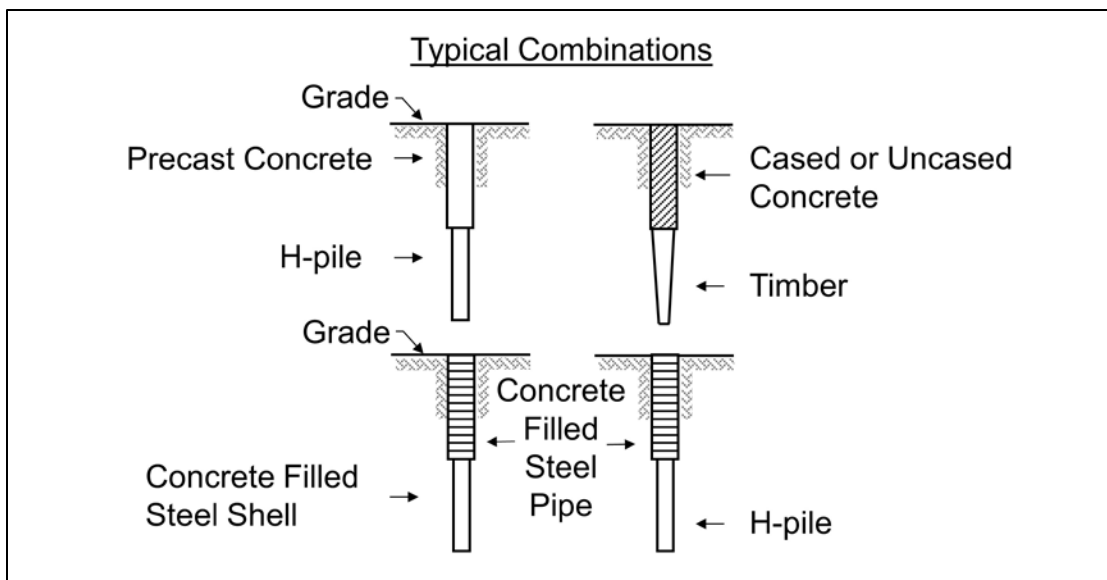


Figure 6-8 Composite piles typical illustration.

6.2 TIMBER PILES

Timber piles are usually of round, tapered cross section made from tree trunks of Southern Pine or Douglas Fir driven with the smaller end used as the pile toe. Southern Pine timber piles can be found to lengths up to 75 feet, and some west coast Douglas fir may be up to 120 feet in length. Oak and other timber types have also been used for piles, but their use is infrequent today. ASTM D25, Standard Specification for Round Timber Piles, presents guidelines on minimum timber pile dimensions, straightness, knot sizes, etc. AWWA C3, Piles - Preservative Treatment by Pressure Process, contains penetration and retention values for the various preservatives. Figure 6-9 presents a photograph of timber piles.



Figure 6-9 Timber piles.

Timber piles are best suited to support modest loads as friction piles in sands, silts and clays. The taper of timber piles is effective in increasing the shaft resistance, particularly in loose sands. They are not recommended as piles to be driven through dense gravel, boulders, or till, or for toe bearing piles on rock since they are vulnerable to damage at the pile head and toe in hard driving. Overdriving of timber piles can result in the crushing of fibers or brooming at the pile head. This can be controlled by using a helmet with cushion material and/or metal strapping around the head of the pile. In hard driving situations, a metal shoe should be attached to the pile toe. Timber piles are favored for the construction of bridge fender systems and small jetties due to the good energy absorption properties of wood.

Timber pile splices are difficult and undesirable. AASHTO (2010) LRFD Bridge Construction Specifications state that timber piles should not be spliced unless specified in the contract documents and approved by the engineer.

Durability is generally not a design consideration if a timber pile is below the permanent water table. However, when a timber pile is subjected to alternate wetting and drying cycles or located above the water table, damage and decay by insects may result. Bacteria and fungi attack can also result in pile damage and decay. Such damage reduces the service life of timber piles significantly unless the pile is treated with a wood preservative. The most common treatments for timber piling are Chromated Copper Arsenate (CCA) for Southern Pine, and Ammoniacal Copper Zinc Arsenate (ACZA) for Douglas Fir. Creosote remains a common treatment option in some areas of the United States but prohibited in others. Creosote cannot be used alone in southern waters due to attack by limnoria tripunctata, but should be used as part of a dual treatment with CCA or ACZA. If cracking of the pile shaft or head occurs and extends below the prescribed pile cut-off level, the initial preservative treatment will not be effective, and the trimmed end of the pile should be treated a second time.

According to Graham (1995), the durability of round timber piling is a function of site-specific conditions:

1. Foundation piles permanently submerged in ground water will typically last indefinitely.
2. Fully embedded, treated foundation piles partially above the ground water with a concrete cap will typically last on the order of 100 years or longer.
3. Treated trestle piles over land will generally last as long as utility poles in the area, i.e., about 75 years in northern areas and about 40 years in southern areas of the United States.
4. Treated piles in fresh water will typically last about five to ten years less than land trestle piles in the same area.
5. For treated piles in brackish water, the longevity should be determined by the experience in the area.
6. Treated marine piles will typically last about 50 years in northern climates and 25 years in southern climates of the United States.

6.3 STEEL H-PILES

Steel H-piles consist of rolled wide flange sections that have flange widths approximately equal to the section depth. In most H-piles sections, the flange and web thicknesses are the same. They are manufactured in standard sizes ranging from 8 to 18 inches. In some cases, W-sections have also been used for piles. However, this is generally customized on a project to project basis. Figure 6-10 contains a photograph of H-piles with driving shoes.



Figure 6-10 H-piles with driving shoes.

H-piles produced today meet the requirements of ASTM A572, Grade 50 steel, as ASTM A36 steel H-piles are no longer readily available. Steel sections meeting the requirements of ASTM A588 and ASTM A690 are also available. These are high strength, low alloy steels developed for improved corrosion resistance in atmospheric (ASTM A588) and marine (ASTM A690) environments. However, ASTM A588 and A690 steels are typically hard to obtain, and long lead times may be necessary if they are specified. ASTM A572, A588 and A690 are all Grade 50 steels. Some H-piles can also be obtained in A572 Grade 60 steel. Therefore, it is possible to use the higher strength of Grade 50 or 60 steel if the pile can be installed to maximize the geotechnical resistance in the project soil conditions. Steel H-piles

are very effective when driven into soft rock. They can be driven very hard with modern high impact velocity hammers with little likelihood of pile toe damage.

H-piles can develop their nominal resistance through shaft resistance, toe resistance or a combination of both. Since H-piles generally displace a minimum amount of soil, they can be driven more easily through dense granular layers and very stiff clays than displacement piles. In addition, problems associated with soil heave during foundation installation are often reduced by using H-piles. However, sometimes H-piles will "plug". That is, the soil being penetrated will adhere to the web and the inside flange surfaces creating a closed end, solid section. The pile will then drive as if it were a displacement pile below the depth of plug formation. Plugging can have a substantial effect on both the soil resistance during driving and the nominal geotechnical resistance. H-piles can be problematic when used as friction piles in some granular deposits. In these conditions they often don't plug during driving, have low dynamic resistances during installation, and result in excessive pile lengths.

Experience indicates that corrosion is not a practical problem for steel piles driven in natural soil, due primarily to the absence of oxygen in the soil. However, in fill materials at or above the water table, moderate corrosion may occur and protection may be needed. In 2013, an H-pile supported pier at the I-43 Leo Frigo Bridge suddenly settled due severe corrosion. While the concurrent factors that lead to the corrosion were considered highly unusual, this occurrence emphasizes the need for identifying corrosive environments during the design stage. As noted previously, high strength, low allow steels are available for improved corrosion resistance. Another common protection method requires the application of pile coatings before and after driving. Coal-tar epoxies, fusion bonded epoxies, metallized zinc, metallized aluminum and phenolic mastics are some of the pile coatings available. Encasement by cast-in-place concrete, precast concrete jackets, or cathodic protection can also provide protection for piles extending above the water table. Another design option for piles subject to corrosion is to select a heavier section than that required by the design loads, anticipating the loss of material caused by corrosion. Corrosion losses can be estimated using the information provided in Section 6.14.1. However, even with the corrosion protection options or allowances mentioned above, certain aggressive soil conditions will preclude the use of steel piles altogether.

One of the key advantages of H-piles is the ease of extension or reduction in pile length. This makes them suitable for nonhomogeneous soils with layers of hard strata or natural obstructions. Splices are commonly made by full penetration

groove welds so that the splice is as strong as the pile in both compression and bending. The welding should always be done by qualified welders in accordance with approved procedures. Proprietary splices are also commonly used for splicing H-piles and Chapter 16 presents additional information on typical splices. A steel load transfer cap is not required by AASHTO if the pile head is embedded 12 inches into the concrete pile cap. Pile toe reinforcement using commercially manufactured pile shoes is recommended for H-piles driven through or into very dense soil or soil containing boulders or other obstructions. Pile shoes are also used for H-piles driven to rock, particularly for penetration into sloping rock surfaces. Chapter 16 provides details on available driving shoes.

The disadvantages of H-piles include a tendency to deviate when natural obstructions are encountered. Nominal resistance verification of H-piles used as friction piles in granular soils based on the observed blow count can also be problematic, and can result in significant length overruns. An H-pile in a granular profile will often not plug during the dynamic loading of pile installation but may plug under the slower static loading condition. Length for length, steel piles tend to be more expensive than concrete piles. On the other hand, steel's high factored resistance for a given weight can reduce pile driving costs.

6.4 STEEL PIPE PILES

6.4.1 Closed End Steel Pipe

Closed end steel pipe piles consist of seamless, welded or spiral welded steel pipes in diameters typically ranging from 8 to 30 inches. Larger pipe pile sizes are available, but larger diameters are more commonly driven open ended. Typical wall thicknesses for closed end pipe piles range from 0.188 to 1 inch. Pipe piles should be specified by grade with reference to ASTM A252, API-5L, or API-2B. In some situations, a contractor may propose to supply used pipe not produced under ASTM standards. Used pipe piles not meeting ASTM standards must be evaluated by an engineer for general condition, drivability, and weldability prior to approval.

A closed end pipe pile is generally formed by welding a 0.75 to 2 inch thick flat steel plate to the pile toe. The toe plate thickness generally increases with pile diameter and/or with anticipated harder driving conditions. When pipe piles are driven to weathered rock or through boulders, a cruciform-reinforced end plate or a conical point with rounded nose is often used to minimize pile toe distortion. Figure 6-11 presents a picture of a typical closed end pipe pile with a flat closure plate.



Figure 6-11 Typical 16 inch closed end pipe pile.

Closed end steel pipe piles can be used as friction piles, toe bearing piles, a combination of both, or as rock socketed piles. They are commonly used where variable pile lengths are required since splicing is relatively easy. With the increased ductility requirements for earthquake resistant design, pipe piles are being used extensively in seismic areas.

Pipe piles may be left open or filled with concrete. If concrete filled, the piles can also have a reinforcing steel cage or structural shape such as an H-section inserted into the concrete. Reinforcing steel is required only when the concrete in the pile may be under tension from such conditions as uplift, high lateral loads, or for unsupported pile lengths.

Most often, pipe piles are driven from the pile head. However, thin wall, closed end pipe piles can also be bottom driven using a mandrel. A mandrel is usually a heavy tubular steel section inserted into the pile that greatly improves pile drivability. After driving, the mandrel is removed and the pile is inspected internally before concrete is placed. Typically, pipe piles are spliced using full penetration groove welds. Proprietary splicing sleeves are available and should be used only if the splice can provide full strength in bending and tension (unless the splice will be located at a distance below ground where bending moments and tension loads are small). Typical pile splices are described in Chapter 16. The corrosion discussion on H-piles is also applicable to steel pipe piles.

6.4.2 Open End Steel Pipe

Open end pipe piles are frequently installed when hard driving conditions, significant penetration depths, or debris is expected. Open end pipe piles are available in diameters that range from 8 to 160 inches. When pipe piles are driven open ended, wall thicknesses of 0.5 inches or greater are commonly used. Similar to closed end pipe piles, the open end piles can be seamless, rolled and welded, or spiral welded steel pipes. Open end pipe piles should be specified by grade with reference to ASTM A252, API-5L, or API-2B. In some situations, a contractor may propose to supply used pipe not produced under ASTM standards. Used pipe piles not meeting ASTM standards must be evaluated by an engineer for general condition, drivability, and weldability prior to approval.

Large diameter open end pipe piles are defined as greater than 36 inches in diameter (Brown and Thompson 2015). These are often selected due to their ability to resist significant vessel impacts and overturning moments, and/or due to scour, ice, or seismic design considerations. Other common applications of large diameter open end pipe include fender systems, mooring dolphins, and offshore facilities. Large diameter open end pipe piles are frequently used to support main piers on major river bridges or other structures with large lateral resistance demands. Large diameter open end pipes are typically driven to bear in dense sand or soft rock, or are installed as long friction piles. Figure 6-12 shows a group of 42 inch diameter, spiral weld, open end pipe piles for a main bridge pier support. A photo of a 12 foot diameter open end pipe is presented in Figure 6-13.

Open end pipe piles can be socketed into bedrock (rock socketed piles), or when driving through dense materials, may form a soil plug. The plug makes the pile act like a closed end pile and can significantly increase the pile toe resistance. Plugging is discussed in greater detail in Section 7.10.7 and is a complex phenomenon. The soil plug should not be removed unless the pile is to be internally cleaned out and filled with concrete or unless the soil plug is preventing the pile from achieving the required penetration depth.

Large diameter open end pipe typically core through the soil during driving due to mass soil inertia effects. However, under static loading conditions, these piles generally plug providing significant toe bearing resistance. Some recent large diameter open end pipe pile projects have incorporated a constrictor plate inside the pile to force plugged behavior during driving. A diagram of a constrictor plate design and a companion photograph are presented in Figures 6-14 and 6-15, respectively. Constrictor plates are also discussed in Section 16.3.3.



Figure 6-12 42 inch diameter, spiral weld, open end, pipe for main river pier.



Figure 6-13 Large diameter open end pipe piles.

Open end pipe piles are seldom cleaned out full length unless a rock socket is planned or short pile lengths are used. Before concrete placement, steel reinforcement and uplift resisting dowels can be added, as necessary.

Open ended piles can also be equipped with internal or external steel cutting shoes to reduce the potential for toe damage. When hard driving conditions are expected such as sloping rock, cobbles and boulders, etc., large diameter open end pipes are frequently designed with a thicker wall pipe section over the bottom two diameters to lessen the risk of toe damage from high localized stresses.

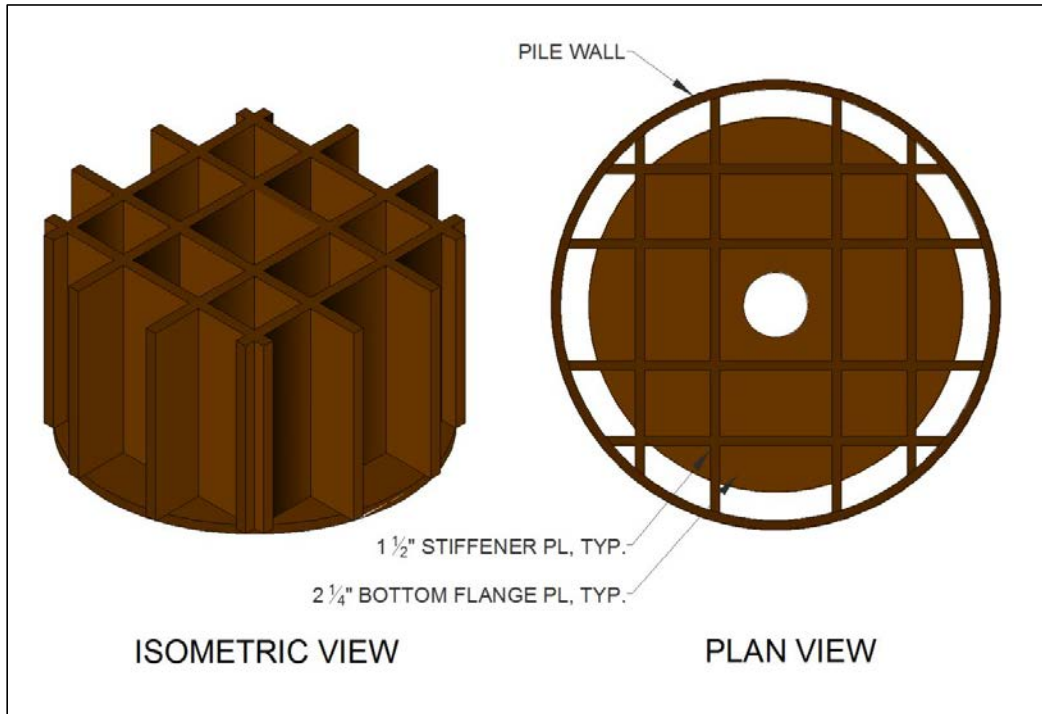


Figure 6-14 Constrictor plate.

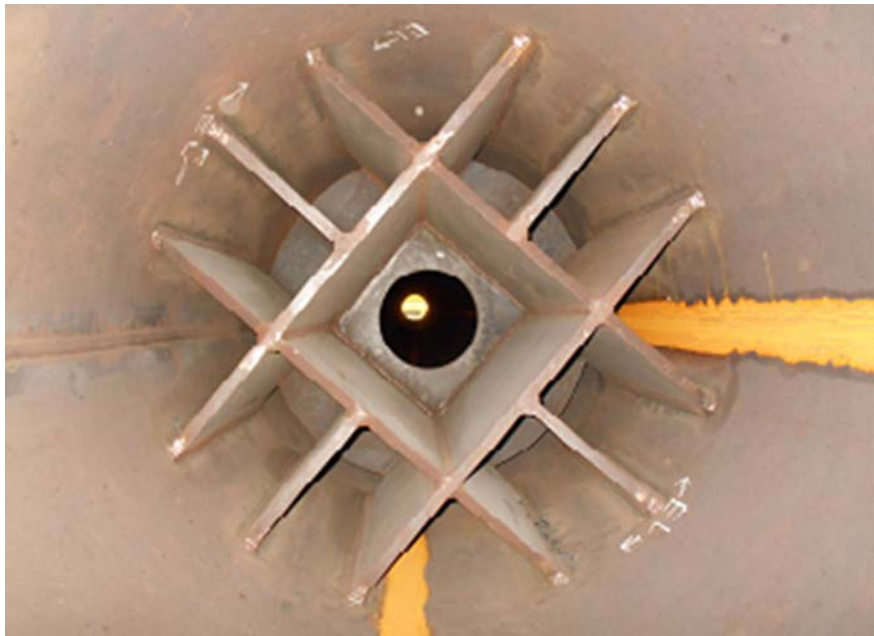


Figure 6-15 Constrictor plate installed inside pipe pile.

6.5 MONOTUBE PILES

The Monotube pile, shown in Figure 6-16, is a proprietary pile driven without a mandrel. Monotubes are longitudinally fluted and are tapered over the lower pile section. Depending upon the pile section selected nominal pile toe diameters of 8 or 8.5 inches taper to a butt diameter of 12, 14, 16, or 18 inches over tapered section lengths of 10 to 75 feet. Non-tapered extensions are available in 20 and 40 feet for splicing to the lower tapered section. Monotube piles are available in 9 to 3 gage shell thicknesses or roughly 0.15 to 0.24 inches. Monotube sections are spliced by inserting the slightly smaller bottom section of the extension into the top of the previously driven section. A fillet weld is then used along the interface between the extension and the lower pile section into which it is inserted. Four V shaped notches cut into the lower pile section at 90 degree locations are often added to increase weld length and splice strength. After driving, Monotube piles are filled with concrete.

The fluted and tapered design of Monotube piles has several functional advantages. The flutes add stiffness necessary for handling and driving lightweight piles. These also increase the surface area while the tapered section improves the soil resistance per unit length in compression loading. The flutes are formed by cold working when the pile is manufactured as this increases the yield point of the steel to more than 50 ksi, further improving the pile drivability.



Figure 6-16 Tapered Monotube section (right) with add-on sections (left).

6.6 TAPERTUBE PILES

This pile consists of a tapered, 12 sided polygon over the lower section with conventional steel pipe pile material as the upper add-on sections. The 15 to 30 feet long tapered section steel is available with pile toe diameters ranging from 8 to 14 inches and pile head diameters of 12 to 24 inches. Wall thickness of the tapered sections ranged from 0.1875 to 0.625 inches. The tapered tube bottom section has a yield strength of 50 ksi, and the upper pipe pile sections conform to ASTM A252 Grade 3 steel with a yield strength of 45 ksi. The tapered and pipe sections are connected using a full penetration weld.

Tapertube piles are driven from the top and filled with concrete after driving. Specialty sleeve splices may be used as an alternative to welding sections together. Please see Chapter 16 for more information. A photo of Tapertube piles is presented in Figure 6-17.



Figure 6-17 Tapertube piles (courtesy DFP Foundation Products, LLC).

6.7 SPIN FIN PILES

The Spin Fin pile is a variation of a pipe pile introduced on the west coast in 1983. It is a pipe pile with an outside “thread” made of fins that gradually wind around a bottom portion of the pile. These fins cause the pile to rotate into the ground during driving. Following driving, the pile is incorporated into a pile cap. Pile rotation is

then restrained by the cap preventing the pile from twisting. This results in a plugging effect that increases the pile's resistance to tension loads as depicted in Figure 6-18. The Spin Fin pile is particularly attractive on projects needing increased uplift resistance such as for seismic events or in soils with limited overburden materials overlying a hard bearing layer such as a glacial till over bedrock. The fins also increase the compression resistance by increasing the bearing area in the pile section having fins. A photograph of a 30 inch diameter spin fin pile is presented in Figure 6-19.

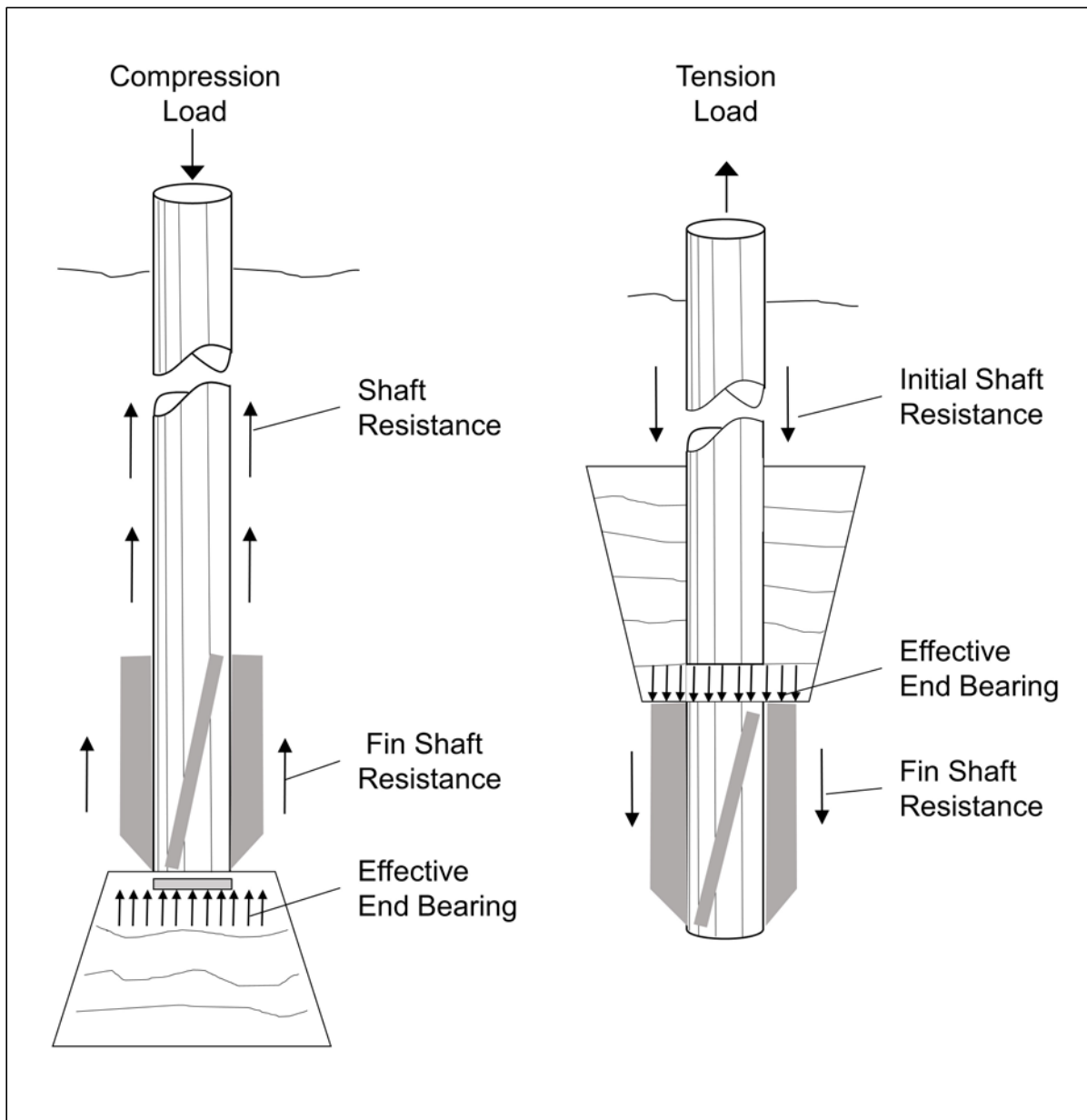


Figure 6-18 Spin Fin pile load transfer illustration.



Figure 6-19 30 inch diameter Spin Fin pile.

6.8 PRESTRESSED CONCRETE PILES

Prestressed concrete piles vary from the most common solid square section to a solid octagonal section. As sections increase in size, they are often cast with an internal void to reduce handling weight. Prestressed piles can either be pre-tensioned or post-tensioned. Pre-tensioned piles are usually cast to their full length in permanent casting beds. Post-tensioned piles are usually manufactured in sections, most commonly cylindrical, and assembled and prestressed to the required pile lengths at the manufacturing plant or on the job site. Figure 6-20 depicts common prestressed concrete pile sections and Figure 6-21 presents a photograph of prestressed piles stored on a barge prior to driving.

The prestressing steel may be in the form of strands or wires which are enclosed in a conventional steel spiral and placed in tension. Prestressing steel must conform to ASTM A416, A421, and A882. Due to the effects of prestressing, these piles can usually be made lighter and longer than reinforced concrete piles of the same size. In cases of extreme environmental conditions, an epoxy coating has been used on prestressing strands. If this coating is used, it should be dusted with sand before the epoxy sets. Then the strand will have sufficient bond strength to carry the prestress

development bond stresses. If an epoxy coating has been used on the strand, it should also be used on the tie or spiral reinforcement. However, epoxy coating is generally not necessary for prestressed piles since the prestressing force will keep the concrete in compression making deterioration less likely.

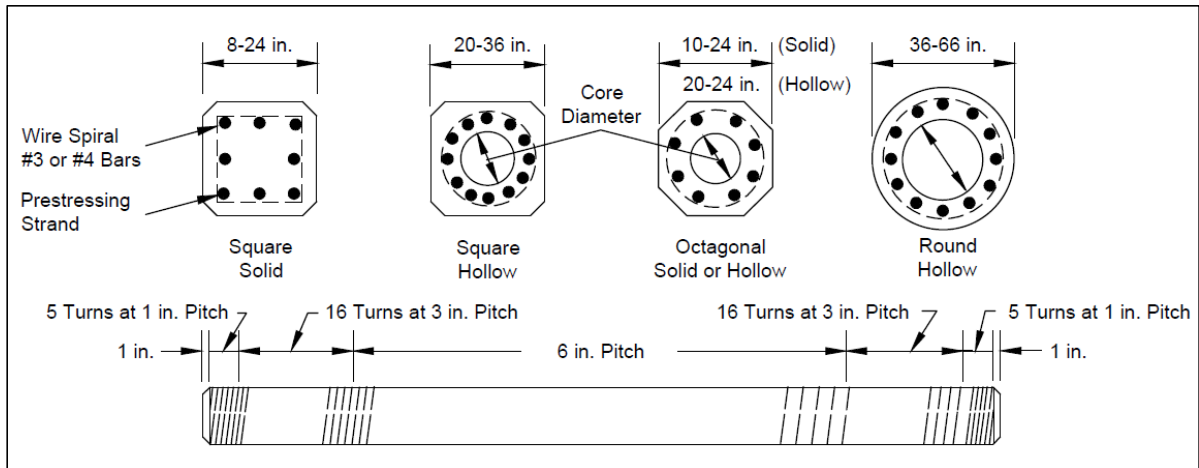


Figure 6-20 Typical prestressed concrete piles.



Figure 6-21 Square prestressed concrete piles.

The primary advantage of prestressed concrete piles compared to conventional reinforced concrete piles is durability. Since the concrete is under continuous compression, hairline cracks are kept tightly closed and thus prestressed piles are usually more resistant to weathering and corrosion than conventionally reinforced piles. This characteristic of prestressed concrete removes the need for special steel coatings since corrosion is not as serious a problem as for reinforced concrete.

Another advantage of prestressing is that the tensile stresses which can develop in the concrete under certain driving and handling conditions are less critical.

Prestressed concrete piles are more vulnerable to damage from striking hard layers of soil or obstructions during driving than reinforced concrete piles. This is due to the decrease in axial compression strength due to the application of the prestressing force. When driven in soft soils, care must also be used since large tension stresses can be generated in easy driving.

Prestressed concrete piles cutoff and splicing problems are considered much more serious by contractors that drive them infrequently than by those that drive only this pile type. Special reinforcement required at the pile head in seismic areas can pose problems if actual lengths vary significantly from the planned length. In these cases, a splice detail must be included so that the seismic reinforcement is extended into the pile cap.

Concrete used for most prestressed concrete piles typically has a 28 day compressive strength between 5 and 6 ksi. Recent developments in prestressed concrete piles include studies on the use of high performance concrete (e.g., Moser 2011) to improve pile durability, or ultra-high performance concrete (e.g., Vande Voort et al. 2008) for improved durability and load support relative to steel H-piles. Belk (2013) studied the use of lightweight aggregate on prestressed concrete piles relative to drivability, load support and weight. At the present time, these developments have not progressed into mainstream practice.

6.9 CONCRETE CYLINDER PILES

Concrete cylinder piles include spun cast, non-spun cast, and Industrial Concrete Products pile types. Each of these cylinder piles types is discussed further below. Cylinder piles are sometimes difficult to drive. However, they usually extend directly to the superstructure support level avoiding the need for a pile cap, which can result in substantial cost savings. Jetting is often used to install cylinder piles to the near the desired depth followed by impact driving to attain the required nominal resistance. When jetting is used, it must be controlled to minimize degradation of the lateral soil resistance and disturbance and removal of soils below the specified jetting elevation. The design of the pile wall often includes periodic vent holes that are used to reduce the build-up of internal water pressure during driving as well as to later avoid build-up of internal gas pressure from organic soil decomposition during service life.

6.9.1 Spun-Cast Cylinder Piles

Spun-cast concrete cylinder piles are hollow concrete piles which are cast in 8, 12, or 16 foot sections. Depending on the manufacturer, cylinder piles are generally available in diameters of 36, 42, 54 and 66 inches. Wall thicknesses of 5, 6, or 6.5 inches are available depending on the pile diameter. Cylinder pile sections are spun centrifugally during the casting process to obtain a high density, durable concrete that is virtually impervious to moisture. The concrete quality from the spun-casting process is unique to spun-cast cylinder piles and concrete compressive strengths of 8 ksi can routinely be achieved. Once cured, sections are assembled to form a pile with the desired pile length. An adhesive joint compound is used between sections. The assembled pile is post tensioned and then the post tensioning ducts grouted.

Results of chloride ion penetration and permeability tests on prestressed cylinder piles indicate that the spun-cast cylinder piles have excellent resistance to chloride intrusion. The post-tensioning process results in a typical prestress level of 1.5 ksi. Figure 6-22 shows the typical configuration of this cylinder pile type. A photograph of concrete cylinder piles is presented in Figure 6-23.

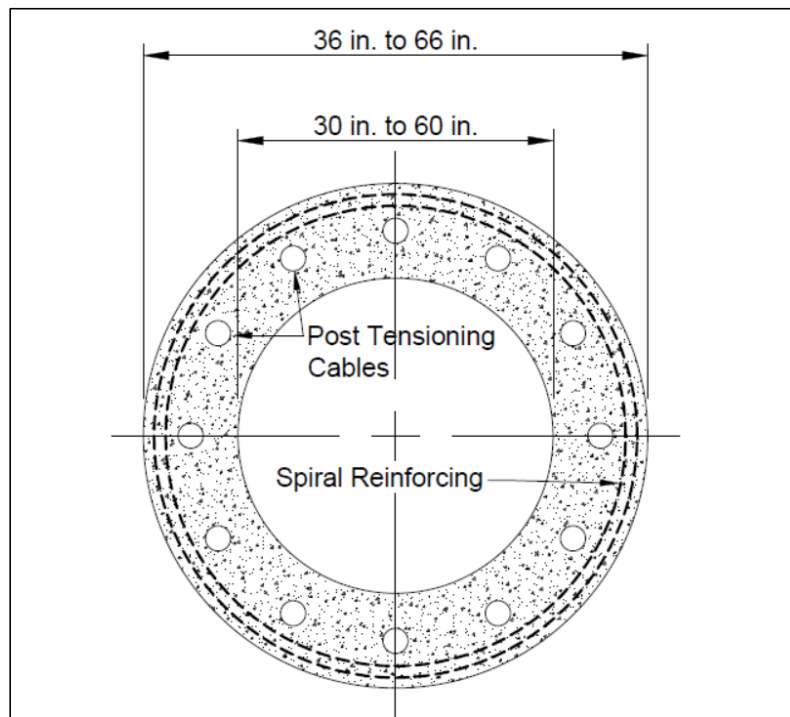


Figure 6-22 Typical spun-cast concrete cylinder pile section.

Generally spun-cast cylinder piles are used for marine structures or land trestles and have high resistance to corrosion and high lateral resistance. To prevent freeze-thaw degradation, air entrainment and adequate spiral reinforcement are important

considerations. The piles typically extend above ground and are designed to resist a combination of axial loads and bending moments. Additional design and installation considerations associated with concrete cylinder piles are summarized in Hartman et al. (2007).



Figure 6-23 Concrete cylinder pile.

6.9.2 Bed-Cast Cylinder Piles

Cylinder piles can also be cast in a bed with forms rather than centrifugally spun cast. These piles are produced to the required length in a single piece and are pretensioned instead of being post tensioned like the spun-cast piles. Due to the differences in the casting process, these piles do not have the high density, low porosity concrete that is characteristic of spun-cast cylinder piles and will therefore not have the same resistance to chloride intrusion. Bed-cast cylinder piles have typical specified concrete compressive strengths of 5.5 ksi, a diameter of 60 inches, and a wall thickness of 7.5 inches.

6.9.3 Industrial Concrete Products (ICP) Piles

These cylindrical piles are pretensioned and spun to compact concrete while curing. The spinning process creates a high density mix by forcibly removing water during the hydration process while pretension adds tensile strength. Typically, ICP piles are cast in sections with steel end plates. Field splices are made by welding the section end plates. Sizes range from 10 inch diameter with a 2.25 inch thick wall to a 48 inch diameter with a 5.9 inch wall. ICP section lengths vary with the pile diameter from 20 to 39 feet on the smallest diameter section up to 33 to 138 feet on the largest diameter section. Piles are supplied open end with a flat shoe or with an X-pointed shoe.

6.10 COMPOSITE PILES

In general, a composite pile is made up of two or more sections of different materials or different pile types. Depending upon the soil conditions, various composite sections may be used. The upper pile section is often precast concrete, steel pipe, or corrugated shell. The lower pile section may consist of steel H, steel pipe, or timber pile. Composite piles have limited application and are generally used only under special conditions. Some of the more common composite piles are discussed below.

6.10.1 Precast Concrete - Steel H-pile Composite Piles

One of the more commonly used composite piles consists of a lower section of steel H-pile or pipe pile embedded in an upper pile section of precast concrete. These concrete-steel composite piles are often used when scour or uplift requirements dictate pile penetration depths that a displacement pile cannot achieve, in subsurface conditions where surficial soil layers have high corrosion potential, or in other conditions that dictate their use. A photograph of composite square concrete piles each with H-pile stinger is presented in Figure 6-24.



Figure 6-24 Precast concrete piles each with H-pile stinger.

6.10.2 Steel Pipe - H-pile Composite Piles

Steel pipe - H-pile composite piles are comprised of a steel pipe upper section with a transition to an H-pile lower section. This composite selection may be applicable where lateral load demands require the bending resistance of a pipe pile in the upper pile length and dense soil conditions necessitate a low displacement pile over the lower pile length to satisfy minimum pile penetration depth or bearing layer requirements. A steel pipe - H-pile composite piles are shown in Figure 6-25.



Figure 6-25 Steel pipe - H-pile composite piles.

6.10.3 Corrugated Shell - Timber Composite Piles

Corrugated shell - timber composite piles are sometimes used as foundation piles. For this composite pile the timber pile section is permanently located below the groundwater level. A concrete filled shell pile is used above the treated or untreated timber pile. In the case of the composite corrugated shell - timber pile, the timber pile is driven below the water table. A corrugated steel shell is connected to the pile

head of the timber section with a wedge ring driven into the wood. The shell is filled with concrete to the cutoff elevation and the pile is complete.

6.10.4 Corrugated Shell - Pipe Composite Piles

This composite pile consists of a pipe pile for the lower section and a corrugated shell for the upper portion of the pile. A variety of pipe and shell diameters can be used to accommodate a range of loading conditions. The corrugated shell - pile composite pile is mandrel driven. The mandrel provides a guide for alignment of the two pile sections provided it extends to the pipe pile head or partially into the pipe pile. Possible pile joints include: a sleeve joint, a welded joint, and a drive-sleeve joint. Once the pipe and shell are driven and connected, they are filled with concrete to cutoff grade and any excess shell is removed.

6.11 PILE TYPES INFREQUENTLY USED ON TRANSPORTATION PROJECTS

Additional pile types exist that are sometimes used in specialty applications. Others were used more frequently in the past and could be encountered if existing foundations are re-used on reconstruction projects. These include Fundex piles, Tubex piles, mandrel driven piles, reinforced concrete piles, and pressure injected footings. Experience and field testing (load and integrity tests) should be used in new designs using these systems or in re-use of existing foundations.

6.11.1 Fundex Piles

The Fundex pile is a unique form of a pipe-cased, cast-in-place concrete displacement pile. Instead of the pile being driven into the ground with a hammer, it is screwed into the ground with a special 18 inch diameter boring tip. The boring tip is fitted to a 14 inch diameter drilling mandrel with a chuck assembly. A drill table forces the drilling mandrel into the ground utilizing a constant vertical load and torque. When the bearing layer or required penetration depth is reached, a reinforcing cage is suspended within the mandrel and concrete is placed. The drilling mandrel is then oscillated out of the ground leaving the drill point behind. This process results in a cast-in place pile typically installed for unfactored design loads in the 40 to 125 ton range.

Some of the advantages of the Fundex piles include minimal vibrations and very low noise during installation, drilling equipment that can be used in confined places, and a removable mast that allows installation with only 20 feet of overhead clearance.

6.11.2 Tubex Piles

Tubex piles are installed similarly to Fundex piles. A pipe-cased hole is created for the Tubex pile as the drill point is advanced into the soil. Pipe sections may be spliced if additional length is required or if required by headroom limitations. Since the steel casing is in place after drilling to the final installation depth, an internal inspection can also be performed prior to concrete and reinforcement placement. However, unlike the Fundex pile, this casing is then left in place along with the drill point. A grout injected version of the Tubex pile is also available. Typically Tubex pile diameters are 14 inches or greater. If grouted, this pile is typically installed for unfactored design loads of up to 230 tons.

Some of the advantages of the Tubex piles include minimal vibrations and very low noise during installation, drilling equipment that can be used in confined places, and a removable mast that allows installation with only 20 feet of overhead clearance. In addition, the grout injected Tubex pile can be used to insulate the steel casing from corrosive environments.

6.11.3 Pressure Injected Footings (PIF)

This type of driven, cast-in-place pile is often referred to as a Franki pile or pressure injected footing. The best site conditions for these piles are loose to medium dense granular soils.

This pile type is installed by bottom driving a temporary steel casing into the ground using a drop weight driving on a zero slump concrete plug at the bottom of the casing. When the required depth has been reached, the steel casing is restrained from above and the concrete plug is driven out the bottom of the tube. An enlarged base is formed by adding and driving out small batches of zero slump concrete.

Steel reinforcing is then installed prior to adding more concrete to the shaft. It is suggested that widely spaced bars be used to allow the low workability mix to penetrate to the exterior of the piles. After the base is formed and reinforcement is placed, concrete continues to be added and the uncased shaft is formed by compacting the concrete with a drop weight in short lifts as the casing is being withdrawn. Alternatively, if a high workability mix is used to complete the pile, a vibrator can be clamped to the top of the tube and used to compact the concrete into place as the casing is withdrawn.

6.11.4 Mandrel Driven Piles

In the past, mandrel driven piles were used in many soil conditions except where obstacles such as cobbles and boulders were present that could damage the thin shells during driving. The thin shells were susceptible to collapse under hydrostatic pressure prior to concrete placement. They were best suited for friction piles in granular material. Thin shell mandrel driven piles are rarely used today for new construction. They may however be encountered when widening or rehabilitating existing structures so a general overview of their characteristics remains useful.

The pile shells for mandrel driven piles were generally produced from sections of corrugated steel and were either of constant diameter, steadily decreasing in diameter from the pile head to the pile toe, or diameter decreasing in discrete steps over the pile length. Typical tapers were on the order of 1 inch per 8 foot length. It was also possible to have different lengths for each section. Separate shell sections were usually screw-connected and waterproofed with an O-ring gasket. The Raymond Step Taper, Armco Hel-Cor, Republic Corwel, and Guild pile were among the pile types previously driven with mandrels. However most of these corrugated shell type piles are no longer manufactured. Thin wall pipe piles have also been mandrel driven with the mandrel driving on a reinforced section at the pile toe.

The properties of the reusable mandrels dictated the drivability of these shell or thin wall pipe pile sections. This resulted in a significant cost advantage for a mandrel driven pile since the mandrels result in improved pile drivability and soil resistance at low material costs. Construction control of mandrel driven piles should include a wave equation analysis that accounts for the improved pile drivability from the mandrel. A dynamic formula should not be used for construction control of mandrel driven piles. Mandrel driven piles may be costly if it is necessary to drive piles to an unanticipated depth that exceeds the mandrel length available at the job site.

6.11.5 Reinforced Concrete Piles

Prestressed concrete piles have replaced reinforced concrete piles in the U.S. market. Reinforced concrete piles were manufactured from concrete and had reinforcement consisting of a steel cage made up of several longitudinal bars and lateral or tie steel in the form of individual hoops or a spiral. While they are no longer used in the U.S., a limited discussion on them is presented in case they are encountered on a rehabilitation or widening project. Steel reinforcing for reinforced concrete piles was governed by ASTM A82, A615, and A884. High yield strength steel reinforcement to resist uplift loads had to conform to ASTM A722.

Reinforced concrete piles were more susceptible to damage during handling and driving because of tensile stresses compared to prestressed piles. Advantages of reinforced concrete piles included their lower net compressive stress during driving and under foundation loads, and a reduced danger of pile head cracking. In addition, these piles were easier to splice than prestressed piles. To reduce corrosion of the reinforced concrete joints, splices were located below the ground surface, or if under water, the mudline. Segmental pile sections were used to produce piles with varied lengths to accommodate variable soil conditions, and were easily transported to job sites.

The most common type of jointed pile was a square cross section made of high density concrete with each successive unit of shorter length. Typical pile cross sections ranged from 10 to 16 inches, but sizes above and below this range were produced. Joints between these pile sections were of the mechanical type, including bayonet fittings or wedges. The joints had to be well aligned or energy was lost during driving and bending stresses would be introduced due to an eccentric connection. These piles were best suited for friction piles in sand, gravel and clay.

Another jointed reinforced concrete pile type utilized a hexagonal section. The advantages of this cross sectional shape were an improved stress distribution over the pile section and an improved resistance to torsional loading.

Special precautions had to be taken when placing piles during cold weather. If piles were driven through ice and water before reaching soil, the air and concrete may have been at low temperatures relative to the soil and water. Such temperature gradients could cause concrete to crack due to non-uniform shrinkage and expansion. Although most reinforced concrete piles were jointed, there were occasions when non-jointed piles were more economical due to the cost of pile segments. Often for a very large project when thousands of piles were used, the piles were economically cast on site. Most non-jointed piles had a square cross section and were difficult to change in length. Only a few splicing procedures existed if a situation arose where a reinforced concrete pile needed to be lengthened. The first method of pile lengthening involved the breakdown of the projecting pile head to provide a suitable lap for reinforcing steel. Concrete was cast to form a joint. A second option was to butt the two piles together within a steel sleeve, and use an epoxy cement to join the two piles. The last lengthening method involved the use of dowel bars to be inserted into drilled holes with epoxy cement to form the joint. If piles were lengthened, the connecting pile sections had to be carefully aligned, since excessive bending stresses would result if any eccentricity

existed. Splicing problems tended to become less severe or even non-existent when contractors developed experience and techniques. Special reinforcement required at the pile head in seismic areas posed problems if actual lengths varied significantly from the planned length. In these cases, a splice detail had to be included so that the seismic reinforcement was extended into the pile cap.

Reinforced concrete piles are no longer used in the United States. However, they are routinely used in Europe, Australia, and many Asian countries for economic reasons.

6.12 DESIGN CONSIDERATIONS IN AGGRESSIVE SUBSURFACE ENVIRONMENTS

For every design, consideration should be given to the possible deterioration of the pile over its design life due to the surrounding environment. This section will address design considerations in aggressive subsurface environments where corrosion, chemical attack, abrasion, and other factors can adversely affect pile durability after installation. An assessment of the in-situ soil conditions, fill materials, and groundwater properties is necessary to completely categorize an aggressive subsurface condition.

An aggressive environment can generally be identified by soil resistivity and pH tests. If either the pH or soil resistivity tests indicate the subsurface conditions are aggressive, then the pile selection and foundation design should be based on an aggressive subsurface environment. The design of pile foundations in an aggressive environment is a developing field. Therefore, a corrosion/degradation specialist experienced in underground corrosion should be retained for major projects with pile foundations in aggressive environments.

Whenever the pH value of the soil or water is less than 4.5, the foundation design should be based on an aggressive subsurface environment. Alternatively, if the resistivity is less than 2000 ohms-cm the site should also be treated as aggressive. When the soil resistivity test results are between 2000 and 5000 ohms-cm then chloride ion content and sulfate ion content tests should be performed. If these test results indicate a chloride ion content greater than 100 parts per million (ppm) or a sulfate ion content greater than 200 ppm, then the foundation design should be based on an aggressive subsurface environment. Resistivity values greater than 5000 ohms-cm are considered non-aggressive environments. Electro chemical classification tests for aggressive environments are described in Chapter 5.

Contaminated soil and groundwater can cause significant damage to foundation piles in direct contact with the aggressive chemicals. Acidic groundwater is common at sites with organic soils, industrial contamination, or mine runoff. The subsurface exploration program should indicate if the soil or groundwater is contaminated. If industrial contamination is found, the maximum likely concentrations should be determined as well as an estimate of the lateral and vertical extent of the contamination.

6.12.1 Corrosion of Steel Piles

Steel piles driven through contaminated soil and groundwater conditions may be subject to high corrosion rates and should be designed appropriately. Corrosion of steel or steel reinforced piles may also occur if piles are driven into disturbed ground, landfills or cinder fills, or low pH soils. Corrosion should also be evaluated for piles located in a marine environment, or if piles are subject to alternate wetting and drying from tidal action. Corrosion rates are a function of the ambient temperature, pH, access to oxygen, and chemistry of the aqueous environment surrounding the steel member.

6.12.1.1 Corrosion in Non-Marine Environments

AASHTO Standard R 27-01 (2010) provides a recommended assessment procedure for evaluating corrosion of steel piling in non-marine applications. This recommended procedure consists of a Phase I and Phase II assessment. In the Phase I assessment, information on the location of the pile cap relative to the groundwater table, the soil characteristics, and soil contaminants is obtained. This information is used to determine if a Phase II assessment is required.

If the pile cap is at or above the water table, a Phase II assessment is performed to evaluate the corrosivity of the site. The Phase II assessment consists of collecting continuous soil samples to a depth of 3 feet below the water table and conducting laboratory tests on the recovered samples. The site sampling and testing protocol is outlined in Figure 6-26. After collecting the necessary information, the possibility of uniform or macro cell corrosion is evaluated using the flow chart presented in Figure 6-27. The final step in the evaluation process includes determining the necessity for electrochemical testing, corrosion monitoring, and mitigation techniques. A flow chart of this process is presented in Figure 6-28.

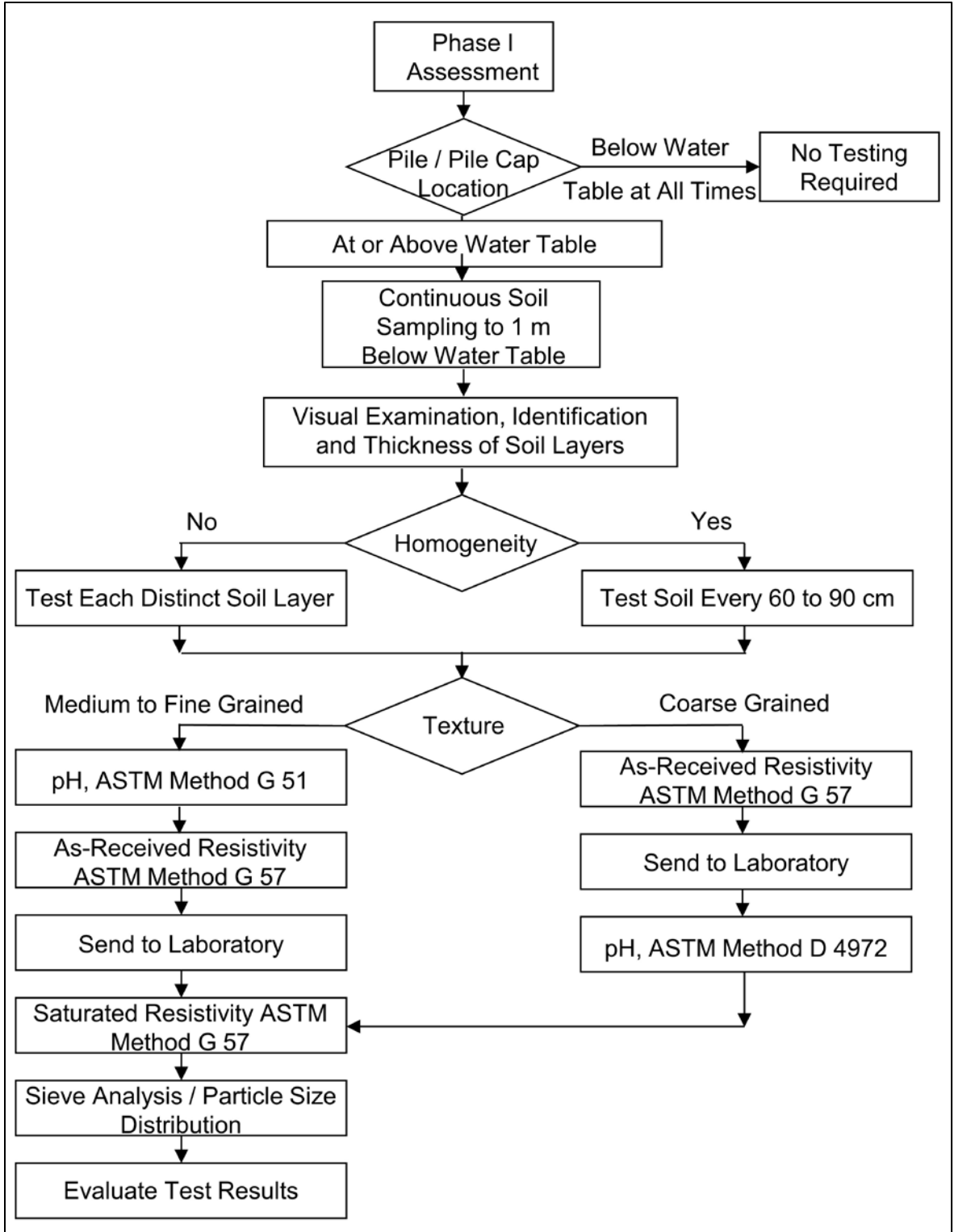


Figure 6-26 Soil sampling and testing protocol for corrosion assessment of steel piles in non-marine applications.

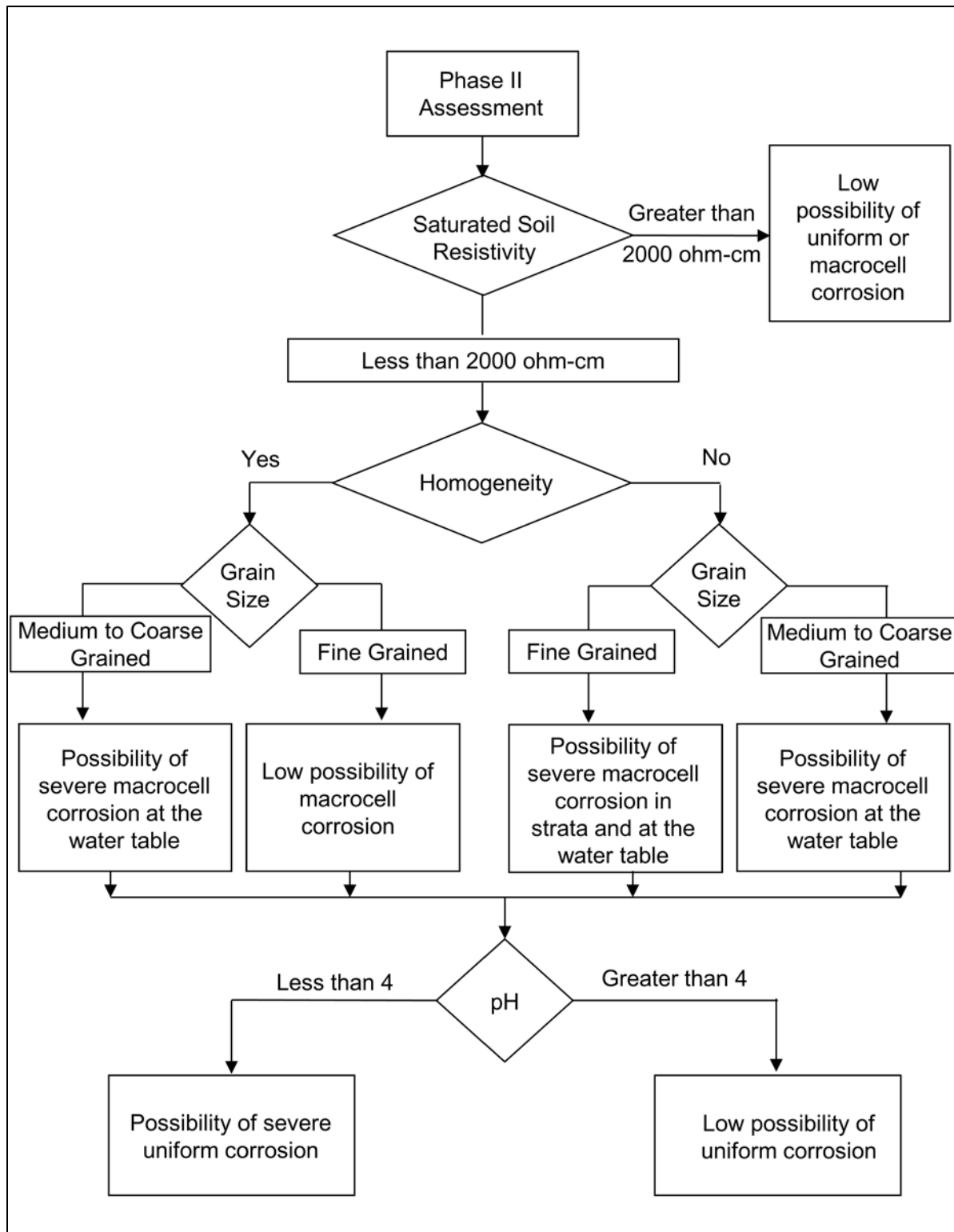


Figure 6-27 Procedure for uniform or macrocell corrosion assessment of steel piles in non-marine applications.

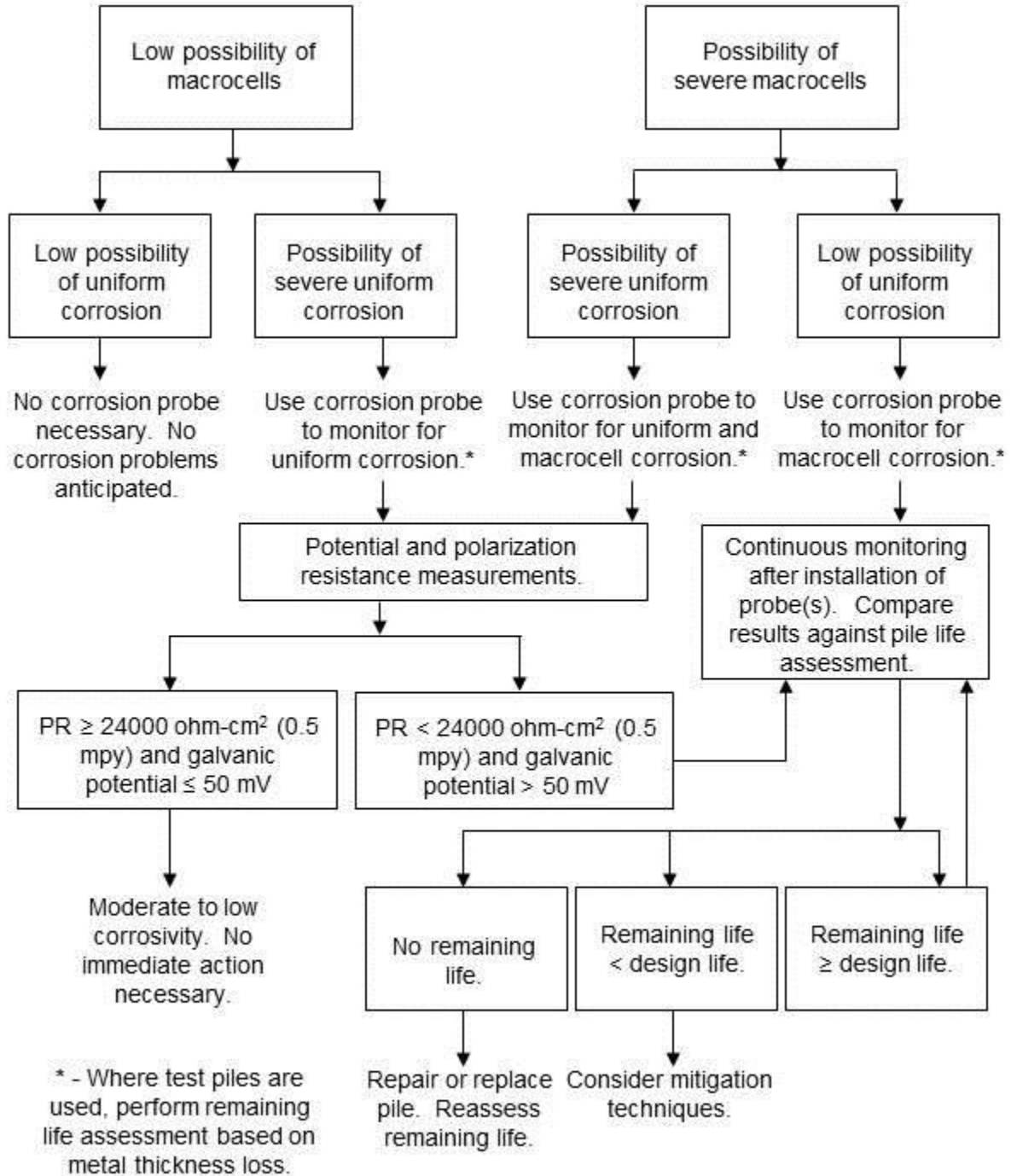


Figure 6-28 Procedure for determination of electrochemical testing, corrosion monitoring and corrosion mitigation techniques.

It should be noted that the flow charts do not cover all possibilities for corrosion of steel piling at a site. Factors not addressed include chemical contamination, stray DC currents, and the presence of high concentrations of microbes. When these conditions are present on a project, an underground corrosion specialist should be consulted.

For steel piles buried in fill or disturbed natural soils, a conservative estimate of the corrosion rate is 0.003 inches per year. Morley (1979) reported corrosion rates of 0.002 inches per year for steel piles immersed in fresh water, except at the waterline in canals where the rate was as high as 0.013 inches per year. The high rate of corrosion at the water line was attributed to debris abrasion and/or cell action between other parts of the structure.

AASHTO Standard R 27-01 (2010) should be consulted for a detailed step by step procedure of corrosion evaluation process and estimation of remaining service life. Additional insight into the corrosion of steel piles in non-marine environments is also presented in NCHRP Report 408 by Beavers and Dunn (1998).

6.12.1.2 Corrosion in Marine Environments

For steel piles in marine environments (salt water), separate zones, each with a different corrosion rate, are present along the length of the pile. Tomlinson (1994) identifies these zones as follows:

1. Atmospheric zone: exposed to the damp atmospheric conditions above the highest water level or subject to airborne spray.
2. Splash zone: above the mean high tide, but exposed to waves, spray, and wash from passing ships.
3. Intertidal zone: between mean high and low tides.
4. Continuous immersion zone: below lowest low tide.
5. Underground zone: below the mudline.

Figure 6-29, after Morley and Bruce (1983), summarizes average and maximum probable marine corrosion rates in these zones as well as in the low water zone. In corrosive environments, the designer should apply one of the design options for piles in corrosive environments discussed in Section 6.12.4.

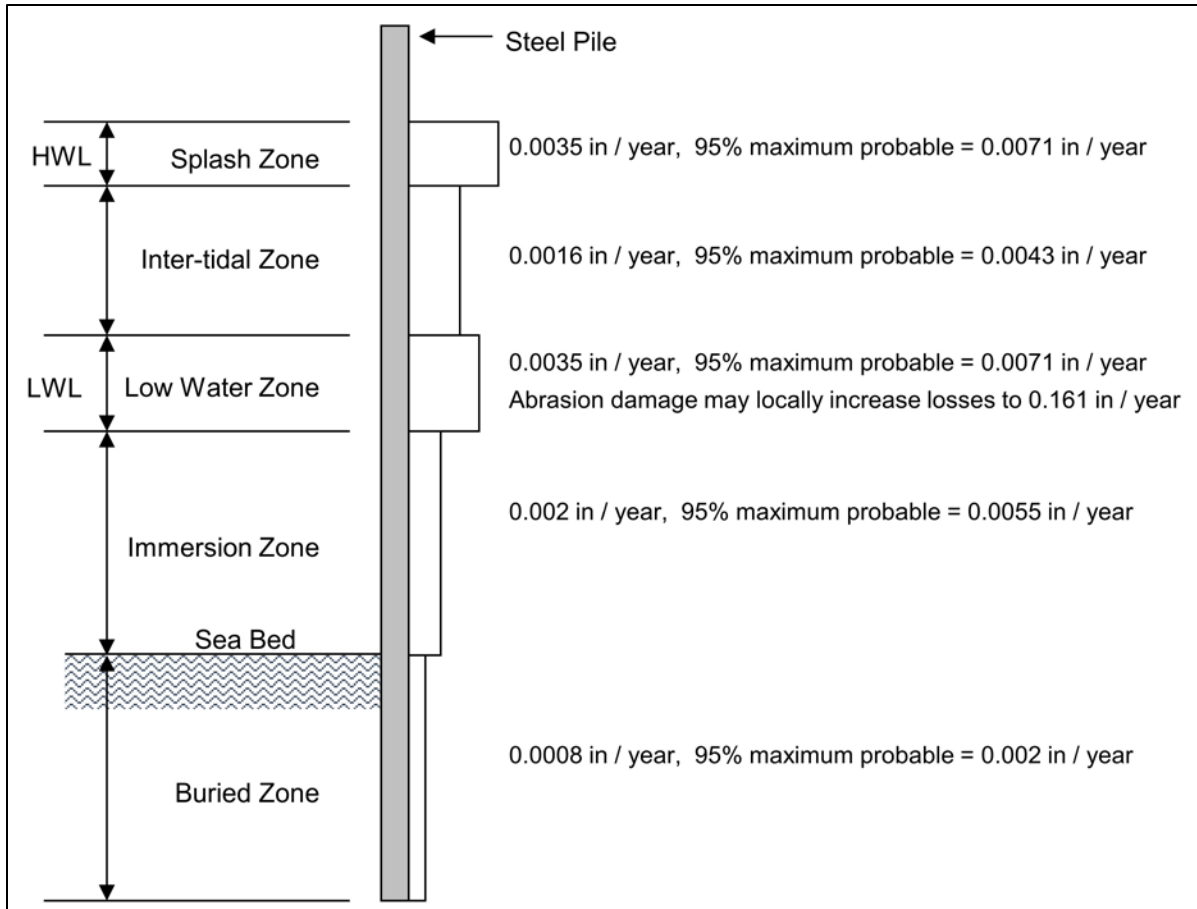


Figure 6-29 Loss of thickness by corrosion for steel piles in seawater (after Morley and Bruce 1983).

6.12.2 Sulfate and Chloride Attack on Concrete Piles

Attack on precast and cast-in-place concrete occurs in soils with high sulfate or chloride concentrations. Factors influencing the rate of deterioration on concrete piles include the pH of the soil, the solubility of the sulfate or chloride, the movement of the groundwater relative to the piles, and the density of the pile concrete.

The reaction between concrete and sulfate begins with sulfate ions in solution. Once the sulfate ions in the groundwater come in contact with Portland cement, an expansive chemical reaction takes place. Expansion of concrete often leads to cracking and spalling which can significantly reduce the available structural resistance of a pile foundation.

One method of reducing sulfate attack is to use a dense concrete which is less permeable to sulfate ions. Other possible deterrents include using sulfate-resisting

cement, using cement with 25% pozzolanic material, or creating a physical barrier between the concrete and the groundwater with some form of pile sleeve.

Chlorides are commonly found in soils, groundwater, or industrial wastes. Instead of attacking concrete, chlorides cause corrosion of reinforcement steel with consequential expansion and bursting of concrete as the products of steel corrosion are formed. Once corrosion begins, it continues at an accelerated rate. This can lead to a loss of bond between steel and concrete and extreme reduction of pile structural resistance. Protective measures which can reduce corrosion include increased concrete cover around the reinforcing steel, and the use of galvanized, or epoxy coated reinforcement.

6.12.3 Bacteria, Fungi, Insect, and Marine Borer Attacks on Timber Piles

Timber piles are subject to attack on land by bacteria, fungi, termites, and beetles, or in water by bacteria, fungi, and marine borers. Incidences of marine borer attack on timber piles have re-emerged in some areas as previously polluted water has improved. As mentioned in Section 6.2, arsenate and creosote pressure treatments are the most effective means of protecting timber piles from premature deterioration. In southern waters, creosote must be combined with other preservative treatments because of attack by *limnoria tripuncata*. Table 6-8 provides a summary of AWPI recommended preservative treatments depending upon foundation use, preservative, and wood species. Any environmental restrictions or regulations on a preservative treatment in a given situation must be considered.

When designing with timber piles, the wood species is usually not specified unless a specific species of wood is more suitable for design loads and/or environmental conditions. Certain species are not suitable for preservative treatment, while others may provide increased durability. As expected, ASTM standards for timber piles vary with geologic region, as land and fresh water piles have less stringent preservative treatment requirements than piles used in marine environments.

If timber piles are installed in other aggressive environments such as environments containing chemical wastes, a timber pile specialist should be consulted in determining the appropriate preservative treatment.

Table 6-8 Preservative Retention Requirements (after Collin 2002)

Pile Use Category	Southern Pine Creosote (pcf)	Douglas Fir Creosote (pcf)	Southern Pine CCA (pcf)	Douglas Fir ACZA (pcf)
Foundation	12	17	0.8	1.0
Land & Fresh Water	12	17	0.8	1.0
Marine (Saltwater) N. of Delaware ¹ or San Francisco ¹	16	16	1.5	1.5
Marine (Saltwater) S. of New Jersey ² or San Francisco ²	20	20	2.5	2.5
Marine (Saltwater) Dual Treatment ³	20	20	1.0	1.0

¹ Where Teredo is expected and Limnoria tripunctata is not expected, creosote or creosote solutions provide adequate protection.

² Where Teredo and Limnoria tripunctata are expected and where pholad attack is not expected, either dual treatment, or high retentions of CCA for Southern Pine or ACZA for Douglas Fir provide maximum protection.

³ In those areas where Limnoria tripunctata and pholad attack is expected or known, dual treatment provides the maximum protection.

6.12.4 Design Options for Piles Subject to Degradation or Abrasion

When a pile must be installed in an aggressive or abrasive environment, several design options can be considered. These design options include:

1. A heavier steel section than required can be used to provide extra thickness (H and pipe sections). This method is not effective in running water with active bedload to scour the corroded surface.

2. Cathodic protection of steel piles in soil below the water table or in marine environments. Note that this method of protection tends to be a costly solution and requires periodic anode replacement.
3. Concrete encasement of steel piles above the mud line. This method may alter the impact absorbing properties of the pile.
4. Use of copper-bearing steel is effective against atmospheric corrosion but the cost is greater than conventional steel.
5. Sleeving or encapsulating of reinforced, cast-in-place piles by using metal casings, polymer or fiberglass jackets isolates contaminants from concrete.
6. Use of a low water/cement ratio, resistant aggregate, and minimum air content consistent with the environment to improve abrasion resistance of precast concrete piles.
7. Use of a protective metallic or epoxy paint (isocyanate-cured) or fusion bonded epoxy coating on exposed sections of the pile. These options may not as effective in running water with active bedload.
8. Use of coal-tar epoxies for corrosion protection in marine environments. This method can also lose effectiveness in running water with active bedload.

Protective coatings cannot be replaced after a pile is driven. Therefore, if a protective coating is used, the coating should be designed to be durable enough to remain undamaged during pile transportation, handling, and placement in the leads for driving as well as resistant to the abrasion resulting from pile driving. The designer should also note that the shaft resistance on a coated pile may be significantly different than on an uncoated pile, depending on the coating.

6.13 SELECTION OF PILE TYPE AND SIZE FOR FURTHER EVALUATION

The selection of appropriate pile types for any project involves the consideration of several design and installation factors including pile characteristics, subsurface conditions and performance criteria. This selection or elimination process should consider the factors listed in Tables 6-1 to 6-7, 6-9, and 6-10. Tables 6-1 to 6-7 summarize typical pile characteristics and uses. Table 6-9 provides pile type recommendations for various subsurface conditions. Table 6-10 presents the placement effects of pile shape characteristics.

In addition to the considerations provided in the tables, the problems posed by the specific project location and topography must be considered in any pile selection process. Following are some of the usually encountered issues:

1. Vibrations from driven pile installation may affect pile type selection, dictate installation equipment selection and/or use of special installation techniques such as predrilling, and/or necessitate vibration monitoring of adjacent structures.
2. Urban areas, remote areas, or other locations with limited access may restrict driving equipment size and, therefore, pile type and size.
3. Local availability of certain materials and capability of contractors may have decisive effects on pile selection.
4. Waterborne operations may dictate use of shorter pile sections due to pile handling limitations.
5. Steep terrain may make the use of certain pile equipment costly or impossible.

Often several different pile types meet all the requirements for a particular structure. In such cases, the final choice should be made on the basis of a cost analysis that assesses the over-all cost of the foundation alternatives. This requires that candidate pile types be carried forward in the design process for determination of the pile section requirements for design loads and constructability. The cost analysis should also include time and space limitations, time delays, cost of load testing programs, as well as the differences in the cost of pile caps and other elements of the structure that may differ among alternatives. For major projects, alternate foundation designs should be considered for inclusion in the contract documents if there is a potential for cost savings.

Table 6-9 Pile Type Selection Based on Subsurface and Hydraulic Conditions.

TYPICAL PROBLEM	RECOMMENDATIONS
Boulders overlying bearing stratum	Use heavy non-displacement pile with a cast steel driving shoe and include contingent predrilling item in contract.
Loose cohesionless soil	Use a tapered pile to develop the maximum unit shaft resistance.
Downdrag and Drag Force	Avoid use of battered piles due to ground settlement. A pile-soil bond breaker such as a bitumen coating or plastic wrap (if feasible) can be used to reduce large drag forces.
Deep soft clay	Use rough concrete piles to increase adhesion and rate of pore water dissipation.
Artesian pressure	Use solid prestressed concrete pile, tapered piles with sufficient collapse strength, or thick wall closed end pipe with flush boot plate depending upon local practice. H-piles without driving shoes may also be viable selection. Do not use mandrel driven thin-wall shells, as generated hydrostatic pressure may cause shell collapse. Pile heave also common to closed end pile.
Scour	Use uniform section pile with sufficient structural resistance to act as a column through scour zone. Do not use tapered piles unless a large part of the taper extends well below scour depth.
Coarse gravel deposits	Use prestressed concrete piles where hard driving is expected. In coarse soils, use of H-piles and open end pipe piles often results in excessive pile lengths and cost overruns due to pile running during installation.

* Table modified and reproduced (Cheney and Chassie 1993).

Table 6-10 Pile Type Selection Based on Pile Shape Effects.

SHAPE CHARACTERISTICS	PILE TYPE	PLACEMENT EFFECT
Displacement	Closed end pipe Precast concrete	Increases lateral ground stress. Densifies cohesionless soils, remolds and weakens cohesive soils temporarily. May cause heave and lateral displacement of previously driven piles. Setup time for large pile groups in sensitive clays may be up to six months.
Non-displacement	Steel H Open end pipe	Minimal disturbance to soil. Not suited for friction piles in coarse granular soils. Piles often have low dynamic resistances in these deposits making resistance verification in the field difficult thereby often resulting in excessive pile lengths.
Tapered	Timber Monotube Tapertube	Increased densification of soil, high soil resistance for short penetration lengths in granular soils.

* Table modified and reproduced (Cheney and Chassie 1993).

6.14 HISTORICAL PRICE INFORMATION

Many state transportation agencies post project bid and award information. This media may be downloaded for use by designers, contractors, and project managers to aid in cost estimating. The corresponding agency standard specifications are also typically available to download and should be reviewed to determine the description of the work as well as the method of measurement and payment. Tables 6-11 to 6-17 present recent historical statewide price information for several state agencies.

The description of the work requirements vary from state to state. Prices for furnishing piles and driving piles are listed separately for some state agencies, while a combined bid price is used by others. Items such as pile shoes, splices, sleeves, load tests and mobilization may or may not be incidental, and vary by agency.

6.14.1 California

According to the CALTRANS specification, furnished cost includes any length of pile installed in the ground, including splices and materials to splice. Driving costs included installing and cutting off piles, providing pile tips or shoes and any predrilling involved. Table 6-11 presents costs tabulated from 2014 for various pile types, including the quantity, weighted unit price per linear foot and number of projects for each. Both steel and concrete piles are driven in California and are presented in this table. Pile class 90, 140, or 200 identifies the axial compression resistance in kips for the prestressed concrete piles in the service limit state.

Table 6-11 CALTRANS, 2014 Contract Cost Data

Description	Quantity ^{1,2}	Weighted Unit Price	No. of Projects
FURNISH STEEL PILING (HP 10 X 57)	12,882	\$30.53	3
FURNISH STEEL PILING (HP 14 X 89)	12,100	\$45.55	1
FURNISH STEEL PILING (HP 14 X 117)	22,593	\$63.69	2
FURNISH 24" CIS SHELL PIPE PILING	8,497	\$135.31	3
FURNISH 30" CIS SHELL PIPE PILING	1,262	\$145.00	1
FURNISH 48" CIS SHELL PIPE PILING	1,242	\$448.19	2
FURNISH PILING (CLASS 90)	3,729	\$50.00	1
FURNISH PILING (CLASS 140)	25,583	\$25.00	1
FURNISH PILING (CLASS 200)	19,256	\$62.87	2
DRIVE STEEL PILE (HP 10 X 57)	280	\$2,034.57	3
DRIVE STEEL PILE (HP 14 X 89)	310	\$1,050.00	1
DRIVE STEEL PILE (HP 14 X 117)	424	\$1,283.02	2
DRIVE 24" STEEL PIPE PILE	132	\$5,863.63	3
DRIVE 30" STEEL PIPE PILE	18	\$20,200.00	1
DRIVE 48" STEEL PIPE PILE	23	\$23,130.43	2
DRIVE PILE (CLASS 90)	94	\$1,550.00	1
DRIVE PILE (CLASS 140)	336	\$3,100.00	1
DRIVE PILE (CLASS 200)	261	\$2513.22	2

¹Furnished Units in Linear Feet.

²Driven Units in Individually Driven Sections.

<http://www.dot.ca.gov/hq/esc/oe/awards/2014CCDB/2014ccdb.pdf>

6.14.2 Florida

Although prestressed concrete piles are primarily driven in Florida, steel piles are also included by the Florida Department of Transportation in their 2015 Historical Cost Summary. Costs are summarized on a statewide basis on a moving 12 month average. The data presented below is for the 12 month period ending January 31, 2016. Prices include furnishing and driving piles, per linear foot, with splices included in the per foot price. Pile points or driving shoes are paid per each. Table 6-12 presents the piling related costs.

Table 6-12 FDOT 2015 Historical Cost Information

Description	Quantity ^{1,2}	Weighted Average Price	No. of Projects
PRESTRESSED CONCRETE PILING, 14" SQ	460	\$230.00	1
PRESTRESSED CONCRETE PILING, 18" SQ	21,755	\$93.73	7
PRESTRESSED CONCRETE PILING, 24" SQ	105,468	\$90.12	10
STEEL PILING, HP 12 X 53	28,113	\$49.11	1
STEEL PILING, HP 14 X 89	5,185	\$90.57	2
STEEL PILING, 24" DIA. PIPE	560	\$224.28	1
POINT PROTECTION , HP 12 X 53	297	\$240.24	1
POINT PROTECTION , HP 14 X 89	61	\$262.55	1
POINT PROTECTION , 24" PIPE	20	\$340.69	1
STEEL PILING, 24" DIA. PIPE	7,936	\$121.27	5
TEST PILES - PREST CONCRETE,18" SQ	4,335	\$198.65	6
TEST PILES - PREST CONCRETE,24" SQ	9,650	\$181.58	9
TEST PILES - STEEL, HP 12 X 53	1,783	\$85.63	1
TEST PILES - STEEL, HP 14 x 89	535	\$128.69	1
TEST PILES - STEEL, 24" DIA. PIPE	140	\$521.59	1

¹Units in Linear Feet for Piles.

²Units in Per Each for Point Protection.

<http://www.fdot.gov/programmanagement/Estimates/HistoricalCostInformation/HistoricalCost.shtm>

6.14.3 Indiana

Steel piles are used almost exclusively across the Midwest. Table 6-13 presents the weighted average unit bid price for Indiana Department of Transportation pile driving items in 2015. This information is tabulated annually and is available on their website. Pile costs are per linear foot and include furnishing and driving the piles including splices. For closed end steel pipe piles, the price includes the flat end plate and concrete fill. Conical tip protection or inside cutting shoes for pipe piles, driving shoes for H-piles, and mobilization of the driving system are separate pay items. Piles are priced per linear foot installed.

Table 6-13 INDOT 2015 Unit Price Summaries

Description	Quantity ^{1,2}	Weighted Average Price
PILE, STEEL PIPE, 14 IN O.D. X 0.250 IN WALL	5,370	\$48.45
PILE, STEEL PIPE, 14 IN O.D. X 0.312 IN WALL	13,352	\$42.10
PILE, STEEL PIPE, 14 IN O.D. X 0.375 IN WALL	3,318	\$55.39
PILE, STEEL PIPE, 14 IN O.D. X 0.50 IN WALL	2,861	\$58.51
PILE, STEEL PIPE, 18 IN O.D. X 0.50 IN WALL	1,254	\$95.00
PILE, STEEL PIPE, 24 IN O.D. X 0.50 IN WALL	838	\$65.00
PILE, STEEL PIPE, 24 IN O.D. X 0.75 IN WALL	7,700	\$75.00
PILE, STEEL H, HP 12 X 53	17,314	\$44.21
PILE, STEEL H, HP 12 X 74	8,362	\$67.82
PILE, STEEL H, HP 12 X 84	3,548	\$64.39
PILE, STEEL H, HP 14 X 73	59	\$325.00
PILE, STEEL H, HP 14 X 89	669	\$109.50
CONICAL PILE TIP, 14 IN	327	\$277.81
CONICAL PILE TIP, 16 IN	15	\$1000.00
PILE SHOE, 24 IN INSIDE CUTTING SHOE	102	\$400.00
PILE SHOE, HP 12 X 53	286	\$123.43
PILE SHOE, HP 12 X 74	152	\$113.85
PILE SHOE, HP 12 X 84	22	\$118.17
PILE SHOE, HP 14 X 73	4	\$125.00
PILE SHOE, HP 14 X 89	12	\$140.00

¹ Units in Linear Feet.

² Tip Reinforcement Unit Price for Each.

<http://www.in.gov/dot/div/contracts/pay/>

6.14.4 Maryland

The Maryland State Highway administration maintains a price index that is updated twice per year. The piling items, quantities and associated unit costs summarized in the July 2015 price index are presented in Table 6-14. In Maryland, furnishing and driving pile are included in the same pay item and are priced per linear foot.

Mobilization of the pile driving system and pile splices are incidental items included in the per foot price. However H-pile shoes (pile points) are a separate bid item, unless specified and are priced per item. Projects for the Maryland State Highway Administration primarily utilize steel piles.

Table 6-14 MDSHA Price Index Published July 2015

Description	Quantity ^{1,2}	Weighted Average Price	Projects
UNTREATED TIMBER PILE	25,855	\$21.19	6
STEEL HP 8 X 36 BEARING PILE	188	\$65.00	1
STEEL HP 12 X 53 BEARING PILE	17,703	\$47.74	4
STEEL HP 12 X 63 BEARING PILE	2,460	\$85.00	1
STEEL HP 12 X 74 BEARING PILE	7,472	\$55.00	1
STEEL HP 14 X 73 BEARING PILE	4,328	\$55.32	1
STEEL HP 14 X 89 BEARING PILE	66,092	\$60.25	9
STEEL HP 14 X 102 BEARING PILE	1,020	\$106.51	1
STEEL HP 8 X 36 BEARING TEST PILE	13	\$180.00	1
STEEL HP 12 X 53 BEARING TEST PILE	568	\$110.30	4
STEEL HP 12 X 63 BEARING TEST PILE	260	\$85.00	1
STEEL HP 12 X 74 BEARING TEST PILE	285	\$85.00	1
STEEL HP 14 X 73 BEARING TEST PILE	183	\$100.00	1
STEEL HP 14 X 89 BEARING TEST PILE	2,250	\$87.13	9
STEEL HP 14 X 102 BEARING TEST PILE	255	\$196.19	1
PILE POINT FOR 12 INCH HP BEARING PILE	144	\$119.63	2
PILE POINT FOR 14 INCH HP BEARING PILE	48	\$126.00	1

¹ Pile Units in Linear Feet.

² Pile Point Unit Price for Each.

http://www.roads.maryland.gov/ohd2/MDSHA_PriceIndex_Jul2015.pdf

6.14.5 North Carolina

Multiple geologic conditions dictate that both concrete and steel piles are driven in North Carolina. Table 6-15 presents the 2015 average bid prices compiled by the North Carolina Department of Transportation. Piles are priced per linear foot, while pile points and pile plates are separate items. More detailed information on the scope of measurement and payment may be found in the most recent agency standard specification.

Table 6-15 2015 NCDOT Bid Quantities and Averages

Description	Quantity ^{1,2}	Weighted Average Price
12" PRESTRESSED CONCRETE PILE	18,220	\$58.94
16" PRESTRESSED CONCRETE PILE	28,315	\$73.39
24" PRESTRESSED CONCRETE PILE	6,076	\$144.80
HP12X53 PILES	43,983	\$49.45
HP14X53 GALVANIZED PILES	680	\$85.00
HP14X73 PILES	10,016	\$62.42
HP14X73 GALVANIZED PILES	1,660	\$71.52
HP14X89 PILES	1,195	\$75.00
14 IN O.D. X 0.50 STEEL PIPE	3,000	\$67.37
36 IN O.D. X 0.625 STEEL PIPE	95	\$230.00
14 IN O.D. X 0.50 GALVANIZED STEEL PIPE	480	\$145.87
16 IN O.D. X 0.50 GALVANIZED STEEL PIPE	400	\$124.53
18 IN O.D. X 0.50 GALVANIZED STEEL PIPE	3,570	\$101.47
24 IN O.D. X 0.50 GALVANIZED STEEL PIPE	7,680	\$152.39
30 IN O.D. X 0.50 GALVANIZED STEEL PIPE	8,560	\$193.34
30 IN O.D. X 0.625 GALVANIZED STEEL PIPE	4,850	\$212.30
36 IN O.D. X 0.625 GALVANIZED STEEL PIPE	770	\$215.00
PREDRILLING FOR PILES	13,169	\$20.38
STEEL PILE POINTS	673	\$386.19
PIPE PILE PLATES	262	\$168.74

¹ Pile Units in Linear Feet.

²Pile Point & Plate Unit Price for Each.

6.14.6 Pennsylvania

Price history for the Pennsylvania Department of Transportation is presented in Table 6-16. The latest PennDOT price history covers projects let between April 2013 and April 2015. The majority of PennDot projects involve steel piles, many of which are H-piles driven to rock due to local geology. For bearing piles, the unit price per linear foot includes furnished and driven pile including splices and cutoff. Driving shoes (tips) are a separate pay item. Shoes for timber piles are included in the unit price.

Table 6-16 2015 PennDOT Bid Quantities and Averages

Description	Quantity ^{1,2}	Weighted Average Price	No. of Projects
TREATED TIMBER BEARING PILES	14,800	\$40.00	1
CAST-IN-PLACE CONCRETE PILES	4,907	\$74.37	7
CAST-IN-PLACE CONCRETE PILE TIP	22	\$804.23	3
STEEL BEAM BEARING PILES, HP10X42	150	\$144.50	1
STEEL BEAM BEARING PILES, HP10X57	10,376	\$63.01	8
STEEL BEAM BEARING PILES, HP12X53	673	\$60.49	3
STEEL BEAM BEARING PILES, HP12X63	3,350	\$54.79	3
STEEL BEAM BEARING PILES, HP12X74	63,600	\$70.31	47
STEEL BEAM BEARING PILES, HP 12X84	5,278	\$96.46	5
STEEL BEAM BEARING PILES, HP14X73	4,497	\$71.95	3
STEEL BEAM BEARING PILES, HP14X89	134,174	\$85.00	19
STEEL BEAM BEARING PILES, HP14X102	126,960	\$68.90	15
STEEL BEAM BEARING PILES, HP14X117	26,458	\$91.33	3
NORMAL DUTY PILE TIP - HP 10X57	56	\$118.58	2
NORMAL DUTY PILE TIP - HP 12X63	44	\$151.59	2
NORMAL DUTY PILE TIP - HP 12X74	410	\$151.17	13
NORMAL DUTY PILE TIP - HP 14X73	50	\$149.04	2
NORMAL DUTY PILE TIP - HP 14X89	26	\$129.00	1
HEAVY DUTY PILE TIP - HP 12X74	405	\$141.92	11
HEAVY DUTY PILE TIP - HP 12X84	49	\$104.08	2
HEAVY DUTY PILE TIP - HP 14X89	1,388	\$134.28	18
HEAVY DUTY PILE TIP - HP 14X117	254	\$135.00	1

¹ Pile Units in Linear Feet.

²Tip Reinforcement Unit Price for Each.

<https://www.dot.state.pa.us/public/Bureaus/design/Pub287/Pub%20287.pdf>

6.14.7 Texas

A 12-month statewide moving average of bid prices and quantities from the Texas Department of Transportation is presented below in Table 6-17. The weighted average prices cover the period from March 1, 2015 to February 28, 2016. The unit bid price for piling is per linear foot in place. However, splices and pile tips, when necessary, are a separate bid item. The majority of driven piles in Texas are concrete piles. Please consult the most recent Texas Department of Transportation Standard Specification for further information on measurement and payment items, as well as the average project bid awards as these values are updated monthly.

Table 6-17 TxDOT 12-Month Project Bid Averages

Description	12 Month Quantity ¹	12 Month AVG BID	No. of Projects
STEEL H-PILING (HP 12 X 53)	640	\$150.00	1
STEEL H-PILING (HP 14 X 117)	201	\$20.00	1
PRESTR CONCRETE PILING (16 IN SQ)	48,679	\$113.38	17
PRESTR CONCRETE PILING (18 IN SQ)	7,133	\$100.20	8
PRESTR CONCRETE PILING (20 IN SQ)	8,151	\$118.80	3
PRESTR CONCRETE PILING (24 IN SQ)	3,304	\$135.00	1

¹ Units in Linear feet.

<http://www.txdot.gov/business/letting-bids/average-low-bid-unit-prices.html>

A brief summary of pay items was presented for selected state agencies covering a range of pile types and installation conditions. The designer should consult the most current price information from the appropriate agency as price histories and specifications change over time.

REFERENCES

- American Concrete Institute (ACI), (2012). Guide to Design, Manufacture and Installation of Concrete Piles. ACI-543R-12, 64 p.
- American Association of State Highway and Transportation Officials (AASHTO). (2001). Standard Recommended Practice for Assessment of Corrosion of Steel Piling for Non-Marine Applications. AASHTO Standard Specifications for Transportation Materials and Methods of Sampling and Testing, Part 1B: Specifications, 24th Edition, 13 p.
- American Association of State Highway and Transportation Officials (AASHTO). (2014). AASHTO LRFD Bridge Design Specifications, US Customary Units, Seventh Edition, with 2015 Interim Revisions. American Association of State Highway and Transportation Officials, Washington, D.C., 1960 p.
- Beavers, J.A. and Durr, C.L. (1998). Corrosion of Steel Piling in Non-Marine Applications. NCHRP Report 408, National Cooperative Highway Research Program, Transportation Research Board, Washington, D.C., 35 p.
- Belk, N.A. (2013). Evaluation of Lightweight Aggregate Concrete for Precast, Prestressed Driven Piles. PhD Dissertation, Auburn University, 215 p.
- Brown, D.A., Dapp, S.D., Thompson, W.R., and Lazarte, C.A. (2007). Design and Construction of Continuous Flight Auger (CFA) Piles. FHWA-HIF-07-03, Geotechnical Engineering Circular (GEC) No. 8. U.S. Dept. of Transportation, Federal Highway Administration, 289 p.
- Brown, D. A., Turner, J.P. and Castelli R.J. (2010). Drilled Shafts: Construction Procedures and LRFD Design Methods, FHWA-NHI-10-016, Geotechnical Engineering Circular (GEC) No. 10. U.S. Dept. of Transportation, Federal Highway Administration, 970 p.
- Brown, D.A., and Thompson III, W.R. (2015). Current Practices for Design and Load Testing of Large Diameter Open-End Driven Pipe Piles. Final Report. NCHRP Report 20-05, Topic 45-05, National Cooperative Highway Research Program, Washington, D.C., 175 p.

- Chellis, R.D. (1961). *Pile Foundations*. Second Edition, McGraw-Hill Book Company, New York, NY, 704 p.
- Cheney, R.S. and Chassie, R.G. (2000). *Soils and Foundations Workshop Reference Manual*. FHWA HI-00-045, U.S. Department of Transportation, National Highway Institute, Federal Highway Administration, Washington, D.C., 358 p.
- Collin, J.G. (2002). *Timber Pile Design and Construction Manual*. American Wood Preservers Institute (AWPI), 122 p.
- Department of the Navy, (1982). *Foundations and Earth Structures Design Manual*. DM 7.2. Naval Facilities Engineering Command, (NAVFAC), Alexandria, VA, 279 p.
- Fleming, W.G.K., Weltman, A.J., Randolph, M.F. Elson, W.K. (2008). *Piling Engineering*, Third Edition, Taylor and Francis, New York, New York, NY, 398 p.
- Fuller, F.M. (1983). *Engineering of Pile Installations*. McGraw-Hill, New York, NY, 286 p.
- Graham, J. (1995). Personal Communication.
- Hartman, J.J., Castelli, R.J., and Malhotra, S. (2007). *Design and Installation of Concrete Cylinder Piles*. Proceeding of GeoDenver 2007, GSP 158 Contemporary Issues in Deep Foundations, ASCE, pp. 1-14.
- Moser, R., Holland, B. Kahn, L., Singh, P., and Kurtis, K. (2011). *Durability of Precast Prestressed Concrete Piles in Marine Environment: Reinforcement Corrosion and Mitigation Part 1*. GDOT Research Project No. 07-30. Office of Materials and Research Georgia Department of Transportation, 243 p.
- Morley, J. (1979). *The Corrosion and Protection of Steel Piling*, British Steel Corporation, Teesside Laboratories, Report No. T/CS/906/4/78/C.
- Morley, J. and Bruce, D.W. (1983). *Survey of Steel Piling Performance in Marine Environments*, Final Report, Commission of the European Communities, Document EUR 8492 EN, 25 p.

- Portland Cement Association (PCA). (1951). Concrete Piles: Design, Manufacture and Driving, 80 p.
- Prakash, S. and Sharma, H. (1990). Pile Foundations in Engineering Practice. John Wiley and Sons, Inc., New York, NY, 768 p.
- Rausche, F. (1994). Design, Installation and Testing of Nearshore Piles. Proceedings of the 8th Annual Symposium on Deep Foundations, Vancouver.
- Sabatini, P.J., Tanyu, B., Armour., P., Groneck, P., and Keeley, J. (2005). Micropile Design and Construction, FHWA-NHI-05-039. National Highway Institute, U.S. Dept. of Transportation, Federal Highway Administration, Washington, D.C., 436 p.
- Tomlinson, M.J. (1994). Pile Design and Construction Practice, Fourth Edition, E & FN Spon, London, 432 p.
- Transportation Research Board. (1977). Design of Pile Foundations. NCHRP Synthesis of Highway Practice No. 42, 68 p.
- Vande Voort, T., Suleiman, M. T., and Sritharan, S. (2008). Design and Performance Verification of Ultra-High Performance Concrete Piles for Deep Foundations. Final Report, Iowa DOT, IHRB Project TR-558, CTRE Project 06-264, Iowa Dept. of Transportation, Ames, IA, 206 p.

CHAPTER 7

GEOTECHNICAL ASPECTS AND LIMIT STATE DESIGN

7.1 INTRODUCTION

Static analysis methods can be categorized as analytical methods that use geomaterial strength and compressibility properties to determine nominal geotechnical resistance and deformation. This chapter will focus on analysis methods for determining the nominal geotechnical resistance of single piles and pile groups in axial compression, uplift, and lateral loading as well as the resulting vertical and lateral deformations. Important considerations are as follows:

1. Static analysis methods are an integral part of the design process. Static analysis methods are necessary to determine the most cost effective pile type and to estimate the number of piles and the required pile lengths for the design of substructure elements. The foundation designer must have knowledge of the design loads and the project performance criteria in order to perform the appropriate static analyses.
2. Many static analysis methods are available. The methods presented in this chapter are relatively simple methods that have proven to provide reasonable agreement with full scale field results. Many of these methods are also included in the AASHTO (2014) design specifications. Other more sophisticated analysis methods may be used and in some cases may provide better results. Regardless of the method used, it is important to continually apply experience gained from past field performance of the analysis method.
3. Designers should fully understand the basis for, the limitations of, and the applicability of a chosen method. This is particularly true of computer solutions where some underlying assumptions may not be readily apparent. A selected method should also have a proven agreement with full scale field results.
4. Evaluation and confirmation of pile drivability is an integral part of limit state design. Foundation designs with fewer, larger, pile sections having greater nominal resistances are more frequently being used. The ability of these piles to achieve the required pile penetration depths necessary to satisfy all nominal resistance and deformation requirements is a critical design check. A pile drivability analysis requires combining the geotechnical aspects detailed in this chapter with the wave equation analysis procedures described

in Chapter 12. A drivability analysis should be performed by the engineer during the design stage to assess the constructability of the pile design.

Construction procedures can have a significant influence on the behavior of pile foundations. The analysis methods described in this chapter lead to successful designs of deep foundations only if appropriate construction techniques and construction monitoring methods are used. Construction monitoring should be an integral part of the design and construction of any foundation. Static load tests, wave equation analysis or dynamic monitoring for construction control should, whenever possible, be used to confirm the results of a static design method. These topics are discussed in detail in subsequent chapters.

The first few sections of this chapter will briefly cover background information. Static analysis procedures for piles subject to compression, uplift, and lateral loads will be covered, as well as pile group settlement. The influence of special design events on driven pile designs will also be discussed. Limited guidance on design in liquefaction susceptible soils is provided. Detailed seismic design is beyond the scope of this manual and is covered in GEC-3 by Kavazanjian et.al (2011). Finally, this chapter will address construction issues pertinent to static analysis methods and foundation design. In all cases, existing character notation for soil resistances as well as load and resistance factors utilized by AASHTO (2014) will be presented.

7.1.1 Static Analysis Methods in Limit State Design

There are four general types of static analyses addressed in this chapter. Static analyses are performed to determine:

1. Nominal resistance in axial compression of a pile or pile group. These calculations are performed to determine the long term resistance of a foundation as well as to determine the soil resistance provided from soil layers subject to scour, liquefaction, downdrag, or that are otherwise unsuitable for long term load support. Static analyses are used to establish minimum pile penetration requirements, pile lengths for bid quantities, as well as to estimate the soil resistance at the time of driving (SRD) and the required nominal driving resistance, R_{ndr} .
2. Nominal resistance in axial tension of a pile or pile group. These calculations are performed to determine the soil resistance to uplift or tension loading which, in some cases, may also determine the minimum pile penetration requirements.

3. Nominal lateral resistance and lateral deformation of a pile or pile group. These soil-structure interaction analysis methods consider the soil strength and deformation behavior as well as the pile structural properties and are used in pile section selection.
4. Settlement of a pile group. These calculations are performed to estimate the vertical foundation deformation under the structure's service loads.

The factored geotechnical resistance of a pile can be defined as the sum of geomaterial resistances along the pile shaft and at the pile toe available to support the factored loads on the pile. As noted above, static analyses are performed to determine the factored resistance of an individual pile and of a pile group as well as the deformation response of a pile group to the factored loads. The factored resistance of an individual pile and of a pile group is the smaller of: (1) the factored geotechnical resistance of surrounding soil/rock medium to support the loads transferred from the pile(s) or, (2) the factored structural resistance of the pile(s). Soil-structure interaction analysis methods are used to determine the deformation response of a pile and pile groups to lateral loads. The results from these analyses in conjunction with pile group settlement analysis are compared to the performance criteria established for the structure. Both vertical (settlement) and lateral deformation analyses of pile groups are computed using factored loads at the service limit state.

The static pile resistance from the sum of the soil/rock resistances along the pile shaft and at the pile toe can be estimated from geotechnical engineering analysis using:

1. Laboratory determined shear strength parameters of the soil and rock surrounding the pile.
2. In-situ test data (i.e., SPT, CPT).
3. Back analysis of geomaterial design parameters based on performance data.

Prior to discussing static design methods for estimating pile resistance in detail, it is desirable to review events that occur in the pile soil system during and after pile driving as well as basic load transfer mechanisms.

7.1.2 Events During and After Pile Driving

The soil and some weaker rocks in which a pile foundation is installed are almost always disturbed. Several factors influence the degree of disturbance. These include the soil and rock type and density, the pile type (displacement, low-displacement), and the method of pile installation (driven, vibrated, drilled, jetted). For driven piles, substantial disturbance and remolding is unavoidable in soils and weaker rocks where the in-situ stresses and rock structure are changed during pile installation.

Over the long term, scour, settlement, pore pressure fluctuations, seismic and other extreme events may occur. These situations should be addressed in the applicable strength, extreme, and service limit states such that sufficient embedment and foundation stiffness is achieved. These topics, among others, will be discussed throughout this chapter.

7.1.2.1 Cohesionless Soils

The resistance of piles driven into cohesionless soil depends primarily on the relative density of the soil. During driving, the relative density of loose to medium dense cohesionless soil is increased close to the pile due to vibrations and lateral displacement of soil. This effect is most pronounced in the immediate vicinity of displacement piles. Broms (1966) and more recent studies found the zone of densification extends as far as 3 to 5.5 diameters away from the pile shaft and 3 to 5 diameters below the pile toe as depicted in Figure 7-1.

The increase in relative density increases the resistance of single piles and pile groups. The pile type selection also affects the amount of change in relative density. Piles with large displacement characteristics such as closed end pipe and precast concrete piles increase the relative density of cohesionless material more than low-displacement open end pipe or steel H-piles. Similarly, vibratory installation may increase the relative density of loose to medium dense cohesionless material more than driving with an impact hammer.

In dense cohesionless soil, the relative density may actually decrease since dense soils will dilate during shear and displacement. As a result, negative pore pressures

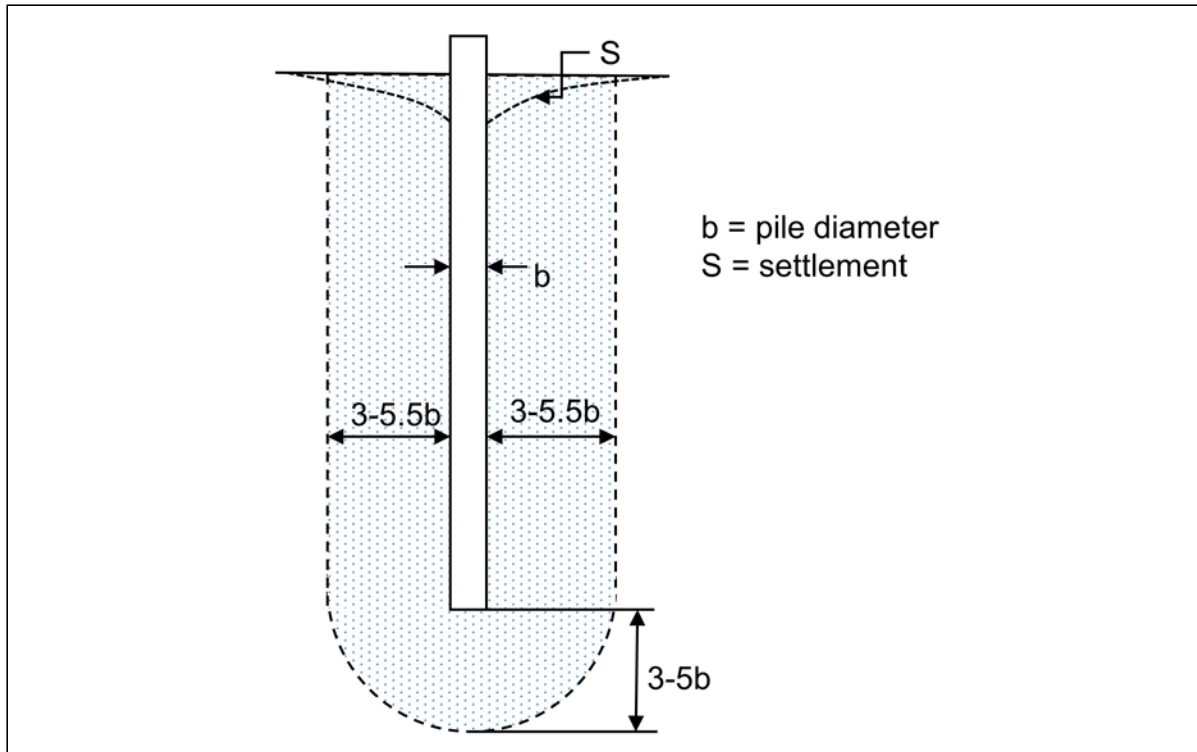


Figure 7-1 Compaction of cohesionless soils during pile driving (after Broms 1966).

may temporarily be generated during driving which could lead to a temporarily increased resistance. The increase in stress, which can occur adjacent to the pile shaft and/or below the pile toe during the driving process, can be lost by relaxation in dense sand and gravels as the negative pore pressures generated during driving are dissipated. The phenomena can be explained by the shear strength equation presented in Equation 7-1.

$$\tau = c + (\sigma - u) \tan \phi \quad \text{Eq. 7-1}$$

Where:

- τ = shear strength of soil.
- c = cohesion.
- σ = total normal stress (pressure) on plane of failure.
- u = pore water pressure.
- ϕ = angle of internal friction.

Negative pore pressures temporarily increase the soil shear strength, and therefore pile resistance, by changing the $(\sigma - u) \tan \phi$ component of shear strength to $(\sigma + u) \tan \phi$. As negative pore pressures dissipate, the shear strength and pile resistance decrease.

The pile driving process can also generate high positive pore water pressures in saturated cohesionless silts and loose to medium dense fine sands. Positive pore pressures temporarily reduce the soil shear strength and the pile resistance. This phenomena is identical to the one described below for cohesive soils. The gain in resistance with time or soil setup is generally quicker for sands and silts than for clays because the pore pressures dissipate more rapidly in cohesionless soils than in cohesive soils.

7.1.2.2 Cohesive Soils

When piles are driven into saturated cohesive materials, the soil near the piles is disturbed and radially compressed. For soft or normally consolidated clays, the zone of disturbance is generally within one pile diameter around the pile. For piles driven into saturated stiff clays, there are also significant changes in secondary soil structure (closing of fissures) with remolding and loss of previous stress history effects in the immediate vicinity of pile. Figure 7-2 illustrates the disturbance zone for piles driven in cohesive soils as observed by Broms (1966). This figure also notes the heave that can occur when driving displacement piles in cohesive soils.

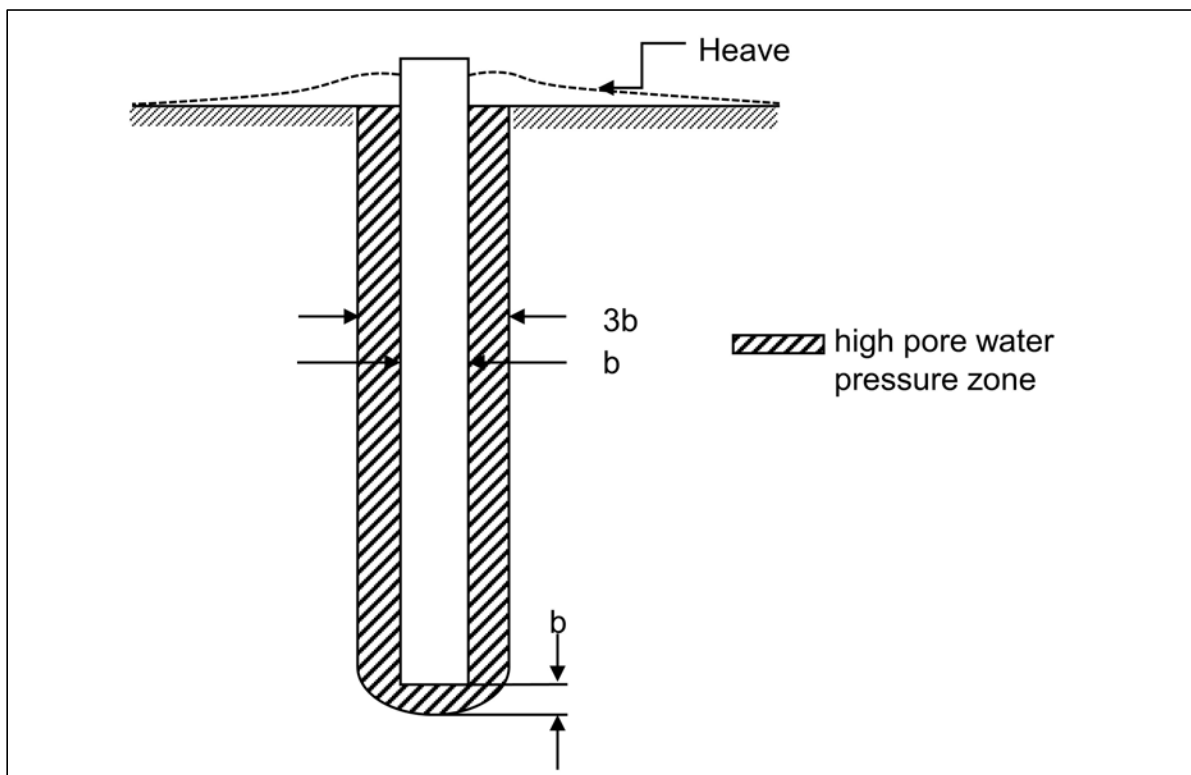


Figure 7-2 Disturbance of cohesive soils during pile driving (after Broms 1966).

The disturbance and radial compression generate high pore pressures (excess positive pore pressures) which temporarily reduce soil shear strength, the nominal geotechnical resistance, and therefore the pile penetration resistance or blow count. As reconsolidation of cohesive soils around the pile occurs, the high pore pressures are diminished, which leads to an increase in shear strength and pile resistance (setup). This phenomenon is opposite to "relaxation" described for cohesionless soils. The zone and magnitude of soil disturbance are dependent on the soil properties of soil sensitivity, driving method, and the pile foundation geometry. Limited data available for partially saturated cohesive soils indicates that pile driving does not generate high pore pressures and hence significant soil setup does not occur.

7.1.2.3 Additional Soil Resistance Considerations

On many driven pile projects, multiple static analyses are required for a design. First, a static analysis is necessary to determine the number and length of piles necessary to support the structure loads. A second static analysis may also be required to determine the nominal resistance the pile will encounter during installation. This second analysis enables the design engineer to determine the necessary capability of the driving equipment and the minimum pile section requirements based on drivability. Figures 7-3 and 7-4 illustrate situations that require two static analyses.

Figure 7-3 shows a situation where piles are to be driven for a bridge pier. In this case, the first static analysis performed should neglect the soil resistance in the soil zone subject to scour, since this resistance may not be available for long term support. The number of piles and pile lengths determined from this analysis will then be representative of the long term conditions in the event of scour. At the time of pile driving however, the scour zone soil will provide resistance to pile penetration. Therefore, a second static analysis is required to estimate the nominal resistance encountered by the pile during driving to the embedment depth determined in the first analysis. The second static analysis includes the soil resistance in the materials above the scour depth as well as the underlying strata.

Figure 7-4 shows another frequently encountered situation in which piles are driven through loose uncompacted fill material into the natural ground. The loose fill material offers unreliable resistance and is usually neglected in determining the number of piles and the pile lengths required. A second static analysis is then performed to determine nominal resistance encountered by the pile during driving, which includes the resistance in the fill material.

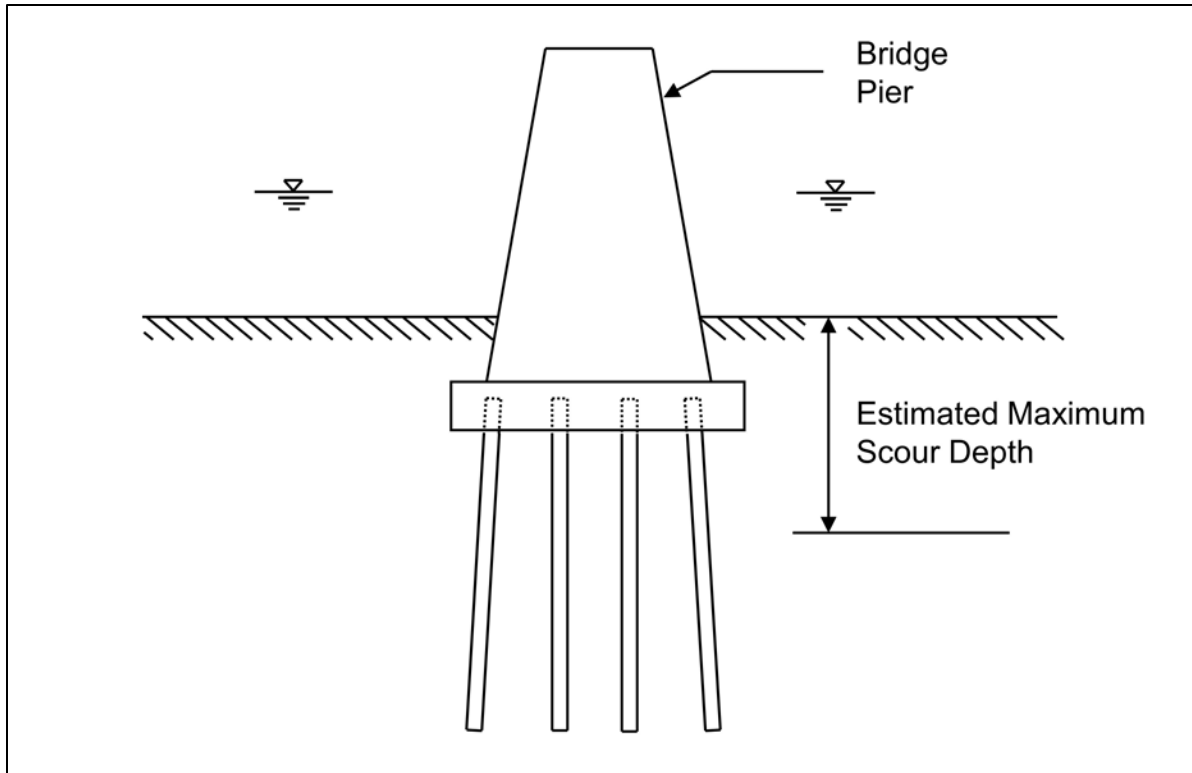


Figure 7-3 Situation where two static analyses are necessary due to scour.

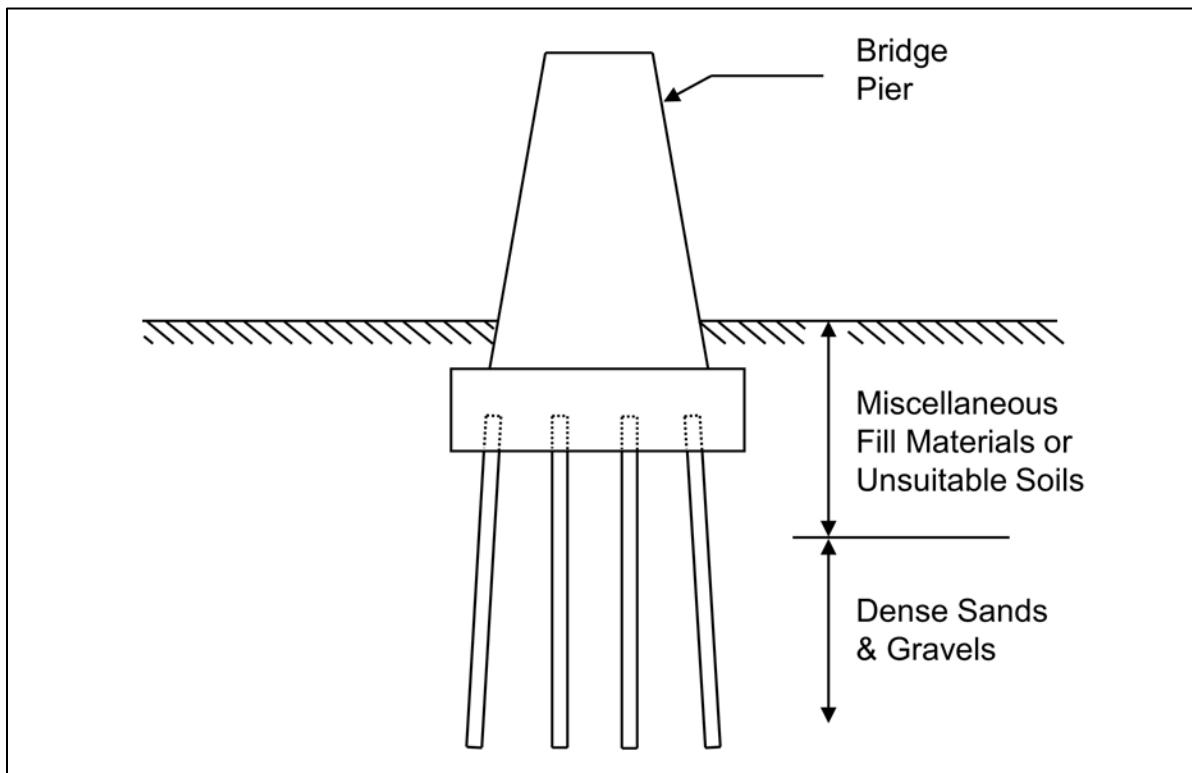


Figure 7-4 Situation where two static analyses are necessary due to fill materials.

In both examples, the soil resistance to be overcome during driving will be substantially greater than the required nominal resistance, R_n . The geotechnical resistance computed in the scourable or unsuitable layer, determined from static analysis, is then added to the required nominal resistance when determining the required nominal driving resistance, R_{dnr} .

The results of multiple static analyses should be considered in the development of project plans and specifications. For example, consider a case where scour, uplift loading, or some other design consideration (e.g., seismic event) dictates that a greater pile penetration depth be achieved than that required for support of the axial compressive loads. The static analyses indicate that a soil resistance of 420 kips must be overcome to obtain the minimum penetration depth needed for a 300 kip nominal resistance in axial compression. This information is germane to the drivability assessment for pile section selection. It should also be conveyed in the construction documents so that the driving equipment can be properly sized and so that the intent of the design is clearly and correctly interpreted by the contractor and construction personnel. Specifying only the 300 kip nominal resistance or providing only the factored load on the plans could easily be misinterpreted and can lead to construction claims. In the above example, the controlling factored load, the nominal resistance, the required nominal driving resistance, and the minimum penetration depth should all be provided. A more in depth discussion on driving criteria is presented in Chapter 17.

7.1.3 Load Transfer

The nominal resistance, R_n , of a pile in homogeneous soil may be expressed by the sum of the shaft resistance R_s and toe resistance R_p , or

$$R_n = R_s + R_p \quad \text{Eq. 7-2}$$

The above equation for nominal resistance assumes that both the pile toe and the pile shaft have moved sufficiently with respect to the adjacent soil to simultaneously develop the nominal shaft and toe resistances. Generally, the displacement needed to mobilize the shaft resistance is smaller than that required to mobilize the toe resistance. This simple rational approach has been commonly used for all piles except very large piles greater than 36 inches in diameter or width.

Figure 7-5 illustrates typical load transfer profiles for a single pile. The load transfer distribution can be obtained from a static load test where strain gages or telltale rods

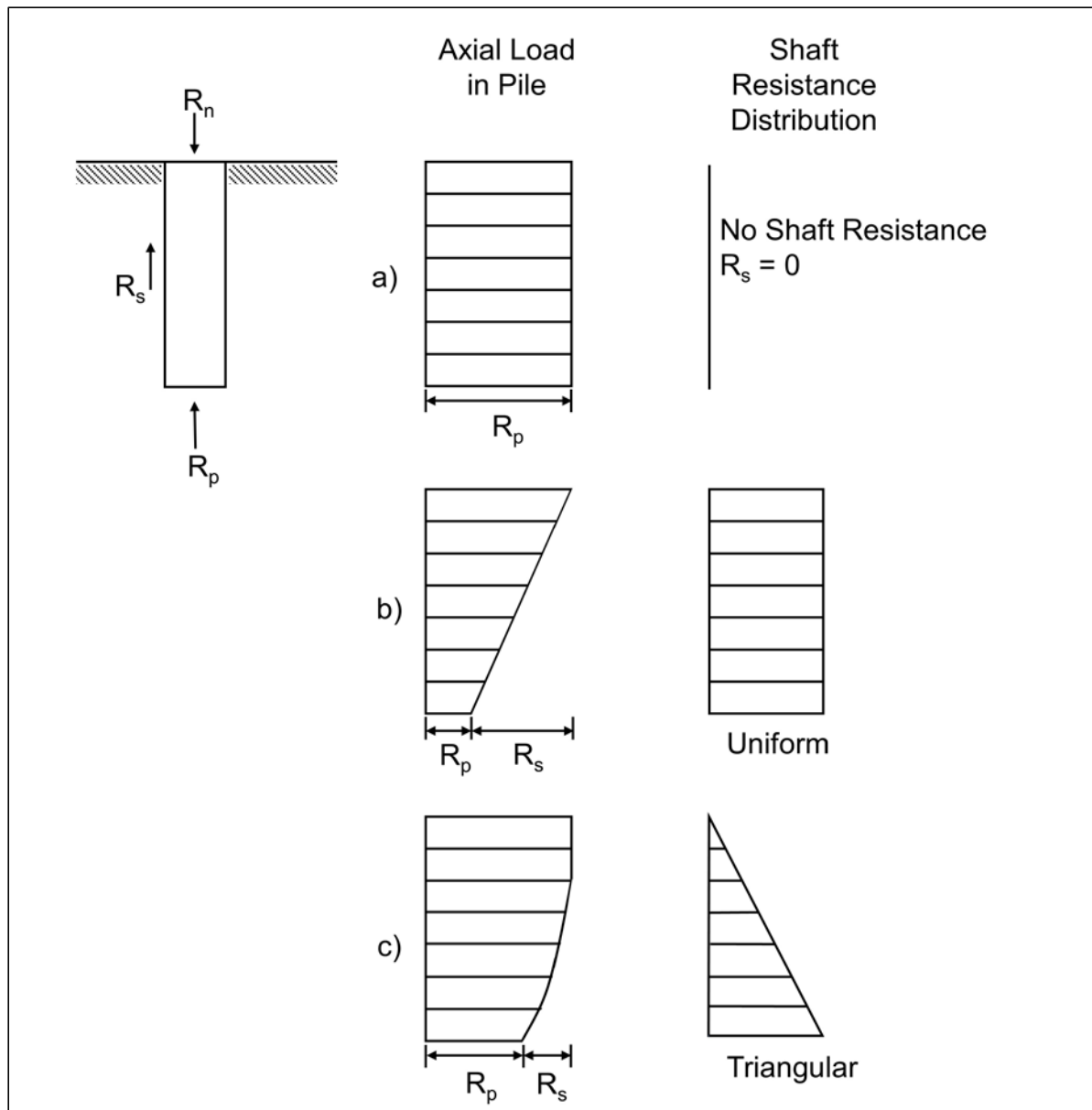


Figure 7-5 Typical load transfer profiles.

are attached to a pile at different depths along the pile shaft. Figure 7-5 shows the nominal resistance, R_n , in the pile plotted against depth. The shaft resistance transferred to the soil is represented by R_s , while R_p represents the resistance at the pile toe. In Figure 7-5(a), the load transfer distribution for a pile with no shaft resistance is illustrated. In this case the full axial load at the pile head is transferred to the pile toe. In Figure 7-5(b), the axial load versus depth for a uniform shaft resistance distribution typical of a cohesive soil is illustrated. Figure 7-5(c) presents the axial load in the pile versus depth for a triangular shaft resistance distribution and is typical of cohesionless soils.

7.1.4 Effective Stress

The vertical effective stress at a given depth below ground surface is the vertical stress at that depth due to the weight of the overlying soils. An Effective Stress Diagram plots the vertical effective stress versus depth, and is used in many static resistance and settlement calculations. An understanding of how to construct and use an Effective Stress Diagram is therefore important.

Information needed to construct an Effective Stress Diagram includes the total unit weight and thickness of each soil layer as well as the depth of the water table. The soil layer thickness and depth of the water table should be available from the project boring logs. The total unit weight of each soil layer may be obtained from density tests on undisturbed cohesive samples or estimated from Standard Penetration Test (SPT) N values in conjunction with the soil visual classification.

The first step in constructing an Effective Stress Diagram is to calculate the total vertical stress, σ_{vo} , versus depth. This is done by summing the product of the total unit weight times the layer thickness versus depth which was demonstrated in Section 5.2.2. Similarly, the pore water pressure, u , is summed versus depth by multiplying the unit weight of water, $\gamma_w = 62.4 \text{ lb/ft}^3$, times the water height. The vertical effective stress, σ'_{vo} , at any depth is then the total vertical stress minus the pore water pressure at that depth.

The vertical effective stress at any depth is determined by summing the weights of all layers above that depth as follows:

1. For soil deposits above the static water table:
 $\sigma'_{vo} = (\text{total soil unit weight, } \gamma)(\text{thickness of soil layer above the desired depth}).$
2. For soil deposits below the static water table:
 $\sigma'_{vo} = (\text{total soil unit weight, } \gamma)(\text{depth}) - (\text{unit weight of water, } \gamma_w)(\text{height of water, } h_w).$

The design water table elevation should be carefully selected. It should be compared to the water level determined in the subsurface exploration and consider seasonal variations.

Figures 7-6 and 7-7 present examples of Effective Stress Diagrams for cases where the water table is above and below the ground surface level.

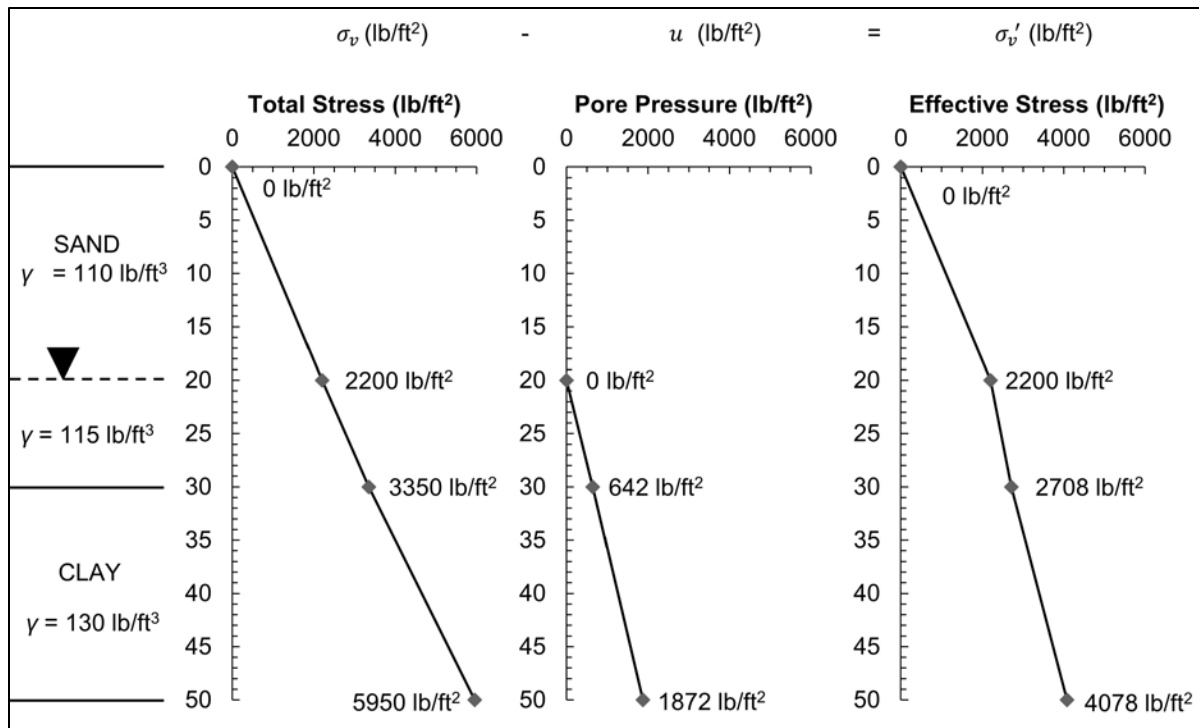


Figure 7-6 Effective stress diagram – water table below ground surface.

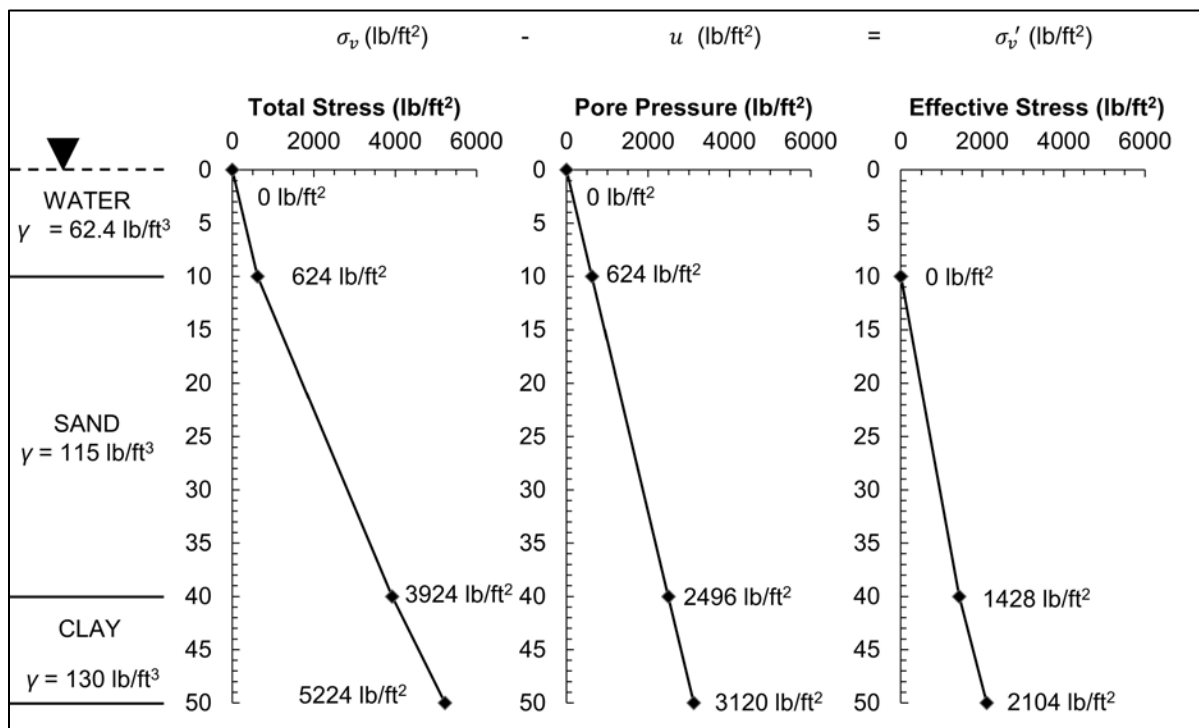


Figure 7-7 Effective stress diagram – water table above ground surface.

7.1.5 Resistance Factors

As discussed in Chapter 2, limit state design for highway structures in the U.S. has been mandated since 2007, and is specified to achieve objectives of safety, serviceability, constructability, and economy. Resistance factors applicable to driven pile design are contained in AASHTO (2014) Table 10.6.5.2.3-1. Section 7.2 of this chapter reviews nominal resistance methods for the strength limit state, while Section 7.3 describes lateral deflection and group settlement for the service limit state. Section 7.4 discusses extreme limit state design which must address strength and serviceability requirements for the respective factored loads and performance requirements.

Resistance factors should not be viewed as a direct replacement for the factor of safety previously used in the allowable stress design (ASD) platform. As discussed in Chapter 2, a resistance factor is a statistically based multiplier applied to the nominal resistance determined from a specific analysis method or analysis procedure. It may be a value determined by national practice (i.e. AASHTO) or it may be a locally calibrated value determined from past practice, databases, and correlation studies. Similarly, load factors are applied to address the uncertainty on the load side, with the load factor also acting as a statistically based multiplier on the force effect. Both the load and resistance factors are tied to a target reliability index, β , which quantifies the probability of non-performance or failure.

Resistance factors to determine the factored resistance via static analysis calculations are summarized in Table 7-1. Several static analysis methods are documented in the literature. However, only those most commonly used in the US transportation industry will be presented in this chapter. Table 7-1 includes several static analysis methods that are presented in this manual that do not have calibrated resistance factors in AASHTO. The presented resistance factors are the best guidance available at the present time. Further research and calibration studies are needed in this area. Brown and Thompson (2015) noted that the AASHTO resistance factor calibration study considered few large diameter pipe piles. Therefore the designer should consider this factor if performing analyses for piles larger than 24 inches in diameter regardless of pile type.

Where a static analysis method is used to determine nominal resistance, the factored resistance, R_r , shall be less than or equal to the sum of the shaft resistance multiplied by the resistance factor associated with the shaft resistance computation method plus the toe resistance multiplied by the resistance factor for the toe resistance computation method as presented in Equation 7-3.

$$R_r \leq \phi R_n = \phi_{stat} R_s + \phi_{stat} R_p \quad \text{Eq. 7-3}$$

Where:

- R_r = factored resistance (kips).
- ϕ_{stat} = resistance factor (based on the static analysis method).
- R_n = nominal resistance (kips).

Table 7-1 Resistance Factors for Static Analysis Methods Presented in this Manual (modified from AASHTO 2014)

Condition	Resistance Determination Method	Resistance Factor
Nominal Geotechnical Resistance of Single Piles in Compression - Static Analysis Methods, ϕ_{stat}	Shaft Resistance and Toe Resistance: Clay and Mixed Soils α -method β -method (1991) Brown (2001) API RP2A (1993) Elsami and Fellenius Schmertmann (1975)	0.35 Differs in Manual ¹ not in AASHTO not in AASHTO not in AASHTO 0.50
	Shaft Resistance and Toe Resistance: Sand Nordlund Method	0.45
Block Failure, ϕ_{bl}	Cohesive	0.60
Nominal Geotechnical Resistance of Single Piles in Tension, ϕ_{up}	Nordlund Method	0.35
	α -method	0.25
	β -method (1991)	0.20
	λ -method	0.30
	SPT-method	0.25
	CPT-method	0.40
Group Uplift Resistance, ϕ_{ug}	Sand and Clay	0.50
Lateral Geotechnical Resistance of Single Pile or Pile Group	All Soils and Rock	1.0

Note: 1 – AASHTO based on Skempton (1951), manual based on Fellenius (1991).

The pile shaft resistance, R_s , and pile toe resistance, R_p , can further be expressed in terms of unit resistance values as shown in Equations 7-4 and 7-5.

$$R_s = f_s A_s \quad \text{Eq. 7-4}$$

$$R_p = q_p A_p$$

Eq. 7-5

Where:

- f_s = unit shaft resistance over the pile surface area (ksf).
- A_s = pile shaft surface area (ft²).
- q_p = unit toe resistance over the pile toe area (ksf).
- A_p = pile toe area (ft²).

The range in the resistance factors has primarily depended upon the reliability of the particular analysis method with consideration of the following items.

1. The level of confidence in the input parameters. This is a function of the type and extent of the subsurface exploration and laboratory testing program. It is assumed that AASHTO Section 10.4 on soil and rock properties is followed.
2. Variability of the soil and rock deposits.
3. Method of static analysis. Resistance factors for some static analysis methods are tied to specific correlation procedures for soil properties.
4. Effects of and consistency of the proposed pile installation method.

AASHTO (2014) Article C10.5.5.2.3 notes that where the nominal resistance is determined by static load test, dynamic testing, wave equation analysis or dynamic formulas, the uncertainty in the nominal resistance is solely due to the reliability of the field resistance determination method. Therefore, the resistance factor for the field method, ϕ_{dyn} , should be used to determine the number of piles of a given factored resistance needed to resist the factored loads in the strength limit state. Table 7-2 summarizes resistance factors for field resistance determination methods. Individual chapters provide expanded details on the field test methods as well as associated performance, analysis, and interpretation information. Chapter 9 covers static load tests, Chapter 10 dynamic pile testing, Chapter 11 rapid load tests, Chapter 12 wave equation analysis, and Chapter 13 dynamic formulas.

If the pile foundation design consists of a small group (i.e. less than 3 piles per substructure unit in this manual) AASHTO (2014) recommends the resistance factors in Tables 7-1 and 7-2 be reduced by 20% to reflect the limited ability of the small group to accommodate the overstressing of one pile. The definition of a small group ranges from 2 or 3 according to Isenhower and Long (1997) to 5 according to Paikowsky et al. (2004).

Table 7-2 Resistance Factors for Field Determination Methods
(after AASHTO 2014)

Condition	Resistance Determination Method	Resistance Factor
Nominal Geotechnical Resistance of Single Pile in Compression Dynamic Analysis and Static Load Test Methods, ϕ_{dyn}	Driving criteria established by successful static load test of at least one pile per site condition and dynamic testing* of at least two piles per site condition, but no less than 2% of the production piles.	0.80
	Driving criteria established by successful static load test of at least one pile per site condition without dynamic testing.	0.75
	Driving criteria established by dynamic testing* conducted on 100% of production piles.	0.75
	Driving criteria established by dynamic testing,*quality control by dynamic testing* of at least two piles per site condition, but no less than 2% of the production piles.	0.65
	Wave equation analysis, without pile dynamic measurements or load test, at End of Drive conditions only.	0.50
	FHWA Modified Gates dynamic pile formula (End of Drive condition only).	0.40
	Engineering News (as defined in AASHTO) dynamic pile formula (End of Drive condition only).	0.10
Nominal Geotechnical Resistance of Single Pile in Tension, ϕ_{dyn}	Static load test.	0.60
	Dynamic testing* with signal matching.	0.50

* - Dynamic testing requires signal matching, and best estimates of nominal resistance are made from a restrrike test. Dynamic tests are calibrated to the static load test, when available.

7.1.6 Interdiscipline Communication and Coordination

The design and construction process requires clear and concise communication among the project professionals practicing in the structural, geotechnical, geologic, hydraulic, and construction fields. Figure 2-3 in Chapter 2 presented a flow chart of the driven pile design and construction process that highlighted the major corroboration areas required in LRFD design and construction of surface transportation projects. The content of the interdiscipline communication was further detailed in Tables 2-4 and 2-5. Effective communication is essential to achieve a cost effective foundation meeting all of the strength, extreme, and service limit state design requirements.

7.2 STRENGTH LIMIT STATES

The strength limit state ensures local and global strength and stability against statistically significant load combinations occurring during the structure design life. Strength limit state design includes an evaluation of the nominal geotechnical and structural resistances as well as the loss of lateral and vertical support in the design flood event due to scour. Geotechnical aspects of strength limit state design includes:

- axial compression resistance of single piles,
- axial compression resistance of pile groups,
- uplift resistance of single piles,
- uplift resistance of pile groups,
- bearing stratum punching failure, and
- constructability including drivability.

7.2.1 Determination of Nominal Resistance for Single Piles

7.2.1.1 General

Numerous static analysis methods are available for calculating the nominal geotechnical resistance of a single pile. Section 7.2.1.3 of this chapter will detail analysis methods for piles in cohesionless, cohesive, and layered soil profiles using readily available SPT or laboratory test information. Additional methods based on cone penetration test results are also presented. As noted earlier, designers should fully understand the basis for, the limitations of, and the applicability of a chosen method. The selected method should also have a proven agreement with full scale

field results in soil conditions similar to the project being designed, with the pile type being evaluated, and the pile installation conditions (impact driving, vibratory driving, etc.) to be used. The AASHTO resistance factors for some static analysis methods require specific procedures for determining soil strength properties.

To perform a static analysis, a pile depth is iteratively assumed based on geomaterial design parameters and selected design methods. This manual presents several design methods with AASHTO (2014) specified resistance factors. However, regional geologic settings or construction control techniques may offer unique conditions not accounted for in these provided methods, therefore reliability calibrations for design methods and resistance factors are encouraged, and may supersede the presented guidelines herein if justified. Table 7-3 compares the static analysis methods presented in AASHTO (2014) design specifications with those contained in this manual. Methods shaded in gray are presented in both documents and have a static analysis resistance factor, ϕ_{stat} . Methods without a static analysis resistance factor require local calibration or must rely on the resistance factor for the field verification method.

Table 7-3 Summary of Static Analysis Methods in GEC-12 and AASHTO (2014) for Determination of Nominal Resistance

Analysis Method	Soil Type	Soil Information Required	Presented in GEC-12	Presented in 2014 AASHTO Code	AASHTO ϕ_{stat}
Meyerhof (1976)	Cohesionless	SPT N	No	Yes	0.30
Nordlund (1963)	Cohesionless	ϕ'	Yes	Yes	0.45
α -method (1980)	Cohesive	s_u	Yes	Yes	0.35
β -method (1951)(1979)*	Cohesive	s_u	No	Yes	0.25
λ -method (1972)	Cohesive	s_u	No	Yes	0.40
API RP2A (1993)	Mixed	s_u, ϕ'	Yes	No	---
β -method (1991)**	Mixed	ϕ'	Yes	No	Differs ¹
Brown (2001)	Mixed	SPT N	Yes	No	---
Elsami & Fellenius (1997)	Mixed	CPT _u	Yes	No	---
Schmertmann (1975)	Mixed	CPT	Yes	Yes	0.50

Notes: ϕ' = effective stress friction angle
 s_u = undrained shear strength
SPT = standard penetration test
CPT = cone penetration test
¹ = β -method in AASHTO uses Skempton (1951), Ersig and Kirby (1979)*;
 β -method in GEC-12 based on Fellenius (1991)**

7.2.1.2 Static Analysis Overview

Agencies often specify the use of select design methodologies based on experience. The design methods presented in this chapter should be used based on applicability to soil conditions, pile type and laboratory testing or subsurface exploration in-situ data. Tables 7-4 and 7-5 present an overview of design methods commonly used for calculating the nominal resistance of piles in cohesionless and cohesive soils, respectively. In layered profiles, the nominal resistance can be calculated by using the applicable cohesionless and cohesive static analysis methods in appropriate soil layers. Table 7-3 identified additional methods that may be used to estimate the nominal resistance in mixed profiles as well as commonly used CPT methods.

Static analysis methods are typically used to estimate the required pile length for a given nominal resistance to establish pile length quantities in the contract documents. The estimated pile lengths and nominal resistance are then confirmed during construction using a field resistance determination method. A driving criterion as discussed in Chapter 17 is established from these results and used to install the remaining production piles. In some cases, static analyses alone are used as the resistance determination method and piles are driven to a predetermined toe elevation. In this latter case, site variability must be addressed in the design pile lengths. Regardless of the static analysis method used, the designer should clearly understand the applications and limitations of the selected method, the soil strength parameters needed to properly use the method, and the procedures and/or correlations used to determine those soil parameters for the method.

The FHWA recommended static analysis methods are the Nordlund method in cohesionless soils (Section 7.2.1.3.1), the α -method in cohesive soils (Section 7.2.1.3.2), and the API method for large diameter pipe piles (Section 7.2.1.3.3). The Nordlund and α -method are recommended methods based on FHWA experience with their reliability in estimating pile length and the associated nominal resistance for conventional pile types in most subsurface conditions. The API method was specifically developed for large diameter pipe piles, and thus is the recommended static analysis method for evaluating highway structure foundations of this pile type.

Table 7-4 Methods of Static Analysis for Piles in Cohesionless Soils

Method	Approach	Method of Obtaining Design Parameters	Advantages	Disadvantages	Remarks
Nordlund Method.	Semi-Empirical.	Charts provided by Nordlund. Estimate of soil friction angle is needed.	Allows for increased shaft resistance of tapered piles and includes effects of pile-soil friction coefficient for different pile materials.	No limiting value on unit shaft resistance is recommended. Soil friction angle often estimated from SPT data. Limit on pile sizes.	Good approach to design that is widely used. Method is based on field observations. Details provided in Section 7.2.1.3.1.
API RP2A.	Empirical, effective stress analysis.	N_q selected from Table 7-8 based on soil type.	Developed specifically for large diameter open end pipe.	Application to non-LDOEPs is limited.	Used almost exclusively for offshore pile design.
Effective Stress Method.	Semi-empirical.	β and N_t selected based on soil classification and estimated friction angle.	β value considers pile-soil friction coefficient for different pile materials. Soil resistance related to effective vertical stress.	Results affected by range in β values and in particular by range in N_t chosen.	Good approach for design. Details provided in Section 7.2.1.3.3.
Brown Method.	Empirical.	Results of SPT tests based of N_{60} values.	Widespread use of SPT test and input data availability. Simple method to use.	Relies solely on N_{60} values, which may not always be available.	Simple method based on correlations with 71 static load test results. Details provided in Section 7.2.1.3.5.
Methods based on Cone Penetration Test (CPT) data.	Empirical.	Results of CPT tests.	Testing analogy between CPT and pile. Reliable correlations and reproducible test data.	Limitations on pushing cone into dense strata.	Good approach for design. Details provided in Sections 7.2.1.3.6 and 7.2.1.3.7.

Table 7-5 Methods of Static Analysis for Piles in Cohesive Soils

Method	Approach	Method of Obtaining Design Parameters	Advantages	Disadvantages	Remarks
α -Method (Tomlinson Method).	Empirical, total stress analysis.	Undrained shear strength estimate of soil is needed. Adhesion calculated from Figures 7-17 and 7-18.	Simple calculation from laboratory undrained shear strength values to adhesion.	Wide scatter in adhesion versus undrained shear strengths in literature. Limits on s_u strengths in soft and medium cohesive soils.	Widely used method described in Section 7.2.1.3.2.
API RP2A.	Empirical, effective stress analysis.	Undrained shear strength estimate of soil is needed.	Developed specifically for large diameter open end pipe piles.	Application to non-LDOEPs is limited.	Used almost exclusively for offshore pile design.
Effective Stress Method.	Semi-Empirical, based on effective stress at failure.	β and N_t values are selected from Table 7-9 based on drained soil strength estimates.	Ranges in β and N_t values for most cohesive soils are relatively small.	Range in N_t values for hard cohesive soils such as glacial tills can be large.	Good design approach theoretically better than undrained analysis. Details in Section 7.2.1.3.3.
Methods based on Cone Penetration Test data.	Empirical.	Results of CPT tests.	Testing analogy between CPT and pile. Reproducible test data.	Cone can be difficult to advance in very hard cohesive soils such as glacial tills.	Good approach for design. Details in Section 7.2.1.3.6 and Section 7.2.1.3.7.

7.2.1.3 Nominal Resistance of Single Piles in Soils

The nominal resistance of a single pile is taken as the sum of shaft and toe resistances ($R_n = R_s + R_p$). The calculation assumes that the shaft resistance and toe resistance can be determined separately and that these two factors do not affect each other. Many analytical and empirical methods have been developed for estimating the nominal resistance of piles using this approach. For typical pile sizes 18 inches and smaller in diameter or width, the nominal resistance is often calculated using the Nordlund Method in cohesionless soils and the α -method in cohesive materials. The Nordlund Method is described in Section 7.2.1.3.1 and the α -method is detailed in Section 7.2.1.3.2. It should be noted that piles larger than 18 inches were not in the correlation database for either the Nordlund Method or the α -method. In layered soil profiles, the nominal resistance can be calculated by combining these methods in cohesionless and cohesive layers as applicable. Table 7-3 identified additional methods that may be used to estimate the nominal resistance in mixed profiles as well as commonly used CPTu and CPT methods.

7.2.1.3.1 Nordlund Method – Cohesionless Soils

The Nordlund Method (1963) is based on field observations and considers the shape of pile taper and its soil displacement in calculating the shaft resistance. This method also accounts for the differences in soil-pile coefficient of friction for different pile materials, and is based on the results of load test programs in cohesionless soils. Several pile types were used in these test programs including timber, H, closed end pipe, Monotube, and Raymond step taper piles. These piles, which were used to develop the method's design curves, had pile widths generally in the range of 10 to 20 inches. The larger pile types used today including large diameter open end pipe piles, concrete cylinder piles, 24 inch and greater square prestressed concrete piles as well as 16 and 18 inch H-pile sections are not in the calibration database. The Nordlund Method tends to over predict the nominal resistance for piles widths larger than 24 inches. Alternative static analysis methods should be evaluated for these other pile types and larger pile sizes.

According to the Nordlund Method, the shaft resistance is a function of the following variables:

1. The friction angle of the soil.
2. The friction angle on the sliding surface.
3. The taper of the pile.
4. The effective unit weight of the soil.

5. The pile length.
6. The minimum pile perimeter.
7. The volume of soil displaced.

These factors are considered in the Nordlund equation as illustrated in Figure 7-8. The Nordlund Method equation for computing the nominal resistance of a pile is as follows:

$$R_n = \sum_{d=0}^{d=D} K_{\delta} C_F \sigma'_d \frac{\sin(\delta + \omega)}{\cos(\omega)} C_d \Delta d + \alpha_t N'_q A_p \sigma'_p \quad \text{Eq. 7-6}$$

Where:

- d = depth (feet).
- D = embedded pile length (feet).
- K_{δ} = coefficient of lateral earth pressure at depth d .
- C_F = correction factor for K_d when $\delta \neq \phi$.
- σ'_d = vertical effective stress at the center of depth increment d .
- δ = friction angle between pile and soil.
- ω = angle of pile taper from vertical.
- C_d = pile perimeter at depth d (feet).
- Δd = length of pile segment.
- α_t = dimensionless factor (dependent on pile depth width relationship).
- N'_q = bearing capacity factor.
- A_p = pile toe area (feet).
- σ'_p = vertical effective stress at the pile toe (ksf).

For a pile of uniform cross section ($\omega=0$) and embedded length D , driven in soil layers of the same effective unit weight and friction angle, the Nordlund equation becomes:

$$R_n = K_{\delta} C_F \sigma'_d \sin(\delta) C_d \Delta d + \alpha_t N'_q A_p \sigma'_p \quad \text{Eq. 7-7}$$

The soil angle of internal friction, ϕ , influences most of the calculations in the Nordlund method. In the absence of laboratory test data, ϕ can be estimated from corrected SPT N values. Section 5.2.3 provides several means of estimating soil friction angle based on these corrected SPT N values. Figures 7-8 to 7-14 should be used to include associate parameters for design. In addition, Table 7-6 and 7-7 provide factors to evaluate the coefficient of lateral earth pressure with depth.

Nordlund developed this method in 1963 with updates in 1979 and did not place a limiting value on the shaft resistance. However, Nordlund recommended that the vertical effective stress at the pile toe, σ'_p , used for computing the pile toe resistance be limited to 3 ksf.

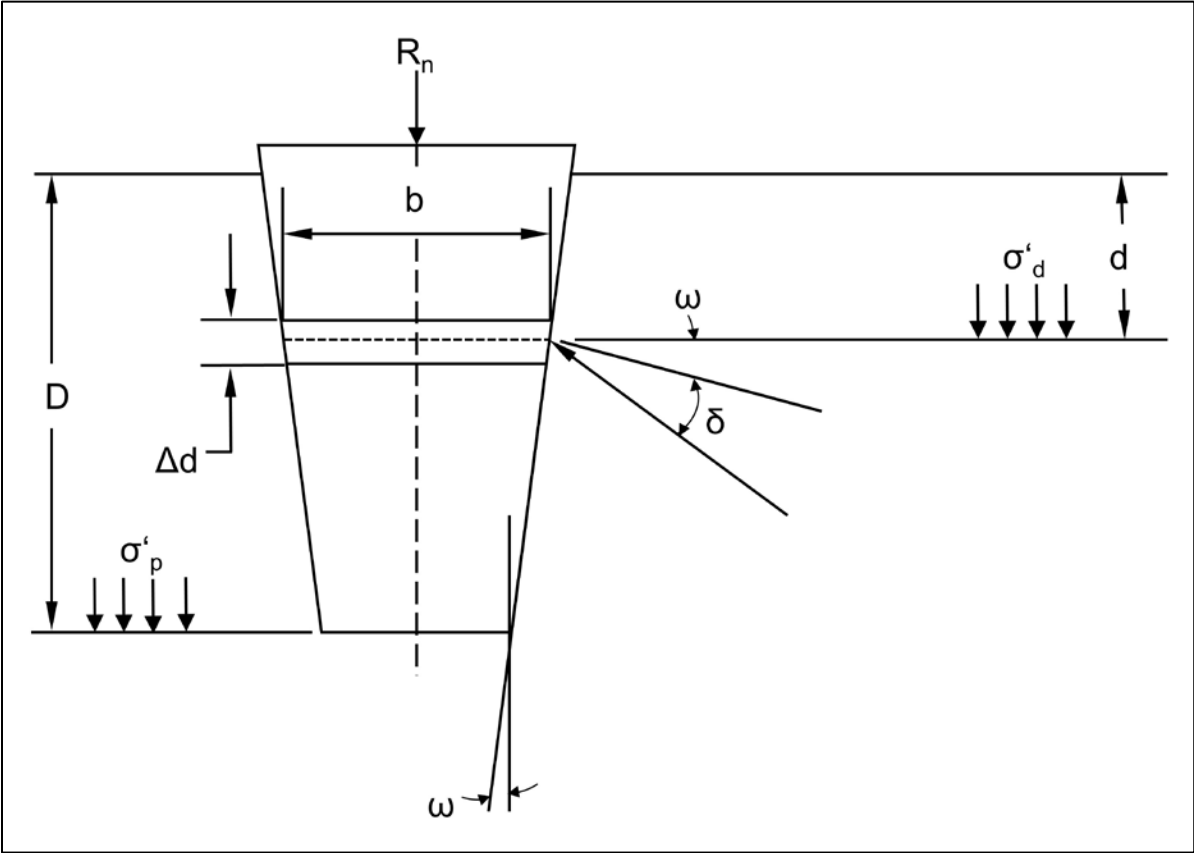
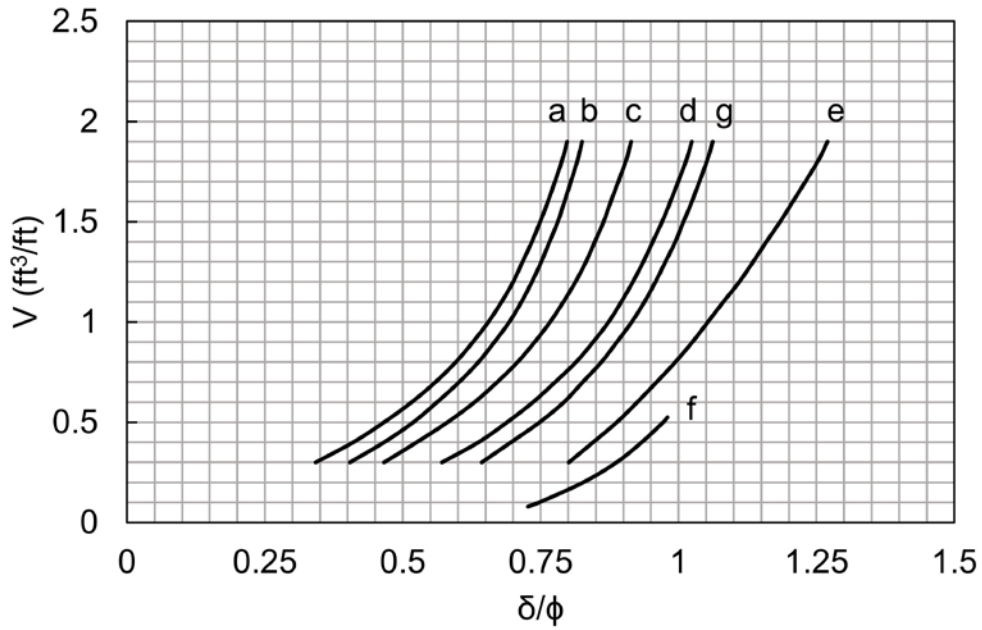


Figure 7-8 Nordlund's general equation diagram for nominal resistance.



- a. Pipe piles and non-tapered portion of monotube piles
- b. Timber piles
- c. Precast concrete piles
- d. Raymond step-taper piles
- e. Raymond uniform taper piles
- f. H-piles and augercast piles
- g. Tapered portion of monotube piles

Figure 7-9 Relationship of δ/ϕ and pile soil displacement, V , for various pile types (after Nordlund 1979).

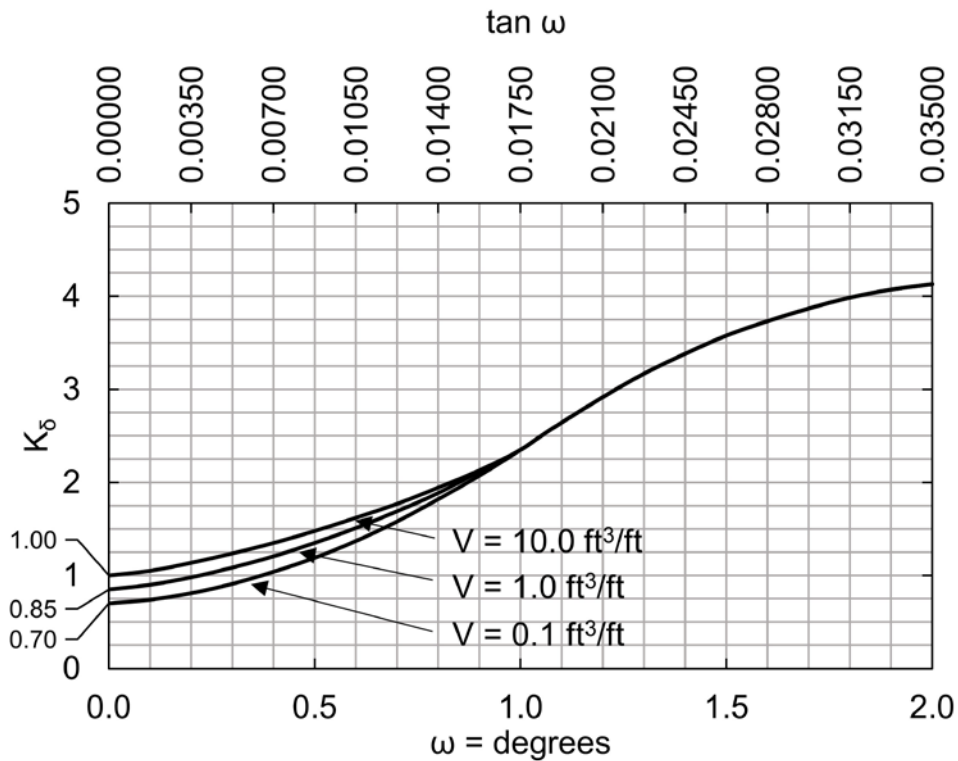


Figure 7-10 Design curve for evaluating K_δ for piles when $\phi = 25^\circ$ (after Nordlund 1979).

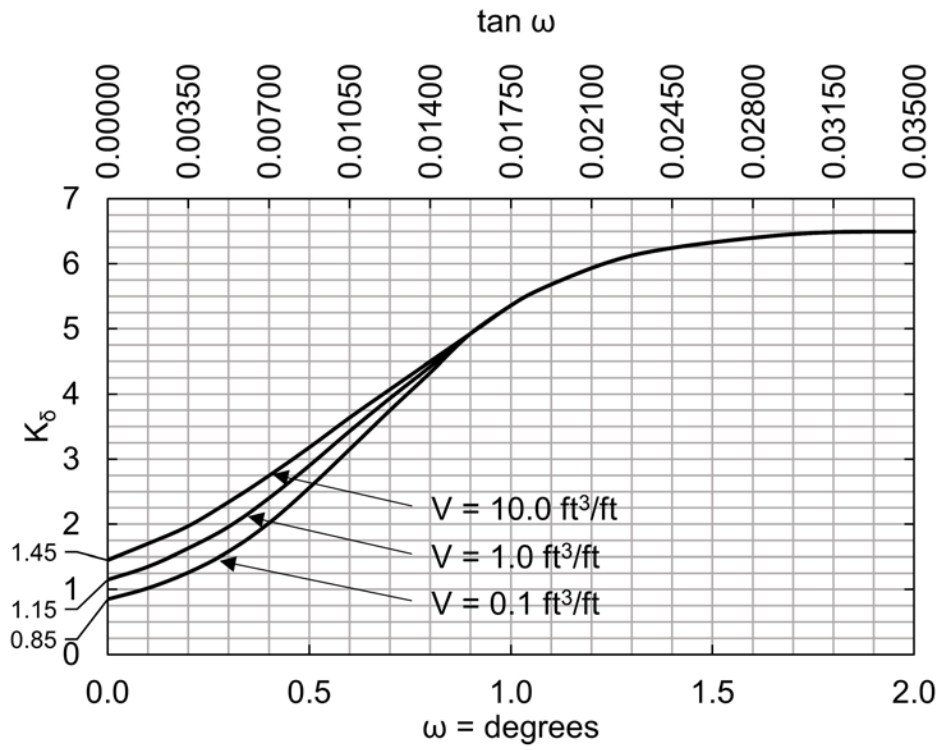


Figure 7-11 Design curve for evaluating K_δ for piles when $\phi = 30^\circ$ (after Nordlund 1979).

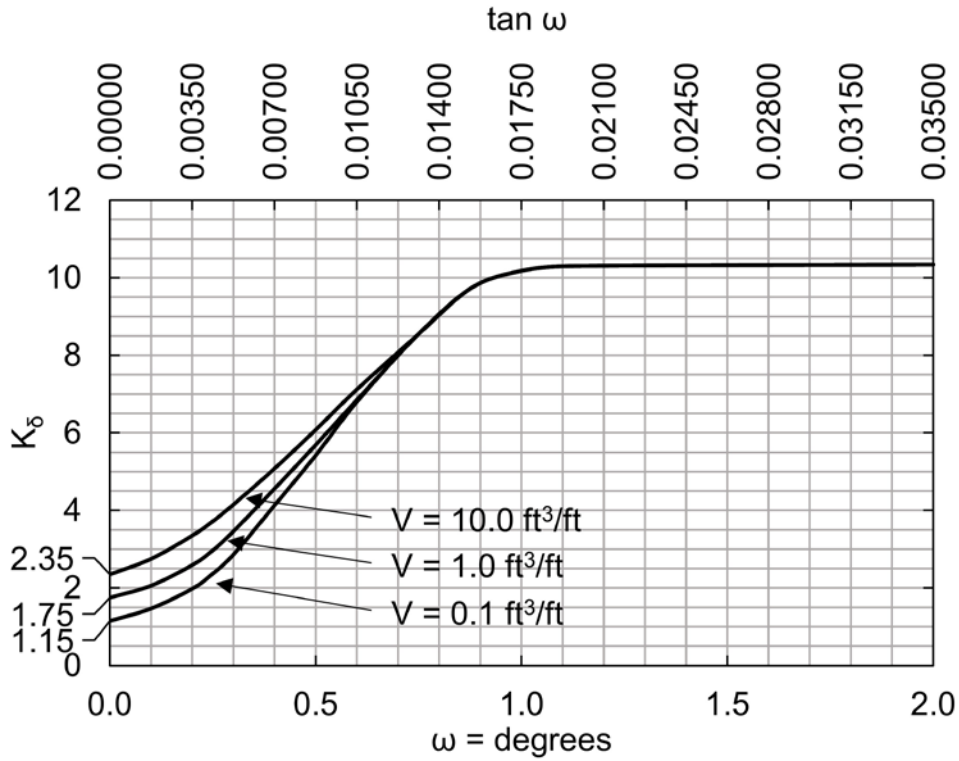


Figure 7-12 Design curve for evaluating K_{δ} for piles when $\phi = 35^{\circ}$ (after Nordlund 1979).

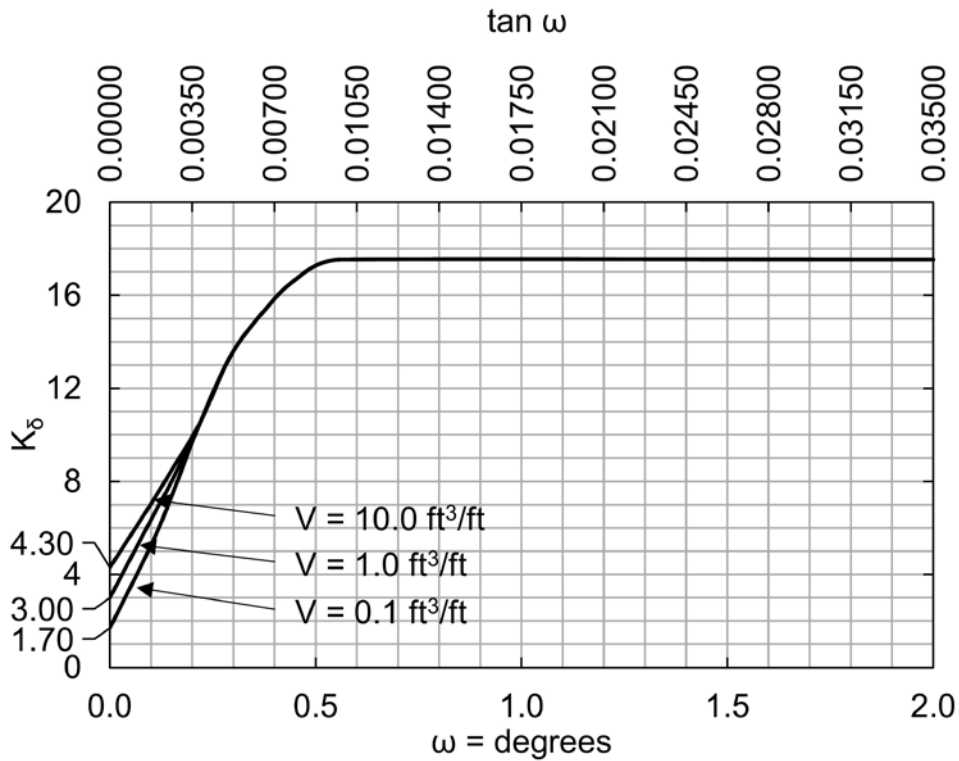


Figure 7-13 Design curve for evaluating K_{δ} for piles when $\phi = 40^{\circ}$ (after Nordlund 1979).

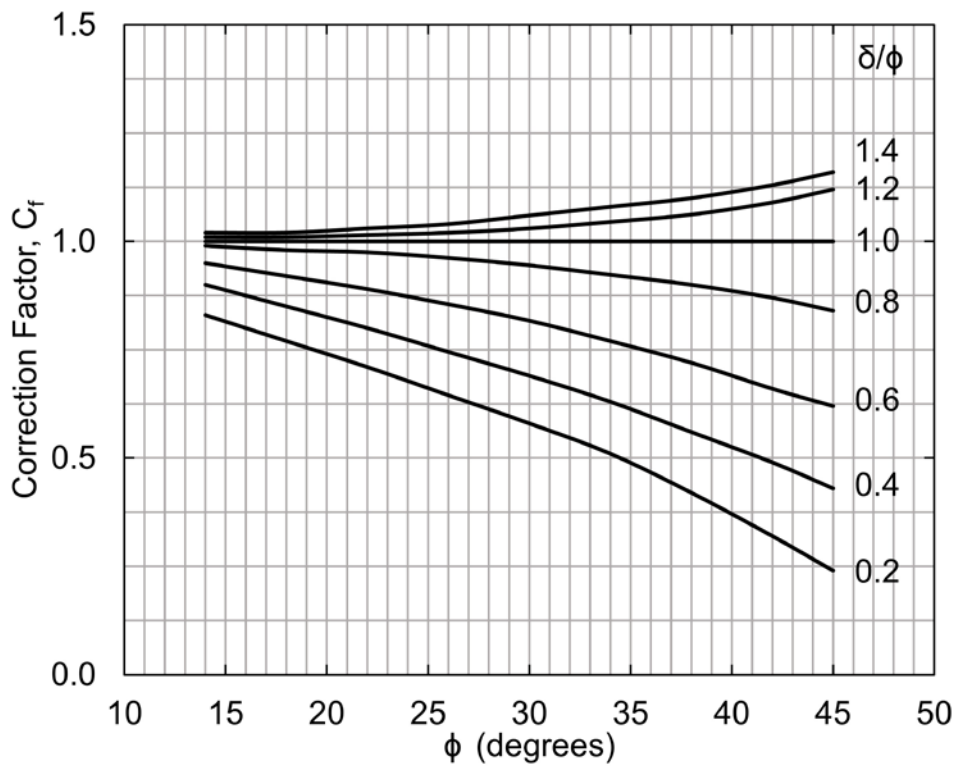


Figure 7-14 Correction factor for K_δ when $\delta \neq \phi$ (after Nordlund 1979).

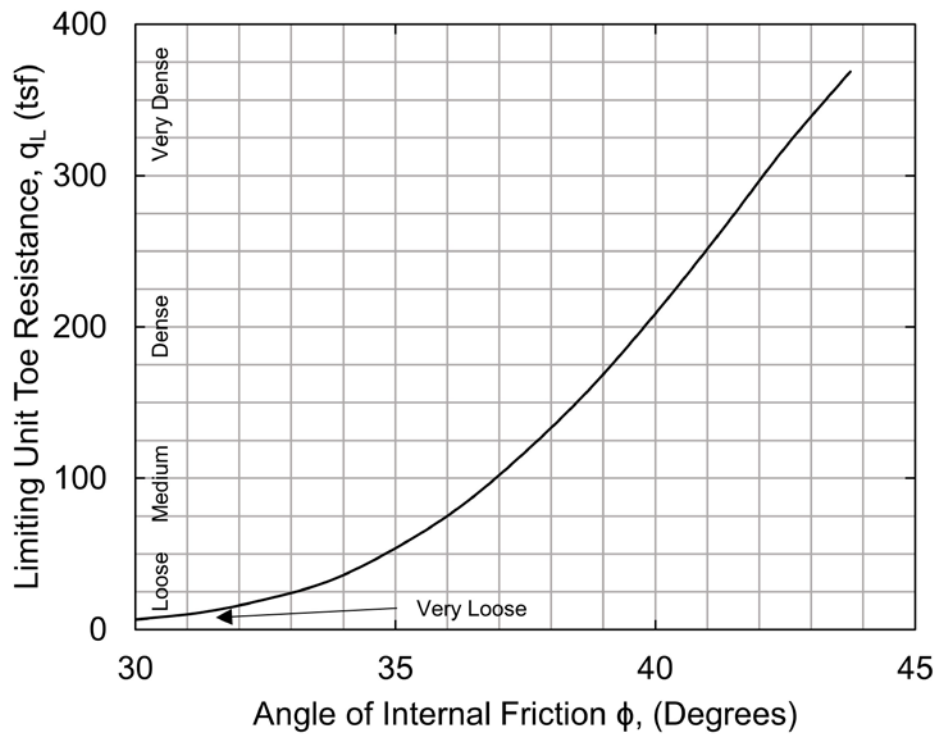


Figure 7-15 Relationship between maximum unit toe resistance and friction angle for cohesionless soils (after Meyerhof 1976).

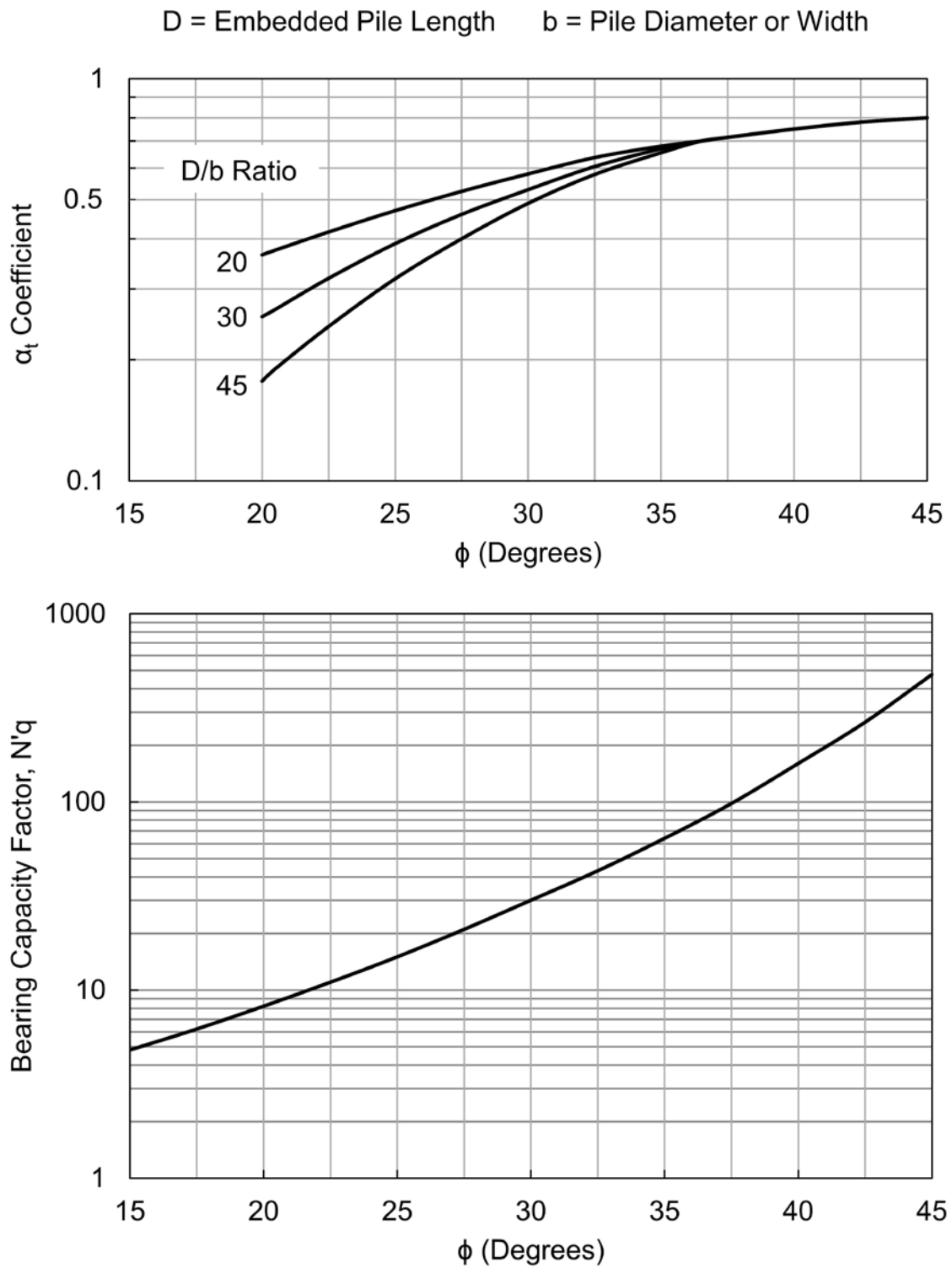


Figure 7-16 Chart for estimating α_t coefficient and bearing capacity factor N'_q (after Bowles 1977).

Table 7-6 Design Table for Evaluating K_s for Piles when $\omega = 0^\circ$ and Displaced Volume $-V = 0.10$ to $1.00 \text{ ft}^3/\text{ft}$

Φ	0.10	0.20	0.30	0.40	0.50	0.60	0.70	0.80	0.90	1.00
25	0.70	0.75	0.77	0.79	0.80	0.82	0.83	0.84	0.84	0.85
26	0.73	0.78	0.82	0.84	0.86	0.87	0.88	0.89	0.90	0.91
27	0.76	0.82	0.86	0.89	0.91	0.92	0.94	0.95	0.96	0.97
28	0.79	0.86	0.90	0.93	0.96	0.98	0.99	1.01	1.02	1.03
29	0.82	0.90	0.95	0.98	1.01	1.03	1.05	1.06	1.08	1.09
30	0.85	0.94	0.99	1.03	1.06	1.08	1.10	1.12	1.14	1.15
31	0.91	1.02	1.08	1.13	1.16	1.19	1.21	1.24	1.25	1.27
32	0.97	1.10	1.17	1.22	1.26	1.30	1.32	1.35	1.37	1.39
33	1.03	1.17	1.26	1.32	1.37	1.40	1.44	1.46	1.49	1.51
34	1.09	1.25	1.35	1.42	1.47	1.51	1.55	1.58	1.61	1.63
35	1.15	1.33	1.44	1.51	1.57	1.62	1.66	1.69	1.72	1.75
36	1.26	1.48	1.61	1.71	1.78	1.84	1.89	1.93	1.97	2.00
37	1.37	1.63	1.79	1.90	1.99	2.05	2.11	2.16	2.21	2.25
38	1.48	1.79	1.97	2.09	2.19	2.27	2.34	2.40	2.45	2.50
39	1.59	1.94	2.14	2.29	2.40	2.49	2.57	2.64	2.70	2.75
40	1.70	2.09	2.32	2.48	2.61	2.71	2.80	2.87	2.94	3.0

Table 7-7 Design Table for Evaluating K_s for Piles when $\omega = 0^\circ$
and Displaced Volume $-V = 1.0$ to $10 \text{ ft}^3/\text{ft}$

ϕ	1.0	2.0	3.0	4.0	5.0	6.0	7.0	8.0	9.0	10.0
25	0.85	0.90	0.92	0.94	0.95	0.97	0.98	0.99	0.99	1.00
26	0.91	0.96	1.00	1.02	1.04	1.05	1.06	1.07	1.08	1.09
27	0.97	1.03	1.07	1.10	1.12	1.13	1.15	1.16	1.17	1.18
28	1.03	1.10	1.14	1.17	1.20	1.22	1.23	1.25	1.26	1.27
29	1.09	1.17	1.22	1.25	1.28	1.30	1.32	1.33	1.35	1.36
30	1.15	1.24	1.29	1.33	1.36	1.38	1.40	1.42	1.44	1.45
31	1.27	1.38	1.44	1.49	1.52	1.55	1.57	1.60	1.61	1.63
32	1.39	1.52	1.59	1.64	1.68	1.72	1.74	1.77	1.79	1.81
33	1.51	1.65	1.74	1.80	1.85	1.88	1.92	1.94	1.97	1.99
34	1.63	1.79	1.89	1.96	2.01	2.05	2.09	2.12	2.15	2.17
35	1.75	1.93	2.04	2.11	2.17	2.22	2.26	2.29	2.32	2.35
36	2.00	2.22	2.35	2.45	2.52	2.58	2.63	2.67	2.71	2.74
37	2.25	2.51	2.67	2.78	2.87	2.93	2.99	3.04	3.09	3.13
38	2.50	2.81	2.99	3.11	3.21	3.29	3.36	3.42	3.47	3.52
39	2.75	3.10	3.30	3.45	3.56	3.65	3.73	3.80	3.86	3.91
40	3.00	3.39	3.62	3.78	3.91	4.01	4.10	4.17	4.24	4.30

STEP BY STEP PROCEDURE FOR: "NORDLUND METHOD"

Steps 1 through 6 are for computing the shaft resistance and Steps 7 through 9 are for computing the pile toe resistance.

- STEP 1 Delineate the soil profile into layers and determine the ϕ angle for each layer.
- Construct Effective Stress Diagram using procedure described in Section 7.1.4.
 - Correct SPT field N values for vertical stress using methods from Section 5.1.1 to obtain corrected SPT N values, $(N_1)_{60}$. Delineate soil profile into layers based on corrected SPT N values.
 - Determine ϕ angle for each layer from laboratory tests or in-situ data.
 - In the absence of laboratory or in-situ test data, determine the average corrected SPT N value, $(N_1)_{60}$, for each soil layer and estimate ϕ angle from Table 5-5 in Chapter 5.
- STEP 2 Determine δ , the friction angle between pile and soil based on displaced soil volume, V , and the soil friction angle, ϕ .
- Compute volume of soil displaced per unit length of pile, V .
 - Use Figure 7-9 with V and determine δ/ϕ ratio for pile type.
 - Calculate δ from δ/ϕ ratio.
- STEP 3 Determine the coefficient of lateral earth pressure, K_δ , for each ϕ angle.
- Determine K_δ for ϕ angle based on displaced volume, V , and pile taper angle, ω , using either Figure 7-10, 7-11, 7-12, or 7-13 and the appropriate procedure described in Step 3b, 3c, 3d, or 3e.
 - If the displaced volume is 0.1, 1.0 or 10.0 ft³/ft, which correspond to one of the curves provided in Figures 7-10 through 7-13 and the ϕ

angle is one of those provided, K_δ can be determined directly from the appropriate figure.

- c. If the displaced volume is 0.1, 1.0 or 10.0 ft³/ft which correspond to one of the curves provided Figures 7-10 through 7-13 but the ϕ angle is different from those provided, use linear interpolation to determine K_δ for the required ϕ angle. Tables 7-6 and 7-7 also provide interpolated K_δ values at selected displaced volumes versus ϕ angle for uniform piles ($\omega = 0$).
- d. If the displaced volume is other than 0.1, 1.0 or 10.0 ft³/ft which corresponds to one of the curves provided in Figures 7-10 through 7-13 but the ϕ angle corresponds to one of those provided, use log linear interpolation to determine K_δ for the required displaced volume. Tables 7-6 and 7-7 also provide interpolated K_δ values at selected displaced volumes versus ϕ angle for uniform piles ($\omega = 0$).
- e. If the displaced volume is other than 0.1, 1.0 or 10.0 ft³/ft which correspond to one of the curves provided in Figures 7-10 through 7-13 and the ϕ angle does not correspond to one of those provided, first use linear interpolation to determine K_δ for the required ϕ angle at the displaced volume curves provided for 0.1, 1.0 or 10.0 ft³/ft. Then use log linear interpolation to determine K_δ for the required displaced volume. Tables 7-6 and 7-7 also provide interpolated K_δ values at selected displaced volumes versus friction angle for uniform piles ($\omega = 0$).

STEP 4 Determine the correction factor, C_F , to be applied to K_δ if $\delta \neq \phi$.

Use Figure 7-14 to determine the correction factor for each K_δ . Enter figure with ϕ angle and δ/ϕ value to determine C_F .

STEP 5 Compute the average vertical effective stress at the midpoint of each soil layer, σ'_d (psf).

Note: A limiting value is not applied to σ'_d .

STEP 6 Compute the shaft resistance in each soil layer. Sum the shaft resistance from each soil layer to obtain the nominal shaft resistance, R_s (kips).

$$R_s = K_\delta C_F \sigma'_d \sin(\delta) C_d D \quad \text{Eq. 7-8}$$

(for uniform pile cross section)

For H-piles in cohesionless soils, the "box" area should generally be used for shaft resistance calculations. An additional discussion on the behavior of open pile sections is presented in Section 7.10.7.

STEP 7 Determine the α_t coefficient and the bearing capacity factor, N'_q , from the ϕ angle near the pile toe.

- a. Enter Figure 7-16(a) with ϕ angle near the pile toe to determine α_t coefficient based on pile length to diameter ratio.
- b. Enter Figure 7-16(b) with ϕ angle near the pile toe to determine N_q .
- c. If ϕ angle is estimated from SPT data, compute the average corrected SPT N value, $(N_1)_{60}$, over the zone from the pile toe to 3 diameters below the pile toe. Use this average corrected SPT N value to estimate ϕ angle near pile toe.

STEP 8 Compute the vertical effective stress at the pile toe, σ'_p (ksf).

Note: The limiting value of σ'_p is 3 ksf.

STEP 9 Compute the nominal toe resistance, R_p (kips).

$$R_p = \alpha_t N'_q A_p \sigma'_p \quad \text{Eq. 7-9}$$

a. While limiting $R_p = q_L A_p$ where q_L value is obtained from:

1. Entering Figure 7-15 with ϕ angle near pile toe determined from laboratory or in-situ test data.

2. Entering Figure 7-15 with ϕ angle near the pile toe estimated and the average corrected SPT N value, $(N_1)_{60}$, near toe as described in Step 7.

b. Use lesser of the two R_p values obtained in steps a and b.

For steel H and open end pipe piles, the selection of the pile toe area (steel area only or full cross sectional area of steel and enclosed soil) for toe resistance calculations should be based on past experience and local correlations with static load test results.

STEP 10 Compute the nominal resistance, R_n , from the sum of the shaft and toe resistances, $R_n = R_s + R_p$.

STEP 11 Compute the factored resistance, R_r (kips), using select resistance factors provided in Section 7.1.5 and Equation 7-3.

AASHTO (2014) provides a recommended resistance factor for this method in Table 7-1 for the nominal resistance determined by static analysis. The nominal resistance at the strength limit state could also be determined using the resistance factor associated with the field verification method, ϕ_{dyn} , as recommended in Table 7-2.

7.2.1.3.2 α -Method - Cohesive Soils

For piles in clay, a total stress analysis is often used where nominal resistance is calculated from the undrained shear strength of the soil. This approach assumes that the shaft resistance is independent of the vertical effective stress and that the unit shaft resistance can be expressed in terms of an empirical adhesion factor times the undrained shear strength.

The unit shaft resistance, f_s , is equal to the adhesion which is the shear stress between the pile surface and the soil at failure. This may be expressed in equation form as:

$$f_s = C_a = \alpha s_u \quad \text{Eq. 7-10}$$

Where:

- C_a = adhesion (ksf).
- s_u = undrained shear strength (ksf).
- α = adhesion factor.

The adhesion factor α depends on the nature and strength of the clay, pile dimension, method of pile installation, and time effects. The values of α vary within wide limits and decreases rapidly with increasing shear strength.

It is recommended that Figure 7-17 generally be used for adhesion calculations, unless one of the special soil stratigraphy cases identified in Figure 7-18 is present at a site. In cases where either Figures 7-17 or 7-18 could be used, the inexperienced user should select and use the smaller value obtained from either figure. The undrained shear strengths addressed in the design charts ranges from approximately 0.5 ksf on the low end to 3.5 to 5.0 ksf on the high end, depending on the design chart. All users should confirm the applicability of a selected design chart in a given soil condition with local correlations between static resistance calculations and static load tests results. This is particularly for cases where the shear strength approaches either the upper or lower limit of the design chart.

In Figure 7-17, the pile adhesion, C_a , is expressed as a function of the undrained shear strength, s_u , with consideration of both the pile type and the embedded pile length, D , to pile diameter, b , ratio. The embedded pile length used in Figure 7-17 should be the minimum value of the length from the ground surface to the bottom of the clay layer, or the length from the ground surface to the pile toe.

Figure 7-18 presents the adhesion factor, α , versus the undrained shear strength of the soil as a function of unique soil stratigraphy and pile embedment. The adhesion factor from these soil stratigraphy cases should be used only for determining the adhesion in a stiff clay layer in that specific condition. For a soil profile consisting of clay layers of significantly different consistencies such as soft clays over stiff clays, adhesion factors should be determined for each individual clay layer.

The top graph in Figure 7-18 may be used to select the adhesion factor when piles are driven through a sand or sandy gravel layer and into an underlying stiff clay stratum. This case results in the highest adhesion factors as granular material is dragged into the underlying clays. The greater the pile penetration into the clay stratum, the less influence the overlying granular stratum has on the adhesion factor. Therefore, for the same undrained shear strength, the adhesion factor decreases with increased pile penetration into the clay stratum.

The middle graph in Figure 7-18 should be used to select the adhesion factor when piles are driven through a soft clay layer overlying a stiff clay layer. In this case, the soft clay is dragged into the underlying stiff clay stratum thereby reducing the adhesion factor of the underlying stiff clay soils. The greater the pile penetration into

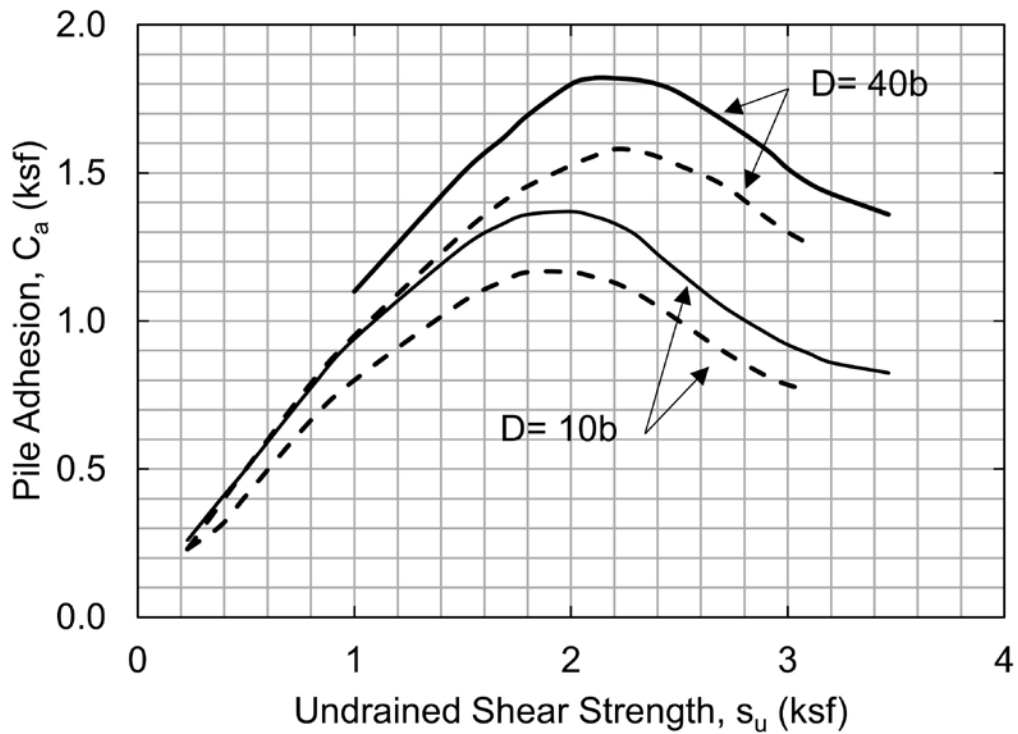
the underlying stiff clay soils, the less the influence the overlying soft clays have on the stiff clay adhesion factor. Therefore, the stiff clay adhesion factor increases with increasing pile penetration into the stiff clay soils.

Last, the bottom graph in Figure 7-18 may be used to select the adhesion factor for piles driven in stiff clays without any different overlying strata. In stiff clays, a gap often forms between the pile and the soil along the upper portion of the pile shaft. In this case, the shallower the pile penetration into a stiff clay stratum the greater the effect the gap has on the shaft resistance that develops. Hence, the adhesion factor for a given shear strength is reduced at shallow pile penetration depths and increased at deeper pile penetration depths.

In highly overconsolidated clays, undrained shear strengths may exceed the upper limits of Figures 7-17 and 7-18. In these cases, it is recommended that adhesion factor, α , be calculated according to API Recommended Practice 2A (1993). Further information for this is provided in Section 7.2.1.3.3 of this chapter.

In the case of H-piles in cohesive soils, the shaft resistance should not be calculated from the surface area of the pile, but rather from the "box" area of the four sides. The shaft resistance for H-piles in cohesive soils consists of the sum of the adhesion, C_a , times the flange surface area along the exterior of the two flanges, plus the undrained shear strength of the soil, s_u , times the area of the two remaining sides of the "box", due to soil-to-soil shear along these faces. This computation can be approximated by determining the adhesion using the appropriate corrugated pile curve in Figure 7-17 and multiplying the adhesion by the H-pile "box" area. Additional information on the behavior of open pile sections is presented in Section 7.10.7.

In clays with large shrink-swell potential, static resistance calculations should ignore the shaft resistance from the adhesion in the shrink-swell zone. During dry times, shrinkage will create a gap between the clay and the pile in this zone and therefore the shaft resistance should not be relied upon for long term support.



Legend

D = Distance from Ground Surface to Bottom of Clay Layer

b = Pile Diameter

———— Concrete, Timber, Corrugated Steel Piles

----- Smooth Steel Piles

Figure 7-17 Adhesion values for piles in cohesive soils (after Tomlinson 1979).

The unit toe resistance, q_p , in a total stress analysis for homogeneous cohesive soil can be expressed as:

$$q_p = N_c s_u \quad \text{Eq. 7-11}$$

Where:

N_c = bearing capacity factor.

s_u = undrained shear strength (ksf).

The term N_c is a dimensionless bearing capacity factor which depends on the pile diameter and the depth of embedment. The bearing capacity factor, N_c , is usually taken as 9 for deep foundations.

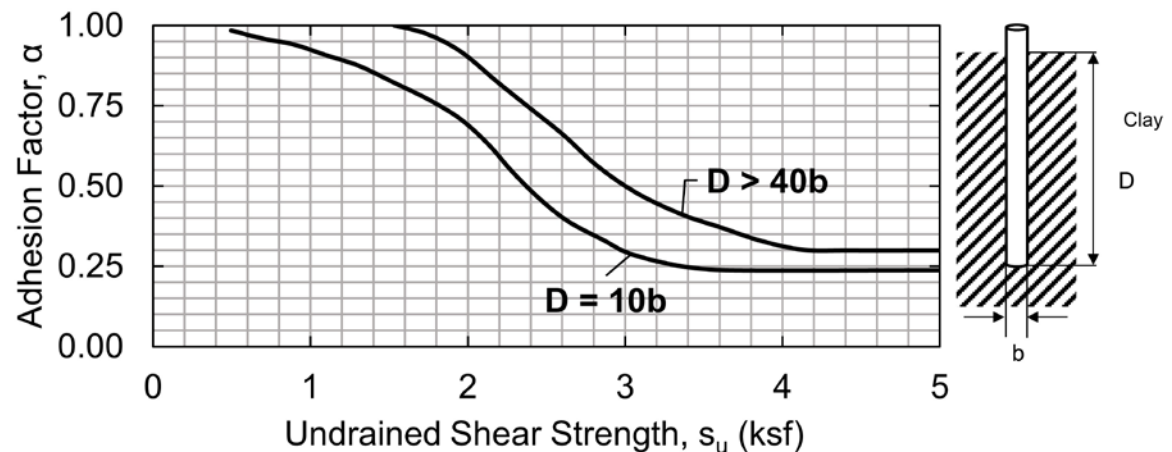
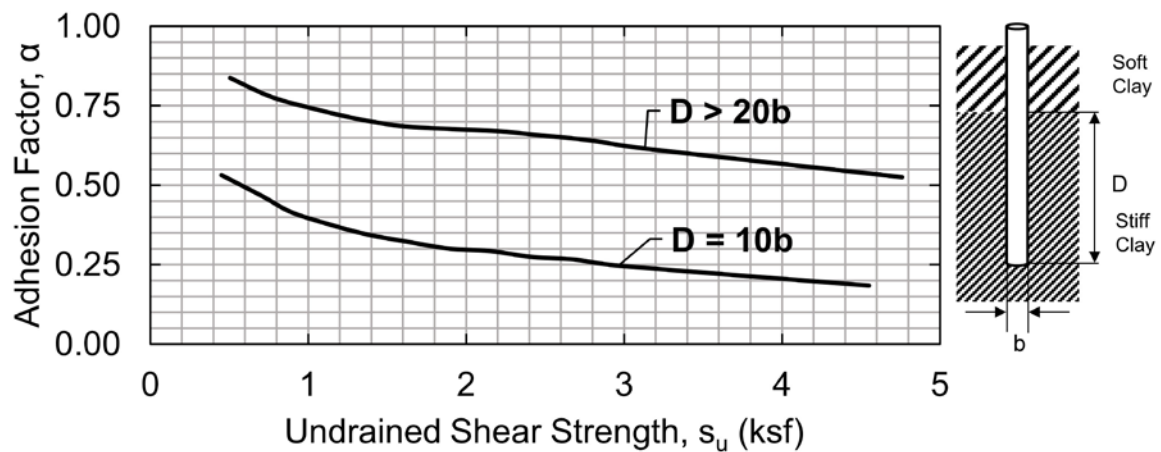
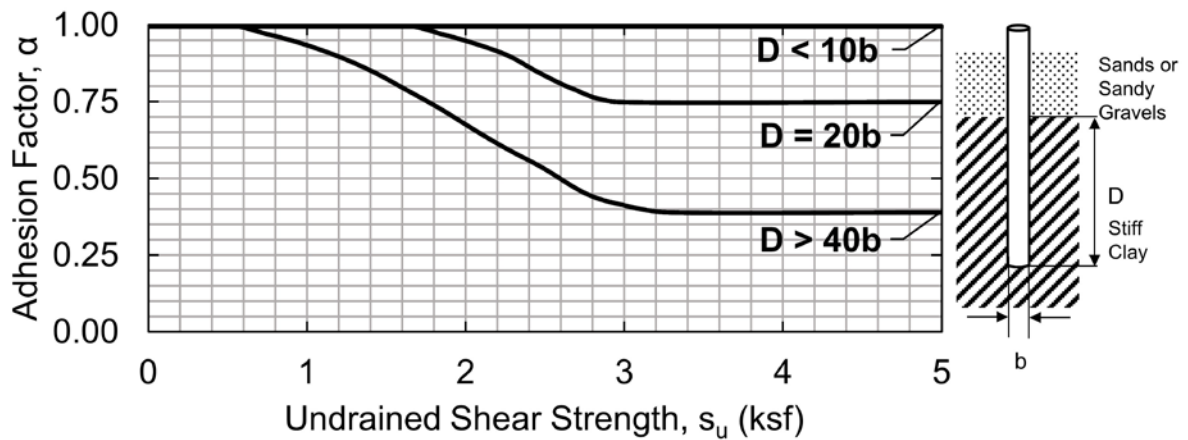


Figure 7-18 Adhesion factors for driven piles in clay (Tomlinson 1980).

On smaller piles in cohesive soils, the toe resistance contribution to the nominal resistance is a low percentage of the overall resistance and is therefore sometimes ignored. On larger piles, the movement required to mobilize the toe resistance is

several times greater than that required to mobilize the shaft resistance. At the movement required to fully mobilize the toe resistance, the shaft resistance may have decreased to a residual value. These factors should be considered when performing nominal resistance assessments of various pile sections.

STEP BY STEP PROCEDURE FOR: "α-METHOD"

STEP 1 Delineate the soil profile into layers and determine the pile adhesion, C_a , from Figure 7-17 or adhesion factor, α , from Figure 7-18 for each layer.

Enter appropriate figure with the undrained shear strength of the soil, s_u , and determine pile adhesion or adhesion factor based on the embedded pile length in clay, D , and pile diameter, b . Use the curve for the appropriate soil and embedment condition. For highly overconsolidated clays where s_u exceeds the chart values, see Section 7.2.1.3.3 for guidance on α .

STEP 2 For each soil layer, compute the unit shaft resistance, f_s (ksf), using Equation 7-10.

STEP 3 Compute the shaft resistance in each soil layer and the nominal shaft resistance, R_s (kips), from the sum of the layer shaft resistances.

STEP 4 Compute the unit toe resistance, q_p (ksf) using Equation 7-11.

STEP 5 Compute the nominal toe resistance, R_p (kips).

For open pile sections, refer to the discussion of pile plugging presented in Section 7.10.7.

STEP 6 Compute the nominal pile resistance, R_n , from the sum of the shaft and toe resistances, $R_n = R_s + R_p$.

STEP 7 Compute the factored resistance, R_r (kips), using the resistance factors provided in Section 7.1.5 and Equation 7-3.

AASHTO (2014) provides a recommended resistance factor for this method in Table 7-1 for the nominal resistance determined by static analysis. The nominal resistance in the strength limit state could also be determined using the resistance factor associated with the field verification method, ϕ_{dyn} , as recommended in Table 7-2.

7.2.1.3.3 P2A Method – Mixed Soil Profiles

The American Petroleum Institute (API) provides a static analysis procedure design developed for offshore construction. These projects almost exclusively use large diameter, open-end, steel pipe piles which are driven by impact hammer to final penetration (API 1993). In NCHRP Report 20-05 on large diameter pipe piles by Brown and Thompson (2015), large diameter open end pipe piles are defined as having a diameter of 36 inches or greater. Large diameter open end pipe piles can be either steel pipe piles or concrete cylinder piles. Recently, large diameter open end pipe pile usage has increased significantly on transportation projects. This has heightened the need for more accurate nominal resistance estimates on these larger piles.

Similar to other design methodologies, the API approach gives consideration to soil type. For cohesive soil, shaft resistance, f_s , can be determined from Equation 7-12.

$$f_s = \alpha s_u \quad \text{Eq. 7-12}$$

Where:

α = dimensionless adhesion factor.

s_u = undrained shear strength at the location in question (ksf).

The factor α_f varies based on effective stress and may be calculated using Equations 7-13 through 7-15 below.

$$\alpha = 0.5\psi^{-0.5} \quad \text{when } \psi \leq 1.0 \quad \text{Eq. 7-13}$$

$$\alpha = 0.5\psi^{-0.25} \quad \text{when } \psi > 1.0 \quad \text{Eq. 7-14}$$

$$\psi = \frac{s_u}{\sigma'_{vo}} \quad \text{Eq. 7-15}$$

Where:

- α = dimensionless factor.
- s_u = undrained shear strength at the sample depth (ksf).
- σ'_{vo} = vertical effective stress at the sample depth (ksf).

An α value of 1.0 is recommended for unconsolidated clays. Reductions in resistance may be practical for very long piles where residual soil strength values are approached due to extended driving and subsequent soil displacement. For these cases, API (1993) recommends the use of engineering judgment.

The unit toe resistance, q_p , for piles in cohesive soil can be determined using Equation 7-16.

$$q_p = 9s_u \quad \text{Eq. 7-16}$$

Because of the dynamic events during driving, the pile may be installed in an unplugged condition, however when static loads are applied, a plugged condition may exist. Consideration should be given to these cases when performing a static analysis and drivability study.

When installing piles in cohesionless soils, the unit shaft resistance may be determined with Equation 7-17.

$$f_s = K_\delta \sigma'_{vo} \tan \delta \quad \text{Eq. 7-17}$$

Where:

- K_δ = coefficient of lateral earth pressure.
- σ'_{vo} = vertical effective stress (ksf).
- δ = friction angle between the soil and pile wall.

API (1993) notes that assuming $K_\delta = 0.8$ for both tension and compression loading of unplugged, open ended pipe pile is appropriate. In addition, for the plugged or closed end case the assumption of $K_\delta = 1.0$ is recommended.

The unit toe resistance, q_p for piles in cohesionless soils may be determined using the following relationship:

$$q_p = \sigma'_{vo} N_q \quad \text{Eq. 7-18}$$

Where:

σ'_{vo} = vertical effective stress (ksf).

N_q = dimensionless bearing capacity factor.

Table 7-8 is modified from API (1993) and presents guidelines for design parameters using steel pipe piles installed in cohesionless soils. Subsurface exploration and testing data for sites in question should be considered where necessary, in lieu of these guidelines.

Table 7-8 Design Parameter Guidelines for Cohesionless Siliceous Soil
(after API 1993)

Density	Soil	Soil-Pile Friction Angle, δ	Limiting Unit Shaft Resistance, (ksf)	N_q	Limiting Unit Toe Resistance, (ksf)
Very loose Loose Medium	Sand Sand-Silt* Silt	15	1.0	8	40
Loose Medium Dense	Sand Sand-Silt* Silt	20	1.4	12	60
Medium Dense	Sand Sand-Silt*	25	1.7	20	100
Dense Very Dense	Sand Sand-Silt*	30	2.0	40	200
Dense Very Dense	Gravel Sand	35	2.4	50	250

* - In sand-silt soils (soils with significant fractions of both sand and silt), the strength values generally increase with increasing sand fractions and decrease with increasing silt fractions.

STEP BY STEP PROCEDURE FOR: "API METHOD"

STEP 1 Delineate the soil profile into cohesive and cohesionless layers.

For cohesive layers, determine the average undrained shear strength, s_u , for the layer and the vertical effective stress σ'_{vo} , at the mid-point of the layer. Determine the adhesion factor, α , based on the s_u/σ'_{vo} ratio and Equation 7-13 or 7-14.

For cohesionless layers, determine the soil-pile friction angle, δ , for the layer and the vertical effective stress σ'_{vo} , at the mid-point of the layer. Determine the coefficient of lateral earth pressure, K_δ , based on the pile type and loading direction.

STEP 2 For each soil layer, compute the unit shaft resistance, f_s (ksf) using Equation 7-12 in cohesive soil layers and Equation 7-17 in cohesionless soil layers.

Note: A limiting unit shaft resistance is applied in cohesionless soils.

STEP 3 Using Equation 7-4, compute the shaft resistance in each soil layer and the nominal shaft resistance, R_s , from the sum of the shaft resistance from each layer.

STEP 4 Compute the unit toe resistance, q_p (ksf).

For piles terminated in a cohesive layer, use the average undrained shear strength, s_u , in Equation 7-16.

For piles terminated in a cohesionless layer, determine bearing capacity factor, N_q , from Table 7-8 and Equation 7-18.

Note: A limiting unit toe resistance is applied in cohesionless soils.

STEP 5 Compute the nominal toe resistance, R_p (kips) using Equation 7-5.

For open pile sections, refer to the discussion of pile plugging presented in Section 7.10.7.

STEP 6 Compute the nominal pile resistance, R_n from the sum of the shaft and toe resistances, $R_n = R_s + R_p$.

STEP 7 Compute the factored resistance, R_r (kips), using the applicable resistance factor for the field verification method.

In NCHRP Report 507, Paikowsky (2004) evaluated the reliability of the API method in cohesive soils but not in sands or mixed profiles. AASHTO (2014) also does not provide a recommended resistance factor for the nominal resistance determined by the API method. Therefore, the nominal resistance at the strength limit state should be determined using the resistance factor associated with the field verification method, ϕ_{dyn} , as recommended in Table 7-2.

7.2.1.3.4 Effective Stress β -Method – Mixed Soil Profiles

Static resistance calculations in cohesionless, cohesive, and layered soils can also be performed using an effective stress method. Effective stress methods were developed to model the long term drained shear strength conditions. Therefore, the effective stress friction angle, ϕ' , should be used in parameter selection.

In an effective stress analysis, the unit shaft resistance is calculated from the following expression:

$$f_s = \beta \sigma'_{vo} \quad \text{Eq. 7-19}$$

Where:

- β = Bjerrum-Burland beta coefficient = $K_\delta \tan \delta$.
- σ'_{vo} = average vertical effective stress along the pile shaft (ksf).
- K_δ = coefficient of lateral earth pressure.
- δ = friction angle between pile and soil.

The unit toe resistance is calculated from:

$$q_p = N_t \sigma'_p \quad \text{Eq. 7-20}$$

Where:

N_t = toe resistance coefficient.

σ'_p = vertical effective stress at the pile toe (ksf).

Recommended ranges of β and N_t coefficients as a function of soil type and ϕ' angle from Fellenius (2014) are presented in Table 7-9. Fellenius notes that factors affecting the β and N_t coefficients consist of the soil composition including the grain size distribution, angularity and mineralogical origin of the soil grains, the original soil density and density due to the pile installation technique, the soil strength, as well as other factors. While Table 7-9 provides the approximate range of β coefficients for various soil types, Fellenius noted that values can deviate significantly from those in the table. β coefficients seldom exceed 1.0.

For sedimentary cohesionless deposits, Fellenius states N_t ranges from about 30 to a high of 120. In very dense deposits such as glacial tills, N_t can be much higher, but can also approach the lower bound value of 30. In clays, Fellenius notes that the toe resistance calculated using an N_t of 3 is similar to the toe resistance calculated from a traditional analysis using undrained shear strength. Therefore, the use of a relatively low N_t coefficient in clays is recommended unless local correlations suggest higher values are appropriate.

As with any design method, the user should also confirm the appropriateness of selected coefficients in a given soil condition with local correlations between static resistance calculations and load tests results.

It should be noted that the effective stress method places no limiting values on either the shaft or toe resistance.

Table 7-9 Approximate Range of β and N_t Coefficients
(after Fellenius 2014)

Soil Type	ϕ'	β	N_t
Clay	25-30	0.15-0.35	3-30
Silt	28-34	0.25-0.50	20-40
Sand	32-40	0.30-0.90	30-150
Gravel	35-45	0.35-0.80	60-300

STEP BY STEP PROCEDURE FOR: "EFFECTIVE STRESS β -METHOD"

- STEP 1 Delineate the soil profile into layers and determine ϕ' angle for each layer.
- Construct Effective Stress Diagram using previously described procedure in Section 7.1.4.
 - Divide soil profile throughout the pile penetration depth into layers and determine the vertical effective stress, σ'_{vo} , (ksf) at the midpoint of each layer.
 - Determine the ϕ' angle for each soil layer from laboratory or in-situ test data.
 - In the absence of laboratory or in-situ data for cohesionless layers, determine the average corrected SPT N value, $(N_1)_{60}$, for each layer and estimate ϕ' angle from a select method in Section 5.2.3 of Chapter 5.

- STEP 2 Select the β coefficient for each soil layer.

- Use local experience to select β coefficient for each layer.
- In the absence of local experience, use Table 7-9 to estimate β coefficient from ϕ' angle for each layer.

- STEP 3 For each soil layer compute the unit shaft resistance, f_s (ksf) using Equation 7-19.

- STEP 4 Compute the shaft resistance in each soil layer and the nominal shaft resistance, R_s (kips), from the sum of the shaft resistance from each soil layer.

Refer to Section 7.10.7 for additional information on the behavior of open pile sections.

- STEP 5 Compute the unit toe resistance, q_p (ksf) using Equation 7-20.
- Use local experience to select N_t coefficient.
 - In the absence of local experience, estimate N_t from Table 7-9 based on ϕ' angle.
 - Calculate the vertical effective stress at the pile toe, σ'_p (ksf).

STEP 6 Compute the nominal toe resistance, R_p (kips) using Equation 7-5.

For open pile sections, refer to the discussion of pile plugging presented in Section 7.10.7.

STEP 7 Compute the nominal pile resistance, R_n from the sum of the shaft and toe resistances, $R_n = R_s + R_p$.

STEP 8 Compute the factored resistance, R_r (kips), using resistance factors provided in Section 7.1.5 and Equation 7-3.

AASHTO (2014) does not provide a recommended resistance factor for the nominal resistance determined by the β -Method by Fellenius. Therefore, the nominal resistance at the strength limit state should be determined using the resistance factor associated with the field verification method, ϕ_{dyn} , as recommended in Table 7-2.

7.2.1.3.5 Brown Method – Mixed Soil Profiles – SPT Data

The Brown Method (2001) is a simple empirical method that uses SPT N_{60} values for calculating unit shaft resistance and unit toe resistance values. The Brown Method was based on resistance correlations with 71 static load tests from Caltrans projects in a wide variety of soil types. The pile types included closed end pipe, open end pipe, H-piles, and precast concrete piles. The method considers compression and uplift loading as well as pile installation method (impact driving and partial vibratory installation).

Brown reported that the average unit shaft resistance, f_s , (ksf) is:

$$f_s = F_{vs} (A_b + B_b N_{60}) \quad \text{Eq. 7-21}$$

Where:

- F_{vs} = factor for pile driving method (1.0 for impact or 0.68 for vibratory).
- A_b = Brown's regression analysis factor based on soil type in (ksf).
- B_b = Brown's regression analysis factor based on soil type in (ksf/bpf).
- N_{60} = SPT N-Value corrected for 60% energy transfer.

Limits on the value of N_{60} were also recommended. If N_{60} is greater than 50, a value of 50 should be used and if N_{60} is less than 3, use 3. Brown recommended that the shaft resistance, R_s , be calculated by multiplying the unit shaft resistance times the pile perimeter with the "box" perimeter used for H-piles rather than the actual pile/soil contact area and for open end pipe piles only the external surface area. Regression factors A_b and B_b , as well as the pile installation factor, F_{vs} , are given in Table 7-10.

Brown (2001) recommended that for impact driven piles, the unit toe resistance, q_p (ksf) is calculated:

$$q_p = 3.55N_{60} \quad \text{Eq. 7-22}$$

For vibratory installed piles this unit toe resistance should then be multiplied by 0.56. The pile toe resistance, R_p , in kips is then calculated as follows:

$$R_p = q_p (A_p + A_{pp} F_p) \quad \text{Eq. 7-23}$$

Where:

- A_p = cross sectional area of the pile material at pile toe (ft²).
- A_{pp} = cross sectional area of soil plug (ft²) for open end pipe piles or H-piles at pile toe.
- F_p = plug mobilization factor, 0.42 for pipe piles or 0.67 for H-piles.

Brown recommended the actual steel area at the pile toe be used for A_p on H-piles and open end pipe piles.

While the simplicity of Brown's method is attractive, it is recommended that the method be used only for preliminary length estimates until a greater experience base is obtained with the method results. Caltrans continues to study and expand on Brown's work as reported by Olson and Shantz (2004). AASHTO (2014) does not provide a recommended resistance factor for the nominal resistance determined by this method. Therefore, the resistance factor for the applicable field verification method, ϕ_{dyn} , should be used if this method is used.

Table 7-10 Input Factors for Brown's Method

Loading Condition	Installation Method	Soil Type	F _{vs}	A _b (ksf)	B _b (ksf/bpf)
Compression	Impact	Clay to Sand	1.0	0.555	0.040
"	"	Gravelly Sand to Boulders	1.0	0.888	0.888
"	"	Rock	1.0	2.89	2.89
Tension	Impact	Clay to Sand	1.0	0.522	0.0376
"	"	Gravelly Sand to Boulders	1.0	0.835	0.0
"	"	Rock	1.0	2.71	0.0
"	Vibratory	Clay to Sand	0.68	0.522	0.0376
"	"	Gravelly Sand to Boulders	0.68	0.835	0.0
"	"	Rock	0.68	2.71	0.0

7.2.1.3.6 Eslami and Fellenius Method – CPT Data

In the Eslami and Fellenius method, the unit shaft resistance is correlated to the average effective cone tip resistance with a shaft correlation coefficient applied based on the soil profile. The unit shaft resistance, f_s , (ksf) is calculated from:

$$f_s = C_s q_E \quad \text{Eq. 7-24}$$

In Which:

$$q_E = q_t - U2 \quad \text{Eq. 7-25}$$

$$q_t = q_c + U2(1 - a) \quad \text{Eq. 7-26}$$

Where:

- C_s = shaft correlation coefficient from Table 7-11.
- q_E = Eslami cone stress.
- $U2$ = pore water pressure measured at cone shoulder.
- q_c = measured cone tip stress.
- a = ratio between shoulder area (cone base) unaffected by the pore water pressure to total area.

Table 7-11 C_s Values for Eslami and Fellenius Method (after Fellenius 2014)

Soil Type	C_s (%)
Soft sensitive soil	8.0
Clay	5.0
Silty clay, stiff clay and silt	2.5
Sandy silt and silt	1.5
Fine sand or silty sand	1.0
Sand	0.4

The unit toe resistance is computed using geometric averaging of the cone tip resistance over the influence zone at the pile toe, after the cone tip resistances have been corrected for pore pressure on the cone shoulder and effective stress. The zone of influence at the pile toe is based on the pile diameter, b , and ranges from $4b$ below the pile toe to $8b$ above the pile toe when the pile is installed through a weak zone overlying a dense zone. When a pile is driven through a dense soil into a weak soil, the zone of influence is from $4b$ below the pile toe to $2b$ above the pile toe. The unit toe resistance is calculated from:

$$q_p = C_p q_{Eg} \quad \text{Eq. 7-27}$$

Where:

C_p = toe correction coefficient equal to 1.0 in most cases.

q_{Eg} = geometric average of the cone tip resistance in ksf over the influence zone after correction for pore pressure on shoulder and adjustment to effective stress.

The toe correction coefficient is a function of the pile size since larger piles require greater movement to mobilize the pile toe resistance. For pile diameters greater than 16 inches, the toe correction coefficient should be calculated as follows:

$$C_p = \frac{12}{b} \quad \text{Eq. 7-28}$$

Where:

b = pile width or diameter (inches).

STEP BY STEP PROCEDURE FOR: “ESLAMI AND FELLENIUS METHOD”

- STEP 1 Obtain CPT test results with outputs of cone stress and pore pressure measurements.
- STEP 2 For each depth increment, compute the unit shaft resistance, f_s (ksf) using Equation 7-24 and coefficients provided in Table 7-11.
- STEP 3 Compute the shaft resistance in each soil layer and the nominal shaft resistance, R_s (kips), from the sum of the shaft resistance from each layer using Equation 7-4.
- STEP 4 Compute the unit toe resistance, q_p (ksf), using Equation 7-27.
- STEP 5 Compute the nominal toe resistance, R_p (kips) using Equation 7-5.
- STEP 6 Compute the nominal pile resistance, R_n from the sum of the shaft and toe resistances, $R_n = R_s + R_p$.
- STEP 7 Compute the factored resistance, R_r (kips), using select resistance factors provided in Section 7.1.5 and Equation 7-3.

AASHTO (2014) does not provide a recommended resistance factor for this method. Therefore, the nominal resistance in the strength limit state should be determined using the resistance factor associated with the field verification method, ϕ_{dyn} , as recommended in Table 7-2.

7.2.1.3.7 Nottingham and Schmertmann Method – CPT Data

One empirical procedure used in U.S. practice was derived from work originally published by Nottingham and Schmertmann (1975), and summarized in publication FHWA-TS-78-209, "Guidelines for Cone Penetration Test, Performance and Design" by Schmertmann (1978).

The nominal shaft resistance, R_s , in cohesionless soils may be derived from unit sleeve friction of the CPT using the following expression:

$$R_s = K_s \left[\frac{1}{2} (f_s A_s)_{0 \text{ to } 8b} + (f_s A_s)_{8b \text{ to } D} \right] \quad \text{Eq. 7-29}$$

Where:

- K_s = ratio of unit pile shaft resistance to unit cone sleeve friction from Figure 7-20 as a function of the full penetration depth, D .
- f_s = average unit sleeve friction over the depth interval indicated by subscript.
- A_s = pile shaft surface area over f_s depth interval.
- b = pile width or diameter.
- D = embedded pile length.
- $0 \text{ to } 8b$ = range of depths for segment from ground surface to a depth of $8b$.
- $8b \text{ to } D$ = range of depths for segment from a depth equal to $8b$ to the pile toe.

The transfer function, K_s , relating pile shaft resistance to CPT sleeve friction, varies as a function of total pile penetration (depth of embedment/pile diameter), pile material type, and type of cone penetrometer used. No limit was imposed on sleeve friction values in the procedure originally proposed by Nottingham and Schmertmann (1975).

If cone sleeve friction data is not available, R_s can be determined from the cone tip resistance as follows:

$$R_s = C_f \sum q_c A_s \quad \text{Eq. 7-30}$$

Where:

- C_f = correction obtained from Table 7-12.
- q_c = average cone tip resistance along the pile length.
- A_s = pile shaft surface area (length).

For shaft resistance in cohesive soils, the nominal shaft resistance, R_s , is obtained from the sleeve friction values using the following expression:

$$R_s = \alpha' f_s A_s \quad \text{Eq. 7-31}$$

Where:

- α' = ratio of pile shaft resistance to cone sleeve friction, patterned after Tomlinson's α -method.
- f_s = unit sleeve friction.
- A_s = pile shaft surface area (length).

The value of α' varies as a function of sleeve friction, f_s , as shown in Figure 7-20. It is expected that this method of calculating pile shaft resistance is less appropriate in sensitive soils as the friction sleeve of the cone encounters severely disturbed soils behind the cone tip.

The estimation of pile toe resistance is described in Figure 7-21. In essence, an elaborate averaging scheme is used to weigh the cone tip resistance values, from 8 pile diameters above the pile toe, to as much as 3.75 pile diameters below the pile toe, favoring the lower cone tip resistance, q_c , values within the depth range. The authors make reference to a "limit" value of q_c between 105 to 315 ksf, that should be applied to the nominal unit pile toe resistance, q_p , unless local experience warrants use of higher values. In the case of mechanical cone soundings in cohesive soils, the q_p value is reduced by 40 percent to account for toe resistance effects on the base of the friction sleeve. As discussed in Section 7.10.7, careful consideration of soil plugging phenomena is needed in choosing the cross-sectional area over which q_p is applied for low displacement open ended pipe and H-piles.

Table 7-12 CPT C_f VALUES

Type of Piles	C_f
Precast Concrete	0.012
Timber	0.018
Steel Displacement	0.012
Open End Steel Pipe	0.008

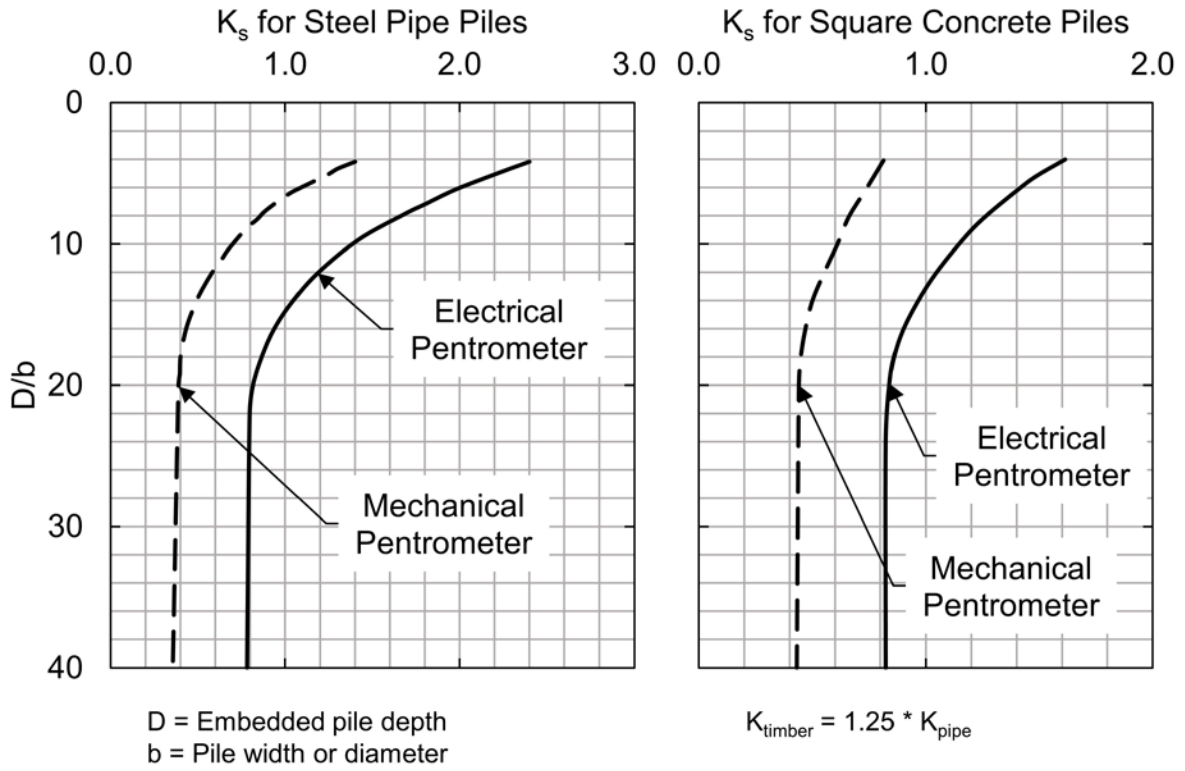


Figure 7-19 Penetrometer design curves for pile shaft friction in sand (after FHWA Implementation Package, FHWA-TS-78-209).

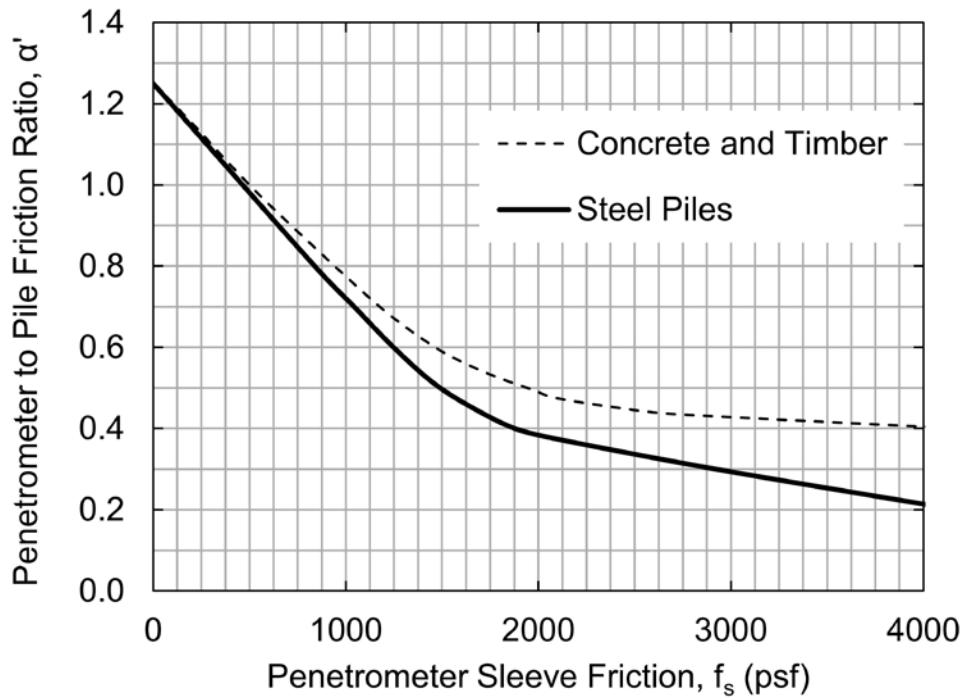


Figure 7-20 Design curve for pile shaft friction in clay (after Schmertmann 1978).

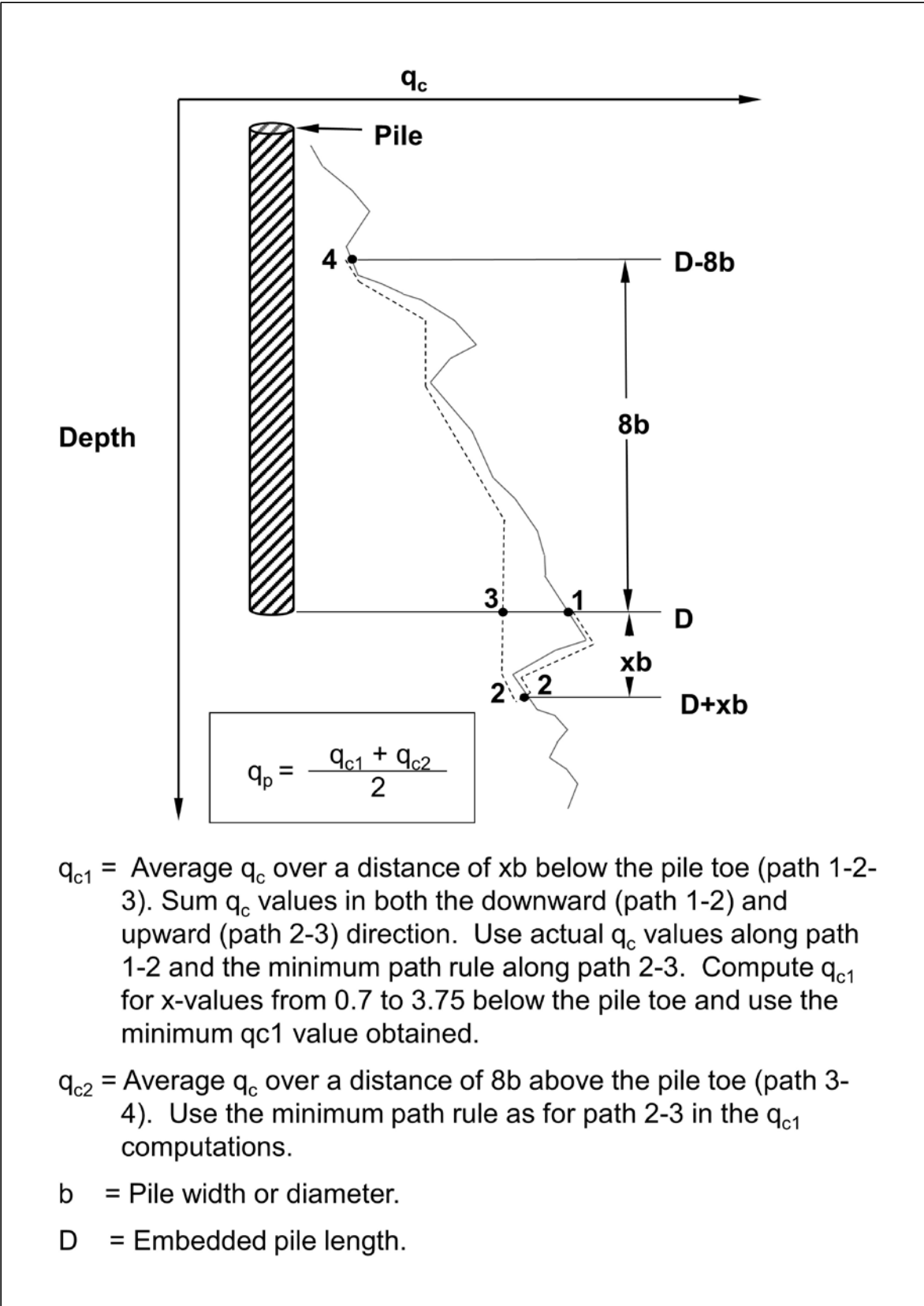


Figure 7-21 Illustration of Nottingham and Schmertmann Procedure for estimating pile toe resistance (FHWA-TS-78-209).

STEP BY STEP PROCEDURE FOR: "NOTTINGHAM AND SCHMERTMANN METHOD"

- STEP 1 Delineate the soil profile into layers using the cone tip resistance, q_c , and sleeve friction, f_s , values.
- STEP 2 Compute the shaft resistance for each soil layer, R_s (kips).
- For piles in cohesionless soils, compute shaft resistance, R_s , using the average sleeve friction value for the layer, f_s , and the K value. Note that K should be determined using the full pile penetration depth to diameter ratio from Figure 7-19, and not the penetration depth for the layer. Conversely, the depth d corresponds to the pile toe depth, or the depth to the bottom of the layer, whichever is less. For H-piles in cohesionless soils, the pile-soil surface area A_s , should be the "box" area.

For cohesionless layers below a depth of $8b$, Equation 7-29 for shaft resistance in a layer reduces to:

$$R_s = K_s f_s A_s \quad \text{Eq. 7-32}$$

Where:

- K_s = ratio of unit pile shaft resistance to unit cone sleeve friction from Figure 7-19 as a function of the full penetration depth, D .
- f_s = average unit sleeve friction over the depth interval indicated by subscript.
- A_s = pile shaft surface area over f_s depth interval.

For piles in cohesionless soils without sleeve friction data, compute the shaft resistance from Equation 7-30.

- For piles in cohesive soils, compute the shaft resistance using the average sleeve friction value for the layer and Equation 7-31.

STEP 3 Compute the shaft resistance in each soil layer and the nominal shaft resistance, R_s (kips), from the sum of the shaft resistance from each layer.

STEP 4 Compute the unit pile toe resistance, q_p (ksf) using Equation 7-33.

$$q_p = \frac{q_{c1} + q_{c2}}{2} \quad \text{Eq. 7-33}$$

Where:

q_{c1} = average q_c over a distance of xb below the pile toe (path 1-2-3 from Figure 7-21). Sum q_c values in both the downward (path 1-2) and upward (path 2-3) direction. Use actual q_c values along path 1-2 and the minimum path rule along path 2-3. Compute q_{c1} for x -values from 0.7 to 3.75 below the pile toe and use the minimum q_{c1} value obtained.

q_{c2} = average q_c over a distance of $8b$ above the pile toe (path 3-4 from Figure 7-21). Use the minimum path rule as for path 2-3 in the q_{c1} computations.

b = pile width or diameter.

D = embedded pile length.

STEP 5 Compute the nominal toe resistance, R_p (kips).

For steel H and unfilled open ended pipe piles, use only the steel cross section area at the pile toe unless there is reasonable assurance and previous experience that a soil plug would form. For a plugged condition use the "box" area of the H-pile and the full cross section area for pipe pile. Additional information on the plugging of open pile sections is presented in Section 7.10.7.

STEP 6 Compute the nominal resistance, R_n from the sum of the shaft and toe resistances, $R_n = R_s + R_p$.

STEP 7 Compute the factored resistance, R_r (kips), using select resistance factors provided in Section 7.1.5 and Equation 7-3.

AASHTO (2014) provides a recommended resistance factor for this method in Table 7-1 for the nominal resistance determined by static analysis. The nominal resistance in the strength limit state could also be determined using the resistance factor associated with the field verification method, ϕ_{dyn} , as recommended in Table 7-2.

7.2.1.4 Nominal Resistance of Single Piles to Rock

Pile foundations on rock are normally designed to carry large loads. For pile foundations driven to rock, which include steel H-piles, pipe piles or precast concrete piles, the exact area in contact with the rock, the depth of penetration into rock, as well as the quality of rock in the immediate pile contact area are largely unknown. Pile installation can also alter the characteristics of the rock formation, further complicating design procedures.

The distinction between soft rock and hard rock is not well defined. The AASHTO definition of soft and hard rock for driven pile foundation design is limited. In general, soft rock is defined as rock that can be penetrated by pile driving and hard rock is defined as rock that cannot be penetrated. Hence, piles are driven into soft rock and driven to hard rock. In many intact rock classification systems, the transition between soft rock and hard rock occurs between an unconfined compression strength of 200 and 1000 ksf. Kulhawy (1991) proposed 400 ksf as the an unconfined compression strength denoting the transition between weak and moderate rock. AASHTO notes that a definition of hard rock based on measureable rock characteristics has not been widely accepted.

Likins and Goble (1978) reported on the results of an Ohio DOT and FHWA sponsored research study on HP 10x42 H-piles driven to shallow bedrock with multiple, similarly sized pile hammers. Static and dynamic load tests were conducted at the two sites, one with hard rock and one with soft rock. The H-piles were driven to a penetration resistance of 20 blows per inch on rock at both sites. At the hard rock site, hard limestone with an unconfined compression strength of up to 1094 ksf was encountered around 22 feet. At the soft rock site, weathered shale with unconfined compressive strength of 172 to 316 ksf was encountered around 15 feet. The A-36 steel H-piles at the hard limestone site were statically load tested to as high as $0.93F_y$ without reaching the Davisson load test failure criteria which is described in Chapter 9. At the weathered shale site, significantly lower nominal resistances were achieved with failure occurring between 0.28 to $0.71F_y$. Relaxation occurred on the H-piles driven at the weathered shale site and higher nominal resistances were observed on piles that penetrated deeper into the shale. This study, even though it was performed with smaller hammers and piles than commonly used today, demonstrates that geotechnical aspects control soft rock design and structural aspects control hard rock design.

Tomlinson and Woodward (2015) state that piles driven to rock can create very high concentrated loads on the rock beneath the pile toe. The ability of the rock to

support the concentrated load depends in part on the compressive strength of the rock, the frequency of fissures and joints in the rock mass, and whether the fissures and joints are tightly closed or are open and filled with weathered material. They further note that very high loads can be supported if the rock is strong and has closed joints or joints on a shallow angle to horizontal. Conversely, steeply inclined and open joints may provide little resistance as the rock beneath the pile toe slides until the joints are closed or the rock mass becomes locked together. The driving of piles through weak or broken rock to hard rock can shatter weak rock such that shaft resistance is significantly reduced or eliminated. The resulting concentrated load may be acceptable for strong intact rock but it may be excessive for a strong but closely jointed rock mass.

Published results as well as empirical values for nominal shaft resistances are presented in Table 7-13. These results may be used for preliminary estimating purposes or as a check of values obtained from field tests. However, they are not intended to be used as final design values without the user determining the applicability of the underlying method or the suitability of a reported nominal resistance value to a given site or geologic formation.

Table 7-13 Published Nominal Shaft Resistance Values in Weak Rock Materials

Rock Description	Pile Type	Nominal Unit Shaft Resistance (ksf)	Source
Moderately strong, slightly weathered, Slaty Mudstone	H-pile	0.6	1.
Moderately strong, slightly weathered, Slaty Mudstone	H-pile	3.3	1.
Faintly to moderately weathered , moderately strong to strong, Mudstone	Pipe Pile	2.6	2.
Very weak, closely fissured argillaceous Siltstone (Mercia Mudstone)	Precast Concrete	2.7	3.
Very weak, coral detrital Limestone (carbonate sandstone/siltstone)	Pipe pile	0.9	2.
Limestone	H-pile	24.0	4.
Weak calcareous Sandstone	Pipe Pile	0.9	2.
Sandstone	H-pile	20.0	4.
Shale	H-pile	12.0	4.

- Information sources:
- 1) George et al. (1976)
 - 2) Tomlinson and Woodward (2015)
 - 3) Leach and Mallard (1980)
 - 4) Illinois DOT Geotechnical Pile Design Guide, AGMU 10.2 (2011)

Published results and recommended empirical values for nominal toe resistances are presented in Table 7-14. Once again these values may be used for preliminary estimating purposes or as a check of values obtained from field tests. However, they are not intended to be used as final design values without the user determining the applicability of the underlying method or the suitability of a reported nominal resistance value to a given site or geologic formation.

Table 7-14 Published Nominal Toe Resistance Values in Weak Rock Materials

Rock Description	Pile Type	Nominal Unit Toe Resistance (ksf)	Source
Weak carbonate Siltstone/Sandstone (coral detrital limestone)	N.A.	106.7	1.
Limestone	H-pile	240.0	2.
Weak calcareous Sandstone	Pipe Pile	62.6	1.
Sandstone	H-pile	200.0	2.
Shale	H-pile	120.0	2.

Information sources: 1) Tomlinson and Woodward (2015)
 2) Illinois DOT Geotechnical Pile Design Guide, AGMU 10.2 (2011)

Based on the above discussion and information, the determination of nominal shaft and toe resistances of piles driven into or on rock is best made on the basis of static or dynamic load tests in conjunction with pile driving observations and local experience. In general, the design of small diameter piles supported on fair to excellent quality rock will be controlled by their nominal structural resistance as described in Chapter 8. A pile on hard intact rock will fail structurally before hard intact rock failure. Piles supported in soft, weakly laminated or weathered rock should be designed based on the results of static or dynamic load tests.

7.2.1.4.1 Piles Driven into Soft and Weak Rock

Tomlinson and Woodward (2015) note that the shaft resistance on piles driven into weak weathered rocks cannot always be calculated from the results of laboratory tests on rock cores. Factors such as degradation of the weak rock, reduction in shaft resistance due to shattering of the rock structure from driving adjacent piles, and formation of an enlarged hole around the pile hamper analytical methods.

The design of axial loaded piles in soft rock should be performed using the same procedures and methods used for piles in soil as presented in Section 7.2.2. Static and dynamic tests are recommended for design verification until local correlations

and design methods are available. The empirical values provided above for H-piles in shale, sandstone, and limestone were developed by Illinois DOT for their practice and have been found to yield reasonable estimates of pile length and nominal resistance in the regional geology.

The nominal toe resistance of piles in soft and hard rocks can also be computed according to Equation 7-34 in Section 7.2.1.4.2 below. For this calculation, the rock friction angle, undrained shear resistance, and effective density are needed from laboratory tests.

It is recommended that unit resistance values calculated from this equation be compared to values obtained from static or dynamic tests and that these comparisons be compiled in a local or regional database. This will assist and improve foundation design procedures in soft and weak rocks. Piles driven into soft rock may not require pile toe protection (i.e. driving shoe).

7.2.1.4.2 Piles Driven to Hard Rock

For piles driven to hard rock, the nominal resistance is generally controlled by the structural limit state. In hard rock designs, the nominal structural resistance will generally be less than the nominal geotechnical resistance of hard rock.

Where laboratory tests can be made on undisturbed samples of weak or hard rock and the undrained shear strength, s_u , and the rock friction angle, ϕ , can be obtained, the nominal unit toe resistance, q_p , in ksf can be calculated using Equation 7-34.

$$q_p = P_s s_u N_c + \gamma D N_q + P_t \gamma \left(\frac{b N_\gamma}{2} \right) \quad \text{Eq. 7-34}$$

Where:

- s_u = undrained shear resistance of the rock (ksf).
 - γ = effective density of the rock mass (kcf).
 - D = pile penetration below the rock surface (ft).
 - b = pile width or diameter (ft).
 - P_s = pile toe shape factor of 1.25 for square pile or 1.2 for a circular pile.
 - P_t = pile base factor of 0.8 for a square pile or 0.7 for a circular pile.
- N_c , N_q , and N_γ are bearing capacity factors from Figure 7-22.

Equation 7-34 represents wedge failure below a foundation modified with shape factors and it should not be confused with Terzaghi's equation for a spread footing

foundation. Tomlinson and Woodward (2015) added the recommended correction factors P_s and P_t for driven pile shapes.

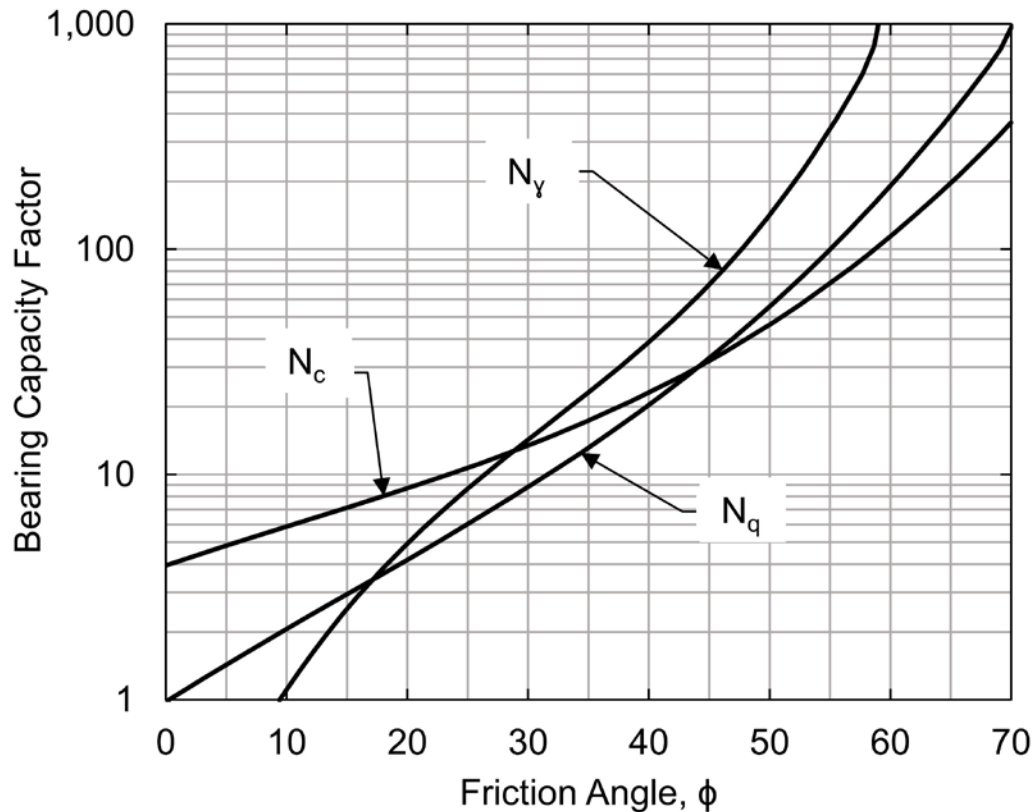


Figure 7-22 Bearing capacity factors for foundations on rock (modified from Pells and Turner 1980).

Data from Kulhawy and Goodman (1980; 1987) showed that the unit toe resistance, q_p , can also be estimated from the Rock Quality Designation (RQD) value of the intact rock mass and the unconfined compression strength of the rock, q_u . RQD was described previously in Chapter 4. For RQD values of 0 to 70%, the nominal unit toe resistance can be estimated as $0.33q_u$. For RQD values of 70 to 100%, the nominal unit toe resistance can be linearly interpolated from $0.33q_u$ at an RQD value of 70% to $0.80q_u$ at an RQD value of 100%. In hard rock cases, pile toe protection should be considered in the design.

A static analysis resistance factor, ϕ_{stat} , for any of the above nominal resistance calculation methods for rock is not available. Therefore, the calculated nominal resistance should be verified during construction using a nominal resistance field verification method and its associated resistance factor, ϕ_{dyn} .

7.2.1.5 Software for Single Pile Nominal Resistance Computations

The FHWA previously sponsored the development and use of the DRIVEN computer program for static analysis computations. This program used the FHWA recommended Nordlund Method and α -method as presented in this manual for calculation of the nominal resistance. The public domain version of the DRIVEN program is no longer available from the FHWA. However, a commercial version of the program, DrivenPiles, was released in 2015. Numerous other static analysis programs are also commercially available. Table 7-15 summarizes the static analysis methods incorporated in commercially available programs. It should be emphasized that the FHWA does not endorse any particular analysis program and the programs are listed alphabetically in Table 7-15.

Table 7-15 Summary of Computer Analysis Software for Axial Single Pile Analysis

Computer Program	Static Analysis Methods in Program	Method Presented in GEC-12 (2016)	Method Presented in AASHTO 7 th Edition (2014)
AllPile	Navfac DM-7	No	No
A-Pile	API-RP2A	Yes	No
A-Pile	US Army COE	No	No
A-Pile	FHWA (alpha / Nordlund)	Yes	Yes
A-Pile	Lambda Method	No	Yes
A-Pile	NGI (CPT)	No	No
A-Pile	ICP (CPT)	No	No
DrivenPiles	Alpha Method	Yes	Yes
DrivenPiles	Nordlund Method	Yes	Yes
FB-Deep	FDOT SPT Method	No	No
FB-Deep	Schmertmann (CPT)	Yes	Yes
FB-Deep	UF (CPT)	No	No
FB-Deep	LCPC (CPT)	No	No
Unipile	Alpha Method	Yes	Yes
Unipile	Beta Method	Yes	Yes, but differs
Unipile	Elsami and Fellenius (CPT)	Yes	No
Unipile	Schmertmann (CPT)	Yes	Yes
Unipile	LCPC (CPT)	No	No
Unipile	Meyerhof (SPT)	No	Yes

An example soil profile is presented in Figure 7-23 along with the necessary soil input parameters for the selected static analysis software programs. Figure 7-24 presents DRIVEN results of nominal resistance, shaft resistance, and toe resistance versus depth. For comparison purposes, results for the same soil profile are presented in Figures 7-25 and 7-26 for the APILE using the Nordlund and alpha Methods and UNIPILE using the Beta Method, respectively.

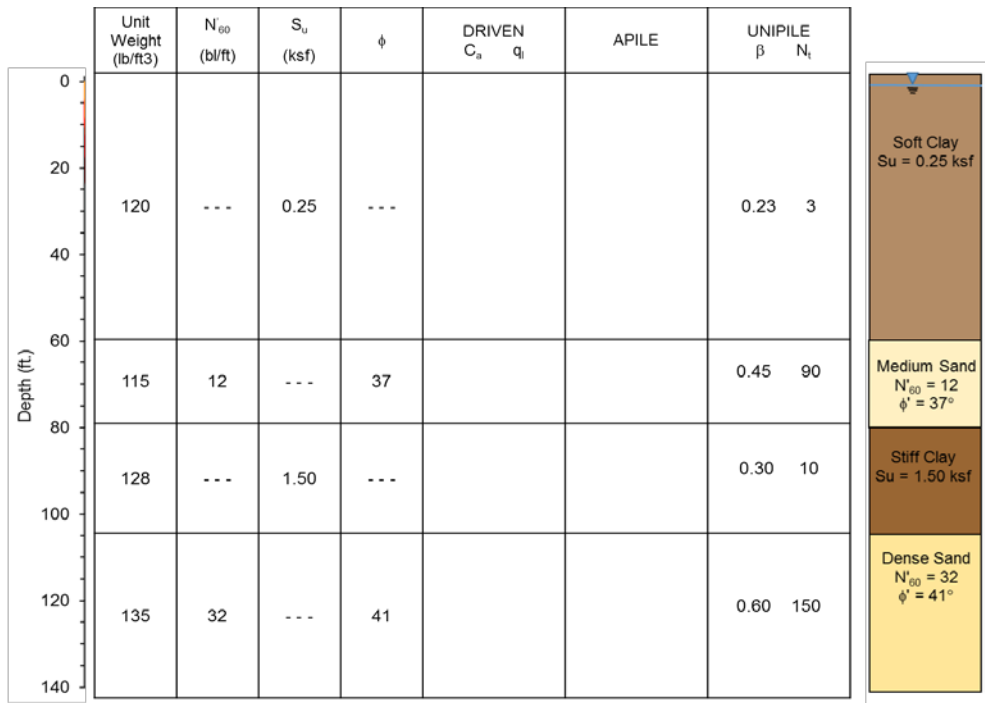


Figure 7-23 Soil profile for computer software comparison.

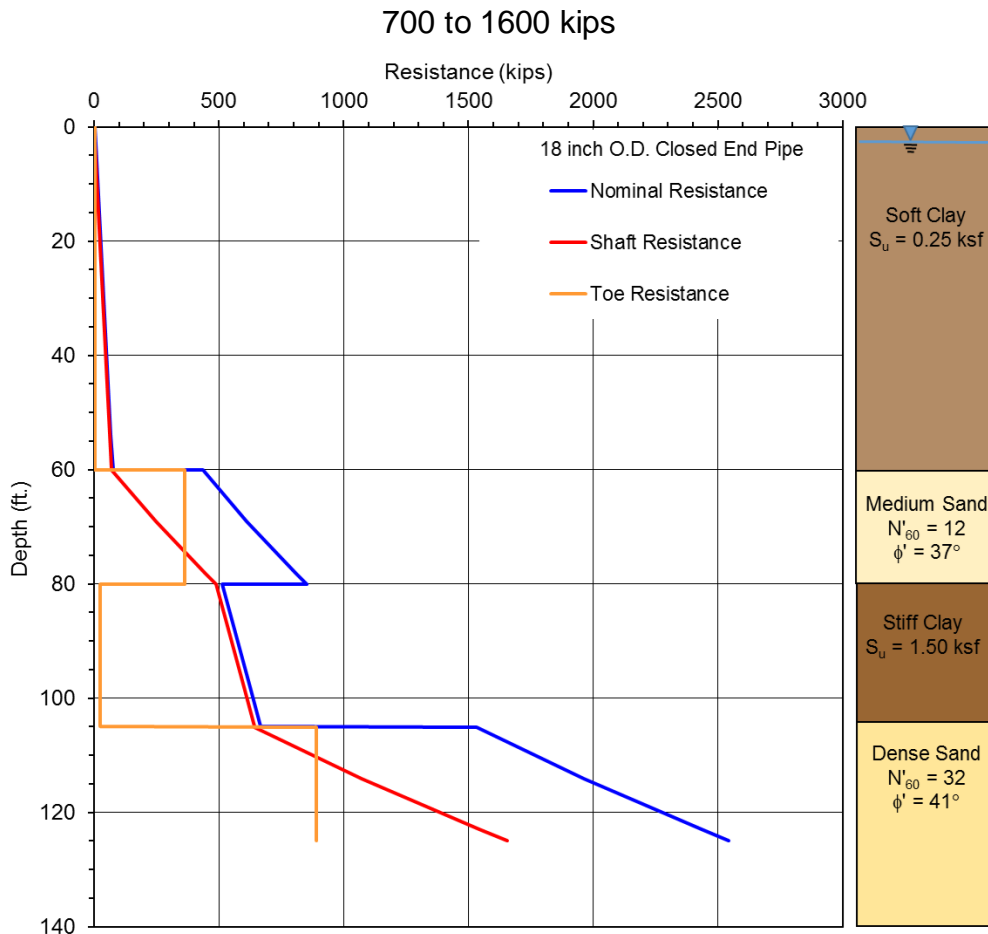


Figure 7-24 Nominal resistance from DRIVEN program using FHWA method.

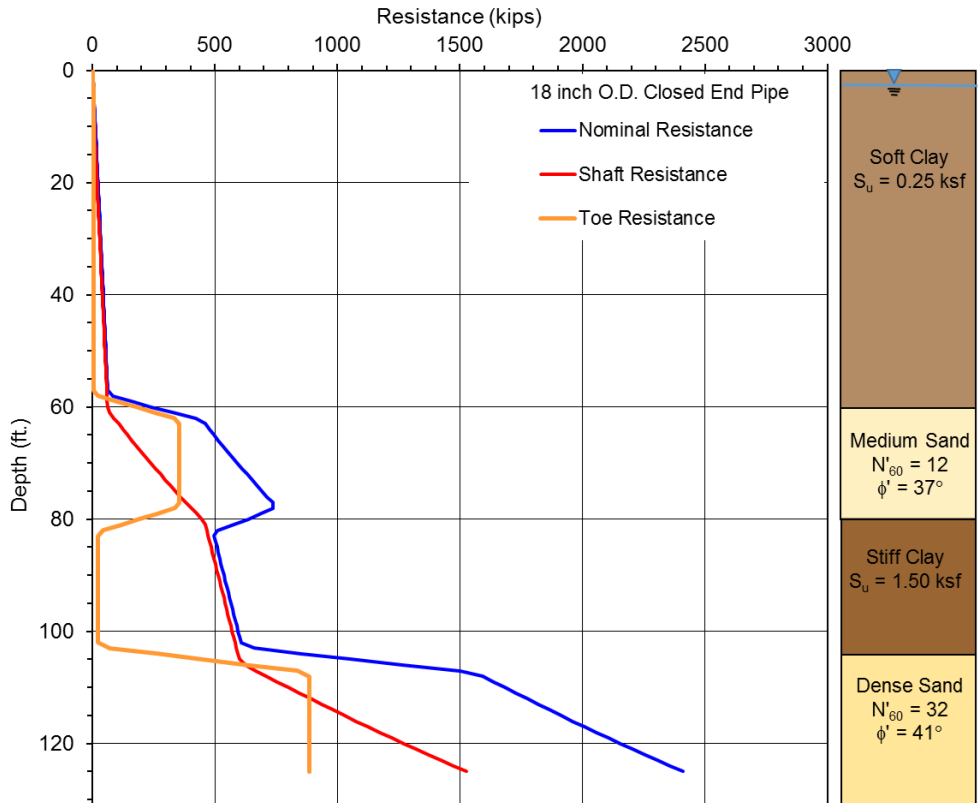


Figure 7-25 Nominal resistance from APILE program using FHWA Method.

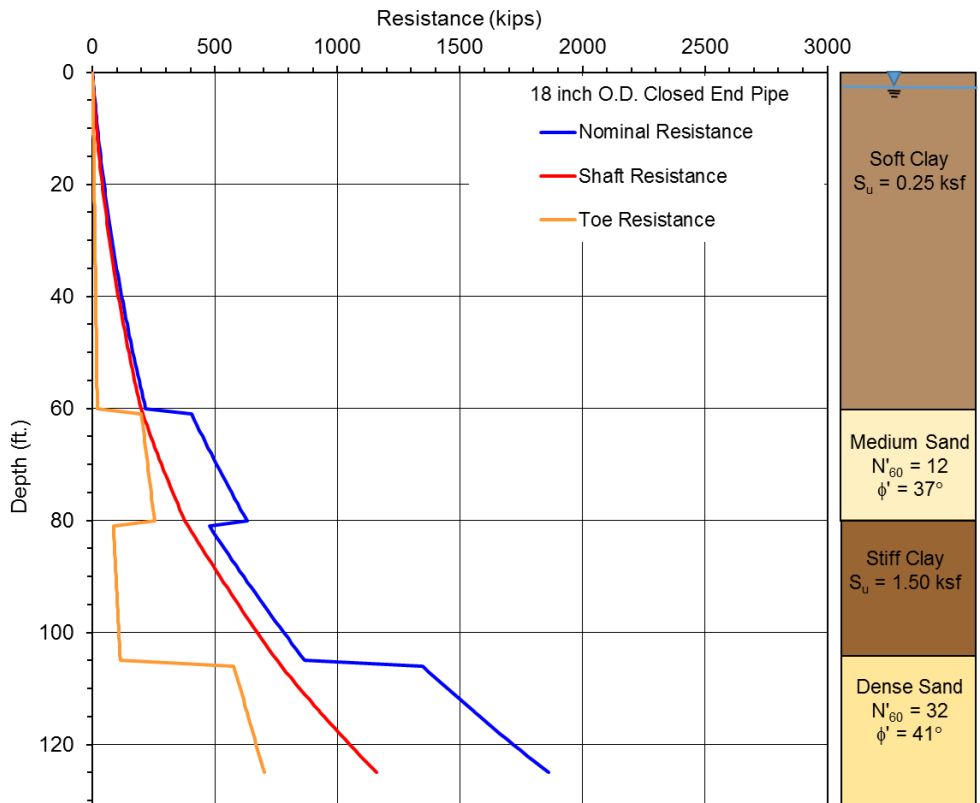


Figure 7-26 Nominal resistance from UNIPILE program using Beta Method.

Of particular note is the difference between the DRIVEN results and the APILE FHWA method results. One could reasonably expect both programs to yield the same results. However, subtle differences in software coding results in about a 10% variation in the toe resistance and nominal resistance at the final 125 foot penetration depth. The programs also have differences in the toe resistance and nominal resistance at the transition depths between soil layers. The APILE program uses an averaging of the toe resistance around layer transitions whereas the DRIVEN program does not. The results from the UNIPILE program which calculates the resistance using effective stresses in all layers yields a lower resistance solution.

Figure 7-27 presents nominal resistance results generated by the APILE - FHWA method for three different pile types in the same soil profile. The pile types include an HP 18 x 204 H-pile, a 18 inch O.D. closed end pipe pile, an a 24 inch square prestressed concrete pile. Note the displaced volume of a 24 inch concrete pile exceeds the 2.0 pcf volume limit in Figure 7-9.

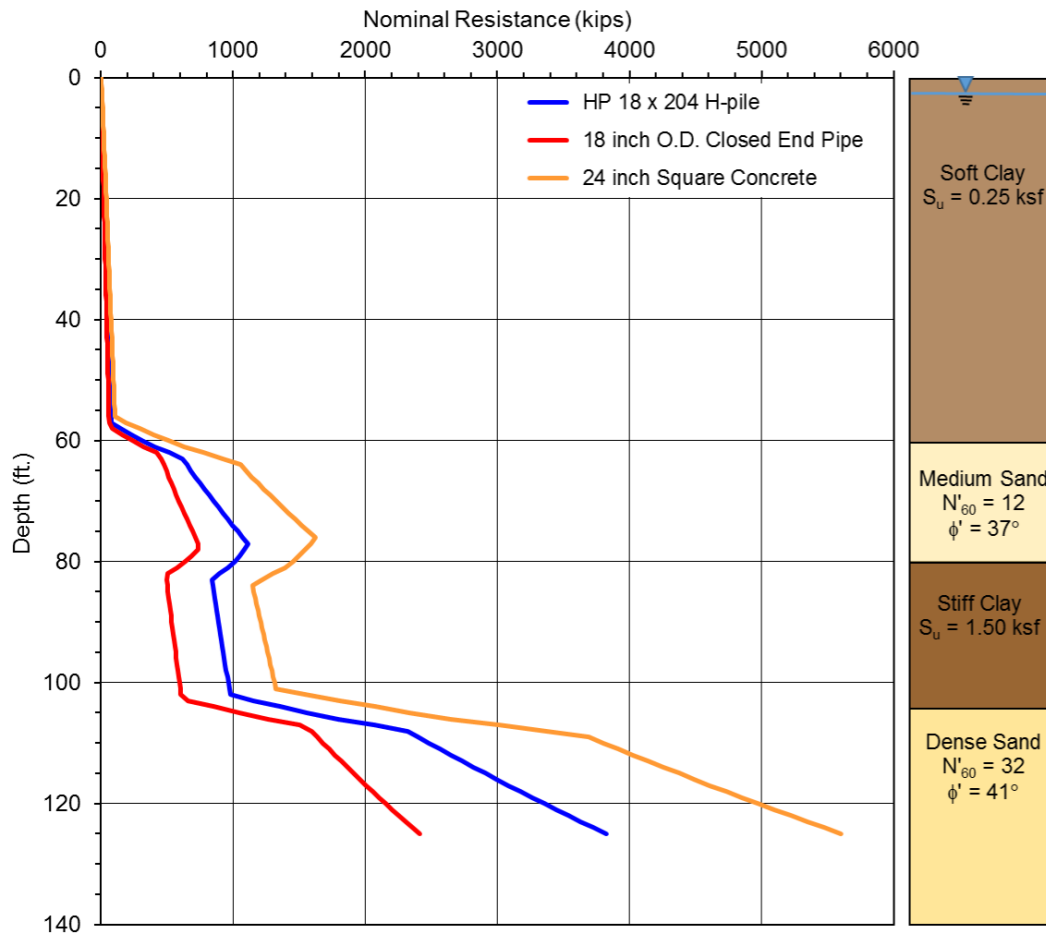


Figure 7-27 Nominal resistance versus depth for three pile types calculated by the APILE program with the FHWA Method.

Both of these examples emphasize the importance of the program user to fully understand the methodology behind a given program, its accuracy, and its limitations in a given application.

In Figure 7-28, a design chart for an 18 inch diameter closed-end pipe pile is presented. The nominal resistance results versus depth were calculated using the APILE - FHWA method. In the same figure, the factored resistance versus depth is presented for different field verification methods. For a factored resistance of 1000 kips in the soil conditions depicted, a relatively small difference exists between the estimated pile penetration depth of 106 feet based on a resistance factor of 0.80 (static load test and dynamic tests on 2% of the production piles) and the estimated pile penetration depth of 108 feet based on a resistance factor of 0.65 (dynamic tests on 2% of the production piles). Hence, a static load test may not be justifiable based on cost in this situation. Conversely, a significant difference exists between the estimated pile penetration depth of 108 feet based on a resistance factor of 0.65 (dynamic tests on 2% of the production piles) and the estimated pile penetration depth of 117 feet based on a resistance factor of 0.50 (wave equation analysis) or 127 feet based on a resistance factor of 0.40 (Modified Gates formula). An evaluation of the nominal and factored resistances versus depth considering the cost of the pile length as well as the field verification method allows the designer to determine the most appropriate method of field verification for the design.

The design chart in Figure 7-28 allows an evaluation of the nominal and factored resistances versus depth considering the cost of the pile length as well as the field verification method. This type of analysis allows the designer to determine the most appropriate method of field verification for the design.

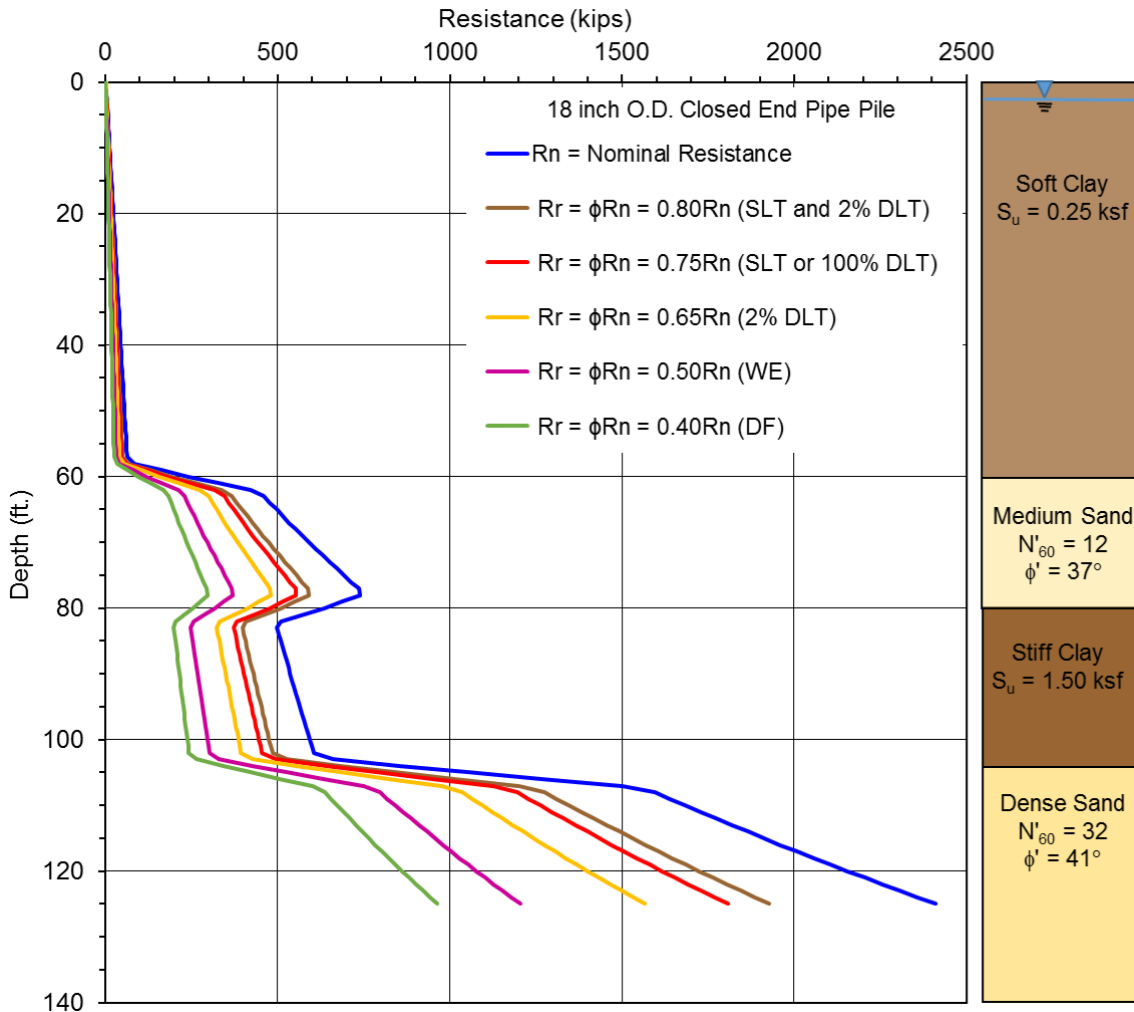


Figure 7-28 Design chart of nominal resistance, R_n , and factored resistance, R_r , versus depth for one pile type with different field control methods.

7.2.2 Resistance of Pile Groups in Axial Compression

The previous sections dealt with design procedures for single piles. However piles for almost all highway structures are installed in groups, due to the heavy foundation loads. The following sections of this chapter will address foundation design procedures for evaluating the nominal resistance in axial compression of pile groups. The nominal resistance in axial compression and settlement of pile groups are interrelated; settlement will be further discussed in Section 7.3.2 of this chapter. Pile group design computations are primarily performed using computer programs designed for this purpose such as FB-Pier or Group 6.0 rather than the simple hand calculations presented in this manual.

The efficiency of a pile group in supporting the foundation load is defined as the ratio of the nominal resistance of the group to the sum of the nominal resistance of the individual piles comprising the group. This may be expressed in equation form as:

$$\eta_g = \frac{R_{ng}}{nR_n} \quad \text{Eq. 7-35}$$

Where:

- η_g = pile group efficiency.
- R_{ng} = nominal resistance of pile group.
- n = number of piles in pile group.
- R_n = nominal resistance of each individual pile in pile group.

If piles are driven into relatively weak cohesive soil or in dense cohesionless material underlain by weaker soil, then the nominal resistance in axial compression of a pile group may be less than that of the sum of the nominal resistance in axial compression of the individual piles. In this case, the pile group has a group efficiency of less than 1. In cohesionless soils, the nominal resistance in axial compression of a pile group is generally greater than the sum of the nominal resistance in axial compression of the individual piles comprising the group. In this case, the pile group has group efficiency greater than 1.

Guidance on the group efficiency for piles driven to or into rock is not contained in AASHTO. Provided the pile group is driven to or into rock with equally strong material beneath, the pile group efficiency should be 1 or greater. Group efficiency of groups driven into highly weathered, karst, or other variable conditions should be further evaluated by the designer based on local conditions.

The soil medium supporting a pile group is also subject to overlapping stress zones from individual piles in the group. The overlapping effect of stress zones for a pile group supported by shaft resistance is illustrated in Figure 7-29.

Piles are typically driven into mixed soil and rock profiles. For pile group analysis, the stratum that provides the majority of the nominal geotechnical resistance may be considered the controlling stratum.

7.2.2.1 Pile Groups in Cohesionless Soils

In cohesionless soils, the nominal group resistance of driven piles with a center to center spacing of less than 3 pile diameters is greater than the sum of the nominal resistance of the individual piles. The greater group resistance is due to the overlap of individual soil compaction zones around each pile which increases the shaft resistance due to soil densification. Piles in groups at center to center spacings greater than three times the average pile diameter generally act as individual piles.

Design recommendations for estimating group resistance for driven piles in cohesionless soil are as follows:

1. The nominal group resistance for driven piles in cohesionless soils not underlain by a weak deposit may be taken as the sum of the individual nominal pile resistances, provided jetting or predrilling was not used in the pile installation process. Jetting or predrilling can result in group efficiencies less than 1. Therefore, jetting or predrilling should be avoided whenever possible and controlled by detailed specifications when necessary.
2. If a pile group founded in a firm bearing stratum of limited thickness is underlain by a weak deposit, then the nominal group resistance is the smaller value of either the sum of the nominal resistances of the individual piles, or the group resistance against block failure of an equivalent pier, consisting of the pile group and enclosed soil mass punching through the firm stratum into the underlying weak soil. From a practical standpoint, block failure in cohesionless soils can only occur when the center to center pile spacing is less than 2 pile diameters, which is less than the minimum center to center spacing of 2.5 diameters allowed by AASHTO (2014). The method shown for cohesive soils in the Section 7.2.2.3 may be used to evaluate the possibility of a block failure.
3. Piles in groups should not be installed at center to center spacing less than 3 times the average pile diameter unless dictated otherwise by pile size, site constraints, pile cap requirements, and construction costs. The minimum center to center spacing of 3 diameters is recommended to optimize nominal group resistance and to minimize pile installation problems associated with a center to center pile spacing of 2.5 diameters.

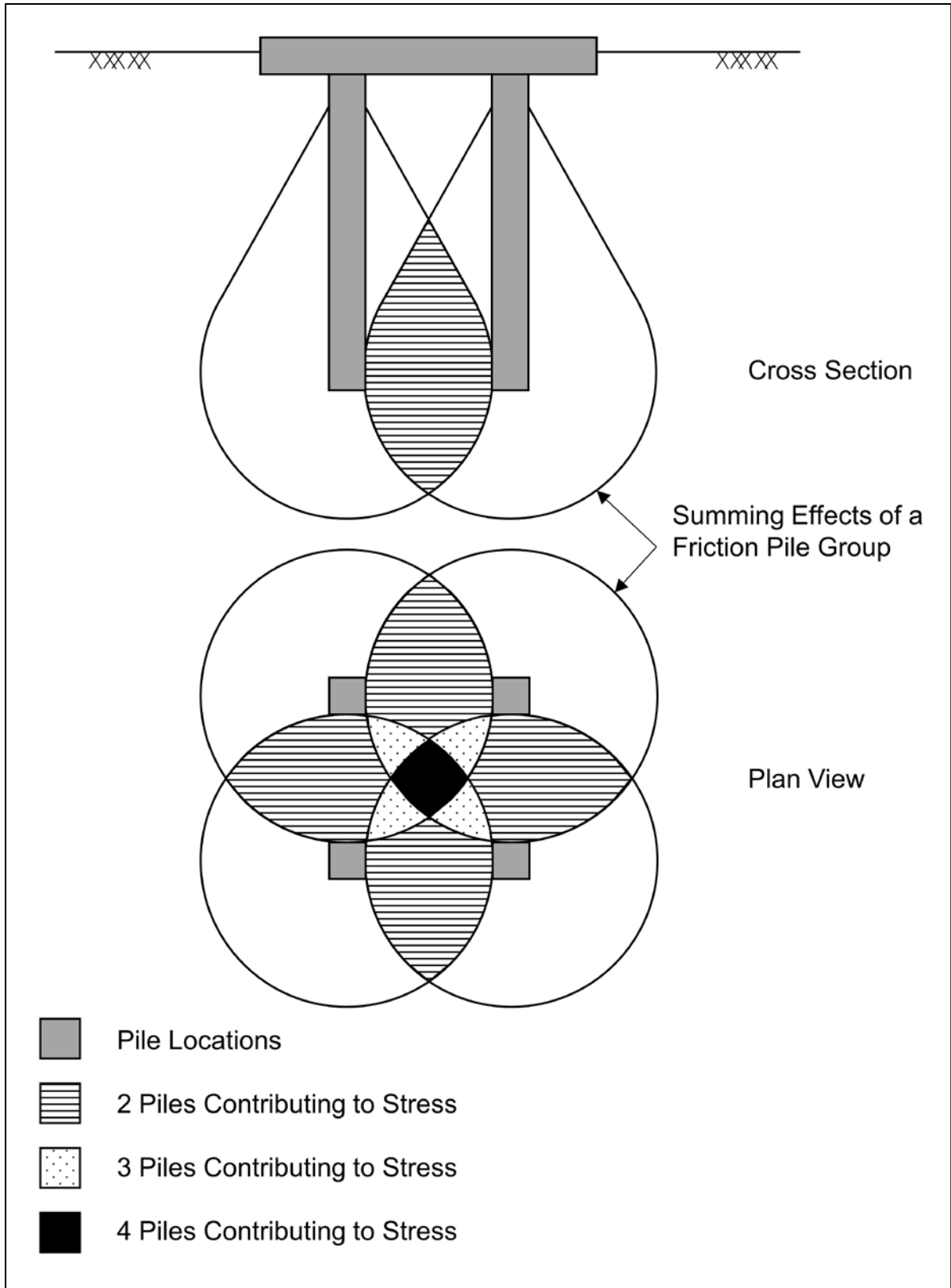


Figure 7-29 Overlap of stress zones for friction pile group (after Bowles 1988).

7.2.2.2 Pile Groups in Cohesive Soils

The nominal group resistance in cohesive soil is usually governed by the sum of the nominal resistance of the individual piles, with some reduction due to overlapping zones of shear deformation in the surrounding soil. AASHTO (2014) design specifications states that the group resistance is influenced by whether the pile cap is in firm contact with the ground. If the pile cap is in firm contact with the ground, the soil between the piles and the pile group act as a unit.

The following design recommendations are for estimating nominal group resistance in cohesive soils. The lesser value of the nominal group resistance, calculated from Steps 1 to 4, should be used.

1. For pile groups driven in clays with undrained shear strengths of less than 2 ksf and the pile cap not in firm contact with the ground, a group efficiency of 0.65 should be used for center to center pile spacing of 2.5 times the average pile diameter. If the center to center pile spacing is greater than 6 times the average pile diameter, then a group efficiency of 1.0 may be used. Linear interpolation should be used for intermediate center to center pile spacing.
2. For piles in clays with undrained shear strengths less than 2 ksf, and the pile cap in firm contact with the ground, a group efficiency of 1.0 may be used.
3. For pile groups in clays with undrained shear strength in excess of 2 ksf, a group efficiency of 1.0 may be used regardless of the pile cap - ground contact.
4. Calculate the nominal pile group resistance against block failure using the procedure described in Section 7.2.2.3.
5. Piles in cohesive soils should not be installed at center to center pile spacing less than 3 times the average pile diameter unless dictated otherwise by pile size, site constraints, pile cap requirements, and construction costs. The center to center pile spacing should also not be less than 3 feet.

It is important to note that the driving of pile groups in cohesive soils can generate large excess pore water pressures. This can result in short term (1 to 2 months after

installation) group efficiencies on the order of 0.4 to 0.8. As these excess pore pressures dissipate, the pile group efficiency will increase. Figure 7-30 presents observations on the dissipation of excess pore water pressure versus time for pile groups driven in cohesive soils. Depending upon the group size, the excess pressures typically dissipate within 1 to 2 months after driving. However, in very large groups, full pore pressure dissipation may take up to a year.

If a pile group will experience the full group load shortly after construction, the foundation designer must evaluate the reduced group resistance that may be available for load support. In these cases, piezometers should be installed to monitor pore pressure dissipation with time. Effective stress resistance calculations can then be used to determine if the increase in pile group resistance versus time during construction meets the load support requirements.

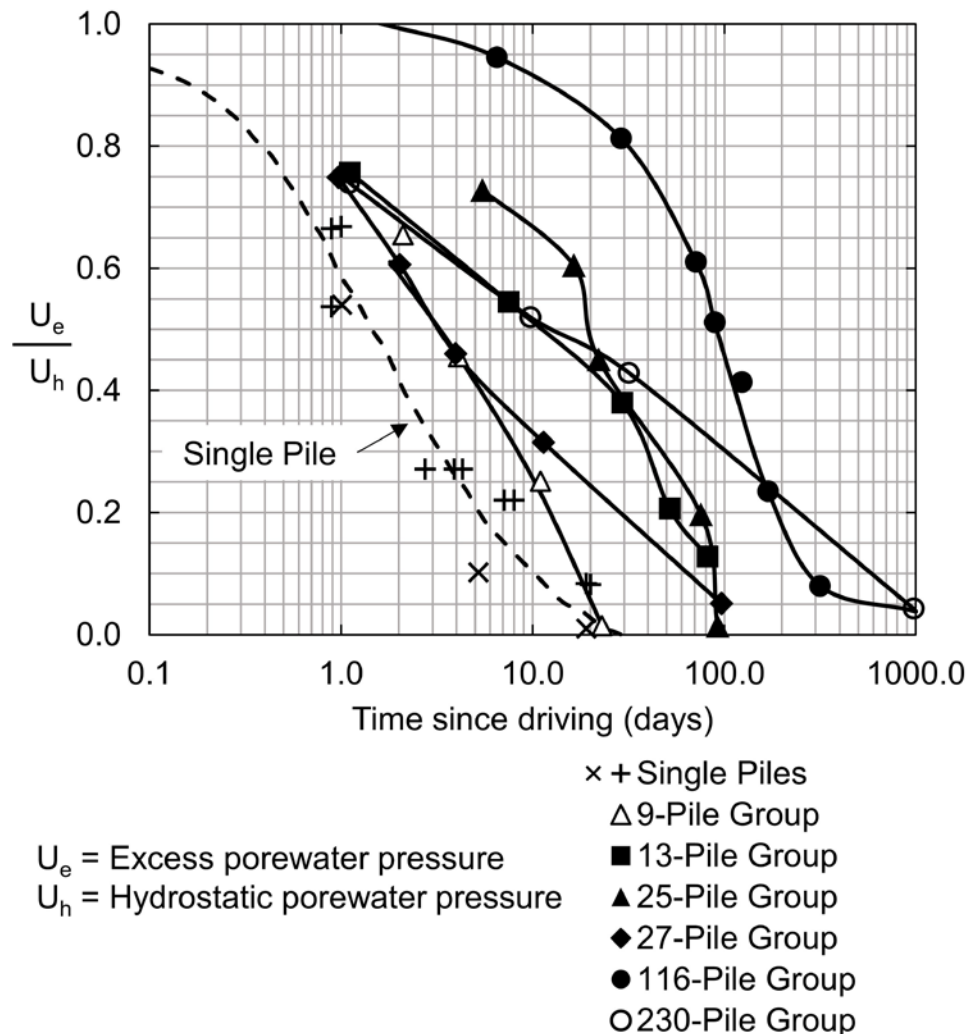


Figure 7-30 Measured dissipation of excess pore water pressure in soil surrounding full scale pile groups (after O'Neill 1983).

7.2.2.3 Block Failure of Pile Groups

Block failure of pile groups is generally only a design consideration for pile groups in soft cohesive soils or in cohesionless soils underlain by a weak cohesive layer. For a pile group in cohesive soil as shown in Figure 7-31 the nominal resistance of the pile group against a block failure is provided by the following expression:

$$R_{ng} = 2D(B + Z)s_{u1} + BZs_{u2}N_c \quad \text{Eq. 7-36}$$

Where:

- R_{ng} = nominal resistance of the pile group.
- D = pile embedded length.
- B = width of pile group.
- Z = length of pile group.
- s_{u1} = weighted average of the undrained shear strength over the depth of pile embedment for the cohesive soils along the pile group perimeter.
- s_{u2} = average undrained shear strength of the cohesive soils at the base of the pile group to a depth of $2B$ below pile toe level.
- N_c = dimensionless bearing capacity factor.

If a pile group will experience the full group load shortly after construction, the nominal group resistance against block failure should be calculated using the remolded or reduced shear strength rather than the average undrained shear strength for s_{u1} .

The bearing capacity factor, N_c , for a rectangular pile group is generally 9. However, for pile groups with small pile embedment depths and/or large widths, N_c should be calculated from the following equation:

$$N_c = 5 \left[1 + \frac{D}{5B} \right] \left[1 + \frac{B}{5Z} \right] \leq 9 \quad \text{Eq. 7-37}$$

Where:

- N_c = dimensionless bearing capacity factor.
- D = pile embedded length.
- B = width of pile group.
- Z = length of pile group.

When evaluating possible block failure of pile groups in cohesionless soils underlain by a weak cohesive deposit, the weighted average unit shaft resistance for the cohesionless soils should be substituted for s_{u1} in calculating the nominal group resistance. The pile group base strength determined from the second part of the nominal group resistance equation should be calculated using the strength of the underlying weaker layer.

Additional guidance can be found in AASHTO (2014) Article 10.6.3.1.2d on the punching failure of a footing situated in a strong layer overlying a weak layer. The equivalent footing concept for the pile group can be used in conjunction with the spread footing guidance.

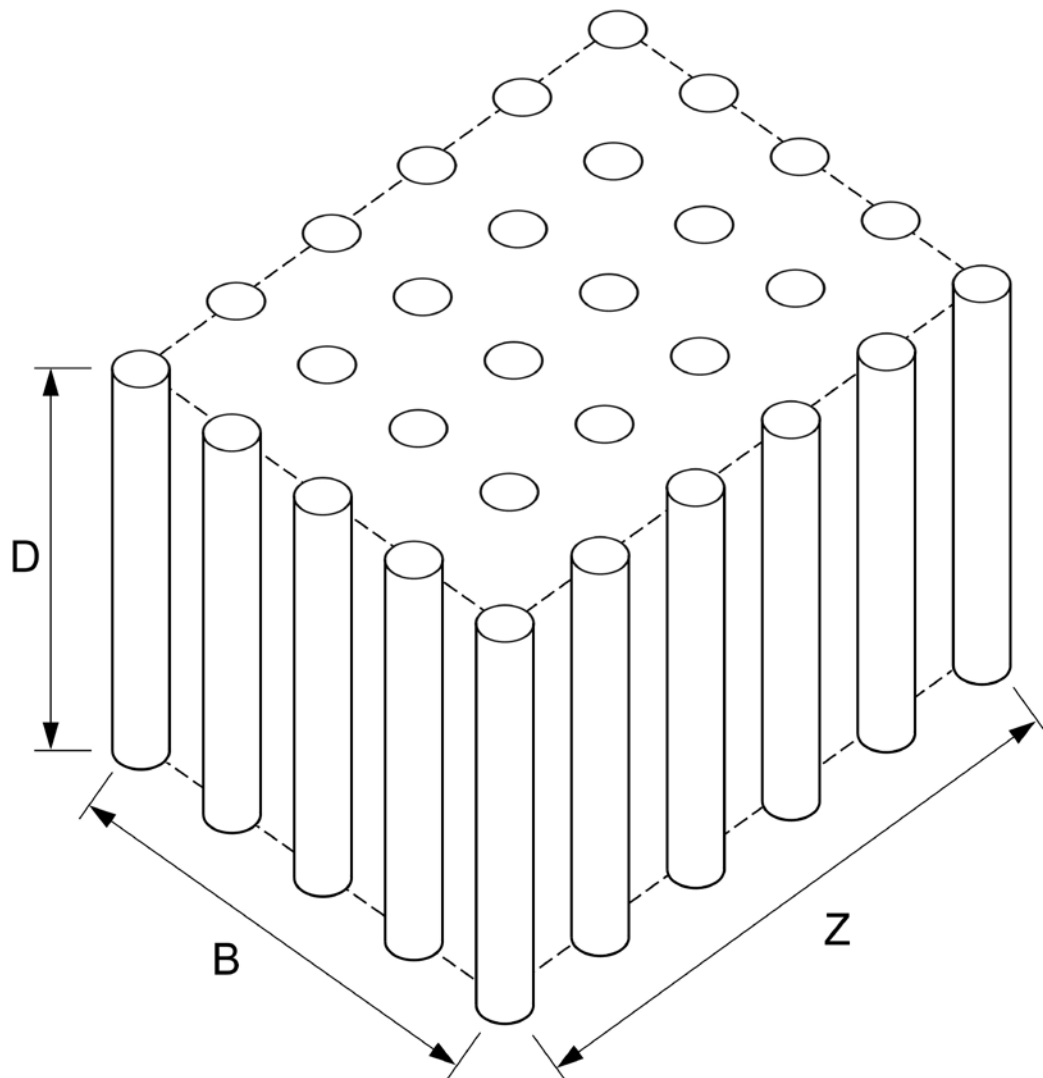


Figure 7-31 Three dimensional pile group configuration (after Tomlinson 1994).

7.2.3 Design for Axial Tension Resistance

The design of piles for axial tension or uplift loading conditions has become increasingly important for structures subject to seismic loading. In some cases, the uplift resistance determines the minimum pile penetration requirements. In those situations, axial tension load tests may be very cost effective as the higher resistance factor as a result of testing may reduce minimum pile penetration requirements and overall pile lengths. Tension load test procedures are described by Kyfor et al. (1992) in FHWA-SA-91-042 as well as in Chapter 9.

7.2.3.1 Axial Tension Resistance of Single Piles

De Nicola and Randolph (1993) note that in fine grained cohesive soils, where loading is assumed to occur under undrained conditions, the shaft resistance is generally considered equal in compression and in uplift.

In non-cohesive or free draining soils, the uplift resistance of a pile has been more controversial. De Nicola and Randolph (1993) state that it has been customary to assume that the shaft resistance in uplift is approximately 70% of the shaft resistance in compression. Based upon a finite difference parametric study, they concluded that a reduction in shaft resistance for uplift in free draining soils should be used, and that piles have lower uplift resistance than their compression shaft resistance. Conversely, the American Petroleum Institute's (1993) recommended design practice considers the pile shaft resistance to be equal in uplift and compression loading. Likewise, Altaee et al. (1992) presented a case of an instrumented pile in sand where the shaft resistance was approximately equal in compression and uplift when residual stresses were considered.

Tomlinson (1994) notes that the shaft resistance under cyclic loading is influenced by the rate of application of load as well as the degree of degradation of soil particles at the soil-pile interface. Under cyclic or sustained uplift loading in clays, the uplift resistance can decrease from the peak value to a residual value. In sands, particle degradation or reorientation can also result in decrease in uplift resistance under cyclic or sustained uplift loading. Therefore, the designer should consider what effect, if any, sustained or cyclic uplift loading will have on soil strength degradation.

Based on the above issues, the factored uplift resistance of a single pile should be taken as that of the nominal shaft resistance calculated from any of the AASHTO static analysis methods with a resistance factor for uplift, ϕ_{up} , from Table 7-1. From AASHTO (2014) Article C10.7.3.10, the uplift resistance factor from static analysis

methods is reduced to 80 percent of the resistance factor for static shaft resistance in compression. Therefore, the shaft resistance does not need to be further reduced for the uplift case.

Equation 7-38 is modified from the general static analysis equation to account for uplift. Selection of the factored uplift resistance should also consider the potential for soil strength degradation due to the duration or frequency of uplift loading, which may not be apparent in the short term static or dynamic test results.

$$R_r = \phi R_n = \phi_{up} R_s \quad \text{Eq. 7-38}$$

Where:

- R_r = factored resistance (Equation 7-3).
- R_s = nominal shaft resistance (Equation 7-4).
- ϕ_{up} = resistance factor for uplift analysis method per Table 7-1.

If a tension static load test is performed for design confirmation, a design uplift resistance factor of up to 0.60 may be used. Dynamic tests with signal matching can also be used to determine uplift resistance per AASHTO (2014) Article 10.7.3.10. Based on a dynamic test, an uplift resistance factor of up to 0.50 is recommended.

Figure 7-32 illustrates a design chart for uplift loading. The nominal resistance and nominal shaft resistance in the figure were calculated using the FHWA method (Nordlund / α -method) in APILE. The nominal shaft resistance has also been factored by 0.60 to yield the factored resistance in axial tension expected based on a static load test, 0.50 for a dynamic test with signal matching, and by 0.25 in the clay layers (α -method) and 0.35 (Nordlund Method) in the sand layers to yield the factored resistance in axial tension based solely on static analysis.

For a factored resistance in axial tension of 100 kips, the uplift design chart indicates estimated pile lengths of 72, 74, and 78 feet for a tension load test, dynamic test with signal matching, and static analysis. Hence, a static analysis may be the most cost effective approach for this factored load for a project with a limited number of piles. On the other hand, the uplift design chart indicates estimated pile lengths of 81, 84, and 112 feet for a factored uplift resistance of 200 kips based on a tension load test, dynamic test with signal matching, and static analysis. In this case, the pile length savings from either static load testing or dynamic testing may be economically justified.

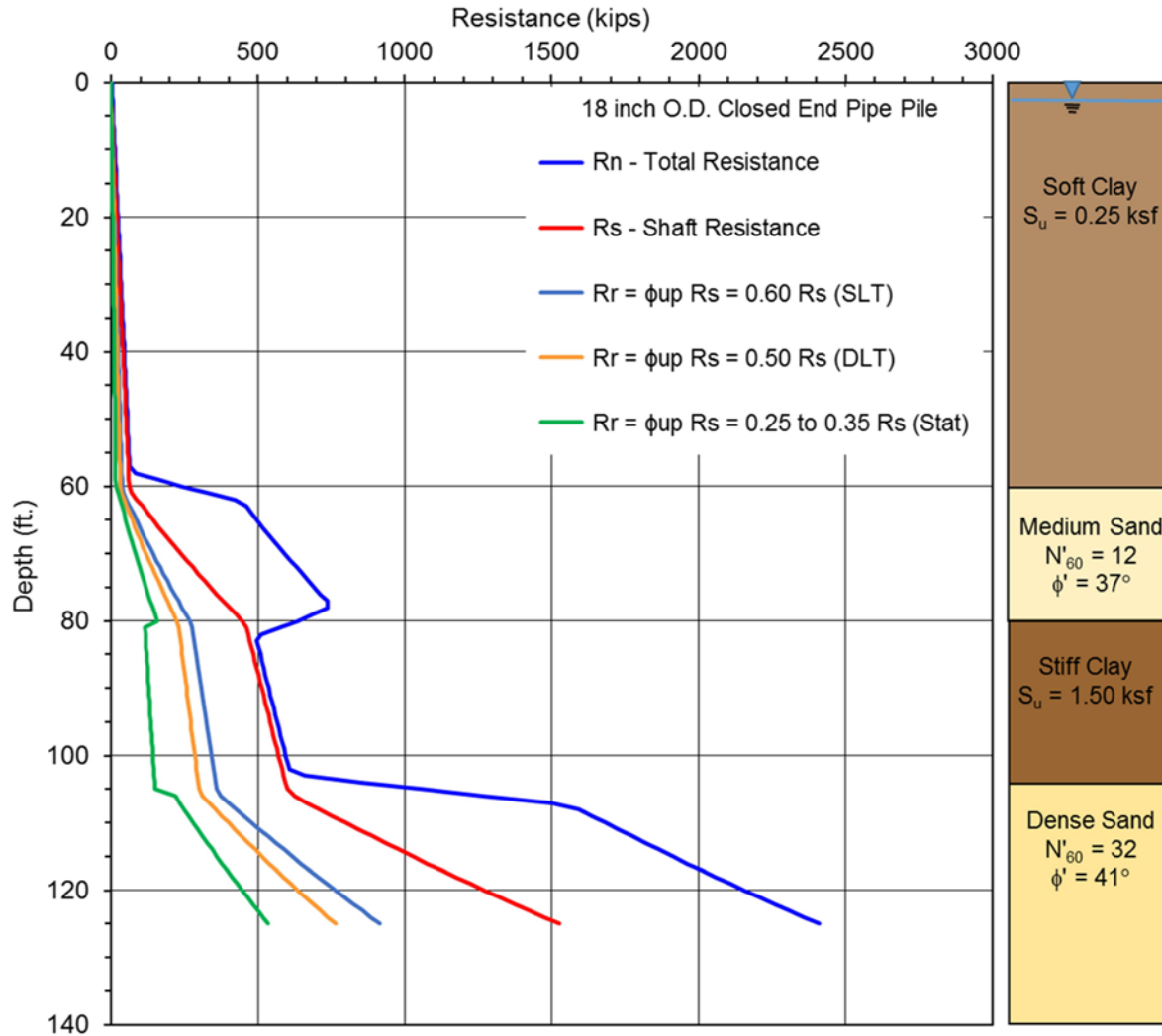


Figure 7-32 Design chart for nominal and factored resistance in axial tension.

7.2.3.2 Axial Tension Resistance of Pile Groups

Axial tension or uplift resistance of a pile group is often a significant factor in determining the minimum pile penetration requirements and in some cases can control the foundation design. A few common conditions where group uplift resistance may significantly influence the foundation design include cofferdam seals that create large buoyancy forces, cantilever segmental bridge construction, and seismic, vessel impact, or debris loading. When piles with uplift loads are driven to a relatively shallow bearing stratum, uplift resistance may control the foundation design. AASHTO (2014) specifications for group uplift resistance are considered relatively conservative, particularly in cohesionless soils.

AASHTO specifications (2014) limit uplift resistance of a pile group to the lesser of:

1. The sum of individual pile resistance in axial tension.
2. The resistance in axial tension of the pile group considered as a block.

Equation 7-39 is modified for factored uplift which considers the total resistance of a pile group. Meanwhile, the group uplift resistance is determined differently for cohesive and cohesionless soils, which is described in the following two sections.

$$R_r = \phi R_n = \phi_{ug} R_{ug} \quad \text{Eq. 7-39}$$

Where:

- R_r = factored resistance in axial tension (Eq. 7-4).
- R_{ug} = nominal resistance in axial tension of the pile group.
- ϕ_{ug} = resistance factor for axial tension, 0.50 per Table 7-1.

7.2.3.2.2 Axial Tension Resistance of Groups in Cohesionless Soils

In cohesionless soils, AASHTO (2014) Article 10.7.3.11 limits the nominal group resistance in axial tension to the lesser of two resistances. The first resistance is the sum of the individual pile nominal shaft resistance times the analysis method resistance factor for uplift, times the number of piles in the group. This is expressed in Equation 7-40.

$$R_r = \phi R_{ug} = \phi_{up} R_s n \quad \text{Eq. 7-40}$$

Where:

- R_{ug} = nominal resistance in axial tension of pile group.
- R_s = nominal shaft resistance.
- ϕ_{up} = resistance factor for uplift analysis method per Table 7-1.
- n = number of piles in group.

The second resistance is defined by the weight of soil contained with the pile group block depicted by Figure 7-33. This approach outlined by Tomlinson (1994), uses the effective weight of the block of soil extending upward from the pile toe level at a slope of 1H:4V. For simplicity in performing the calculation, the weights of the piles within the soil block are considered equal to the weight of the soil. The group uplift resistance is the lesser resistance determined from Equation 7-40 or Figure 7-33.

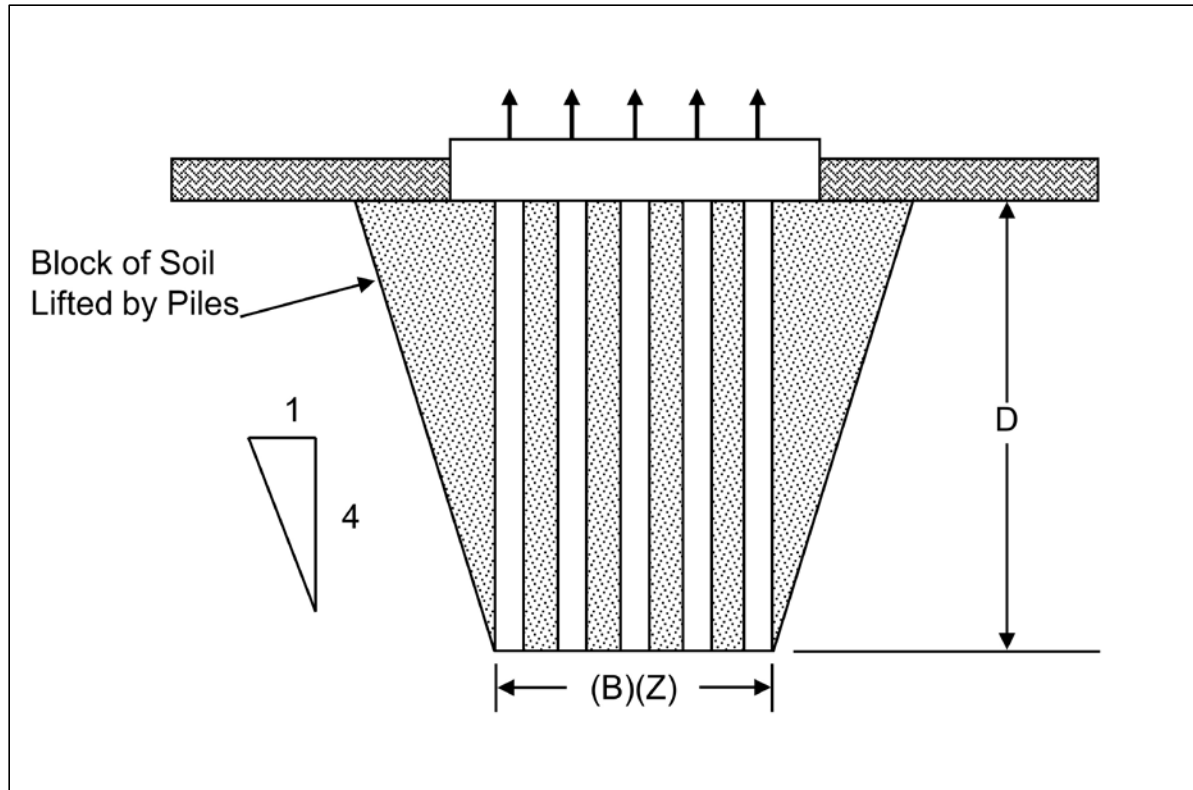


Figure 7-33 Uplift of pile group in cohesionless soil (after Tomlinson 1994).

7.2.3.2.3 Axial Tension Resistance of Groups in Cohesive Soils

Similarly in cohesive soils, AASHTO (2014) Article 10.7.3.11 limits the nominal group uplift resistance to the lesser of the resistance computed by Equation 7-40 or Equation 7-41. Figure 7-34 depicts the nominal group resistance provided by the soil weight contained within the pile group block and the soil shear resistance along the group perimeter, as should be used for Equation 7-41.

$$R_n = R_{ug} = 2D(B + Z)s_u + W_g \quad \text{Eq. 7-41}$$

Where:

- R_n = nominal resistance (kips).
- R_{ug} = nominal resistance in axial tension of the pile group (kips).
- D = pile embedded length (feet).
- B = width of pile group (feet).
- Z = length of pile group (feet).
- s_u = weighted average of the undrained shear strength over the depth of pile embedment along the pile group perimeter (ksf).
- W_g = effective weight of the pile/soil block including pile cap weight (kips).

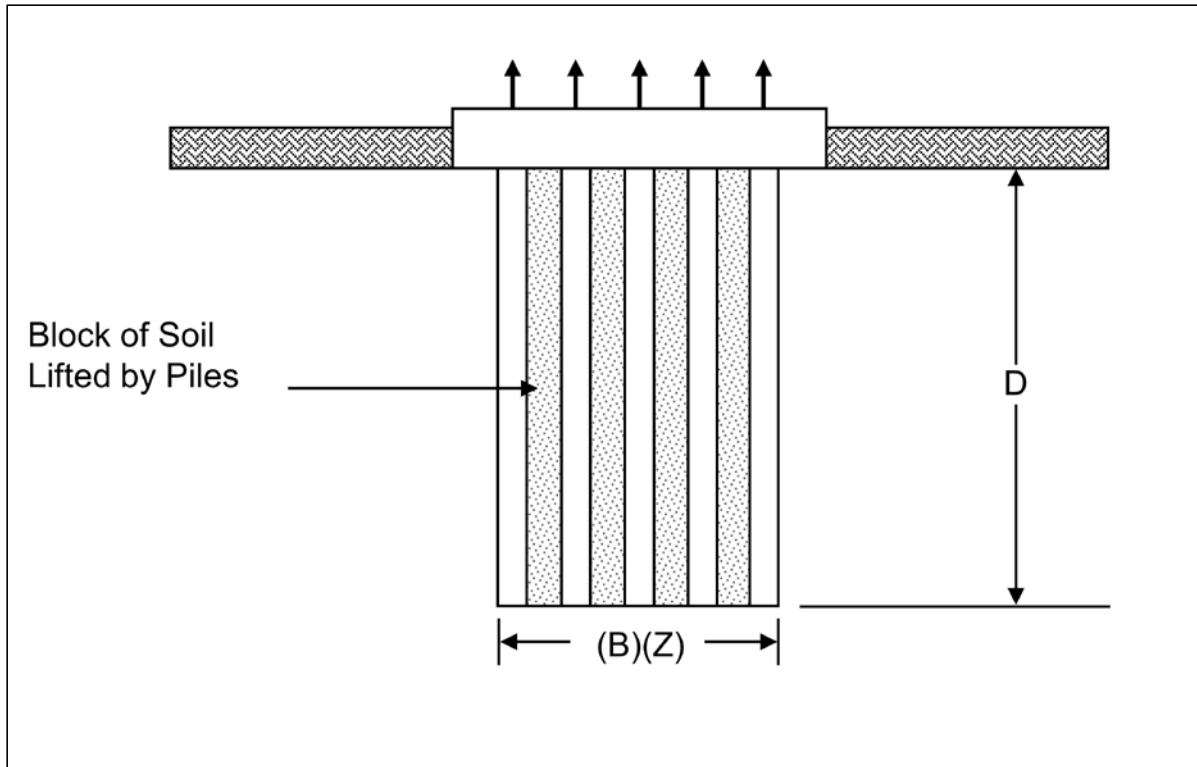


Figure 7-34 Uplift of pile group in cohesive soils (after Tomlinson 1994).

7.2.4 Nominal Axial Resistance Changes after Pile Driving

The surrounding soil is greatly disturbed when a pile is driven into it. As the soil surrounding the pile regains strength following the installation disturbance, a time dependent change in geotechnical resistance occurs. Frequently piles driven in saturated clays, and loose to medium dense silts or fine sands gain significant resistance after driving has been completed. This phenomenon is called soil setup. Occasionally piles driven into dense saturated fine sands, dense silts, or weak laminated rocks such as shale, will exhibit a decrease in resistance after the driving has been completed. This phenomenon is called relaxation. Case history discussions on soil setup and relaxation may be found in Fellenius et al. (1989), and Thompson and Thompson (1985), respectively.

7.2.4.1 Relaxation

The nominal resistance of driven piles can decrease with time following driving. This decrease in nominal resistance is known as relaxation. Relaxation has been observed in dense, saturated, fine grained soils such as non-cohesive silts and fine sands. In these cases, the driving process is believed to cause the dense soil near the pile toe to dilate (tendency for volume increase), thereby generating negative

pore pressures (suction). The negative pore pressures temporarily increase the effective stresses acting on the pile, resulting in a temporarily higher soil strength and driving resistance. When these pore pressures dissipate, the effective stresses acting on the pile decrease, as does the nominal resistance. Several cases of relaxation in silts and fine sands have been reported in the literature including Yang (1970), York et al. (1994), Morgano and White (2004), and Richardson (2011).

Relaxation in weak laminated rocks has also been reported. Thompson and Thompson (1985) attributed this to a release of locked in horizontal stresses. Rock formations reported in the literature to exhibit relaxation include shales; Thompson and Thompson (1985), Hussein et al. (1993), Morgano and White (2004); and phyllite, Seidel et al. (1992). However, relaxation is possible in other weak laminated rock formations such as mudstone, claystone, and siltstone among others.

Because the nominal resistance may decrease (relaxation) after the end of driving, nominal resistance assessments from static load testing or dynamic test restrikes should be made after equilibrium conditions in the soil have been re-established. In the absence of site specific pore pressure data from piezometers, it is suggested that static load testing or restriking of piles in dense silts and fine sands be delayed for a few days to a week after driving, or longer if possible. In relaxation prone shales, it is suggested that static load testing or restrike testing be delayed a minimum of ten days to two weeks after driving.

Published cases of the relaxation magnitude of various soil types are quite limited. However, data from Thompson and Thompson (1985) as well as Hussein et al. (1993) suggest relaxation factors for piles founded in some shales can range from 0.5 to 0.9. The relaxation factor is defined as the static load test failure load divided by the nominal resistance at the end of initial driving. Relaxation factors of 0.5 and 0.8 have also been observed in two cases where piles were founded in dense sands and extremely dense silts, respectively. The importance of evaluating time dependent decreases in nominal resistance for piles founded in these materials cannot be over emphasized. AASHTO (2014) Article 10.7.3.4.2 states that a restrike test should be done after a sufficient time for relaxation to develop if relaxation is possible in the soils at the site.

7.2.4.2 Soil Setup

When saturated cohesive soils are compressed and disturbed due to pile driving, large excess pore pressures develop. These excess pore pressures are generated partly from the shearing and remolding of the soil and partly from radial compression

as the pile displaces the soil. The excess pore pressures cause a reduction in the effective stresses acting on the pile, and a reduction in the soil shear strength. This results in a reduced nominal resistance during, and for a period of time after, driving.

After driving, the excess pore pressures will dissipate primarily through radial flow of the pore water away from the pile (Randolph et al. 1979). With the dissipation of pore pressures, the soil reconsolidates and increases in shear strength. This increase in soil shear strength results in an increase in the nominal resistance and is called soil setup. A similar decrease in resistance to pile penetration with subsequent soil setup may occur in loose to medium dense, saturated, fine grained sands or silts. The magnitude of the gain in nominal resistance depends on soil characteristics, pile material and pile dimensions.

Because the nominal resistance may increase after the end of driving, nominal resistance assessments should be made from static load tests, dynamic testing, or hammer restrike events performed after equilibrium conditions in the soil have been re-established. The time for the return of equilibrium conditions is highly variable and depends on soil type and degree of soil disturbance.

In research studies, piezometers installed within three diameters of the pile can be used to monitor pore pressure dissipation with time. Effective stress static nominal resistance calculations can be used to evaluate the increase in resistance with time once pore pressures are quantified.

To quantify the largest magnitude of soil setup, static load testing or restrike dynamic testing of piles in fine grained soils should be delayed until pore pressures dissipate and return to equilibrium. In the absence of site specific pore pressure data or local experience, it is preferable that static load testing or dynamic restrike tests of piles in clays and other predominantly fine grained soils be delayed for two weeks after driving or longer if possible. Unfortunately, delays of this magnitude to quantify or confirm the soil setup magnitude are not frequently feasible on most routine projects. Therefore, it is best to quantify the soil setup magnitude and time rate of setup in a design stage test program in high setup locales. The design stage program should include multiple restrike events on dynamic test piles and static load test(s) so that both the time rate of setup as well as the setup magnitude can be determined and later used for production driving where only shortened restrike intervals can be accommodated due to the construction schedule. In sandy silts and fine sands, pore pressures generally dissipate more rapidly. In these more granular deposits, three to seven days is often a sufficient time delay.

Hannigan et al. (2012) presented a case history multiple dynamic monitoring events on test piles were used to quantify the time dependent soil setup magnitude and its spatial variation for a four-level interchange project. Static load tests were also used to confirm the nearly five-fold increase in shaft resistance over time.

Several methods have been proposed to predict soil setup effects. A study by Skov and Denver (1988) looked at predicting the nominal resistance in cohesive and cohesionless soils sometime after initial driving based on initial driving measurements using Equation 7-42.

$$R_n = R_{no} \left(1 + A_1 \log \frac{t}{t_o} \right) \quad \text{Eq. 7-42}$$

Where:

- R_n = nominal resistance after time “t” of driving (kips).
- R_{no} = initial nominal resistance at “t_o” of driving (kips).
- A_1 = constant based on soil type and subsurface condition.
(0.2 for sand and 0.6 for clay).
- t = time after driving (days).
- t_o = time after driving from which the increase in resistance is linear in logarithmic time (days) (typically 0.5 for sand, 1.0 for clay).

Komurka et al. (2003) summarized the state of the practice in estimating and measuring soil setup in a report to the Wisconsin Highway Research Program. This report summarizes the mechanisms associated with soil setup development and reviews several empirical relationships for estimating setup.

A study by Bullock et al. (2005) assessed five square prestressed concrete piles driven in various soils throughout Florida. Resistance was measured through initial drive and restrike dynamic testing followed by subsequent O-cell tests. For this, they expanded upon the Skov and Denver approach.

$$R_s = R_{so} \left[\left(\frac{m_s}{R_{so}} \right) \log \left(\frac{t}{t_o} \right) + 1 \right] \quad \text{Eq. 7-43}$$

Where:

- R_s = shaft resistance after time “t” of driving (kips).
- R_{so} = initial shaft resistance at “t_o” of driving (kips).
- m_s = semilog-linear slope of R_s vs t from multiple restrike tests.
- t = time after driving (days).
- t_o = time of driving (days) (1 day for all tests).

Ng (2011) investigated soil setup on steel HP 10x42 piles driven into cohesive soils throughout Iowa. Initial drive and restrike dynamic testing was performed to assess time dependent resistance changes. This dissertation was presented in SI units, therefore the pore water dissipation factor, C_h , should be determined first using Equation 7-44, and then converted to English units for inclusion in Equation 7-45.

$$C_h = \frac{3.179}{N^{2.08}} \text{ (cm}^2\text{/min)} \quad \text{Eq. 7-44}$$

In which:

$$\frac{R_s}{R_{so}} = \left[\left(\frac{f_c C_h}{N_a r_p^2} + f_r \right) \log \frac{t}{t_o} + 1 \right] \frac{L_t}{L_o} \quad \text{Eq. 7-45}$$

Where:

- R_s = shaft resistance after time “t” of driving (kips).
- R_{so} = initial shaft resistance at “ t_o ” of driving (kips).
- f_c = consolidation factor (non-dimensional regression factor).
- C_h = pore water pressure dissipation factor (in²/min for Equation 7-45).
- N_a = average SPT N-Value over pile length.
- N = SPT N-Value.
- r_p = equivalent pile radius (inches).
- f_r = remolding recovery rate (non-dimensional regression factor).
- L_t = embedded pile length at time “t” after initial driving (feet).
- L_o = embedded pile length at the time of initial driving (feet).
- t = time after initial driving (days).
- t_o = time of driving (days) (0.00694 days for all tests).

Another recent study comparing the nominal resistance from initial drive and restrike dynamic testing was performed by Reddy and Stuedlein (2014). They reviewed data from 76 piles in the Puget Sound Lowlands of Oregon, with restrikes varying from 5 to 310 hours. Both closed (CEP) and open end (OEP) steel pipe piles, as well as prestressed concrete piles (PSC) were utilized. The setup prediction model developed followed a hyperbolic curve and is presented as Equation 7-46.

$$R_s = \frac{R_{so} A_2 \log \left(\frac{t}{t_o} \right)}{k_1 + k_2 R_{so} A_2 \log \left(\frac{t}{t_o} \right)} + R_{so} \quad \text{Eq. 7-46}$$

Where:

- R_s = shaft resistance after time “t” of driving (kips).
- R_{s0} = initial shaft resistance at “ t_0 ” of driving (kips).
- A_2 = constant based on pile type (1.72 for PSC piles, 0.70 for CEP, and 0.77 for OEP).
- t = time after driving (hours).
- t_0 = time of driving (hours) (1 hour for all tests).
- k_1 = regression factor (0.17 for PSC, 0.12 for CEP and 0.15 for OEP).
- k_2 = regression factor (0.00044 for PSC piles, 0.00078 for CEP piles, 0.00060 for OEP piles).

For the studies presented above, specific contributing factors were explored (i.e. regional soil, pile type, etc.). Therefore, these predictive methods may not translate to other areas with different conditions unless modified by local correlation experience. However, many of these studies provide a suggested approach for agencies to generate a database of tested piles with initial driving, restrrike testing and static load tests are available to better assess the time dependent changes.

Limited information is available regarding soil setup in unsaturated soils. However, it is anticipated that setup would occur in these deposits.

Rausche et al. (1996) calculated general soil setup factors based on the predominant soil type along the pile shaft. The soil setup factor was defined as the static load test failure load divided by the end-of-drive wave equation resistance. These results are presented in Table 7-16. The database for this study was comprised of 99 test piles from 46 sites. The number of sites and the percentage of the database in a given soil condition is included in the table. While these soil setup factors may be useful for preliminary estimates, soil setup is better estimated based on site specific data gathered from pile restriking, dynamic measurements, static load testing, and local experience.

Table 7-16 Soil Setup Factors (after Rausche et al. 1996)

Predominant Soil Type Along Pile Shaft	Range in Soil Setup Factor	Recommended Soil Setup Factors*	Number of Sites and (Percentage of Database)
Clay	1.2-5.5	2.0	7 (15%)
Silt - Clay	1.0-2.0	1.0	10 (22%)
Silt	1.5-5.0	1.5	2 (4%)
Sand - Clay	1.0-6.0	1.5	13 (28%)
Sand - Silt	1.2-2.0	1.2	8 (18%)
Fine Sand	1.2-2.0	1.2	2 (4%)
Sand	0.8-2.0	1.0	3 (7%)
Sand - Gravel	1.2-2.0	1.0	1 (2%)

* Confirmation with Local Experience Recommended.

7.2.4.2.1 Estimation of Pore Pressures During Driving

According to Lo and Stermac (1965), the maximum pore pressure induced from pile driving may be estimated from the following equation.

$$\Delta_{um} = \left[(1 - K_o) + \left(\frac{\Delta u}{\sigma'_{v_m}} \right) \right] \sigma'_{vi} \quad \text{Eq. 7-47}$$

Where:

- Δ_{um} = maximum excess pore pressure (ksf).
- K_o = at rest earth pressure coefficient.
- σ'_{vi} = initial vertical effective stress prior to pile driving (ksf).
- $(\Delta u / \sigma'_{v_m})_m$ = maximum value of the pore pressure ratio, $\Delta u / \sigma'_{v_o}$, measured in a CU triaxial test with pore pressure measurements.

Ismael and Klym (1979) presented a case history where the above procedure was used. They reported good agreement between measured excess pore pressures with estimates from the Lo and Stermac procedure.

Poulos and Davis (1980) summarized measurements of excess pore pressures due to pile driving from several case histories. In this compilation, the reported excess pore pressure measurements divided by the vertical effective stress were plotted versus the radial distance from the pile surface divided by the pile radius. These

results are presented in Figure 7-35 and indicate that the excess pore pressure at the pile-soil interface can approach 1.4 to 1.9 times the vertical effective stress, depending upon the clay sensitivity.

The foundation designer should evaluate the potential change in nominal resistance with time. Once pore pressures are measured or estimated, effective stress static resistance calculation methods can be used to quantify the probable change in nominal resistance with time.

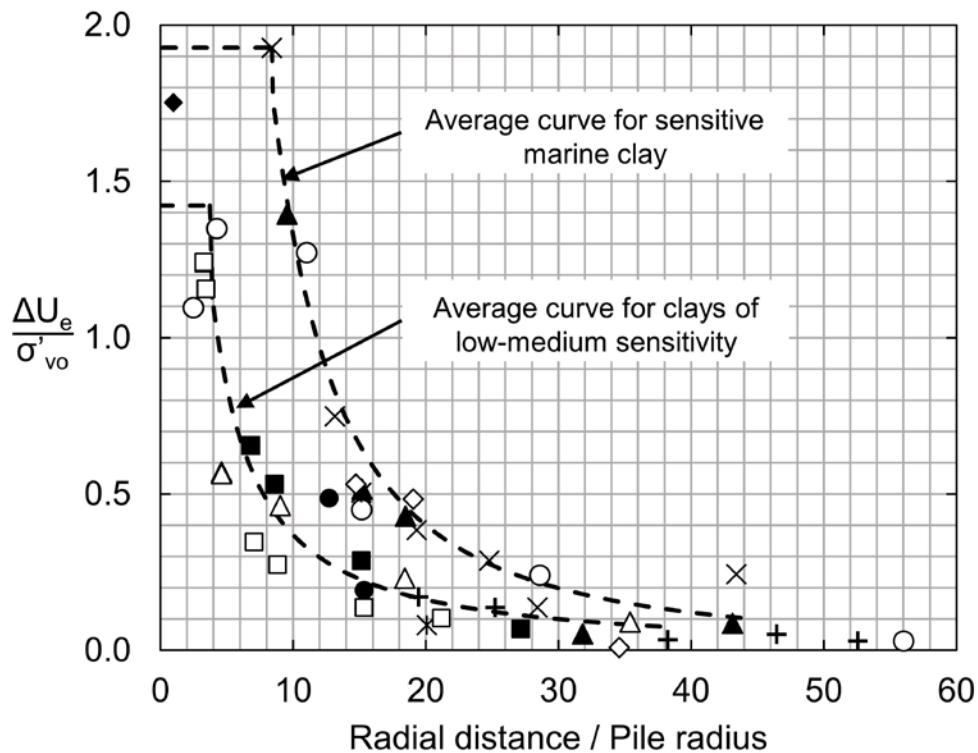


Figure 7-35 Excess pore water pressure due to pile driving (after Poulos and Davis 1980).

7.2.4.3 Implementation of Time Effects During Construction

As discussed above in the relaxation and soil setup sections, changes in nominal resistance occur after driving. These are permanent physical changes to the nominal resistance. Significant cost savings can be achieved when soil setup is effectively used. Many state transportation agencies are aware of soil setup effects, and as mentioned in Komurka et al. (2003), if setup effects could be predicted in the design phase, it may be possible to reduce pile lengths, reduce pile sections (use smaller-diameter or thinner-wall pipe piles, or smaller-section H-piles), or reduce the size of driving equipment (use smaller hammers and/or cranes).

Conversely, relaxation effects have been studied to a lesser degree, and in areas with known weathered shale or weak laminated bedrock, initial drive and restrike dynamic testing can prove useful to evaluate the extent of resistance loss (Long and Anderson 2014). Potentially problematic pile installations can be avoided when relaxation is identified early on and modified construction procedures adopted.

7.2.5 Nominal Lateral Resistance

In addition to axial compression and uplift loads, piles are routinely subjected to lateral loads. Potential sources of lateral loads on bridge structures include vehicle acceleration and braking forces, wind loads, wave and current forces, debris loading, ice forces, vessel impact loads, construction procedures, thermal expansion and contraction, earth pressures on the back of abutment walls, slope movements, and seismic events. These lateral loads can be of the same magnitude as axial compression loads and therefore warrant careful consideration during design.

AASHTO (2014) Article 10.7.3.12 addresses the nominal resistance of piles subjected to lateral loads. For a long pile, the nominal lateral resistance is controlled by the strength of the pile material since the pile will fail structurally before soil failure occurs along the entire pile length. The nominal lateral resistance of a short pile, defined as a pile with insufficient embedment to prevent toe rotation, is controlled by the soil. While short and rigid piles with very large lateral loads are relatively uncommon in practice, when encountered, they should be further evaluated in a p-y analysis considering both the properties of the geomaterials and the pile's structural resistance. The p-y method is described in detail in Section 7.3.7.3.

AASHTO (2014) notes that the strength limit state for nominal lateral resistance is, in most cases, only structural for the reasons described above. Chapter 8 provides guidance on structural limit states. The foundation deformation under lateral loading must also be within the established performance criterion for the structure. Section 7.3.7 discusses horizontal pile deflection under the service limit state.

7.2.6 Pile Length Estimates for Contract Documents

Pile length estimates and contract pile quantities should be carefully established using a combination of the site subsurface information, static analysis methods, and preconstruction test pile programs. Sometimes, pile length estimates can be determined from an obvious bearing layer. In other cases, construction control or static analysis methods may be relied upon, but the potential bias in either method

should be considered. Local pile driving experience should also be reviewed when determining the pile length estimates.

Minimum pile penetration requirements for effects of uplift, settlement, scour, lateral deflection, or downdrag should also factor into the contract pile length estimates. In cases where the depth of penetration required to achieve the nominal resistance in axial compression is less than the depth to satisfy these strength, service or extreme limit state requirements, the minimum pile penetration required to satisfy all limit state requirements should be used for contract pile quantities. The contract documents should also explicitly note the minimum pile penetration depth and the required nominal resistance below that depth during driving, R_{ndr} , to avoid construction control problems if the required nominal resistance is achieved above the minimum pile penetration depth. It is important to note that a minimum pile penetration depth is not always required and that the estimated length may be all that is necessary for contract documents.

7.2.7 Groundwater Effects and Buoyancy

The nominal resistance in axial compression and tension as well as the lateral resistance can be influenced by groundwater elevation changes and the resulting change in vertical effective stress. Groundwater elevation changes can be influenced by droughts, regional construction events such as construction of tunnels, or by local site events such as excavation dewatering. Events which cause temporary lowering of the groundwater elevation increases vertical effective stresses and thus the effective stress acting on the pile. Hence, a pile driven for the required nominal resistance in a temporarily lowered groundwater condition will have a nominal resistance less than required when the groundwater returns to its normal elevation.

Buoyant forces should also be considered in driven pile foundation design. A closed-end pipe pile driven through soft soils to rock or a hard bearing layer may need a thicker wall section or other measures to counter-act buoyancy effects. In this situation, buoyancy effects can raise a sealed closed-end pile from the bearing layer if the shaft resistance alone is insufficient to resist buoyancy forces.

7.2.8 Site Dewatering

When a site is dewatered during construction, a temporary increase in effective stresses will occur. This causes a corresponding temporary increase in soil shear strength that will result in piles driven in a dewatered site to develop a greater

resistance at a shallower pile penetration depth as compared to the non-dewatered condition. The soil resistance to be overcome to reach a specified penetration depth will also be greater than in the non-dewatered condition. If not considered in the design stage, the selected pile type may not be drivable to the required penetration depth in the dewatered construction condition. When dewatering is terminated, the effective stresses acting on the pile will decrease as the water table rises. This will result in a decrease in the soil shear strength and a decrease in long term nominal resistance. Hence piles driven to the nominal resistance in the dewatered condition would have less than the required nominal resistance once dewatering is terminated.

For projects where significant dewatering is required, the effects of the dewatering on nominal resistance and pile drivability should be evaluated. In these cases, multiple static analyses should be performed to determine the nominal resistance and drivability requirements under the short term dewatered condition, as well as the long term nominal resistance after dewatering has been terminated.

Dewatering can also have negative impacts on nearby structures supported on deep and shallow foundations. The increase in effective stress can cause or increase drag force on deep foundations or cause consolidation settlements that affect the performance of deep and shallow foundations systems. The potential dewatering effects on adjacent structures should be evaluated during the design phase.

7.2.8.1 Artesian Conditions

Artesian conditions develop where a permeable soil layer or aquifer is confined by two impermeable layers and the permeable soil layer outcrops at an elevation higher than where it is encountered in-situ. In this situation the effective stresses acting on the pile are directly related to the head of water. Artesian conditions can result in lower than expected nominal resistance in the soil layer as well as potential vertical groundwater migration issues along the pile-soil interface. Harris et al. (2003) describe a driven pile case history where the back calculated effective stress design parameters from a static load test program were significantly lower than expected due to artesian conditions. A detailed subsurface exploration program can aid in identifying artesian conditions. Nominal resistances that require pile lengths that punch through confining layers should be avoided in design. Artesian conditions should be noted on foundation plans to reduce the risk of construction problems.

7.2.9 Scour

Scour is defined as the erosion of soil and rock materials from the streambed and/or stream banks due to flowing water. Foundations subject to scour require input from all disciplines; hydraulics, structures, geotechnical, and construction. Multidiscipline input and communications are required to achieve the most cost effective design.

Though often considered as being localized, scour may consist of multiple components including long term aggradation and degradation, local scour, and contraction scour. Aggradation and degradation involve the long term streambed elevation changes due to an abundance or deficit, respectively, in upstream sediment supply. Local scour involves the removal of material from the immediate vicinity of a substructure unit and can be either clear-water (free of disturbed upstream sediment), or live-bed scour, complicated by the transport of upstream sediment into the scour hole following the storm event. In contrast, contraction scour occurs due to a constriction of the flow and involves erosion across all or most of the channel width and relates directly with the stream stratigraphy at the scour location. Contraction scour may be cyclic and or relate to the passing of a flood.

Different materials, subject to any of the above mentioned types of scour, erode at different rates. In a flood event, loose granular soils can be eroded away in a few hours. Cohesive or cemented soils typically erode more gradually and over several cycles of flooding but can experience the same nominal scour depths as those of cohesionless deposits. As noted earlier in this chapter, the nominal resistance of a driven pile is due to soil resistance along the pile shaft and at the pile toe. Therefore, the erosion of the soil materials providing pile support can have significant detrimental effects on nominal resistance and must clearly be evaluated during the design stage.

Depending on the type of scour and the scour susceptibility of the streambed soils, multiple static resistance calculations may be required to evaluate the nominal resistance of a pile and to establish minimum pile penetration requirements. In the case of local scour, the soil in the scour zone provides resistance at the time of driving that cannot be counted on for long term support. Hence, shaft resistance in the scour zone, although included for drivability considerations, is ignored for design purposes. However, because the erosion is localized, nominal resistance calculations should assume that the vertical effective stress is unchanged. The effects of non-localized scour on long term pile resistance are more severe. In all of degradation, contraction scour, and general scour, a reduction in both the scour zone soil resistance and the vertical effective stress is applied to long term

resistance calculations, due to the widespread removal of the streambed materials. This added reduction in effective stresses can have a significant effect on the calculated shaft and toe resistances. Figure 7-36 provides an illustration of localized and non-localized scour. Table 7-17 presents HEC-18 recommended minimum scour design flood frequencies and scour design check flood frequencies as a function of the hydraulic design flood frequencies.

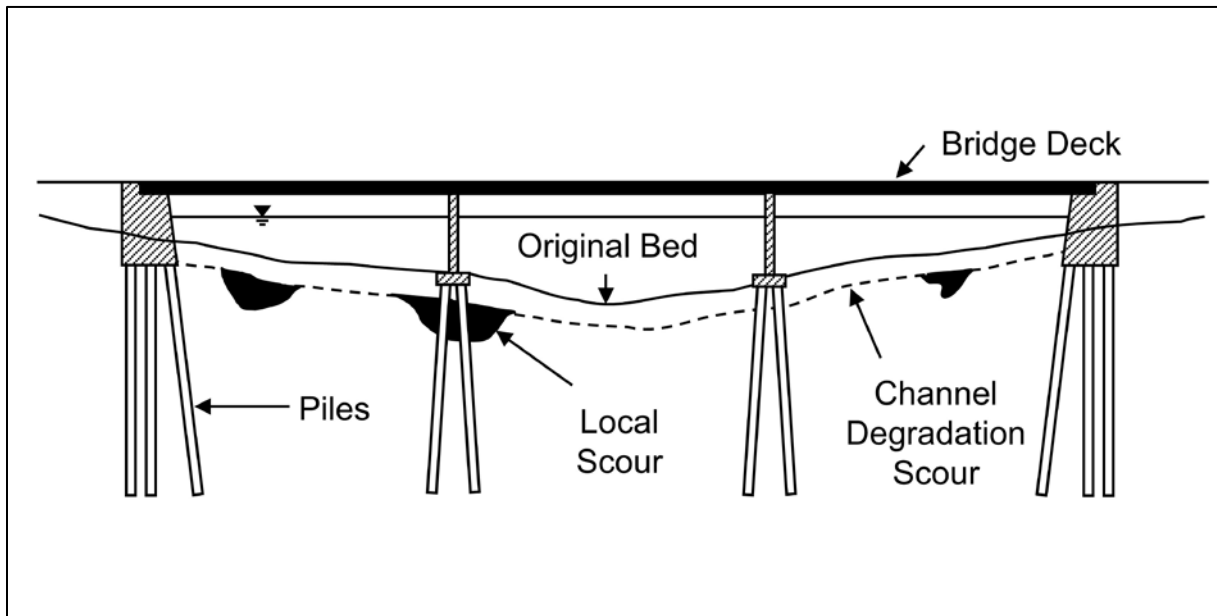


Figure 7-36 Local and channel degradation scour.

Table 7-17 Hydraulic Design, Scour Design, and Scour Design Check Flood Frequencies per HEC-18 (after Arneson et al. 2012)

Hydraulic Design Flood Frequency, Q_D	Scour Design Flood Frequency, Q_S	Scour Design Check Flood Frequency, Q_C
Q_{10}	Q_{25}	Q_{50}
Q_{25}	Q_{50}	Q_{100}
Q_{50}	Q_{100}	Q_{200}
Q_{100}	Q_{200}	Q_{500}

The FHWA publication FHWA HIF-12-003, "Evaluating Scour at Bridges" by Arneson et al. (2012) more commonly known as HEC-18, recommends that the following pile design issues also be considered at bridge sites subject to scour.

1. For pile supported substructures subjected to scour, a reevaluation of the foundation design may require a change in the pile length, number, cross-sectional dimension and type based on the loading and performance requirements and site-specific conditions.
2. Piling should be designed for additional lateral restraint and column action because of the increase in unsupported pile length after scour. The unsupported pile length is discussed in Chapter 8.
3. Local scour holes at piers and abutments may overlap one another in some instances. If local scour holes do overlap, the scour is indeterminate and may be deeper. The top width of a local scour hole on each side of the pier ranges from 1.0 to 2.8 times the depth of local scour. A top width value of 2.0 times the depth of local scour on each side of a pier is recommended.
4. Perform the bridge foundation analysis on the basis that all streambed material in the scour prism above the total scour line has been removed and is not available for nominal resistance or lateral support. In areas where the local scour is confined to the proximity of the footing, the lateral ground stresses on the pile length which remains embedded may not be significantly reduced from the pre-local scour conditions.
5. Placing the top of the footing or pile cap below the streambed a depth equal to the estimated long term degradation and contraction scour depth will minimize obstruction to flood flows and resulting local scour. Even lower footing elevations may be desirable for pile supported footings when the piles could be damaged by erosion and corrosion from exposure to river or tidal currents. However, in deep water situations, it may be more cost effective to situate the pile cap above the mudline and design the foundation accordingly.
6. Stub abutments positioned in the embankment should be founded on piling driven below the elevation of the thalweg including long term degradation and contraction scour in the bridge waterway to assure structural integrity in the event the thalweg shifts and the bed material around the piling scours to the thalweg elevation.

AASHTO (2014) Article 10.7.3.6 notes that scour effects must be considered in determining the minimum pile embedment depth and the required nominal driving resistance, R_{ndr} . The pile penetration depth after the design scour event must satisfy the required nominal resistance for axial and lateral loading. Therefore, the piles need to be driven to the required nominal resistance plus the shaft resistance lost due to scour. The shaft resistance in the scour zone should be calculated using the same static analysis procedure used for design except the scour zone resistance should not be included in the long term nominal resistance. The bias of the static analysis method should also be considered.

If restrike dynamic measurements with signal matching are performed during construction, the shaft resistance in the scour zone materials can be determined and that resistance subtracted from the nominal resistance. The material below the scour elevation must provide the required nominal resistance after the scour event.

7.2.10 Downdrag

Downdrag is ground settlement, or downward soil movement, relative to a pile. Current AASHTO (2014) guidance treats downdrag and the resulting drag force as an additional load that must be supported by the pile foundation. Therefore, downdrag is addressed in AASHTO under the geotechnical strength limit state. The AASHTO approach has generally been conservative in practice as there have been relatively few transportation structures where drag forces have been problematic and corrective action required. However, a design procedure that addresses the effects of downdrag in the geotechnical service limit state and in the pile structural strength limit state is preferred to the current AASHTO geotechnical strength limit state approach. The recommended design approach for downdrag is presented under the service limit state in Section 7.3.6.1.

7.3 SERVICE LIMIT STATES

Service limit states for foundations include settlement, lateral movement, overall stability and scour at the design flood. Foundation movement should be limited to structural tolerances for both the total and differential deformations. As mentioned in AASHTO (2014), the economics of limiting settlement, rotation and horizontal movements should be compared with the cost of designing the respective superstructure to tolerate such movement. This includes maintenance of either structural or roadway elements. Deformations should be computed assuming scour will occur at the design flood.

The service limit state provides limits on stress, deformation, and cracking under regular service conditions. Service limit state geotechnical considerations in driven pile foundation designs include:

- vertical deformation – settlement,
- horizontal movements,
- rotation,
- overall stability, and
- deformations due to scour at the design flood (100 year event).

Settlements should be determined using the Service I Load combination which includes normal operational factors only. If the pile foundation is supported in or on cohesive deposits subject to time dependent consolidation settlement, transient loads may be excluded from the settlement analysis. Settlement methods are covered in Section 7.3.5.

Load combinations for all applicable service limit states should be evaluated for horizontal movement and foundation rotation. Horizontal movement is measured at the foundation top, and should be within structural limits based on column length and stiffness. Sufficient geotechnical resistance and structural stiffness to resist shear and overturning loads should be checked during design. Lateral loading from the structure or earthen elements is covered in Section 7.3.7. Rotational movement is likewise measured at the foundation top and should be restricted.

Service limit state considerations are further discussed in AASHTO (2014) Articles 10.5.2.1 through 10.5.2.4 and associated commentary. All applicable service limit state load combinations must be evaluated.

7.3.1 Tolerable Vertical Deformations and Angular Distortion

Tolerable deformations are limited by the structure type and function, design service life, and anticipated performance at respective displacement levels. Vertical, horizontal, and rotational displacements should be considered during design, where tolerable movement criteria shall be established by empirical procedures, structural analysis, or both (AASHTO 2014).

Agencies often limit tolerable vertical deformations to restrictive values such as 1 inch or less without a rational basis. While there are no technical reasons to set arbitrary deformation limits, there are practical reasons for limits such as the deformation tolerances of attached structures and utilities. Drainage, ride quality, and safety are additional considerations in evaluating the deformation magnitude that can be tolerated by the design.

Moulton (1985) performed a detailed study of 314 bridges to develop a tolerable movement criterion for highway bridges. He recommended limiting values of angular distortion for multi-span and simple span structures. Angular distortion is illustrated in Figure 7-37, and is defined by the differential settlement of the foundation, S_d , relative to the span length, L_s . Both the differential settlement and span length should be expressed in the same units. The tolerable movement criteria recommend by Moulton and illustrated in SHRP 2 Project R19B is presented in Table 7-18. Moulton also recommended that lateral deformations be limited to 1.5 inches for all structures.

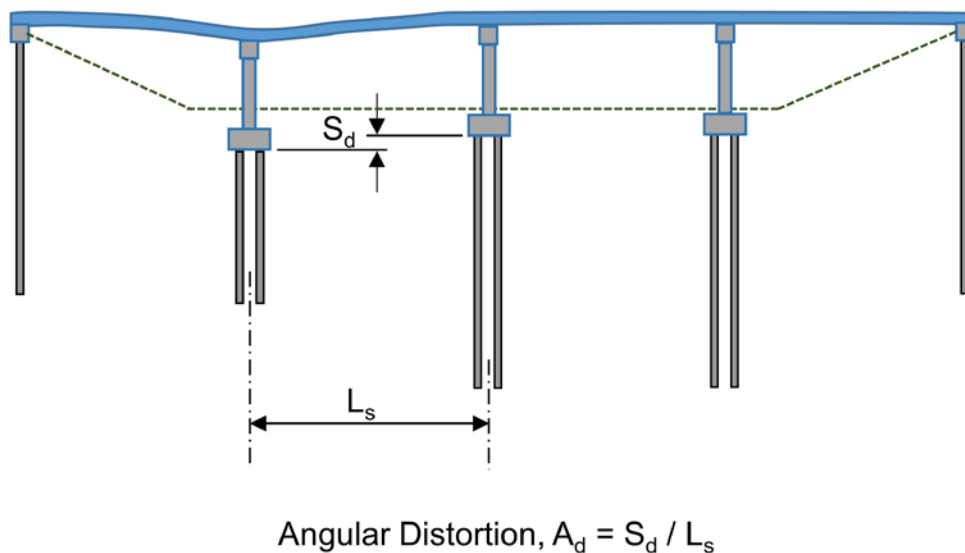


Figure 7-37 Angular distortion due to non-uniform bridge settlement.

Table 7-18 Tolerable Movement Criteria for Bridges

Type of Bridge	Limiting Angular Distortion, S_d/L_s (radians)
Multi-span bridges	0.004
Simple-span bridges	0.005

Note the limiting angular distortion criterion was developed for tolerable bridge movements in the longitudinal direction and should not be used for tolerable bridge movements in the transverse direction.

7.3.1.1 Load Factor for Vertical Deformations

AASHTO (2014) specifications include a load factor for vertical deformations or settlement, γ_{SE} , which is to be considered on a project-specific basis. AASHTO specifications currently recommend a value of 1.0 for this load factor in lieu of project-specific information to the contrary. This load factor is used to assess force effects from settlement on the structural design such as the generation of secondary moments within a given span due to settlement of a substructure support. For example, a settlement load factor of 1.25 does not indicate the computed settlements from a given method should be multiplied by 25% to limit the probability of exceeding tolerable settlements. Rather, the settlement load factor is applied to the limit state load combinations to determine the settlement effects on service and strength limit states. A research effort is in progress to develop additional guidance on application and use of the γ_{SE} load factor.

7.3.2 S-0 Concept for Vertical Deformations

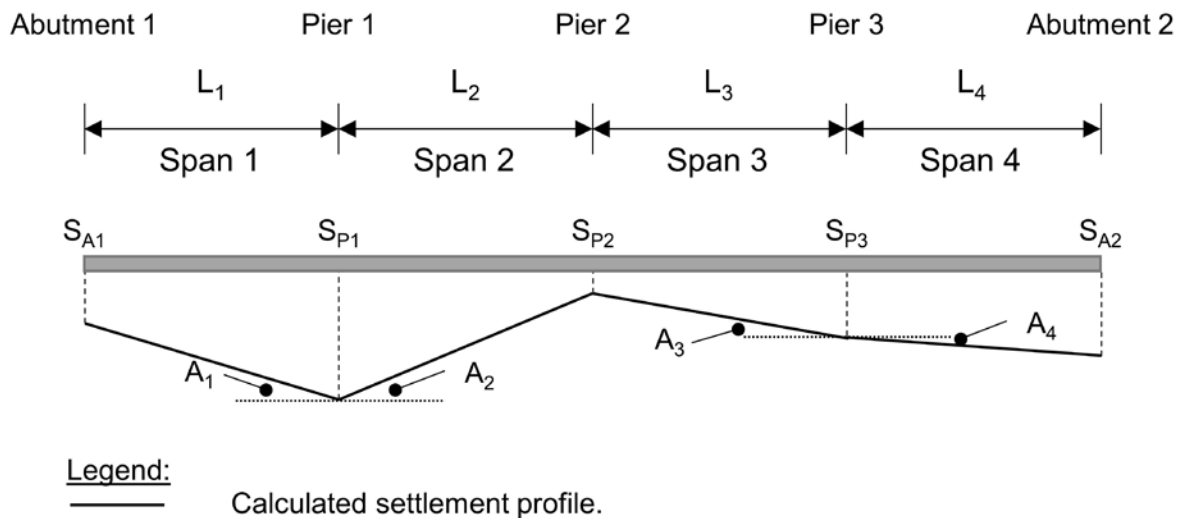
Due to the variability of subsurface conditions, the vertical deformation that occurs at each substructure location will generally vary. In addition, the predicted deformation and actual deformation will differ. Therefore, a bridge structure should be designed to accommodate a realistic value of differential settlement and angular distortion in the longitudinal direction using the S-0 concept proposed by Duncan and Tan (1991). The key points of this method are as follows:

1. The actual settlement of a substructure unit can be as large as the value calculated by a given method.

2. The actual settlement of an adjacent substructure unit can be zero instead of the value calculated using the same method.

The maximum differential settlement between two adjacent foundations using this approach is therefore the maximum total settlement calculated for either foundation unit supporting the span. The maximum angular distortion is then the maximum total settlement divided by the span length. These values represent the design differential settlement, DS_d , and the design angular distortion, DA , respectively.

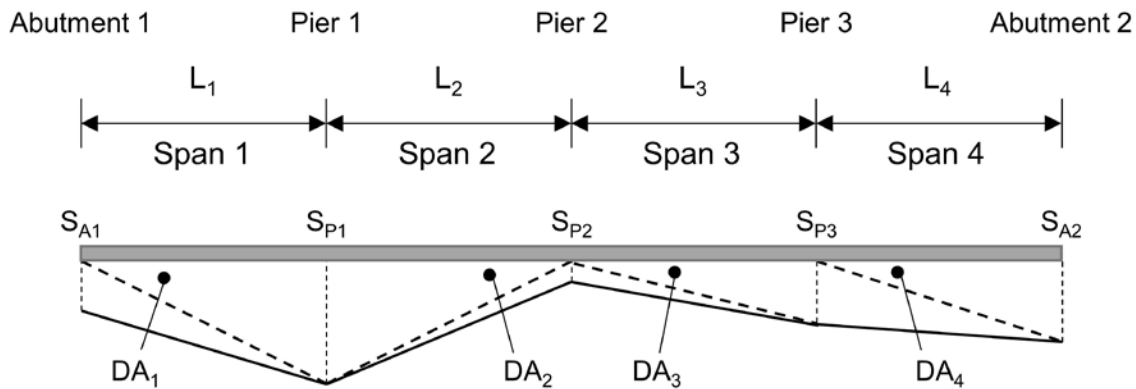
Figure 7-38 illustrates the computed settlement and associated computed angular distortion for a four span bridge supported by two abutments and three piers. The design differential settlement and design angular distortion using the S-0 concept are illustrated in Figure 7-39.



Support Element	Settlement, S
Abutment 1	S_{A1}
Pier 1	S_{P1}
Pier 2	S_{P2}
Pier 3	S_{P3}
Abutment 2	S_{A2}

Span	Differential Settlement	Angular Distortion, A
1	$ S_{A1} - S_{P1} $	$A = S_{A1} - S_{P1} /L_1$
2	$ S_{P1} - S_{P2} $	$A = S_{P1} - S_{P2} /L_2$
3	$ S_{P2} - S_{P3} $	$A = S_{P2} - S_{P3} /L_3$
4	$ S_{P3} - S_{A2} $	$A = S_{P3} - S_{A2} /L_4$

Figure 7-38 Example settlement and angular distortion profile (after Modjeski and Masters 2015).



Legend:

- Calculated settlement profile (refer to Figure 7-38).
- Hypothetical settlement profile assumed for computation of maximum angular distortion, based on $S = 0$ concept.

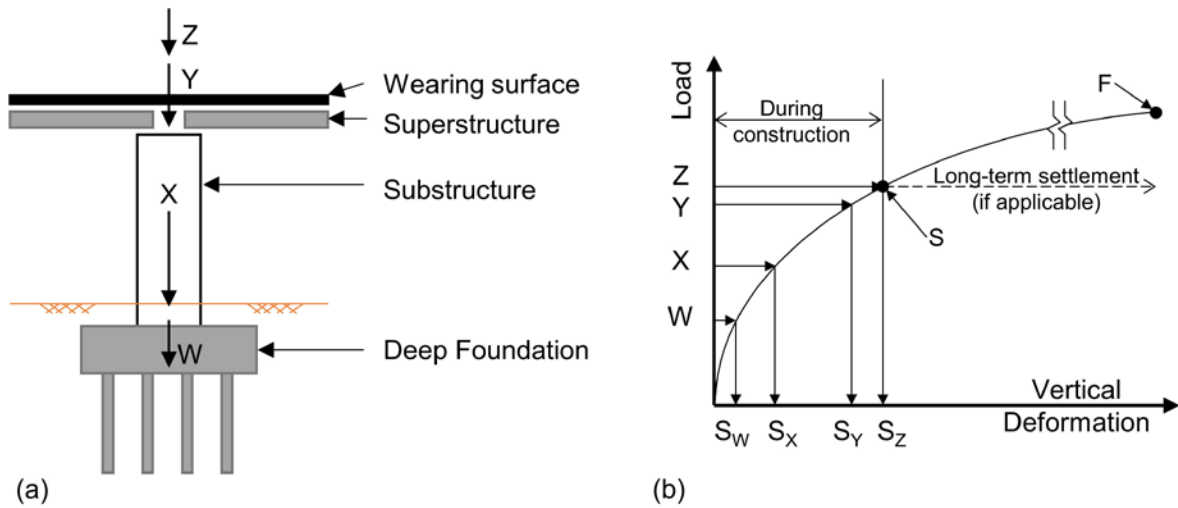
Span	Design Differential Settlement, $D\delta$	Design Angular Distortion, DA
1	$DS_{P1} = S_{P1}$ (assume $S_{A1} = 0$)	$DA_1 = S_{P1}/L_1$
2	$DS_{P1} = S_{P1}$ (assume $S_{P2} = 0$)	$DA_2 = S_{P1}/L_2$
3	$DS_{P3} = S_{P3}$ (assume $S_{P2} = 0$)	$DA_3 = S_{P3}/L_3$
4	$DS_{A2} = S_{A2}$ (assume $S_{P3} = 0$)	$DA_4 = S_{A2}/L_4$

Figure 7-39 Settlement profile with design differential settlement and design angular distortion from S-0 concept (after Modjeski and Masters 2015).

7.3.3 Construction Point Concept

In the example presented in Figure 7-39, the computed settlements and resultant angular distortion are based on the foundation loads applied instantaneously at the same time. In reality, the loads on the foundation are gradually applied. Similarly, settlements from those incrementally applied loads occur as construction progresses. Therefore, settlement and angular distortion relative to several critical points during construction process should be evaluated separately by the designer.

Figure 7-40(a) illustrates the typical sequences in the construction of a bridge pier, while Figure 7-40(b) shows the associated applied load from each sequence and resulting vertical deformation. Plotting the load and deformation results as shown in this figure allow settlement and resulting distortion to be assessed relative to a given



Legend:

W	Load after foundation construction
X	Load after pier column and wall placement
Y	Load after superstructure construction
Z	Load after wearing surface construction
S	Service load (service limit state)
F	Factored load (strength limit state)

S_W	Settlement under load W
S_X	Settlement under load X
S_Y	Settlement under load Y
S_Z	Settlement under load Z

Figure 7-40 Construction point concept: (a) identification of key construction points, (b) estimated load-deformation behavior (after Modjeski and Masters 2015).

point in the construction process. In a typical bridge structure project, settlement that occurs after pier column and superstructure construction but prior to wearing surface construction is often the most relevant. For example, settlement occurring prior to superstructure construction may not be significant to the superstructure design.

Vertical deformation and angular distortion should be determined and evaluated using the construction point concept in limit state designs. The four span bridge example from Figure 7-38 is revisited to illustrate the construction point concept. In Figure 7-41, the calculated settlements (solid line), and hypothetical maximum angular distortion (dashed line) from the S-0 concept are once again plotted. Using construction point load and deformation data similar to Figure 7-40, the range in anticipated settlement and the resulting range in angular distortion are then computed. The results are then depicted by the hatched zone pattern in Figure 7-41.

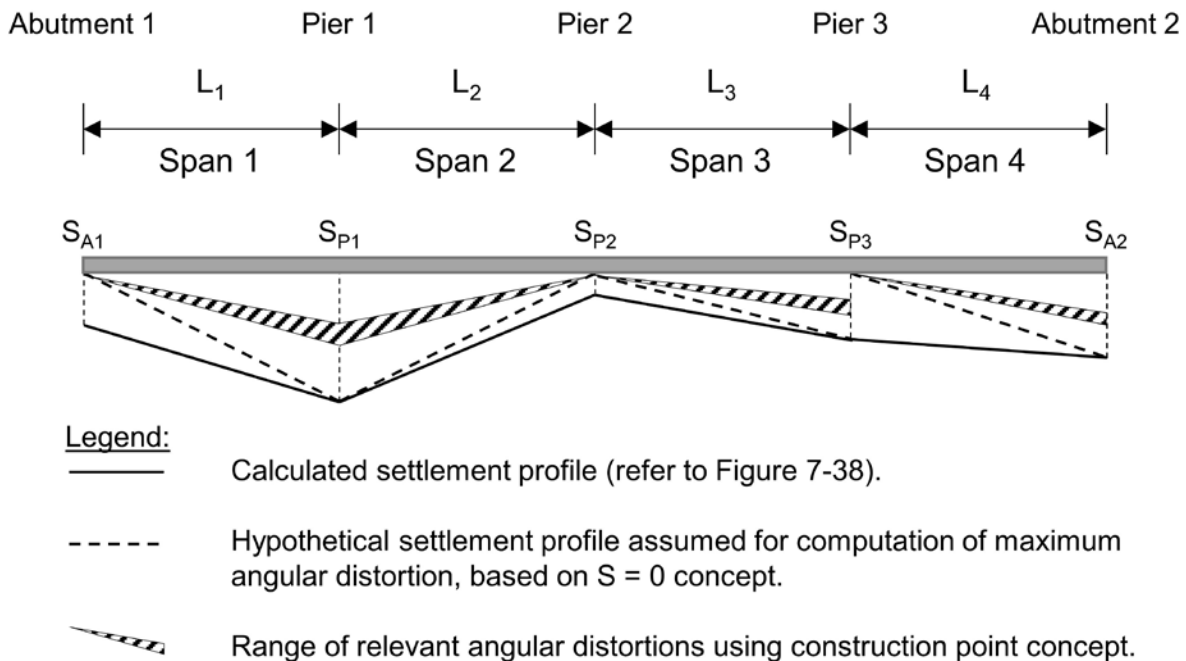


Figure 7-41 Settlement profile with angular distortion from construction point concept (after Modjeski and Masters 2015).

7.3.4 Recommended Procedure for Vertical Deformation Analysis

Modjeski and Masters, Inc., et al. (2015) in SHRP2 Report S2-R19B-RW-1 presented a recommended design procedure for determining vertical deformations or settlement. Their recommended procedure can be summarized as follows:

1. The total foundation settlement should be computed at each substructure location using an appropriate analysis method. Several appropriate analysis methods are described in detail in Section 7.3.5.
 - a. Calculate the total foundation settlement, S_{ta} , using all applicable loads in the Service I load combination.
 - b. Calculate the total foundation settlement, S_{tp} , before construction of the bridge superstructure using all applicable substructure loads in the Service I load combination.
 - c. Calculate, S_{tr} , the relevant total settlement: $S_{tr} = S_{ta} - S_{tp}$.

2.
 - a. Assume that the relevant settlement at each substructure support location can be as large as the magnitude calculated from an appropriate analysis method and that the settlement at the adjacent substructure support is zero. Hence, the differential settlement, S_d , for a bridge span is the maximum relevant settlement value of either support location.
 - b. As illustrated in Figure 7-37, calculate the angular distortion, A , in radians from the ratio of the differential settlement, S_d , divided by the span length, L_s , or: $A_d = S_d / L_s$.
3. Compute the modified angular distortion, A_m , by multiplying A from step 2b by the load factor for settlement, γ_{SE} .
4. Check the modified angular distortion with the owner-specified criteria. Alternatively, angular distortion should be limited to 0.004 radians for multi-span bridges and 0.005 radians for single span bridges if no owner-specified criteria are provided. Other angular distortion limits may be applicable or appropriate due to:
 - vertical clearance,
 - cost of mitigation via larger foundations, realignment, ground improvement, or surcharge,
 - rideability,
 - tolerable deformation limits of other associated structures,
 - roadway drainage,
 - aesthetics, and
 - safety.
5. Evaluate the ramifications of the computed angular distortions on the structure. Modify the foundation design if necessary based on the structural ramifications.
6. The above procedure is also recommended for structures where foundations have been designed for equal total settlement due to the uncertainty in the settlement prediction from any given method.

7.3.5 Pile Group Settlement

Pile groups supported in and underlain by cohesionless soils will produce only immediate settlements. This means the settlements will occur immediately as the pile group is loaded. Pile groups supported in and underlain by cohesive soils may produce both immediate settlements and primary consolidation and secondary compression settlements that occur over a period of time. In highly over-consolidated clays, the majority of the foundation settlement will occur immediately. Primary consolidation settlements will generally be the major source of foundation settlement in normally consolidated clays.

The settlement of a pile group is likely to be many times greater than the settlement of an individual pile carrying the same load per pile as each pile in the pile group. Figure 7-42 illustrates that for a single pile, only a small zone of soil around and below the pile toe is subjected to vertical stress. This also illustrates that for a pile group, a considerable depth of soil around and below the pile group is stressed. The settlement of the pile group may be large, depending on the compressibility of the soils within the stressed zone.

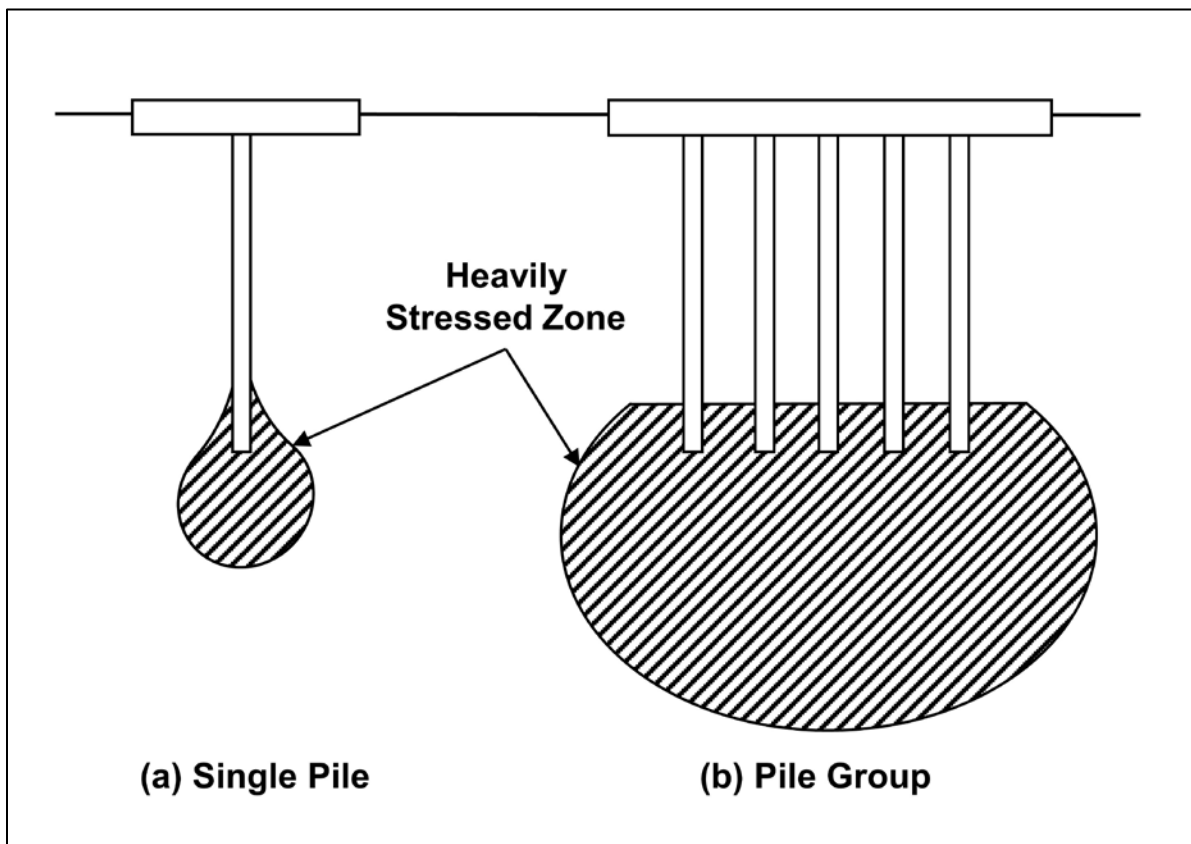


Figure 7-42 Stress zone from single pile and pile group (after Tomlinson 1994).

Methods for estimating settlement of pile groups are provided in the following sections. Methods for estimating single pile settlements are not provided because piles are usually installed in groups.

7.3.5.1 Elastic Compression of Piles

The pile group settlement methods discussed in the following sections only consider soil settlements and do not include the settlement caused by elastic compression of pile material due to the imposed axial load. Therefore, the elastic compression should also be computed and this settlement added to the group settlement estimates of soil settlement. The elastic compression, Δ , can be computed by the following expression:

$$\Delta = \frac{QL}{AE} \quad \text{Eq. 7-48}$$

Where:

- Q = unfactored axial load (kips).
- L = total pile length (inches).
- A = pile cross sectional area (in²).
- E = elastic modulus of pile material (ksi).

The modulus of elasticity for steel piles is 29,000 ksi. For concrete piles, the modulus of elasticity varies with concrete compression strength and is generally on the order of 4,000 ksi. The elastic compression of short piles is usually quite small and can often be neglected in design. For pile with significant shaft resistance, much of the load will be transferred to the soil over the length of the pile. In those cases, the elastic compression will be overestimated by Equation 7-48.

7.3.5.2 Group Settlement in Cohesionless Soils

Settlement in cohesionless soils is generally considered elastic for deformation calculations. Meyerhof (1976) provided elastic settlement correlations based on SPT and CPT test data as described in 7.3.5.2.1 and 7.3.5.2.2, respectively. Elastic settlement may also be estimated by the Hough (1959) method shown in Equation 7-49. The stress increase in a soil layer due to the foundation loads should be determined using the equivalent footing method with consideration of the soil stratigraphy.

$$S = H_o \left[\frac{1}{C'} \log \frac{\sigma'_{vo} + \Delta\sigma}{\sigma'_{vo}} \right] \quad \text{Eq. 7-49}$$

Where:

- S = total layer settlement (feet).
- H_o = initial soil layer thickness (feet).
- C' = dimensionless bearing capacity index from Figure 7-43, determined from the average corrected SPT N value for the layer with consideration of the SPT hammer type.
- σ'_{vo} = vertical effective stress at midpoint of layer prior to stress increase (ksf).
- $\Delta\sigma$ = average change in vertical stress in the layer in (ksf).

Cheney and Chassie (2002) report that FHWA experience with this method indicates the method is usually conservative and can overestimate settlements by a factor of 2. This conservatism is attributed to the use of the original bearing capacity index chart from Hough (1959) which was based upon SPT donut hammer data. Based upon average energy variations between SPT donut, safety, and automatic hammers reported in technical literature, Figure 7-43 now includes a correlation between SPT N values from safety and automatic hammers and bearing capacity index. The safety hammer values are considered N_{60} values. This modification should improve the accuracy of settlement estimates with this method.

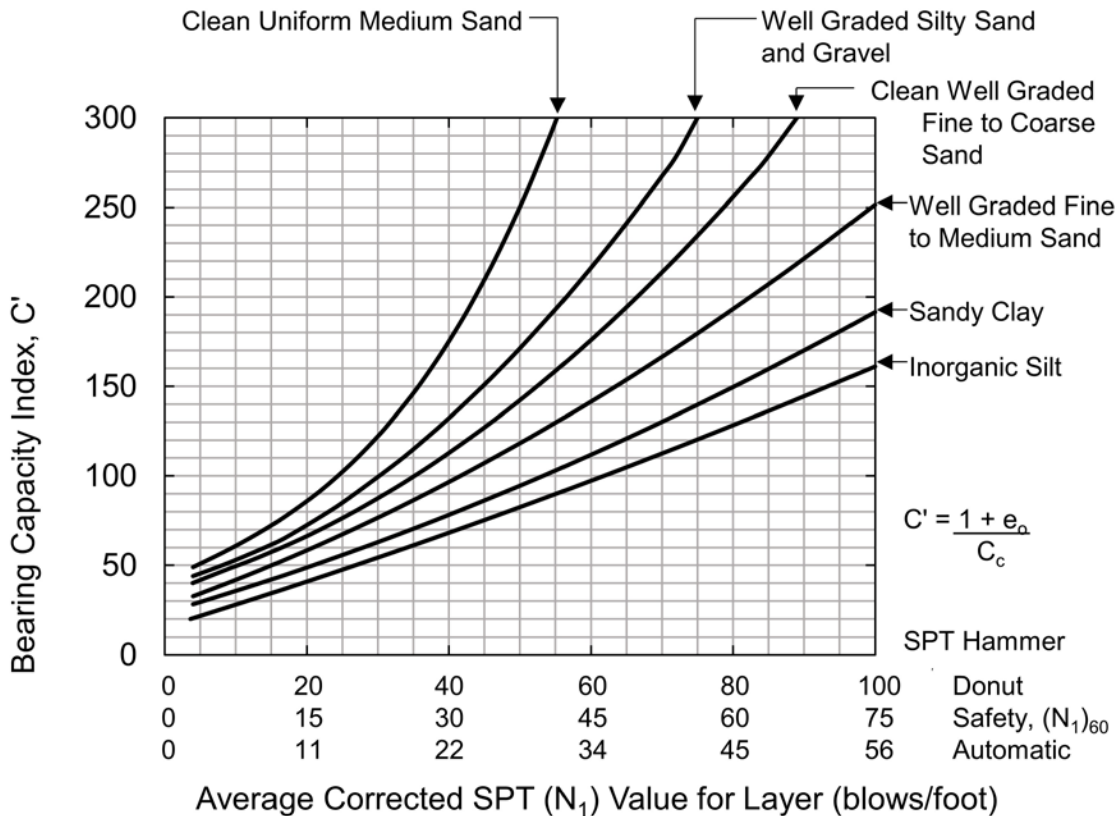


Figure 7-43 Values of the bearing capacity index, C' , for granular soil (data from Hough 1959).

7.3.5.2.1 Method Based on SPT Test Data

Meyerhof (1976) recommended that the settlement of a pile group in a homogeneous sand deposit not underlain by a more compressible soil at a greater depth may be conservatively estimated by the following expression:

$$S = \frac{4p_f I_f \sqrt{B}}{N_{1(60)}} \quad \text{Eq. 7-50}$$

For silty sand, use:

$$S = \frac{8p_f I_f \sqrt{B}}{N_{1(60)}} \quad \text{Eq. 7-51}$$

In which

$$I_f = 1 - \frac{D'}{8B} \geq 0.5 \quad \text{Eq. 7-52}$$

Where:

- S = estimated total settlement (inches).
- p_f = design foundation pressure (ksf).
- B = width of pile group (feet).
- $N_{1(60)}$ = average corrected SPT N value within a depth B below pile toe.
- D' = 2/3 pile embedded length (feet).
- I_f = influence factor for group embedment.

For piles in cohesionless soils underlain by cohesive deposits, the method presented in Sections 7.3.5.3 should be used.

7.3.5.2.2 Method Based on CPT Test Data

Meyerhof (1976) recommended the following relationship to estimate maximum settlements using cone penetration test results for saturated cohesionless soils.

$$S = \frac{p_f B I_f}{2q_{ca}} \quad \text{Eq. 7-53}$$

In which

$$I_f = 1 - \frac{D'}{8B} \geq 0.5 \quad \text{Eq. 7-54}$$

Where:

- S = estimated total settlement (inches).
- p_f = design foundation pressure (ksf).
- B = width of pile group (feet).

- I_f = influence factor for group embedment.
- q_{ca} = average cone tip resistance within depth of B below the pile toe (ksf).
- D' = $2/3$ pile embedded length (feet).

7.3.5.3 Group Settlement in Cohesive Soils

Terzaghi and Peck (1967) proposed that pile group settlements could be evaluated using an equivalent footing situated at a depth of $1/3 D$ above the pile toe. This concept is illustrated in Figure 7-44. For a pile group consisting of only vertical piles, the equivalent footing has a plan area $(B)(Z)$ that corresponds to the perimeter dimensions of the pile group as depicted previously in Figure 7-31. The pile group load over this plan area is then the stress transferred to the soil through the equivalent footing. The load is assumed to spread within the frustum of a pyramid with side slopes at 30° and to cause uniform additional vertical stress at lower levels.

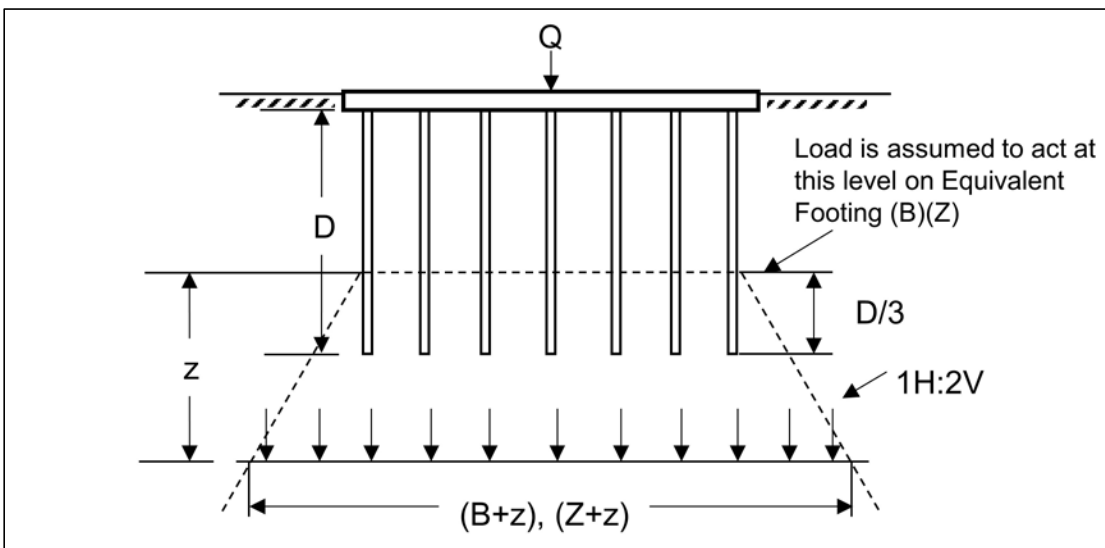


Figure 7-44 Equivalent footing concept.

The stress at any level is equal to the load carried by the group divided by the plan area of the base of the frustum at that level. AASHTO (2014) Article 10.7.2.3.1 states that the load used in calculating group settlement is the permanently applied load. Equation 7-55 should be used to calculate the change in stress for a given depth, z , below the equivalent footing.

$$\Delta\sigma'_d = \frac{Q}{(B+z)(Z+z)} \quad \text{Eq. 7-55}$$

Where:

$\Delta\sigma'_d$ = change in stress below equivalent footing (inches).

- Q = unfactored permanent load (kips).
 B = width of pile group (feet).
 Z = length of pile group (feet).
 z = depth below equivalent footing.

Rather than fixing the equivalent footing at a depth of a D above the pile toe for all soil conditions, the depth of the equivalent footing should be adjusted based upon soil stratigraphy and load transfer mechanism to the soil. Figure 7-45 presents the recommended equivalent footing location and stress distribution proposed by Duncan and Buchignani, (1976) for a pile group driven through a soft clay layer and into a medium or firm layer.

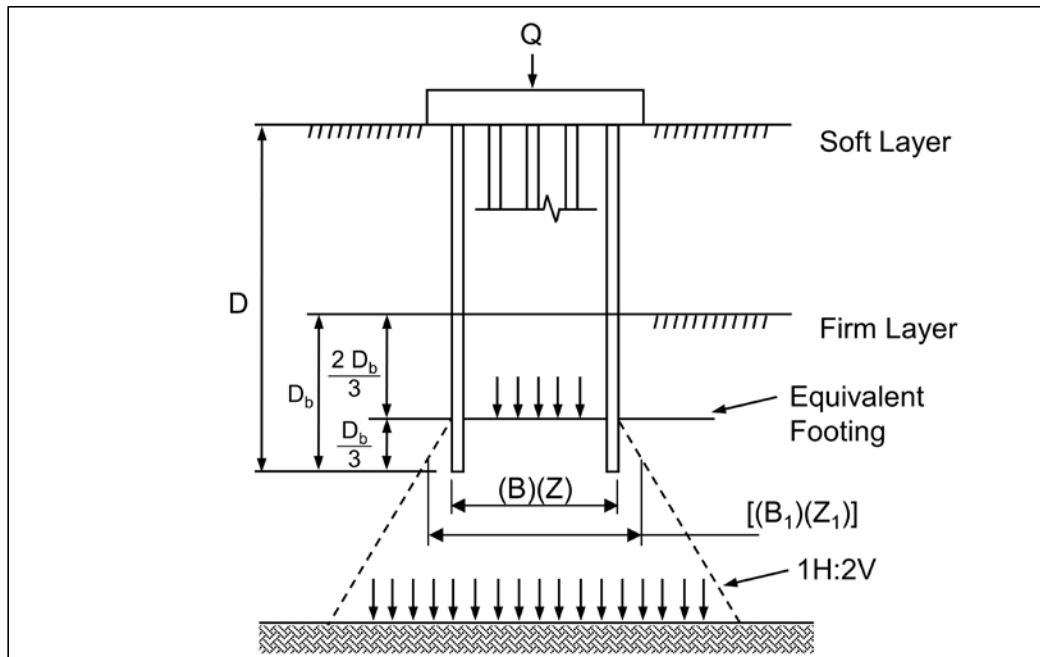


Figure 7-45 Stress distribution below equivalent footing for a pile group in firm clay (after Duncan and Buchignani, 1976).

Figure 7-46 presents other recommended locations of the equivalent footing for the following load transfer and soil resistance conditions:

- toe resistance piles in hard clay or sand underlain by soft clay,
- piles supported by shaft resistance in clay,
- piles supported by shaft resistance in sand underlain by clay, and
- piles supported by shaft and toe resistance in layered soil profile.

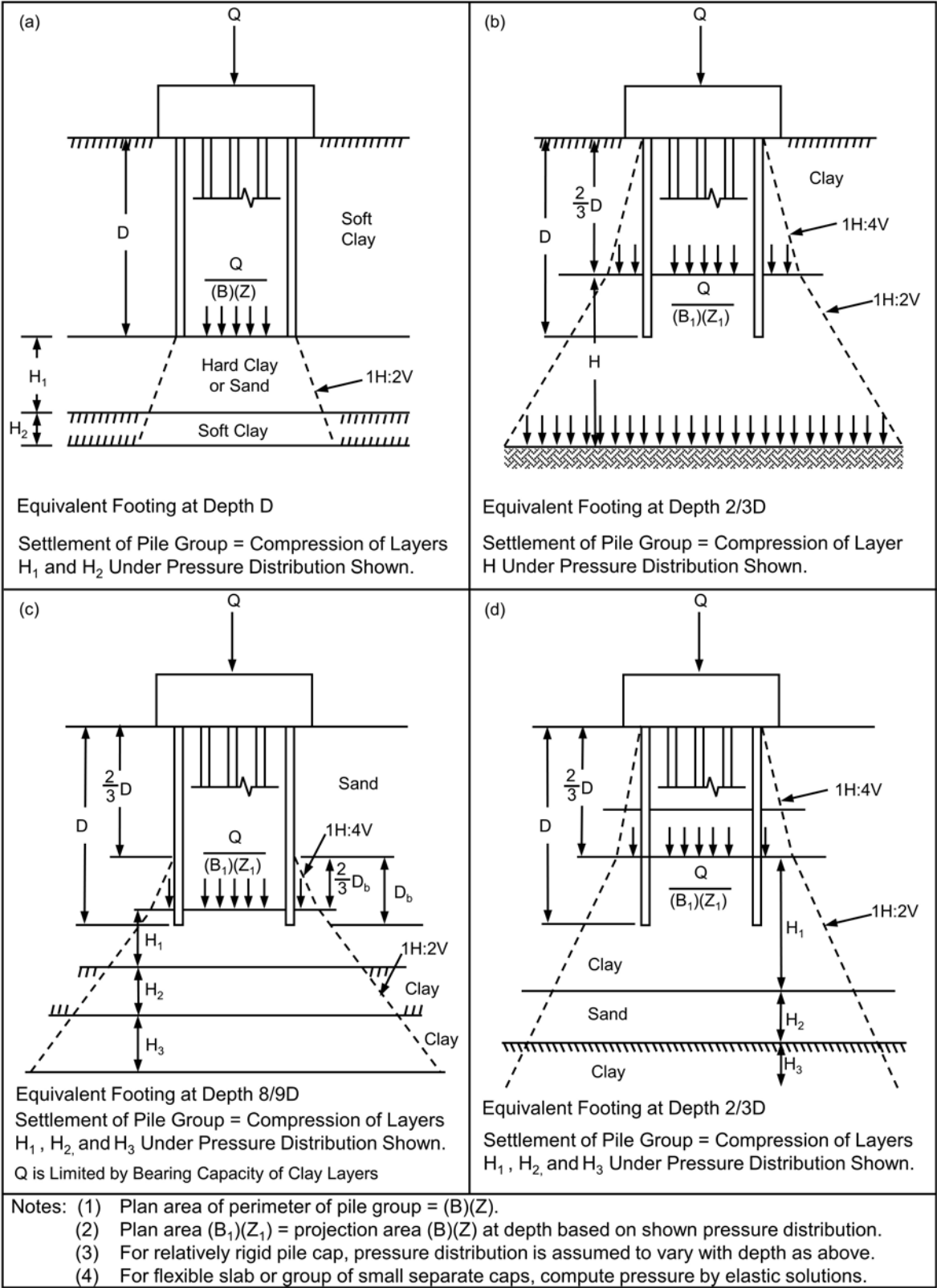


Figure 7-46 Stress distribution below equivalent footing for a pile group (modified from Cheney and Chassie 2000).

Consolidation settlements are calculated based on the stress increase in the underlying layers. Equations 7-56 through 7-58 provide primary consolidation settlement estimations for cohesive soil. Parameters determined from a consolidation test are shown in the plot of void ratio versus vertical effective stress in Figure 7-47.

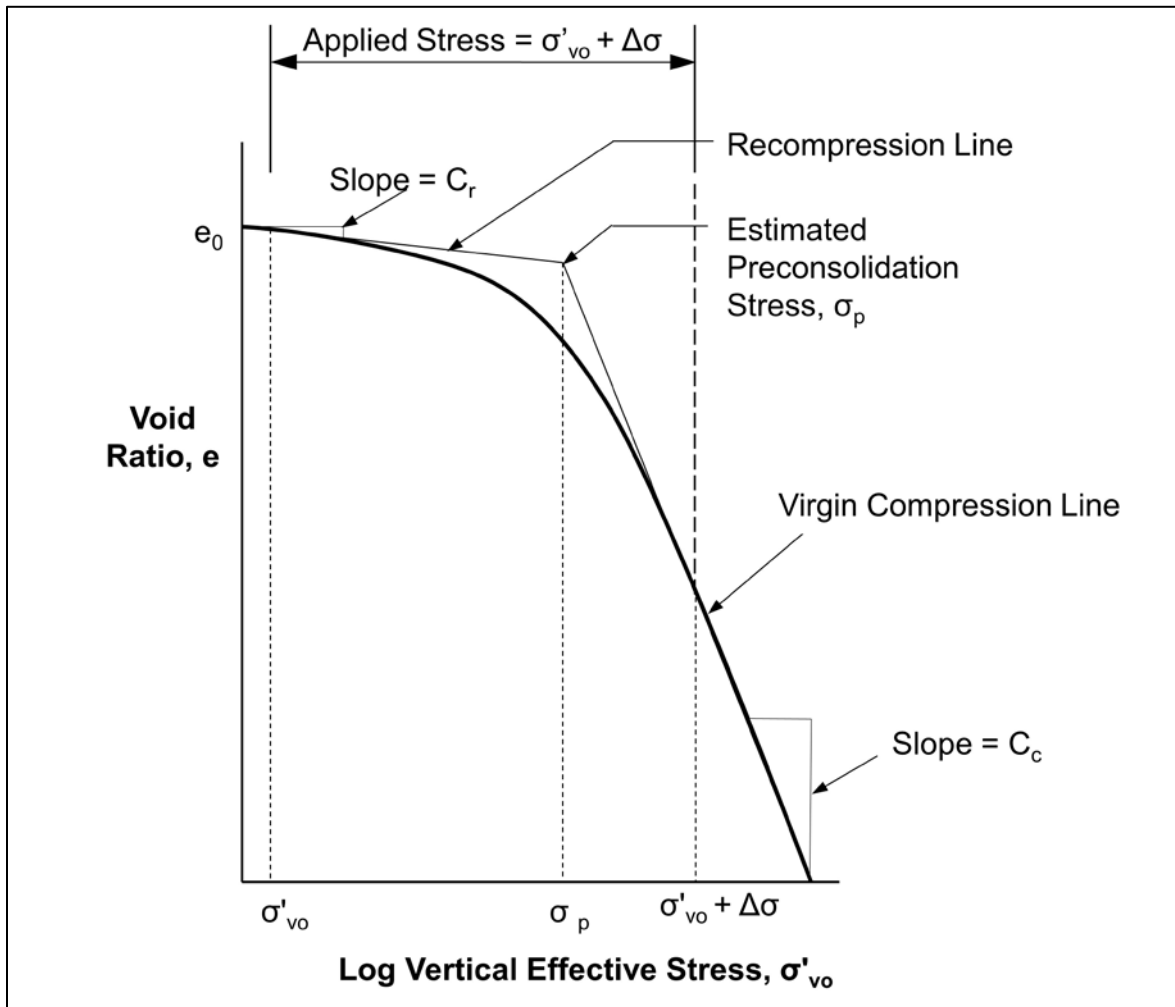


Figure 7-47 Plot of void ratio vs. vertical effective stress from consolidation test. For normally consolidated ($\sigma'_{vo} = \sigma_p$) cohesive soil layers:

$$S_c = \sum_i^n \frac{C_c}{1 + e_o} H_o \log \left(\frac{\sigma'_{vo} + \Delta\sigma}{\sigma'_{vo}} \right) \quad \text{Eq. 7-56}$$

For overconsolidated soil with ($\sigma'_{vo} + \Delta\sigma \leq \sigma_p$):

$$S_c = \sum_i^n \frac{C_r}{1 + e_o} H_o \log \left(\frac{\sigma'_{vo} + \Delta\sigma}{\sigma'_{vo}} \right) \quad \text{Eq. 7-57}$$

For overconsolidated soil with $(\sigma'_{vo} + \Delta\sigma > \sigma_p)$:

$$S_c = \sum_i^n \frac{C_r}{1+e_o} H_o \log\left(\frac{\sigma_p}{\sigma'_{vo}}\right) + \frac{C_c}{1+e_o} H_o \log\left(\frac{\sigma'_{vo} + \Delta\sigma}{\sigma_p}\right) \quad \text{Eq. 7-58}$$

Where:

- S_c = settlement estimate from primary consolidation (feet).
- e_o = initial soil layer void ratio.
- H_o = initial soil layer height (feet).
- σ_p = preconsolidation stress (psf).
- σ'_{vo} = vertical effective stress at midpoint of each layer prior to loading (psf).
- $\Delta\sigma$ = additional pressure from structural loading (psf).
- C_r = recompression index from consolidation test.
- C_c = compression index from consolidation test.

STEP BY STEP PROCEDURE FOR GROUP SETTLEMENT IN COHESIVE SOILS

- STEP 1 Determine the new load imposed on soil by the pile group.
- a. Determine the location of the equivalent footing. For pile groups supported primarily by toe resistance, the equivalent footing is placed at the pile toe as illustrated in Figure 7-46 (a). For pile groups supported primarily by shaft resistance, the equivalent footing is placed at a depth of $\frac{2}{3} D$ as shown in Figure 7-46 (b, c, and d).
 - b. Determine the dimensions of the equivalent footing. For pile groups consisting only of vertical piles, the equivalent footing (unless modified for load transfer as in Figure 7-46) has the same dimensions as the length and width of the pile group from Figure 7-31. For pile groups supported primarily by shaft resistance that include batter piles, the plan area of the footing should be calculated from the dimensions of the pile group at depth $\frac{2}{3} D$, including the plan area increase due to the pile batter. For toe resistance groups with batter piles, the equivalent footing area should be the dimensions of the pile group at depth D , including the area increase due to pile batter.
 - c. Determine the stress distribution to soil layers below the equivalent footing up to the depth at which the stress increase from the equivalent footing is less than 10% of existing vertical effective stress at that depth. Remember that the equivalent footing size may be increased and the

footing stress correspondingly reduced as a result of load transfer above the footing location or in groups with batter piles. The depth at which the stress increase is less than 10% will provide the total thickness of cohesive soil layer or layers to be used in performing settlement computations. AASHTO (2014) Article 10.7.2.3.1 states that the load used in calculating settlement is the permanently applied load.

- d. Divide the cohesive soil layers in the affected stress increase zone into several thinner layers with thickness of 5 to 10 feet. The thickness of each layer is the thickness H for the settlement computation for that layer.
- e. Determine the existing vertical effective stress, σ'_{vo} , at the midpoint of each layer.
- f. Determine the imposed stress increase, $\Delta\sigma$, at the midpoint of each affected soil layer based on the appropriate stress distribution.

STEP 2 Determine consolidation test parameters.

Plot the results of consolidation test(s) as shown in Figure 7-47 followed by determination of settlement parameters.

STEP 3 Compute settlements.

Using the appropriate settlement equation, Equation 7-56, 7-57 or 7-58, compute the settlement of each affected soil layer. Sum the settlements of all layers to obtain the total estimated soil settlement from the pile group. Add the elastic compression of the pile under the design load to obtain the total estimated pile group settlement.

7.3.5.4 Time Rate of Settlement in Cohesive Soils

Settlement analyses in cohesive soils should also evaluate the time required for the anticipated settlement to occur. In time rate computations, the time for 90% consolidation to occur is typically used to determine the total time required for primary settlement. The time rate of settlement of a cohesive soil deposit can be calculated from:

$$t = \frac{TH_v^2}{C_v} \quad \text{Eq. 7-59}$$

Where:

- t = time for settlement to occur (days).
- T = theoretical time factor for percentage of primary consolidation to occur (Table 7-19).
- H_v = maximum vertical drainage path in the cohesive layer (feet).
- C_v = coefficient of consolidation (ft²/day).

The term H_v should not be confused with the term H_o used in the settlement equations for cohesive soils. H_v is the maximum distance water must travel from the compressible cohesive deposit to reach a more permeable layer. In the case of a cohesive layer overlain and underlain by a permeable granular layer, H_v would be ½ the cohesive layer thickness. However, if the cohesive layer were overlain by a permeable granular layer and underlain by a non-permeable rock layer, H_v would be the full thickness of the cohesive deposit. Additional discussion on time rate of consolidation can be found in Samtani and Nowatzki (2006).

Table 7-19 Time Factors for Settlement

Primary Settlement (%)	Time Factor (T)
10	0.008
20	0.031
30	0.071
40	0.126
50	0.197
60	0.287
70	0.403
80	0.567
90	0.848

7.3.5.5 Group Settlement in Layered Soils

Piles are often installed in a layered soil profile consisting of cohesionless and cohesive soils or in soil profiles where an underlying soil stratum of different consistency is affected by the pile group loading. In these cases, group settlement will be influenced by the stress increase in and compressibility of the affected layers.

Figures 7-46(a), 7-46(c) and 7-46(d) may be used to determine the location of the equivalent footing and to evaluate the resulting stress increase in a soil layer. The settlement of each layer is then calculated using the appropriate settlement equation presented in Section 7.3.5.2 or Section 7.3.5.3.

STEP BY STEP PROCEDURE FOR GROUP SETTLEMENT IN LAYERED SOIL PROFILES

STEP 1 Determine the new load imposed on soil by the pile group.

- a. Determine the location of the equivalent footing. For pile groups supported primarily by toe resistance, the equivalent footing is placed at the pile toe as illustrated in Figure 7-46 (a). For pile groups supported primarily by shaft resistance in sands underlain by cohesive soils, the equivalent footing is placed at a depth of $8/9 D$ as shown in Figure 7-46 (c). For pile groups in layered soils supported by a combination of shaft and toe resistance, the equivalent footing is placed at $2/3 D$ as shown in Figure 7-46 (d).
- b. Determine the dimensions of the equivalent footing. For pile groups consisting only of vertical piles, the equivalent footing (unless modified for load transfer as in Figures 7-46 (c) and 7-46 (d)) has the same dimensions as the length and width of the pile group from Figure 7-31. For pile groups supported primarily by shaft resistance that include batter piles, the plan area of the footing should be calculated from the dimensions of the pile group at the equivalent footing depth that includes the plan area increase due to the pile batter. For toe resistance groups with batter piles, the equivalent footing area should be calculated from the dimensions of the pile group at depth D , including the plan area increase due to the pile batter.
- c. Determine the stress distribution to soil layers below the equivalent footing up to the depth at which the stress increase from the equivalent footing is less than 10% of existing vertical effective stress at that depth. Remember that the equivalent footing size may be increased and the footing stress correspondingly reduced as a result of load transfer above the footing location or in groups with batter piles. The depth at which the stress increase is less than 10% will provide the total thickness of soil to be evaluated in the settlement

computations. AASHTO (2014) Article 10.7.2.3.1 states that the load used in calculating settlement is the permanently applied load.

- d. Divide the soil layers in the affected stress increase zone into several thinner layers of 5 to 10 feet in thickness. The thickness of each layer is the thickness H for the settlement computation for that layer.
- e. Determine the existing vertical effective stress, σ'_{vo} , at the midpoint of each soil layer.
- f. Determine the imposed stress increase, $\Delta\sigma$, at the midpoint of each affected soil layer based on the appropriate stress distribution.

STEP 2 Determine consolidation test parameters for each cohesive layer.

Plot results of consolidation test(s) as shown in Figure 7-47.

Determine σ_p , e_o , C_r and C_c values from the consolidation test data.

STEP 3 Determine bearing capacity index for each cohesionless layer.

Determine the average corrected SPT N value, for each cohesionless layer. Use N_{60} or the appropriate SPT hammer type in Figure 7-43 to obtain the bearing capacity index for each layer. The safety hammer N values in Figure 7-43 are considered representative N_{60} values.

STEP 4 Compute settlements.

Using the appropriate settlement equation, compute the settlement of each affected soil layer. Sum the settlements of all layers to obtain the total estimated soil settlement from the pile group. Add the elastic compression of the pile under the design load to obtain the total estimated pile group settlement.

7.3.5.6 Group Settlement Using the Janbu Tangent Modulus Approach

The previous methods of group settlement analyses assume a linear relationship between induced stress and soil strain. However except at very small strains, a non-linear relationship exists between stress and strain. Figure 7-48 illustrates that a stress increase at a small original stress will result in a larger strain than the same stress increase applied at a greater original stress.

Janbu (1963, 1965) proposed a tangent modulus approach that is referenced in the Canadian Foundation Engineering Manual (1985). In this method, the stress strain relationship of soils is expressed in terms of a dimensionless modulus number, m , and a stress exponent, j . Values of the modulus number can be determined from conventional laboratory triaxial or oedometer tests. The stress exponent, j , can generally be taken as 0.5 for cohesionless soils and 0 for cohesive soils.

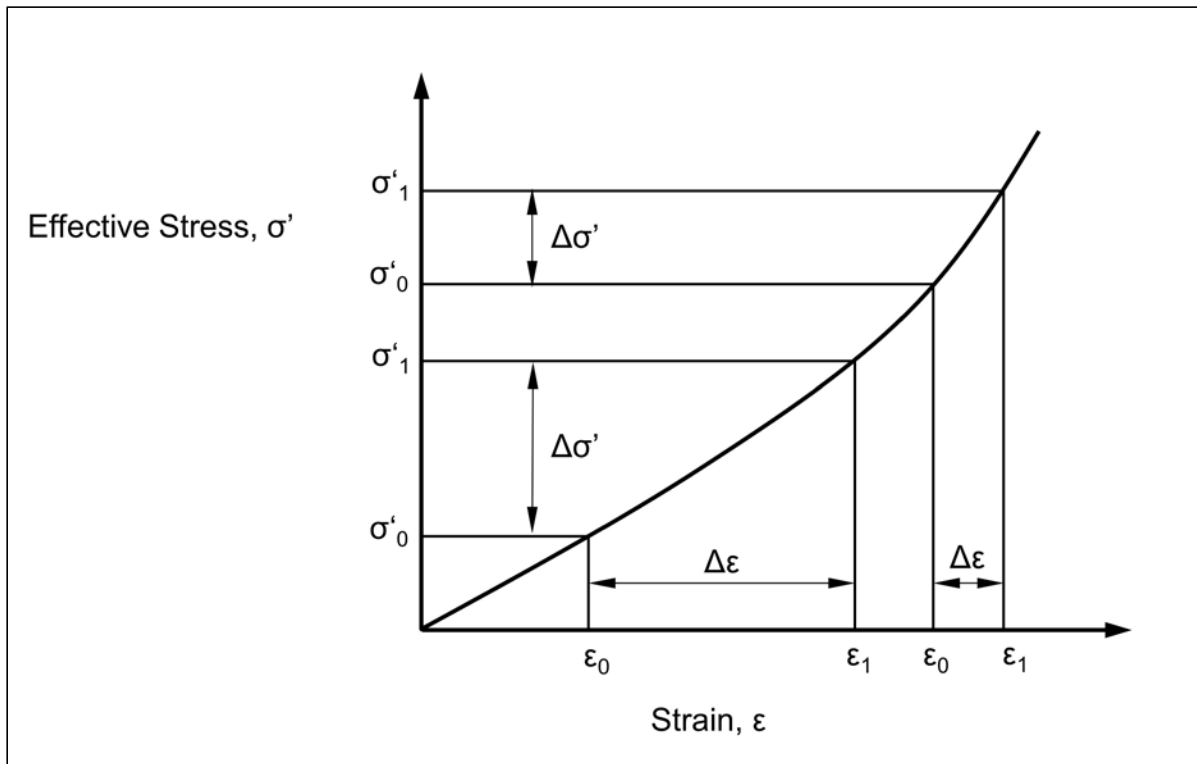


Figure 7-48 Non-linear relation between stress and strain in soil (after Fellenius 1990).

The following seven equations are used to calculate the strain for normally and over consolidated, cohesionless and cohesive soils. The terms used in these four equations are as follows:

- ε = strain from the increase in effective stress.
- E_s = elastic modulus of soil (ksf).
- m_n = dimensionless modulus number.
- m_{nr} = dimensionless recompression modulus number.
- j = stress exponent in Table 7-20.
- σ'_1 = new effective stress after stress increase (ksf).
- σ'_0 = effective stress prior to stress increase (ksf).
- σ'_p = preconsolidation stress (ksf).
- σ_r = constant reference stress = 2 ksf.

For cohesionless soils ($j > 0$), the strain induced by an increase in effective stress may be expressed as shown in Equation 7-60:

$$\varepsilon = \frac{1}{m_n j} \left[\left(\frac{\sigma'_1}{\sigma_r} \right)^j - \left(\frac{\sigma'_o}{\sigma_r} \right)^j \right] \quad \text{Eq. 7-60}$$

For dense coarse grained soils ($j = 1$), the following equation should be used to calculate the strain induced by an increase in effective stress:

$$\varepsilon = \frac{1}{E_s} [\sigma'_1 - \sigma'_o] \quad \text{Eq. 7-61}$$

For sandy or silty soil ($j = 0.5$), the Equation 7-62 should be used to calculate the strain induced by an increase in effective stress:

$$\varepsilon = \frac{\sqrt{2}}{m_n} \left[\sqrt{\sigma'_p} - \sqrt{\sigma'_o} \right] \quad \text{Eq. 7-62}$$

For overconsolidated sandy or silty soil, where the final stress will exceed the preconsolidation stress, Equation 7-63 should be used to calculate the induced strain:

$$\varepsilon = \frac{\sqrt{2}}{m_{nr}} \left[\sqrt{\sigma'_1} - \sqrt{\sigma'_o} \right] + \frac{\sqrt{2}}{m_n} \left[\sqrt{\sigma'_1} - \sqrt{\sigma'_p} \right] \quad \text{Eq. 7-63}$$

For cohesive soils, the stress exponent is zero, ($j = 0$). The strain induced by an increase in effective stress in a normally consolidated cohesive soil is then as follows:

$$\varepsilon = \frac{1}{m_n} \ln \left[\left(\frac{\sigma'_1}{\sigma'_o} \right) \right] \quad \text{Eq. 7-64}$$

For overconsolidated cohesive soils, if the applied foundation stress exceeds the preconsolidation stress, the following equation should be used to calculate the strain:

$$\varepsilon = \frac{1}{m_{nr}} \ln \left[\left(\frac{\sigma'_p}{\sigma'_o} \right) \right] + \frac{1}{m_n} \ln \left[\left(\frac{\sigma'_1}{\sigma'_p} \right) \right] \quad \text{Eq. 7-65}$$

For overconsolidated cohesive soils, if the applied foundation stress does not exceed the preconsolidation stress, the following equation should be used to calculate strain:

$$\varepsilon = \frac{1}{m_{nr}} \ln \left[\left(\frac{\sigma'_1}{\sigma'_{vo}} \right) \right] \quad \text{Eq. 7-66}$$

In cohesionless soils, the modulus number can be calculated from the soil modulus of elasticity, E_s (ksf), and the previously described terms using Equation 7-67:

$$m_n = \frac{\sqrt{2}E_s}{(\sqrt{\sigma'_1} + \sqrt{\sigma'_o})} \quad \text{Eq. 7-67}$$

In cohesive soils, the modulus number, m_n , or recompression modulus number, m_{nr} , can be calculated from the initial void ratio, e_o , and the compression index, C_c , or recompression index, C_r . The modulus number is calculated from:

$$m_n = 2.30 \left[\frac{1+e_o}{C_c} \right] \quad \text{Eq. 7-68}$$

The recompression modulus number, m_{nr} , is calculated by substituting the recompression index, C_r , for the compression index, C_c , as follows:

$$m_{nr} = 2.30 \left[\frac{1+e_o}{C_r} \right] \quad \text{Eq. 7-69}$$

The Janbu tangent modulus approach is quite adaptable to calculating pile group settlements in any soil profile. For reference purposes, typical and normally conservative modulus number and stress exponent values from the Canadian Foundation Engineering Manual (1985) are presented in Table 7-20. These values may be useful for preliminary settlement estimates. A step by step procedure for this method follows.

STEP BY STEP PROCEDURE FOR PILE GROUP SETTLEMENT BY JANBU METHOD

- STEP 1 Determine the new load imposed on soil by the pile group.
- a. Determine the location of the equivalent footing. For pile groups supported primarily by toe resistance, the equivalent footing is placed at the pile toe as illustrated in Figure 7-46 (a). For pile groups supported primarily by shaft resistance in sands underlain by cohesive soils, the equivalent footing is placed at a depth of $8/9 D$ as shown in Figure 7-46(c). For pile groups in layered soils supported by a combination of shaft and toe resistance, the equivalent footing is placed at $2/3 D$ as shown in Figure 7-46 (d).

- b. Determine the dimensions of the equivalent footing. For pile groups consisting only of vertical piles, the equivalent footing (unless modified for load transfer as in Figures 7-46 (c) and 7-46 (d) has the same dimensions as the length and width of the pile group from Figure 7-31. For pile groups supported primarily by shaft resistance that include batter piles, the plan area of the footing should be calculated from the dimensions of the pile group at the equivalent footing depth that includes the plan area increase due to the pile batter. For toe resistance groups with batter piles, the equivalent footing area should be calculated from the dimensions of the pile group at depth D , including the plan area increase due to the pile batter.
- c. Determine the stress distribution to soil layers below the equivalent footing up to the depth at which the stress increase from the equivalent footing is less than 10% of existing vertical effective stress at that depth. Remember that the equivalent footing size may be increased, and the footing stress correspondingly reduced, as a result of load transfer above the footing location, or in groups with batter piles. The depth at which the stress increase is less than 10% will provide the total thickness of the soil to be analyzed and the number of soil layers for settlement calculations. AASHTO (2014) Article 10.7.2.3.1 states that the load used in calculating settlement is the permanently applied load.
- d. Divide the soil layers in the affected stress increase zone into several thinner layers of 5 to 10 feet in thickness. The thickness of each layer is the thickness H for the settlement computation for that layer.
- e. Determine the existing effective stress, σ'_{vo} , at the midpoint of each soil layer.
- f. Determine the preconsolidation stress, σ_p , at the midpoint of each soil layer and whether the soil layer is overconsolidated or normally consolidated.
- g. Determine the new effective stress, σ'_1 , at the midpoint of each affected soil layer based on the equivalent footing stress distribution.

Table 7-20 Typical Modulus and Stress Exponent Values
(after Canadian Geotechnical Society 1985)

Soil Type	Consistency	Range in Modulus Number, m_n	Stress Exponent, j
Glacial Till	Very Dense to Dense	1000-300	1.0
Gravel	---	400-40	0.5
Sand	Dense	400-250	0.5
Sand	Medium Dense	250-150	0.5
Sand	Loose	150-100	0.5
Silt	Dense	200-80	0.5
Silt	Medium Dense	80-60	0.5
Silt	Loose	60-40	0.5
Silty Clay & Clayey Silt	Hard-Stiff	60-20	0
Silty Clay & Clayey Silt	Stiff-Firm	20-10	0
Silty Clay & Clayey Silt	Soft	10-5	0
Marine Clay	Soft	20-5	0
Organic Clay	Soft	20-5	0
Peat	---	5-1	0

STEP 2 Determine modulus number and stress exponent for each soil layer.

Use laboratory test data to compute modulus number for each layer. Preliminary settlement estimates can be made by using assumed modulus numbers based on soil type as indicated in Table 7-20.

STEP 3 Select the appropriate strain computation equation for each layer.

Select the strain equation applicable to each layer depending upon whether the soil layer is cohesive or cohesionless, and overconsolidated or normally consolidated.

STEP 4 Compute settlements.

Using the appropriate strain computation equation, compute the settlement, S , of each affected soil layer of thickness, H_o . Sum the settlements of all layers until the stress increase is less than 10% of the

existing vertical effective stress at that depth obtain the total estimated soil settlement from the pile group. Add the elastic compression of the pile under the design load to obtain the total estimated pile group settlement.

7.3.5.7 Group Settlement Using the Neutral Plane Method

As the previous sections demonstrate, most of the group settlement methods select the depth of the equivalent footing based upon the assumed load transfer behavior. A preferred solution is to determine the depth of the neutral plane, and place the equivalent footing at or below the neutral plane location. The neutral plane occurs at the depth where the unfactored permanent load plus the load from negative shaft resistance is equal to the positive shaft resistance plus the toe resistance. The design should aim to locate the neutral plane in competent soils. When this is done, group settlements are usually well within acceptable limits.

The position of the neutral plane and the resulting negative shaft resistance can be determined from a static calculation. As previously stated, the neutral plane is the depth at which the sum of the unfactored permanent load plus the negative shaft resistance is equal to the positive shaft resistance plus the toe resistance. Above the neutral plane, the settlement of the soil is greater than the settlement of the pile. Any shaft resistance above the neutral plane is negative shaft resistance, since by definition the soil settlement is greater than the pile settlement. Therefore, the soil settlement transfers load to the pile. Below the neutral plane, the settlement of the soil is less than the settlement of the pile and load is transferred from the pile to the soil. Accordingly, pile settlement equals soil settlement at the neutral plane. Therefore, pile settlement is controlled by the soil compressibility below the neutral plane.

The following step by step procedure adapted from Goudreault and Fellenius (1994) is recommended for determination of the neutral plane.

STEP BY STEP PROCEDURE FOR DETERMINING THE NEUTRAL PLANE DEPTH

STEP 1 Perform a static resistance calculation.

- a. Determine the nominal resistance, R_n , from a static resistance calculation.

- b. Plot the load transfer versus depth by subtracting the shaft resistance at a given depth from the nominal resistance. This computation is identified as Curve A in Figure 7-49.

STEP 2 Determine the load transfer to the pile above the neutral plane.

- a. Determine the unfactored permanent load, Q_d .
- b. Plot the load transfer to the pile versus depth by adding the shaft resistance at a given depth to the sustained load. This computation is labeled as Curve B in Figure 7-49.

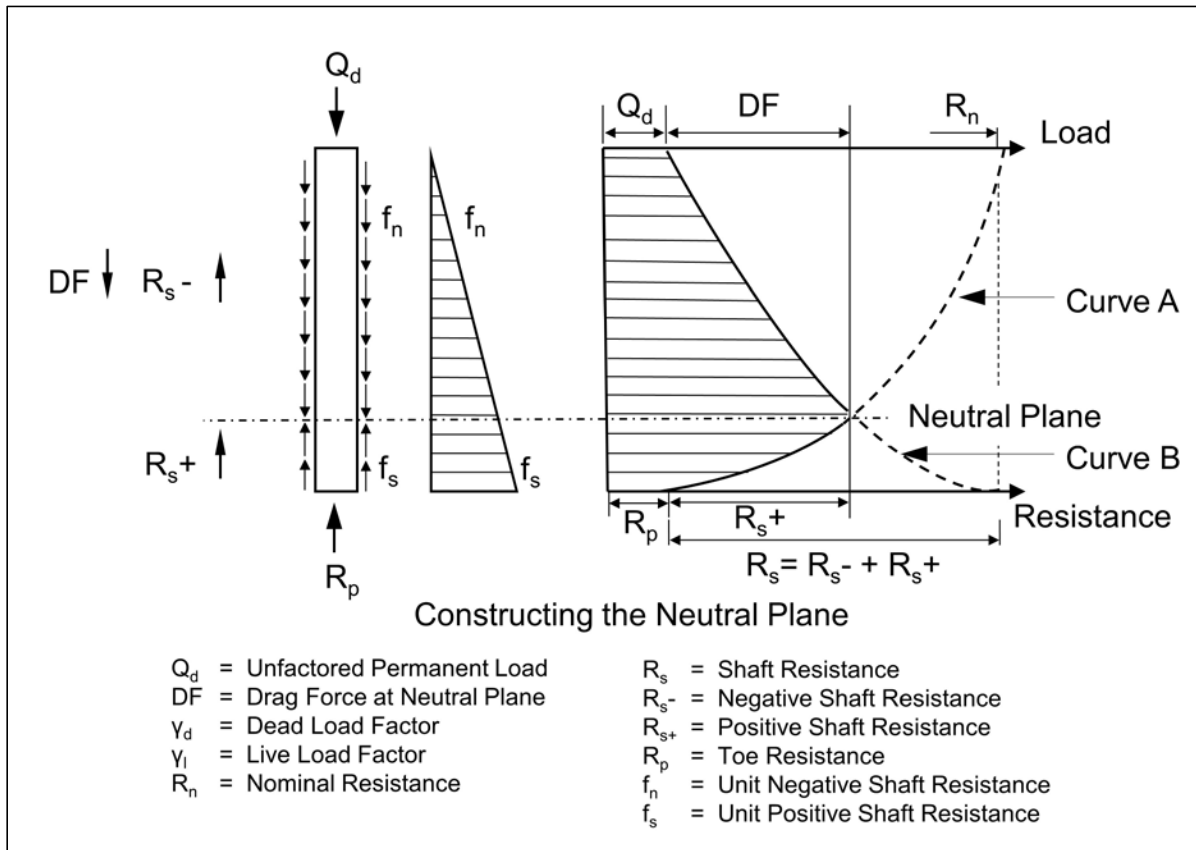


Figure 7-49 Neutral plane (after Goudreault and Fellenius 1994).

STEP 3 Determine the depth of the neutral plane.

- a. The neutral plane is at the depth of where Curves A and B intersect.
- b. The location of the neutral plane will move if the permanent load is changed or the soil resistance versus depth is altered. Hence, design or construction decisions altering the permanent load, or soil

resistance versus depth, will require reevaluation of the neutral plane location under the changed conditions. Preaugering, jetting, use of bitumen coatings, etc. are but a few of the factors that can change the soil resistance versus depth and thus the neutral plane location.

Goudreault and Fellenius (1994), note that the magnitude of group settlement between the neutral plane and the pile toe level is generally small. This is because the piles below the neutral plane act as reinforcing elements and the compression of the pile-reinforced soil is small. Therefore, for most cases they recommend calculating the pile group settlements based on locating the neutral plane at the pile toe.

The group load is distributed below the neutral plane at a slope of 1H:2V. As in the previous methods, the soil materials below the neutral plane should be evaluated for settlement until the stress increase is less than 10%. Group settlements are generally calculated based upon the stress increase and the resulting strain as presented for the Janbu method in Section 7.3.5.6. However, the methods presented for layered soils in Section 7.3.5.5 could also be used.

7.3.6 Settlement Due to Downdrag

When soil moves downward relative to the pile, it creates a drag force on, and therefore within, the pile. The downward soil movement creates the potential for downward pile movement. This downward pile movement is referred to as downdrag. The subsurface conditions, pile installation methods, pile loading sequences, as well as the pile and ground surface configuration determine the magnitude of the drag force and the downdrag movement.

The design approach for downdrag specified by AASHTO treats drag force as an additional load to be resisted in a geotechnical strength limit state analysis. However, drag force does not affect geotechnical strength. As the pile head axial compression load approaches the nominal geotechnical resistance, all shaft resistance is positive or acting upward, hence no drag force exists. This section provides further explanation of these concepts and a recommended approach for calculating drag force and downdrag movement is presented in Section 7.3.6.1. The recommended approach is based on the neutral plane method developed by Fellenius (1989), and modified by Siegel et al. (2013). The recommended method should be used in evaluating the structural strength and geotechnical service limit states, respectively.

The drag force and/or the downdrag movement may be large or small, but for practical consideration they always exist primarily due to the contrasting stiffness between the pile and the surrounding geomaterials as well as due to soil disturbance and soil stress changes caused by pile installation. This is an important realization. It means that drag force and downdrag are not design considerations in only special circumstances. Rather, drag force and downdrag should be evaluated in all driven pile designs. The determination of drag force and its effect on the structural resistance should be considered in the structural strength limit state analysis. Determination of the downdrag movement, since it contributes to pile head settlement, should be part of a geotechnical service limit state analysis.

Negative shaft resistance occurs as the soil moves downward relative to the pile. The accumulation of negative shaft resistance with depth produces the drag force on the pile. When piles are installed through a soil deposit undergoing consolidation, a large drag force can develop. Battered piles should be avoided in soil conditions where large soil settlements are expected because of the additional bending forces imposed on the piles which can cause pile deformation and damage.

There exists a depth along the pile where the sum of the permanent load on the pile plus the negative shaft resistance is equal to the positive shaft resistance on the pile plus the toe resistance. This depth is the location of the neutral plane. The maximum drag force and the maximum axial compression stress in the pile occur at the neutral plane.

Figure 7-50 presents plots of the calculated load in a pile versus depth as a function of time. This data set was collected by the Minnesota Department of Transportation (MnDOT) using sister bar mounted vibrating wire strain gages embedded in a 12.75 inch O.D. concrete filled pipe pile. A large abutment footing and wall were constructed atop the pile concurrent with abutment backfilling. As the sustained pile head load increased, the development and location of the neutral plane 30 feet above the pile toe is readily apparent. The maximum compression force in the pile and the drag force at the neutral plane are also easily identified. The effects of any residual driving stresses are not included in the load versus depth profiles due to installation of the embedded instrumentation following pile driving.

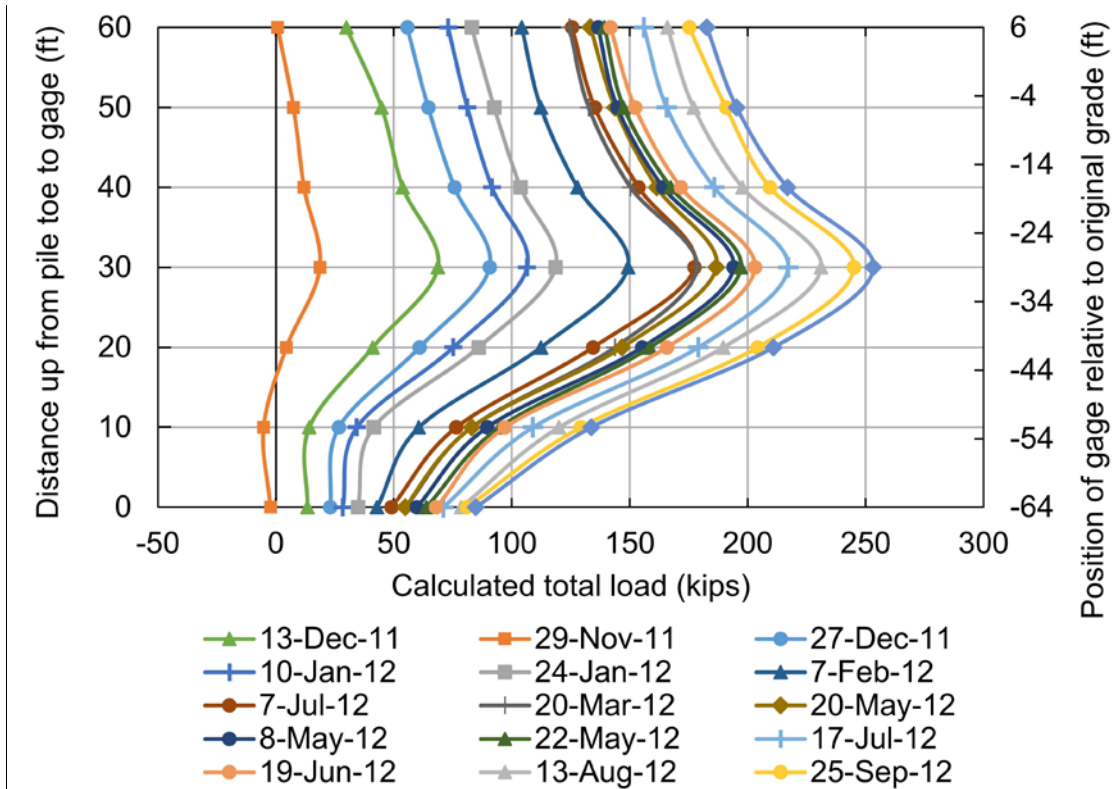


Figure 7-50 Calculated load versus depth in 12.75 inch O.D. concrete filled pipe pile as a function of time (after MnDOT Geotechnical Manual).

Figure 7-51 illustrates the changes that occur as the pile approaches the geotechnical strength limit state. Note that the location of the neutral plane moves up the pile toward the ground surface. This results in a reduction in the magnitude of the negative shaft resistance as well as the drag force in the pile. At the geotechnical strength limit state, geotechnical failure, all shaft resistance is positive as the entire pile is moving downward relative to the soil during plunging failure. Hence, drag force does not alter the geotechnical strength limit state.

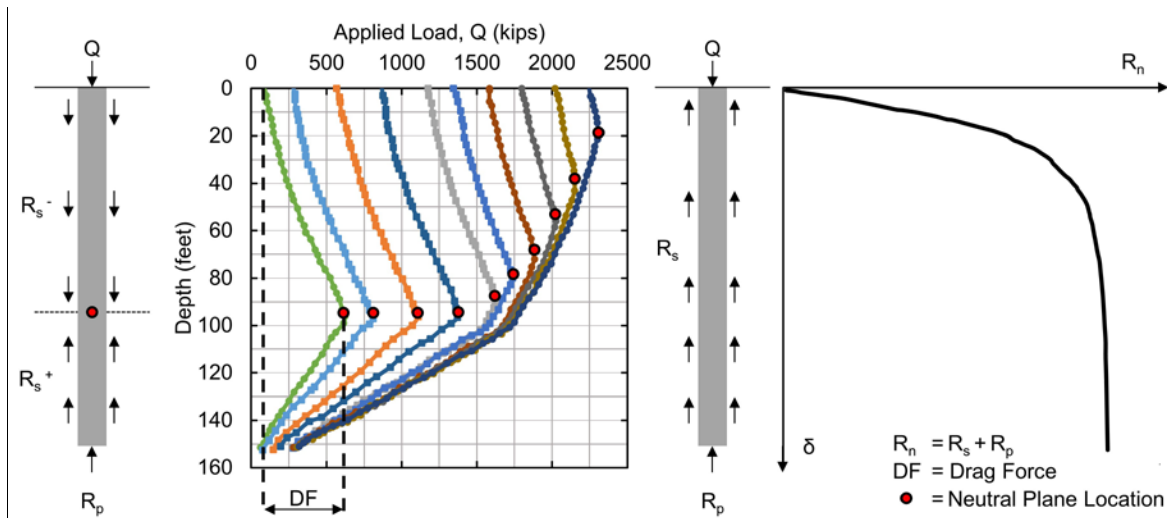


Figure 7-51 Change in neutral plane, negative shaft resistance, and drag force during transition to geotechnical strength limit (after MnDOT Geotechnical Manual).

The recommended design procedure for downdrag is presented in Section 7.3.6.1. The recommended approach addresses settlement considerations due to downdrag in the geotechnical service limit state and pile structural considerations in the structural limit state. Figure 7-52 presents a conceptual illustration of soil and pile movement and resulting pile forces.

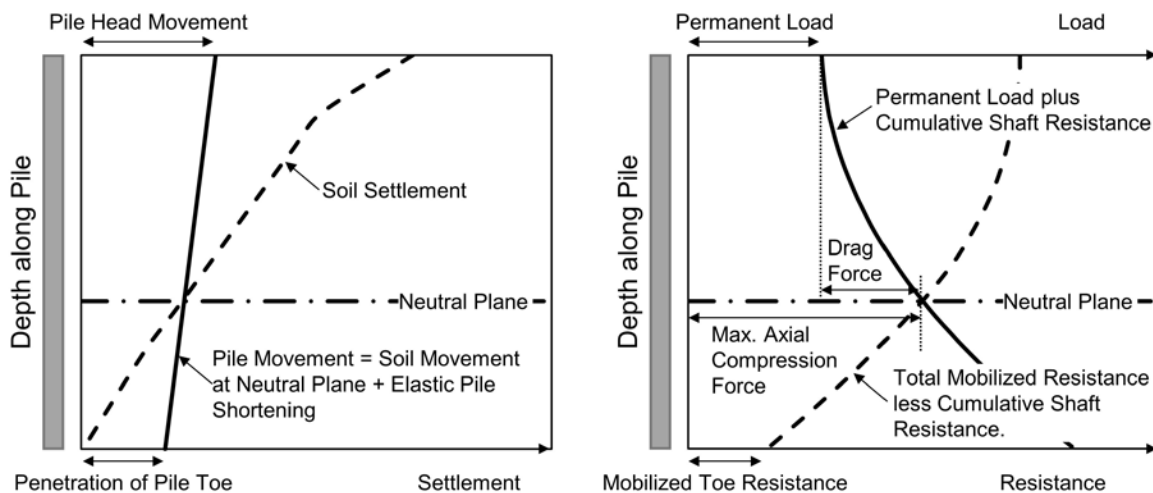


Figure 7-52 Conceptual illustration of soil and pile movement (left) and resulting neutral plane and pile forces (right) (adapted from Siegel et al. 2013).

Figure 7-53 illustrates the most common situation where large negative shaft resistance develops when fill is placed over a compressible layer immediately prior to, or after, piles are driven. Effective stress changes due to dewatering can also cause negative shaft resistance to develop such as shown in Figure 7-54.

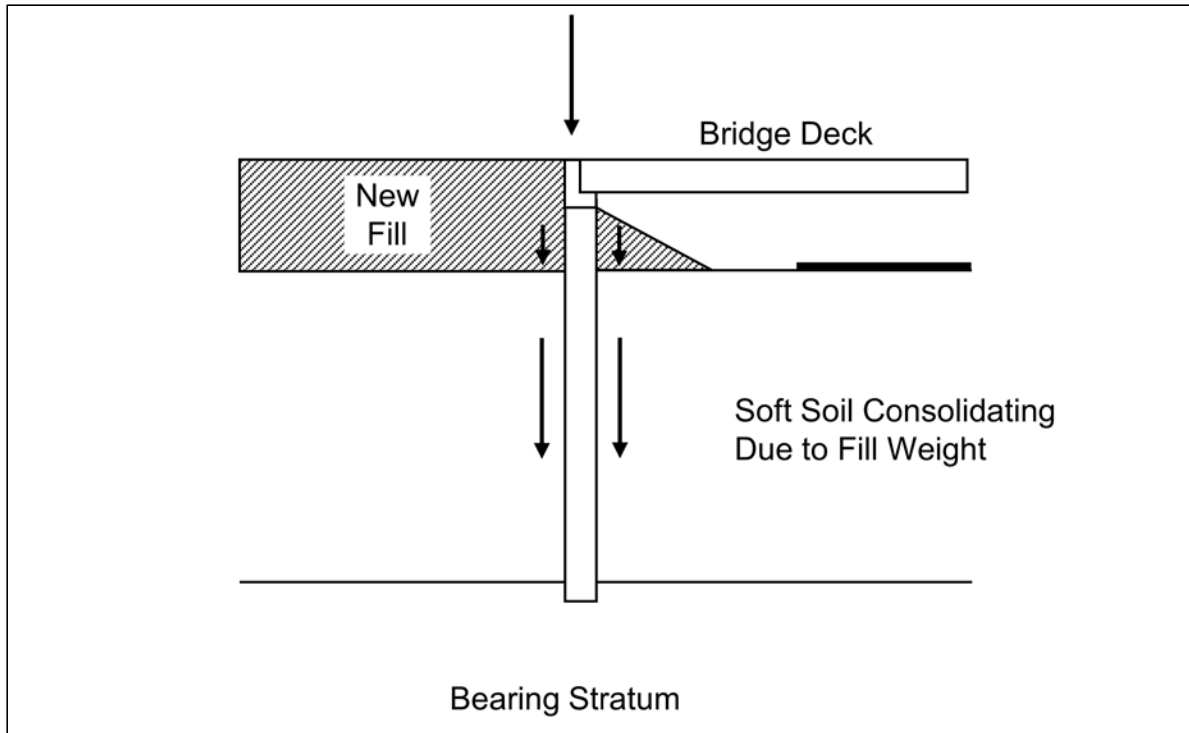


Figure 7-53 Common downdrag situation due to fill weight.

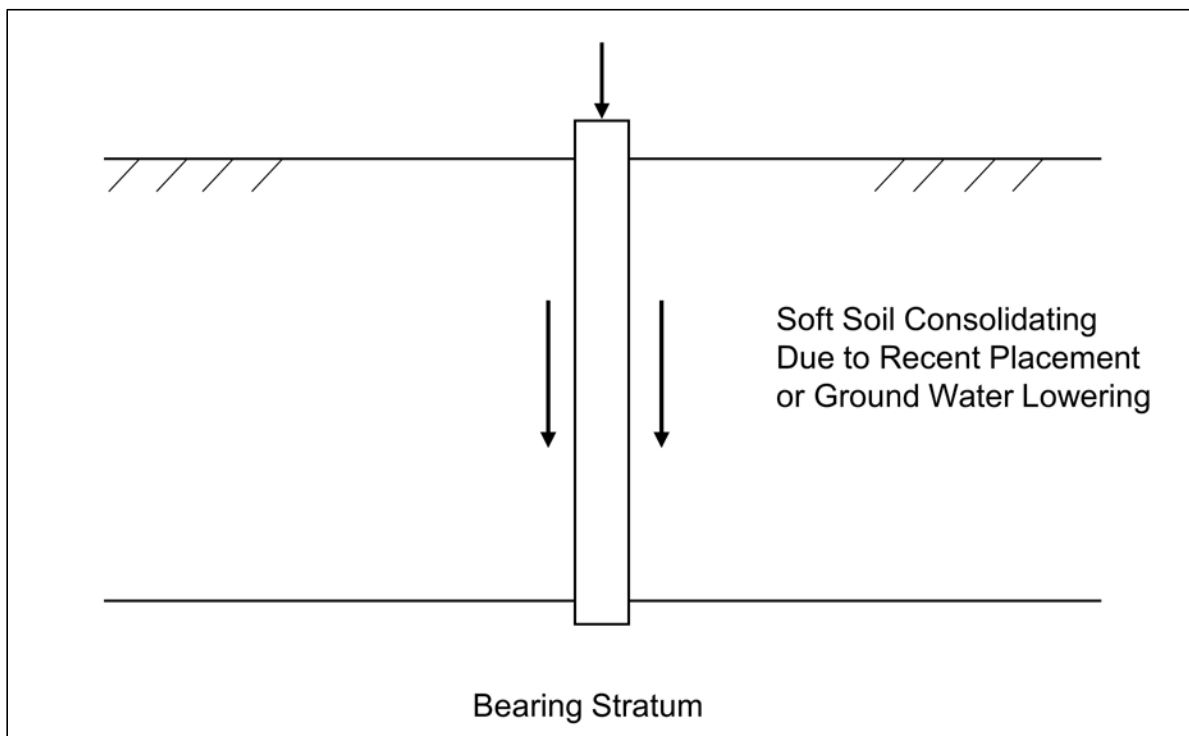


Figure 7-54 Common downdrag situation due to ground water lowering.

Briaud and Tucker (1993) presented the following criteria to assist in identifying situations where drag force and downdrag may be significant and should be carefully

evaluated in the design. This list is not meant to be all inclusive and other situations can also cause significant drag force and downdrag. Ultimately the designer must determine when the magnitude of the drag force and/or downdrag movement must be addressed in the design. Briaud and Tucker listed the following events for where significant drag force and downdrag merits careful consideration in the design:

1. The total settlement of the ground surface will be larger than 4 inches.
2. The settlement of the ground surface after the piles are driven will be larger than 0.4 inches.
3. The height of the embankment placed on the ground surface exceeds 5 feet.
4. The thickness of the soft compressible layer is larger than 30 feet.
5. The water table will be lowered by more than 10 feet.
6. The piles will be longer than 80 feet.

7.3.6.1 Recommended Approach for Downdrag

Siegel et al. (2013) proposed a downdrag design approach using the neutral plane method within the LRFD framework. This approach is the FHWA recommended design method for downdrag. It does not treat the drag force as an additional load that must be supported. Rather, drag force is a settlement consideration in the geotechnical service limit state and is a structural consideration in the pile structural limit state. The approach recognizes that drag force develops on all piles, regardless of soil and loading conditions.

The information necessary to implement the downdrag analysis procedure includes:

- Unfactored structural loads to determine the permanent load.
- Defined subsurface stratigraphy with appropriate parameters for all layers.
- Soil behavior models to characterize load-deformation response, (instrumented load tests, or t-z and q-z models).
- Information on fill placement including amount, lateral extent, and timeline.

In the recommended approach, all loads and resistances should be unfactored. The use of factored loads or factored resistances will distort load-transfer relationships and lead to erroneous predictions of settlement and drag force.

STEP BY STEP PROCEDURE FOR DOWNDRAG ANALYSIS

- STEP 1 Assume soil consolidation and ground settlement will occur.
- STEP 2 Using an appropriate static analysis method for the pile type and subsurface conditions, determine the nominal shaft, mobilized toe, and total mobilized resistance as a function of pile penetration depth.

Shaft resistance is typically fully mobilized at relatively small pile movements of 0.10 inches or less. The full toe resistance however may require a toe movement as much as 4 to 5% of the pile diameter depending on the geomaterial at the pile toe. An assessment of the mobilized toe resistance magnitude can be made using engineering judgment along with t-z and q-z behavior in static analysis software, or from t-z and q-z values derived from instrumented static load tests.

Example output of the required static analysis results versus pile penetration depth is included in Figure 7-55. An illustration of the percentage toe resistance mobilized relative to the toe movement normalized by the pile diameter is presented in Figure 7-56.

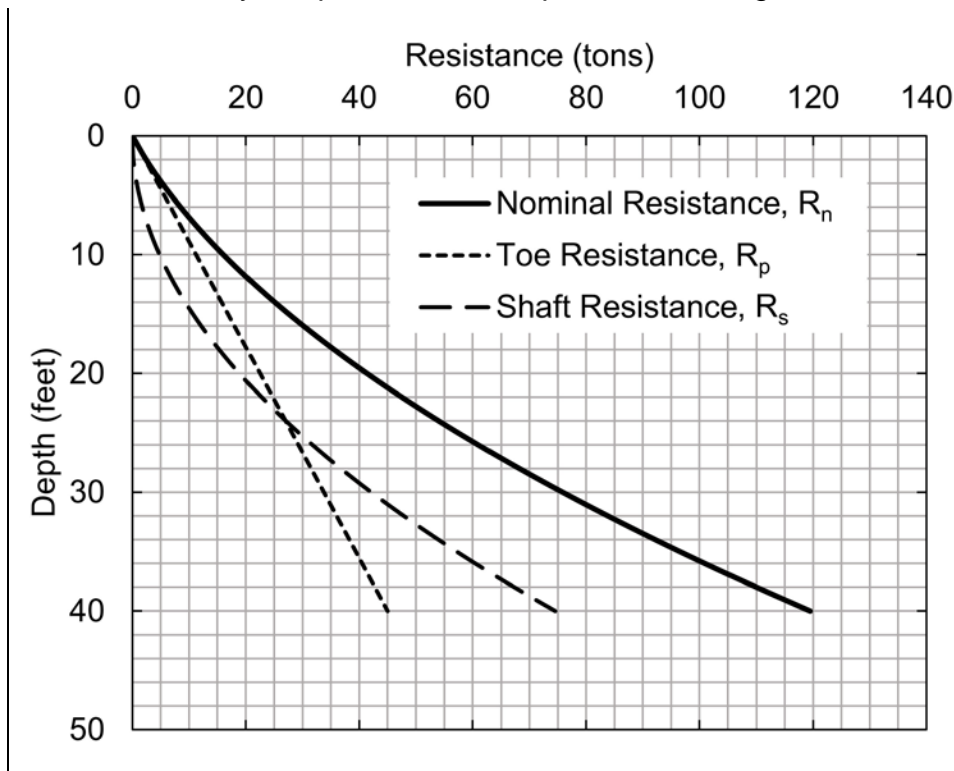


Figure 7-55 Plot of static analysis results (after Siegel et al. 2013).

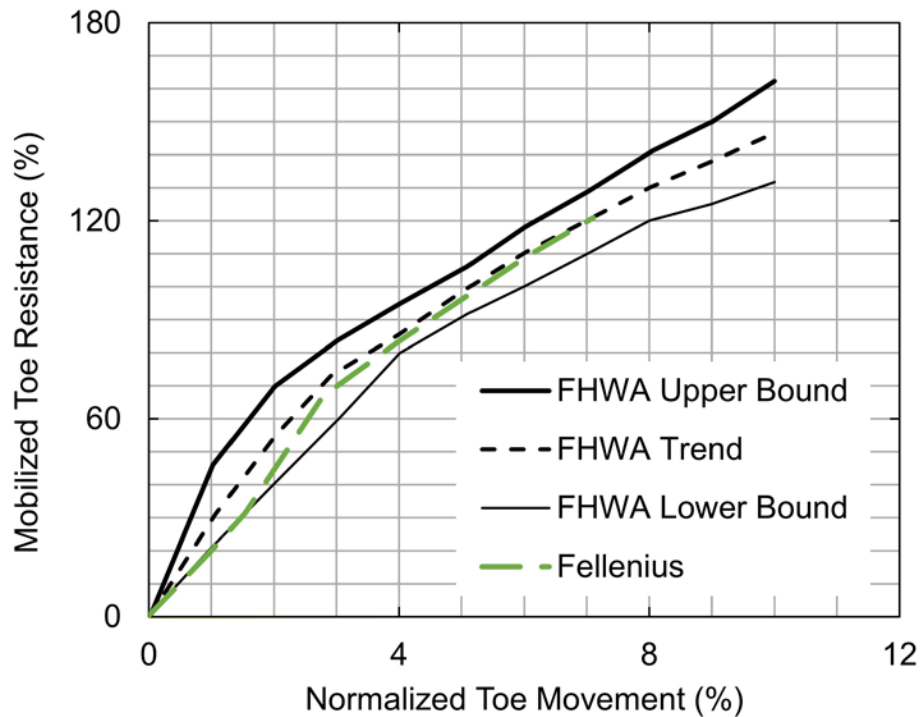


Figure 7-56 Plot of normalized toe resistance versus toe movement (after Siegel et al. 2013).

STEP 3 Select the pile toe elevation for analysis.

STEP 4 Develop the axial load and resistance versus depth diagram at the selected pile toe elevation.

Plot the accumulated shaft resistance versus depth ($\sum R_s$) from Step 2 on the load and resistance diagram. This is depicted by the solid line in Figure 7-57.

Determine the unfactored permanent load on the pile. Add the unfactored permanent load to the accumulated shaft resistance versus depth. This is indicated by the solid line in Figure 7-58.

Subtract the sum of the accumulated shaft resistance at a given depth from the nominal resistance at the selected the pile toe elevation ($R_n - \sum R_s$). Plot this resistance on the load and resistance diagram. This is denoted by dashed lines in Figure 7-59. Graphs a, b, and c, represent the total mobilized resistance based on the shaft resistance plus a

mobilized toe resistance of 100%, 50%, and 0% of the nominal toe resistance, respectively.

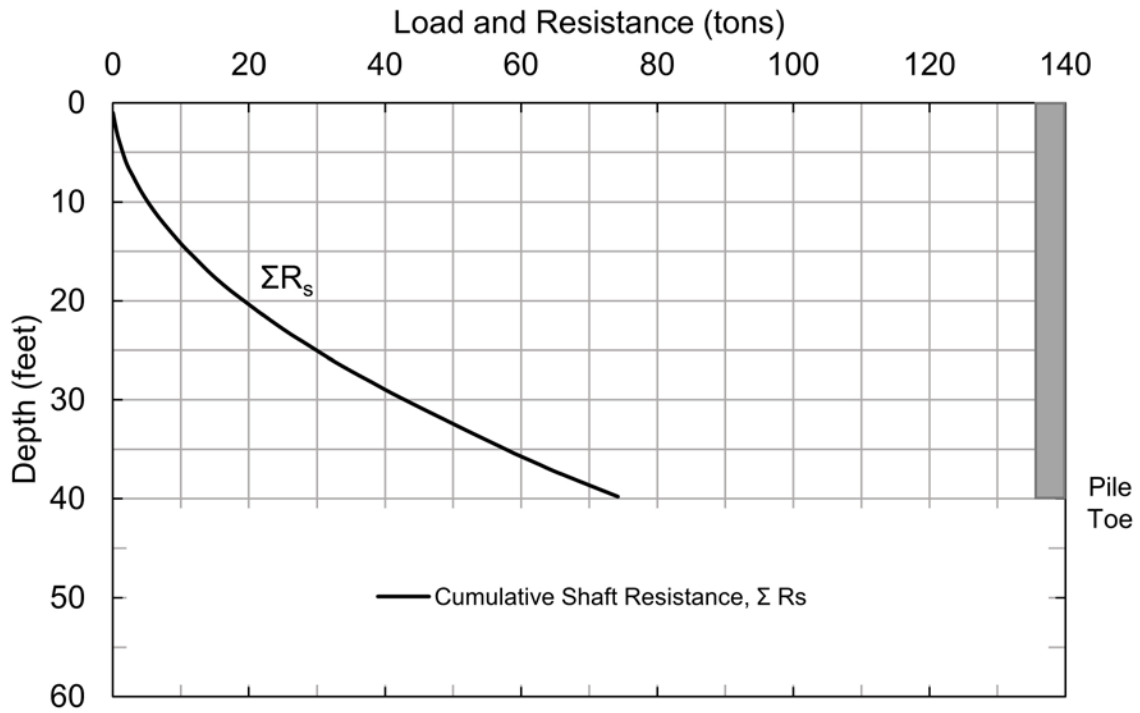


Figure 7-57 Axial load and resistance plot of cumulative shaft resistance vs. depth (after Siegel et al. 2013).

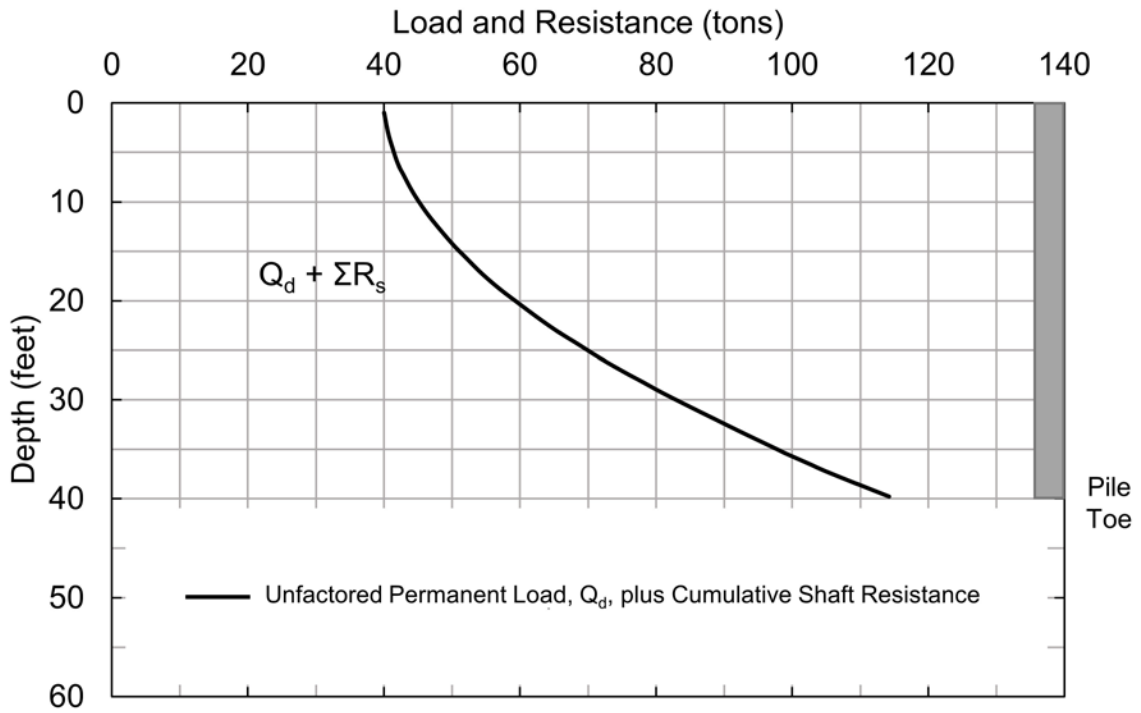


Figure 7-58 Axial load and resistance plot of unfactored permanent load plus cumulative shaft resistance vs depth (after Siegel et al. 2013).

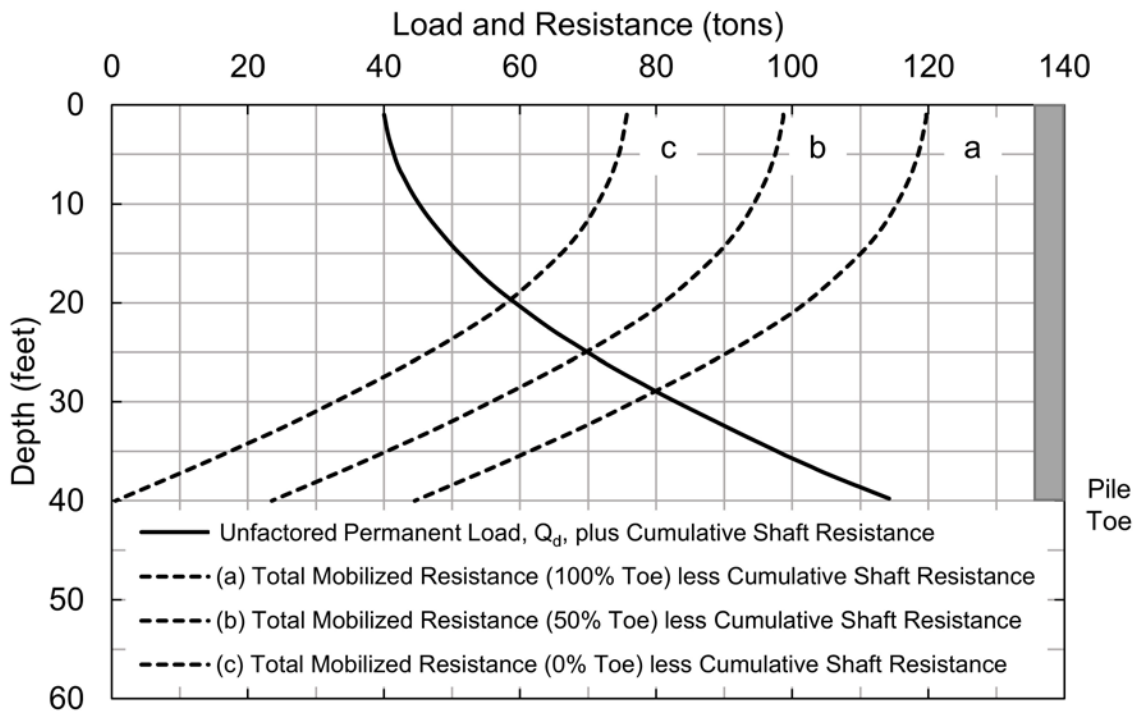


Figure 7-59 Axial load and resistance plot including mobilized resistances (after Siegel et al. 2013).

STEP 5 Determined the location of the neutral plane, the magnitude of the maximum axial compression load in the pile, and the magnitude of the drag force.

For the example given in Figure 7-60, the neutral plane occurs at depth A, B, or C, depending on the magnitude of the mobilized toe resistance. If 100% of the toe resistance is mobilized, the neutral plane occurs at a depth of 30 feet (point A), the maximum axial load in the pile is 80 tons, and the drag force is 40 tons (80 tons – 40 ton permanent pile head load). Conversely, if no toe resistance is mobilized, the neutral plane occurs at a depth of 20 feet (point C), the maximum axial load in the pile is 60 tons, and the drag force is 20 tons (60 tons – 40 ton permanent pile head load).

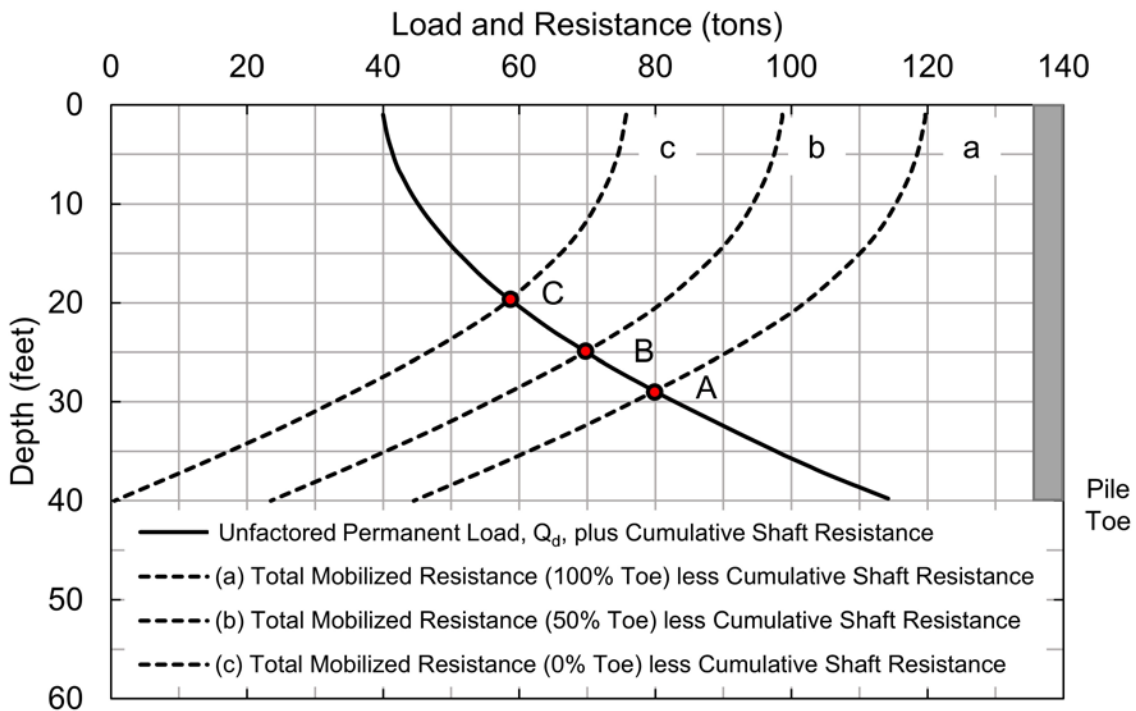


Figure 7-60 Axial Load and resistance plot including neutral plane location based on mobilized toe resistance (after Siegel et al. 2013).

STEP 6 Check the structural strength limit state due to loading conditions including drag force. The factored structural resistance of the pile in the strength limit state in axial compression, P_r , must exceed the factored permanent load and factored drag force per Equation 7-70.

$$1.25(Q_d) + \gamma_p (DF) < P_r \quad \text{Eq. 7-70}$$

Where:

- Q_d = permanent load on pile (kips).
- DF = drag force on pile (kips).
- γ_p = load factor for drag force in neutral plane analysis.
- P_r = factored axial compression resistance of pile (kips).

An AASHTO load factor for drag force, γ_p , determined by static analysis methods using the neutral plane procedure is not yet available. Therefore, local calibration is required for implementation of this approach. The Minnesota DOT has adopted a load factor of 1.1 for drag force with the neutral plane downdrag procedure while a local calibration effort is in progress. This load factor was based on an equivalent minimum factor of safety 1.5 for material strength evaluation.

STEP 7 Calculate the settlement due to downdrag with respect to the neutral plane.

- a. Calculate the thickness of compressible soil, t_{soil} , beneath the neutral plane.

$$t_{soil} = D_{il} - D_{np} \quad \text{Eq. 7-71}$$

Where:

- t_{soil} = thickness of compressible soil beneath neutral plane (feet).
- D_{il} = depth from reference to top of incompressible layer (feet).
- D_{np} = depth from reference to neutral plane (feet).

- b. Determine settlement due to downdrag from stress increase.

$$S_{dd} = t_{soil} \left(\frac{\gamma_p \Delta \sigma}{E_s} \right) \quad \text{Eq. 7-72}$$

Where:

- S_{dd} = settlement due to downdrag (feet).
- t_{soil} = thickness of compressible soil beneath neutral plane (feet).
- γ_p = load factor for downdrag.
- $\Delta \sigma$ = increase in vertical stress (ksf).
- E_s = elastic modulus of in-situ soil (ksf).

It should be noted that effective stress changes such as approach fill placement after pile driving will alter the plot of the permanent load plus cumulative shaft resistance. This will in turn alter the location of the neutral plane, the maximum compression force in the pile, the magnitude of the drag force, and calculated settlement due to downdrag. Similarly, changes in the permanent load to be applied to the pile or changes in the pile toe elevation will also alter the analysis results.

7.3.6.2 Methods for Reducing Downdrag and Drag Force

In situations where the permanent load and drag force exceed the structural strength limit state, or where pile settlement exceeds the geotechnical service limit state, methods for mitigating the drag force should be evaluated. The following techniques have been used in cases with large drag forces:

- a. Increase the structural resistance

In cases where the factored structural resistance is insufficient, the pile structural resistance may be increased by using a pile section with greater structural resistance. The use of a thicker wall section in a steel pipe pile, a heavier H-pile section of the same size, or use of higher strength pile materials are possible solutions. A larger pile size can also be evaluated although this will also increase the pile surface area and therefore drag force.

- b. Increase the number of piles

An increase in the number of piles will result in a decrease in the permanent load carried per pile. This will reduce the maximum axial compression force carried by the pile section.

- c. Reduce soil settlement by preloading

Preconsolidation of compressible soils can be achieved by preloading and consolidating the soils prior to pile installation. This approach is often used for bridge foundations in fill sections. Prefabricated vertical drains are often used in conjunction with preloading to shorten the time required for consolidation. Additional information on prefabricated vertical drains is available in "Prefabricated Vertical Drains," FHWA RD 86/168 by Rixner et al. (1986) and in "Ground Improvement Methods" manual by Elias et al. (2004).

d. Use lightweight fill material

Construct structural fills using lightweight fill material to reduce the drag forces. Lightweight fill materials often used, depending upon regional availability, include geofoam, foamed concrete, wood chips, blast furnace slag, and expanded shales. Additional information on lightweight fills is available in Elias et al. (2004). Geofoam blocks being placed for embankment construction are shown in Figure 7-61.

e. Use a friction reducer

Bitumen coating and plastic wrap are two methods commonly used to reduce the friction at the pile-soil interface. Bitumen coatings should only be applied to the portion of the pile which will be embedded in the negative shaft resistance zone. Case histories on bitumen coatings have reported reductions in negative shaft resistance from as little as 47% to as much as 90%. Goudreault and Fellenius (1994) suggest that the reduction effect of bitumen may be analyzed by using an upper limit of 200 psf as the pile-soil shear resistance or adhesion in the bitumen coated zone.



Figure 7-61 Geofoam block approach embankment (courtesy MnDOT).

One of the major problems with bitumen coatings is protecting the coating during pile installation, especially when driving through coarse soils. An inexpensive solution to this problem is to weld an oversized collar around the pile where the bitumen ends. The collar opens an adequate size hole to permit passage of the bitumen for moderate pile lengths in fine grained soils. Figure 7-62 presents a photograph on an over-sized collar between the uncoated lower pile section and white washed bitumen coating on the upper pile section.

Bitumen coatings can also present additional construction problems associated with field coating and handling. The bitumen coating used must have relatively low viscosity to permit slippage during soil consolidation, yet high enough viscosity and adherence to insure the coating will stick to the pile surface during storage and driving. The bitumen must also have sufficient ductility to prevent cracking and spalling of the bitumen during handling and driving. Therefore, the climate at the time of pile installation should be considered in selection of the proper bitumen coating. The use of bitumen coatings can be quite successful provided proper construction control methods are followed. However, bitumen coatings should not be casually specified as the solution to drag forces.

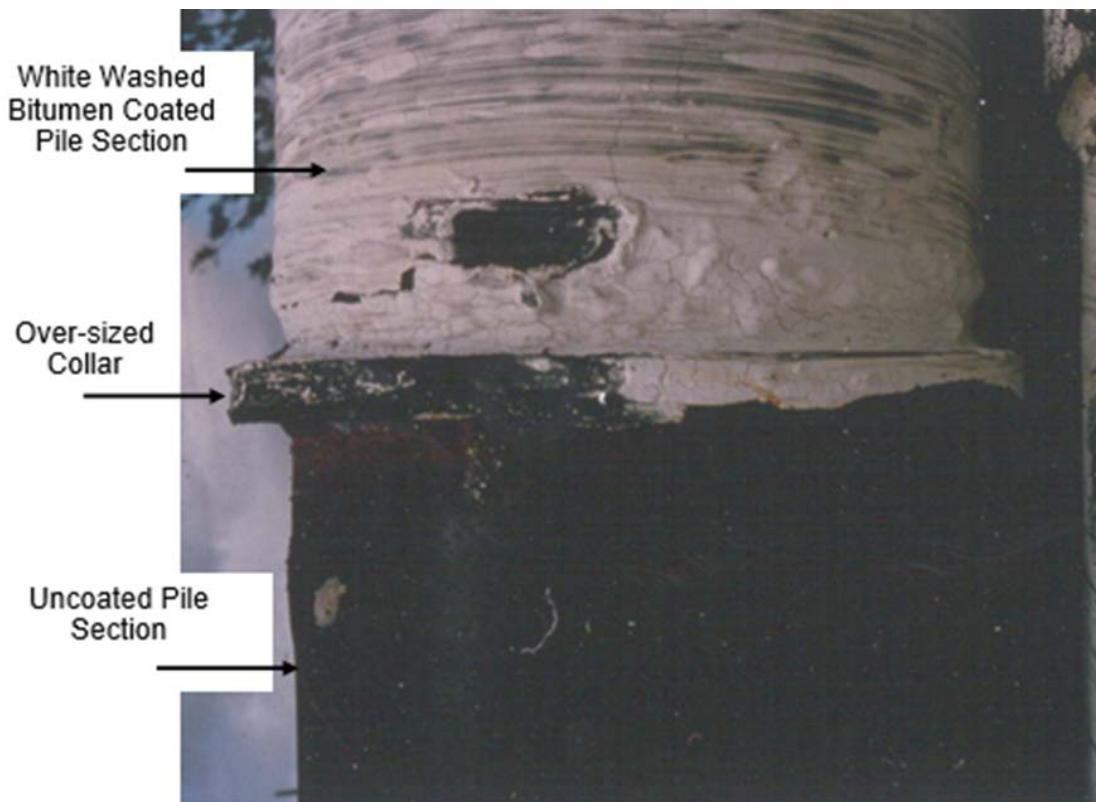


Figure 7-62 Over-sized collar for bitumen coating protection.

Plastic wrap has proven to be an economically attractive friction reducer, particularly for abutment piles driven behind and before construction of MSE walls. Tawfig (1994) performed laboratory tests on 0.006 inch thick polyethylene sheets used as a friction reducer. The laboratory test results indicated plastic wraps reduced the pile-soil shear resistance from between 78% for a one wrap layer to 98% for a two layer wrap with mineral oil lubricant. The laboratory test data indicated the pile-soil shear resistance of a one wrap layer was about 200 psf and only 20 psf for the lubricated two wrap system.

f. Prevent direct contact between soil and pile

Pile sleeves are sometimes used to eliminate direct contact between pile and soil. Bentonite slurry has been used in the past to achieve the same purpose. However these methods are generally more expensive and less effective than other solutions.

7.3.7 Horizontal Pile Foundation Deflection

Historically, designers often used prescriptive values for the lateral load resistance of vertical piles, or have added batter piles to increase a pile group's lateral resistance when it was believed that vertical piles could not provide the needed lateral resistance. However, vertical piles can be designed to withstand significant lateral loads. Modern analysis methods should be employed in the selection of the pile type and pile section.

Coduto (1994) notes that a foundation system consisting of only vertical piles designed to resist both axial and lateral loads is more flexible, and thus more effective at resisting dynamic loads, as well as less expensive to build. Bollman (1993) reported that the Florida Department of Transportation often uses only vertical piles to resist lateral loads, including ship impact loads because vertical piles are often less expensive than batter piles. In areas where seismic lateral loading is a serious concern, batter piles can deliver excessively large horizontal forces to the structure during the earthquake event. This phenomenon was observed during the Loma Prieta earthquake of 1989 in California and discussed in greater detail by Hadjian et al. (1992). In earthquake areas, lateral loads should be resisted by ductile vertical piles, and batter piles should be avoided whenever possible.

Sophisticated analysis methods are now readily available that allow the lateral load-deflection behavior of piles to be rationally evaluated. Lateral loads and moments on a vertical pile are resisted by the flexural stiffness of the pile and mobilization of resistance in the surrounding soil as the pile deflects. The flexural stiffness of a pile

is defined by the pile's modulus of elasticity, E , and moment of inertia, I . The geomaterial resistance to an applied lateral load is a combination of geomaterial compression and shear resistance, as shown in Figure 7-63.

The design of laterally loaded piles must evaluate both the pile structural response and geomaterial deformation to lateral loads. The nominal structural resistance must be determined. In addition, the pile deformation under the service loading conditions must be calculated and compared to foundation performance criteria.

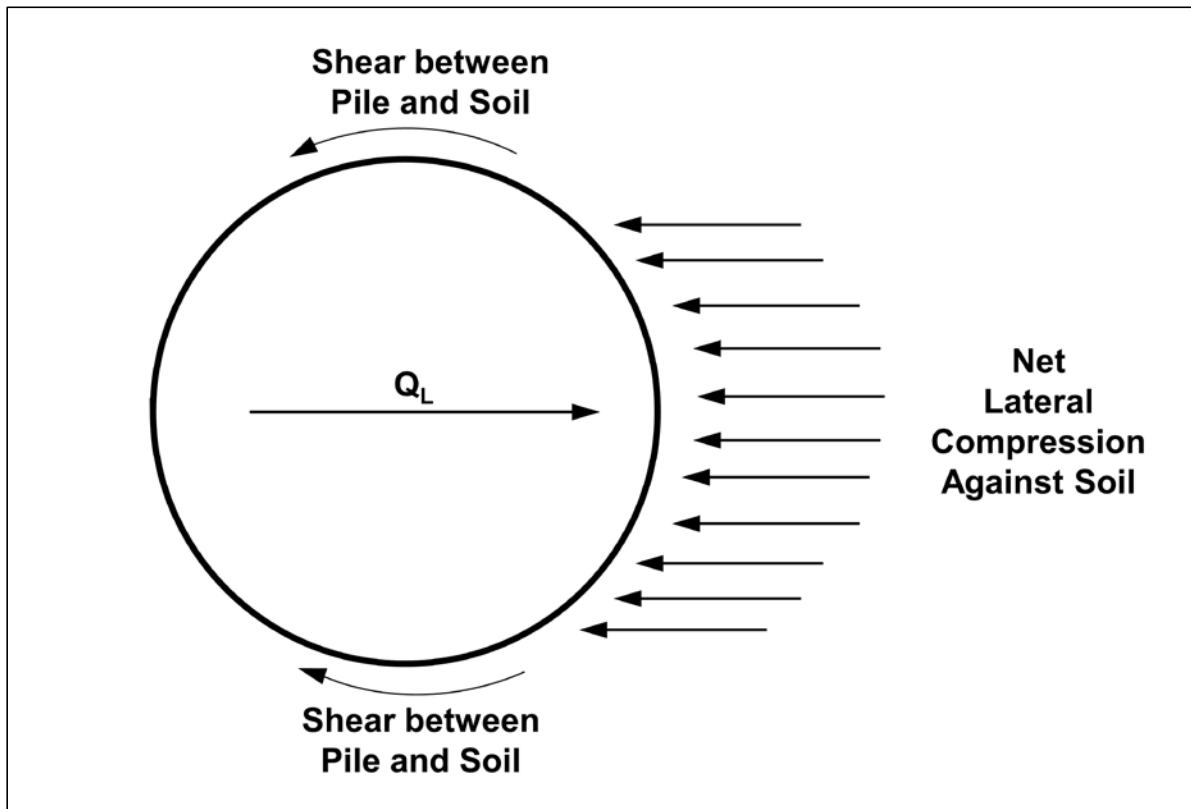


Figure 7-63 Soil resistance to a lateral pile load (after Smith 1989).

The design of laterally loaded piles requires the combined skills of the geotechnical and structural engineer. It is inappropriate for the geotechnical engineer to analyze a laterally loaded pile without a full understanding of pile-structure interaction. Likewise it is inappropriate for the structural engineer to complete a laterally loaded pile design without a full understanding of how pile section or spacing changes may alter the geotechnical response. Because of the interaction of pile structural and geotechnical considerations, the economical solution of lateral pile loading problems requires interdisciplinary coordination between the structural and geotechnical engineer.

Soil, pile, and load parameters have significant effects on the lateral resistance of piles. The factors influencing these parameters are as follows:

1. Geomaterial Parameters

- a. Soil or rock type and physical properties such as shear strength, friction, density, groundwater level, and moisture content.
- b. Coefficient of horizontal subgrade reaction in (pcf). This coefficient is defined as the ratio between a horizontal stress per unit area of vertical surface (psf) and the corresponding horizontal displacement (inches). For a given deformation, the greater the coefficient, the greater the lateral load resistance.

2. Pile Parameters

- a. Physical properties such as shape, material, and dimensions.
- b. Pile head conditions (rotational constraint, if any).
- c. Method of pile placement such as driving, jetting, etc.
- d. Group action.

3. Lateral Load Parameters

- a. Static (monotonic or cyclic) or dynamic.
- b. Eccentricity (moment coupled with shear force).

7.3.7.1 Pile Head Fixity

The pile to pile cap connection can behave as a pinned connection, fixed connection, or somewhere in between depending on the design detail. Wilson et al. (2006) summarized the design effect of pile to pile cap connection. If the pile extends only a nominal distance into the pile cap, it will behave as a pinned connection. A pinned connection provides restraint against translational movements but does not restrain rotation of the pile head relative to the cap. Conversely, a fixed connection requires the pile to be embedded two to three diameters into pile cap or

to be fitted with a specially designed connection. A fixed connection provides restraint against rotation and all directions of movement of the pile head relative to the pile cap.

At the service limit state, a pinned connection will typically have more horizontal movement than a fixed connection as illustrated in Figure 7-64. At the strength limit state, Figure 7-65 illustrates that a fixed head condition will generally result in a larger bending moment at the pile head compared to a pinned connection, but may or may not have larger bending moments below the pile head.

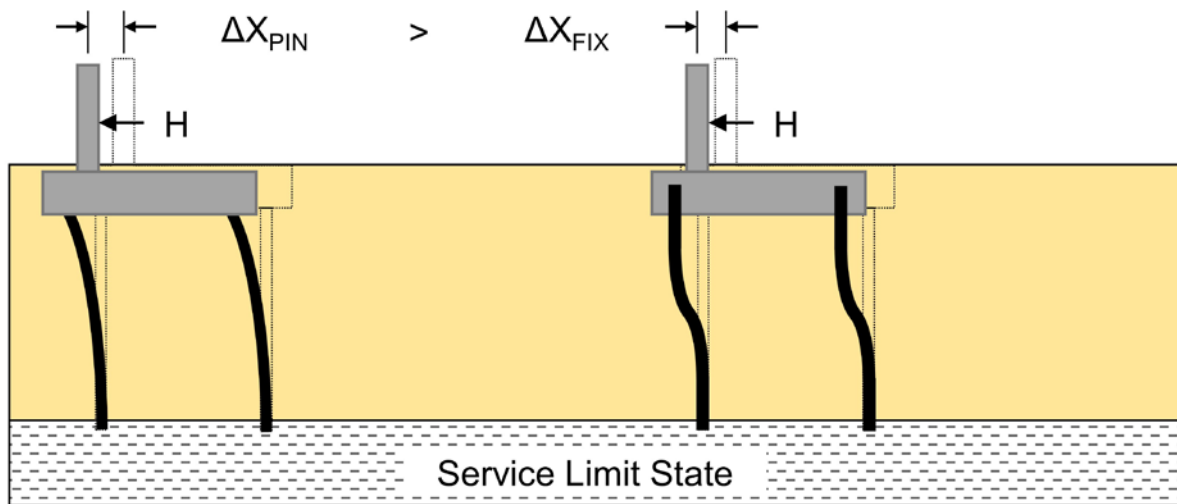


Figure 7-64 Effect of pile head fixity on translation at service limit state (after Wilson et al. 2006).

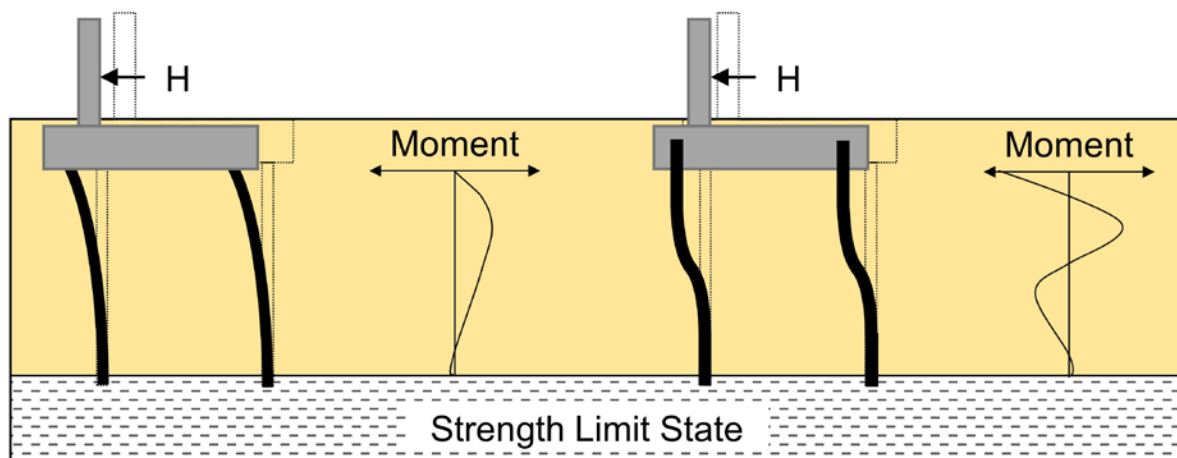


Figure 7-65 Effect of pile head fixity on moment in piles at strength limit state (after Wilson et al. 2006).

7.3.7.2 Lateral Design Methods

The basic design approaches for lateral soil resistance analysis of vertical piles consist of lateral load tests or analytical methods. Both of these approaches are described in greater detail in the following sections.

1. Lateral Load Tests

Full scale lateral load tests can be conducted at a site during either the design or construction stage. The load-deformation data obtained is used to finalize or confirm the design for the particular site. Factors such as loading rate, cyclic (single or multi-directional) versus monotonic application of design forces, and magnitude of axial load should be considered in developing appropriate field testing procedures. Lateral load tests may not be economically justifiable on many projects but are essential on projects controlled by lateral load demand. Chapter 9 provides additional details on lateral load test procedures and interpretation.

2. Analytical Methods

The analytical methods are based on theory and empirical data and permit the rational consideration of various site parameters. Two common approaches are Broms' (1964a, 1964b) hand calculation method, and Reese's (1984) computer solution. Both approaches consider the pile to be analogous to a beam on an elastic foundation. FHWA IP-84-11 by Reese (1984) presents details of both methods.

Broms' method provides a relatively easy hand calculation procedure to determine lateral loads and pile deflections at the ground surface. Broms' method also ignores the axial load on the pile. As lateral load demand has increased along with the need for improved deformation estimates more detailed load-deformation computer analyses have become the norm.

Reese's p-y method is a more rigorous computer analysis that was originally available in the 1993 DOS based COM624 computer program which was developed under an FHWA research grant. That method is now incorporated in that program's proprietary successor, the LPILE program (Isenhower and Wang 2014). The p-y method permits the inclusion of more complete modeling parameters of a specific problem. The program output provides distributions versus depth of moment, shear, soil and pile moduli, and soil resistance for the entire length of pile, including moments and shears in above ground sections.

For the design of all major pile foundation projects, the p-y method should be used. Some of the more common software programs that perform lateral loading analysis using the p-y method include LPILE, FBPIER, and ALLPILE. It should be emphasized that the FHWA does not endorse the use of any particular software program. However the p-y method, described further in the following section, is the FHWA recommended analysis method for lateral load design.

7.3.7.3 p-y Method

The interaction of a pile-soil system subjected to lateral load has long been recognized as a complex function of nonlinear response characteristics of both pile and soil. The most widely used nonlinear analysis method is the p-y method, where p is the soil resistance per unit pile length and y is the lateral soil or pile deflection. This method, illustrated in Figure 7-66, models the soil resistance to lateral load as a series of nonlinear springs. As noted previously, some of the more common software programs that perform lateral loading analysis using the p-y method include LPILE, FBPIER, and ALLPILE.

Reese (1984, 1986) has presented procedures for describing the soil response surrounding a laterally loaded pile for various soil conditions by using a family of p-y curves. The procedures for constructing these curves are based on experiments using full sized, instrumented piles and theories for the behavior of soil and rock under stress.

The geomaterial modulus subgrade reaction is defined as follows:

$$k = -\frac{p}{y} \quad \text{Eq. 7-73}$$

Where:

- k = modulus of subgrade reaction (psi).
- p = soil resistance per unit pile length (lbs/inch).
- y = lateral deflection (inch).

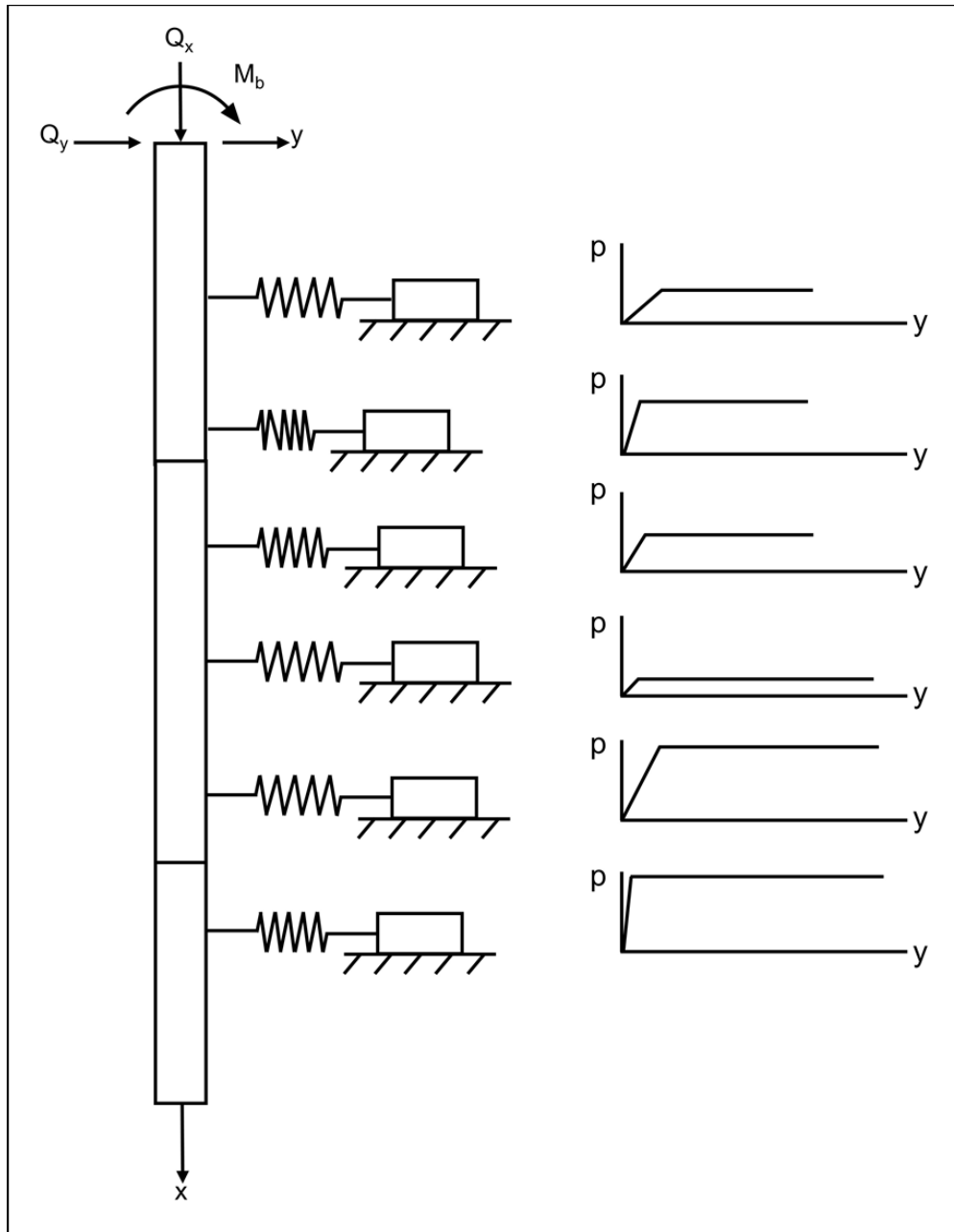


Figure 7-66 Typical lateral analysis pile-soil model.

The negative sign indicates that the ground resistance opposes pile deflection. The ground's modulus is the secant modulus of the p - y curve and is not constant except over a small range of deflections. Typical p - y curves are shown in Figure 7-67. Ductile p - y curves, such as curve A, are typical of the response of soft clays under static loading and sands. Brittle p - y curves, such as curve B, can be found in some stiff clays under dynamic loading conditions.

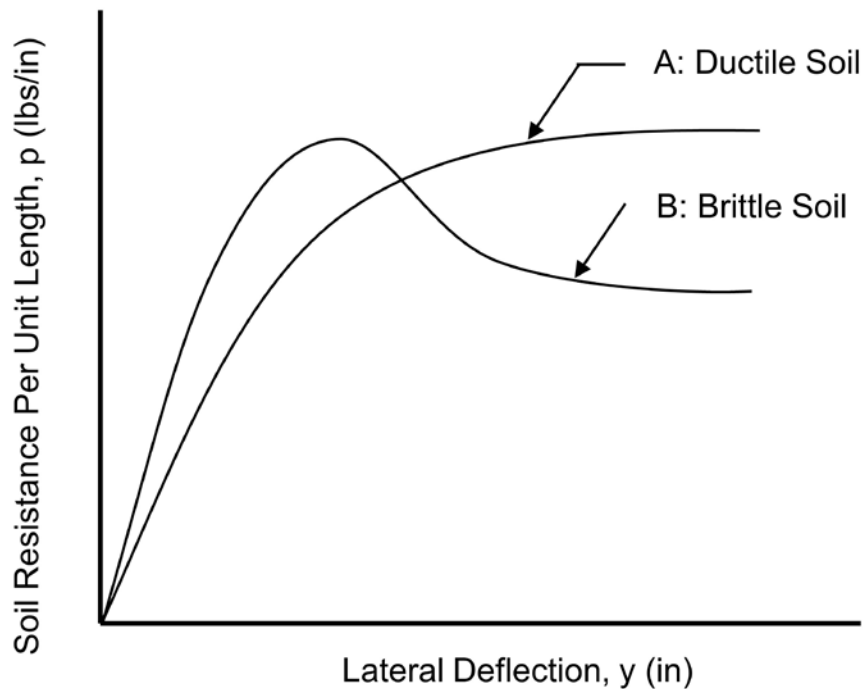


Figure 7-67 Typical p-y curves for ductile and brittle soil (after Coduto 1994).

The factor most influencing the shape of the p-y curve is the soil properties. However, the p-y curves also depend upon depth, soil stress strain relationships, pile width, water table location, and loading conditions (static or cyclic). Representative values for the clay ϵ_{50} strain parameter are provided in Table 7-21 while modulus of subgrade reaction values for clays and sand are shown in Table 7-22. Procedures for constructing p-y curves for various soil and water table conditions as well as static or cyclic loading conditions are typically provided in the p-y program documentation.

Table 7-21 Representative Values of ϵ_{50} for Clays

Clay Consistency	Average Undrained Shear Strength, s_u , (ksf)	ϵ_{50}
Soft Clay	0.25-0.50	0.02
Medium Clay	0.50-1.0	0.01
Stiff Clay	1.0-2.0	0.007
Very Stiff Clay	2.0-4.0	0.005
Hard Clay	4.0-8.0	0.004

Table 7-22 Representative Modulus of Subgrade Reaction Values, k_s and k_c , for Clays and Sands

Soil Type	Avg. Undrained Shear Strength, s_u , (ksf)	Soil Condition Relative to Water Table	k_s -Static Loading (pci)	k_c -Cyclic Loading (pci)
Soft Clay	0.25-0.50	---	30	---
Medium Clay	0.50-1.0	---	100	---
Stiff Clay	1.0-2.0	---	500	200
Very Stiff Clay	2.0-4.0	---	1000	400
Hard Clay	4.0-8.0	---	2000	1000
Loose Sand	---	Submerged	20	20
Loose Sand	---	Above	25	25
Med Dense Sand	---	Submerged	60	60
Med Dense Sand	---	Above	90	90
Dense Sand	---	Submerged	125	125
Dense Sand	---	Above	225	225

The p-y programs solve the nonlinear differential equations representing the behavior of the pile-soil system to lateral (shear and moment) loading conditions in a finite difference formulation using Reese's p-y method of analysis. The strongly nonlinear reaction of the surrounding soil to pile-soil deflection is represented by the p-y curve prescribed to act on each discrete element of the embedded pile. For each set of applied boundary (static) loads the program performs an iterative solution which satisfies static equilibrium and achieves an acceptable compatibility between force and deflection (p and y) in every element.

The shape and discrete parameters defining each individual p-y curve may be input by the user or generated by the program. Layered soil systems are characterized by conventional geotechnical data including soil type, shear strength, density, depth, and stiffness parameters, and whether the loading conditions are monotonic or cyclic in nature.

For batter piles, Awoshika and Reese (1971) proposed a modifying constant ranging from 0 to 2 be applied to the p_{ult} value based on the direction of the applied lateral load relative to the orientation of the pile batter. This modifying constant proportionally modifies the p-values. If the pile head is inclined away from the

direction of the horizontal load, the modifying constant ranges from 1 to 2. If the pile head is inclined toward the applied horizontal load the modifying constant ranges from 1 to 0. With this approach, predicted behavior has been reported to reasonably agree with lateral test results on outwardly battered piles but less successful for inwardly battered piles. Hence, full scale load tests to better evaluate batter pile response should be considered on important projects.

The influence of applied loads (axial, lateral and moment) at each element can be modeled with flexural rigidity varying as a function of applied moment. In this manner, progressive flexural damage such as cracking in a reinforced concrete pile can be treated more rigorously. Programs typically include a subroutine which calculates the value of flexural rigidity at each element under the boundary conditions and resultant pile-soil interaction conditions.

Typical p-y analysis output summarizes the input information and the analysis results. The input data summarized includes the pile geometry and properties, and soil strength data. Output includes the generated p-y curves at various depths below the pile head and the computed pile deflections, bending moments, stresses and soil moduli as functions of depth below the pile head. This information allows an analysis of the pile's structural resistance. Internally generated (or input) values of flexural rigidity for cracked or damaged pile sections are also output. Graphical output presentations versus depth include the computed deflection, slope, moment, and shear in the pile, and soil reaction forces similar to those illustrated in Figure 7-68.

The p-y analyses characterize the behavior of a single pile under lateral loading conditions. A detailed view is obtained of the load transfer and structural response mechanisms to design conditions. Considerable care is required in extrapolating the results to the behavior of pile groups (pile-soil-pile interaction, etc.), and accounting for the effects of different construction processes such as predrilling or jetting.

In any lateral analysis case, the analyst should verify that the intent of the modeling assumptions, all elastic behavior for example, is borne out in the analysis results. When a lateral load test is performed, the measured load-deflection results versus depth should be plotted and compared with the analysis predicted behavior so that an evaluation of the validity of the p-y curves used for design can be made. Figure 7-69 illustrates a comparison between the measured load-deflection curve and one predicted by COM624P.

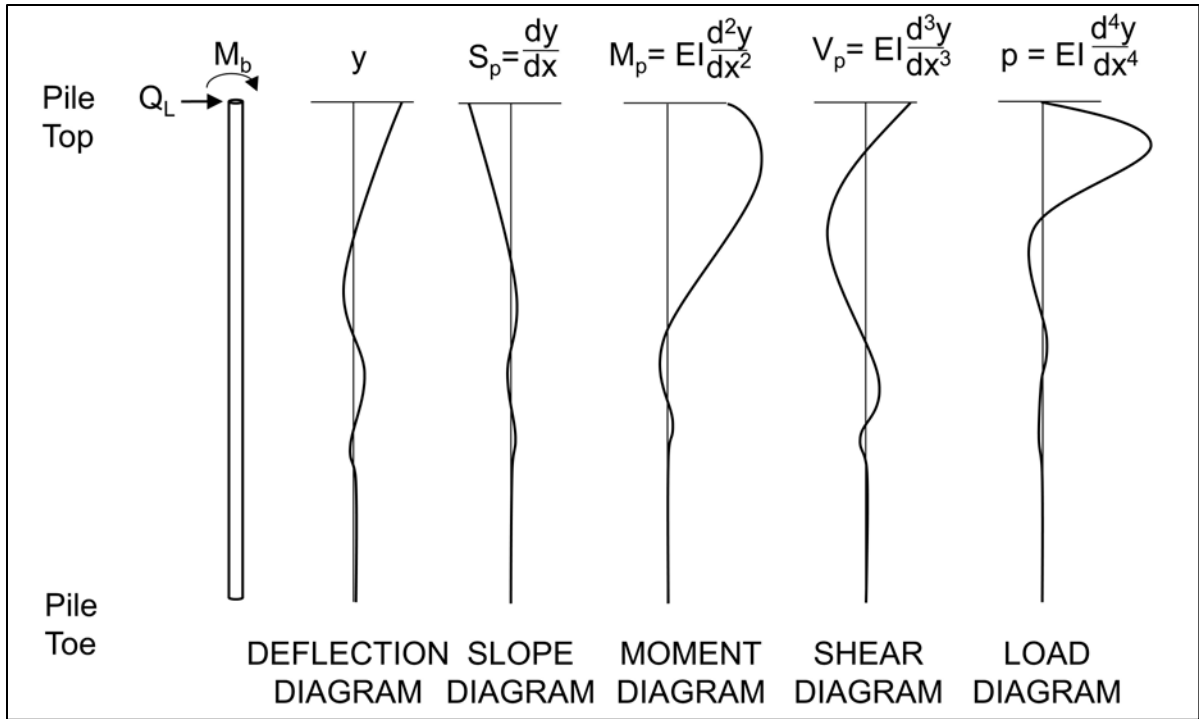


Figure 7-68 Graphical presentation of p-y analysis results (after Reese 1986).

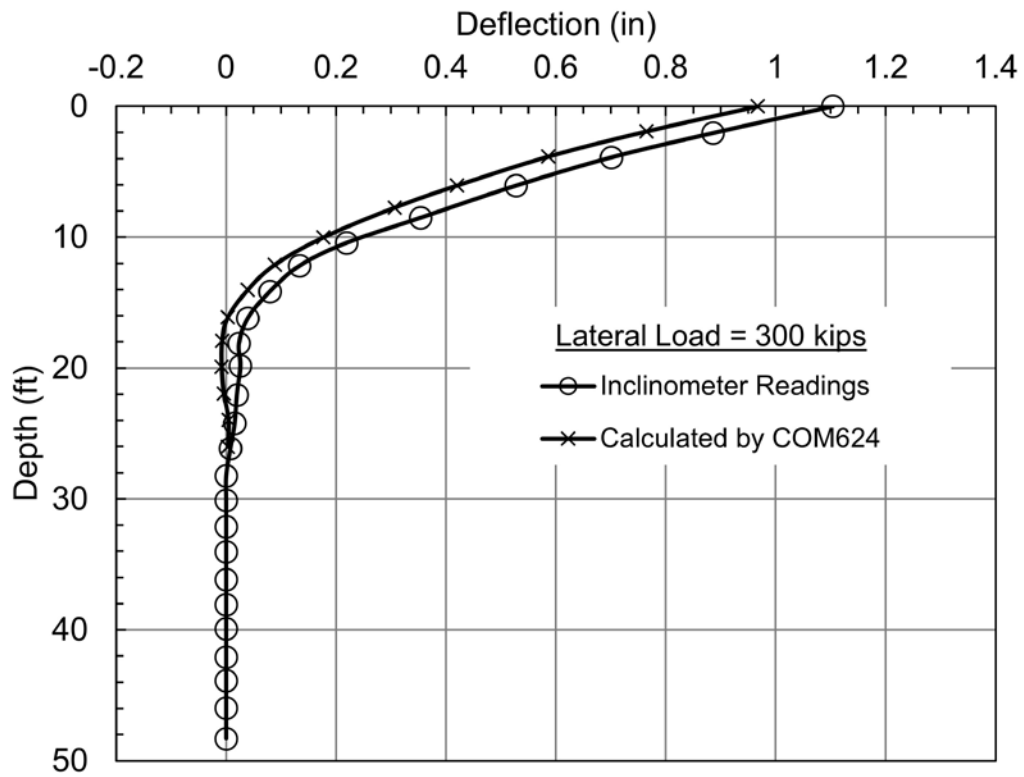


Figure 7-69 Comparison of measured and COM624P predicted load-deflection behavior versus depth (after Kyfor et al. 1992).

7.3.7.4 Strain Wedge Method

The p-y methods are generally applicable to piles that have the ability to bend and deflect. For short, stiff, piles, the strain wedge (SW) method may be a more realistic modeling approach as a short stiff pile tends to rotate rather than bend. Background details on the strain wedge method are provided in Norris (1986) and Ashour et al. (1998a).

In the strain wedge method, a passive soil wedge is modelled to resist lateral pile loads. A three dimensional wedge is incorporated into the beam on elastic foundation problem and can accommodate variations in shape, depth, loading and pile deflection due to changes in strain. Additional research with this model has added the use of multiple soil layers and the effect of pile head conditions (Ashour et al. 2002). Within the wedge, the mobilized strains form the relationship between passive resistance and horizontal displacement as shown in Figure 7-70.

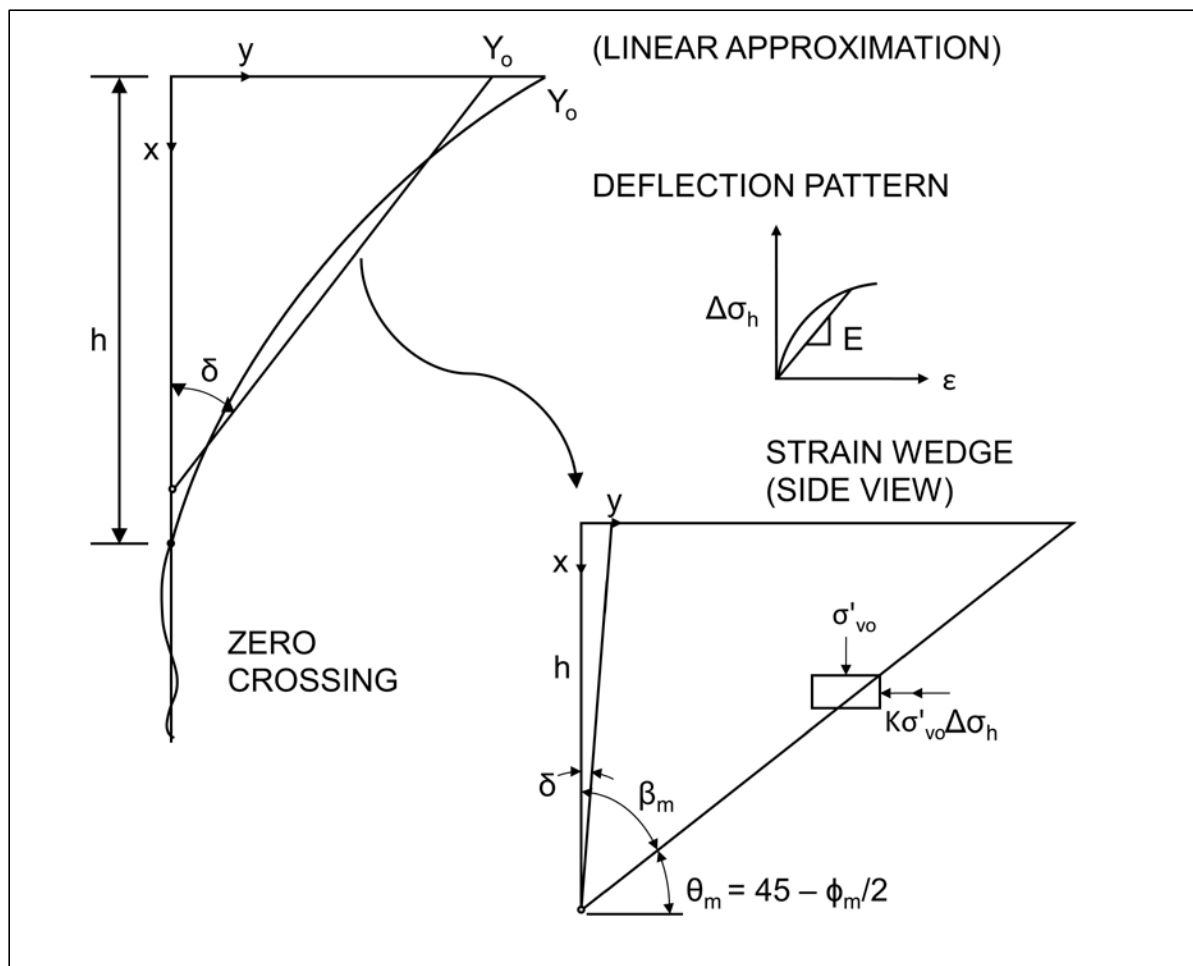
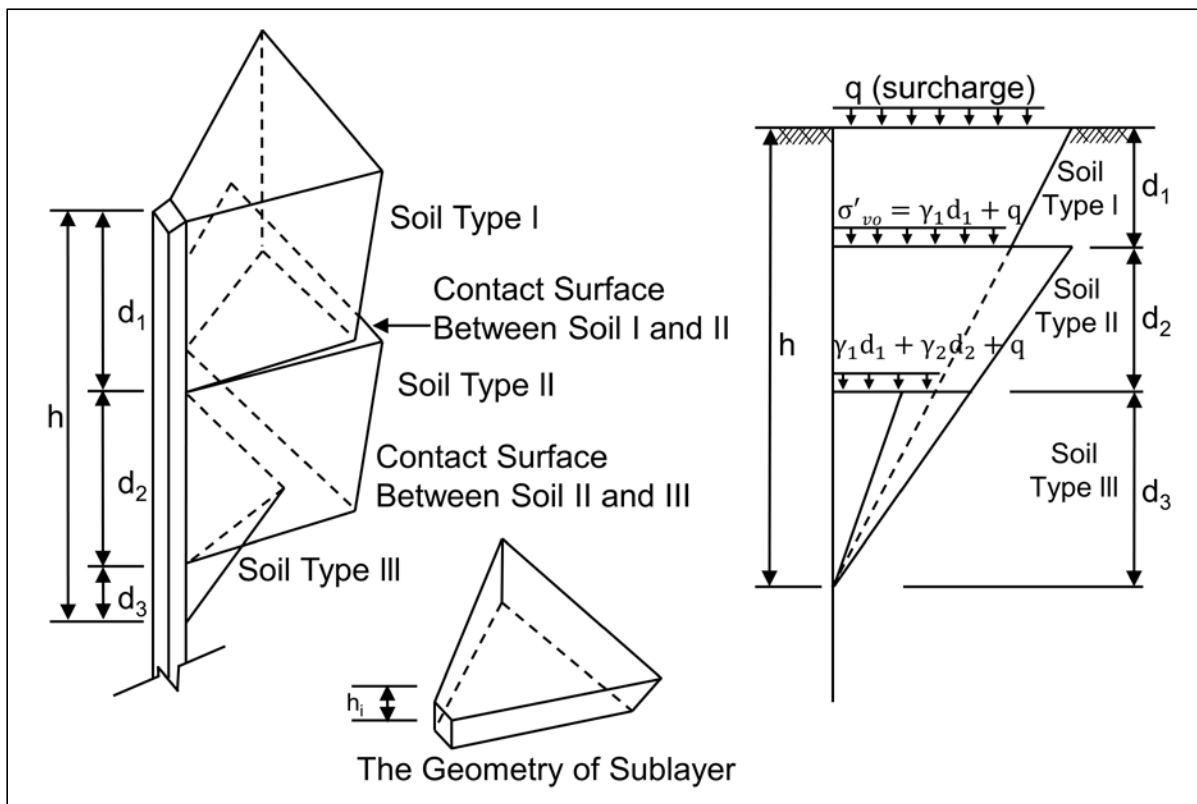


Figure 7-70 Strain wedge developed in soil (after Ashour et al. 1998a).

The soil stress-strain behavior can be estimated or directly incorporated from laboratory tests and included in the wedge profile. For the so called multi-sublayer technique, individual soil parameters are assigned for each respective soil layer in the wedge. The wedge shape changes with variations in soil properties as depicted in Figure 7-71. This analysis method therefore offers a potential benefit over traditional p-y modeling; the elastic springs are not independently modeled along the continuous pile length as shown in Figure 7-72. In addition, pile group effects are addressed from the overlapping wedges of each pile in the group.

Implementation of the SW method may be performed with software such as the Deep Foundation System Analysis Program (DFSAP), and has shown positive correlation with measured pile response from field tests (Ashour et al. 1998a). However widespread use of DFSAP has yet to occur, and many transportation agencies continue to use p-y based lateral pile analyses.



Table

Figure 7-71 Proposed geometry of compound passive wedge (after Ashour et al. 1998a).

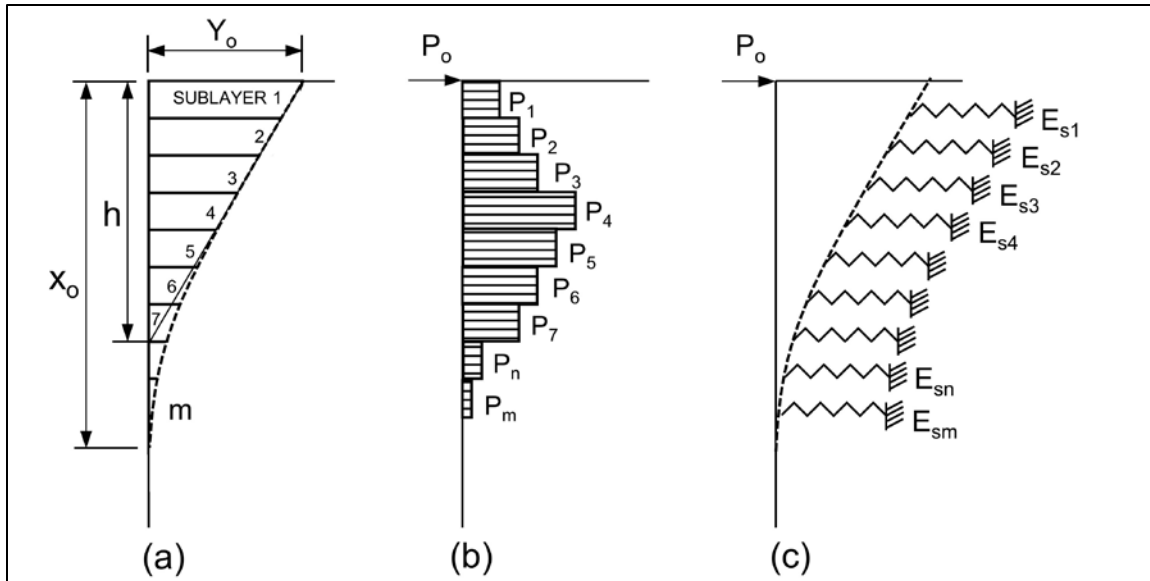


Figure 7-72 Soil-pile interaction with multiple soil layers (after Ashour et al. 1998a).

7.3.7.5 Single Piles

Lateral analysis software readily performs lateral analysis for a single pile. The applied loads to be analyzed should be factored loads (at the respective strength, service, and extreme event limit states) while the geotechnical resistance has a resistance factor of 1.0 per AASHTO (2014). Pile bents frequently consist of a single row of piles. Therefore, these are modeled as a single pile along the alignment of a bridge, and as a pile group in the perpendicular axis. More frequently, piles are installed in groups with two or more rows of piles. The following section addresses lateral pile analysis in greater detail with content applicable to both a single pile (lead row) and pile groups.

7.3.7.6 Pile Groups

The ability of a pile group to resist lateral loads from vessel impact, debris, wind, or wave loading, seismic events, and other sources is a significant design issue. The deflection of a pile group under a lateral load is typically 2 to 3 times larger than the deflection of a single pile loaded to the same intensity. Holloway et al. (1981) and Brown et al. (1988) reported that piles in trailing rows of pile groups (nearest the point of load application) have significantly less resistance to a lateral load than piles in the lead row, and therefore exhibit greater deflections. This is due to the pile-soil-pile interaction that takes place in a pile group. The pile-soil-pile interaction results in the lateral resistance of a pile group being less than the sum of the lateral resistance of the individual piles comprising the group. Hence, laterally loaded pile groups have a group efficiency of less than 1.

The lateral resistance of an individual pile in a pile group is a function of its position in the group and the center to center pile spacing. Brown et al. (1988) proposed a p-multiplier, P_m , be used to modify the p-y curve of an individual pile based upon the piles row position. An illustration of the p-multiplier concept is presented in Figure 7-73. For piles in a given row, the same P_m value is applied to all p-y curves along the length of the pile. In a lateral load test of a 3 by 3 pile group in very dense sand with a center to center pile spacing of $3b$, Brown found the leading row of piles had a P_m of 0.8 times that of an individual pile. The P_m values for the middle and back row of the group were 0.4 and 0.3, respectively.

McVay et al. (1995) performed centrifuge model tests on a 3 by 3 pile group having center to center pile spacings of $3b$ and $5b$. A dense and loose sand condition was simulated in the centrifuge model tests. For the dense sand case at a center to center spacing of $3b$, the centrifuge model test results were similar to Brown's field results. However, McVay also found that the P_m values were influenced by soil density and the center to center spacing. The P_m results from McVay's centrifuge tests as well as other recent results for vertical piles in 3 x 3 pile groups are summarized in Table 7-23. McVay's centrifuge tests indicated lateral load group efficiencies in sands on the order of 0.74 for a center to center pile of $3b$ and 0.93 for a center to center spacing of $5b$. Field studies in cohesive soils have also shown that pile-soil-pile interaction occurs. Brown et al. (1987) reported P_m values of 0.7, 0.5, and 0.4 for the lead, second, and third row of a laterally loaded pile group in stiff clays.

Additional work on this topic has included full scale lateral load testing of a 16 pile group in loose sand by Ruesta and Townsend (1997), and a 9 pile group in clayey silt by Rollins et al. (1998). A scaled model study of a cyclically laterally loaded pile group in medium clay has also been reported by Moss (1997). The center to center pile spacing, P_m results, and pile head deflections reported in these studies are included in Table 7-23. NCHRP Project 24-09 entitled "Static and Dynamic Lateral Loading of Pile Groups" was also completed by Brown et al. (2001). The objective of this study was to develop and validate an improved design method for pile groups subjected to static and dynamic lateral loads. The information summarized in Table 7-23 has been averaged and incorporated into AASHTO (2014). However, the distinction between soil type and test type is not made. The designer should consider if other p-multiplier, P_m , values may be more applicable in situations similar to those described in Table 7-22 which have comparatively lower P_m values than AASHTO.

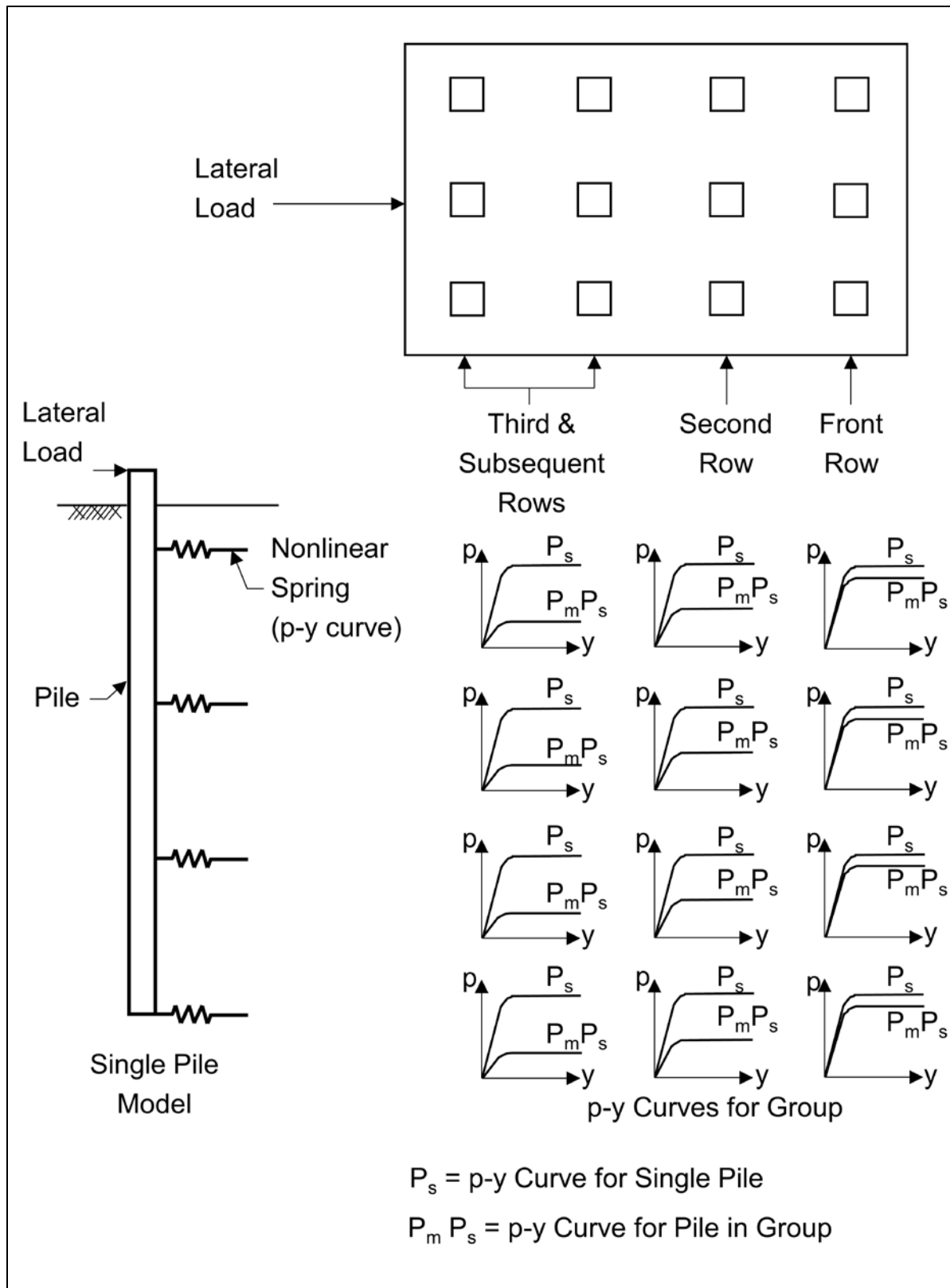


Figure 7-73 Illustration of p-multiplier concept for lateral group analysis.

Table 7-23 Laterally Loaded Pile Group Studies

Soil Type	Test Type	Center to Center Pile Spacing	Calculated p-Multipliers, P_m For Rows 1, 2, & 3+	Deflection, inches	Reference
Stiff Clay	Field Study	3b	0.70, 0.50, 0.40	2	Brown <i>et al.</i> (1987)
Stiff Clay	Field Study	3b	0.70, 0.60, 0.50	1.2	Brown <i>et al.</i> (1987)
Stiff Clay	Field Study	3.3b	0.82, 0.61, 0.45	3.5	Rollins <i>et al.</i> (2006)
Stiff Clay	Field Study	4.4b	0.90, 0.80, 0.69	1.6	Rollins <i>et al.</i> (2006)
Stiff Clay	Field Study	5.65b	0.95, 0.88, 0.77	2.6	Rollins <i>et al.</i> (2006)
Medium Clay	Scale Model-Cyclic Load	3b	0.60, 0.45, 0.40	2.4 at 50 cycles	Moss (1997)
Clayey Silt	Field Study	3b	0.60, 0.40, 0.40	1.0-2.4	Rollins <i>et al.</i> (1998)
V. Dense Sand	Field Study	3b	0.80, 0.40, 0.30	1	Brown <i>et al.</i> (1988)
M. Dense Sand	Centrifuge Model	3b	0.80, 0.40, 0.30	3	McVay <i>et al.</i> (1995)
M. Dense Sand	Centrifuge Model	5b	1.0, 0.85, 0.70	3	McVay <i>et al.</i> (1995)
Loose M. Sand	Centrifuge Model	3b	0.65, 0.45, 0.35	3	McVay <i>et al.</i> (1995)
Loose M. Sand	Centrifuge Model	5b	1.0, 0.85, 0.70	3	McVay <i>et al.</i> (1995)
Loose F. Sand	Field Study	3b	0.80, 0.70, 0.30	1-3	Ruesta <i>et al.</i> (1997)

Brown and Bollman (1993) proposed a p-multiplier procedure for the design of laterally loaded pile groups. It is recommended that this approach, outlined in the step by step procedure that follows, be used for the design of laterally loaded pile groups. For a center to center pile spacing of 3b, AASHTO (2014) design specifications recommend p-multiplier, P_m , values of 0.8 for the lead row, 0.4 for the second row, and 0.3 for the third and subsequent rows. For a center to center pile spacing of 5b, the AASHTO specified P_m values are 1.0 for the lead row, 0.85 for the second row, and 0.7 for the third and subsequent rows. For center to center pile spacing between 3B and 5B, interpolation is recommended to determine the

appropriate P_m value. Figure 7-74 shows typical load and moment versus deflection plots from this procedure which can be performed using multiple individual analyses with a p-y software program. The analyses can also be performed with less effort using pile group software such as the FB-Pier, FB-MultiPier or GROUP computer programs.

The computer program FB-Pier was developed with FHWA support as the primary design tool for analysis of pile groups under axial and lateral loads. This program, which is a successor of the LPGSTAN program by Hoit and McVay (1994) is a non-linear, finite element analysis, soil structure interaction program. FB-Pier uses a p-multiplier approach in evaluation of laterally loaded pile groups under axial, lateral, and combined axial and lateral loads. The program is capable of analyzing driven pile and drilled shaft foundation supported sound walls, retaining walls, signs and high mast lighting. FB-MultiPier replaced FB-Pier and functions similarly. FB-MultiPier contains additional features and can apply loading variations from multiple piers connected by bridge spans.

Fayyazi et al. (2012) studies the effects of the center to center pile spacing between rows as well as the spacing between piles within the same row in two model pile groups in sand. They observed that the spacing within a row can have a significant effect of the lateral pile group resistance due to the edge effects from overlapping zones of influence between two piles in the same row. They found that edge effects can result in overestimating the lateral load resistance by as much as 30%. Their research is ongoing with the goal of providing a procedure of p-multiplier selection that considers both row and inter row pile spacing within a group.

STEP BY STEP DESIGN PROCEDURE FOR LATERALLY LOADED PILE GROUPS USING LATERAL SINGLE PILE ANALYSIS

STEP 1 Obtain factored lateral loads.

STEP 2 Develop p-y curves for single pile.

- a. Obtain site specific single pile p-y curves from instrumented lateral pile load test at site.
- b. Use p-y curves based on published correlations with soil properties.
- c. Develop site specific p-y curves based on in-situ test data.

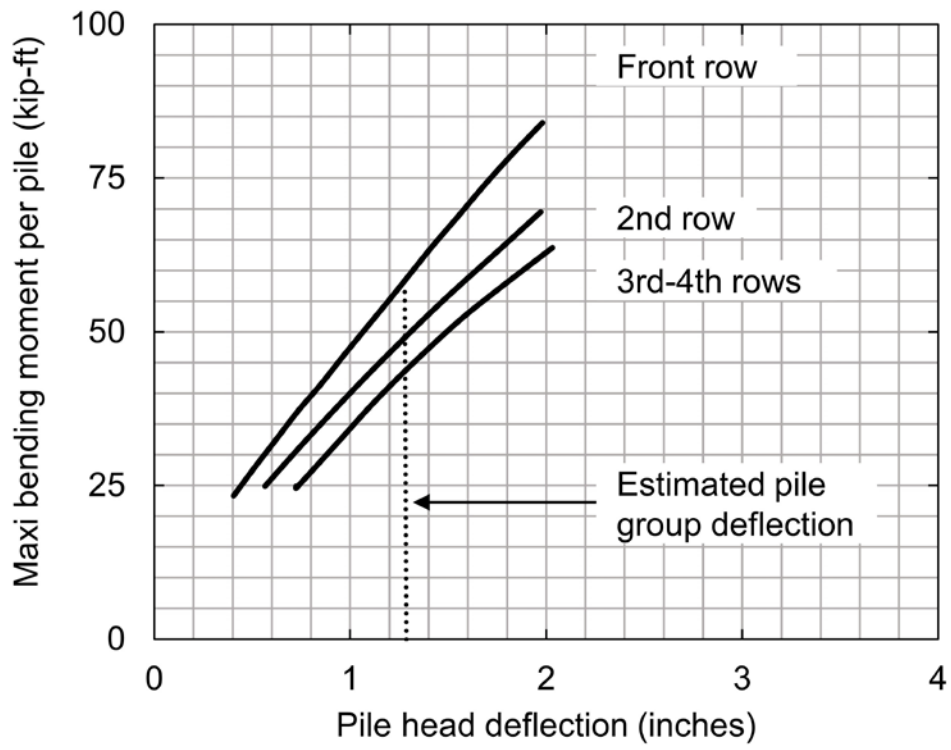
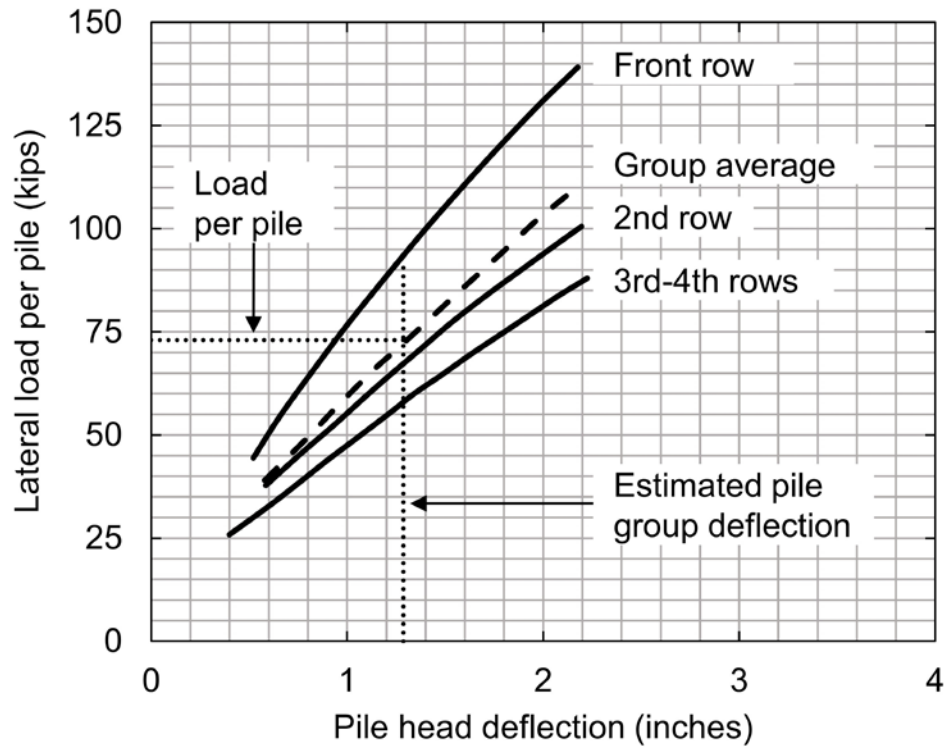


Figure 7-74 Typical plots of (a) Load versus deflection and (b) Bending moment versus deflection for pile group analysis (adapted from Brown and Bollman 1993).

STEP 3 Run software analyses.

- a. Perform p-y analyses using the P_m value for each row position to develop load-deflection and load-moment data.
- b. Use AASHTO (2014) design specification recommendations for P_m values. For a center to center pile spacing of $3b$, recommended P_m values are 0.8 for the lead row, 0.4 for the second row, and 0.3 for the third and subsequent rows. For a center to center pile spacing of $5b$, recommended P_m values are 1.0 for the lead row, 0.85 for the second row, and 0.7 for the third and subsequent rows. Interpolate for center to center pile spacing between $3b$ and $5b$ to determine for the appropriate P_m value.
- c. Determine shear load versus deflection behavior for piles in each row. Plot load versus pile head deflection results similar to as shown in Figure 7-74(a).

STEP 4 Estimate group deflection under lateral load.

Average the load for a given deflection from all piles in the group (i.e. each of the four rows) to determine the average group response to a lateral load as shown in Figure 7-74(a).

Divide the lateral load to be resisted by the pile group by the number of piles in the group to determine the average lateral load resisted per pile.

Enter load-deflection graph similar to Figure 7-74(a) with the average load per pile to estimate group deflection using the group average load deflection curve.

STEP 5 Evaluate pile structural acceptability.

- a. Plot the maximum bending moment determined from p-y software analyses versus deflection for each row of piles as illustrated in Figure 7-74(b).
- b. Check the pile structural adequacy for each p. Use the estimated group deflection under the lateral load per pile to determine the maximum bending moment for an individual pile in each row.

- c. Determine maximum pile stress from p-y software output associated with the maximum bending moment.
- d. Compare maximum pile stress with pile yield stress.

STEP 6 Perform refined pile group evaluation that considers superstructure-substructure interaction.

7.3.7.6.1 Lateral Resistance Increases Through Ground Improvement

Methods to improve the lateral resistance of pile groups in weak near surface soils were evaluated by Rollins and Brown (2011) in NCHRP Report 698, Design Guidelines for Increasing the Lateral Resistance of Highway-Bridge Pile Foundations by Improving Weak Soils. This study concluded that significant increases in lateral resistance in soft clays and loose sands can be achieved through soil replacement or ground improvement techniques. Figure 7-75 illustrates the appropriate treatment areas to improve lateral resistance around new foundations in weak soils as well as the treatment areas around existing foundations to improve their lateral resistance.

Tables 7-24 and 7-25 summarize the treatment options studied, the improvement in lateral resistance achieved, the treatment costs, and the cost savings. The standard alternative to ground improvement is to add more piles in order to resist the same lateral load. This option would also require a larger pile cap. The approximate cost of the additional piles and larger cap necessary to resist the same lateral load was estimated for each ground improvement technique and is reported in the third column of Table 7-25. The difference between this cost and the ground improvement cost in column 2 is the reported cost savings in column 4. For more detailed information, please refer to the NCHRP study.

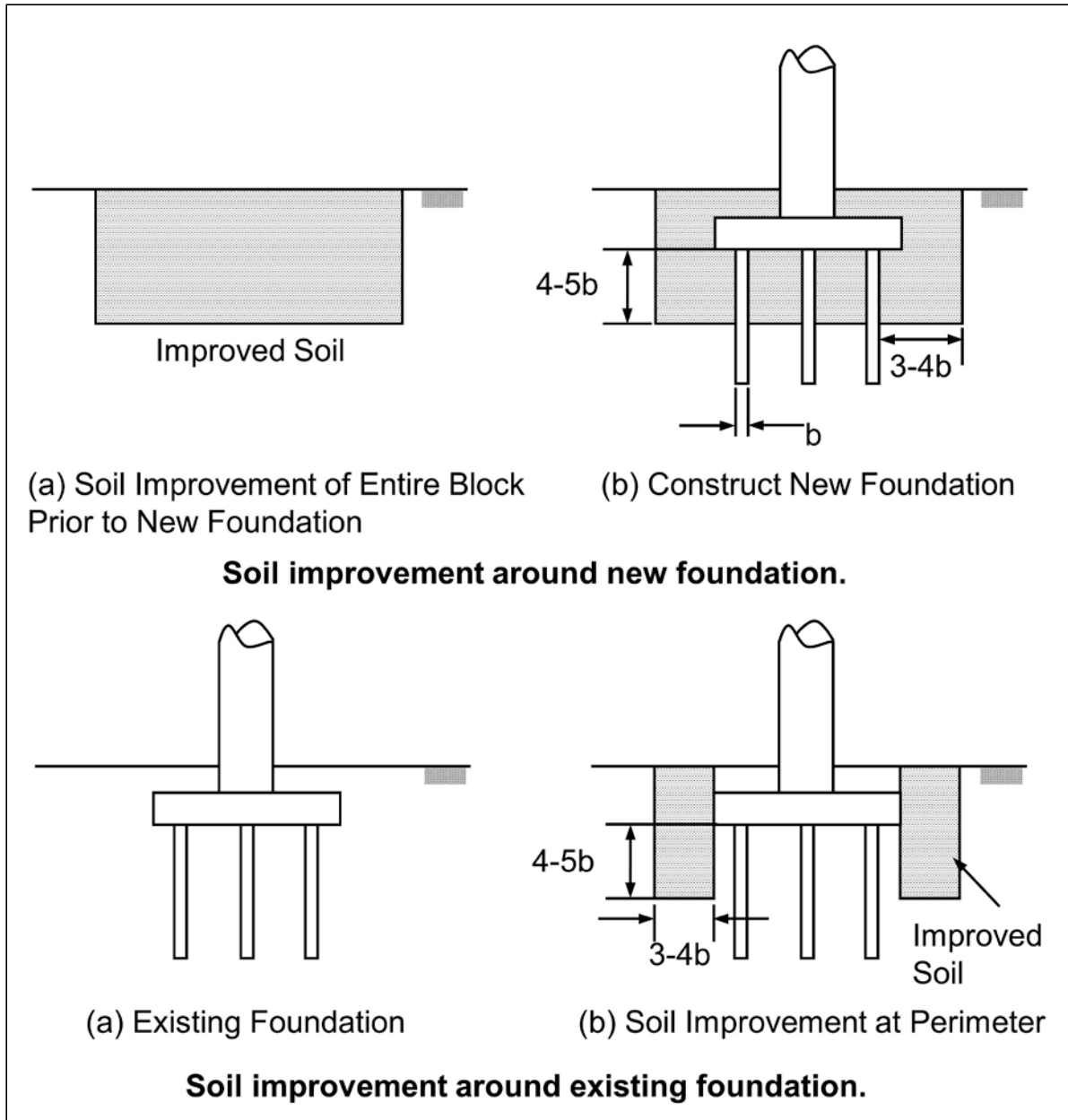


Figure 7-75 Ground improvement treatment areas for increased lateral resistance of pile groups in weak soils (Rollins and Brown 2011).

Table 7-24 Summary of Ground Improvement Method and Increase in Lateral Resistance (after Rollins and Brown 2011)

Treatment Method	Treatment Dimensions (LxWxD)	Treatment Volume (yd ³)	Untreated Lateral Resistance (kips)	Increase in Lateral Resistance (kips)	Percent Increase in Resistance
Jet grouting below cap.	15' x 10.5' x 10'	58.3	282	500	160
Jet grouting adjacent to cap.	6,6' x 13' x 12'	38.1	214	398	185
Soil mixing adjacent to cap.	4' x 11' x 10'	16.3	282	170	60
Weak flowable fill below cap.	13.5' x 8.8' x 6'	26.4	232	24	10
Flowable fill adjacent to cap.	6' x 12' x 6'	16.0	265	145	55
Compacted fill to edge of cap.	9.6' x 8.75' x 3.5'	10.9	232	23	10
Compacted fill 5 feet beyond edge of cap.	14.6' x 8.75' x 3.5'	16.6	232	40	18
Rammed aggregate piers adjacent to cap top.	13, 2.5 dia x 13' deep	29.5	285	40	14
Rammed aggregate piers adjacent to cap top.	13, 2.5' dia. X 10.5 deep	23.6	50	35	70

Table 7-25 Summary of Ground Improvement Method and Associated Costs for Increase in Lateral Resistance after (Rollins and Brown 2011)

Treatment Method	Ground Improvement Cost	Pile and Pile Cap Cost for Same Lateral Load Increase	Savings Relative to Adding Additional Piles	Ground Improvement Lateral Support Cost (\$ / kip)
Jet grouting below cap.	\$28,500	\$84,200	\$55,700	57
Jet grouting adjacent to cap.	\$38,000	\$69,360	\$31,360	95
Soil mixing adjacent to cap.	\$10,000	\$30,345	\$20,345	59
Weak flowable fill below cap.	\$3,180	\$4,335	\$1,155	133
Flowable fill adjacent to cap.	\$3,600	\$26,010	\$22,410	25
Compacted fill to edge of cap.	\$544	\$4,335	\$3,791	24
Compacted fill 5 feet beyond edge of cap.	\$828	\$8,670	\$7,842	21
Rammed aggregate piers adjacent to cap top.	\$4,225	\$8,670	\$4,445	106
Rammed aggregate piers adjacent to cap top.	\$4,225	\$8,670	\$4,445	121

7.3.8 Lateral Squeeze of Foundation Soil and Solutions

Bridge abutments supported on piles driven through soft compressible cohesive soils may tilt forward or backward depending on the geometry of the backfill and the abutment. This problem is illustrated in Figure 7-76. Large horizontal movements may cause damage to the structure. The unbalanced fill loads displace the soil laterally. This lateral displacement may bend the piles, causing the abutment to tilt toward or away from the fill. Lateral squeeze can similarly adversely affect pier locations if stockpiles are placed adjacent to a pier location.

The following rules of thumb are recommended for determining whether tilting will occur, as well as estimating the magnitude of horizontal movement.

1. Lateral squeeze and abutment tilting can occur if:

$$\gamma_f h_f > 3s_u \quad \text{Eq. 7-74}$$

Where:

- γ_f = unit weight of fill (pcf).
- h_f = height of fill (feet).
- s_u = undrained shear strength of soft cohesive soil (psf).

2. If abutment tilting can occur, the magnitude of the horizontal movement can be estimated by the following formula:

$$S_h = 0.25S_v \quad \text{Eq. 7-75}$$

Where:

- S_h = horizontal abutment movement (inches).
- S_v = vertical fill settlement (inches).

Mitigation of lateral squeeze may be provided by several means. The four solutions below represent primary methods to prevent lateral squeeze.

- a. Delay installation of abutment piling until after fill settlement has stabilized (best solution).
- b. Provide expansion shoes large enough to accommodate the movement.
- c. Use steel H-piles to provide high tensile strength in flexure.
- d. Use lightweight fill materials to reduce driving forces.

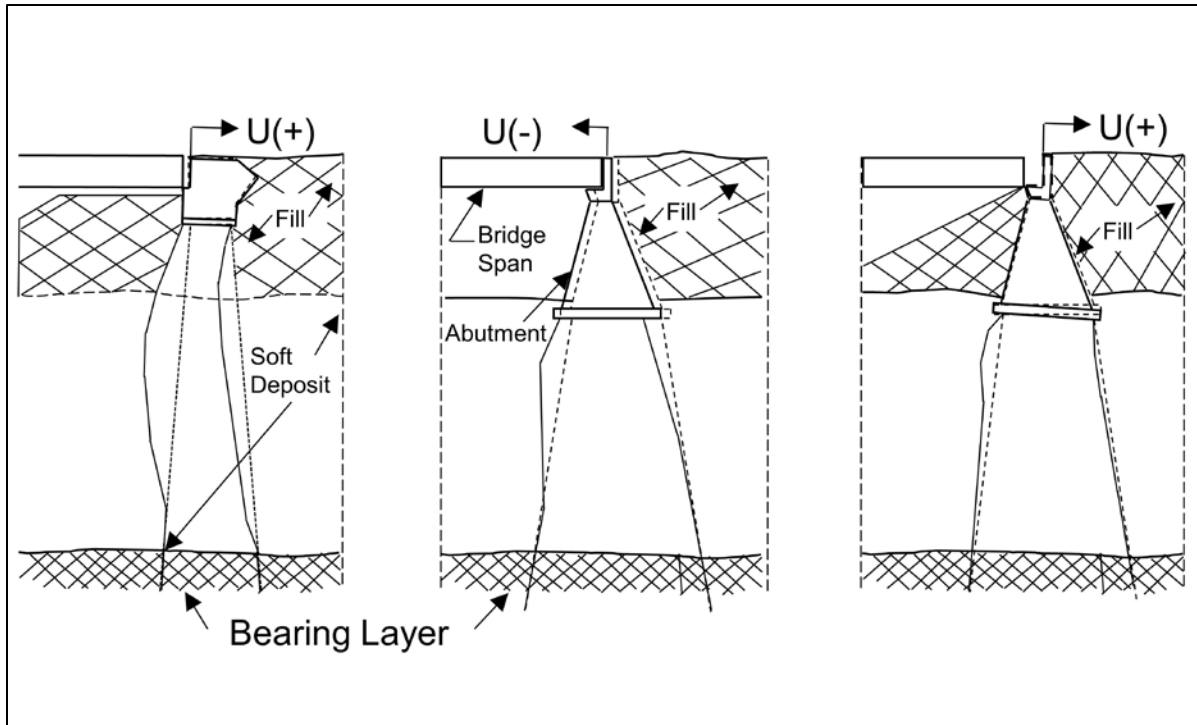


Figure 7-76 Examples of abutment tilting due to lateral squeeze.

7.3.9 Overall Stability

Abutments are often supported by a deep foundation system and are also subject to the potential for overall stability failure. Although the stiffness of deep foundations may provide resistance against this shear loading, if the slip surface is below the pile tip elevation, or if large earthen loads are generated, global stability failure should be evaluated. To a lesser extent, this situation may apply to walls or other cut slopes which are also founded on structural elements. Per AASHTO (2014), the Service I Load Combination and load factor should be used to assess global stability. When the stabilizing system includes a structural element (deep foundation), a resistance factor of 0.65 for sliding is recommended for use in stability calculations. As provided in the AASHTO (2014) commentary, the 0.65 resistance factor is taken as the inverse of the typical 1.5 safety factor used in the ASD approach. A detailed discussion on the mechanisms of shear failure and slope stability is beyond the scope of this manual. References can be made to Sabatini et al. (1997), Duncan and Wright (2005) and Tanyu et al. (2008).

7.4 EXTREME EVENT LIMIT STATES

Extreme event limit states involve events with a low occurrence probability. However, these events can have a detrimental impact on the foundation and structure if not considered in design. As noted in AASHTO (2014), the extreme event limit state exists to protect against structural collapse and preserve life. Furthermore, AASHTO (2014) provides guidance on extreme event loading cases, including ice loading and vehicle and vessel impacts. Arneson et al. (2012) details scour development near bridge piers and abutments, while Kavazanjian et al. (2011) provides an in depth discussion on seismic events. Background information on ice loads can be found in Montgomery et al. (1984). In depth coverage for vessel impact design is available in AASHTO (2009) Guide Specifications and Commentary for Vessel Collision Design of Highway Bridges. The following sections provide a discussion on these event types, while the documents referenced above address these topics in greater detail.

Extreme event limit state evaluations ensure structural survival of a bridge under unique major occurrences such as earthquakes, floods, and vehicle or vessel collisions having return periods significantly greater than the bridge design life. Extreme event limit states for driven pile foundation design include:

- the check flood for scour,
- vessel collision,
- vehicle collision,
- seismic loading,
- ice and debris loading, and
- other site-specific situations determined by the design engineer.

7.4.1 Extreme Event Scour During Check Flood

Many bridges are constructed over rivers, bodies of water, and tidal areas where scour is a consideration in the foundation design. These structures encounter repeated aggradation or degradation of material in the scour zone which affects the foundation resistance. The check flood is an extreme event that is unlikely to happen during the design life of the structure. Arneson et al. (2012) details design requirements for the check flood where soil materials within the scour zone are assumed to be removed and provide no geotechnical resistance for lateral, axial compression, or tension loads.

For the applicable factored loads, the pile foundation must have adequate factored axial and lateral resistance. In the extreme event limit state, the check flood for scour differs from the design flood as follows:

1. The 500-year check flood has a different and typically deeper scour prism.
2. The loads used for structural modeling in the extreme event limit state are unfactored.
3. Resistance factors of 1.0 are used for the geotechnical resistances on lateral and axial compression loads, and 0.8 or less for uplift loads.

Overall stability of the bridge should be evaluated during the check flood, where storm surges, tides or other floods can detrimentally impact the foundation and overall structure. Debris loads during the check flood should likewise be included in this analysis. Piles should be driven to penetration depths to overcome the loss of shaft resistance within the scour prism.

Loading combinations with the check flood are further explained in Section 7.4.4, as well as in HEC-18 (Arneson et al. 2012). Section 7.2.9 also provides additional background on scour design considerations.

7.4.2 Seismic and Seismic Induced Downdrag

The design issues associated with pile foundation design for seismic events are significant and include liquefaction effects on soil resistance, ground movements, seismic induced foundation loads, and seismic induced drag forces. As noted in AASHTO (2014) design specifications, bridges shall be designed for a low probability of collapse but may suffer significant damage or disruption of service as a result of earthquake loading. A pseudo-static analysis approach is commonly utilized for many bridges and will be covered in this section. In addition, subsequent sections of this manual will discuss seismic action effects with respect to the extreme event limit states. However, more detailed references should be consulted on the seismic design procedure including Geotechnical Engineering Circular No. 3 by Kavazanjian et al. (2011) and FHWA-NHI-15-004 LRFD Seismic Analysis and Design of Bridges by Marsh et al. (2014).

7.4.2.1 AASHTO Recommendations for the Equivalent Static Seismic Force

For earthquake loads, the horizontal ground displacements are transmitted from the foundation to superstructure where accelerations occur. As a result, inertial forces are generated and applied back to the foundation which must then resist these loads. The superstructure must be designed to resist brittle failure as a result of seismic loading (Marsh et al. 2014) while the foundation must resist effects of liquefaction, ground movement, drag forces and the increased superstructure loads. Before defining the required nominal geotechnical resistance, the increased loads resulting from seismic action must first be determined.

STEP BY STEP PROCEDURE FOR: “EVALUATION OF EARTHQUAKE LOAD”

The seismic hazard of a site contributes to expected loads that can develop for a 1000 year design earthquake (AASHTO 2014). AASHTO Article 3.10 outlines steps to determine the elastic seismic coefficient, C_{sm} . However the end goal is to define the equivalent static horizontal seismic force, $P_e(x)$. This relationship is shown in Equation 7-76, with the following steps providing a discussion of this process.

$$P_e(x) = C_{sm} W \quad \text{Eq. 7-76}$$

Where:

- $P_e(x)$ = equivalent static horizontal seismic force acting on superstructure.
- C_{sm} = elastic seismic response coefficient (dimensionless).
- W = equivalent weight of the superstructure.

STEP 1 Define the Site Ground Coefficient and Spectral Coefficients.

The site peak ground acceleration coefficient, PGA, short period spectral coefficient, S_s and long period spectral coefficient, S_l , are determined by inspecting contour seismic maps developed for such a purpose. These maps were developed by the U.S. Geological Survey for AASHTO and may be found in the Chapter 3 of AASHTO (2014) design specifications. In addition, the U.S. Geological Survey website includes an application (<http://earthquake.usgs.gov/designmaps/us/application.php>) which performs a search and presents these output values, after the user enters the site location and site classification.

STEP 2 Determine the Site Classification.

Using results of the subsurface investigation, the site is classified as A to F. The upper 100 feet of the subsurface profile is to be averaged to define the shear wave velocity, SPT N-Value, and undrained shear strength. Table 7-26 should be used for this determination.

Table 7-26 Site Class Definition

Site Class	Soil Type and Profile
A	Hard rock with measured shear wave velocity, $\bar{v}_s > 5,000$ ft/s.
B	Rock with $2,500$ ft/sec $< \bar{v}_s < 5,000$ ft/s.
C	Very dense soil and soil rock with $1,200$ ft/sec $< \bar{v}_s < 2,500$ ft/s, or with either $\bar{N} > 50$ blows/ft, or $\bar{s}_u > 2.0$ ksf.
D	Stiff soil with 600 ft/s $< \bar{v}_s < 1,200$ ft/s, or with either $15 < \bar{N} < 50$ blows/ft, or $1.0 < \bar{s}_u < 2.0$ ksf.
E	Soil profile with $\bar{v}_s < 600$ ft/s or with either $\bar{N} < 15$ blows/ft or $\bar{s}_u < 1.0$ ksf, or any profile with more than 10 ft of soft clay defined as soil with $PI > 20$, $w > 40$ percent and $\bar{s}_u < 0.5$ ksf.
F	Soils requiring site-specific evaluations, such as: <ul style="list-style-type: none"> • Peats or highly organic clays ($H > 10$ ft of peat or highly organic clay where H = thickness of soil). • Very high plasticity clays ($H > 25$ ft with $PI > 75$). • Very thick soft/medium stiff clays ($H > 120$ ft).

\bar{v}_s = average shear wave velocity

\bar{N} = average SPT N- value

\bar{s}_u = average undrained shear strength

w = moisture content

PI = Plasticity Index

STEP 3 Determine the Site Factors.

Site factors corresponding to the zero, short and long periods of acceleration should be determined using Table 7-27 to Table 7-29. Straight line interpolation should be used for intermediate values in any of the three tables. If the site is classified as Class F, a site-specific geotechnical investigation with dynamic response analysis should be performed to determine these acceleration period parameters.

Table 7-27 Site Factor Values, F_{pga} , at Zero Period Acceleration

Site Class	PGA < 0.1	PGA = 0.2	PGA = 0.3	PGA = 0.4	PGA > 0.5
A	0.8	0.8	0.8	0.8	0.8
B	1.0	1.0	1.0	1.0	1.0
C	1.2	1.2	1.1	1.0	1.0
D	1.6	1.4	1.2	1.1	1.0
E	2.5	1.7	1.2	0.9	0.9
F	*	*	*	*	*

Table 7-28 Site Factor Values, F_a , for Short Period Coefficient S_s

Site Class	$S_s < 0.25$	$S_s = 0.5$	$S_s = 0.75$	$S_s = 1.0$	$S_s > 1.25$
A	0.8	0.8	0.8	0.8	0.8
B	1.0	1.0	1.0	1.0	1.0
C	1.2	1.2	1.1	1.0	1.0
D	1.6	1.4	1.2	1.1	1.0
E	2.5	1.7	1.2	0.9	0.9
F	*	*	*	*	*

Table 7-29 Site Factor Values, F_v , for Long Period Coefficient, S_1

Site Class	$S_1 < 0.1$	$S_1 = 0.2$	$S_1 = 0.3$	$S_1 = 0.4$	$S_1 > 0.5$
A	0.8	0.8	0.8	0.8	0.8
B	1.0	1.0	1.0	1.0	1.0
C	1.7	1.6	1.5	1.4	1.3
D	2.4	2.0	1.8	1.6	1.5
E	3.5	3.2	2.8	2.4	2.4
F	*	*	*	*	*

STEP 4 Characterize the Design Response Spectrum and Determine the Elastic Seismic Response Coefficient, C_{sm}

The Design Response Spectrum as shown in Figure 7-77 is created using the zero, short, and long period acceleration values as well as the site factor values determined from the steps above.

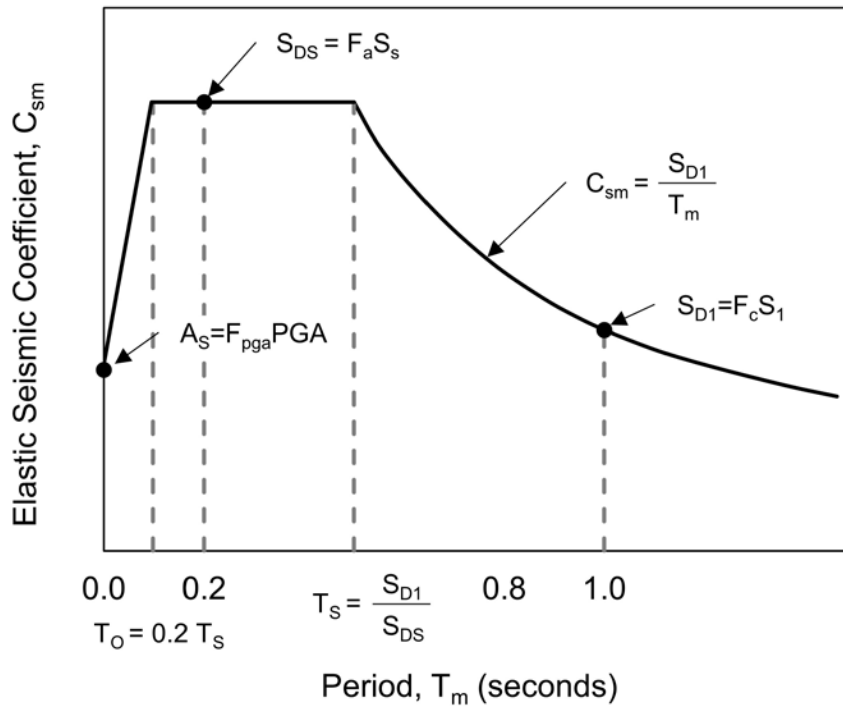


Figure 7-77 Design response spectrum (after AASHTO 2014).

The elastic seismic response coefficient is a function of the Design Response Spectrum and a hand calculation may be used to determine this exact value. Equation 7-77 to Equation 7-79 should be employed for this purpose.

$$C_{sm} = A_s + (S_{DS} - A_s) \left(\frac{T_m}{T_o} \right) \quad \text{Eq. 7-77}$$

In which

$$A_s = F_{PGA} PGA \quad \text{Eq. 7-78}$$

$$S_{DS} = F_a S_s \quad \text{Eq. 7-79}$$

Where:

C_{sm} = elastic seismic response coefficient (dimensionless).

A_s = peak seismic ground acceleration coefficient modified by short-period site factor (dimensionless).

S_{DS} = C_{sm} value with a period of 0.2 second = $F_a S_s$

T_m = period of vibration of m th mode(s).

T_o = reference period to define spectral shape = $0.2T_s$.

T_s = corner period when spectrum changes from independent to inversely proportional = S_{D1} / S_{DS}

F_{PGA} = zero period site factor.

- PGA= peak ground acceleration coefficient.
- F_a = short period site factor.
- S_s = short period spectral coefficient.
- S_{D1} = C_{sm} value with a period of 1.0 seconds = $F_v S_1$.

The elastic seismic response coefficient, C_{sm} , is then substituted into Equation 7-76 as noted to determine the equivalent static force. The structural engineer applies this force to the superstructure using a method outlined in Article 4.7.4.3 of the AASHTO (2014) design specifications. The minimum analysis requirement depends on the seismic zone in which the bridge exists, as well as the bridge regularity and operational classification. Table 7-30 classifies the site as Seismic Zone 1 through 4 depending on the acceleration coefficient, S_{D1} . If the site is classified as Seismic Zone 2 through 4, a liquefaction assessment is required for multispan bridges.

Table 7-30 Seismic Zones

Acceleration Coefficient, S_{D1}	Seismic Zone
$S_{D1} \leq 0.15$	1
$0.15 < S_{D1} \leq 0.30$	2
$0.30 < S_{D1} \leq 0.50$	3
$0.50 < S_{D1}$	4

For the Extreme Event I check, the factored loads resulting from seismic action are then applied to the foundation for an axial, lateral and overturning analysis. A resistance factor of 1.0 is used on the resistances for axial compression loads and 0.8 or less for lateral and uplift loads as recommended by AASHTO (2014).

7.4.2.2 Liquefaction

Liquefaction is defined as a loss of shear strength and stiffness which results from built-up pore water pressure during cyclic loading. Soil types most susceptible to liquefaction are saturated, very loose to medium dense, fine to medium grained sands and non-plastic silts. However, liquefaction has also occurred in saturated, very loose to medium dense gravels.

In seismically active areas where peak earthquake acceleration will be greater than 0.1g, the soil susceptibility to liquefaction should be evaluated. A commonly used procedure for identification of liquefaction susceptible soils was proposed by Seed et al. (1983). This liquefaction evaluation approach is detailed in Lam and Martin

(1986), the Commentary for Article 10.5.4 of AASHTO (2014), and Chapter 6 of GEC-3 by Kavazanjian et al. (2011). If the soils are found to be subject to liquefaction during the design event, the pile foundation must be designed to accommodate the following resulting behavior: the loss of resistance in the liquefied zone, the seismic induced loads, as well as the anticipated vertical and horizontal displacements, and the resulting drag force. Alternatively, the liquefaction potential may be mitigated through ground improvement techniques.

Pile foundations in liquefiable soils must penetrate through the zone of liquefaction and develop adequate resistance in the underlying deposits. Evaluation of compression and uplift resistances during the seismic event can be made by assigning residual strength properties to the liquefiable layers. Appropriate residual strengths should be used to analyze axial and lateral loading. Residual strengths of sands and silty sands can be approximated from SPT resistance values using a correlation proposed by Seed (1987) and updated by Seed and Harder (1990). Additional correlations on the residual strengths of sands and silty sands have been reported by Olson and Stark (2002), as well as Idriss and Boulanger (2007). Figure 7-78 presents the correlation developed by Idriss and Boulanger between the equivalent clean sand SPT corrected blow count and the ratio of the residual shear strength, s_r , divided by the vertical effective stress, σ'_{vo} .

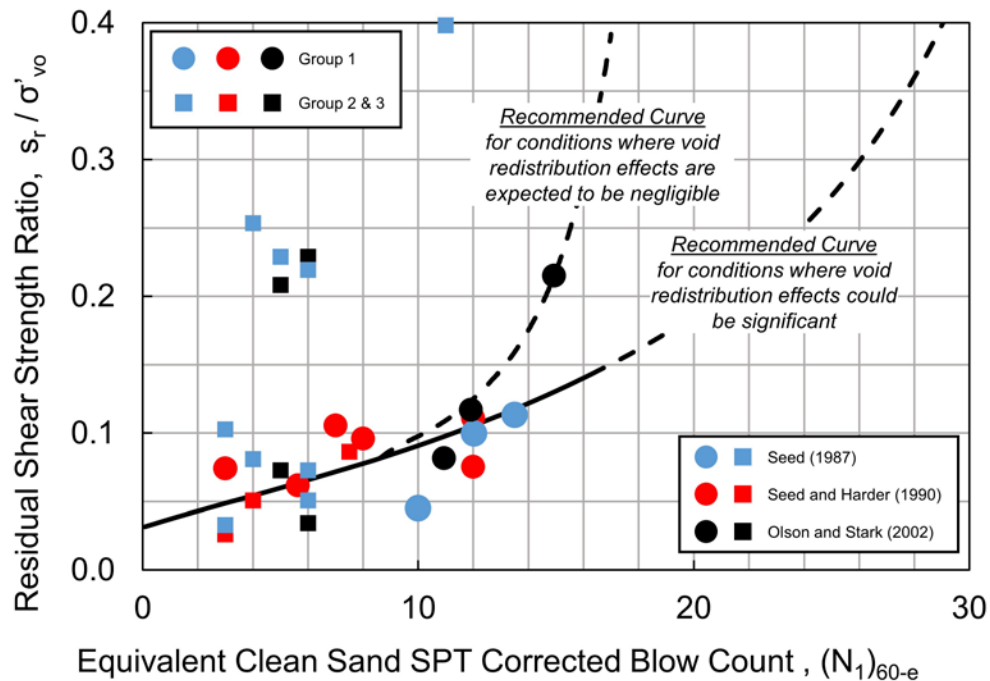


Figure 7-78 Correlation between the Residual Undrained Strength Ratio, s_r / σ'_{vo} and equivalent clean sand SPT blow count, $(N_1)_{60-e}$ (Idriss and Boulanger 2007).

The SPT N-value used for the equivalent clean sand in Figure 7-78 should be corrected for both energy and vertical effective stress as well as for the percent fines, as described by Seed and Harder (1990). The correction for the percent fines is provided in Table 7-31.

Table 7-31 Blow Count Correction, N_{corr} , for the Equivalent Clean Sand Blow Count, $(N_1)_{60-e}$

Percent Passing #200 Sieve	N_{corr}
0-9	0
10-24	1
25-49	2
50-74	4
> 75	5

The equivalent clean sand blow count is then determined using Equation 7-80 below.

$$(N_1)_{60-e} = (N_1)_{60} + N_{corr} \quad \text{Eq. 7-80}$$

Where:

- $(N_1)_{60-e}$ = equivalent clean sand blow count.
- $(N_1)_{60}$ = SPT N value corrected for energy and overburden stress.
- N_{corr} = correction for percent fines from Table 7-31.

In a Washington State research report, Kramer (2008) proposed an alternate approach for estimating the residual strength of liquefied soil. This approach estimated the residual strength based on a weighted value determined by four methods. This residual strength was based on 20% of the value determined following Idriss (1998), 20% of the value determined in accordance with from Olson and Stark (2002), 20% of the value determined following Idriss and Boulanger (2007), and 40% of the value determined using the Kramer-Wang hybrid model, Kramer and Wang (2007).

Following a seismic event that induces soil liquefaction, the liquefied layer will generally consolidate as pore water pressure dissipates. Settlement magnitude can be estimated using procedures in Kavazanjian et al. (2011). Fellenius and Siegel (2008) noted that the location of the zone of liquefaction relative to the neutral plane is very important. If liquefaction occurs in soil layers above the location of the neutral plane before liquefaction, the liquefaction event will have limited effect on the

pile. If liquefaction occurs in soil layers located below the pre-liquefaction location of the neutral plane, it will increase the axial compression load in the pile as well as result in additional pile settlement. The structural design of the pile section and the settlement resulting from liquefaction occurring below the neutral plane should be evaluated in the design. The pile foundation must be structurally capable of supporting the increased drag force and foundation settlement occurring after liquefaction must be within the structure's performance criteria.

Liquefaction induced lateral spread can impose significant bending moments in piles driven through liquefiable soils. Therefore, piles in liquefiable soils should be flexible and ductile in order to accommodate lateral loads. The maximum bending moment of piles in liquefiable soils is often evaluated in a p-y analysis by assigning Reese's soft clay p-y curve with low residual shear strengths and high ϵ_{50} values to the liquefiable layer. Brandenberg et al. (2007) performed centrifuge model tests and found p-multiplier values of 0.05 in loose sand and 0.30 in dense sand could be used to model pile p-y response in fully liquefied granular layers.

7.4.3 Ice and Collisions

Vehicle and vessel collision as well as ice loads are included in the Extreme Event II load combination provided in AASHTO (2014). Each is treated as an independent extreme event. However they often occur in tandem with other loading cases such as large wind loads and vessel impact. Since these loads are typically applied to the superstructure, they are analyzed for structural loading cases, and therefore do not directly alter the geotechnical resistance as with scour and earthquakes. The Extreme Event II limit state equation can be expressed as Equation 7-81 below.

$$\sum \gamma_i Q_i = \gamma_p DL + 0.5LL + 1.0WA + 1.0FR + 1.0(IC \text{ or } CT \text{ or } CV) \quad \text{Eq. 7-81}$$

Where:

- γ_i = load factor.
- Q_i = force effect.
- γ_p = load factor for permanent loads (from Table 2-3 of Chapter 2).
- DL = dead loads.
- LL = live loads.
- WA = water load.
- FR = friction load.
- IC = ice load.
- CT = vehicular collision force.
- CV = vessel collision force.

From the equation above, ice loads as well as vehicle and vessel collisions are treated as separate events. Therefore they will be independently discussed.

7.4.3.1 Ice Loads

AASHTO (2014) provides consideration for ice loading that occurs in freshwater bodies such as lakes and rivers. Specific mention of saltwater ice loading is left to specialists in that area, and are thus beyond the scope of this manual. The expected ice forces are assumed to act directly on piers. Four loading conditions may occur including; 1) dynamic impact from ice sheet collision with the bridge pier, 2) static load resulting from thermal expansion of ice sheets around piers, 3) load from hanging dams or ice jams and 4) static uplift or vertical loads that result from ice adhesion when water levels fluctuate.

Section 3.9 of AASHTO (2014) provides in depth detail on the magnitude and application of ice loads resulting from the above mentioned factors. A discussion of dynamic forces resulting from ice collisions is mainly provided by Montgomery et al. (1984), where forces depend on the flow size, the ice strength and thickness, and pier geometry. Meanwhile, presumed values are noted in AASHTO (2014) as to ice crushing strength.

Static loads applied from thermal expansion and hanging dams or ice jams are accounted for in the structural design of superstructure members. Increased forces are therefore applied during a static structural analysis, where they generate alternative loading conditions for the foundations. To account for vertical forces from ice adhesion in rapid water level fluctuations, AASHTO (2014) recommends Equation 7-82 to determine the vertical force surrounding circular piers. Equation 7-83 should be used for oblong piers.

$$F = 80t_i^2 \left(0.35 + \frac{0.03R}{t_i^{0.75}} \right) \quad \text{Eq. 7-82}$$

$$F = 0.2t_i^{1.25} C + 80t_i^2 \left(0.35 + \frac{0.03R}{t_i^{0.75}} \right) \quad \text{Eq. 7-83}$$

Where:

- F = vertical force.
- t_i = ice thickness (feet).
- C = perimeter of pier excluding half circles at ends of oblong pier (feet).
- R = radius of pier (feet).

7.4.3.2 Vehicle Collision

When bridge piers are within 30 feet of the roadway edge or within 50 feet of the railway centerline, vehicular collision should be evaluated. In the absence of crash protection, an equivalent 600 kip static force is to be applied 5 feet above grade and at an angle of 0 to 15 feet from the edge of pavement. This loading condition is based on full scale tractor trailer collision tests. A distributed load of no more than 5 feet wide by 2 feet high may be alternatively applied for wall piers, if considered a suitable replacement for an anticipated vehicle.

The designer may also utilize a barrier to redirect or absorb the vehicular collision. For this, an embankment, guardrail or other crash protection system may be used. AASHTO (2014) requires this barrier to be structurally independent of the pier and ground mounted. If within 10 feet of the pier, the barrier must be 54 inches high, while a height of 42 inches must be reached if outside of this distance.

7.4.3.3 Vessel Collision

Bridges that span navigable bodies of water should be designed for vessel impact. Bow, deck house, or mast impacts are typically applied to superstructure elements. A head on collision with piers may occur and should consider the full vessel mass. Based on an assessment of vessels passing the bridge, a design vessel is selected and given a deadweight tonnage (DWT) value of representative size and weight. The head on collision force to the pier may be calculated as follows.

$$P_s = 8.15V\sqrt{DWT} \quad \text{Eq. 7-84}$$

Where:

- P_s = equivalent static vessel impact force (kips).
- DWT = deadweight tonnage (tonne).
- V = vessel impact velocity (ft/s).

After determination of the equivalent static impact force, the load is to be applied as either 100 percent in the direction parallel to the channel centerline or 50 percent in the direction normal to the channel centerline. Both loading cases should be evaluated. Overall stability is determined by applying a point load at the mean high water level as shown in Figure 7-79. AASHTO (2014) notes that all substructure components exposed to direct impacts shall be designed to resist the applied loads.

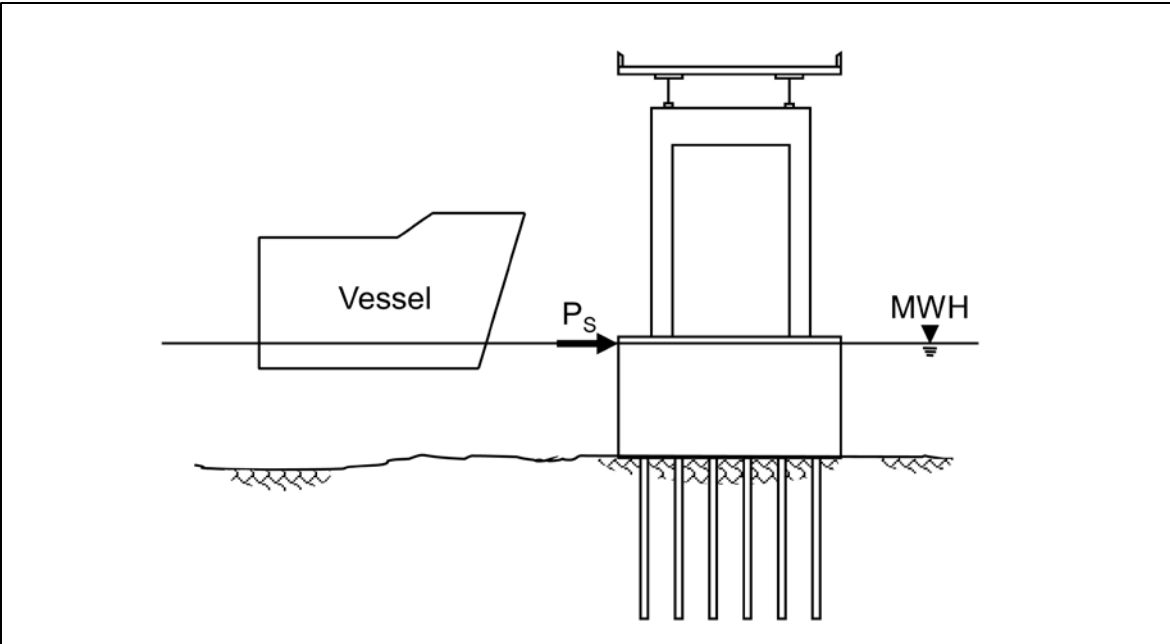


Figure 7-79 Application of equivalent impact force (after AASHTO 2014).

7.4.4 Combined Extreme Events

Two extreme event combinations with scour are given in AASHTO (2014). Extreme Event I is in combination with earthquake loading, while the Extreme Event II combination includes ice, vessel and vehicle collisions and hydraulic loads. As noted in Arneson et al. (2012), the Extreme Event I combination has a low occurrence probability for both the check flood and earthquake loading. Therefore scour for the mean discharge or normal non-flood flow may be applied to this event combination. For the Extreme Event II combination, research is ongoing to assess the probability of joint loading conditions during the check flood, and judgement should be used based on site-specific factors. If ice or debris jams near the structure dictates the use of a more extreme flood event than the check flood, this may be used to assess the extreme event limit state.

7.5 DETERMINATION OF MINIMUM PILE PENETRATION

Foundation settlement and resultant structure deformation should be kept within tolerable limits as described in Section 7.3.1. Once all limit state analyses have been performed, minimum pile penetration depths should be specified, if necessary. Minimum pile penetration depths may be required to limit structure vertical or lateral deformations under applied loads.

A minimum pile penetration depth should be specified only if needed. In many cases, the inclusion of only an estimated length is satisfactory with recognition that once piles achieve their required nominal driving resistance, driving may be terminated shorter than the estimated length. The ability of an appropriately sized pile hammer to drive piles to the specified minimum penetration depth should be evaluated during the design phase in a wave equation drivability analysis. The drivability analysis is used to check constructability and viability of achieving the minimum pile penetration depth. An alternative pile type or use of pile installation aids may need to be specified if the drivability analysis indicates the minimum pile penetration depth is not obtainable using conventional driving procedures.

AASHTO (2014) design specifications state that the minimum pile penetration depth shall be the pile toe elevation needed to satisfy the following requirements, as applicable, to the site and loading conditions. Additional guidance on each topic affecting the minimum pile penetration requirement is provided in the noted sections.

- a. Single pile and pile group settlement (service limit state – Section 7.3.5).
- b. Lateral deflection (service limit state – Section 7.3.7).
- c. Uplift (strength limit state – Section 7.2.3).
- d. Penetration depth into soils to accommodate drag forces from static settlement stresses (service limit state – Section 7.3.6).
- e. Penetration depth into soils due to liquefaction (strength and extreme event limit states – Section 7.4.2).
- f. Penetration depth into soils needed to provide adequate pile axial (compression and uplift) and lateral resistance after scour (strength limit state – Section 7.2.9, and extreme event limit states – Section 7.4.1).
- g. Penetration depth into soils necessary to achieve fixity for resisting the applied lateral loads (strength limit state – Section 7.2.5, and service limit state – Section 7.3.7). It should be noted that AASHTO is silent on the definition of fixity, which can vary if defined by the deflection profile, the bending moment profile, or the pile head deflection.
- h. Axial uplift and lateral resistance to resist extreme event limit states loads (extreme event limit state – Section 7.4).

7.6 DETERMINATION OF R_{ndr} TO ESTABLISH CONTRACT DRIVING CRITERIA

The required nominal driving resistance, R_{ndr} , is used to establish the driving criteria. This resistance along with the field method for resistance verification should be specified in contract documents. The nominal driving resistance includes many factors such as the axial compression loads, resistance from scourable or liquefiable layers, as well as time dependent soil strength changes. Some of these conditions result in an increased soil resistance at the time of installation. In these cases, the pile should be driven to a higher nominal resistance to accommodate these future resistance losses. Inclusion of the R_{ndr} in conjunction with the factored load and the field verification method can reduce the risk of contractor claims. A minimum penetration depth may also be required in addition to the R_{ndr} to also satisfy uplift or lateral loading requirements and/or serviceability.

An example calculation for determining R_{ndr} is illustrated in Equation 7-85 based on the project information provided in Table 7-32. The factored axial load, Q , is 200 kips in compression. Given the site conditions, some resistance will be lost in a soil layer subject to scour. The resistance lost in the scour zone should be determined by an appropriate static analysis method and should not be factored per AASHTO (2014) Article 10.7.3.6. For this example, it is estimated that 50 kips of resistance will be lost in the scour zone. The pile will also be driven into a weathered shale formation that historically has exhibited a loss in toe resistance following initial driving. The resistance lost to relaxation should be factored based the resistance verification method. For this example, it is estimated that 100 kips of toe resistance will be lost. Based on field verification by dynamic testing with signal matching, the resistance loss from relaxation is then 154 kips.

Equations 7-85 and 7-86 are simplified from AASHTO (2014) to provide the necessary calculation steps.

Table 7-32 Summary of Load and Resistance Information

Q (kips)	200
ϕ_{dyn}	0.65
R_n (kips)	308
R_{scour} (kips)	50
R_{relax} (kips)	154
R_{ndr} (kips)	512

Example computation of R_n

$$R_n = \frac{Q}{\phi_{dyn}} \quad \text{Eq. 7-85}$$

$$R_n = \frac{200}{0.65} = 308 \text{ kips}$$

Example computation of R_{ndr}

$$R_{ndr} = R_n + R_{scour} + R_{relax} \quad \text{Eq. 7-86}$$

$$R_{ndr} = 308 + 50 + \left(\frac{100}{0.65} \right) = 512 \text{ kips}$$

Table As shown in the above example, R_{ndr} is considerably higher than the nominal resistance due to the site specific considerations of scour and relaxation. The load and resistance factors used in this determination may be found respectively in Table 2-3 in Chapter 2 and Table 7-2 of this chapter.

7.7 DRIVABILITY ANALYSIS

Greater pile penetration depths are increasingly being required to satisfy minimum penetration depth requirements due to extreme events such as scour, vessel impact, ice and debris loading, as well as seismic events. Therefore, the ability of a pile to be driven to the required penetration depth has become increasingly more important. AASHTO (2014) Article 10.7.8 states that a drivability analysis should be performed by the engineer and that it be conducted during the design stage. Pile drivability refers to the ability of a pile to be driven to the required pile penetration depth and/or to the required resistance, and within specified material strength limits. All of the previously described static analysis methods are meaningless if the pile cannot be driven to the required depth and nominal resistance without sustaining damage. The limit of pile drivability is the maximum soil resistance a pile can overcome at a reasonable blow count without being damaged while being driven by an appropriately sized and properly operating driving system.

Primary factors controlling the nominal geotechnical resistance of a pile are the pile type and length, the soil conditions, and the method of installation. Since the pile type, length and method of installation can be specified, it is often erroneously assumed that the pile can be installed as designed to the estimated penetration depth. However, the pile must have sufficient drivability to overcome the soil

resistance encountered during driving to reach the estimated or specified pile penetration depth. If a pile section does not have a drivability limit in excess of the soil resistance to be overcome during driving, it will not be drivable to the desired pile penetration depth. The failure to adequately evaluate pile drivability is one of the most common deficiencies in driven pile design practice.

In evaluating the drivability of a pile, the soil disturbance during installation and the time dependent soil strength changes should be considered. Both soil setup and relaxation have been described earlier in this chapter. For economical pile design, the foundation designer must match the soil resistance to be overcome at the time of driving with the pile impedance (discussed below), the pile material strength, and the pile driving equipment.

7.7.1 Factors Affecting Drivability

A pile must satisfy two aspects of drivability. First, the pile must have sufficient stiffness to transmit driving forces large enough to overcome soil resistance. Second, the pile must have sufficient structural strength to withstand the driving forces without damage.

The primary controlling factor on pile drivability is the pile impedance, EA/C . Once the pile material is selected, and thus the pile modulus of elasticity, E , and the pile wave speed, C , only increasing the pile cross sectional area, A , will improve the pile drivability. For steel H-piles, the designer can improve pile drivability by increasing the H-pile section without increasing the H-pile size. This will increase the area and impedance without significantly changing the soil resistance on the section. The drivability of steel pipe piles can be improved by increasing the pipe wall thickness. This again increases the pile impedance without increasing the soil resistance. For open ended pipe piles, an inside-fitting cutting shoe can improve drivability by delaying the formation of a soil plug and thereby reducing the soil resistance to be overcome. Most concrete piles are solid cross sections. Therefore, increasing the pile area to improve drivability is usually accompanied by an increase in the soil resistance to driving.

A lesser factor influencing pile drivability is the pile material strength. The influence of pile material strength on drivability is limited, since strength does not alter the pile impedance. However, a pile with a higher pile material strength can tolerate higher driving stresses that may allow a larger pile hammer to be used. This may allow a slightly higher nominal resistance to be obtained before refusal driving conditions or pile damage occurs.

Other factors that may affect pile drivability include the driving system characteristics such as ram weight, stroke, and speed, as well as the actual system performance in the field. The dynamic soil response can also affect pile drivability. Soils may have higher damping characteristics or elasticity than assumed, both of which can reduce pile drivability. Dynamic soil response is discussed in greater detail in Chapters 10, 11, and 12. Pile installation aids such as predrilling, jetting and spudding, can assist in meeting project pile penetration requirements. However, these installation aids do not change the drivability of the pile section.

Even if the geotechnical and structural resistance both indicate a large geotechnical resistance could be used, this large geotechnical resistance may still not be obtainable because driving stresses may exceed material driving stress limits. A pile cannot be driven to a static nominal resistance that is as high as the structural resistance of the pile because of the additional dynamic resistance or damping forces generated during pile driving. Pile structural resistance and driving stresses are presented in Chapter 8.

7.7.2 Methods for Determining Pile Drivability

There are three available methods for predicting and/or checking pile drivability. As design tools, all of the methods have advantages and disadvantages and are therefore presented in order of increasing cost and reliability.

1. Wave Equation Analysis

This computer program accounts for pile impedance and calculates estimated driving stresses as well as the relationship of pile penetration resistance (blow count) versus nominal resistance (Goble and Rausche 1986). Wave equation analyses performed in the design stage require assumptions on the hammer type and performance level, the drive system components, as well as the soil response during driving. These shortcomings are reflected in variations between predicted and actual field behavior. Even with these shortcomings, the wave equation is a powerful design tool that can and should be used to check drivability in the design stage, to design an appropriate pile section, or to specify driving equipment characteristics. As noted previously, AASHTO (2014) design specification state that a wave equation drivability analysis should be performed during design in the strength limit state. Additional information on the wave equation, including its use as a construction control tool, is presented in Chapter 12.

2. Dynamic Testing and Analysis

Dynamic measurements can be made during pile installation to calculate driving stresses and to estimate nominal resistance at the time of driving. Time dependent changes in nominal resistance can be evaluated during restrike tests. Signal matching analysis of the dynamic test data can provide soil parameters for a refined wave equation analysis. A shortcoming of this method as a design tool is that it must be performed during pile driving. Therefore, in order to use dynamic testing information to confirm drivability or to refine a design, a test program is required during the design stage. Additional details on dynamic testing and analysis, including its use as a construction control tool, is presented in Chapter 10.

3. Static Load Tests

Static load tests are useful for confirming pile drivability and the nominal resistance prior to production pile driving (Kyfor et al. 1992). Test piles are normally driven to estimated lengths and load tested. The confirmation of pile drivability through static load test programs is the most accurate method of confirming drivability and nominal resistance since a pile is actually driven and statically load tested. However, this advantage also illustrates one of its shortcomings as a design tool, in that a test program is required during the design stage. Other shortcomings associated with static load tests for determining drivability include:

- a. cost and time delay that limit their suitability to certain projects.
- b. assessment of driving stresses and the extent of pile damage, if any, is not provided by the test.
- c. can be misleading on projects where soil and/or rock conditions are highly variable.

Additional details on static load tests, including its use as a construction control tool, are presented in Chapter 9. Rapid load tests can also be used to evaluate nominal resistance and are discussed in Chapter 11.

As design and construction control tools, methods 1 and 2 offer additional information and complement static load tests. Used properly, methods 1 and 2 can yield significant savings in material costs or reduction of construction delays and

risks of claims. These methods can be used to reduce the number of static load tests and increase the usefulness and applicability of the static load test performed. A determination of the increase (soil setup) or decrease (relaxation) in geotechnical resistance with time can also be made if piles are tested under restrike conditions after initial driving.

7.7.3 Drivability versus Pile Type

Drivability should be checked during the design stage of all driven piles. It is particularly important for closed end steel pipe piles where the impedance of the steel casing may limit pile drivability. Although the designer may attempt to specify a thin wall pipe in order to save material cost, a thin wall pile may lack the drivability to develop the required nominal resistance or to achieve the necessary pile penetration depth. This concept is illustrated in the wave equation example problem presented in Section 12.5.8 of Chapter 12. Wave equation drivability analyses should be performed in the design stage to select the pile section and wall thickness per AASHTO (2014) design specifications. An example of a wave equation drivability assessment is presented in Section 12.5.3.

Steel H-piles and open pipe piles, prestressed concrete piles, and timber piles are also subject to drivability limitations. This is particularly true as extreme events and the trend to use larger nominal resistances require increased pile penetration depths. The drivability of long prestressed concrete piles can be limited by the pile's tensile strength.

7.8 CONSIDERATIONS FOR BATTER PILE DESIGN AND CONSTRUCTION

Battered or inclined piles are piles that are driven on an inclination from vertical and are often considered when large static lateral loads are expected or where structural rigidity is required. A battered pile can typically resist larger horizontal loads and experience less deflection than their vertical counterparts at the same loading levels. When static loads are applied, battered piles generally perform well. However under dynamic horizontal loads or for seismic events, the increased structural stiffness benefit decreases. In seismic design particularly, earthquake induced displacements generate load, and as force is a function of stiffness, the increased stiffness from battered piles results in larger applied horizontal forces to the structure. Where significant drag forces are expected, battered piles should be avoided due to the increased bending moment loads along the pile length.

The response of a pile group to applied loads will differ if the pile group consists solely of vertical piles, or if the pile group consists of a combination of vertical and batter piles. Figure 7-80 illustrates the response of a foundation unit subjected to a horizontal load and an overturning moment. In Case A, the foundation unit is supported by a single pile that rotates about a point below the ground surface in response to the applied load and moment. In Case B, the foundation unit is supported by two vertical piles and it translates horizontally and displaces vertically downward in response to the applied load and overturning moment. In Case C, the foundation unit is supported by an outwardly battered lead pile and a trailing vertical pile. This foundation unit translates horizontally and displaces vertically upward in response to the applied load and overturning moment. Hence, the influence of batter piles on the foundation response must be considered in the foundation design.

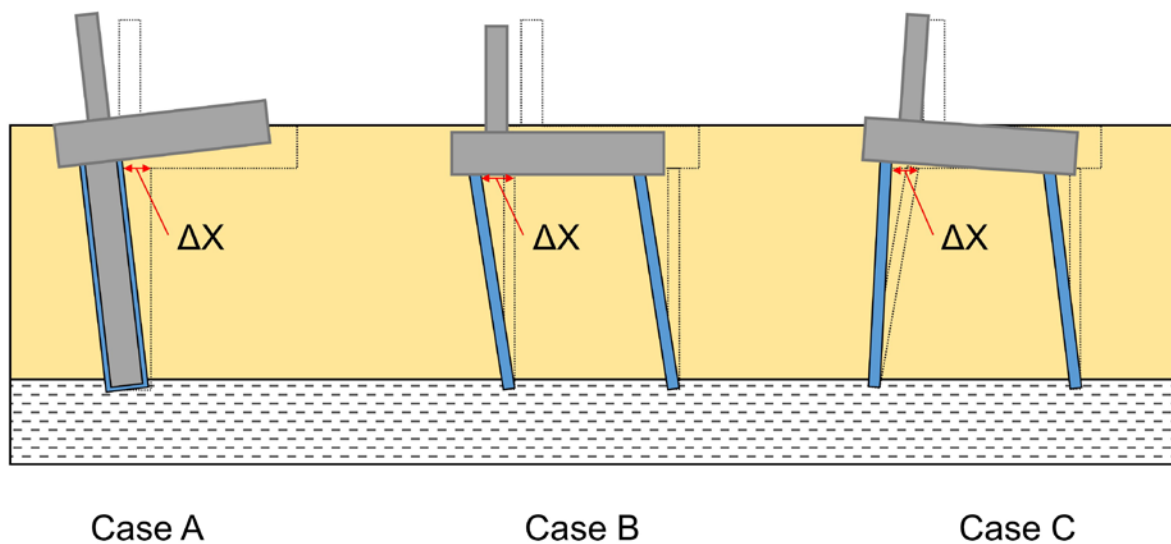


Figure 7-80 Variation of foundation response depending on group configuration and batter (after Wilson et al. 2006).

For batter piles, the horizontal component of the axial load contributes to, or subtracts from the horizontal resistance of the group depending on the batter pile direction relative to the applied load. Wilson et al. (2006) noted that the analysis for a pile group containing batter piles is similar to the procedures described earlier in Section 7.3.7.5 with the following exceptions:

1. Using a rigid cap assumption, the vertical load at the head of each pile is resolved into the axial pile load based on the batter angle. The horizontal component of the axial pile load is then computed.
2. The sum of all horizontal components is computed, and the total compared to the applied horizontal load. If the sum of the horizontal components is less than the applied horizontal load, the remainder of the horizontal load must be resisted through pile bending computed in a p-y analysis. If the sum of the horizontal components are greater and opposite of the applied horizontal load, the piles will bend in the opposite direction of the applied load.
3. If no vertical load is applied to a batter pile by the pile cap, the batter pile will have no axial load. Without an axial load, it will have no horizontal component to resist an applied horizontal load. A battered pile in this scenario behaves as a vertical pile and the horizontal resistance is provided by pile bending.

Careful assessment of the direction of the applied horizontal loads and corresponding need, location, and orientation of batter piles is required when batter piles are incorporated into a foundation design. As noted above, adding batter piles to resist horizontal loads is inefficient and could be more economically handled by vertical piles if the batter pile receives no vertical load from the pile cap.

Batter pile interference with the surrounding environment should be carefully reviewed during the design. The selected batter angle as well as pile deviation from the selected batter angle should be evaluated for potential conflicts with adjacent in-use foundations, cofferdams and excavation support systems, utilities, abandoned deep foundations from previous construction, tunnels, and other constraint posed by the surrounding environment. In situations where an offshore lead and template system are used with batter piles, additional bending stresses from the weight of the pile hammer and the unsupported portion of the pile above the template can cause additional stresses that must be considered in addition to the axially oriented driving stresses. From a constructability standpoint, batter angles greater than 1H:3V should be avoided.

7.9 CORROSION AND DETERIORATION

Corrosion and deterioration of all pile types must be considered for the respective environmental conditions. Section 6.12 of Chapter 6 provides extensive detail on

design considerations for aggressive subsurface environments. AASHTO (2014) recommends at minimum, an evaluation for steel corrosion particularly in fill soils, low pH soils, and marine environments. For concrete piles, sulfate, chloride and acid attack should be evaluated. Timber piles are subject to decay from wetting and drying cycles as well as attack from marine bores and insects. Additional details can be found in AASHTO (2014) Article 10.7.5 and associated commentary.

7.10 ADDITIONAL DESIGN AND CONSTRUCTION CONSIDERATIONS

The previous sections of this chapter addressed typical geotechnical design and analysis procedures for pile foundation design. However, the designer should be aware of additional design and construction considerations that can influence the reliability of static analysis procedures in estimating nominal resistance. These issues include the influence of time, predrilling or jetting, driving piles through embankments, soil densification, and the plugging of open pile sections on soil resistance. Pile driving induced vibrations can also influence the final design and resistance calculation results if potential vibration levels dictate changes in pile type or installation procedures. These final sections serve to fill the gaps between design and construction events that may influence long term resistance and/or construction procedures.

7.10.1 Minimum Pile Spacing, Clearance, and Cap Embedment

AASHTO (2014) design specifications recommend a minimum center-to-center pile spacing of no less than 30 inches or 2.5 pile diameters. In addition, the pile cap edge should be greater than 9 inches from the side of the nearest pile. As discussed previously in this chapter, center-to-center spacing less than 3.0 diameters can create construction difficulties and lower pile group axial and lateral resistances. Therefore, the benefit of a smaller cap size should be weighed against the reduced resistances and constructability issues that can arise with the smaller spacing.

The pile head should extend a minimum of 12 inches into the pile cap. Any damaged portions of the pile head should be trimmed and the damaged portion removed down to undamaged material before pouring the cap. If piles are attached to the cap by embedded bars or strands, the piles should extend a minimum of 6 inches into the pile cap.

When a reinforced concrete bent cap is cast in place atop piles, the concrete cover should be a minimum of 6 inches on all sides of the piles. Pile misalignment may occur. Therefore an additional allowance should be given for cover in conjunction with specified maximum permissible pile misalignment and its remedy. Where pile reinforcement is anchored into the cap satisfying AASHTO (2014) Article 5.13.4.1 requirements, the projection may be less than 6.0 inches.

7.10.1.1 Special Considerations for Large Pile Sizes

AASHTO design specifications do not address minimum pile spacing requirements or pile cap embedment for large diameter open end pipe piles. The synthesis study on large diameter pipe piles by Brown and Thompson (2015) presents limited details on this subject and most state agencies do not currently have standard plan details for these large pile sizes.

One detail used to connect large diameter pipe piles into the pile cap consists of internally cleaning out the pipe pile to the desired depth, if necessary, and then inserting a reinforcing cage into the pile that also extends up into the pile cap. The pile is then filled with a concrete plug. In some cases, design details require the internal cleanout extended to the scour depth or mudline, and in other instances, the concrete plug extends only for the length needed for load transfer.

Another design approach is use an internal reinforcing cage in conjunction with welded shear studs on the exterior surface of the pile that extends into the pile cap. At least two rows of shear studs are frequently used to develop sufficient load transfer from the pile to cap. In addition to the use of rebar cages or cages and shear studs, large diameter piles heads typically extend on the order of 3 feet into the pile cap to develop the required structural connection.

Little information was provided with respect to center to center pile spacing. However because of the large diameter, comparison with drilled shaft minimum spacing guidelines may be appropriate. The presented pile layout in Brown and Thompson (2015) shows the minimum spacing to be on the order of 3 pile diameters center-to-center. Since large diameter open end piles are often selected for a foundation design due to their high lateral load resistance, greater center-to-center pile spacing may be applicable for the lateral load demand.

7.10.2 Identification of High Rebound Soils

During pile driving, the hammer impact causes temporary compression of the soil and pile system. For certain soil types, the deformed soil system can spring back close to its original position. When this occurs, it proves difficult to continue pile driving operations and to achieve the nominal resistance (Hussein et al. 2006). This effect is known as high rebound, or elastic rebound, and is generally due to increased pore water pressure from driving occurring near the pile toe. As driving continues, pore water pressure increases and causes a larger rebound, leading to refusal like driving conditions. If pile driving is paused, the pore water pressure dissipates and subsequently smaller rebound occurs.

Studies have shown that for dense silty sand, hard silty clay, glacial tills, silt and other fine grained saturated soils, high elastic rebound can occur when using displacement piles (Likins 1983; Hussein et al. 2006; Cosentini et al. 2010). Research is ongoing to determine what specific soil properties or in-situ tests may be used to locate and quantify high rebound soils beyond a basic assessment of soil types and saturation. Local experience may be of great value in areas where these soil conditions exist, as recommendations on pile drivability may provide a significant cost savings in design and construction. Pile driving equipment with heavy rams operating at short hammer strokes is helpful in these installation conditions.

7.10.3 Soil and Pile Heave

As noted by Haggerty and Peck (1971), whenever piles are driven, soil is displaced. This can result in both upward movement (pile heave) and lateral movements of previously driven piles. These soil movements can be detrimental to the resistance of previously driven piles as well as to adjacent facilities. Obviously, the greater the volume of soil displaced by pile driving, the greater the potential for undesirable movements of previously driven piles, or damage to adjacent structures. Heave of piles primarily supported by toe resistance is particularly troublesome since the pile may be lifted from the bearing stratum, thereby greatly reducing the soil resistance and increasing the foundation settlement when loaded. Haggerty and Peck noted that saturated, insensitive clays display incompressible behavior during pile driving and have the greatest heave potential.

When piles are to be installed in cohesive soils, it is recommended that the potential magnitude of vertical and lateral soil movements be considered in the design stage. If calculations indicate that movements may be significant, use of an alternate low displacement pile, or specifying a modified installation procedure (such as predrilling

to reduce the volume of displaced soil) should be evaluated. A step by step procedure adapted from Haggerty and Peck for estimating soil and pile heave in saturated insensitive clay follows. The procedure assumes a regular pile driving sequence and a level foundation surface. The paper by Haggerty and Peck should be consulted for modifications to the recommended procedure for conditions other than those stated.

STEP BY STEP PROCEDURE FOR ESTIMATING SOIL AND PILE HEAVE

STEP 1 Calculate the estimated soil heave at the ground surface.

- a. Divide the volume of inserted piles by the volume of soil enclosed by the pile foundation to obtain the volumetric displacement ratio.
- b. Estimate the normalized soil heave (soil heave / pile length) from $\frac{1}{2}$ the volumetric displacement ratio calculated in Step 1a.
- c. Calculate the soil heave at the ground surface by multiplying the normalized soil heave in Step 1b by the average length of piles.

STEP 2 Determine the depth of no pile-soil movement.

- a. Figure 7-81 illustrates that an equilibrium depth, d , exists where the potential upward pushing and downward resisting forces on the pile shaft are equal.
- b. Calculate the pile-soil adhesion along the entire pile shaft using the α -method described in Section 7.2.1.3.2.
- c. Through multiple iterations determine the equilibrium depth, d , where the adhesion from the upward pushing force equals the adhesion from the downward resisting force. Note that only shaft resistance is considered in calculating the downward resisting force.

STEP 3 Calculate the estimated pile heave.

- a. Calculate the percentage of pile length resisting heaving soil.

$$L\% = \frac{D-d}{D} \quad \text{Eq. 7-87}$$

Where:

- $L\%$ = percentage of pile length resisting heaving soil (%).
- D = pile embedded length (feet).
- d = equilibrium depth (feet).

- b. Calculate the estimated pile heave by multiplying the estimated soil heave from Step 1c by the percentage of pile length resisting heave from Step 3a.

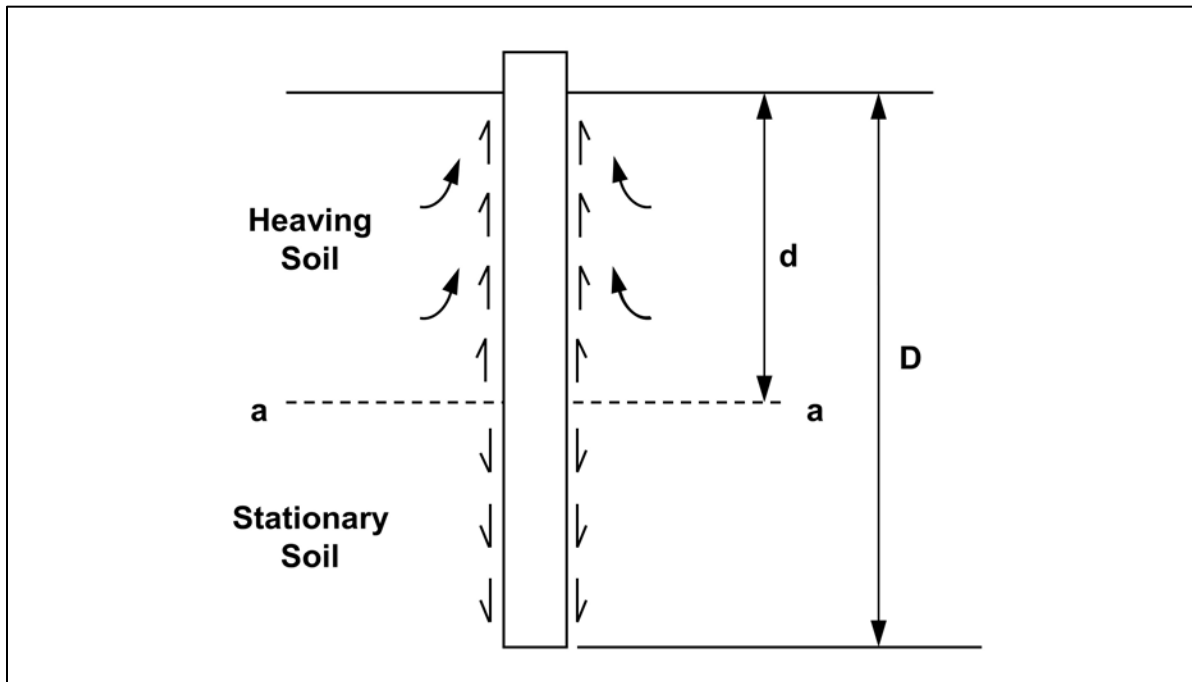


Figure 7-81 Balance of forces on pile subject to heave (after Haggerty and Peck 1971).

More recent work on this topic was present in Sagaseta and Whittle (2001) where the shallow strain path method (SSPM) was used to predict ground movements due to pile driving in clay. Results from this method typically yield a reasonable first estimate of pile heave.

7.10.4 Piles Driven Through Embankment Fills

Approach embankments are frequently constructed before the commencement of pile driving operations. Piles driven through embankment fills should penetrate a minimum of 10 feet below original grade unless refusal driving conditions are

encountered on bedrock or a competent bearing layer. An alternative foundation type may be more effective in cases where refusal driving conditions occur at a pile penetration depth less than 10 feet below the embankment base. Ideally, bedrock or a bearing layer that may cause refusal driving conditions is identified by the subsurface exploration program performed before foundation construction begins. To minimize drag forces, piles should not be driven through embankments or constructed over compressible materials until after 90% primary settlement is complete.

7.10.5 Effect of Predrilling, Jetting and Vibratory Installation on Nominal Resistance

Piles are sometimes predrilled or jetted to a prescribed depth in order to attain the pile penetration depths required, as well as to reduce other foundation installation concerns, such as ground vibrations. Jetting is usually performed in cohesionless soils that can be freely eroded by water jets. Jetting, which can be very effective in sands, is usually ineffective in cohesive soils. For clays, and other drillable materials, such as thin layers of rock, predrilling the pile locations is more effective. The predrilled hole can be slightly smaller, equal to, or slightly larger than the pile diameter.

The use of predrilling or jetting will result in greater soil disturbance than considered in standard static pile resistance calculations. Therefore, when predrilling or jetting is contemplated, the effect of either of these construction procedures on calculated compression, uplift, and lateral soil resistance should be considered. Poulos and Davis (1980) reported that the shaft resistance should be reduced by 50% of the originally calculated resistance in the jetted zone, if the pile is jetted and then driven to the final penetration. McClelland et al. (1969) reported that a decrease in shaft resistance over a predrilled depth can range from 50 to 85% of that calculated without predrilling, depending upon the size of the predrilled hole. Hence, the probable reduction in compression, uplift, and lateral resistance from jetting or predrilling should be evaluated whenever predrilling or jetting is being considered.

Agencies are often requested to allow pile installation with a vibratory pile hammer instead of an impact hammer. Mosher (1987) summarized the results from five sites where piles were installed by both impact and vibratory hammers. This study concluded that for a majority of the cases, piles installed in sand with a vibratory hammer had a lower nominal resistance than impact driven piles at the same site. Mosher also concluded that time dependent soil strength changes occurred equally for both installation methods. Hence, even with soil setup, the resistance of the

vibratory installed piles did achieve the resistance of the impact driven piles. However, it was also observed that impact driving a vibratory installed pile would increase the resistance of the vibratory installed pile to that of an impact driven pile.

O'Neill and Vipulanandan (1989) performed a laboratory evaluation of piles installed with vibratory hammers. This laboratory study found impact driven piles had a 25% greater unit shaft resistance and a 15 to 20% higher unit toe resistance than vibratory installed piles in medium dense to dense, uniform, fine sand. However, in very dense, uniform, fine sand, the impact driven pile had a 20 to 30% lower unit shaft resistance and approximately a 30% lower unit toe resistance than the vibratory installed pile.

Ghose-Hajra et al. (2015) compared the effects of pile installation using an impact and a vibratory hammer on the long term soil setup on two H-piles and two open-end pipe piles driven in a soft clay formation in southeast Louisiana. This study found that the impact driven piles always had a greater soil resistance than the companion vibratory installed pile at comparable time intervals.

The above studies indicate use of vibratory pile installation rather than impact driving will affect the nominal pile resistance that can be achieved at a given pile penetration depth. Therefore, communication between design and construction personnel should occur, and the influence of vibratory pile installation be evaluated when it is proposed. Impact driving a specific final depth of vibratory installed piles may provide a foundation that meets the engineer's performance requirements at reduced installation cost.

7.10.6 Densification Effects on Nominal Resistance and Installation Conditions

As illustrated in the previously presented Figure 7-1, driving a pile in cohesionless soil influences the surrounding soils to a distance of about 3 to 5 pile diameters away from the pile. The soil displacement and vibrations resulting from driving pile groups in cohesionless soils can further densify cohesionless materials. The use of displacement piles also intensifies group densification effects in cohesionless soils.

Densification can result in the soil resistance as well as the resistance during pile driving being significantly higher than that calculated for a single pile in static analysis calculations. The added confinement provided by cofferdams or the sequence of pile installation can further aggravate a group densification issue. Piles should be installed from the center of the group outward in order to reduce group densification effects due to installation sequence. Densification can cause

significant construction problems if scour, seismic, or other considerations require achieving pile penetration depths that cannot be achieved.

Potential densification effects should be considered in the design stage. Studies by Meyerhof (1959) and Kishida (1967) indicate that an increase in the soil friction angle of up to 4 degrees would not be uncommon for piles in loose to medium dense sands. It is expected that the increase in soil friction angle would be less for dense sands or cohesionless soils with a significant fine content. Densification affects the nominal resistance to be overcome during driving. As a constructability check, static analyses should be performed using higher soil strength parameters than used for design to assess nominal resistance due to densification. Results from these static analyses may indicate that a low displacement pile should be used, the pile spacing should be increased, or that a pile installation aid should be specified in order to obtain the required pile penetration depth.

7.10.7 Plugging of Open Pile Sections

Open pile sections include open end pipe piles and H-piles. The use of open pile sections has increased, particularly where special design events dictate large pile penetration depths. When open pile sections are driven, they may behave as low displacement piles and "core" through the soil, or act as displacement piles if a soil plug forms near the pile toe. It is generally desired that open sections remain unplugged during driving and plugged under static loading conditions.

Stevens (1988) reported that plugging of pipe piles in clays does not occur during driving if pile accelerations (along the plug zone) are greater than 22g's. Holloway and Beddard (1995) reported that hammer blow size (impact force and energy) influenced the dynamic response of the soil plug. With a large hammer blow, the plug "slipped" under the dynamic event, whereas under a lesser hammer blow the pile encountered toe resistance typically of a plugged condition. From a design perspective, these cases indicate that pile penetration of open sections can be facilitated if the pile section is designed to accommodate a large pile hammer. Wave equation analyses can provide calculated accelerations at selected pile segments.

Static soil resistance calculations must determine whether an open pile section will exhibit plugged or unplugged behavior. Studies by O'Neill and Raines (1991), Raines et al. (1992), as well as Paikowsky and Whitman (1990) suggest that plugging of open pipe piles in medium dense to dense sands generally begins at a pile penetration to pile diameter ratio of 20, but can be as high as 35. For pipe piles

in soft to stiff clays, Paikowsky and Whitman (1990) reported plugging can occur at penetration-to-pile diameter ratios of 10 to 20.

The above studies suggest that plugging in any soil material may occur under static loading conditions once the penetration to pile diameter ratio exceeds 20 in dense sands and clays, or 20 to 30 in medium sands. However, plugging is difficult to predict with certainty in all cases. For large diameter open ended pipe piles, plugging during driving is significantly less likely to occur particularly for piles larger than 36 inches in diameter. Plugging of large diameter pipe piles under static loading conditions is more likely than in the dynamic conditions. However, it is still subject to uncertainty. Forced plugging of large diameter pipe piles using an internal constrictor plate as illustrated in Figures 6-14 and 6-15 is sometimes used to reduce this uncertainty.

NCHRP Report 20-05 by Brown and Thompson (2015) provides a summary of the current industry practices with large diameter open end piles and provides an in depth discussion on plugging. This report postulates that large inertial effects prevent plug development during driving. Under static loading conditions, plug or unplugged behavior for these large diameter piles is uncertain. Further research is ongoing regarding design methods on large diameter pipe piles.

An illustration of the difference in the soil resistance mechanism that develops on a pipe pile with an open and plugged toe condition is presented in Figure 7-83. Paikowsky and Whitman (1990) recommend that the static resistance of an open end pipe pile be calculated from the lesser of the following equations:

Plugged Condition:

$$R_n = f_{so} A_{so} + q_p A_{pp} \quad \text{Eq. 7-88}$$

Unplugged Condition:

$$R_n = f_{so} A_{so} + f_{si} A_{si} + q_p A_p - W_p \quad \text{Eq. 7-89}$$

Where:

- R_n = nominal resistance (kips).
- f_{so} = exterior unit shaft resistance (ksf).
- A_{so} = pile exterior surface area (ft²).
- f_{si} = interior unit shaft resistance (ksf).
- A_{si} = pile interior surface area (ft²).

- q_p = unit toe resistance (ksf).
- A_{pp} = cross sectional area of pile and soil plug at pile toe (ft²).
- A_p = cross sectional area of pile material at pile toe (ft²).
- W_p = weight of soil plug (kips).

The soil stresses and displacements induced by driving an open pile section and a displacement pile section are not the same. Hence, a lower unit toe resistance, q_p , should be used for calculating the toe resistance of open end pipe piles compared to a typical closed end condition. The value of the interior unit shaft resistance in an open end pipe pile is typically on the order of 1/3 to 1/2 the exterior unit shaft resistance, and is influenced by soil type, pile diameter, and pile shoe configuration. These factors will also influence the length of soil plug that may develop.

For open end pipe piles in cohesionless soils, Tomlinson (1994) recommends that the static soil resistance be calculated using a limiting value of 105 ksf for the unit toe resistance, regardless of the pile size or soil density. Tomlinson states that higher unit toe resistances do not develop, because yielding of the soil plug rather than geotechnical failure of the soil below the plug governs the resistance.

For open end pipe piles driven in stiff clays, Tomlinson (1994) recommends that the static soil resistance be calculated as follows when field measurements confirm a plug is formed and carried down with the pile:

$$R_n = 0.8C_a A_s + 4.5s_u A_p \quad \text{Eq. 7-90}$$

Where:

- R_n = nominal resistance (kips).
- C_a = pile adhesion from Figure 7-17 (ksf).
- A_s = pile shaft surface area (ft²).
- s_u = average undrained shear strength at the pile toe (ksf).
- A_p = toe area of a plugged pile (ft²).

Static soil resistance calculations for open end pipe piles in cohesionless soils should be performed using the Paikowsky and Whitman equations. Toe resistance should be calculated using the Tomlinson limiting unit toe resistance of 105 ksf, once Meyerhof's limiting unit toe resistance, determined from Figure 7-15, exceeds 105 ksf. For open end pipe piles less than 24 inches in diameter, and in predominantly cohesive soils, the Tomlinson equation should be used. Conversely, for moderate (24 to 36 inch O.D.) and large (36+ inch) diameter open ended pipe piles, plugging is less certain under static conditions and should be carefully analyzed.

The API method incorporated into the APILE program calculates the plugged and unplugged resistance of a open end pipe pile. The program also contains an automated routine that calculates whether a plugged or unplugged condition will develop. The results for a 30 inch open end pipe along with the analyzed soil profile are presented in Figure 7-82.

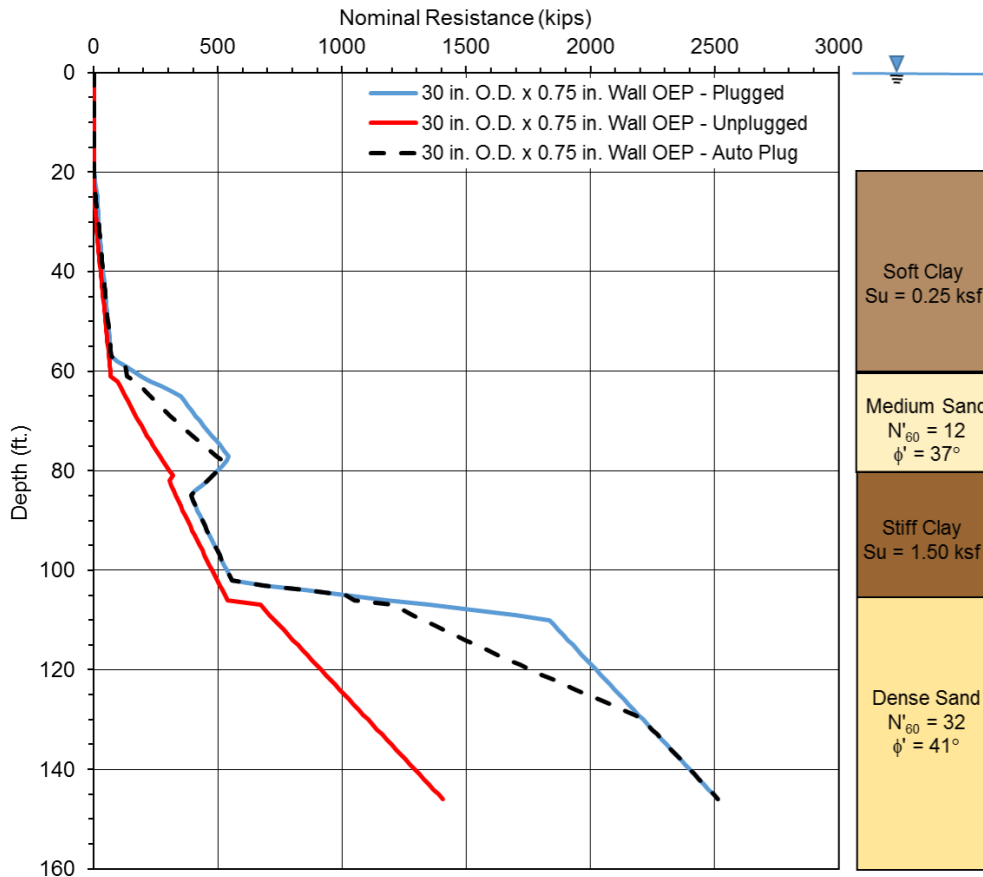


Figure 7-82 Variation in expected static resistance from APILE API method based on plugged, unplugged, and automatic calculated plugging.

The plugging phenomenon in H-piles can be equally difficult to analyze. However, the distance between flanges of an H-pile is smaller than the inside diameter of most open end pipe piles. Therefore, an H-pile is more likely to be plugged under static loading conditions where the “box” area of the pile toe is used for static calculation of the toe resistance in cohesionless and cohesive soils. The toe resistance for H-piles driven to rock is usually governed by the pile structural strength, calculated based on the steel cross sectional area, and should not include the area of a soil plug, if any.

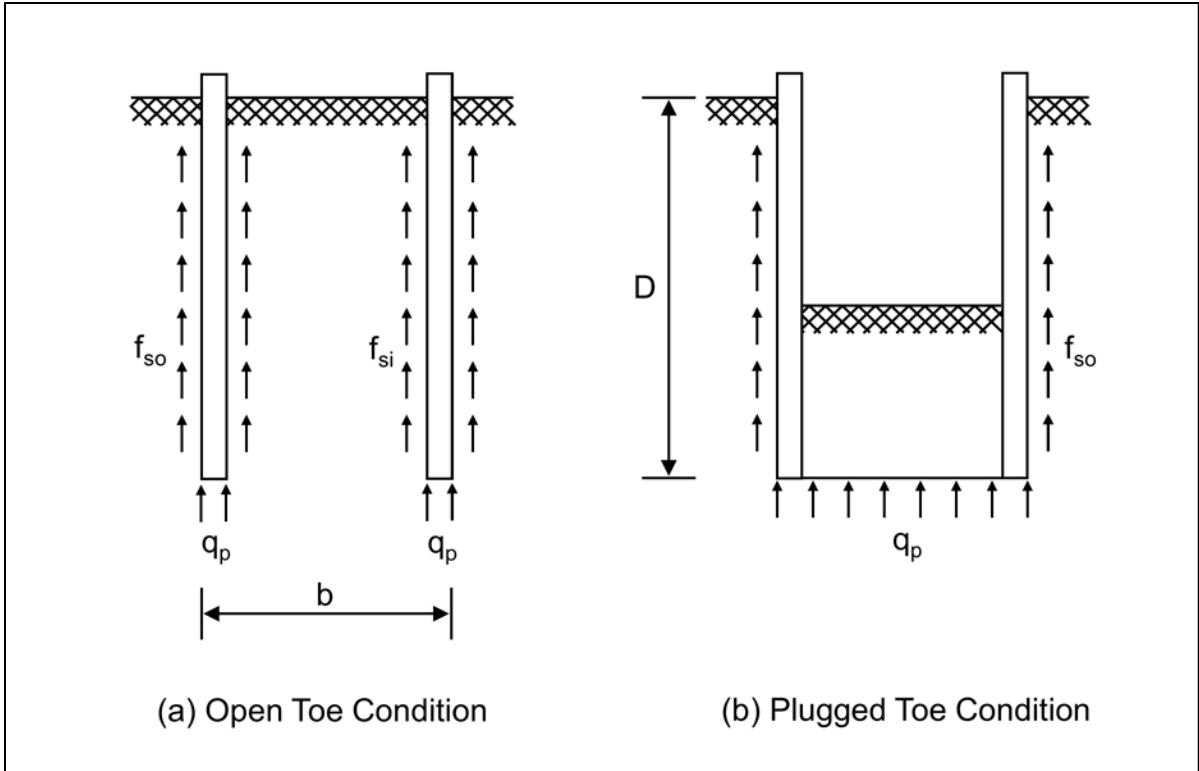


Figure 7-83 Plugging of open end pipe piles (after Paikowsky and Whitman 1990).

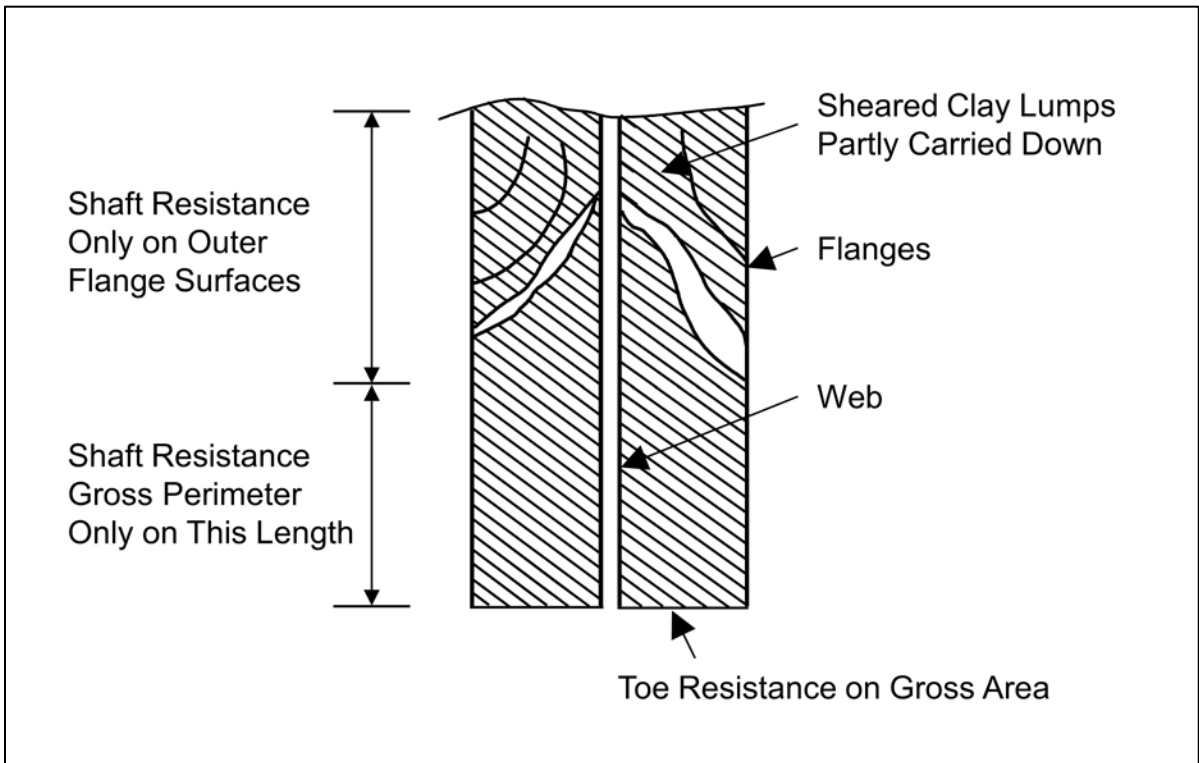


Figure 7-84 Plugging of H-piles (after Tomlinson 1994).

For H-piles in cohesionless soils, arching between the flanges may occur, and the "box" perimeter can be used for shaft resistance calculations. In most cohesive soils, the shaft resistance is calculated from the sum of the adhesion, C_a , along the exterior of the two flanges plus the undrained shear strength of the soil, s_u , times the surface area of the two remaining sides of the "box" due to soil-to-soil shear along these two faces. Figure 7-84 illustrates that the calculation of shaft resistance in H-piles in stiff clays can still be problematic. Sheared clay lumps can develop above the plug zone, in which case the shaft resistance may only develop along the exterior surfaces of the flanges in the sheared lump zone.

The above discussions highlight the point that a higher degree of uncertainty often exists for static soil resistance calculations of open pile sections than for displacement piles. Soil plug formation and plug response is often different under static and dynamic loading. This can complicate nominal resistance evaluations of open pile sections with all dynamic methods (wave equation, dynamic testing, and dynamic formulas). Therefore, for large diameter open end pipe piles, greater than 18 inches, or for H-piles designed to carry their load primarily in shaft resistance, a static load test is recommended for resistance verification.

REFERENCES

- Altaee, A., Evgin, E. and Fellenius, B.H. (1992). Axial Load Transfer for Piles in Sand, I: Tests on an Instrumented Precast Pile. *Canadian Geotechnical Journal*, Vol. 29, No. 1, pp. 11-20.
- American Association of State Highway and Transportation Officials (AASHTO). (2010). *LRFD Guide Specifications and Commentary for Vessel Collision Design of Highway Bridges*, Second Edition, with 2010 Interim, CVCB-2-M. American Association of State Highway and Transportation Officials, Washington, D.C., 244 p.
- American Association of State Highway and Transportation Officials (AASHTO). (2014). *AASHTO LRFD Bridge Design Specifications, US Customary Units, Seventh Edition, with 2015 Interim Revisions*. American Association of State Highway and Transportation Officials, Washington, D.C., 1960 p.
- American Petroleum Institute (API). (1993). *Recommended Practice for Planning, Designing and Constructing Fixed Offshore Platforms – Load and Resistance Factor Design*. API Recommended Practice 2A-LRFD (RP 2A-LRFD), First Edition, Reaffirmed 2003, 242 p.
- Arneson, L.A., Zevenbergen, L.W., Lagasse, P.F., and Clopper, P.E. (2012). *Evaluating Scour at Bridges*, Fifth Edition, FHWA-HIF-12-003, Hydraulic Engineering Circular (HEC) No. 18. U.S. Dept. of Transportation, Federal Highway Administration, 340 p.
- Ashour, M., Norris, G., and Pilling, P., (1998a). Lateral Loading of a pile in Layered Soil Using the Strain Wedge Model. *American Society of Civil Engineers, (ASCE) Journal of Geotechnical and Geoenvironmental Engineering*, Vol. 124, No.4, pp. 303-315.
- Ashour, M., Norris, G., and Pilling P., (2002). Strain Wedge Model Capability of Analyzing Behavior of Laterally Loaded Isolated Piles, Drilled Shafts, and Pile Groups. *American Society of Civil Engineers, (ASCE) Journal of Bridge Engineering*, Vol. 7, No. 4, pp. 245-254.

- Awoshika, K., and Reese, L. C., (1971). Analysis of Foundation with Widely-Spaced Batter Piles, Research Report 11 7-3F, Center for Highway Research, The University of Texas at Austin, 321 p.
- Bollman, H.T. (1993). Notes on Designing Deep Foundations for Lateral Loads. Proceedings of Design of Highway Bridges for Extreme Events, Crystal City, VA, pp. 175-199.
- Bowles, J.E. (1977). Foundation Analysis and Design. Second Edition, McGraw-Hill Book Company, Blacklick, OH, 750 p.
- Bowles, J.E. (1988). Foundation Analysis and Design. Fourth Edition, McGraw Hill, New York, NY, 1023 p.
- Brandenberg, S.J., Boulanger, R.W., Kutter, B.L., and Chang, D. (2007). Static Pushover Analyses of Pile Groups in Liquefied and Laterally Spreading Ground in Centrifuge Tests. American Society of Civil Engineers (ASCE), Journal of Geotechnical and Geoenvironmental Engineering, Vol. 133, No. 9, pp. 1055-1066.
- Briaud J-L. and Miran, J. (1992). The Cone Penetration Test, FHWA-SA-91-043. U.S. Department of Transportation, Federal Highway Administration, Office of Technology Applications, Washington, D.C., 161 p.
- Briaud, J. L. and Tucker, L.M. (1993). Downdrag on Bitumen-Coated Piles, NCHRP 24-5. National Cooperative Highway Research Program, (NCHRP), Washington, D.C., 245 p.
- Broms, B.B. (1964a). Lateral Resistance of Piles in Cohesive Soils. American Society of Civil Engineers, (ASCE), Journal for Soil Mechanics and Foundation Engineering, Vol. 90, SM2, pp. 27-63.
- Broms, B.B. (1964b). Lateral Resistance of Piles in Cohesionless Soils. American Society of Civil Engineers, (ASCE), Journal for Soil Mechanics and Foundation Engineering., Vol. 90, SM3, pp. 123-156.
- Broms, B.B. (1966). Methods of Calculating the Ultimate Bearing Capacity of Piles – A Summary. Soils-Soils, No. 18-19, pp. 21-32.

- Brown, D.A., Reese, L.C. and O'Neill, M.W. (1987). Cyclic Lateral Loading of a Large-Scale Pile Group in Sand. American Society of Civil Engineers (ASCE), Journal of Geotechnical Engineering., Vol. 113, No. 11, Reston, VA, pp. 1326-1343.
- Brown, D.A., Morrison, C. and Reese, L.C. (1988). Lateral Load Behavior of Pile Group in Sand. American Society of Civil Engineers (ASCE), Journal of Geotechnical Engineering , Vol. 114, No. 11, Reston, VA, pp. 1261-1276.
- Brown, D.A. and Bollman, H.T. (1993). Pile-Supported Bridge Foundations Designed for Impact Loading. Appended Document to the Proceedings of Design of Highway Bridges for Extreme Events, Crystal City, VA, pp. 265-281.
- Brown, D.A., O'Neill, M.W., Hoit, M., McVay, M., El Naggar, M.H., and Chakraborty, S. (2001). Static and Dynamic Lateral Loading of Pile Groups. NCHRP Report 461, Transportation Research Board – National Research Council, Washington, D.C., 50 p.
- Brown, D. A., Turner, J.P. and Castelli R.J. (2010). Drilled Shafts: Construction Procedures and LRFD Design Methods, FHWA-NHI-10-016, Geotechnical Engineering Circular (GEC) No. 10. U.S. Dept. of Transportation, Federal Highway Administration, 970 p.
- Brown, D.A., and Thompson III, W.R. (2015). Current Practices for Design and Load Testing of Large Diameter Open –End Driven Pipe Piles. Final Report. NCHRP Report 20-05, Topic 45-05 National Cooperative Highway Research Program, Washington, D.C., 175 p.
- Brown, R. P. (2001). Predicting the Ultimate Axial Resistance of Single Driven Piles. PhD Dissertation (supervisor: Prof. Roy E. Olson), Department of Civil Engineering, The University of Texas at Austin, 168 p.
- Bullock, P.J., Schmertmann, J. H., McVay, M. C., Townsend, F., March (2005). Side Shear Setup. II: Results From Florida Test Piles. American Society of Civil Engineers (ASCE), Journal of Geotechnical Engineering, Vol. 131, No. 3, Reston, VA, pp. 301-310.
- Canadian Geotechnical Society. (1985). Canadian Foundation Engineering Manual, Second Edition. Technical Committee on Foundations, BiTech Publishers, Vancouver, B.C., 456 p.

- Cheney, R.S. and Chassie, R.G. (2000). Soils and Foundations Workshop Reference Manual. FHWA HI-00-045, U.S. Department of Transportation, National Highway Institute, Federal Highway Administration, Washington, D.C., 358 p.
- Cheney, R.S. and Chassie, R.G. (2002). Soils and Foundation Workshop Manual. Second Edition, Report No. HI-88-009. U.S. Department of Transportation, Federal Highway Administration, Office of Engineering, Washington, D.C., 395 p.
- Coduto, D.P. (1994). Foundation Design: Principles and Practice. Prentice-Hall, Inc., Englewood Cliffs, NJ, 796 p.
- De Nicola, A. and Randolph, M. (1993). Tensile and Compressive Shaft Capacity of Piles in Sand. *Journal of Geotechnical Engineering.*, Vol. 19, No. 12, pp. 1952-1973.
- Duncan, J.M., and Buchignani, A.L (1976). An Engineering Manual for Settlement Studies, Department of Civil Engineering, University of California, Berkeley, CA, 94 p.
- Duncan, J. M., and S. G. Wright. (2005). Soil Strength and Slope Stability, John Wiley, Hoboken, N.J, 297 p.
- Elias, V., Welsh, J.P., Warren, J., Lukas, R.G., Collin J.G., and Berg, R.R. (2006). Ground Improvement Methods Volumes I and II, FHWA-NHI-06-019 and FHWA NHI-06-020. National Highway Institute, Federal Highway Administration, U.S. Department of Transportation, Washington D.C.
- Eslami, A., and Fellenius, B. H. (1997). Pile Capacity by Direct CPT and CPTu Methods Applied to 102 Case Histories. *Canadian Geotechnical Journal*, Vol. 34, No. 6, pp. 880-898.
- Fayyazi, M.S., Taiebat, M., Finn, W.D.L., and Ventura, C.E. (2012). Evaluation of P-Multiplier Method for Performance Based Design of Pile Groups. Second International Conference on Performance Based Design in Earthquake Geotechnical Engineering, Taormina, Italy. , Vol. 34, No. 6, pp. 880-898.

- Fellenius, B.H., Riker, R.E., O'Brien, A.J. and Tracy, G.R. (1989). Dynamic and Static Testing in a Soil Exhibiting Set Up. American Society of Civil Engineers (ASCE), Journal of Geotechnical Engineering, Vol. 115, No. 7, pp. 984-1001.
- Fellenius, B.H. (1991). Foundation Engineering Handbook, Chapter 13 - Pile Foundations. Second Edition. Van Nostrand Reinhold Publisher, New York, NY, pp. 511-536.
- Fellenius, B.H. and Siegel, T.C., (2008). Pile Design Considerations in a Liquefaction Event. American Society of Civil Engineers (ASCE), Journal of Geotechnical and Geoenvironmental Engineering, Vol. 132, No. 9, pp. 1412-1416.
- Fellenius, B.H. (2014). Basics of foundation Design. Electronic Edition. <http://www.Fellenius.net> , 410 p.
- Goble, G.G. and Rausche, F. (1986). Wave Equation Analysis of Pile Driving - WEAP86 Program. U.S. Department of Transportation, Federal Highway Administration, Implementation Division, McLean, Volumes I-IV.
- Ghose-Hajra, M., Jensen, R., and Hulliger, L. (2015). Pile Setup and Axial Capacity Gain for Driven Piles Installed Using Impact Hammer versus Vibratory System. Proceedings of the International Foundations Conference and Equipment Exposition 2015, San Antonio, TX, pp. 1064-1074.
- Gouderault, P. and Fellenius, B.H. (1994). UNIPILE Program Background and Manual. Unisoft, Ltd., Ottawa, Canada, 120 p.
- Hadjian, A.H., Fallgren, R.B. and Tufenkjian, M.R. (1992). Dynamic Soil-Pile-Structure Interaction, The State-of-Practice. American Society of Civil Engineers (ASCE), Geotechnical Special Publication No. 34, Piles Under Dynamic Loads, pp. 1-26.
- Hagerty, D.J. and Peck, R.B. (1971). Heave and Lateral Movements Due to Pile Driving. American Society of Civil Engineers (ASCE), Journal of the Soil Mechanics and Foundations Division, Vol. 97, No.11, pp. 1513-1532.

- Harris, D.E., Anderson, D.G., Butler, J.J., Fellenius, B.H., Fisher, G.S., and Hinman, J. (2003). Design of Pile Foundations for the Sand Creek Byway, Sandpoint, Idaho. Proceedings of the Deep Foundation Institute Annual Meeting, Miami, FL, 11 p.
- Haque, M., Chen, Q., Abu-Farsakh, M., and Tsai, C. (2014). Effects of Pile Size on Setup Behavior of Cohesive Soils. Proceedings of Geo-Congress 2014: Geo-Characterization and Modeling for Sustainability, Atlanta, GA, pp. 1743-1749.
- Hoit, M.I. and McVay, M. (1994). LPGSTAN User's Manual. University of Florida, Gainesville, FL, 27 p.
- Holloway, D.M. and Beddard, D.L. (1995). Dynamic Testing Results Indicator Pile Test Program - I-880. Proceedings of the 20th Annual Members Conference of the Deep Foundations Institute. Charleston, SC, pp. 105-126.
- Holloway, D.M., Moriwaki, Y., Stevens, J.B. and Perez, J-Y. (1981). Response of a Pile Group to Combined Axial and Lateral Loading. Proceedings of the 10th International Conference on Soil Mechanics and Foundation Engineering, Boulimia Publishers, Stockholm, Sweden, pp. 731-734.
- Hough, B.K. (1959). Compressibility as the Basis for Soil Bearing Value. American Society of Civil Engineers (ASCE), Journal for Soil Mechanics and Foundation Division, Vol. 85, No. 4, pp. 11-40.
- Hussein, M.H., Likins, G.E. and Hannigan, P.J. (1993). Pile Evaluation by Dynamic Testing During Restrike. Eleventh Southeast Asian Geotechnical Conference, Singapore, pp. 535-539.
- Hussein, M., Woerner, II, W., Sharp, M., and Hwang, C. (2006). Pile Driveability and Bearing Capacity in High-Rebound Soils. Proceeding of Geocongress 2006: Geotechnical Engineering in the Information Technology Age. Atlanta, GA, February 26-March 1, 2006, ASCE, Reston, VA, pp. 1-4.
- Idriss, I.M. and Boulanger, R.W. (2007). SPT and CPT-based Relationships for the Residual Shear Strength of Liquefied Soils. Proceedings of the 4th International Conference on Earthquake Geotechnical Engineering. The Netherlands, pp. 1-22.

- Isenhower, W.M. and Wang, S.T. (2014). User's Manual for LPILE 2013: A Program to Analyze Deep Foundations Under Lateral Loading, ENSOFT. Austin, TX, 177 p.
- Ismael, N.F. and Klym, T.W. (1979). Pore-Water Pressures Induced by Pile Driving. American Society of Civil Engineers, Journal of Geotechnical Engineering, Vol. 105, No.11, pp.1349-1354.
- Kramer. S.L. and Wang, C.-H. (2007). Estimation of the residual strength of liquefied soil, in preparation.
- Kramer, S.L. (2008). Evaluation of Liquefaction Hazards in Washington State. Washington State Research Report WA-RD 668.1, Washington State Department of Transportation, Olympia, WA, 329 p.
- Janbu, N. (1963). Soil Compressibility as Determined by Oedometer and Triaxial Tests. European Conference on Soil Mechanics and Foundation Engineering, Wiesbaden, Germany, Vol. 1, pp. 19-25.
- Janbu, N. (1965). Consolidation of Clay Layers Based on Non-linear Stress-Strain. Proceedings of the Sixth International Conference on Soil Mechanics and Foundation Engineering, Montreal, Canada, Vol. 2, pp. 83-87.
- Kavazanjian, E., Wan, J-N. J., Martin, G.R., Shamsabadi, A., Lam, I., Dickenson, S.E., and Hung, C.J. (2011). LRFD Seismic Analysis and Design of Transportation Geotechnical Features and Structural Foundations, FHWA-NHI-11-032, Geotechnical Engineering Circular (GEC) No. 3. U.S. Dept. of Transportation, Federal Highway Administration, Washington, D.C., 592 p.
- Kishida, H. (1967). Ultimate Bearing Capacity of Piles Driven in Loose Sands. Japanese Society of Soil Mechanics and Foundation Engineering, Soils and Foundations. Vol. 7, No. 3, pp. 20-29.
- Komurka, V.E., Wagner, A.B., and Edil, T.B. (2003). Estimating Soil/Pile Setup, Final Report. Wisconsin Highway Research Program, Report No. 0305, Wisconsin Department of Transportation, Madison, WI, 42 p.
- Kulhawy, F.H. and Goodman, R.E. (1980). Design of Foundations on Discontinuous Rock, Proceedings of the International Conference on Structural Foundation on Rock, Sydney, Australia, Vol. 1, pp. 209-220.

- Kulhawy, F.H. and Goodman, R.E. (1987). Foundations in Rock, Ground Engineering, Chapter 15, London, UK.
- Kyfor, Z.G., Schnore, A.R., Carlo, T.A. and Bailey, P.F. (1992). Static Testing of Deep Foundations, FHWA-SA-91-042. U.S. Department of Transportation, Federal Highway Administration, Office of Technology Applications, Washington, D.C., 174 p.
- Likins, G.E. and Goble, G.G. (1978). Tests on H-piles Driven to Rock. Proceedings of the Thirty Second Annual Ohio Transportation Engineering Conference, pp. 57-67.
- Lo, K.Y. and Stermac, A.G. (1965). Induced Pore Pressures During Pile Driving Operations. Proceedings of the Sixth International Conference on Soil Mechanics and Foundation Engineering, Vol. 2, Montreal, Canada, pp. 285-289.
- Long, J., and Anderson, A. (2014). Improved of Driven Pile Installation and Design in Illinois: Phase 2, FHWA-ICT-14-019. Illinois Department of Transportation, Bureau of Material and Physical Research, Springfield, IL, 84 p.
- Marsh, M.L., Buckle, I.G., and Kavazanjian Jr, E. (2014). LRFD Seismic Analysis and Design of Bridges, FHWA-NHI-15-004. National Highway Institute, U.S. Dept. of Transportation, Federal Highway Administration, Washington, D.C., 608 p.
- Modjeski and Masters, Inc. (2015). Bridges for Service Life Beyond 100 Years: Service Limit State Design. SHRP2 Report S2-R19B-RW-1. Transportation Research Board, Washington D.C., 268 p.
- McClelland, B., Focht, J.A. and Emrich, W.J. (1969). Problems in Design and Installation of Offshore Piles. American Society of Civil Engineers (ASCE), Journal of the Soil Mechanics and Foundations Division, Vol. 94, No.6, pp. 1491-1514.
- McVay, M., Casper, R. and Shang, T-I. (1995). Lateral Response of Three-Row Groups in Loose to Dense Sands at 3D and 5D Pile Spacing. American Society of Civil Engineers (ASCE), Journal of Geotechnical Engineering, Vol. 121, No. 5, pp. 436-441.

- Meyerhof, G. G. (1956). Penetration Tests and Bearing Capacity of Piles, American Society of Civil Engineers (ASCE), Journal of the Soil Mechanics and Foundation Division, Vol. 82, No. 1, Paper 886, pp. 1-29 .
- Meyerhof, G.G. (1976). Bearing Capacity and Settlement of Pile Foundations, American Society of Civil Engineers (ASCE), Journal of Geotechnical Engineering, Vol. 102, No. 3, pp. 195-228.
- Montgomery, C.T., Gerard R., Huiskamp, W.J., and Kornelson, R.W. (1984) Application of Ice Engineering to Bridge Design Standards. Proceedings of the Cold Regions Engineering Specialty Conference, Canadian Society for Civil Engineering, Montreal, QC, Canada, pp. 795-810.
- Morgano, C.M., White, B. (2004). Identifying Soil Relaxation from Dynamic Testing. Proceedings of the Seventh International Conference on the Application of Stresswave Theory to Piles 2004, Petaling Jaya, Selangor, Malaysia, pp. 415-421.
- Mosher, R.L. (1987). Comparison of Axial Capacity of Vibratory Driven Piles to Impact Driven Piles, ITL-87-7. Department of the Army, Waterways Experiment Station, Vicksburg, MS, 36 p.
- Moss, R.E.S. (1997). Cyclic Lateral Loading of Model Pile Groups in Clay Soil, Phase 2B. Department Civil and Environmental Engineering, Geotechnical Division, Utah State University, Logan, UT, 700 p.
- Kuthy, R.A., Ungerer, R.P, Renfrew, W.W., Hiss, J.G.F., and Rizzuto, I.F. (1977). Lateral Load Capacity of Vertical Pile Groups. ERD 77 RR47. New York State Department of Transportation, Engineering Research and Development Bureau. Albany, NY, 49 p.
- Ng, K. W. (2011). Pile Setup, Dynamic Construction Control, and Load and Resistance Factor Design of Vertically-Loaded Steel H Piles. Theses and Dissertations. Paper 11924. Iowa State University, Ames, IA, 299 p.
- Ng, K., Roling, M., AbdelSalam, S., Suleiman, M., and Sritharan, S. (2013). Pile Setup in Cohesive Soil. I: Experimental Investigation. American Society of Civil Engineers (ASCE), Journal of Geotechnical and Geoenvironmental Engineering, Vol. 139, No. 2, pp. 199-209.

- Nordlund, R.L. (1963). Bearing Capacity of Piles in Cohesionless Soils. American Society of Civil Engineers, ASCE, Journal of the Soil Mechanics and Foundations Division, Vol. 98, No. 12, pp. 1291-1310.
- Nordlund, R.L. (1979). Point Bearing and Shaft Friction of Piles in Sand. Missouri-Rolla 5th Annual Short Course on the Fundamentals of Deep Foundation Design, Rolla, MO.
- Norris, G. M. (1986). Theoretically based BEF laterally loaded pile analysis. Proceedings of the Third International Conference on Numerical Methods in Offshore Piling, Nates, France, pp. 361-386.
- Nottingham, L.C. (1975). Use of Quasi-Static Friction Cone Penetrometer to Predict Load Capacity of Displacement Piles. Ph.D. dissertation to the Department of Civil Engineering, University of Florida, Gainesville, FL, 552 p.
- Olson, R.E., and Shantz T.J., (2004). Axial Load Capacity of Piles in California in Cohesionless Soils. Geotechnical Special Publication No. 125, Current Practices and Future Trends in Deep Foundations, American Society of Civil Engineers (ASCE), Reston, VA, pp. 1-15.
- Olson, S.M. and Stark, T.D. (2002). Liquefied Strength ratio from Liquefaction Flow Failure Case Histories. Canadian Geotechnical Journal, Vol 39, No.5, pp. 629-647.
- O'Neill, M.W. (1983). Group Action in Offshore Piles. Proceedings of the Conference on Geotechnical Practice in Offshore Engineering, Houston, TX, pp. 25-64.
- O'Neill, M.W. and Vipulanandan, C. (1989). Laboratory Evaluation of Piles Installed with Vibratory Drivers. NCHRP Report 316, National Cooperative Highway Research Program, Transportation Research Board, Washington, D.C., 51 p.
- O'Neill, M.W. and Raines, R.D. (1991). Load Transfer for Pipe Piles in Highly Pressured Dense Sand. American Society of Civil Engineers, (ASCE), Journal of Geotechnical Engineering, Vol. 117, No. 8, pp. 1208-1226.

- Paikowsky, S.G. (2004), with contributions from Birgisson, B., McVay, M., Nguyen, T., Kuo, C., Baecher, G., Ayyub, B., Stenersen, K., O'Malley, K., Chernauskas, L., and O'Neill, M., Load and Resistance Factor Design (LRFD) for Deep Foundations. NCHRP Report 507, Transportation Research Board, Washington, D.C., 76 p.
- Paikowsky, S.G. and Whitman, R.V. (1990). The Effects of Plugging on Pile Performance and Design. Canadian Geotechnical Journal, Vol. 27, No. 4, pp. 429-440.
- Poulos, H.G. and Davis, E.H. (1980). Pile Foundation Analysis and Design. John Wiley and Sons, New York, NY, pp. 18-51.
- Preim, M.J., March, R., and Hussein, M.H. (1989). Bearing Capacity of Piles in Soils with Time Dependent Characteristics. Proceedings of the International Conference on Piling and Deep Foundations, London, England, pp. 363-370.
- Raines, R.D., Ugaz, O.G. and O'Neill, M.W. (1992). Driving Characteristics of Open-Toe Piles in Dense Sand. American Society of Civil Engineers (ASCE), Journal of Geotechnical Engineering, Vol. 118, No. 1, pp 72-88.
- Randolph, M. F., Carter, J. P., and Wroth, C. P. (1979). Driven Piles in Clay—The Effects of Installation and Subsequent Consolidation. Geotechnique, Vol. 29, No. 4, pp. 361-393.
- Rausche, F., Thendean, G., Abou-matar, H., Likins, G. and Goble, G. (1996). Determination of Pile Drivability and Capacity from Penetration Tests, DTFH61-91-C-00047, Final Report. U.S. Department of Transportation, Federal Highway Administration, McLean, VA, 432 p.
- Reddy, S. and Stuedlein, A. (2014) Time-Dependent Capacity Increase of Piles Driven in the Puget Sound Lowlands. Geotechnical Special Publication No. 233, From Soil Behavior Fundamentals to Innovations in Geotechnical Engineering, pp. 464-474.
- Reese, L.C. (1984). Handbook on Design of Piles and Drilled Shafts Under Lateral Load, FHWA-IP-84-11. U.S. Department of Transportation, Federal Highway Administration, Office of Implementation, Washington, D.C., 392 p.

- Reese, L.C. (1986). Behavior of Piles and Pile Groups Under Lateral Load, FHWA-RD-85-106. U.S. Department of Transportation, Federal Highway Administration, Office of Engineering and Highway Operations Research and Development, Washington, D.C., 311 p.
- Reese, L.C., Wang, T.C., Arrellaga, J.A., and Vasquez, L.G. (2014). APILE 2014 User's Manual: A Program for the Study of Driven Piles under Axial Load. ENSOFT. Austin, TX, 223 p.
- Rixner, J.J., Kraemer, S.R. and Smith, A.D. (1986). Prefabricated Vertical Drains Volume I, Engineering Guidelines, FHWA-RD-86-168. U.S. Department of Transportation, Federal Highway Administration, Office of Engineering and Highway Operations Research and Development, McLean, VA, 117 p.
- Rollins, K.M., Peterson, K.T., and Weaver, T.J. (1998) Lateral Load Behavior of a Full-Scale Pile Group in Clay. American Society of Civil Engineers (ASCE), Journal of Geotechnical and Geoenvironmental Engineering, Vol. 124, No. 6, pp. 468-478.
- Rollins, K. M., Olsen, R. J., Egbert, J. J., Jensen, D. H., Olsen, K. G., and Garrett, B. H. (2006a). Pile Spacing Effects on Lateral Pile Group Behavior: Load Tests American Society of Civil Engineers (ASCE), Load tests. Journal of Geotechnical and Geoenvironmental Engineering, Vol. 132, No. 10, pp. 1262-1271.
- Rollins, K.M., and Brown, D.A., (2011). Design Guidelines for Increasing the Lateral Resistance of Highway-Bridge Pile Foundations by Improving Weak Soils. NCHRP Report No. 697, Washington, D.C., 98 p.
- Ruesta, P.F. and Townsend, F.C. (1997). Evaluation of Laterally Loaded Pile Group at Roosevelt Bridge. American Society of Civil Engineers (ASCE), Journal of Geotechnical and Geoenvironmental Engineering, Vol. 123, No. 12, pp. 1153-1161.
- Sabatini, P. J., Elias, V., Schmertmann, G. R., and Bonaparte, R. (1997). Earth Retaining Systems, FHWA-SA-96-038. Geotechnical Engineering Circular (GEC) No. 2. U.S. Department of Transportation, Federal Highway Administration, Washington, D.C.

- Sagaseta, C., and Whittle, A. J. (2001). Prediction of Ground Movements Due to Pile Driving in Clay. American Society of Civil Engineers (ASCE), Journal of Geotechnical and Geoenvironmental Engineering, Vol. 127, No. 11, pp. 939-949.
- Schmertmann, J.H. (1975). Measurement of In Situ Shear Strength. Proceedings of the Conference on In Situ Measurement of Soil Properties, Vol. 2, ASCE, New York, NY, pp. 57-138.
- Schmertman, J.H. (1978). Guidelines For Cone Penetration Test, Performance, and Design, FHWA-TS-78-209. U.S. Department of Transportation, Federal Highway Administration, Washington, D.C., 145 p.
- Seed, H.B., Idriss, I.M. and Arango, I. (1983). Evaluation of Liquefaction Potential Using Field Performance Data. American Society of Civil Engineers (ASCE), Journal of Geotechnical Engineering, Vol. 109, No. 3, pp. 458-482.
- Seed, H.B. (1987). Design Problems in Soil Liquefaction. American Society of Civil Engineers (ASCE), Journal of Geotechnical Engineering, Vol. 113, No. 8, pp. 827-845.
- Seed, R.B. and Harder, L.F., Jr. (1990). SPT-Based Analysis of Cyclic Pore Pressure Generation and Undrained Residual Strength. Proceedings of the H.B. Bolton Seed Memorial Symposium, BiTech Publishers, Vol. 2, pp. 351-376.
- Seidel, J.P., Anderson, G.D., and Morison, N.J. (1992). The Effects of Pile Relaxation on Toe Capacity and Stiffness. Proceedings of the Fourth International Conference on the Application of Stress-Wave Theory to Piles. The Hague, Netherlands, pp 153-158.
- Siegel, T.C., Lamb, R., Dasenbrock, D., and Axtell, P.J. (2013). Alternative Design Approach for Drag Load and Downdrag with the LRFD Framework. Proceedings of the 38th Annual Conference on Deep Foundations 2013, Phoenix, AZ, pp. 23-39.
- Smith, T.D. (1989). Fact or Friction: A Review of Soil Response to a Laterally Moving Pile. Proceeding of the Foundation Engineering Congress, Evanston, IL, pp. 588-598.

- Stevens, R.F. (1988). The Effect of a Soil Plug on Pile Drivability in Clay. Proceedings of the Third International Conference on the Application of Stress Wave Theory to Piles, BiTech Publishers, Vancouver, Canada, pp. 861-868.
- Tanyu B.F., Sabatini, P. J., and Berg, R.R. (2008). Earth Retaining Structures, FHWA-NHI-07-07. U.S. Department of Transportation, Federal Highway Administration, Washington, D.C., 792 p.
- Tawfig, K.S. (1994). Polyethylene Coating for Downdrag Mitigation on Abutment Piles. Proceedings of the International Conference on Design and Construction of Deep Foundations, Vol. 2, pp. 685-698.
- Terzaghi, K., and Peck, R.B. (1967). Soil Mechanics in Engineering Practice, Second Edition, Wiley and Sons, Inc., New York, NY, 729 p.
- Terzaghi, K., Peck, R.B., and Mesri, G. (1996). Soil Mechanics in Engineering Practice, Third Edition, Wiley and Sons, Inc., New York, NY, 592 p.
- Thompson, C.D. and Thompson, D.E. (1985). Real and Apparent Relaxation of Driven Piles. American Society of Civil Engineers (ASCE), Journal of Geotechnical Engineering, Vol. 111, No. 2, pp. 225-237.
- Tomlinson, M.J. (1980). Foundation Design and Construction, Fourth Edition. Pitman Advanced Publishing Program, Boston, MA, 793 p.
- Tomlinson, M.J. (1994). Pile Design and Construction Practice, Fourth Edition, E & FN Spon, London, 432 p.
- Wilson, K.E., Kimmerling, R.E., Goble, G.G., Sabatini, P.J., Zang, S.D., Zhou, J.Y., Amrhein, W.A., Bouscher, J.W., and Danovich, L.J. (2006). LRFD for Highway Bridge Substructures and Earth Retaining Structures, FHWA-NHI-05-094. U.S. Dept. of Transportation, Federal Highway Administration, 1730 p.
- Yang, Nai C. (1970). Relaxation of Piles in Sand and Inorganic Silt. American Society of Civil Engineers (ASCE), Journal of the Soil Mechanics and Foundations Division, March, Vol. 96, No. 2, pp. 395-409.

York, D., Brusey, W., Clémente, F., and Law, S. (1994). Setup and Relaxation in Glacial Sand. American Society of Civil Engineers (ASCE), Journal of Geotechnical Engineering, Vol 120, No. 9, pp. 1498-1513.

CHAPTER 8

STRUCTURAL ASPECTS AND LIMIT STATES

Driven piles resist a variety of vertical loads, moments and lateral loads. The previous chapter discussed a pile's and pile group's geotechnical resistance to these loads. This chapter considers the pile's structural limit states which can govern the design in situations where both lateral and axial loads are applied. The analysis of the effects of vessel impact, wind, scour, and earthquake events in structure design often generates factored loads that can tax the pile's structural resistance.

8.1 INTRODUCTION

This chapter addresses structural limit states, but is not meant to cover structural design in a comprehensive way. Please review AASHTO (2014) for specific structural design equations and requirements. A driven pile must satisfy stress and buckling checks under static loading conditions during its design life as well as under dynamic, driving induced loads. Therefore, the material strength limits are compared to:

1. The factored driving stresses.
2. The factored design loads during the pile's design life.

In almost all cases, the highest stress levels occur in a pile during driving. High driving stresses are necessary to cause pile penetration. The pile must be stressed to overcome the nominal geotechnical resistance, plus any dynamic resistance forces, in order to be driven to support the pile design load. The high strain rate and temporary nature of the loading during pile driving allow a substantially higher driving stress limitation than for the static design case. Wave equation analyses can be used to predict driving stresses prior to installation. During installation, dynamic testing can be used to monitor driving stresses.

Factored loads are briefly considered in Chapter 2. The factored structural resistance is summarized in this chapter, in conformance with the AASHTO (2014) LRFD Bridge Design Specification. AASHTO (2014) provides a discussion on

concrete piles in Article 5, steel piles in Article 6, and timber piles in Article 8. Composite concrete filled steel pipe piles are also discussed.

The factored structural resistances for piles given in AASHTO (2014) are a function of the following variables:

1. Average section yield strength, such as:
 - a. F_y , the yield strength for steel piles or steel reinforcement.
 - b. f'_c , the ultimate compression strength for concrete, typically at 28 days.
 - c. Wood crushing strengths.
2. Factors for incision, loading rate, submersion, cross sectional shape and analysis method for timber piles.
3. Resistance factor, ϕ_i , which allows for variations in loading condition, materials, construction dimensions, and method reliability.
4. Load factor, γ_i , to account for uncertainty in the factored service loads.

Driving stress limits, group layout, preliminary cap design, in-service stress limits, and buckling of piles are addressed in this chapter.

8.2 BASIC STRUCTURAL PROPERTIES OF DRIVEN PILES

8.2.1 Material Properties

Primary pile materials include steel, concrete and timber. The properties of these materials can significantly affect static nominal structural resistance and nominal driving resistance. Steel piles are generally produced to meet a minimum design yield stress which is used during load evaluations. Common steel Pipe pile and H-pile designations are given in Table 8-1 and Table 8-2 respectively, along with the minimum required yield stress. H-pile sections were traditionally available as Grade A-36 steel; however ASTM A572 requires new sections to be produced with a minimum yield stress of 50 ksi. H-piles of grade A-36 are therefore no longer manufactured. For all steel piles, the elastic modulus for static calculations, E_s , is assumed to be 29,000 ksi, per AASHTO (2014) specifications.

Table 8-1 Common Steel Pipe Pile Grades and Yield Stress

Designation/Grade	Yield Stress, F_y , ksi
ASTM A-252 Grade 2	35
ASTM A-252 Grade 3	45
ASTM A-252 Grade 3 (Mod)	50-80

Table 8-2 Common Steel H-pile Grades and Yield Stress

Designation/Grade	Yield Stress, F_y , ksi
A-36	36
ASTM A-572-50	50
ASTM A-572-60	60

For concrete piles, the elastic modulus/concrete strength is likewise a limiting variable. However, reinforcing steel can be added to increase tensile strength. The elastic modulus of concrete is typically estimated based on the compression strength. Without confirming test data, the AASHTO (2014) recommended method to determine the elastic modulus of concrete is presented in Equation 8-1. This approach assumes normal weight concrete with a unit weight of 145 pcf.

$$E_c = 1820\sqrt{f'_c} \quad \text{Eq. 8-1}$$

Where:

- E_c = elastic modulus of concrete (ksi).
- f'_c = concrete compression strength at 28 days, unless otherwise specified (ksi).

Timber pile properties vary by tree species. Douglass-Fir and Southern Pine are the predominant timber pile species used across the United States. However, Red Oak and Red Pine are also used. Reference values for compression stress parallel to grain, F_{co} , and elastic modulus, E_o , are provided in AASHTO (2014) Article 8.4.1.4 and are shown in Table 8-3. These values are typically modified by shape and size factors which are further discussed in Section 8.4.

Table 8-3 Timber Pile Compression Stress and Elastic Modulus Reference Values (after AASHTO 2014)

Species	F_{co} ksi	E_o ksi
Pacific Coast Douglas-Fir	1.25	1500
Red Oak	1.10	1250
Red Pine	0.90	1280
Southern Pine	1.20	1500

8.2.2 Pile Section Definitions

Beyond material properties, the general shape and element dimensions affect modes of structural resistance. The relative thickness of steel generally limits the magnitude of force that can be reasonably transferred to the pile either during driving, or for structural considerations. Axial compression and flexural resistance is also derived from the pile shape, and as relatively large loads are transferred to steel and concrete piles, the element dimensions should be accounted for. Figure 8-1 and Figure 8-3 provide general shape dimensions for H-piles and pipe piles, respectively.

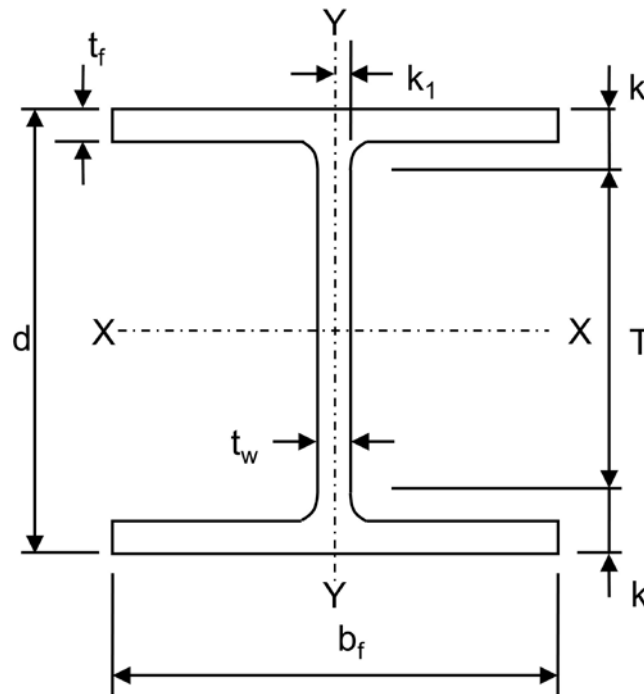


Figure 8-1 H-pile section dimensions.

Section	Weight lb/ft	Area in ²	Depth d in	Flange Width b _f in	Thickness		Properties							
					Web t _w in	Flange t _f in	X- Axis				Y- Axis			
							I in ⁴	Z in ³	S in ³	r in	I in ⁴	Z in ³	S in ³	r in
HP8X36	36	10.6	8.02	8.16	0.445	0.445	119	33.6	29.8	3.36	40.3	15.2	9.9	1.95
HP10X42	42	12.4	9.70	10.10	0.420	0.415	210	48.3	43.4	4.13	71.7	21.8	14.2	2.41
HP10X57	57	16.7	9.99	10.20	0.565	0.565	294	66.5	58.8	4.18	101	30.3	19.7	2.45
HP12X53	53	15.5	11.80	12.00	0.435	0.435	393	74.0	66.7	5.03	127	32.2	21.1	2.86
HP12X63	63	18.4	11.90	12.10	0.515	0.515	472	88.3	79.1	5.06	153	38.7	25.3	2.88
HP12X74	74	21.8	12.10	12.20	0.610	0.605	569	105.0	93.8	5.11	186	46.6	30.4	2.92
HP12X84	84	24.6	12.30	12.30	0.685	0.685	650	120.0	106.0	5.14	213	53.2	34.6	2.94
HP12x89	89	25.9	12.36	12.32	0.720	0.720	689	126.3	111.6	5.16	225	56.2	36.5	2.94
HP12X102	102	29.9	12.56	12.64	0.819	0.819	811	147.6	129.3	5.20	276	67.1	43.7	3.04
HP12X117	117	34.4	12.76	12.87	0.929	0.929	946	170.8	148.2	5.24	331	79.3	51.4	3.11
HP14X73	73	21.4	13.60	14.60	0.505	0.505	729	118	107	5.84	261	54.6	35.8	3.49
HP14X89	89	26.1	13.80	14.70	0.615	0.615	904	146	131	5.88	326	67.7	44.3	3.53
HP14X102	102	30.1	14.00	14.80	0.705	0.705	1050	169	150	5.92	380	78.8	51.4	3.56
HP14X117	117	34.4	14.20	14.90	0.805	0.805	1220	194	172	5.96	443	91.4	59.5	3.59
HP16X88	88	25.8	15.30	15.70	0.540	0.540	1110	161	145	6.56	349	68.2	44.5	3.68
HP16X101	101	29.9	15.50	15.80	0.625	0.625	1300	187	168	6.59	412	80.1	52.2	3.71
HP16X121	121	35.8	15.80	15.90	0.750	0.750	1590	226	201	6.66	504	97.6	63.4	3.75
HP16X141	141	41.7	16.00	16.00	0.875	0.875	1870	264	234	6.70	599	116.0	74.9	3.79
HP16X162	162	47.7	16.30	16.10	1.000	1.000	2190	306	269	6.78	697	134.0	86.6	3.82
HP16X183	183	54.1	16.50	16.30	1.130	1.130	2510	349	304	6.81	818	156.0	100.0	3.89
HP18X135	135	39.9	17.50	17.80	0.750	0.750	2200	281	251	7.43	706	122.0	79.3	4.21
HP18X157	157	46.2	17.70	17.90	0.870	0.870	2570	327	290	7.46	833	143.0	93.1	4.25
HP18X181	181	53.2	18.00	18.00	1.000	1.000	3020	379	336	7.53	974	167.0	108.0	4.28
HP18X204	204	60.2	18.30	18.10	1.130	1.130	3480	433	380	7.60	1120	191.0	124.0	4.31

Figure 8-2 Table of H-pile section properties (modified from Skyline Steel 2015).

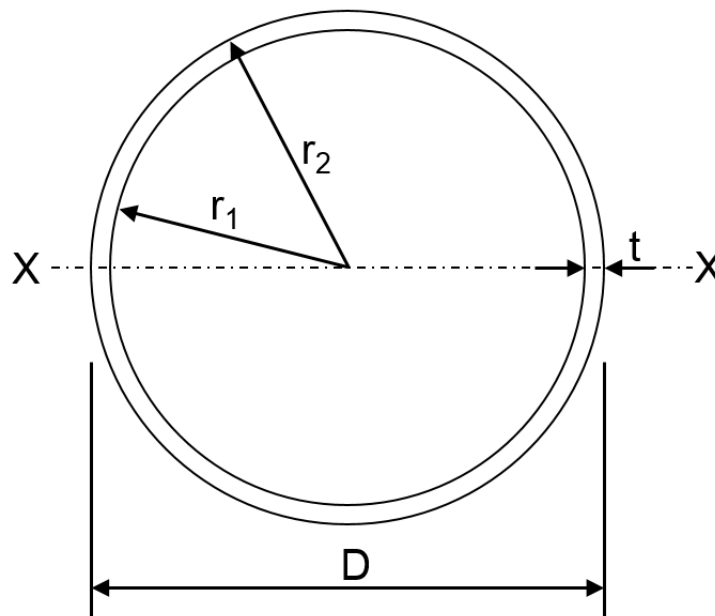


Figure 8-3 Pipe pile section dimensions.

The largest stresses in piles occur at the greatest distance from the neutral axis. This is at the outer edge(s) of a single pile and at the outer edge of the outermost piles of a group. Under combined axial and flexural loading, the pile area, the stiffness or moment of inertia, and distance from neutral axis to the edge of the section, must be defined to check maximum stress.

The moment of inertia, I (in⁴), for various common shapes may be computed with Equation 8-2 to 8-4. A reference should be made to the AISC (2011) shape tables or Figure 8-2 for H-piles, where tabulated structural property values about the strong and weak axis are provided. Sections should be selected from those commonly available from local suppliers. Otherwise, scheduling delays may result as manufacturers do not continuously hold all pile sizes in stock.

For solid, circular sections:

$$I = \frac{\pi(D)^4}{64} \quad \text{Eq. 8-2}$$

For voided circular sections:

$$I = \frac{\pi[(D)^4 - (D_1)^4]}{64} \quad \text{Eq. 8-3}$$

For solid, square sections:

$$I = \frac{b^4}{12} \quad \text{Eq. 8-4}$$

Where:

- D = outside diameter (inches).
- D_1 = inner diameter, $2 r_1 = D - 2 t$, (inches).
- t = pipe pile wall thickness (inches).
- b = width/height of square (inches).

To compute moment induced stresses, it is also convenient to compute the elastic section modulus, S , as in Equation 8-5.

$$S = \frac{I}{c} \quad \text{Eq. 8-5}$$

Where:

- S = elastic section modulus (in^3).
- I = moment of inertia (in^4).
- c = distance from centroid to outer edge (inches).

8.2.3 Effective Length and Buckling

From a structural view, piles act as columns and therefore under axial or moment loads, an effective length could be considered for simplified frame analyses. Pile end conditions are used to approximate an effective length factor, K , as shown in Figure 8-4, where the pile toe is generally assumed fixed for both translation and rotation. In the absence of sufficient bracing, (e.g. very soft soils, piles extended through water, large scour) the pile head may be affected by sidesway, and therefore a fixed rotation and translation condition may not apply. For these conditions, the design value of K should be applied. For example, if a pile extends into a pier cap, which is subject to severe scour, rotation is generally prevented by the pier cap mass and stiffness, while lateral movement may result from reduced soil confining pressure (reduced lateral bracing) in combination with existing loads. In this case, a fixed rotation and free translation condition may exist. In pile bents, depending on the foundation's connection to the superstructure, the bent cap could allow rotation and translation perpendicular to the long axis of the bent cap, but free translation with fixed rotation along the long axis of the bent cap. To have a rotationally fixed pile top condition, Rollins and Stenlund (2010) observed that rather than defining a rule-of-thumb for minimum pile embedment length into the pile cap, the moment capacity of the pile cap to pile connection should be designed with pile embedment and cap reinforcement details such that the moment capacity of the connection exceeds the moment capacity of the pile.

Buckling is generally of concern when piles extend through water or air, or for liquefaction, where an absence of confining stress is clearly recognizable. Concern for buckling has also been expressed for piles extending through very soft soils or peat. However, pile buckling is a function of the confining stress (bracing) and applied load (Davisson 1963).

To characterize buckling in soft soils, a load test program was performed by the Bethlehem Steel Corporation which suggested that even soft soils provide adequate support (Bethlehem Steel Corporation 1970). One such H-pile in this study extended through 31 feet of water and 29 feet of organic silt where the pile sank under its own weight. A load of 200 tons produced a gross settlement of 0.63 inches while net settlement, after unloading, was measured at 0.02 inches. No pile buckling

occurred. In addition, Coduto et al. (2016) suggests that, “even the softest soils provide enough lateral support to prevent underground buckling in piles subject only to axial loads, especially when a cap is present and provides rotational fixity to the pile top.”

Buckled shape of column is shown by dashed line						
Theoretical K value	0.5	0.7	1.0	1.0	2.0	2.0
Design value of K when ideal conditions are approximated	0.65	0.80	1.0	1.2	2.1	2.0
End condition code		Rotation fixed Translation fixed			Rotation free Translation fixed	
		Rotation fixed Translation free			Rotation free Translation free	

Figure 8-4 Effective length factors, K (after AASHTO 2014).

A more conservative approach to this issue is presented in Chance (2003) where the critical buckling load is determined through the use of computer software such as LPILE. For this method, a pile-soil model is generated and incremental loads are applied to evaluate the resulting deflection. This method may provide the design engineer with a deflected pile shape to assess buckling for a given factored load in lieu of using prescriptive minimum soil strength values to characterize an unbraced length.

8.3 STRUCTURAL CONSIDERATIONS AND RESISTANCE FACTORS

The limitations on nominal static design stresses for driven piles in various codes generally represent the static resistance which can be consistently developed with traditional driving equipment and methods.

The factored resistance must be greater than factored loads applied to the pile. The recommended AASHTO limits for factored pile design stresses will generally keep the driving stresses within recommended limits. Factored loads are covered in Article 3 of the AASHTO Specification (2014) while driving stress limits are presented in the respective pile material sections for concrete (Article 5), steel (Article 6), and timber (Article 8).

8.3.1 Depth to Fixity

The unbraced length, l , or laterally unsupported length is defined by AASHTO (2014) as the distance between two braced points that resist buckling or distortion modes. For embedded piles, the unbraced length is considered for scour and pile stickup through air and/or water. For preliminary analysis, when lateral loads are applied, the effective length, K , for flexural or torsional resistance calculations is taken as the total unsupported length, plus an embedded depth to “fixity.” If a lateral pile analysis with p-y curves for soil-structure interaction has been performed as discussed in Chapter 7, the depth to fixity concept is unnecessary. Most software with lateral analysis also includes additional features to determine a pile’s buckling capacity given the soil model and a pile model with the expected stick-up above the ground level.

For preliminary calculations, however, the depth to fixity below the ground may be evaluated based on soil type and soil strength parameters as shown in Equation 8-6 for clays and Equation 8-8 for sands. Table 8-4 contains the rate of increase in soil modulus for sands, n_h , and should be used as applicable in the following depth to fixity estimates.

For clays:

$$d_f = 1.4 \left(\frac{EI_w}{E_s} \right)^{0.25} \quad \text{Eq. 8-6}$$

$$E_s = 0.465s_u \quad \text{Eq. 8-7}$$

For sands:

$$d_f = 1.8 \left(\frac{EI_w}{n_h} \right)^{0.2} \quad \text{Eq. 8-8}$$

Where:

- d_f = depth to fixity below the ground (ft).
- E = elastic modulus of pile material (ksi).

- E_s = elastic modulus of clay soil (ksi).
- s_u = undrained shear strength of clay (ksf).
- I_w = weak axis moment of inertia of pile (ft⁴).
- n_h = rate of increase of soil modulus with depth (Table 8-4) (ksi/ft).

Table 8-4 Rate of Increase of Soil Modulus with Depth for Sands (ksi/ft)
(after AASHTO 2014)

Consistency	Dry or Moist	Submerged
Loose	0.417	0.208
Medium	1.110	0.556
Dense	2.780	1.390

8.3.2 Limiting Slenderness Ratio

Piles extending through air or water are unbraced over some length and therefore, for axial compression, the slenderness ratio should be checked during design. For non-composite steel piles, which are not fully embedded, slenderness ratio limits should be satisfied as follows:

$$\frac{Kl}{r_s} \leq 120 \quad \text{Eq. 8-9}$$

Where:

- K = effective length factor (Figure 8-4) (dimensionless).
- l = unbraced length, or laterally unsupported length plus d_f (inches).
- r_s = minimum radius of gyration, $\sqrt{I/A}$ (inches).

8.3.3 Resistance Factors

A discussion and step by step determination of the nominal structural resistance for timber, steel, and concrete piles is provided in the following sections. The AASHTO (2014) specifications form the basis of these respective sections. Following the Load and Resistance Factor Design (LRFD) approach, a resistance factor is applied to the calculated nominal structural resistance.

In practical terms, the imposed factored load must be less than or equal to the factored resistance. Chapter 2 provides a discussion on load combinations in which load factors are applied to respective load effects. The critical load combination is

applied as axial, shear and moment loads on the structural member and will be described herein as follows:

Factored axial load:

$$\sum(n_i\gamma_i)Q_i = Q \rightarrow P_u \quad \text{Eq. 8-10}$$

Factored moment load:

$$\sum(n_i\gamma_i)Q_i = Q \rightarrow M_u \quad \text{Eq. 8-11}$$

Factored shear load:

$$\sum(n_i\gamma_i)Q_i = Q \rightarrow V_u \quad \text{Eq. 8-12}$$

The nominal structural resistance is specific to pile properties such as material, size, and shape. A separate discussion based on pile material is provided in Section 8.4 through Section 8.7. On the resistance side, the factored structural resistance will be described as shown below.

Factored resistance in axial compression:

$$\sum\phi_i R_i = \phi_c P_n = P_r \quad \text{Eq. 8-13}$$

Factored resistance in flexure:

$$\sum\phi_i R_i = \phi_f M_n = M_r \quad \text{Eq. 8-14}$$

Factored resistance in shear:

$$\sum\phi_i R_i = \phi_v V_n = V_r \quad \text{Eq. 8-15}$$

AASHTO (2014) recommended resistance factors for driving and structural resistance are provided in Table 8-5 and Table 8-6, respectively. As an example, for a steel H-pile with good driving conditions and with the use of a pile tip (e.g. pile point or shoe), $\phi_{da} = 1.0$ would be used in Equation 8-33 (Section 8.5.1) along with the material yield stress to determine the nominal driving stress limits. For nominal structural resistance, $\phi_c = 0.60$, would be entered into Equation 8-34 (Section 8.5.2). A similar procedure is therefore used for alternative pile types, driving conditions, and loading cases.

Table 8-5 Resistance Factors During Pile Driving

Resistance Determination Method	Pile Drivability Resistance Factor
Steel Piles (AASHTO 6.5.4.2)	$\phi_{da} = 1.0$
Concrete Piles (AASHTO 5.5.4.2)	$\phi_{da} = 1.0$
Timber Piles (AASHTO 8.5.4.2)	$\phi_{da} = 1.15$

Table 8-6 Structural Limit Resistance Factors for Piles in Compression

Pile Material	Design Resistance	Resistance Factor
Steel (AASHTO 6.5.4.2)	Axial - Good driving conditions where pile tip is not necessary	
	H-piles	$\phi_c = 0.60$
	Pipe Piles	$\phi_c = 0.70$
	Axial -Pile is subject to damage due to severe driving conditions where pile tip is necessary	
	H-piles	$\phi_c = 0.50$
	Pipe Piles	$\phi_c = 0.60$
	Combined Axial and Flexural for Undamaged Piles	
Axial – H-piles	$\phi_c = 0.70$	
Axial – Pipe Piles	$\phi_c = 0.80$	
Flexure – Both Pile Types	$\phi_f = 1.00$	
Shear	$\phi_v = 1.00$	
Concrete (AASHTO 5.5.4.2)	Tension Controlled	
	Reinforced Concrete	$\phi_c = 0.90$
	Prestressed Concrete	$\phi_c = 1.00$
Compression Controlled		
Prestressed Concrete	$\phi_c = 0.75$	
Timber (AASHTO 8.5.4.2)	Compression Parallel to Grain	$\phi_c = 0.90$
	Flexure	$\phi_f = 0.85$
	Shear	$\phi_v = 0.75$

8.4 TIMBER PILES

Timber piles are typically round, tapered, and used for modest loading levels. Several species of timber are suitable for use as piles, however Douglas Fir and Southern Pine are by far the most common types used in the United States. Equations to assess maximum driving stresses (Section 8.4.1) or axial and flexural stresses (Section 8.4.2) will be subsequently described, while reference design values shown in Table 8-7 are factored into these calculations. For the load cases described herein, the reference value is modified with an adjustment factor specific to the loading case and pile properties.

Table 8-7 Reference Design Values for Timber Piles, ksi (after AASHTO 2014)

Species	F_{co}	F_{bo}	F_{vo}	E_o
Pacific Coast Douglas-Fir ¹	1.25	2.45	0.115	1500
Red Oak ²	1.10	2.45	0.135	1250
Red Pine ³	0.90	1.90	0.085	1280
Southern Pine ⁴	1.20	2.40	0.110	1500

¹ Use Douglas Fir-Larch reference values for connection design.

² Northern and Southern Red Oak.

³ United States grown Red Pine. Use Northern Pine reference values for connection design.

⁴ Reference strengths apply to Loblolly, Longleaf, Shortleaf and Slash Pine.

Where:

F_{co} = reference value for compression stress parallel to grain (ksi).

F_{bo} = reference value for strength in flexure (ksi).

F_{vo} = reference value for strength in shear (ksi).

E_o = reference value elastic modulus (ksi).

The time effect factor, C_λ , shown in Table 8-8 is utilized in consideration of specific limit states. AASHTO (2014) commentary provides that the Strength I condition be used when the cumulative duration of a bridge live load is two months, while the Strength II condition is used for cumulative live loading less than two months. Furthermore for permanent loads, the Strength IV limit state should be used.

Table 8-8 Time Effect Factors (after AASHTO 2014)

Limit State	C_λ
Strength I	0.8
Strength II	1.0
Strength III	1.0
Strength IV	0.6
Extreme Event I	1.0

A size reduction factor, C_F , is applied to timber piles in flexure; however this factor is only applied if the critical section in bending has a diameter greater than 12 inches (i.e. area of 144 in²). This would be the sawn lumber beam equivalent of a depth of 12 inches (i.e. area of 144 in²). If the critical section area is less than 144 in², the shape reduction factor is set equal to 1.0. Conversely, if the critical section area is greater than 144 in², Equation 8-16 should be used to determine the size reduction factor. Considering the AASHTO (2014) criteria, “the equation should be entered with a b equal to the depth of a square beam having the same cross-sectional area as that of a round member” (Showalter 2012).

$$C_F = \left(\frac{12}{b}\right)^{\frac{1}{9}} \quad \text{Eq. 8-16}$$

Where:

C_F = size factor.

b = depth of beam or width of dimension lumber.

The wet service factor, C_M , provides adjustment based upon moisture content and although not all timber piles are submerged, and assumption of wet use conditions may be made. A wet service factor equal to 1.0 is therefore recommended.

Several adjustment factors provided in the AASHTO (2014) specifications do not apply to timber piles such as the volume factor C_v , incising factor C_i , deck factor C_d , flat-use factor C_{fu} . Since AASHTO (2014) design specifications do not provide specific guidance on these values for timber piles, the values are assumed as 1.0 in this manual to prevent unwarranted increases or reductions in the structural resistance limits.

8.4.1 Driving Stresses

Timber piles should be installed to limit excessive pile stress development that may result in shearing or brooming near the pile top. Additional stresses may develop along the pile as well, especially as the tapered section decreases near the pile toe. AASHTO (2014) specifications limit maximum compression and tension driving stresses as Equation 8-17.

$$\sigma_{dr} = \phi_{da} (2.6F_{co}) \quad \text{Eq. 8-17}$$

Where:

σ_{dr} = driving stress (ksi).

φ_{da} = resistance factor during driving (1.15 for timber piles, Table 8-5).

F_{co} = reference value for compression stress parallel to grain (Table 8-7).

8.4.2 Structural Resistance

AASHTO (2014) summarizes axial and flexural loading resistance limits in Article 8.6, 8.8 and 8.10. The following sections provide design checks to determine structural strength limits, where Table 8-7 provides reference values, Table 8-8 contains time effect factors, and Equation 8-16 may be used to determine a size factor. The equations below apply to all timber elements, and therefore several adjustment factors introduced in the AASHTO (2014) specification do not specifically pertain to piles and are assumed to equal 1.0.

8.4.2.1 Axial Compression Parallel to Grain

For axial compression loading, the factored structural limit state is taken as follows:

$$P_r = \varphi P_n \quad \text{Eq. 8-18}$$

Where:

P_r = factored resistance in axial compression (kips).

φ = resistance factor (0.9 for timber pile compression parallel to grain).

P_n = nominal resistance in axial compression (kips).

STEP BY STEP PROCEDURE FOR: "NOMINAL COMPRESSION RESISTANCE"

STEP 1 Determine the adjusted resistance in compression, F_c .

The nominal resistance for axial compression should be evaluated using Equation 8--19 and 8-20 which are provided in AASHTO (2014) Article 8.4.

$$F_c = F_{co} C_{KF} C_M C_F C_i C_\lambda \quad \text{Eq. 8-19}$$

In which:

$$C_{KF} = \frac{2.5}{\varphi} \quad \text{Eq. 8-20}$$

Where:

- F_c = adjusted resistance in compression (ksi).
- F_{co} = reference resistance in compression (Table 8-7) (ksi).
- C_{KF} = format conversion factor where $\phi_c = 0.9$.
- C_M = wet service factor (1.0 for piles).
- C_F = size factor (1.0 for or Equation 8-16 for piles).
- C_i = incising factor (Not Applicable for piles-1.0).
- C_λ = time effect factor (Table 8-8).

STEP 2 Determine the nominal resistance in axial compression, P_n

Following adjustment of the reference resistance in compression, the nominal resistance in axial compression is calculated from Equation 8-21. If the piles are sufficiently braced, the column stability factor, C_p , may be taken as 1.0. However, Equation 8-22 should be used to determine the column stability factor, C_p , if sufficient bracing does not exist.

$$P_n = F_c A_g C_p \quad \text{Eq. 8-21}$$

In which:

$$C_p = \frac{1+B}{2c} - \sqrt{\left(\frac{1+B}{2c}\right)^2 - \frac{B}{c}} \leq 1.0 \quad \text{Eq. 8-22}$$

$$B = \frac{F_{cE}}{F_c} \leq 1.0 \quad \text{Eq. 8-23}$$

$$F_{cE} = \frac{K_{cE} E b^2}{L_e^2} \quad \text{Eq. 8-24}$$

$$E = E_o C_t \quad \text{Eq. 8-25}$$

Where:

- F_c = adjusted resistance in compression parallel to grain (ksi).
- P_n = nominal resistance in axial compression (kips).
- A_g = gross cross-sectional area (in²).
- C_p = column stability factor.
- C_M = wet service factor (1.0 for piles).
- C_i = incising factor (Not Applicable for piles-1.0).
- c = round timber pile factor (0.85).

- K_{cE} = round timber pile factor (0.76).
- b = depth or width (inches).
- L_e = effective length taken as KL (Figure 8-4, inches).
- E_o = reference modulus of elasticity (ksi) (Table 8-7).

8.4.2.2 Flexure

For flexure, the factored structural limit state is taken as:

$$M_r = \phi M_n \quad \text{Eq. 8-26}$$

Where:

- M_r = factored flexural resistance (kip-in).
- ϕ = resistance factor (0.85 for timber pile flexure).
- M_n = nominal flexural resistance (kip-in).

STEP BY STEP PROCEDURE FOR: "NOMINAL FLEXURAL RESISTANCE"

STEP 1 Determine the adjusted resistance in flexure, F_b .

A round timber pile is assumed in this manual for flexure. If alternative pile cross sections are used, consideration should be given to the new shape. To determine the adjusted resistance in flexure, the following equations should be applied.

$$F_b = F_{bo} C_{KF} C_M C_F C_{fu} C_i C_d C_\lambda \quad \text{Eq. 8-27}$$

In which:

$$C_{KF} = \frac{2.5}{\phi} \quad \text{Eq. 8-28}$$

Where:

- F_{bo} = reference resistance in flexure (Table 8-7) (kips).
- C_{KF} = format conversion factor where $\phi_f = 0.85$.
- C_M = wet service factor (1.0 for piles).
- C_F = size factor (1.0 or Equation 8-16 for piles).
- C_{fu} = flat use factor (Not Applicable for piles-1.0).
- C_i = incising factor (Not Applicable for piles-1.0).
- C_d = deck factor (Not Applicable for piles-1.0).
- C_λ = time effect factor (Table 8-8).

STEP 2 Determine the nominal flexural resistance, M_n .

Following adjustment of the reference resistance in flexure, the nominal flexural resistance is calculated as follows.

$$M_n = F_b S \quad \text{Eq. 8-29}$$

Where:

- M_n = nominal flexural resistance (kip-in).
- S = elastic section modulus (in³).
- F_b = adjusted resistance in flexure (Table 8-7) (ksi).

8.4.2.3 Combined Flexure and Axial Compression

For combined flexure and compression, the factored structural limit state must satisfy checks for beam rupture and lateral buckling as shown in Equation 8-30. If the applied loads are not sufficiently resisted by the pile section, an alternative pile design is required.

$$\left(\frac{P_u}{P_r}\right)^2 + \frac{M_u}{M_r \left(1 - \frac{P_u}{F_{cE} A_g}\right)} \leq 1.0 \quad \text{Eq. 8-30}$$

In which:

$$F_{cE} = \frac{K_{cE} E b^2}{L_e^2} \quad \text{Eq. 8-31}$$

$$E = E_o C_M C_i \quad \text{Eq. 8-32}$$

Where:

- P_r = factored resistance in axial compression (kips) (Equation 8-18).
- P_u = factored axial load (kips) (Equation 8-10).
- M_r = factored resistance in flexure (kip-in) (Equation 8-26).
- M_u = factored moment load (kip-in) (Equation 8-11).
- A_g = gross cross-sectional area (in²).
- C_M = wet service factor (N/A -1.0 for piles).
- C_i = incising factor (N/A -1.0 for piles).
- K_{cE} = round timber pile factor (0.76).
- b = pile width or diameter (inches).
- L_e = effective length taken as KL (Figure 8-4, inches).
- E_o = reference modulus of elasticity (ksi) (Table 8-7).

8.5 STEEL PILES

8.5.1 Driving Stresses

Steel piles can handle higher stresses than concrete or timber during driving, and the limit is governed the steel yield strength. Several grades of steel are routinely produced and higher grades may be specified if warranted. Table 8-1 provides an overview of typical steel grades and their respective yield strength. Pile driving does not typically generate sufficiently high tensile stresses to yield steel piles, therefore a stress limit is only required in compression. For steel piles, AASHTO (2014) specifications limit nominal compression driving stresses as follows:

$$\sigma_{dr} = \phi_{da} (0.9F_y) \quad \text{Eq. 8-33}$$

Where:

- σ_{dr} = driving stress limit (ksi).
- ϕ_{da} = resistance factor during driving (1.0 for steel piles, Table 8-5).
- F_y = yield stress of steel (ksi) (Table 8-1).

8.5.2 Structural Resistance

8.5.2.1 Axial Compression

For axial compression loads, the factored structural limit state is taken as:

$$P_r = \phi_c P_n \quad \text{Eq. 8-34}$$

Where:

- P_r = factored resistance in axial compression (kips).
- ϕ_c = resistance factor (Table 8-6).
- P_n = nominal resistance in axial compression (kips).

To determine the nominal resistance in axial compression, pile strength and buckling failure should be considered. The following step by step procedure should be used to calculate the nominal resistance.

STEP BY STEP PROCEDURE FOR: “NOMINAL COMPRESSION RESISTANCE”

STEP 1 Determine the equivalent nominal yield resistance, P_o .

The equivalent nominal yield resistance, P_o , is a function of the material yield stress, cross sectional area and slenderness reduction factor, if applicable. For non-slender piles in compression, the slenderness reduction factor, Q , is taken as 1.0. However for slender piles, the full nominal yield strength under uniform axial compression is limited by local buckling. This reduction factor is governed by section buildup, pile dimensions and material properties, therefore, a further discussion of slender members and direction for calculating Q may be found in AASHTO (2014) Article 6.9.4.2.2.

$$P_o = QF_y A_g \quad \text{Eq. 8-35}$$

Where:

- A_g = gross cross-sectional area (in²).
- P_o = equivalent nominal axial yield resistance (kips).
- F_y = yield stress of steel (Table 8-1) (ksi).
- Q = slender element reduction factor (dimensionless).

To satisfy the slender element requirement for local buckling, Equation 8-36 is used for H-piles and Equation 8-38 is used for unfilled pipe piles.

$$\frac{b_f}{2t_f} \leq 0.64 \sqrt{\frac{k_c E_{st}}{F_y}} \quad \text{Eq. 8-36}$$

And:

$$0.35 \leq k_c \leq 0.76$$

In which:

$$k_c = \frac{4}{\sqrt{d_w/t_w}} \quad \text{Eq. 8-37}$$

Where:

- b_f = flange width (inches).
- t_f = flange thickness (inches).
- F_y = yield stress of steel (Table 8-1) (ksi).
- E_{st} = elastic modulus of steel (ksi).
- d_w = web depth (inches).
- t_w = web thickness (inches).

$$\frac{D}{t} \leq 0.11 \frac{E_{st}}{F_y} \quad \text{Eq. 8-38}$$

Where:

- D = diameter of pipe (inches).
- t = wall thickness (inches).
- F_y = yield stress of steel (Table 8-1) (ksi).
- E_{st} = elastic modulus of steel (ksi).

STEP 2 Determine the elastic critical buckling resistance, P_e .

In determination of the nominal resistance in axial compression, buckling may occur with a lack of sufficient bracing. This topic is discussed further in Section 8.2.3. AASHTO (2014) requires both flexural and torsional modes of buckling be checked if applicable. For fully embedded piles, the flexural buckling mode will be used. However, when the pile extends through water or air, doubly symmetric open section members (e.g., H-piles) must be evaluated for torsional buckling as well. The critical failure mode is the lesser buckling resistance, and is employed to define the nominal resistance in axial compression.

Flexural buckling:

$$P_e = \frac{\pi^2 E_{st} A_g}{\left(\frac{Kl}{r_s} \right)^2} \quad \text{Eq. 8-39}$$

Where:

- P_e = elastic critical buckling resistance (kips).
- E_{st} = elastic modulus of steel (ksi).
- A_g = gross cross-sectional area (in²).
- K = effective length in the plane of buckling (Figure 8-4) (dimensionless).
- l = unbraced length in the plane of buckling (Section 8.3) (inches).
- r_s = radius of gyration about axis normal to plane of buckling (inches).

Torsional buckling:

$$P_e = \left[\frac{\pi^2 E_{st} C_w}{(K_z l_z)^2} + GJ \right] \frac{A_g}{I_x + I_y} \quad \text{Eq. 8-40}$$

In which:

$$C_w = \frac{I_y h^2}{4} \quad \text{Eq. 8-41}$$

$$G = 0.385 E_{st} \quad \text{Eq. 8-42}$$

Where:

- P_e = elastic critical buckling resistance (kips).
- E_{st} = elastic modulus of steel (ksi).
- C_w = warping torsional constant (doubly symmetric open sections) (in⁶).
- K_z = effective length for torsional buckling (Figure 8-4) (dimensionless).
- l_z = unbraced length for torsional buckling (inches).
- G = shear modulus (ksi).
- J = St. Venant torsional constant (in⁴).
- A_g = gross cross-sectional area (in²).
- I_x, I_y = moments of inertia about the major and minor principal axes of cross section, respectively (in⁴).
- h = distance between flange and centroids (inches).

STEP 3 Determine the nominal resistance in axial compression, P_n .

With the above resistances defined, the nominal resistance for axial compression may be evaluated using the following equations, which are provided in AASHTO (2014) Article 6.9.4.1.

If $\frac{P_e}{P_o} \geq 0.44$:

$$P_n = P_o 0.658 \frac{P_e}{P_o} \quad \text{Eq. 8-43}$$

If $\frac{P_e}{P_o} < 0.44$:

$$P_n = 0.877 P_e \quad \text{Eq. 8-44}$$

Where:

- P_n = nominal resistance in axial compression (kips).
- P_o = equivalent nominal yield resistance (Equation 8-35) (kips).
- P_e = elastic critical buckling resistance (Equation 8-39 or 8-40) (kips).

8.5.2.2 Flexure

The factored resistance in flexure is computed as follows

$$M_r = \phi_f M_n \quad \text{Eq. 8-45}$$

Where:

M_r = factored resistance in flexure (kip-in).

ϕ_f = resistance factor (Table 8-6).

M_n = nominal resistance in flexure (kip-in).

The nominal flexural resistance is a function of pile shape as well as general pile properties. Steel piles are primarily H-piles or pipe piles. Therefore the step by step procedure that follows will consider only these two steel pile types. If alternative sections are used, the engineer is referred to Article 6.12.2.2 of the AASHTO (2014) specifications. Steel H-piles and I-sections are treated equally for flexural resistance. Hence, part A of this procedure applies to both steel H-piles and miscellaneous I sections.

STEP BY STEP PROCEDURE FOR: "NOMINAL FLEXURAL RESISTANCE"

A. Steel H-Sections.

STEP 1 Check flange slenderness ratio and limiting slenderness.

$$\lambda_f = \frac{b_f}{2t_f} \quad \text{Eq. 8-46}$$

$$\lambda_{pf} = 0.38 \sqrt{\frac{E_{st}}{F_{yf}}} \quad \text{Eq. 8-47}$$

$$\lambda_{rf} = 0.83 \sqrt{\frac{E_{st}}{F_{yf}}} \quad \text{Eq. 8-48}$$

Where:

λ_f = slenderness ratio for flange.

λ_{pf} = limiting slenderness ratio for a compact flange.

λ_{rf} = limiting slenderness ratio for a non-compact flange.

- b_f = flange width (inch).
- t_f = flange thickness (inch).
- E_{st} = elastic modulus of steel (ksi).
- F_{yf} = minimum yield strength of lower strength flange (ksi).

STEP 2 Determine the nominal flexural resistance.

To determine the nominal flexural resistance, the above slenderness definitions should first be resolved. These functions serve to define the limiting flexural resistance. In the case where the limiting slenderness ratio of a compact flange is greater than the slenderness ratio, the plastic moment about the weak axis will limit resistance. For H-piles, Eq. 8-49 can be used. Conversely, Eq. 8-51 should be used when the slenderness ratio is greater than the limiting slenderness ratio of a compact flange.

If $\lambda_f \leq \lambda_{pf}$:

$$M_n = M_p \quad \text{Eq. 8-49}$$

In which, for HP-sections about weak axis:

$$M_p = 1.5F_y S_y \quad \text{Eq. 8-50}$$

If $\lambda_{pf} < \lambda_f \leq \lambda_{rf}$, the nominal flexural resistance about the weak axis is:

$$M_n = \left[1 - \left(1 - \frac{S_y}{Z_y} \right) \left(\frac{\lambda_f - \lambda_{pf}}{0.45 \sqrt{\frac{E_{st}}{F_{yf}}}} \right) \right] f_{yf} Z_y \quad \text{Eq. 8-51}$$

Where:

- M_n = nominal resistance in flexure (kip-in).
- M_p = plastic moment about the weak axis (kip-in).
- S_y = elastic section modulus about weak axis (in³).
- Z_y = plastic section modulus about weak axis (in³).
- λ_f = slenderness ratio for flange (Equation 8-46, dimensionless).
- λ_{pf} = limiting slenderness ratio for a compact flange (Equation 8-47, dimensionless).

- E_{st} = elastic modulus of steel (ksi).
- F_y = yield stress of steel (ksi).
- F_{yf} = minimum yield strength of lower strength flange (ksi).

B. Steel Pipe Piles.

STEP 1 Check diameter to thickness ratio.

If the diameter to thickness ratio is sufficiently large, local buckling limits flexural resistance. To determine whether the plastic moment or local buckling will govern flexural resistance, Equation 8-52 should be applied. If Equation 8-52 is satisfied, the plastic moment will yield the steel pile and Step 2a should follow. Conversely, local buckling will limit flexural resistance if Equation 8-2 is not satisfied, and therefore Step 2b should follow.

$$\frac{D}{t} \leq 0.07 \frac{E_{st}}{F_y} \quad \text{Eq. 8-52}$$

Where:

- D = outside diameter of pipe (inch).
- t = pipe thickness (inch).
- E_{st} = elastic modulus of steel (ksi).
- F_y = yield strength of steel (Table 8-1) (ksi).

STEP 2a Determine nominal flexural resistance by plastic moment.

The nominal flexural resistance can be taken as follows:

$$M_n = M_p = F_y Z_y \quad \text{Eq. 8-53}$$

Where:

- M_n = nominal resistance in flexure (kip-in).
- M_p = plastic moment (kip-in).
- Z_y = plastic section modulus about weak axis (in³).
- F_y = yield strength of steel (Table 8-1) (ksi).

STEP 2b Determine nominal flexural resistance by local buckling.

Where local buckling will limit the nominal resistance in flexure, the following checks apply.

If $\frac{D}{t} \leq 0.31 \frac{E_{st}}{F_y}$:

$$M_n = \left(\frac{0.021E_{st}}{\frac{D}{t}} + F_y \right) S_y \quad \text{Eq. 8-54}$$

If $\frac{D}{t} > 0.31 \frac{E_{st}}{F_y}$:

$$M_n = f_{cr} S_y \quad \text{Eq. 8-55}$$

In which:

$$f_{cr} = \frac{0.33E_{st}}{\frac{D}{t}} \quad \text{Eq. 8-56}$$

Where:

- D = outside diameter of pipe (inch).
- t = pipe thickness (inch).
- E_s = elastic modulus of steel (ksi).
- F_y = yield strength of steel (Table 8-1) (ksi).
- M_n = nominal flexural resistance (kip-in).
- S_y = elastic section modulus about weak axis (in^3).
- f_{cr} = elastic local buckling stress (ksi).

8.5.2.3 Combined Axial Compression and Flexure

Combined axial compression and flexure checks are only applied to pile groups with vertical piles. At this time, AASHTO (2014) does not have a recommendation to include battered piles. For combined compression and flexure of vertical piles, AASHTO (2014) requires the factored structural limit state to satisfy the following limit state checks.

If $\frac{P_u}{P_r} < 0.2$:

$$\frac{P_u}{2.0P_r} + \left(\frac{M_{ux}}{M_{rx}} + \frac{M_{uy}}{M_{ry}} \right) \leq 1.0 \quad \text{Eq. 8-57}$$

If $\frac{P_u}{P_r} \geq 0.2$:

$$\frac{P_u}{P_r} + \frac{8.0}{9.0} \left(\frac{M_{ux}}{M_{rx}} + \frac{M_{uy}}{M_{ry}} \right) \leq 1.0 \quad \text{Eq. 8-58}$$

Where:

- P_u = factored load in axial compression (kips).
- P_r = factored resistance in axial compression (kips) (Section 8.5.2.1).
- M_{ux} = factored moment about x-axis (kip-ft).
- M_{rx} = factored resistance in flexure about x-axis (kip-ft) (Section 8.5.2.2).
- M_{uy} = factored moment about y-axis (kip-ft).
- M_{ry} = factored resistance in flexure about y-axis (kip-ft) (Section 8.5.2.2).

8.5.2.4 Shear

Piles used for bridge foundations are generally not also used to resist high shear loads as significant lateral pile deflections may negatively impact bridge serviceability. For shear loads, the factored structural limit state is taken as:

$$V_r = \phi_v V_n \quad \text{Eq. 8-59}$$

Where:

- V_r = factored resistance in shear (kips).
- ϕ_v = resistance factor (Table 8-6).
- V_n = nominal resistance in shear (kips).

A straightforward calculation of the nominal structural resistance in shear is shown in Equation 8-60 and Equation 8-61 for an H-pile section. Reference should be made to the AASHTO (2014) specifications for additional design requirements concerning piles subject to significant shear loads or for alternative non-composite pile sections.

$$V_n = CV_p \quad \text{Eq. 8-60}$$

$$V_p = 0.58F_{yw}d_w t_w \quad \text{Eq. 8-61}$$

Where:

- V_n = nominal resistance in shear (kips).
- C = ratio of shear-buckling resistance to shear yield strength, typically 1.0 for H-piles.
- V_p = plastic shear force (kips).
- F_{yw} = yield strength of web (Table 8-1) (ksi).
- d_w = web depth of pile section (inch).
- t_w = web thickness of pile section (inch).

8.5.3 Example Calculations for H Pile Structural Resistance.

The following example provides calculations for an HP 14x117 which will support an integral abutment. This H-pile section is produced with a yield stress, F_y , of 50 ksi, an elastic modulus, E_{st} , of 29,000 ksi while the radius of gyration in the weak direction, r_s , is 3.59 inches (Figure 8-2). Based upon project specific conditions, an unbraced length, l , of 120 inches is assumed for scour. In addition, rotation is fixed while translation is free at the pile head, whereas both rotation and translation are fixed for at the pile toe, thus an effective length factor of 1.2 results (Figure 8-4).

Under the given conditions, the pile section easily satisfies main member slenderness limits ($kl/r < 120$). However a further inspection of local buckling under compression loads is required. First the buckling coefficient is determined.

$$k_c = \frac{4}{\sqrt{d_w/t_w}} = \frac{4}{\sqrt{14.2\text{inches}/0.805\text{inches}}} = 0.952 \quad [\text{Eq. 8-37}]$$

But, k_c must satisfy:

$$0.35 \leq k_c \leq 0.76$$

Therefore:

$$k_c = 0.76$$

After calculating the buckling coefficient, the following condition is checked.

$$\frac{b_f}{2t_f} \leq 0.64 \sqrt{\frac{k_c E_{st}}{F_y}} \quad [\text{Eq. 8-36}]$$

$$\frac{14.9\text{inches}}{2 * 0.805\text{inches}} \leq 0.64 \sqrt{\frac{0.76 * 29,000\text{ksi}}{50\text{ksi}}}$$

$$9.25 \leq 13.44 \Rightarrow Q = 1.0$$

Based upon Equation 8-36, the pile section is a non-slender element, and therefore the slenderness reduction factor Q is set equal to 1.0. The equivalent nominal yield resistance is determined using Equation 8-35.

$$P_o = QF_y A_g \quad [\text{Eq. 8-35}]$$

$$P_o = 1.0 * 50\text{ksi} * 34.4\text{in}^2$$

$$P_o = 1720 \text{ kips}$$

Next, elastic critical buckling resistance in the section is determined.

$$P_e = \frac{\pi^2 E_{st} A_g}{\left(\frac{Kl}{r_s}\right)^2} \quad [\text{Eq. 8-39}]$$

$$P_e = \frac{\pi^2 * 29,000\text{ksi} * 34.4\text{in}^2}{\left(\frac{1.2 * 120\text{inches}}{3.59\text{inches}}\right)^2}$$

$$P_e = 6120 \text{ kips}$$

From Step 3 of Section 8.5.2.1, the nominal resistance in axial compression, P_n , is determined by applying either Equation 8-43 or 8-44. For this example, the ratio of elastic critical buckling resistance, P_e , to yield resistance, P_o , satisfies criteria for Equation 8-43 and is therefore shown in the following calculations.

$$\text{If } \frac{P_e}{P_o} \geq 0.44 :$$

$$\frac{P_e}{P_o} = \frac{6120\text{kips}}{1720\text{kips}} = 3.56 \geq 0.44$$

Therefore:

$$P_n = P_o 0.658^{\frac{P_o}{P_e}} \quad [\text{Eq. 8-43}]$$

$$P_n = 1720\text{kips} * 0.658^{\frac{1720\text{kips}}{6120\text{kips}}}$$

$$P_n = 1529 \text{ kips}$$

After calculation of the nominal resistance in axial compression, a resistance factor can be applied to determine the factored structural resistance in axial compression. Because good driving conditions were encountered and pile toe protection was not necessary, a resistance factor, $\phi_c = 0.60$, is used (Table 8-6). This factor is applied when only axial compression is considered. When using the combined axial and flexure interaction equations as shown in Section 8.5.2.3, $\phi_c = 0.70$ is used.

$$P_r = \phi_c P_n \quad [\text{Eq. 8-34}]$$

$$P_r = 0.60 * 1,529 \text{ kips}$$

$$P_r = 917 \text{ kips}$$

Continuing with the example, the factored resistance in flexure is determined. To begin, the flange slenderness is inspected for the HP 14x117 pile section. In addition, compact and non-compact flange slenderness ratios are calculated.

Flange slenderness ratio:

$$\lambda_f = \frac{b_f}{2t_f} \quad [\text{Eq. 8-46}]$$

$$\lambda_f = \frac{14.9 \text{ inches}}{2 * 0.805 \text{ inches}}$$

$$\lambda_f = 9.25$$

Limiting slenderness ratio for a compact flange:

$$\lambda_{pf} = 0.38 \sqrt{\frac{E_{st}}{F_{yf}}} \quad [\text{Eq. 8-47}]$$

$$\lambda_{pf} = 0.38 \sqrt{\frac{29,000 \text{ ksi}}{50 \text{ ksi}}}$$

$$\lambda_{pf} = 9.25$$

Limiting slenderness ratio for a non-compact flange:

$$\lambda_{rf} = 0.83 \sqrt{\frac{E_{st}}{F_{yf}}} \quad [\text{Eq. 8-48}]$$

$$\lambda_{rf} = 0.83 \sqrt{\frac{29,000 \text{ ksi}}{50 \text{ ksi}}}$$

$$\lambda_{rf} = 19.98$$

After determining the slenderness ratio functions, a comparison is then made. For this particular pile, Equation 8-48 will be used to define the nominal flexural resistance. Reference should be made to Figure 8-2 for H-pile section properties such as the elastic and plastic section moduli.

If $\lambda_{pf} < \lambda_f \leq \lambda_{rf}$:

$$9.15 < 9.25 \leq 19.98$$

Therefore:

$$M_n = \left[1 - \left(1 - \frac{S_y}{Z_y} \right) \left(\frac{\lambda_f - \lambda_{pf}}{0.45 \sqrt{\frac{E_{st}}{F_{yf}}}} \right) \right] f_{yf} Z_y \quad [\text{Eq. 8-51}]$$

$$M_n = \left[1 - \left(1 - \frac{59.5 \text{ in}^3}{91.4 \text{ in}^3} \right) \left(\frac{9.25 - 9.15}{0.45 \sqrt{\frac{29,000 \text{ ksi}}{50 \text{ ksi}}}} \right) \right] 50 \text{ ksi} * 91.4 \text{ in}^3$$

$$M_n = 4555 \text{ kip-in}$$

Following the calculation of nominal resistance in flexure, a resistance factor can be applied to determine the factored structural resistance in flexure. The AASHTO recommended resistance factor for flexure is, $\phi_f = 1.0$, is used (Table 8-6).

$$M_r = \phi_f M_n \quad [\text{Eq. 8-45}]$$

$$M_r = 1.0 * 4555 \text{ kip-in}$$

$$M_r = 4555 \text{ kip-in}$$

Finally, the nominal resistance in shear of the pile section is determined using Equations 8-60 and 8-61. For the HP 14x117 pile section, the web depth is 14.2 inches and the web thickness is 0.805 inches (Figure 8-2). The plastic shear force is calculated using Equation 8-61.

$$V_p = 0.58F_{yw}d_w t_w \quad [\text{Eq. 8-61}]$$

$$V_p = 0.58 * 50\text{ksi} * 14.2\text{inches} * 0.805\text{inches}$$

$$V_p = 332 \text{ kips}$$

The nominal structural resistance in shear is calculated using Equation 8-60.

$$V_n = CV_p \quad [\text{Eq. 8-60}]$$

$$V_n = 1.0 * 332\text{kips}$$

$$V_n = 332 \text{ kips}$$

By multiplying the nominal structural resistance in shear by the AASHTO (2014) recommended resistance factor, the factored structural resistance in shear is determined.

$$V_r = \phi_v V_n \quad [\text{Eq. 8-59}]$$

$$V_r = 1.0 * 332\text{kips}$$

$$V_r = 332 \text{ kips}$$

8.6 CONCRETE PILES

8.6.1 Driving Stresses

Concrete by nature is strong in compression while tensile strength is mainly derived from reinforcing steel and prestressed longitudinal rebar. The additional tensile strength from prestressing allows for somewhat larger tensile stresses to develop and is therefore featured in nearly all concrete piles manufactured in the United States today. Unlike timber and steel piles, concrete piles are susceptible to damage in both compression and tension under normal driving conditions. The use of a pile cushion (Chapter 15) slows the impact velocity and thus, reduces dynamic forces during driving. Pile cushions are therefore employed when driving piles to lessen the probability of damage.

Driving stress limits are applied to the gross concrete area. In severe corrosive environments, the nominal tension stress is limited to the effective prestress after losses. AASHTO (2014) specifications limit the nominal driving stresses in compression and tension for concrete piles as follows.

For compression:

$$\sigma_{dr} = \phi_{da} (0.85 f'_c - f_{pe}) \quad \text{Eq. 8-62}$$

For tension:

$$\sigma_{dr} = \phi_{da} (0.095 \sqrt{f'_c} + f_{pe}) \quad \text{Eq. 8-63}$$

Where:

- σ_{dr} = driving stress (ksi).
- ϕ_{da} = resistance factor during driving (1.0 for concrete piles, Table 8-5).
- f'_c = concrete compression strength at 28 days, unless otherwise specified (ksi).
- f_{pe} = effective prestressing stress in concrete (ksi).

In Chapter 10 of the AASHTO (2014) specifications, the effective prestressing stress in the concrete is designated as f_{pe} , as shown in Equation 8-62 and 8-63. This value should typically be on the order of 0.5 to 1.0 ksi for most piles on highway projects, and should certainly be less than f'_c .

8.6.2 Structural Resistance

8.6.2.1 Axial Compression

For axial compression loading, the factored structural limit state is taken as:

$$P_r = \phi_c P_n \quad \text{Eq. 8-64}$$

Where:

- P_r = factored resistance in axial compression (kips).
- ϕ_c = resistance factor (Table 8-6).
- P_n = nominal resistance in axial compression (kips).

To determine the nominal resistance in axial compression, a straightforward calculation is performed considering either spiral or tie reinforcement. As mentioned in the ASSHTO (2014) commentary, reduction factors are placed on the respective equations to account for unintended eccentricity. Further details on axial resistance of concrete piles can be found in Article 5.7.4.4 of AASHTO (2014).

For members with spiral reinforcement:

$$P_n = 0.85 \left[0.85 f'_c (A_g - A_{str} - A_{ps}) + F_{yr} A_{str} - A_{ps} (f_{pe} - E_{st} \epsilon_{cu}) \right] \quad \text{Eq. 8-65}$$

For members with tie reinforcement:

$$P_n = 0.80 \left[0.85 f'_c (A_g - A_{str} - A_{ps}) + F_{yr} A_{str} - A_{ps} (f_{pe} - E_{st} \epsilon_{cu}) \right] \quad \text{Eq. 8-66}$$

Where:

- P_n = nominal resistance in axial compression (kips).
- f'_c = concrete compression strength at 28 days, unless otherwise specified (ksi).
- f_{pe} = effective stress in the prestressing steel after losses (ksi).
- F_{yr} = yield stress of reinforcing steel (ksi).
- A_g = gross cross-sectional area (in²).
- A_{str} = cross sectional area of longitudinal reinforcement (in²).
- A_{ps} = cross sectional area of prestressing steel (in²).
- E_{st} = elastic modulus of prestressing steel (ksi).
- ϵ_{cu} = failure strain of concrete in compression (in/in).

8.6.2.2 Biaxial Flexure

For biaxial flexure, the factored structural limit state is taken as:

$$M_r = \phi_f M_n \quad \text{Eq. 8-67}$$

Where:

- M_r = factored resistance in flexure (kip-ft).
- ϕ_f = resistance factor (Table 8-6).
- M_n = nominal resistance in flexure (kip-ft).

Biaxial flexural resistance must satisfy the following checks. Additional information may be found in Article 5.7.4.5 of the AASHTO (2014) specifications.

If $P_u \geq 0.10\phi_c f'_c A_g$:

$$\frac{1}{P_{rxy}} = \frac{1}{P_{rx}} + \frac{1}{P_{ry}} - \frac{1}{\phi P_o} \leq 1.0 \quad \text{Eq. 8-68}$$

In which:

$$P_n = 0.85 f'_c (A_g - A_{str} - A_{ps}) + F_{yr} A_{str} - A_{ps} (f_{pe} - E_{st} \epsilon_{cu}) \quad \text{Eq. 8-69}$$

If $P_u < 0.10\phi_c f'_c A_g$:

$$\left(\frac{M_{ux}}{M_{rx}} + \frac{M_{uy}}{M_{ry}} \right) \leq 1.0 \quad \text{Eq. 8-70}$$

Where:

- P_u = factored axial load.
- P_{rx} = factored resistance in axial compression determined on the basis that only eccentricity, e_y , is present (kips).
- P_{ry} = factored resistance in axial compression determined on the basis that only eccentricity, e_x , is present (kips).
- P_{rxy} = factored resistance axial compression with biaxial flexure (kips).
- M_{ux} = factored moment about x-axis (kip-in).
- M_{rx} = factored resistance in flexure about x-axis (kip-in) (Section 8.5.2.3).
- M_{uy} = factored moment about y-axis (kip-in).
- M_{ry} = factored resistance in flexure about y-axis (kip-in) (Section 8.5.2.3).
- ϕ_c = resistance factor for axial compression (Table 8-6).

- f'_c = concrete compression strength at 28 days, unless otherwise specified (ksi).
- f_{pe} = effective stress in the prestressing steel after losses (ksi).
- F_{yr} = yield stress of reinforcing steel (ksi).
- A_g = gross cross-sectional area (in²).
- A_{str} = cross sectional area of longitudinal reinforcing steel (in²).
- A_{ps} = cross sectional area of prestressing steel (in²).
- E_p = elastic modulus of prestressing steel (in²).
- ϵ_{cu} = failure strain of concrete in compression (in²).

The analysis of the prestressed concrete section response to a combination of an axial load and two orthogonal moments is complex. A successful and practical approach to the analysis of the pile cross section is offered by the FB-Pier Program. The concrete and the prestressing steel stress strain relationships are assumed. For concrete, the FB-Pier program assumes a maximum concrete strength of $0.85f'_c$ to include loading time effects on the concrete strength and all points on the stress strain curve are reduced to 85 percent of the short time values.

Bi-axial interaction diagrams are determined for each of an increasing set of axial loads up to the maximum axial strength condition. An illustration of one of these interaction diagrams for a particular axial load is shown in Figure 8-5. These diagrams are determined for the entire range of axial loads up to the axial failure case. With increasing axial load the maximum moment strength becomes smaller. A three dimensional interaction diagram can then be constructed with the axial load on the vertical axis and a particular interaction diagram at each level of axial load. Imagine a stack of these interaction diagrams. Thus, a three dimensional failure surface is defined. The equation of the failure surface can be generated by fitting a surface through the interaction diagrams at each level.

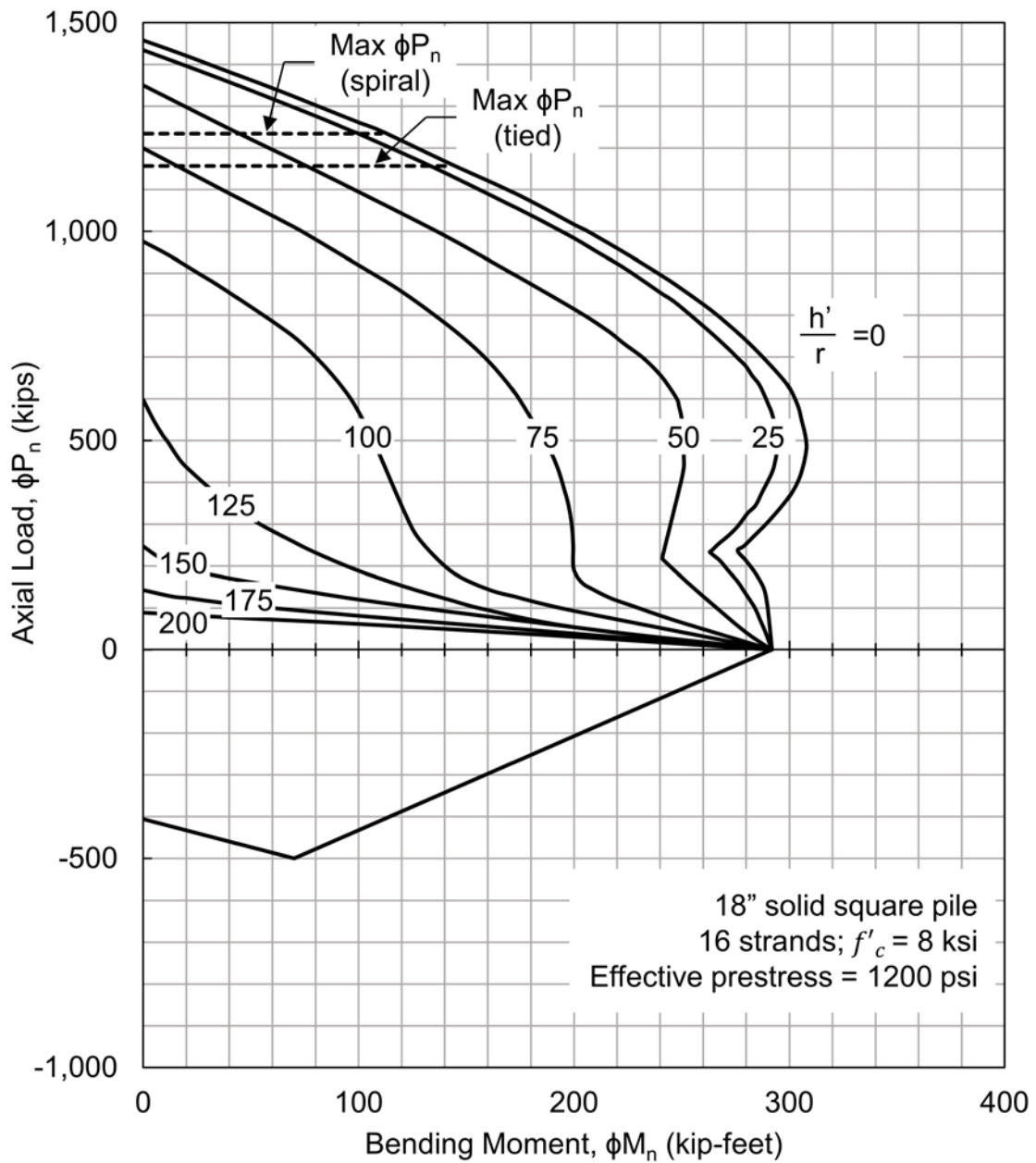


Figure 8-5 Moment interaction diagram.

When the necessary failure surfaces are available, the analysis at a particular load level can be checked by examining whether the vector of the forces on the section (axial, M_x and M_y) falls within or outside the failure envelope. The deformations associated with the three applied forces make it possible to determine the displacements associated with the various load levels. This elegant and powerful

analysis algorithm produces excellent results. Well-designed graphics make it possible for the foundation specialist to easily evaluate the results.

The analysis has been discussed for prestressed concrete piles and they are probably the most challenging to deal with. FB-Pier can also analyze steel piles and concrete filled pipes using the same concepts described above.

8.7 COMPOSITE PILES

Composite piles for structural applications shall be defined as concrete filled steel pipe piles. Guidance for other composite pile types such as a concrete pile with an H-pile stinger is not provided for in AASHTO (2014) specifications. Therefore structural resistances over the length of respective pile materials should be evaluated considering the primary section material.

8.7.1 Driving Stress

Concrete filled steel pipe piles are driven unfilled. Therefore, driving stresses for the non-composite steel section should be used and reference should be made to Section 8.5.1, Driving Stresses: Steel Piles.

8.7.2 Structural Resistance

8.7.2.1 Axial Compression

The behavior of composite sections is somewhat different than non-composite members and is therefore evaluated by alternate means. AASHTO (2014) provides evaluation methods to assess the strength limit state of composite sections, provided the following criteria are met.

1. The cross-sectional area of steel is at least 4 percent of the total cross-sectional area. If the cross sectional area of steel is less than this limit, the pile is considered non-composite and should be evaluated following procedures in Section 8.6 Concrete Piles.
2. The concrete compression strength is between 3.0 ksi and 8.0 ksi. Commentary provided in AASHTO (2014) notes the lower limit is imposed to encourage use of good quality concrete.

3. The yield strength of longitudinal reinforcement to determine the compression resistance cannot exceed 60.0 ksi.

For axial compression loading of concrete filled steel pipes, the factored structural limit state is taken as:

$$P_r = \phi P_n \quad \text{Eq. 8-71}$$

Where:

- P_r = factored resistance in axial compression (kips).
 ϕ = resistance factor (Table 8-6).
 P_n = nominal resistance in axial compression (kips).

STEP BY STEP PROCEDURE FOR: "NOMINAL COMPRESSION RESISTANCE"

STEP 1 Determine the normalized column slenderness factor, λ .

The normalized column slenderness factor is be evaluated using the following equation. However, if the pile is fully embedded, λ may be taken as 0 (AASHTO 2014).

$$\lambda = \left(\frac{Kl}{\pi r_s} \right)^2 \left(\frac{F_e}{E_e} \right) \quad \text{Eq. 8-72}$$

In which:

$$F_e = F_y + C_1 F_{yr} \left(\frac{A_{str}}{A_{st}} \right) + C_2 f'_c \left(\frac{A_c}{A_{st}} \right) \quad \text{Eq. 8-73}$$

$$E_e = E_{st} \left[1 + \left(\frac{C_3}{n} \right) \left(\frac{A_c}{A_{st}} \right) \right] \quad \text{Eq. 8-74}$$

$$n = \frac{E_{st}}{E_c} \quad \text{Eq. 8-75}$$

Where:

- λ = normalized column slenderness factor.
 A_{st} = cross sectional area of steel (in²).
 A_c = cross sectional area of concrete (in²).
 A_{str} = cross sectional area of longitudinal reinforcing steel (in²).
 K = effective length factor (Figure 8-4).
 l = unbraced length in the plane of buckling (inches).
 r_s = radius of gyration about axis normal to plane of buckling (inches).

- F_e = nominal compression resistance of composite section (ksi).
- F_y = yield stress of steel (Table 8-1) (ksi).
- F_{yr} = yield stress of reinforcing steel (ksi).
- f'_c = concrete compression strength at 28 days, unless otherwise specified (ksi).
- E_e = modified elastic modulus of steel for composite column (ksi).
- E_{st} = elastic modulus of steel (ksi).
- E_c = elastic modulus of concrete (Equation 8-1) (ksi).
- C_1 = composite column constant 1 (1.00 for concrete filled pipes).
- C_2 = composite column constant 2 (0.85 for concrete filled pipes).
- C_3 = composite column constant 3 (0.40 for concrete filled pipes).

STEP 2 Determine the nominal resistance in axial compression, P_n .

After determining the normalized column slenderness ratio, a relatively straightforward calculation of the nominal resistance in axial compression is made using either Equation 8-73 or Equation 8-74.

If $\lambda \leq 2.25$:

$$P_n = 0.66^\lambda F_e A_{st} \quad \text{Eq. 8-76}$$

If $\lambda > 2.25$:

$$P_n = \frac{0.88 F_e A_{st}}{\lambda} \quad \text{Eq. 8-77}$$

Where:

- λ = normalized column slenderness factor.
- P_n = nominal resistance in axial compression (kips).
- A_{st} = cross sectional area of steel (in²).
- F_e = nominal resistance in axial compression of composite section (ksi).

8.8 LAYOUT OF PILE GROUPS

A group of piles is typically required to support large structural loads. An initial group layout must be determined to perform in-service stress checks. The possible loads are illustrated in Figure 8-6. The various load combinations, as given in Article 3.4 of the 2014 AASHTO Standard Specification, should be investigated to determine the pile stress conditions. Pile group layouts can be determined through the use of computer software such as GROUP or FB-Pier, which utilize soil structure interaction (t-z and p-y curves) to distribute loads and deflections throughout the pile group. Alternatively, a hand calculation for the Rigid Cap Method may be performed as follows.

STEP BY STEP PROCEDURE FOR: "LAYOUT OF PILE GROUPS"

STEP 1 Estimate the number of piles required to resist structural loads.

An initial, or trial, group layout may be computed by dividing the factored axial load acting on the pile cap/group by the factored geotechnical resistance of a single pile, and then rounding the number up (say, by 15% or more, depending upon magnitude of the moments and lateral loads) to a constructible pile layout. Therefore, the number of piles is estimated as:

$$\frac{P_u}{R_r} \cong n \rightarrow (\text{number of piles, round up}) \quad \text{Eq. 8-78}$$

Where:

- P_u = largest factored, axial load of the superstructure (kips).
- R_r = factored resistance of a single pile (geotechnical) (kips).
- n = number of piles in pile group.

Please note however that for many highway structures, lateral or tension loading may govern the design. Although the Equation 8-78 provides a preliminary guide to estimate the number of piles for axial compression loads, additional piles may be required to resist other loads and limit deflection.

STEP 2 Generate trial pile group configuration.

A trial configuration for the group of piles should be developed with n -piles. Minimum center-to-center pile spacing requirements by AASHTO (2014) specifications is the lesser of 2.5 feet or 2.5 pile diameters. However, as

recommended in the previous edition of this manual, experience with pile group loading and efficiency has shown that 3.0 pile diameters is a more practical pile spacing minimum. Example pile group layouts can be found in CRSI Design Handbook (2002) and other sources.

STEP 3 Determine the maximum single pile axial load.

The trial group configuration consisting of n -piles should be checked for adequate single pile axial resistance under the combined superstructure/substructure axial loads and moments. The various factored load combinations, and not just the combination with the largest axial load, should be checked to determine the critical loading case. If the stiffness of all piles in the group are equal, then the maximum single pile factored axial load, P_{ui} , may be computed with the rigid cap method as:

$$P_{ui} = \frac{P_{uz} + W_c + W_s}{n} + \frac{M_{ux}y}{\sum y^2} + \frac{M_{uy}x}{\sum x^2} \quad \text{Eq. 8-79}$$

Where:

- P_{ui} = maximum single pile factored axial load (kips).
- P_{uz} = factored axial load from superstructure/substructure acting upon pile cap (kips).
- W_c = estimated weight of pile cap (kips).
- W_s = estimated weight of soil above pile cap, if applicable (kips).
- n = number of piles in pile group.
- M_{ux} = factored moment about the x axis acting on the pile cap (kip-ft).
- M_{uy} = factored moment about the y axis acting on the pile cap (kip-ft).
- x = distance along x-axis from the center of the column to each pile center (feet).
- y = distance along y-axis from the center of the column to each pile center (feet).

If the maximum single pile factored axial load exceeds the pile factored structural resistance, add one, or more, piles to the group or increase the pile spacing if $P_{ui} > P_{uz}$ and recompute the maximum single pile factored axial load (P_{ui}). If the moments in one direction are substantially larger than the other, it may be desirable to make the cap unsymmetrical.

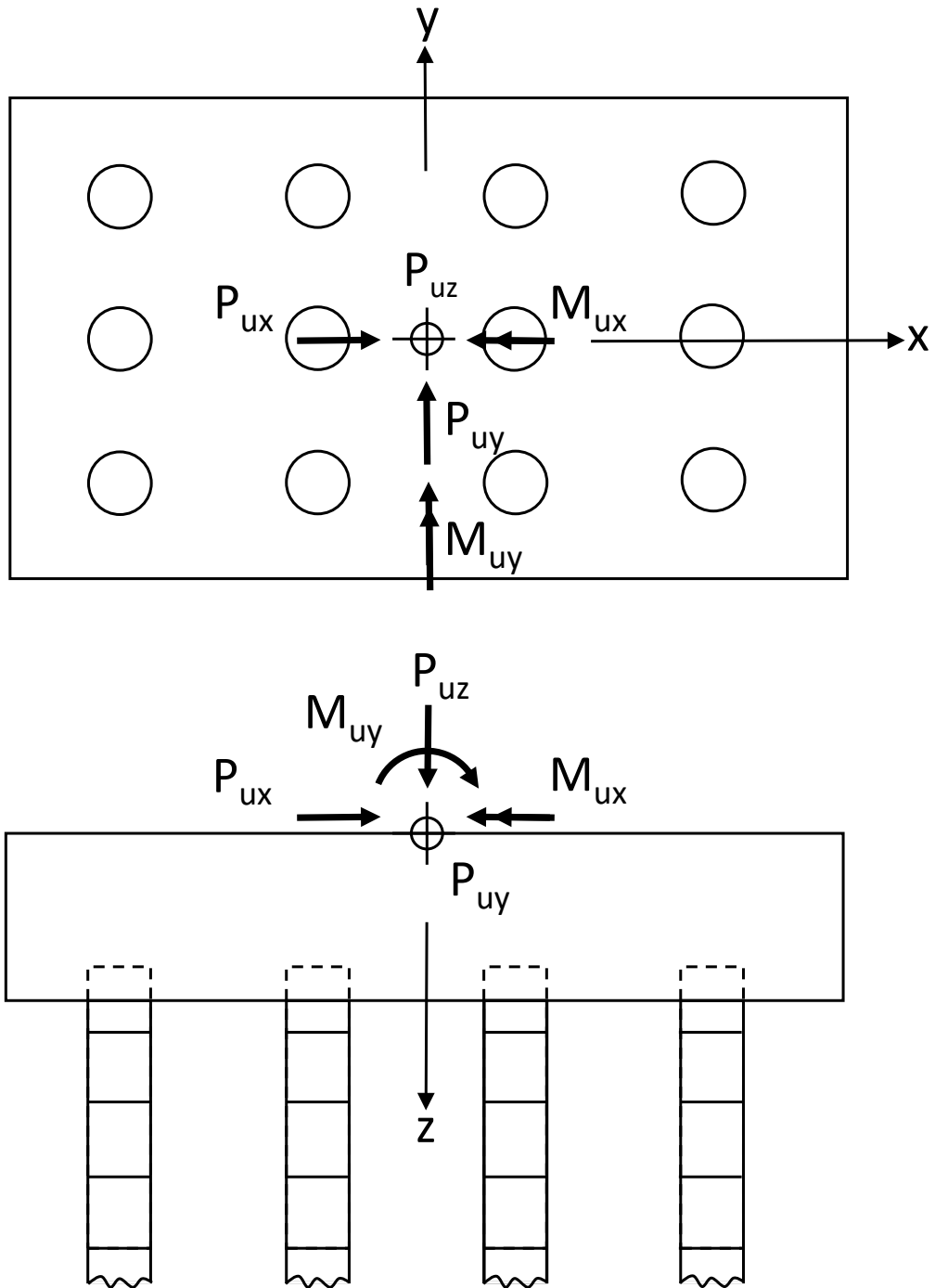


Figure 8-6 Pile group layout.
 (Note: Column supported on pile cap not shown for clarity)

8.9 PRELIMINARY DESIGN OF PILE BENT AND GROUP CAPS

The purpose of this section is to provide guidelines to develop a preliminary size of a pile cap for the purposes of cost estimating. Information for complete, comprehensive structural design, including design for seismic and other extreme events, is beyond the scope of this manual, and not presented herein.

A state-of-the-practice manual on pile cap design was recently published by the Concrete Reinforcing Steel Institute (CRSI). This manual, "Design Guide for Pile Caps" (Mays 2015), was developed to provide the practicing engineer with a detailed overview of pile cap design, analysis methods, and detailing. It follows the American Concrete Institute ACI-14: Building Code Requirements for Structural Concrete and Commentary (ACI 2014) and covers piles with nominal loads up to 400 tons. Design procedure for vertical, lateral/overturning, and seismic loading is presented. Spreadsheets for pile cap design, following ACI-14, are available for download at <http://www.crsi.org/pilecaps.cfm>. This guide and spreadsheets are useful tools to develop a preliminary cap design for detailed analysis following AASHTO (2014).

In bridge design, the LRFD structural design of a concrete pile bent cap is similar to that of structural design for a concrete pier cap (Wilson et al. 2006). However, several design considerations are unique to cap design including: pile embedment into the cap, structural design depth, pile concrete cover requirements, pile misalignment tolerance, concrete pile anchorage, and minimum pile spacing requirements.

The design and size of the pile cap is dependent on the pile group layout, pile loads, and superstructure loads. Thus, an iterative design is required to optimize overall economics. The horizontal dimensions of the pile cap for the trial pile group configuration may be estimated, per AASHTO (2014) Article 10.7.1.2, by using: (i) the minimum center-to-center pile spacing of not less than 30.0 inches or 2.5 pile diameters; and (ii) a minimum edge of cap to side of pile distance of 9 inches. Maximum width and/or length of pile cap may be dictated by project constraints.

The thickness of the pile cap is a sum of the pile embedment into the cap, clear space between the cap reinforcing steel and the top of (embedded) piles, and thickness required for structural support. Per AASHTO (2014) Article 10.7.1.2, the piles shall project at least 12.0 inches into the cap after damaged pile material has been removed. If the piles and cap are attached by embedded bars or strands, this thickness may be reduced to 6.0 inches. The reinforced concrete must be designed with consideration of flexure and shear, for the factored loads. Potential shear

failures include punching about a single pile, punching about a pair of piles, a single pile across the corner of the cap, and punching of the (superstructure) column across the width(s) of the cap.

STEP BY STEP PROCEDURE FOR: "LAYOUT OF PILE GROUPS"

STEP 1 Estimate the total thickness of cap.

An initial, trial total (including pile embedment and 3 inches clear space between top of piles and reinforcing steel) thickness of the pile cap may be estimated from experience, agency guidelines or standards, or with the following equation:

$$t_{cap} = \frac{P_{ui}}{12} + 30 \quad \text{Eq. 8-80}$$

Where:

- t_{cap} = thickness of cap (inches).
- P_{ui} = maximum single pile factored axial load (kips).

This initial, trial thickness should be refined by examining punching shear in the reinforced concrete pile cap. Equations for these preliminary calculation steps are shown below.

STEP 2 Determine dimensions for computations.

1. Determine effective shear depth to concrete reinforcement, d_v . The effective shear depth, d_v , is taken as the distance between the resultants of the tensile and compression forces due to flexure, as illustrated in Figure 8-7, where:

$$d_v = t_{cap} - d_c - d_s - d_f \quad \text{Eq. 8-81}$$

Where:

- d_v = effective depth to reinforcement (inches).
- t_{cap} = thickness of cap (inches).
- d_c = clear space (inches).
- d_s = distance to center of steel (inches).
- d_f = pile embedment into cap (inches).
- h = structural depth, thickness of cap less pile embedment (inches).

The effective shear depth for a regularly reinforced section, per AASHTO (2014) Article 5.8.2.9, need not be taken to be less than the greater of $0.9d_s$ or $0.72h$ (inches). Thus, an assumed value of the effective shear depth, d_v , for preliminary sizing may be taken as the maximum of $0.9d_s$ or $0.72h$ (inches).

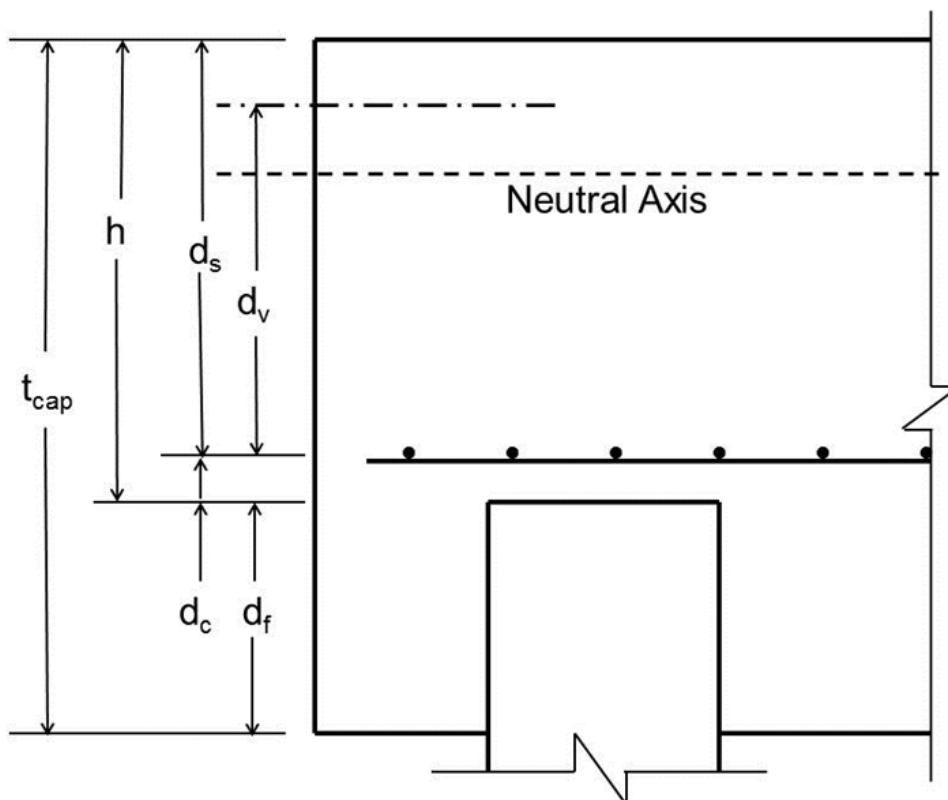


Figure 8-7 Cap section and notation.

2. Determine critical punching shear perimeter, b_o , around the column supported on the pile cap. The shear force applied the shear perimeter is the load acting outside that perimeter.

For square columns:

$$b_o = 4(b_c + d_v) \quad \text{Eq. 8-82}$$

For rectangular columns:

$$b_o = 2(c_1 + c_2 + 2d_v) \quad \text{Eq. 8-83}$$

For circular columns:

$$b_o = c_o + d_v \quad \text{Eq. 8-84}$$

Where:

- b_o = critical punching shear perimeter (inches).
- d_v = effective shear depth (inches).
- b_c = column side for square columns (inches).
- c_1 = small column side for rectangular columns (inches).
- c_2 = large column side for rectangular columns (inches).
- c_o = column diameter (inches).

STEP 3 Check punching (two-way) shear at: (i) at a distance $d/2$ from face of column and at the face of the column, as illustrated in Figure 8-8; and (ii) around individual and pair of piles as illustrated in Figures 8-9 and 8-10.

1. Compute total applied two-way, punching shear stress, V_u , at critical section.

For shear around column:

$$V_u = P_u \quad \text{Eq. 8-85}$$

Where:

- V_u = factored shear force (kips).
- P_u = factored axial load of the superstructure (kips).

For shear around individual or pair of piles:

$$V_u = \gamma_i Q_i = n_i R_r \quad \text{Eq. 8-86}$$

Where:

- V_u = factored shear force (kips).
- R_r = factored (geotechnical) axial resistance of a single pile (kips).
- n_i = number of piles whose centers lie inside the two-way shear critical section.

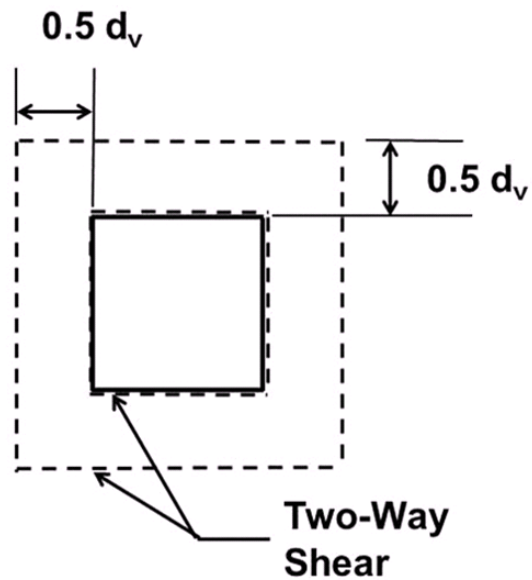


Figure 8-8 Critical punching (two-way) shear sections around column.

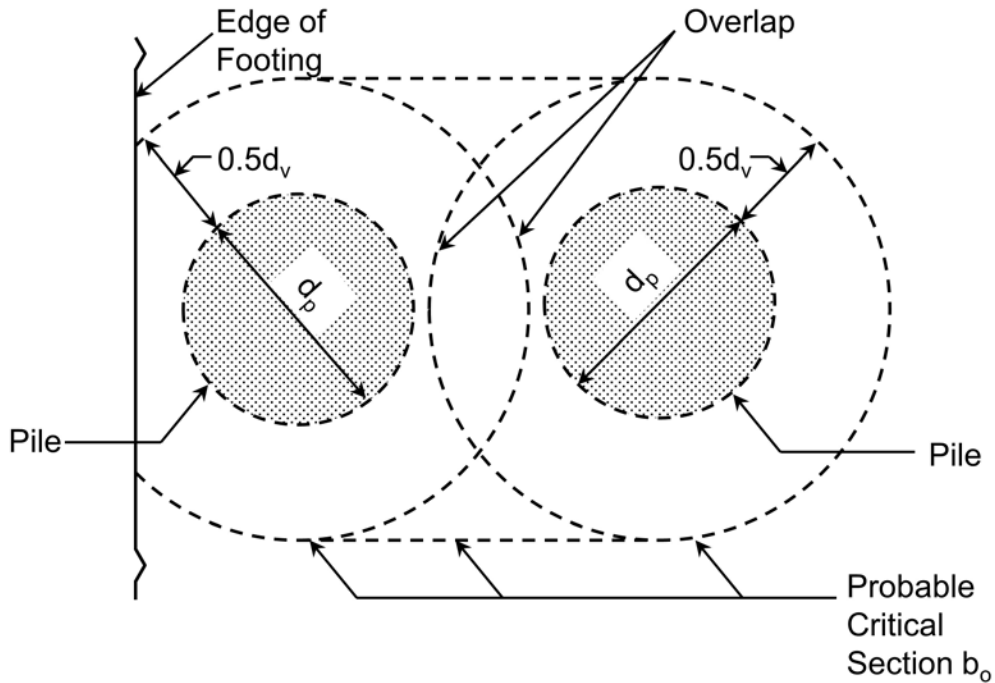


Figure 8-9 Critical section from overlapping critical perimeters (after AASHTO 2014).

2. Determine the nominal shear strength of concrete, per AASHTO Article 5.13.3.6.3, for two way action. Without transverse reinforcement, the nominal resistance is calculated using Equation 8-84. Sections with transverse reinforcement resist shear by means presented in Equation 8-85.

Without Transverse Reinforcement (AASHTO 5.13.3.6.3-1):

$$V_n = \left(0.063 + \frac{0.126}{\beta_c} \right) \sqrt{f'_c} b_o d_v \leq 0.126 \sqrt{f'_c} b_o d_v \quad \text{Eq. 8-87}$$

With Transverse Reinforcement (AASHTO 5.13.3.6.3-2):

$$V_n = V_c + V_s \leq 0.192 \sqrt{f'_c} b_o d_v \quad \text{Eq. 8-88}$$

In which (AASHTO 5.13.3.6.3-3,-4):

$$V_c = 0.0632 \sqrt{f'_c} b_o d_v \quad \text{Eq. 8-89}$$

$$V_s = \frac{A_{stv} F_y d_v}{s} \quad \text{Eq. 8-90}$$

Where:

- V_n = nominal shear resistance (kips).
- V_s = nominal shear resistance provided by steel reinforcement (kips).
- V_c = nominal shear resistance provided by concrete tensile strength (kips).
- β_c = ratio of the long side to the short side of the load.
- f'_c = concrete compression strength at 28 days, unless otherwise specified (ksi).
- F_y = specified yield stress of reinforcement (ksi).
- b_o = critical punching (two-way) shear perimeter (inches).
- d_v = effective shear depth (inches).
- A_{stv} = area of transverse reinforcement within distance, s (in²).
- s = spacing of the transverse reinforcement (inches).

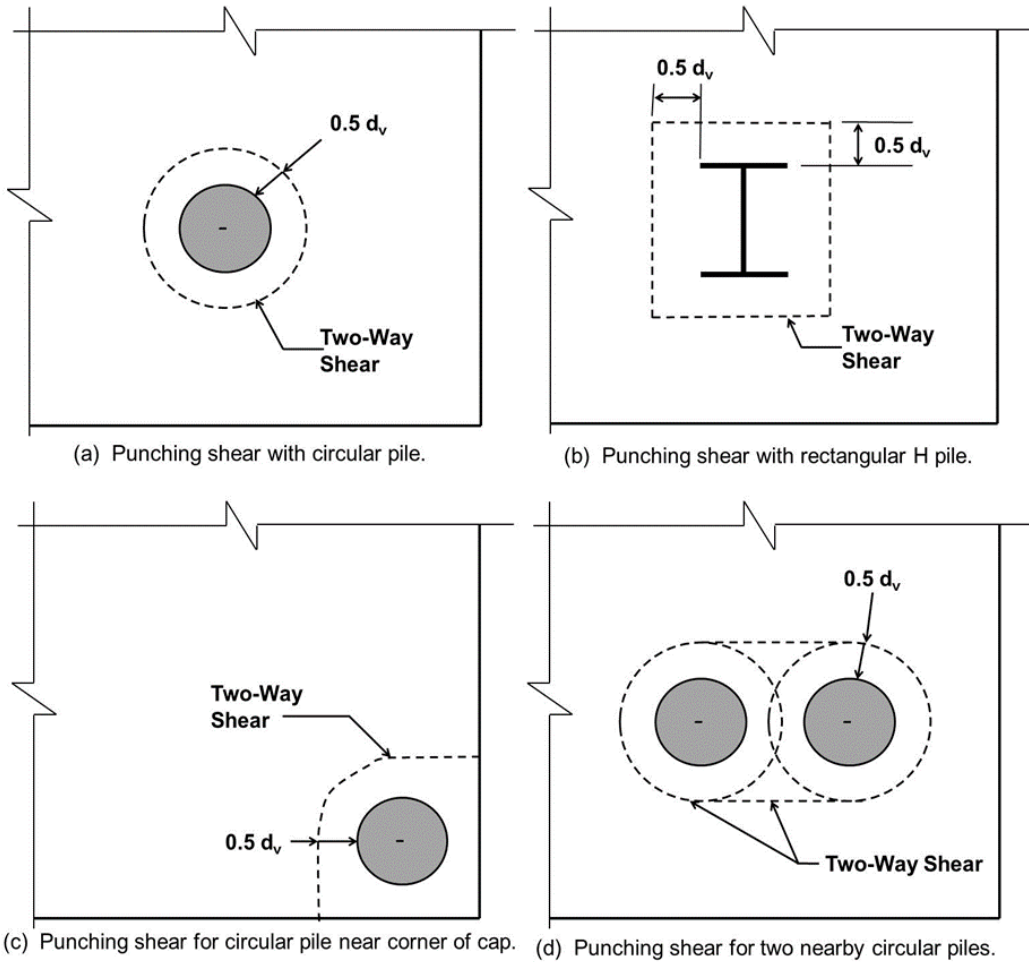


Figure 8-10 Pile punching shear for: (a) circular pile; (b) rectangular H pile; (c) circular pile near corner of cap; and (d) two nearby circular piles.

3. Compute the factored shear resistance from:

$$V_r = \phi_v V_n \quad \text{Eq. 8-91}$$

Where:

- V_r = factored shear resistance (kips).
- ϕ_v = resistance factor (0.9 for normal weight concrete shear).
- V_n = nominal shear resistance (kips).

4. Check that the factored shear resistance is greater than the factored shear load.

$$V_u < V_r \quad \text{Eq. 8-92}$$

Where:

- V_u = factored shear load (kips).
- V_r = factored shear resistance (kips).

If the above condition is not satisfied, increasing shear reinforcement or the effective shear depth should be considered.

STEP 4 Check One-Way Beam Shear, per AASHTO Article 5.13.3.6.2.

1. Compute total applied beam (one-way) shear stress, V_u , at critical sections, per AASHTO (2014) Article 5.8.3.2. Determine the beam shear distance from column to critical section as illustrated in Figure 8-11. Determine beam shear distance from the pile to the critical section(s), as illustrated in Figure 8-12.
2. For each direction of pile cap, check number of piles that lie outside of the critical section. Compute total applied one-way, beam shear stress, V_u , at critical section.

$$V_u = \gamma_i Q_i = n_o R_r \quad \text{Eq. 8-93}$$

Where:

- V_u = factored shear stress (kips).
- R_r = factored nominal resistance of a single pile (geotechnical) (kips).
- n_o = number of piles which lie outside of the one-way critical shear section.

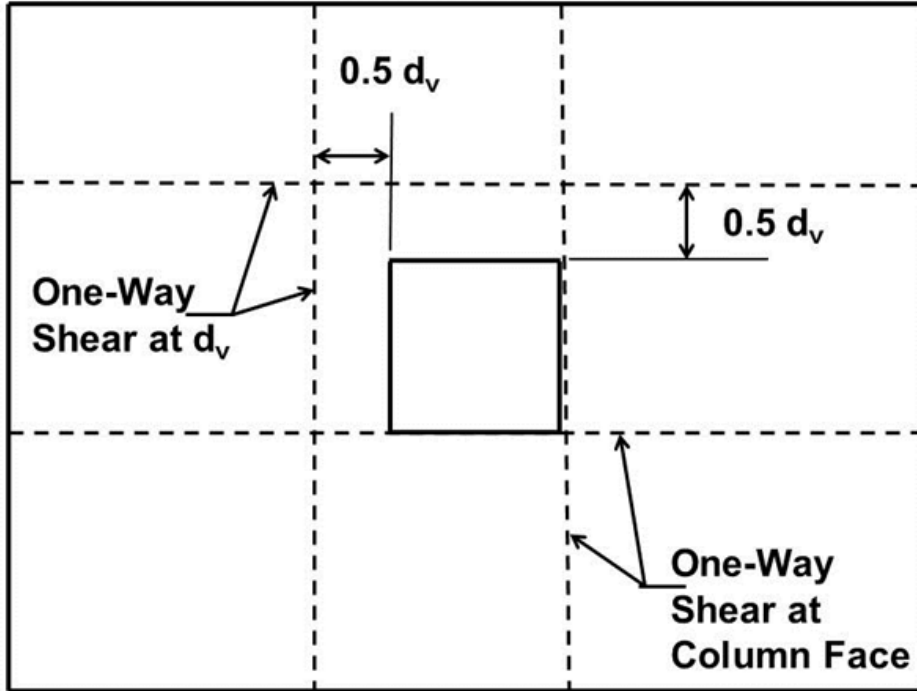


Figure 8-11 One-way beam shear critical sections from column.

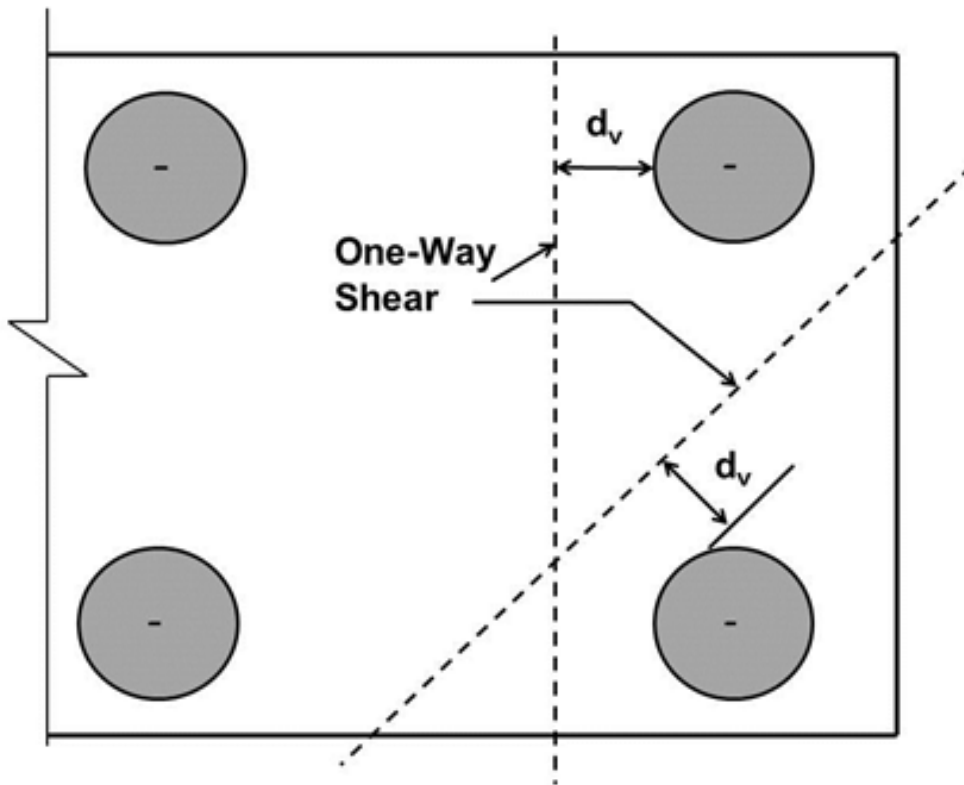


Figure 8-12 One-way beam shear critical sections from pile(s).

3. Determine the nominal shear strength of concrete, per AASHTO Article 5.8.3.3. The nominal shear resistance, V_n , without prestressed reinforcement, is the lesser of Equation 8-91 or 8-92 per AASHTO Article 5.8.3.3-2:

$$V_n = V_c + V_s \quad \text{Eq. 8-94}$$

$$V_n = 0.25 f'_c b_v d_v \quad \text{Eq. 8-95}$$

Where:

- V_n = nominal shear resistance (kips).
- V_s = nominal shear resistance provided by steel reinforcement (kips).
- V_c = nominal shear resistance provided by concrete tensile strength (kips).
- f'_c = concrete compression strength at 28 days, unless otherwise specified (ksi).
- b_v = width of interface (inches).
- d_v = effective depth to reinforcement (inches).

4. Compute the factored shear resistance from:

$$V_r = \phi_v V_n$$

Where:

- V_r = factored shear resistance (kips).
- ϕ_v = resistance factor (0.9 for normal weight concrete shear per AASHTO Article 5.5.4.2.1).
- V_n = nominal shear resistance (kips).

5. Check that the factored shear resistance is greater than the factored shear load.

$$V_u < V_r \quad \text{Eq. 8-96}$$

Where:

- V_u = factored shear force (kips).
- V_r = factored shear resistance (kips)

STEP 5 Check Bending in Cap.

1. Compute factored bending moment, for each direction of pile cap, from piles to edge of column.

$$M_u = \sum R_r(x, y) \leq \phi M_n \quad \text{Eq. 8-97}$$

Where:

- M_u = factored moment load (kip-in).
- R_r = factored (geotechnical) axial resistance of a single pile (kip).
- x, y = distance from edge of column to each pile (in both x and y directions) (inches).
- M_n = nominal flexural resistance (kip-in).
- ϕ = resistance factor (0.9 for normal weight concrete in shear or torsion).

The moment resistance of a reinforced concrete beam is determined based on the assumption of a rectangular distribution of the compression stress in the concrete at failure. The design must fail by yielding the tension steel to assure ductility. The nominal flexural resistance, M_n , for a non-prestressed rectangular section can be computed with the following equation (after AASHTO 5.7.3.2.2-1):

$$M_n = A_{stt} f_{st} \left(d_{st} - \frac{a}{2} \right) - A_{stc} f_{sc} \left(d_{sc} - \frac{a}{2} \right) \quad \text{Eq. 8-98}$$

In which:

$$a = c \beta_1 = \frac{\beta_1 A_s f_s - A'_s f'_s}{\beta_1 0.85 f'_c b} = \frac{A_s f_s - A'_s f'_s}{0.85 f'_c b} \quad \text{Eq. 8-99}$$

Where:

- M_n = nominal flexural resistance (kip-in).
- A_{stt} = area of tension reinforcement (in²).
- f_{st} = stress in the mild steel tension reinforcement at nominal flexural resistance (ksi), as specified in AASHTO Article 5.7.2.1.
- d_{st} = distance from extreme compression fiber to the centroid of the tensile reinforcement (in).
- a = $c \beta_1$, depth of the equivalent stress block (in).
- b = width of the compression face.
- c = distance between the neutral axis and the compression face (in).
- β_1 = stress block factor, which cancels in Equation 8-99.
- A_{stc} = area of compression reinforcement (in²).

- f_{sc} = stress in the mild steel compression reinforcement at nominal flexural resistance (ksi), as specified in AASHTO Article 5.7.2.1.
- d_{sc} = distance from extreme compression fiber to the centroid of the compression reinforcement (in).

The equation for moment strength, M_n , can be solved for the area of steel, A_{st} . However, $a/2$ is small compared with d so an approximate value can be assumed for $a/2$, A_{st} can be calculated and the steel area adjusted to arrive at a satisfactory A_{st} . If $d-a/2$ is assumed to be $0.9d$, A_{st} will be quite close and it will be satisfactory for preliminary design. If an improved A_{st} is desired it can be obtained made by determining an improved a with knowledge of the preliminary A_{st} and with the new a the next cycle of A_{st} can be determined and it will probably be final.

Per AASHTO Article 5.7.3.3.2, the tensile reinforcement should be adequate to develop a factored flexural resistance, M_r of at least 1.33 times the factored moment. See Article 5.7.3.3.2 for more details.

The final, structural design of pile caps is beyond the scope of this manual. See AASHTO (2014), ACI (2014), etc. for guidance on detailed structural design.

8.9.1 Cap Considerations for Large Pile Sizes

For Large Diameter Open-Ended Piles (LDOEPs), general analysis steps in the above section should be followed. No strict guidance can be offered at this time regarding minimum spacing and embedment into the pier cap, specifically for large pile sizes. Case studies presented in Brown and Thompson (2014) present few details on this subject as most state agencies do not currently have standard plans for these pile sizes. Pile tops were however embedded further into the cap, than with smaller pile sections. This was on the order of 3 feet into the pier cap for LDOEPs.

Pile spacing considerations should reflect guidelines proposed for drilled shafts due to the comparable element diameter. The presented pile plan layout in Brown and Thompson (2014) shows a minimum pile spacing on the order of 3 pile diameters (center to center), which is consistent with typical drilled shaft group layouts (Brown et al. 2010).

REFERENCES

- American Association of State Highway and Transportation Officials (AASHTO). (2014). AASHTO LRFD Bridge Design Specifications, US Customary Units, Seventh Edition, with 2015 Interim Revisions. American Association of State Highway and Transportation Officials, Washington, D.C., 1960 p.
- American Institute of Steel Construction (AISC). (2011). Steel Construction Manual, Fourteen Edition, (Third Printing). American Institute of Steel Construction Chicago, IL, 2192 p.
- American Concrete Institute (ACI) (2014). Building Code Requirements for Structural Concrete and Commentary, ACI 318-14. Farmington Hills, MI, 520 p.
- Bethlehem Steel Corporation. (1970). Steel H Piles, Handbook 2196-B. Bethlehem Steel Corporation, Bethlehem, PA, 64 p.
- Brown, D. A., Turner, J.P. and Castelli R.J. (2010). Drilled Shafts: Construction Procedures and LRFD Design Methods, FHWA-NHI-10-016. Geotechnical Engineering Circular (GEC) No. 10, U.S. Dept. of Transportation, Federal Highway Administration (FHWA), Washington D.C., 970 p.
- Brown, D.A., and Thompson III, W.R. (2015). Current Practices for Design and Load Testing of Large Diameter Open-End Driven Pipe Piles. Final Report. NCHRP Report 20-05, Topic 45-05, National Cooperative Highway Research Program, (NCHRP) Washington, D.C., 175 p.
- Coduto, D P., and Kitch, W.A., and Yeung, M.R. (2016). Foundation Design: Principles and Practices, Third Edition. Pearson Education, Upper Saddle River, NJ:, 686 p.
- Davisson, M.T. (1963). Estimating Buckling Loads for Piles. Proceedings of the Second Pan-American Conference on Soil Mechanics and Foundation Engineering, Brazil, Vol. 1, pp. 351-371.

- Davisson, M.T. and K.E. Robinson. (1965). Bending and Buckling of Partially Embedded Piles. Proceedings Sixth International Conference on Soil Mechanics and Foundation Engineering, University of Toronto Press. Montreal, Canada, pp. 243-246.
- Mays, T. (2015). Design Guide for Pile Caps, First Edition. Concrete Reinforcing Steel Institute (CSRI), Schaumburg, IL, 152 p.
- Reese, L.C. (1984). Handbook on Design of Piles and Drilled Shafts Under Lateral Load, FHWA-IP-84-11. U.S. Department of Transportation, Federal Highway Administration, Office of Implementation, Washington, D.C., 392 p.
- Rollins, K. and Stenlund, T. (2010). Laterally Loaded Pile Cap Connections. Utah Department of Transportation, Research Division, Report UT-10.16, 133 p.
- Showalter, J. (2012). Round Timber Poles and Piles. Wood Design Focus, Forest Products Society, Vol. 22, No. 4, pp. 14-18.
- Skyline Steel. (2015). Steel H-pile Technical Datasheets. Skyline Steel, <http://www.skylinesteel.com>.
- White, C.D., and Castrodale, R.W. (2004). Precast/Prestressed Concrete Institute Bridge Design Manual – Chapter 20 Precast Prestressed Concrete Piles, MNL 133. Precast/Prestressed Concrete Institute, Chicago, IL, 171 p.
- Wilson, K.E., Kimmerling, R.E., Goble, G.G., Sabatini, P.J., Zang, S.D., Zhou, J.Y., Amrhein, W.A., Bouscher, J.W. and Danaovich, L.J. (2006). LRFD for Highway Bridge Substructures and Earth Retaining Structures Reference Manual, FHWA NHI-05-094. U.S. Dept. of Transportation, Federal Highway Administration (FHWA), Washington, D.C., 1730 p.

APPENDIX A

LIST OF FHWA/ NHI RESOURCES RELEVANT TO DEEP FOUNDATIONS

- Abu-Hejleh, N., DiMaggio, J.A., Kramer, W.M., Anderson, S., and Nichols, S. (2010). Implementation of LRFD Geotechnical Design for Bridge Foundations: Reference Manual. FHWA-NHI-10-039. National Highway Institute, Federal Highway Administration, Washington, D.C.
- Abu-Hejleh, N., Kramer, W.M., Mohamed, K., Long, J.H., and Zaheer, M.A. (2013). Implementation of AASHTO LRFD Design Specifications for Driven Piles, FHWA-RC-13-001. U.S. Dept. of Transportation, Federal Highway Administration, 71 p.
- Arneson, L.A., Zevenbergen, L.W., Lagasse, P.F., and Clopper, P.E. (2012). Evaluating Scour at Bridges, Fifth Edition, FHWA-HIF-12-003, Hydraulic Engineering Circular (HEC) No. 18. U.S. Dept. of Transportation, Federal Highway Administration, 340 p.
- Aziznamini, A., Power, E.H., Myers, G.F., and Ozyildirim, H.C. (2014). Bridges for Service Life Beyond 100 Years, Innovative Systems Subsystems, and Components, S2-R19A-RW-1 Strategic Highway Research Program 2 (SHRP), Transportation Research Board, Washington, D.C., 248 p.
- Briaud J-L. and Miran, J. (1992). The Cone Penetration Test, FHWA-SA-91-043. U.S. Department of Transportation, Federal Highway Administration, Office of Technology Applications, Washington, D.C., 161 p.
- Brown, D.A., and Thompson, W.R. (2011). Developing Production Pile Criteria from Test Pile Data. National Cooperative Highway Research Program (NCHRP) Synthesis 418, Washington, D.C., 54 p.
- Brown, D. A., Turner, J.P. and Castelli R.J. (2010). Drilled Shafts: Construction Procedures and LRFD Design Methods, FHWA-NHI-10-016, Geotechnical Engineering Circular (GEC) No. 10. U.S. Dept. of Transportation, Federal Highway Administration, 970 p.

- Brown, D.A., Dapp, S.D., Thompson, W.R., and Lazarte, C.A. (2007). Design and Construction of Continuous Flight Auger (CFA) Piles. FHWA-HIF-07-03, Geotechnical Engineering Circular (GEC) No.08. U.S. Dept. of Transportation, Federal Highway Administration, 289 p.
- Cheney, R.S. and Chassie, R.G. (2000). Soils and Foundations Workshop Reference Manual. FHWA HI-00-045, U.S. Department of Transportation, National Highway Institute, Federal Highway Administration, Washington, D.C., 358 p.
- Elias, V., Welsh, J.P., Warren, J., Lukas, R.G., Collin J.G., and Berg, R.R. (2006). Ground Improvement Methods Volumes I and II, FHWA-NHI-06-019 and FHWA NHI-06-020. National Highway Institute, Federal Highway Administration, U.S. Department of Transportation, Washington D.C.
- Federal Highway Administration (FHWA). (1996). Geotechnical Engineering Notebook DT-15. Differing Site Conditions. U.S. Dept. of Transportation, Federal Highway Administration, Washington, D.C. 36 p.
- Federal Highway Administration (FHWA). (2002a). Life-Cycle Cost Analysis Primer, IF-02-047. Federal Highway Administration, U.S. Department of Transportation. Washington, D.C., 24 p.
- Geotechnical Guideline 13 (1985). Geotechnical Engineering Notebook, U.S. Department of Transportation. Federal Highway Administration, Washington, D.C., 37 p.
- Ghosn, M., Moses, F., and Wang, J. (2003). Design of Highway Bridges for Extreme Events, NCHRP Report 489. National Cooperative Highway Research Program. Transportation Research Board, Washington, D.C., 174 p.
- Goble, G.G. and Rausche, F. (1976). Wave Equation Analysis of Pile Driving – WEAP Program, FHWA IP-76-14.3., U.S. Department of Transportation, Federal Highway Administration, Office of Research and Development, Washington, D.C., Volumes I-IV.
- Goble, G.G. and Rausche, F. (1986). Wave Equation Analysis of Pile Driving - WEAP86 Program. U.S. Department of Transportation, Federal Highway Administration, Implementation Division, McLean, Volumes I-IV.

- Hawk, H. (2003). Bridge Life-Cycle Cost Analysis, NCHRP483. Transportation Research Board of the National Academies, Washington, D.C. 96 p.
- Kavazanjian, E., Wan, J-N. J., Martin, G.R., Shamsabadi, A., Lam, I., Dickenson, S.E., and Hung, C.J. (2011). LRFD Seismic Analysis and Design of Transportation Geotechnical Features and Structural Foundations, FHWA-NHI-11-032, Geotechnical Engineering Circular (GEC) No. 3. U.S. Dept. of Transportation, Federal Highway Administration, Washington, D.C., 592 p.
- Kimmerling, R.E. (2002). Shallow Foundations, FHWA-IF-02-054, Geotechnical Engineering Circular (GEC) No. 6. U.S. Dept. of Transportation, Federal Highway Administration, Washington, D.C., 310 p.
- Kyfor, Z.G., Schnore, A.R., Carlo, T.A., and Bailey, P.F. (1992). Static Testing of Deep Foundations, FHWA-SA-91-042. U.S. Department of Transportation, Federal Highway Administration, Office of Technology Applications, Washington, D.C., 174 p.
- Lam, I.P. and Martin, G.R. (1986). Seismic Design of Highway Bridge Foundations. Volume II - Design Procedures and Guidelines, FHWA-RD-86-102. U.S. Department of Transportation, Federal Highway Administration, Office of Engineering and Highway Operations, McLean, VA, 167p.
- Long, J., and Anderson, A. (2014). Improved of Driven Pile Installation and Design in Illinois: Phase 2, FHWA-ICT-14-019. Illinois Department of Transportation, Bureau of Material and Physical Research, Springfield, IL, 84 p.
- Marsh, M.L., Buckle, I.G., and Kavazanjian Jr, E. (2014). LRFD Seismic Analysis and Design of Bridges, FHWA-NHI-15-004. National Highway Institute, U.S. Dept. of Transportation, Federal Highway Administration, Washington, D.C., 608 p.
- Mayne, P.W., Christopher, B., Berg, R., and DeJong, J. (2001). Manual on Subsurface Investigations, FHWA NHI-01-031, U.S. Dept. of Transportation, National Highway Institute, Federal Highway Administration, Washington, D.C., 301 p.
- Munfakh, G., Arman, A., Collin, J.G., Hung, J.C.-J., and Brouillette, R.P. (2001). Shallow Foundations Reference Manual, FHWA-NHI-01-023. National Highway Institute, Federal Highway Administration, Washington, D.C., 222 p.

- Rausche, F., Likins, G.E., Goble, G.G., Hussien, M. (1986). The Performance of Pile Driving Systems; Inspector's Manual. U.S. Department of Transportation, Federal Highway Administration, Washington, D.C., 92 p.
- Rausche, F., Thendean, G., Abou-matar, H., Likins, G.E. and Goble, G.G. (1996). Determination of Pile Drivability and Capacity from Penetration Tests, DTFH61-91-C-00047, Final Report. U.S. Department of Transportation, Federal Highway Administration, McLean, VA, 432 p.
- Reese, L.C. (1984). Handbook on Design of Piles and Drilled Shafts Under Lateral Load. Report No. FHWA-IP-84-11, U.S. Department of Transportation, Federal Highway Administration, Office of Implementation, McLean, VA, 386 p.
- Reese, L.C. (1986). Behavior of Piles and Pile Groups Under Lateral Load, FHWA-RD-85-106. U.S. Department of Transportation, Federal Highway Administration, Office of Engineering and Highway Operations Research and Development, Washington, D.C., 311 p.
- Rixner, J.J., Kraemer, S.R. and Smith, A.D. (1986). Prefabricated Vertical Drains Volume I, Engineering Guidelines, FHWA-RD-86-168. U.S. Department of Transportation, Federal Highway Administration, Office of Engineering and Highway Operations Research and Development, McLean, VA, 117 p.
- Sabatini, P. J., Elias, V., Schmertmann, G. R., and Bonaparte, R. (1997). Earth Retaining Systems FHWA-SA-96-038, Geotechnical Engineering Circular (GEC) No. 2. U.S. Department of Transportation, Federal Highway Administration, Washington, D.C., 161 p.
- Sabatini, P.J., Tanyu, B., Armour., P., Groneck, P., and Keeley, J. (2005). Micropile Design and Construction, FHWA-NHI-05-039. National Highway Institute, U.S. Dept. of Transportation, Federal Highway Administration, Washington, D.C., 436 p.
- Samtani, N.C. and Nowatzki, E.A. (2006). Soils and Foundations: Reference Manual, Vol. 1, FHWA-NHI-06-088, U.S. Dept. of Transportation, National Highway Institute, Federal Highway Administration, Washington, D.C., 462 p.

- Samtani, N.C., Nowatzki, E.A., and Mertz, D.R. (2010). Selection of Spread Footings on Soils to Support Highway Bridge Structures, FHWA-RC TD-10-001. U.S. Department of Transportation, Federal Highway Administration, Washington, D.C., 98 p.
- Schmertmann, J.H. (1978). Guidelines For Cone Penetration Test, Performance, and Design, FHWA-TS-78-209. U.S. Department of Transportation, Federal Highway Administration, Washington, D.C., 145 p.
- Tanyu B.F., Sabatini, P. J., and Berg, R.R. (2008). Earth Retaining Structures, FHWA-NHI-07-07. U.S. Department of Transportation, Federal Highway Administration, Washington, D.C., 792 p.
- Wightman, W., Jalinoos, F., Sirles., and Hanna, K. (2003), Applications of Geophysical Methods to Related Highway Problems. U.S. Dept. of Transportation, Federal Highway Administration (FHWA), Washington D.C., 716 p.
- Wilson, K.E., Kimmerling, R.E., Goble, G.C., Sabatini, P.J., Zang, S.D., Zhou, J.Y. Amrhein, W.A., Bouscher, J.W. and Danaovich, L.J. (2006). LRFD for Highway Bridge Substructures and Earth Retaining Structures Reference Manual, FHWA NHI-05-094. U.S. Dept. of Transportation, Federal Highway Administration, Washington, D.C., 1730 p.

Appendix B

LIST OF ASTM AND AASHTO PILE DESIGN AND TESTING SPECIFICATIONS

- American Association of State Highway and Transportation Offices (AASHTO).
Standard Method of Test for High Strain Dynamic Testing of Piles, AASHTO
Designation T-298-33.
- American Association of State Highway and Transportation Officials (AASHTO).
(1978). Manual on Foundation Investigations Second Edition.. AASHTO
Highway Subcommittee on Bridges and Structures, Washington, D.C., 196 p.
- American Association of State Highway and Transportation Officials (AASHTO).
(2001). Standard Recommended Practice for Assessment of Corrosion of
Steel Piling for Non-Marine Applications. AASHTO Standard Specifications
for Transportation Materials and Methods of Sampling and Testing, Part 1B:
Specifications, 24th Edition, 13 p.
- American Association of State Highway and Transportation Officials (AASHTO).
(2011) Guide Specifications for LRFD Seismic Bridge Design, 2nd Edition,
with 2012, 2014, and 2015 Interim Revisions. American Association of State
Highway and Transportation Officials, Washington, D.C., 331 p.
- American Association of State Highway and Transportation Officials (AASHTO).
(2014). AASHTO LRFD Bridge Design Specifications, US Customary Units,
Seventh Edition, with 2015 Interim Revisions. American Association of State
Highway and Transportation Officials, Washington, D.C., 1960 p.
- ASTM A27-13. (2014). Standard Specification for Steel Castings, Carbon, for
General Application. Book of ASTM Standards, Vol. 1.02, ASTM International,
West Conshohocken, PA, 4 p.
- ASTM A572-15. (2015). Standard Specification for High-Strength Low-Alloy
Columbium-Vanadium Structural Steel. Book of ASTM Standards, Vol. 1.04,
ASTM International, West Conshohocken, PA, 4 p.

- ASTM D1143-07. (2014). Standard Test Methods for Deep Foundations Under Static Axial Compressive Load. Book of ASTM Standards, Vol. 4.08, ASTM International, West Conshohocken, PA, 15 p.
- ASTM D1452-09. (2014). Standard Practice for Soil Exploration and Sampling by Auger Borings. Annual Book of ASTM Standards, Vol. 4.08, ASTM International, West Conshohocken, PA, 6 p.
- ASTM D1586-11. (2014). Standard Test Method for Standard Penetration Test (SPT) and Split-Barrel Sampling of Soils. Annual Book of ASTM Standards, Vol. 4.08, ASTM International, West Conshohocken, PA, 9 p.
- ASTM D1587-12. (2014). Standard Practice for Thin-Walled Tube Sampling of Soils for Geotechnical Purposes. Annual Book of ASTM Standards, Vol. 4.08, ASTM International, West Conshohocken, PA, 4 p.
- ASTM D2113-14. (2014). Standard Practice for Rock Core Drilling and Sampling of Rock for Site Investigation. Annual Book of ASTM Standards, Vol. 4.08, ASTM International, West Conshohocken, PA, 20 p.
- ASTM D2573-08. (2012). Standard Test Method for Field Vane Shear Test in Cohesive Soil. Annual Book of ASTM Standards, Vol. 4.08, ASTM International, West Conshohocken, PA, 8 p.
- ASTM D3689-07. (2014). Standard Test Methods for Deep Foundations Under Static Axial Tensile Load. Book of ASTM Standards, Vol. 4.08, ASTM International, West Conshohocken, PA, 13 p.
- ASTM D4633-10. (2014). Standard Test Method for Energy Measurement for Dynamic Penetrometer. Book of ASTM Standards, Vol. 4.08, ASTM International, West Conshohocken, PA, 7 p.
- ASTM D4719-07. (2014). Standard Test Methods for Prebored Pressuremeter Testing in Soils Annual. Book of ASTM Standards, Vol. 4.08, ASTM International, West Conshohocken, PA, 10 p.
- ASTM D4945-12. (2014). Standard Test Method for High-Strain Dynamic Testing of Piles. Book of ASTM Standards, Vol. 4.08, ASTM International, West Conshohocken, PA, 9 p.

- ASTM D4971-02. (2014). Standard Test Method for Determining the In Situ Modulus of Deformation of Rock Using the Diametrically Loaded 76-mm (3-in.) Borehole Jack. Book of ASTM Standards, Vol. 4.08, ASTM International, West Conshohocken, PA, 7 p.
- ASTM D5778-12. (2014). Standard Test Method for Electronic Friction Cone and Piezocone Penetration Testing of Soils. Book of ASTM Standards, Vol. 4.08, ASTM International, West Conshohocken, PA, 20 p.
- ASTM D5882-07. (2013). Standard Test Method for Low-Strain Dynamic Testing of Piles Annual Book of ASTM Standards, Vol. 4.09, ASTM International, West Conshohocken, PA, 6 p.
- ASTM D6032-08. (2014). Standard Test Method for Determining Rock Quality Designation (RQD) of Rock Core. Annual Book of ASTM Standards, Vol. 4.09, ASTM International, West Conshohocken, PA, 5 p.
- ASTM D6635-07. (2014). Standard Test Method for Performing the Flat Dilatometer. Book of ASTM Standards, Vol. 4.09, ASTM International, West Conshohocken, PA, 16 p.
- ASTM D7012-14. (2014). Standard Tests Method for Compressive Strength and Elastic Moduli of Intact Rock Core Specimens under Varying States of Stress and Temperatures. Annual Book of ASTM Standards, Vol. 4.09, ASTM International, West Conshohocken, PA, 9 p.
- ASTM D7383-10 (2010). Standard Test Methods for Axial Compressive Force Pulse (Rapid) Testing of Deep Foundations. Annual Book of ASTM Standards, Vol. 4.08, ASTM International, West Conshohocken, PA, 9 p. ASTM
- ASTM Vol 4.08. (2014). Soil and Rock I, Vol. 4.08, ASTM International, West Conshohocken, PA, 1826 p.
- ASTM Vol 4.09. (2014). Soil and Rock II, Vol. 4.09, ASTM International, West Conshohocken, PA, 1754 p.

Appendix C

PILE HAMMER INFORMATION

Type	Hammer Make	Hammer Model	Hammer Type	Rated Energy kip-feet	Ram Weight kips	Stroke feet
1	DELMAG	D 5	OED	10.51	1.10	9.55
2	DELMAG	D 8-22	OED	20.10	1.76	11.42
3	DELMAG	D 12	OED	22.61	2.75	8.22
4	DELMAG	D 15	OED	27.09	3.30	8.21
5	DELMAG	D 16-32	OED	40.20	3.52	11.42
6	DELMAG	D 22	OED	40.61	4.91	8.27
7	DELMAG	D 22-02	OED	48.50	4.85	10.00
8	DELMAG	D 22-13	OED	48.50	4.85	10.00
9	DELMAG	D 22-23	OED	51.22	4.85	10.56
10	DELMAG	D 25-32	OED	66.34	5.51	12.04
11	DELMAG	D 30	OED	59.73	6.60	9.05
12	DELMAG	D 30-02	OED	66.20	6.60	10.03
13	DELMAG	D 30-13	OED	66.20	6.60	10.03
14	DELMAG	D 30-23	OED	73.79	6.60	11.18
15	DELMAG	D 30-32	OED	75.44	6.60	11.43
16	DELMAG	D 36	OED	83.82	7.93	10.57
17	DELMAG	D 36-02	OED	83.82	7.93	10.57
18	DELMAG	D 36-13	OED	83.82	7.93	10.57
19	DELMAG	D 36-23	OED	88.50	7.93	11.16
20	DELMAG	D 36-32	OED	90.56	7.93	11.42
21	DELMAG	D 44	OED	90.16	9.50	9.49
22	DELMAG	D 46	OED	107.08	10.14	10.56
23	DELMAG	D 46-02	OED	107.08	10.14	10.56
24	DELMAG	D 46-13	OED	96.53	10.14	9.52
25	DELMAG	D 46-23	OED	107.08	10.14	10.56
26	DELMAG	D 46-32	OED	122.19	10.14	12.05
27	DELMAG	D 55	OED	125.00	11.86	10.54
28	DELMAG	D 62-02	OED	152.45	13.66	11.16
29	DELMAG	D 62-12	OED	152.45	13.66	11.16
30	DELMAG	D 62-22	OED	164.60	13.66	12.05
31	DELMAG	D 80-12	OED	186.24	17.62	10.57
32	DELMAG	D 80-23	OED	212.50	17.62	12.06
33	DELMAG	D100-13	OED	265.68	22.07	12.04
35	DELMAG	D 19-52	OED	43.20	4.00	10.80
36	DELMAG	D 6-32	OED	13.52	1.32	10.23

Type	Hammer Make	Hammer Model	Hammer Type	Rated Energy kip-feet	Ram Weight kips	Stroke feet
37	DELMAG	D 12-32	OED	31.33	2.82	11.11
38	DELMAG	D 12-42	OED	33.30	2.82	11.81
39	DELMAG	D 14-42	OED	34.50	3.09	11.18
40	DELMAG	D 19-32	OED	42.44	4.00	10.61
41	DELMAG	D 19-42	OED	43.24	4.00	10.81
42	DELMAG	D200-42	OED	492.04	44.09	11.16
43	DELMAG	D120-42	OED	301.79	26.45	11.41
44	DELMAG	D150-42	OED	377.33	33.07	11.41
45	DELMAG	D125-42	OED	313.63	27.56	11.38
46	DELMAG	D 21-42	OED	55.75	4.63	12.04
47	DELMAG	D 5-42	OED	10.56	1.10	9.60
48	DELMAG	D160-32	OED	393.45	35.27	11.16
49	DELMAG	D260-32	OED	639.36	57.32	11.16
50	FEC	1200	OED	22.50	2.75	8.18
51	FEC	1500	OED	27.09	3.30	8.21
52	FEC	2500	OED	50.00	5.50	9.09
53	FEC	2800	OED	55.99	6.16	9.09
54	FEC	3000	OED	63.03	6.60	9.55
55	FEC	3400	OED	73.01	7.48	9.76
56	FEC	D-18	OED	39.70	3.97	10.00
61	MITSUBIS	M 14	OED	25.25	2.97	8.50
62	MITSUBIS	MH 15	OED	28.14	3.31	8.50
63	MITSUBIS	M 23	OED	43.01	5.06	8.50
64	MITSUBIS	MH 25	OED	46.84	5.51	8.50
65	MITSUBIS	M 33	OED	61.71	7.26	8.50
66	MITSUBIS	MH 35	OED	65.62	7.72	8.50
67	MITSUBIS	M 43	OED	80.41	9.46	8.50
68	MITSUBIS	MH 45	OED	85.43	10.05	8.50
70	MITSUBIS	MH 72B	OED	135.15	15.90	8.50
71	MITSUBIS	MH 80B	OED	149.60	17.60	8.50
81	LINKBELT	LB 180	CED	8.10	1.73	4.68
82	LINKBELT	LB 312	CED	15.02	3.86	3.89
83	LINKBELT	LB 440	CED	18.20	4.00	4.55
84	LINKBELT	LB 520	CED	26.31	5.07	5.19
85	LINKBELT	LB 660	CED	51.63	7.57	6.82
90	HITACHI	HNC65	ECH	56.42	14.33	3.94
91	HITACHI	HNC80	ECH	69.43	17.64	3.94
92	HITACHI	HNC100	ECH	86.79	22.05	3.94
93	HITACHI	HNC125	ECH	108.49	27.56	3.94
101	KOBE	K 13	OED	25.43	2.87	8.86
103	KOBE	K22-Est	OED	45.35	4.85	9.35
104	KOBE	K 25	OED	51.52	5.51	9.35
107	KOBE	K 35	OED	72.18	7.72	9.35

Type	Hammer Make	Hammer Model	Hammer Type	Rated Energy kip-feet	Ram Weight kips	Stroke feet
110	KOBE	K 45	OED	92.75	9.92	9.35
112	KOBE	KB 60	OED	130.18	13.23	9.84
113	KOBE	KB 80	OED	173.58	17.64	9.84
120	ICE	180	CED	8.13	1.73	4.70
121	ICE	422	CED	23.12	4.00	5.78
122	ICE	440	CED	18.56	4.00	4.64
123	ICE	520	CED	30.37	5.07	5.99
124	ICE	640	CED	40.62	6.00	6.77
125	ICE	660	CED	51.63	7.57	6.82
126	ICE	1070	CED	72.60	10.00	7.26
127	ICE	30-S	OED	22.50	3.00	7.50
128	ICE	40-S	OED	40.00	4.00	10.00
129	ICE	42-S	OED	42.00	4.09	10.27
130	ICE	60-S	OED	59.99	7.00	8.57
131	ICE	70-S	OED	70.00	7.00	10.00
132	ICE	80-S	OED	80.00	8.00	10.00
133	ICE	90-S	OED	90.00	9.00	10.00
134	ICE	100-S	OED	100.00	10.00	10.00
135	ICE	120-S	OED	120.00	12.00	10.00
136	ICE	200-S	OED	100.00	20.00	5.00
137	ICE	205-S	OED	170.00	20.00	8.50
139	ICE	32-S	OED	26.01	3.00	8.67
140	ICE	120S-15	OED	132.45	15.00	8.83
142	MKT	DE-20C	OED	20.00	2.00	10.00
143	MKT	DE-30C	OED	28.00	2.80	10.00
144	MKT	DE-33C	OED	33.00	3.30	10.00
145	MKT	DE333020	OED	40.00	4.00	10.00
146	MKT	DE 10	OED	8.80	1.10	8.00
147	MKT	DE 20	OED	16.00	2.00	8.00
148	MKT	DE 30	OED	22.40	2.80	8.00
149	MKT	DA35B SA	OED	23.80	2.80	8.50
150	MKT	DE 30B	OED	23.80	2.80	8.50
151	MKT	DA 35B	CED	21.00	2.80	7.50
152	MKT	DA 45	CED	30.72	4.00	7.68
153	MKT	DE 40	OED	32.00	4.00	8.00
154	MKT	DE 35	OED	35.00	3.50	10.00
155	MKT	DE 42	OED	42.00	4.20	10.00
157	MKT	DE 50C	OED	50.00	5.00	10.00
158	MKT	DE 70C	OED	70.00	7.00	10.00
159	MKT	DE 50B	OED	42.50	5.00	8.50
160	MKT	DA55B SA	OED	40.00	5.00	8.00
161	MKT	DA 55B	CED	38.20	5.00	7.64
162	MKT	DE 70B	OED	59.50	7.00	8.50

Type	Hammer Make	Hammer Model	Hammer Type	Rated Energy kip-feet	Ram Weight kips	Stroke feet
163	MKT	DE-50B	OED	50.00	5.00	10.00
164	MKT	DE-70B	OED	70.00	7.00	10.00
165	MKT	DE-110C	OED	110.00	11.00	10.00
166	MKT	DE-150C	OED	150.00	15.00	10.00
167	MKT	DA 35C	CED	21.00	2.80	7.50
168	MKT	DA 55C	CED	38.20	5.00	7.64
171	CONMACO	C 50	ECH	15.00	5.00	3.00
172	CONMACO	C 65	ECH	19.50	6.50	3.00
173	CONMACO	C 550	ECH	25.00	5.00	5.00
174	CONMACO	C 565	ECH	32.50	6.50	5.00
175	CONMACO	C 80	ECH	26.00	8.00	3.25
176	CONMACO	C 100	ECH	32.50	10.00	3.25
177	CONMACO	C 115	ECH	37.38	11.50	3.25
178	CONMACO	C 80E5	ECH	40.00	8.00	5.00
179	CONMACO	C 100E5	ECH	50.00	10.00	5.00
180	CONMACO	C 115E5	ECH	57.50	11.50	5.00
181	CONMACO	C 125E5	ECH	62.50	12.50	5.00
182	CONMACO	C 140	ECH	42.00	14.00	3.00
183	CONMACO	C 160	ECH	48.75	16.25	3.00
184	CONMACO	C 200	ECH	60.00	20.00	3.00
185	CONMACO	C 300	ECH	90.00	30.00	3.00
186	CONMACO	C 5200	ECH	100.00	20.00	5.00
187	CONMACO	C 5300	ECH	150.00	30.00	5.00
188	CONMACO	C 5450	ECH	225.00	45.00	5.00
189	CONMACO	C 5700	ECH	350.00	70.00	5.00
190	CONMACO	C 6850	ECH	510.00	85.00	6.00
191	CONMACO	C 160 **	ECH	51.78	17.26	3.00
192	CONMACO	C 50E5	ECH	25.00	5.00	5.00
193	CONMACO	C 65E5	ECH	32.50	6.50	5.00
194	CONMACO	C 200E5	ECH	100.00	20.00	5.00
195	CONMACO	C 300E5	ECH	150.00	30.00	5.00
196	CONMACO	C 1750	ECH	1050.00	175.00	6.00
204	VULCAN	VUL 01	ECH	15.00	5.00	3.00
205	VULCAN	VUL 02	ECH	7.26	3.00	2.42
206	VULCAN	VUL 06	ECH	19.50	6.50	3.00
207	VULCAN	VUL 08	ECH	26.00	8.00	3.25
208	VULCAN	VUL 010	ECH	32.50	10.00	3.25
209	VULCAN	VUL 012	ECH	39.00	12.00	3.25
210	VULCAN	VUL 014	ECH	42.00	14.00	3.00
211	VULCAN	VUL 016	ECH	48.75	16.25	3.00
212	VULCAN	VUL 020	ECH	60.00	20.00	3.00
213	VULCAN	VUL 030	ECH	90.00	30.00	3.00
214	VULCAN	VUL 040	ECH	120.00	40.00	3.00

Type	Hammer Make	Hammer Model	Hammer Type	Rated Energy kip-feet	Ram Weight kips	Stroke feet
215	VULCAN	VUL 060	ECH	180.00	60.00	3.00
220	VULCAN	VUL 30C	ECH	7.26	3.00	2.42
221	VULCAN	VUL 50C	ECH	15.10	5.00	3.02
222	VULCAN	VUL 65C	ECH	19.18	6.50	2.95
223	VULCAN	VUL 65CA	ECH	19.57	6.50	3.01
224	VULCAN	VUL 80C	ECH	24.48	8.00	3.06
225	VULCAN	VUL 85C	ECH	25.99	8.52	3.05
226	VULCAN	VUL 100C	ECH	32.90	10.00	3.29
227	VULCAN	VUL 140C	ECH	35.98	14.00	2.57
228	VULCAN	VUL 200C	ECH	50.20	20.00	2.51
229	VULCAN	VUL 400C	ECH	113.60	40.00	2.84
230	VULCAN	VUL 600C	ECH	179.16	60.00	2.99
231	VULCAN	VUL 320	ECH	60.00	20.00	3.00
232	VULCAN	VUL 330	ECH	90.00	30.00	3.00
233	VULCAN	VUL 340	ECH	120.00	40.00	3.00
234	VULCAN	VUL 360	ECH	180.00	60.00	3.00
235	VULCAN	VUL 505	ECH	25.00	5.00	5.00
236	VULCAN	VUL 506	ECH	32.50	6.50	5.00
237	VULCAN	VUL 508	ECH	40.00	8.00	5.00
238	VULCAN	VUL 510	ECH	50.00	10.00	5.00
239	VULCAN	VUL 512	ECH	60.00	12.00	5.00
240	VULCAN	VUL 520	ECH	100.00	20.00	5.00
241	VULCAN	VUL 530	ECH	150.00	30.00	5.00
242	VULCAN	VUL 540	ECH	200.00	40.90	4.89
243	VULCAN	VUL 560	ECH	300.00	62.50	4.80
245	VULCAN	VUL 3100	ECH	300.00	100.00	3.00
246	VULCAN	VUL 5100	ECH	500.00	100.00	5.00
247	VULCAN	VUL 5150	ECH	750.00	150.00	5.00
248	VULCAN	VUL 6300	ECH	1800.00	300.00	6.00
251	RAYMOND	R 1	ECH	15.00	5.00	3.00
252	RAYMOND	R 1S	ECH	19.50	6.50	3.00
253	RAYMOND	R 65C	ECH	19.50	6.50	3.00
254	RAYMOND	R 65CH	ECH	19.50	6.50	3.00
255	RAYMOND	R 0	ECH	24.38	7.50	3.25
256	RAYMOND	R 80C	ECH	24.48	8.00	3.06
257	RAYMOND	R 80CH	ECH	24.48	8.00	3.06
258	RAYMOND	R 2/0	ECH	32.50	10.00	3.25
259	RAYMOND	R 3/0	ECH	40.63	12.50	3.25
260	RAYMOND	R 150C	ECH	48.75	15.00	3.25
261	RAYMOND	R 4/0	ECH	48.75	15.00	3.25
262	RAYMOND	R 5/0	ECH	56.88	17.50	3.25
263	RAYMOND	R 30X	ECH	75.00	30.00	2.50
264	RAYMOND	R 8/0	ECH	81.25	25.00	3.25

Type	Hammer Make	Hammer Model	Hammer Type	Rated Energy kip-feet	Ram Weight kips	Stroke feet
265	RAYMOND	R 40X	ECH	100.00	40.00	2.50
266	RAYMOND	R 60X	ECH	150.00	60.00	2.50
270	MENCK	MHU 100C	ECH	73.71	11.10	6.64
271	MENCK	MH 68	ECH	49.18	7.72	6.37
272	MENCK	MH 96	ECH	69.43	11.02	6.30
273	MENCK	MH 145	ECH	104.80	16.53	6.34
274	MENCK	MHU 195	ECH	143.74	21.36	6.73
275	MENCK	MHU 220	ECH	162.17	24.84	6.53
276	MENCK	MHU 400	ECH	294.82	51.09	5.77
277	MENCK	MHU 600	ECH	442.28	75.52	5.86
278	MENCK	MHU 1000	ECH	737.38	126.98	5.81
279	MENCK	MHU 1700	ECH	1253.24	207.15	6.05
280	MENCK	MHU 2100	ECH	1548.29	257.18	6.02
281	MENCK	MHU 3000	ECH	2211.90	370.23	5.97
282	MENCK	MRBS 500	ECH	45.07	11.02	4.09
283	MENCK	MRBS 750	ECH	67.77	16.53	4.10
285	MENCK	MRBS 850	ECH	93.28	18.96	4.92
286	MENCK	MRBS1100	ECH	123.43	24.25	5.09
287	MENCK	MRBS1502	ECH	135.59	33.07	4.10
288	MENCK	MRBS1800	ECH	189.81	38.58	4.92
289	MENCK	MRBS2500	ECH	262.11	63.93	4.10
290	MENCK	MRBS2502	ECH	225.95	55.11	4.10
291	MENCK	MRBS2504	ECH	225.95	55.11	4.10
292	MENCK	MRBS3000	ECH	325.36	66.13	4.92
293	MENCK	MRBS3900	ECH	513.34	86.86	5.91
294	MENCK	MRBS4600	ECH	498.94	101.41	4.92
295	MENCK	MRBS5000	ECH	542.33	110.23	4.92
296	MENCK	MRBS6000	ECH	759.23	132.27	5.74
297	MENCK	MRBS7000	ECH	631.40	154.00	4.10
298	MENCK	MRBS8000	ECH	867.74	176.37	4.92
299	MENCK	MRBS8800	ECH	954.53	194.01	4.92
300	MENCK	MBS12500	ECH	1581.83	275.58	5.74
301	MKT	No. 5	ECH	1.00	0.20	5.00
302	MKT	No. 6	ECH	2.50	0.40	6.25
303	MKT	No. 7	ECH	4.15	0.80	5.19
304	MKT	9B3	ECH	8.75	1.60	5.47
305	MKT	10B3	ECH	13.11	3.00	4.37
306	MKT	C5-Air	ECH	14.20	5.00	2.84
307	MKT	C5-Steam	ECH	16.20	5.00	3.24
308	MKT	S-5	ECH	16.25	5.00	3.25
309	MKT	11B3	ECH	19.15	5.00	3.83
310	MKT	C826 Stm	ECH	24.40	8.00	3.05
311	MKT	C826 Air	ECH	21.20	8.00	2.65

Type	Hammer Make	Hammer Model	Hammer Type	Rated Energy kip-feet	Ram Weight kips	Stroke feet
312	MKT	S-8	ECH	26.00	8.00	3.25
313	MKT	MS-350	ECH	30.80	7.72	3.99
314	MKT	S 10	ECH	32.50	10.00	3.25
315	MKT	S 14	ECH	37.52	14.00	2.68
316	MKT	MS 500	ECH	44.00	11.00	4.00
317	MKT	S 20	ECH	60.00	20.00	3.00
318	IHC	S-30	ECH	21.70	3.53	6.15
319	IHC	S-40	ECH	28.93	4.85	5.97
320	IHC	S-35	ECH	25.53	6.63	3.85
321	IHC	S-70	ECH	51.25	7.73	6.63
322	IHC	S-90	ECH	65.90	9.94	6.63
323	IHC	S-120	ECH	89.37	13.48	6.63
324	IHC	S-150	ECH	110.06	16.60	6.63
325	IHC	S-200	ECH	145.64	22.00	6.62
326	IHC	S-280	ECH	205.31	30.06	6.83
327	IHC	S-400	ECH	292.60	44.20	6.62
328	IHC	S-500	ECH	366.09	55.30	6.62
329	IHC	S-600	ECH	443.54	67.00	6.62
330	IHC	S-900	ECH	658.36	99.45	6.62
331	IHC	S-1200	ECH	891.05	134.60	6.62
332	IHC	S-1800-L	ECH	1170.39	166.00	7.05
333	IHC	S-2300	ECH	1681.48	254.00	6.62
334	IHC	S-2000	ECH	1473.97	222.65	6.62
335	IHC	SC-30	ECH	21.81	3.76	5.80
336	IHC	SC-40	ECH	29.86	5.51	5.42
337	IHC	SC-50	ECH	36.82	7.29	5.05
338	IHC	SC-60	ECH	44.95	13.30	3.38
339	IHC	SC-75	ECH	54.80	12.15	4.51
340	IHC	SC-110	ECH	81.89	17.46	4.69
341	IHC	SC-150	ECH	109.35	24.30	4.50
342	IHC	SC-200	ECH	152.51	30.20	5.05
343	IHC	SC-250	ECH	179.80	37.26	4.83
344	IHC	S-750	ECH	550.79	83.11	6.63
345	IHC	S-800	ECH	589.97	88.15	6.69
346	IHC	S-1400	ECH	1033.84	147.94	6.99
347	IHC	S-1800	ECH	1340.21	195.64	6.85
348	IHC	S-2500	ECH	1843.16	275.80	6.68
349	HERA	1900	OED	44.41	4.19	10.60
350	HERA	1250	OED	24.85	2.76	9.02
351	HERA	1500	OED	29.81	3.31	9.02
352	HERA	2500	OED	49.70	5.51	9.02
353	HERA	2800	OED	55.70	6.18	9.02
354	HERA	3500	OED	69.59	7.72	9.02

Type	Hammer Make	Hammer Model	Hammer Type	Rated Energy kip-feet	Ram Weight kips	Stroke feet
355	HERA	5000	OED	99.45	11.03	9.02
356	HERA	5700	OED	113.38	12.57	9.02
357	HERA	6200	OED	123.30	13.67	9.02
358	HERA	7500	OED	149.19	16.54	9.02
359	HERA	8800	OED	174.99	19.40	9.02
360	ICE	I-12obs	OED	30.21	2.82	10.71
361	ICE	I-19obs	OED	43.24	4.02	10.77
362	ICE	I-30obs	OED	71.45	6.62	10.80
363	ICE	I-36obs	OED	90.68	7.94	11.42
364	ICE	I-46obs	OED	107.74	10.15	10.62
365	ICE	I-62obs	OED	164.98	14.60	11.30
366	ICE	I-80obs	OED	212.40	17.70	12.00
367	ICE	I-8v2obs	OED	17.60	1.76	10.00
368	ICE	I-100obs	OED	264.45	23.61	11.20
369	BSP	SL20	ECH	14.11	3.31	4.27
370	BSP	SL30	ECH	21.69	5.51	3.94
371	FAIRCHLD	F-45	ECH	45.00	15.00	3.00
372	FAIRCHLD	F-32	ECH	32.55	10.85	3.00
374	BSP	CX40	ECH	28.21	6.61	4.27
375	BSP	CX50	ECH	37.61	8.82	4.27
376	BSP	CX60	ECH	47.01	11.02	4.27
377	BSP	CX75	ECH	52.08	13.23	3.94
378	BSP	CX85	ECH	60.75	15.43	3.94
379	BSP	CX110	ECH	78.11	19.84	3.94
381	BSP	HH3	ECH	26.02	6.61	3.94
382	BSP	HH5	ECH	43.38	11.02	3.94
383	BSP	HH7	ECH	60.78	15.43	3.94
384	BSP	HH8	ECH	69.50	17.64	3.94
385	BSP	HH9	ECH	78.17	19.84	3.94
386	BSP	HH11-1.2	ECH	95.55	24.25	3.94
387	BSP	HH14-1.2	ECH	121.59	30.86	3.94
388	BSP	HH16-1.2	ECH	138.87	35.27	3.94
391	BSP	HA30	ECH	260.37	66.14	3.94
392	BSP	HA40	ECH	347.16	88.18	3.94
393	BSP	HH11-1.5	ECH	119.31	24.25	4.92
394	BSP	HH14-1.5	ECH	151.83	30.86	4.92
395	BSP	HH16-1.5	ECH	173.54	35.27	4.92
396	BSP	CG180	ECH	131.92	26.45	4.99
397	BSP	CG210	ECH	153.91	30.86	4.99
398	BSP	CG240	ECH	175.90	35.27	4.99
399	BSP	CG270	ECH	197.88	39.68	4.99
400	BSP	CG300	ECH	219.87	44.09	4.99
401	BERMINGH	B23	CED	22.99	2.80	8.21

Type	Hammer Make	Hammer Model	Hammer Type	Rated Energy kip-feet	Ram Weight kips	Stroke feet
402	BERMINGH	B200	OED	18.00	2.00	9.00
403	BERMINGH	B225	OED	29.25	3.00	9.75
404	BERMINGH	B300	OED	40.31	3.75	10.75
405	BERMINGH	B400	OED	53.75	5.00	10.75
406	BERMINGH	B-21	OED	53.25	4.63	11.50
410	BERMINGH	B300 M	OED	40.31	3.75	10.75
411	BERMINGH	B400 M	OED	53.75	5.00	10.75
412	BERMINGH	B400 4.8	OED	43.20	4.80	9.00
413	BERMINGH	B400 5.0	OED	45.00	5.00	9.00
414	BERMINGH	B23 5	CED	22.99	2.80	8.21
415	BERMINGH	B250 5	OED	26.25	2.50	10.50
416	BERMINGH	B3505	OED	47.20	4.00	11.80
417	BERMINGH	B4005	OED	59.00	5.00	11.80
418	BERMINGH	B4505	OED	77.88	6.60	11.80
419	BERMINGH	B5005	OED	92.04	7.80	11.80
420	BERMINGH	B5505	OED	108.56	9.20	11.80
421	BERMINGH	B550 C	OED	88.00	11.00	8.00
422	BERMINGH	B2005	OED	18.00	2.00	9.00
424	BERMINGH	B2505	OED	35.40	3.00	11.80
425	BERMINGH	B3005	OED	35.40	3.00	11.80
431	BERMINGH	B6005	OED	160.95	13.64	11.80
432	BERMINGH	B6505 C	OED	253.00	22.00	11.50
433	BERMINGH	B6505	OED	202.86	17.64	11.50
434	BERMINGH	B-9	OED	21.00	2.00	10.50
435	BERMINGH	B-32	OED	81.08	7.05	11.50
436	BERMINGH	B-64	OED	166.50	14.11	11.80
437	BERMINGH	B-6505HD	OED	220.50	22.05	10.00
441	MENCK	MHF5-5	ECH	38.69	11.02	3.51
442	MENCK	MHF5-6	ECH	46.43	13.23	3.51
443	MENCK	MHF5-7	ECH	54.17	15.43	3.51
444	MENCK	MHF5-8	ECH	61.91	17.64	3.51
445	MENCK	MHF5-9	ECH	69.65	19.84	3.51
446	MENCK	MHF5-10	ECH	77.39	22.05	3.51
447	MENCK	MHF5-11	ECH	85.13	24.25	3.51
448	MENCK	MHF5-12	ECH	92.87	26.45	3.51
449	MENCK	MHF3-3	ECH	24.76	7.05	3.51
450	MENCK	MHF3-4	ECH	30.96	8.82	3.51
451	MENCK	MHF3-5	ECH	38.69	11.02	3.51
452	MENCK	MHF3-6	ECH	46.43	13.23	3.51
453	MENCK	MHF3-7	ECH	54.17	15.43	3.51
454	MENCK	MHF10-15	ECH	124.73	33.06	3.77
455	MENCK	MHF10-20	ECH	166.28	44.07	3.77
456	MENCK	MHF 5-14	ECH	108.34	30.86	3.51

Type	Hammer Make	Hammer Model	Hammer Type	Rated Energy kip-feet	Ram Weight kips	Stroke feet
457	MENCK	MHU135T*	ECH	110.59	17.99	6.15
458	MENCK	MHU500T*	ECH	368.74	65.96	5.59
459	MENCK	MHU 300S	ECH	221.20	35.73	6.19
460	MENCK	MHU 270T	ECH	221.20	35.73	6.19
461	MENCK	MHU 200T	ECH	162.24	26.75	6.07
462	MENCK	MHU 400T	ECH	324.37	52.45	6.18
463	MENCK	MHU 500T	ECH	405.53	65.96	6.15
464	MENCK	MHU 700T	ECH	567.72	92.88	6.11
465	MENCK	MHU 840S	ECH	619.22	92.88	6.67
466	MENCK	MHU 600B	ECH	457.03	65.96	6.93
467	MENCK	MHU 600T	ECH	486.63	80.39	6.05
468	MENCK	MHU 800S	ECH	604.57	99.93	6.05
469	MENCK	MHU1200S	ECH	884.84	145.71	6.07
470	MENCK	MHU1500S	ECH	1106.07	178.94	6.18
471	MENCK	MHU1700T	ECH	1400.86	227.36	6.16
472	MENCK	MHU1900S	ECH	1400.86	227.36	6.16
473	MENCK	MHU 150S	ECH	110.59	17.99	6.15
474	MENCK	MHU2700S	ECH	1990.19	318.77	6.24
475	MENCK	MHU 135T	ECH	110.59	17.99	6.15
476	MENCK	MHU 750T	ECH	604.57	99.93	6.05
477	MENCK	MHU1100T	ECH	899.66	145.71	6.18
478	MENCK	MHU150S*	ECH	110.59	17.99	6.15
479	MENCK	MHU600B*	ECH	457.03	65.96	6.93
481	JUNTTAN	HHK3A	ECH	26.05	6.62	3.94
482	JUNTTAN	HHK4A	ECH	34.73	8.82	3.94
483	JUNTTAN	HHK5A	ECH	43.41	11.03	3.94
484	JUNTTAN	HHK6A	ECH	52.10	13.23	3.94
485	JUNTTAN	HHK7A	ECH	60.75	15.43	3.94
486	JUNTTAN	HHK10A	ECH	86.83	22.05	3.94
487	JUNTTAN	HHK12A	ECH	104.19	26.47	3.94
488	JUNTTAN	HHK14A	ECH	121.56	30.88	3.94
491	JUNTTAN	HHK9A	ECH	78.14	19.85	3.94
494	JUNTTAN	HHK16A	ECH	138.92	35.29	3.94
495	JUNTTAN	HHK18A	ECH	156.29	39.70	3.94
496	JUNTTAN	HHK20A	ECH	173.65	44.11	3.94
497	JUNTTAN	HHK4SL	ECH	43.40	8.82	4.92
498	JUNTTAN	HHK3AL	ECH	17.37	6.62	2.63
499	JUNTTAN	HHK4AL	ECH	23.15	8.82	2.63
500	JUNTTAN	HHK5AL	ECH	28.94	11.03	2.63
501	HPSI	110	ECH	44.00	11.00	4.00
502	HPSI	150	ECH	60.00	15.00	4.00
503	HPSI	154	ECH	61.60	15.40	4.00
504	HPSI	200	ECH	80.00	20.00	4.00

Type	Hammer Make	Hammer Model	Hammer Type	Rated Energy kip-feet	Ram Weight kips	Stroke feet
505	HPSI	225	ECH	90.00	22.50	4.00
506	HPSI	650	ECH	32.50	6.50	5.00
507	HPSI	1000	ECH	50.00	10.00	5.00
508	HPSI	1605	ECH	83.00	16.60	5.00
509	HPSI	2005	ECH	95.10	19.02	5.00
510	HPSI	3005	ECH	154.33	30.87	5.00
511	HPSI	3505	ECH	176.33	35.27	5.00
512	HPSI	2000	ECH	80.00	20.00	4.00
514	UDDCOMB	H2H	ECH	16.62	4.40	3.77
515	UDDCOMB	H3H	ECH	24.88	6.60	3.77
516	UDDCOMB	H4H	ECH	33.18	8.80	3.77
517	UDDCOMB	H5H	ECH	41.47	11.00	3.77
518	UDDCOMB	H6H	ECH	49.76	13.20	3.77
519	UDDCOMB	H8H	ECH	82.19	17.60	4.67
520	UDDCOMB	H10H	ECH	86.88	22.05	3.94
521	DAWSON	HPH1200	ECH	8.72	2.30	3.79
522	DAWSON	HPH1800	ECH	13.72	3.30	4.16
523	DAWSON	HPH2400	ECH	17.32	4.19	4.13
524	DAWSON	HPH6500	ECH	46.98	10.25	4.58
525	DAWSON	HPH4500	ECH	32.56	7.72	4.22
526	DAWSON	HPH9000	ECH	66.30	10.47	6.33
530	BRUCE	SGH-0312	ECH	26.00	6.60	3.94
531	BRUCE	SGH-0512	ECH	43.34	11.00	3.94
532	BRUCE	SGH-0712	ECH	60.68	15.40	3.94
533	BRUCE	SGH-1012	ECH	86.77	22.05	3.94
534	BRUCE	SGH-0412	ECH	34.67	8.80	3.94
535	BANUT	S3000	ECH	26.04	6.62	3.94
536	BANUT	S4000	ECH	34.72	8.82	3.94
537	BANUT	S5000	ECH	43.41	11.03	3.94
538	BANUT	S6000	ECH	52.09	13.23	3.94
539	BANUT	S8000	ECH	69.45	17.64	3.94
540	BANUT	S10000	ECH	86.81	22.05	3.94
541	BANUT	3 Tonnes	ECH	17.35	6.61	2.62
542	BANUT	4 Tonnes	ECH	23.14	8.82	2.62
543	BANUT	5 Tonnes	ECH	28.92	11.02	2.62
544	BANUT	6 Tonnes	ECH	34.72	13.23	2.62
545	BANUT	7 Tonnes	ECH	40.49	15.43	2.62
550	ICE	70	ECH	21.00	7.00	3.00
551	ICE	75	ECH	30.00	7.50	4.00
552	ICE	110-SH	ECH	37.72	11.50	3.28
553	ICE	115-SH	ECH	37.95	11.50	3.30
554	ICE	115	ECH	46.00	11.50	4.00
555	ICE	160-SH	ECH	64.00	16.00	4.00

Type	Hammer Make	Hammer Model	Hammer Type	Rated Energy kip-feet	Ram Weight kips	Stroke feet
556	ICE	160	ECH	64.00	16.00	4.00
557	ICE	220	ECH	88.00	22.00	4.00
558	ICE	275	ECH	110.00	27.50	4.00
559	ICE	DKH-3U	ECH	26.00	6.60	3.94
560	HMC	28A	ECH	28.00	7.00	4.00
561	HMC	28B	ECH	21.00	7.00	3.00
562	HMC	62	ECH	46.00	11.50	4.00
563	HMC	86	ECH	64.00	16.00	4.00
564	HMC	119	ECH	88.00	22.00	4.00
565	HMC	149	ECH	110.00	27.50	4.00
566	HMC	187	ECH	138.00	34.50	4.00
567	HMC	19D	ECH	14.00	3.50	4.00
568	HMC	38D	ECH	28.00	7.00	4.00
569	APE	D 8-42	OED	19.80	1.76	11.25
570	APE	D 1-42	OED	1.32	0.21	6.33
571	APE	D 19-42	OED	47.13	4.19	11.25
572	APE	D 30-42	OED	74.42	6.62	11.25
573	APE	D 36-42	OED	89.30	7.94	11.25
574	APE	D 46-42	OED	114.11	10.14	11.25
575	APE	D 62-42	OED	153.80	13.67	11.25
576	APE	D 80-42	OED	198.45	17.64	11.25
577	APE	D 100-42	OED	248.06	22.05	11.25
579	APE	D 16-42	OED	39.69	3.53	11.25
580	APE	D 16-52	OED	39.69	3.53	11.25
581	APE	D 25-42	OED	62.01	5.51	11.25
582	APE	D 125-42	OED	310.08	27.56	11.25
583	APE	D 50-42	OED	124.03	11.03	11.25
584	APE	D 12-42	OED	29.77	2.65	11.25
585	APE	D 36-26	OED	89.30	7.94	11.25
586	APE	D 128-42	OED	317.25	28.20	11.25
587	APE	D 138-42	OED	342.00	30.40	11.25
588	APE	D 160-42	OED	396.90	35.28	11.25
589	APE	D 180-42	OED	446.51	39.69	11.25
590	APE	D 225-42	OED	558.00	49.60	11.25
591	APE	5.4mT	ECH	26.00	12.00	2.17
592	APE	7.2mT	ECH	51.30	16.20	3.17
593	APE	D 220-42	OED	540.81	48.46	11.16
594	APE	15-60	ECH	150.00	30.00	5.00
595	APE	10-60	ECH	100.00	20.00	5.00
596	APE	400U	ECH	400.00	80.00	5.00
598	APE	750U	ECH	750.00	120.00	6.25
599	APE	D 100-13	OED	300.04	23.70	12.66
600	BSP	DX20	ECH	14.11	3.31	4.27

Type	Hammer Make	Hammer Model	Hammer Type	Rated Energy kip-feet	Ram Weight kips	Stroke feet
601	BSP	DX25	ECH	18.09	4.41	4.10
602	BSP	DX30	ECH	21.71	5.51	3.94
603	BSP	LX2.5-SA	ECH	14.47	5.51	2.63
604	BSP	LX4-SA	ECH	23.15	8.82	2.63
605	BSP	LX5-SA	ECH	28.94	11.03	2.63
606	BSP	CGL370	ECH	271.22	55.11	4.92
607	BSP	CGL440	ECH	325.47	66.14	4.92
608	BSP	CGL520	ECH	379.71	77.16	4.92
609	BSP	CGL590	ECH	433.96	88.18	4.92
610	BSP	LX7-SA	ECH	40.52	15.44	2.63
625	BRUCE	SGH-1212	ECH	104.13	26.46	3.94
626	BRUCE	SGH-1312	ECH	112.81	28.66	3.94
627	BRUCE	SGH-1315	ECH	141.01	28.66	4.92
628	BRUCE	SGH-1412	ECH	121.48	30.87	3.94
629	BRUCE	SGH-1415	ECH	151.85	30.87	4.92
630	BRUCE	SGH-1612	ECH	138.84	35.27	3.94
631	BRUCE	SGH-1615	ECH	173.55	35.27	4.92
632	BRUCE	SGH-1618	ECH	208.26	35.27	5.90
633	BRUCE	SGH-1619	ECH	219.83	35.27	6.23
634	BRUCE	SGH-1812	ECH	156.19	39.68	3.94
635	BRUCE	SGH-1815	ECH	195.24	39.68	4.92
636	BRUCE	SGH-2012	ECH	173.55	44.09	3.94
637	BRUCE	SGH-2015	ECH	216.94	44.09	4.92
638	BRUCE	SGH-2312	ECH	199.58	50.71	3.94
639	BRUCE	SGH-2315	ECH	249.48	50.71	4.92
640	BRUCE	SGH-3012	ECH	260.32	66.14	3.94
641	BRUCE	SGH-3013	ECH	282.02	66.14	4.26
642	BRUCE	SGH-3015	ECH	325.40	66.14	4.92
643	BRUCE	SGH-4012	ECH	347.10	88.19	3.94
644	BRUCE	SGH-4212	ECH	364.45	92.59	3.94
645	BRUCE	SGH-5012	ECH	433.87	110.23	3.94
650	Twinwood	V20B	ECH	35.58	9.04	3.94
651	Twinwood	V100D	ECH	87.66	22.27	3.94
652	Twinwood	V160B	ECH	140.58	35.71	3.94
653	Twinwood	V400A	ECH	263.84	67.02	3.94
656	Pilemast	24-750	ECH	1.50	0.75	2.00
657	Pilemast	24-900	ECH	1.80	0.90	2.00
658	Pilemast	24-2000	ECH	4.00	2.00	2.00
659	Pilemast	24-2500	ECH	5.00	2.50	2.00
660	Pilemast	36-3000	ECH	9.00	3.00	3.00
661	Pilemast	36-5000	ECH	15.00	5.00	3.00
669	MVE	M-12	OED	30.21	2.82	10.71
670	MVE	M-19	OED	49.38	4.02	12.30

Type	Hammer Make	Hammer Model	Hammer Type	Rated Energy kip-feet	Ram Weight kips	Stroke feet
671	MVE	M-30	OED	83.35	6.62	12.60
801	DKH	PH-5	ECH	43.40	11.02	3.94
802	DKH	PH-7	ECH	60.75	15.43	3.94
803	DKH	PH-7S	ECH	60.75	15.43	3.94
804	DKH	PH-10	ECH	86.79	22.05	3.94
805	DKH	PH-13	ECH	112.83	28.66	3.94
806	DKH	PH-20	ECH	216.98	44.09	4.92
807	DKH	PH-30	ECH	325.47	66.14	4.92
808	DKH	PH-40	ECH	433.96	88.18	4.92
809	DKH	DKH-713	ECH	112.92	28.66	3.94
850	PILECO	D8-22	OED	18.66	1.76	10.60
851	PILECO	D12-42	OED	29.89	2.82	10.60
852	PILECO	D19-42	OED	42.51	4.01	10.60
853	PILECO	D25-32	OED	58.41	5.51	10.60
854	PILECO	D30-32	OED	70.07	6.61	10.60
855	PILECO	D36-32	OED	84.16	7.94	10.60
856	PILECO	D46-32	OED	107.48	10.14	10.60
857	PILECO	D62-22	OED	161.31	13.67	11.80
858	PILECO	D80-23	OED	197.57	17.64	11.20
859	PILECO	D100-13	OED	246.85	22.04	11.20
860	PILECO	D125-32	OED	308.67	27.56	11.20
861	PILECO	D225-22	OED	555.34	49.58	11.20
862	PILECO	D250-22	OED	617.06	55.09	11.20
863	PILECO	D138-32	OED	340.61	30.41	11.20
864	PILECO	D180-32	OED	444.27	39.67	11.20
865	PILECO	D280-22	OED	688.55	61.73	11.16
866	PILECO	D160-32	OED	395.08	35.28	11.20
867	PILECO	D400-12	OED	810.10	88.15	9.19
868	PILECO	D600-12	OED	1215.10	132.22	9.19
869	PILECO	D800-22	OED	1620.20	176.30	9.19
921	BRUCE	SGH-0212	ECH	17.34	4.40	3.94
922	BRUCE	SGH-0715	ECH	75.77	15.40	4.92
923	BRUCE	SGH-1015	ECH	108.47	22.05	4.92
924	BRUCE	SGH-1215	ECH	130.16	26.46	4.92
925	BRUCE	SGH-2512	ECH	216.94	55.12	3.94
926	BRUCE	SGH-2515	ECH	271.17	55.12	4.92
927	BRUCE	SGH-3512	ECH	303.71	77.16	3.94
928	BRUCE	SGH-3515	ECH	379.64	77.16	4.92
929	BRUCE	SGH-4015	ECH	433.87	88.19	4.92
930	BRUCE	SGH-4215	ECH	455.56	92.59	4.92
931	BRUCE	SGH-4512	ECH	390.48	99.21	3.94
932	BRUCE	SGH-4515	ECH	488.10	99.21	4.92
933	BRUCE	SGH-4712	ECH	407.84	103.62	3.94

Type	Hammer Make	Hammer Model	Hammer Type	Rated Energy kip-feet	Ram Weight kips	Stroke feet
934	BRUCE	SGH-4715	ECH	509.80	103.62	4.92
935	BRUCE	SGH-4719	ECH	645.74	103.62	6.23
936	BRUCE	SGH-5015	ECH	542.34	110.23	4.92
937	BRUCE	SGH-5715	ECH	618.26	125.66	4.92
938	BRUCE	SGH-6015	ECH	650.80	132.28	4.92
939	BRUCE	SGH-7015	ECH	759.27	154.32	4.92
940	BRUCE	SGH-8015	ECH	867.74	176.37	4.92
949	JUNTTAN	HHK10S	ECH	108.49	22.05	4.92
950	JUNTTAN	HHK28S	ECH	303.78	61.73	4.92
951	JUNTTAN	HHK5S	ECH	54.27	11.03	4.92
952	JUNTTAN	HHK7S	ECH	75.97	15.44	4.92
953	JUNTTAN	HHK9S	ECH	97.68	19.85	4.92
954	JUNTTAN	HHK12S	ECH	130.24	26.47	4.92
955	JUNTTAN	HHK14S	ECH	151.95	30.88	4.92
956	JUNTTAN	HHK16S	ECH	173.65	35.29	4.92
957	JUNTTAN	HHK18S	ECH	195.36	39.70	4.92
958	JUNTTAN	HHK20S	ECH	217.07	44.11	4.92
959	JUNTTAN	HHK25S	ECH	271.22	55.11	4.92
960	JUNTTAN	HHK36S	ECH	390.56	79.36	4.92
961	JUNTTAN	HHU5A	ECH	54.27	11.03	4.92
962	JUNTTAN	HHU7A	ECH	75.94	15.43	4.92
963	JUNTTAN	HHU9A	ECH	97.64	19.84	4.92
964	JUNTTAN	HHU12A	ECH	130.19	26.45	4.92
965	JUNTTAN	HHU14A	ECH	151.88	30.86	4.92
966	JUNTTAN	HHU16A	ECH	173.58	35.27	4.92
968	JUNTTAN	SHK100-3	ECH	26.91	6.61	4.07
969	JUNTTAN	SHK100-3	ECH	35.89	8.82	4.07
970	JUNTTAN	SHK100-3	ECH	44.84	11.02	4.07
971	JUNTTAN	SHK100-3	ECH	53.82	13.23	4.07
972	JUNTTAN	SHK110-5	ECH	44.98	11.02	4.08
973	JUNTTAN	SHK110-5	ECH	53.82	13.23	4.07
974	JUNTTAN	SHK110-5	ECH	65.62	15.43	4.25
975	JUNTTAN	SHK110-5	ECH	77.42	17.64	4.39
976	JUNTTAN	SHK110-5	ECH	87.74	19.84	4.42
977	JUNTTAN	SHK100-5	ECH	44.84	11.02	4.07
978	JUNTTAN	SHK100-5	ECH	53.82	13.23	4.07
979	JUNTTAN	SHK110-7	ECH	65.63	15.43	4.25
980	JUNTTAN	SHK110-7	ECH	77.43	17.64	4.39
981	JUNTTAN	SHK110-7	ECH	87.74	19.84	4.42
998	HYPOTHET	EX 4	OED	23.38	2.75	8.50
999	SELF	Drop/10t	ECH	300.00	20.00	15.00
1001	DFI-Corp	HHA250-4	ECH	25.18	5.51	4.57
1002	DFI-Corp	HHA300-4	ECH	28.75	6.61	4.35

Type	Hammer Make	Hammer Model	Hammer Type	Rated Energy kip-feet	Ram Weight kips	Stroke feet
1003	DFI-Corp	HHA325-4	ECH	30.36	7.16	4.24
1004	DFI-Corp	HHA350-4	ECH	31.80	7.70	4.13
1005	DFI-Corp	HHA400-6	ECH	51.92	8.80	5.90
1006	DFI-Corp	HHA450-6	ECH	57.04	9.92	5.75
1007	DFI-Corp	HHB500-6	ECH	66.66	11.00	6.06
1008	DFI-Corp	HHB600-6	ECH	77.88	13.20	5.90
1020	J&M	70B HIH	ECH	21.00	7.00	3.00
1021	J&M	82 HIH	ECH	32.80	8.20	4.00
1022	J&M	115 HIH	ECH	46.00	11.50	4.00
1023	J&M	160 HIH	ECH	64.00	16.00	4.00
1024	J&M	220 HIH	ECH	88.00	22.00	4.00
1025	J&M	275 HIH	ECH	110.00	27.50	4.00
1026	J&M	345 HIH	ECH	138.00	34.50	4.00
1134	Pilemer	DKH-3U	ECH	26.00	6.60	3.94
1135	Pilemer	DKH 10L	ECH	86.79	22.05	3.94
1201	Liebherr	H 50/3	ECH	28.97	6.60	4.39
1202	Liebherr	H 50/4	ECH	35.02	8.80	3.98
1203	Liebherr	H 85/5	ECH	43.34	11.00	3.94
1204	Liebherr	H 85/7	ECH	60.16	15.43	3.90
1205	Liebherr	H 110/7	ECH	60.16	15.43	3.90
1206	Liebherr	H 110/9	ECH	78.01	19.85	3.93
1251	ICE	I-30 V2	OED	71.71	6.62	10.84
1261	APE	D 19-52	OED	47.13	4.19	11.25
1262	APE	D 16-32	OED	39.69	3.53	11.25
1263	APE	D 19-32	OED	47.13	4.19	11.25
1264	APE	D 25-32	OED	62.01	5.51	11.25
1265	APE	D 30-32	OED	74.42	6.62	11.25
1266	APE	D 36-32	OED	89.30	7.94	11.25
1267	APE	D 46-32	OED	114.11	10.14	11.25
1268	APE	D 62-22	OED	153.80	13.67	11.25
1269	APE	D 80-23	OED	198.45	17.64	11.25
1270	APE	D 100-32	OED	248.06	22.05	11.25
1271	APE	D 120-32	OED	349.69	27.60	12.67
1272	APE	D 70-42	OED	173.64	15.44	11.25
1273	APE	D 25-52	OED	62.01	5.51	11.25
1274	APE	D 30-52	OED	74.42	6.62	11.25
1275	APE	D 36-52	OED	89.30	7.94	11.25
1276	APE	D 46-52	OED	114.11	10.14	11.25
1277	APE	D 50-52	OED	124.03	11.03	11.25
1278	APE	D 62-52	OED	153.80	13.67	11.25
1279	APE	D 70-52	OED	173.64	15.44	11.25
1280	APE	7.5a	ECH	24.00	12.00	2.00
1281	APE	7.5b	ECH	20.40	10.20	2.00

Type	Hammer Make	Hammer Model	Hammer Type	Rated Energy kip-feet	Ram Weight kips	Stroke feet
1282	APE	7.5c	ECH	15.20	7.60	2.00
1283	APE	9.5a	ECH	50.66	16.00	3.17
1284	APE	9.5b	ECH	44.32	14.00	3.17
1285	APE	7-3	ECH	42.00	14.00	3.00
1286	APE	8-3	ECH	48.00	16.00	3.00
1287	APE	8	ECH	16.00	8.00	2.00
1288	APE	8a	ECH	24.00	12.00	2.00
1289	APE	10-4	ECH	80.00	20.00	4.00
1321	MENCK	MHU 240U	ECH	221.20	35.73	6.19
1322	MENCK	MHU 440S	ECH	324.37	52.45	6.18
1323	MENCK	MHU 360U	ECH	324.37	52.45	6.18
1324	MENCK	MHU 550S	ECH	404.06	65.96	6.13
1325	MENCK	MHU 450U	ECH	404.06	65.96	6.13
1326	MENCK	MHU 660S	ECH	485.17	80.39	6.04
1327	MENCK	MHU 540U	ECH	485.17	80.39	6.04
1328	MENCK	MHU 720T	ECH	588.19	99.93	5.89
1329	MENCK	MHU 650U	ECH	588.19	99.93	5.89
1330	MENCK	MHU1000S	ECH	736.48	126.98	5.80
1331	MENCK	MHU 900T	ECH	736.48	126.98	5.80
1332	MENCK	MHU 810U	ECH	736.48	126.98	5.80
1333	MENCK	MHU1700S	ECH	1272.95	207.15	6.15
1334	MENCK	MHU2100S	ECH	1573.92	257.18	6.12
1335	MENCK	MHU3000S	ECH	2216.56	370.23	5.99
1336	MENCK	MHU1400B	ECH	1032.08	145.71	7.08
1337	MENCK	MHU3500S	ECH	2582.43	385.85	6.69
1371	IHC	S-3000	ECH	2211.93	332.44	6.65
1372	IHC	S-4000	ECH	2948.91	444.30	6.64
1401	FAMBO	HR250	ECH	1.81	0.55	3.28
1402	FAMBO	HR500akk	ECH	3.62	1.10	3.28
1403	FAMBO	HR500	ECH	4.34	1.10	3.94
1404	FAMBO	HR1000	ECH	8.68	2.20	3.94
1405	FAMBO	HR1500	ECH	13.02	3.31	3.94
1406	FAMBO	HR2000	ECH	17.36	4.41	3.94
1407	FAMBO	HR2750	ECH	23.87	6.06	3.94
1408	FAMBO	HR3000	ECH	26.04	6.61	3.94
1409	FAMBO	HR4000	ECH	34.72	8.82	3.94
1410	FAMBO	HR5000	ECH	43.40	11.02	3.94
1411	FAMBO	HR7000	ECH	60.75	15.43	3.94
1412	FAMBO	HR8000	ECH	69.45	17.64	3.94
1413	FAMBO	HR10000	ECH	86.79	22.05	3.94
1501	ICE	I-12v2	OED	29.63	2.82	10.50
1502	ICE	I-8v2	OED	18.69	1.76	10.60
1503	ICE	I-19v2	OED	46.14	4.01	11.50

Type	Hammer Make	Hammer Model	Hammer Type	Rated Energy kip-feet	Ram Weight kips	Stroke feet
1504	ICE	I-30v2	OED	76.05	6.61	11.50
1505	ICE	I-36v2	OED	93.73	7.94	11.81
1506	ICE	I-46v2	OED	119.77	10.14	11.81
1507	ICE	I-62v2	OED	172.37	14.59	11.81
1508	ICE	I-80v2	OED	208.30	17.64	11.81
1509	ICE	I-100v2	OED	260.37	22.05	11.81
1510	ICE	I-125v2	OED	310.10	27.56	11.25
1511	ICE	I-160v2	OED	393.45	35.27	11.16
1512	ICE	IP-2	ECH	17.36	4.41	3.94
1513	ICE	IP-3	ECH	26.04	6.61	3.94
1514	ICE	IP-5	ECH	43.40	11.02	3.94
1515	ICE	IP-7	ECH	60.75	15.43	3.94
1516	ICE	IP-10	ECH	86.78	22.04	3.94
1517	ICE	IP-13	ECH	112.83	28.66	3.94
1520	ICE	I-138v2	OED	328.62	30.40	10.81
1531	SPI	D 19-42	OED	42.61	4.02	10.60
1532	SPI	D 30-32	OED	72.08	6.80	10.60
1601	DELMAG	D 2	OED	1.78	0.49	3.61
1602	DELMAG	D 4	OED	3.60	0.84	4.30
1603	DELMAG	D 8-12	OED	20.10	1.76	11.42
1604	DELMAG	D 12-52	OED	33.98	2.82	12.05
1605	DELMAG	D 16-52	OED	40.20	3.52	11.42
1606	DELMAG	D 25-52	OED	66.34	5.51	12.04
1607	DELMAG	D 30-52	OED	75.44	6.60	11.43
1611	DELMAG	D138-32	OED	339.51	30.44	11.16
1612	DELMAG	D180-32	OED	442.64	39.68	11.16
1613	DELMAG	D300-32	OED	737.73	66.14	11.16
1614	DELMAG	D400-32	OED	983.64	88.18	11.16
1620	HMC	TD19	OED	46.09	4.01	11.49
1621	HMC	TD30	OED	69.87	6.61	10.57

Type	Hammer Make	Hammer Model	Hammer Type	Rated Power kW	Ecc. Mass kips	Frequency Hz
620	MAIT	34	VIB	227.00	1.23	33.30
621	MAIT	42	VIB	309.00	1.52	33.30
622	MAIT	54	VIB	450.00	0.98	33.30
623	MAIT	68	VIB	531.00	1.23	33.30
624	MAIT	120	VIB	674.00	1.74	30.00
698	ICE	50B	VIB	432.00	10.42	26.70
699	ICE	3117	VIB	235.00	1.12	28.30
700	ICE	23-28	VIB	21.00	0.10	26.70
701	ICE	216	VIB	130.00	0.46	26.70
702	ICE	216E	VIB	130.00	0.46	26.70
703	ICE	11-23	VIB	164.00	0.46	31.70
704	ICE	223	VIB	242.00	0.46	38.30
705	ICE	416L	VIB	242.00	0.92	26.70
706	ICE	812	VIB	375.00	1.82	26.70
707	ICE	815	VIB	375.00	1.84	26.70
708	ICE	44-30	VIB	242.00	1.30	20.00
709	ICE	44-50	VIB	377.00	1.30	26.70
710	ICE	44-65	VIB	485.00	1.30	27.50
711	ICE	66-65	VIB	485.00	1.95	21.70
712	ICE	66-80	VIB	597.00	1.95	26.70
713	ICE	1412B	VIB	597.00	2.04	21.00
714	ICE	1412C	VIB	470.00	2.02	23.00
715	ICE	V125	VIB	984.00	1.04	25.80
716	ICE	14RF	VIB	242.00	1.01	38.30
717	ICE	14-23	VIB	164.00	1.17	35.00
718	ICE	22-23V	VIB	164.00	0.92	26.90
719	ICE	22-30	VIB	250.00	0.92	26.90
720	HMC	3+28	VIB	21.00	0.11	26.80
721	HMC	3+75	VIB	56.00	0.11	36.10
722	HMC	13+200	VIB	149.00	0.35	26.70
723	HMC	13S+200	VIB	149.00	0.35	26.70
724	HMC	13H+200	VIB	164.00	0.35	29.80
725	HMC	25+220	VIB	164.00	0.61	20.90
726	HMC	26+335	VIB	242.00	0.71	25.60
727	HMC	26S+335	VIB	242.00	0.71	25.60
728	HMC	51+335	VIB	242.00	1.21	19.50
729	HMC	51+535	VIB	377.00	1.21	26.40
730	HMC	51S+535	VIB	377.00	1.21	26.40
731	HMC	51+740	VIB	485.00	1.21	27.50
732	HMC	76+740	VIB	485.00	1.82	21.70
733	HMC	76+800	VIB	597.00	1.82	26.10
734	HMC	115+800	VIB	597.00	1.35	20.40
735	HMC	230+1600	VIB	1193.00	2.69	20.40

Type	Hammer Make	Hammer Model	Hammer Type	Rated Power kW	Ecc. Mass kips	Frequency Hz
750	MKT	V-2B	VIB	52.00	0.15	30.00
751	MKT	V-5C	VIB	138.00	0.43	28.33
752	MKT	V-20B	VIB	242.00	0.20	28.33
753	MKT	V-30	VIB	448.00	1.47	28.33
754	MKT	V-35	VIB	485.00	1.60	28.33
755	MKT	V-140	VIB	1341.00	1.17	23.33
770	APE	3	VIB	10.58	0.00	38.30
771	APE	6	VIB	10.58	0.01	38.30
772	APE	15	VIB	59.67	0.11	30.00
773	APE	20	VIB	59.67	0.15	38.30
774	APE	20E	VIB	59.67	0.15	38.30
775	APE	50	VIB	194.00	0.23	30.00
776	APE	50E	VIB	194.00	0.23	30.00
777	APE	100	VIB	194.00	0.32	30.00
778	APE	100E	VIB	194.00	0.14	30.00
779	APE	100HF	VIB	260.00	0.14	43.00
780	APE	150	VIB	260.00	0.14	30.00
781	APE	150T	VIB	260.00	0.17	30.00
782	APE	150HF	VIB	466.00	0.32	43.00
783	APE	200	VIB	466.00	0.29	30.00
784	APE	200T	VIB	466.00	0.34	30.83
785	APE	200T HF	VIB	738.00	0.34	43.00
786	APE	300	VIB	738.00	0.34	25.00
787	APE	400B	VIB	738.00	0.78	23.33
788	APE	600	VIB	800.00	1.05	23.30
789	APE	Tan 400	VIB	1476.00	1.37	23.33
790	APE	Tan 600	VIB	1800.00	2.11	23.30
791	APE	200-6	VIB	470.00	0.43	30.00
811	MGF	RBH 80	VIB	50.00	0.60	30.00
812	MGF	RBH 140	VIB	85.00	1.04	26.67
813	MGF	RBH 200	VIB	125.00	0.74	26.67
814	MGF	RBH 320	VIB	200.00	0.79	26.67
815	MGF	RBH 460	VIB	255.00	1.13	26.67
816	MGF	RBH 1050	VIB	460.00	1.55	22.50
817	MGF	RBH 1575	VIB	700.00	1.16	22.50
818	MGF	RBH 2400	VIB	975.00	1.77	23.50
880	ICE	23RF	VIB	384.00	0.83	38.30
881	ICE	1412BT	VIB	1193.00	1.67	21.70
882	ICE	23-40	VIB	30.00	0.19	31.80
883	ICE	28-35	VIB	261.00	1.16	27.30
884	ICE	28RF-35	VIB	261.00	1.16	27.30
885	ICE	V360	VIB	783.00	0.94	25.00
886	ICE	V360 T	VIB	1566.00	1.88	25.00

Type	Hammer Make	Hammer Model	Hammer Type	Rated Power kW	Ecc. Mass kips	Frequency Hz
887	ICE	44-30V	VIB	250.00	0.92	26.00
888	ICE	44-70	VIB	585.00	0.92	28.10
889	ICE	66-70	VIB	585.00	0.92	23.00
890	ICE	7RF	VIB	154.00	0.51	38.30
891	ICE	66-70HS	VIB	585.00	0.92	26.70
892	ICE	66-80HS	VIB	597.00	0.92	29.20
893	ICE	100c-Tdm	VIB	1774.00	1.83	26.67
894	ICE	423	VIB	377.00	0.92	38.30
895	ICE	32RF	VIB	391.00	1.16	33.30
896	ICE	36RF	VIB	431.00	1.30	33.30
897	ICE	46RF	VIB	678.00	1.66	38.30
898	ICE	64RF	VIB	663.00	1.16	32.50
899	ICE	44B	VIB	595.00	1.30	30.00
900	Mueller	MS16HF	VIB	219.00	1.16	39.20
901	Mueller	MS25H2	VIB	218.00	0.90	28.00
902	Mueller	MS25H3	VIB	218.00	0.90	28.00
903	Mueller	MS50H2	VIB	419.00	1.20	27.00
904	Mueller	MS50H3	VIB	419.00	1.20	27.00
905	Mueller	MS25HHF	VIB	274.00	0.58	27.30
906	Mueller	MS50HHF	VIB	562.00	1.17	27.30
907	Mueller	MS100HHF	VIB	750.00	2.33	24.90
908	Mueller	MS120HHF	VIB	895.00	2.30	25.60
909	Mueller	MS200HHF	VIB	837.00	4.25	22.90
910	Mueller	MS-10HFV	VIB	203.00	0.39	39.30
911	Mueller	MS-16HFV	VIB	294.00	0.53	39.20
912	Mueller	MS-24HFV	VIB	720.00	0.85	39.20
913	Mueller	MS-32HFV	VIB	551.00	1.05	39.60
914	Mueller	MS-48HFV	VIB	823.00	1.69	39.20
915	Mueller	MS-62HFV	VIB	735.00	1.82	35.00
1039	J&M	11-23	VIB	164.00	0.92	31.70
1040	J&M	1412	VIB	559.00	1.67	21.70
1041	J&M	1412T	VIB	1119.00	1.67	21.70
1042	J&M	216	VIB	149.00	0.92	26.70
1044	J&M	22-23	VIB	164.00	0.92	20.80
1045	J&M	22-30	VIB	261.00	0.92	27.50
1050	J&M	28-35	VIB	261.00	1.17	27.50
1051	J&M	360	VIB	783.00	0.94	21.70
1052	J&M	416	VIB	250.00	0.92	26.70
1053	J&M	416B	VIB	261.00	0.92	26.70
1054	J&M	416S	VIB	250.00	0.92	26.70
1055	J&M	815	VIB	429.00	0.92	26.70
1056	J&M	44-30	VIB	250.00	0.92	20.00
1057	J&M	44-50	VIB	399.00	0.92	26.70

Type	Hammer Make	Hammer Model	Hammer Type	Rated Power kW	Ecc. Mass kips	Frequency Hz
1058	J&M	44-65	VIB	552.00	0.92	27.50
1060	J&M	66-65	VIB	552.00	0.92	21.70
1061	J&M	66-80	VIB	559.00	0.92	26.70
1100	PVE	14M	VIB	190.00	1.01	28.30
1101	PVE	23M	VIB	234.00	1.66	27.50
1102	PVE	25M	VIB	294.00	0.98	28.30
1103	PVE	27M	VIB	294.00	0.98	28.30
1104	PVE	38M	VIB	392.00	0.92	28.30
1105	PVE	50M	VIB	440.00	1.20	28.30
1106	PVE	52M	VIB	564.00	0.75	28.30
1107	PVE	105M	VIB	784.00	1.52	22.50
1108	PVE	110M	VIB	784.00	0.80	22.50
1109	PVE	200M	VIB	1130.00	1.45	23.30
1110	PVE	2307	VIB	190.00	0.47	38.30
1111	PVE	1420	VIB	190.00	1.01	33.30
1112	PVE	2315	VIB	234.00	1.09	38.30
1113	PVE	2520	VIB	294.00	1.81	33.30
1114	PVE	2310VM	VIB	190.00	0.72	38.30
1115	PVE	2315VM	VIB	234.00	1.09	38.30
1116	PVE	2316VM	VIB	294.00	1.16	38.30
1117	PVE	2319VM	VIB	392.00	1.37	38.30
1118	PVE	2323VM	VIB	392.00	0.83	38.30
1119	PVE	2332VM	VIB	564.00	1.16	38.30
1120	PVE	2335VM	VIB	784.00	1.27	38.30
1121	PVE	40VM	VIB	564.00	1.45	33.30
1122	PVE	50VM	VIB	564.00	1.20	30.00
1123	PVE	55M	VIB	403.00	1.17	28.33
1124	PVE	82M	VIB	565.00	1.76	28.33
1125	PVE	300M	VIB	1796.00	6.21	23.33
1126	PVE	16VM	VIB	335.00	0.35	38.33
1127	PVE	20VM	VIB	395.00	0.41	38.33
1128	PVE	24VM	VIB	395.00	0.52	38.33
1129	PVE	28VM	VIB	403.00	0.61	38.33
1130	PVE	2070VM	VIB	1130.00	1.52	33.33
1131	PVE	2312VM	VIB	252.00	0.26	38.33
1132	PVE	2350VM	VIB	790.00	1.09	38.33
1142	PTC	30HP	VIB	196.00	0.87	27.00
1143	PTC	40HD	VIB	269.00	0.87	28.00
1144	PTC	50HD1	VIB	255.00	0.87	25.00
1145	PTC	50HD2	VIB	290.00	0.87	25.00
1146	PTC	65HD	VIB	305.00	0.87	26.00
1147	PTC	60HD	VIB	305.00	0.87	28.00
1148	PTC	75HD	VIB	410.00	0.87	25.00

Type	Hammer Make	Hammer Model	Hammer Type	Rated Power kW	Ecc. Mass kips	Frequency Hz
1149	PTC	100HD	VIB	451.00	0.87	23.00
1150	PTC	100HDS	VIB	564.00	0.87	23.00
1151	PTC	175HD	VIB	611.00	0.87	23.00
1152	PTC	240HD	VIB	988.00	0.87	23.00
1153	PTC	240HDS	VIB	988.00	0.87	30.00
1154	PTC	120HD	VIB	410.00	0.87	23.00
1155	PTC	130HD	VIB	564.00	0.87	23.00
1156	PTC	200HD	VIB	710.00	0.87	23.00
1157	PTC	265HD	VIB	1080.00	0.87	24.00
1340	H&M	H-150	VIB	94.00	0.11	28.30
1341	H&M	H-1700	VIB	165.00	0.20	20.00
1431	BRUCE	SGV-80	VIB	112.20	0.13	33.33
1432	BRUCE	SGV-100	VIB	142.60	0.18	30.00
1433	BRUCE	SGV-200	VIB	184.80	0.31	28.83
1434	BRUCE	SGV-300	VIB	211.20	0.35	27.50
1435	BRUCE	SGV-400	VIB	286.00	0.44	26.67
1436	BRUCE	SGV-450	VIB	323.40	0.48	26.67
1437	BRUCE	SGV-600	VIB	451.50	0.72	26.67
1438	BRUCE	SGV-1000	VIB	569.10	1.03	25.00
1630	LBFoster	4150	VIB	335.00	0.53	25.00